

20

Resurgence, Physics and Numbers

edited by Frédéric Fauvet, Dominique Manchon,
Stefano Marmi and David Sauzin

Resurgence, Physics and Numbers

edited by
Frédéric Fauvet, Dominique Manchon,
Stefano Marmi and David Sauzin



EDIZIONI
DELLA
NORMALE

20

CRM
SERIES

Inês Aniceto
Institute of Physics
Jagiellonian University
Ul. Łojasiewicza 11
30-348 Kraków, Poland

Carl M. Bender
Department of Physics
Washington University
St. Louis, MO 63130, USA

Michael Borinsky
Depts. of Math. and Physics
Humboldt U.
10099 Berlin, Germany

Olivier Bouillot
Institut Villebon-Georges Charpak
Université Paris-Sud
91400 Orsay, France

Ricardo Couso-Santamaría
CAMGSD, Departamento de Matemática,
Instituto Superior Técnico
Universidade de Lisboa
Av. Rovisco Pais 1
1049-001 Lisboa, Portugal

Gerald V. Dunne
Department of Physics
University of Connecticut
Storrs, CT, 06269, USA

Jean Ecalte
Département de mathématiques
Bât. 425 Université Paris-Sud
91405 Orsay Cedex, France

Li Guo
Department of Mathematics
and Computer Science
Rutgers University
Newark, NJ 07102, USA

Javad Komijani
Institute for Advanced Study
Technische Universität München
Garching 85748, Germany

Dirk Kreimer
Depts. of Math. and Physics
Humboldt U.
10099 Berlin, Germany

Frédéric Menous
Laboratoire de Mathématiques
Bâtiment 425
Université Paris-Sud
91405 Orsay Cedex, France

Jean-Christophe Novelli
Université Paris-Est Marne-la-Vallée
Laboratoire d'Informatique Gaspard-Monge
(CNRS - UMR 8049)
77454 Marne-la-Vallée Cedex 2, France

Sylvie Paycha
Universität Potsdam, Mathematik
Campus II - Golm, Haus 9
Karl-Liebknecht-Straße
24-25 D-14476 Potsdam, Germany

Jean-Yves Thibon
Université Paris-Est Marne-la-Vallée
Laboratoire d'Informatique Gaspard-Monge
(CNRS - UMR 8049)
77454 Marne-la-Vallée Cedex 2, France

Mithat Ünsal
Department of Physics
North Carolina State University
Raleigh, NC, 27695
and
Department of Mathematics
Harvard University
Cambridge, MA, 02138, USA

Qing-hai Wang
Department of Physics
National University of Singapore
117542, Singapore

Bin Zhang
School of Mathematics
Yangtze Center of Mathematics
Sichuan University
Chengdu, 610064, P. R. China

Resurgence, Physics and Numbers

edited by
Frédéric Fauvet, Dominique Manchon,
Stefano Marmi and David Sauzin



EDIZIONI
DELLA
NORMALE

© 2017 Scuola Normale Superiore Pisa

ISBN 978-88-7642-612-4

ISBN 978-88-7642-613-1 (eBook)

DOI 10.1007/978-88-7642-613-1

ISSN 2239-4524 (Print)

ISSN 2532-3326 (Online)

Contents

Preface	xi
Inês Aniceto	
Asymptotics, ambiguities and resurgence	1
1 Introduction and summary	2
2 General concepts and definitions	4
2.1 Transseries, resurgence and discontinuities	7
2.2 Some properties of the alien derivative revisited	14
2.3 Bridge equations	16
3 The simplicity of linear differential equations: the Airy function	18
3.1 Saddle-point analysis	18
3.2 Resurgence and Stokes phenomena	21
3.3 Large-order behaviour and Écalles-Borel-Padé resummation	28
4 Non-linear ODEs and the resurgence of the One-parameter Transseries	38
4.1 Alien chain and discontinuities	44
4.2 Large-order relations	49
4.3 Exact results: ambiguity cancellation	51
5 Further directions: multi-parameter transseries, resonance and beyond	57
References	59
Carl M. Bender, Javad Komijani and Qing-hai Wang	
Nonlinear eigenvalue problems	67
1 Introduction	67
2 Nonlinear eigenvalue problems for Painlevé I and II	72
2.1 Eigenvalue problems for Painlevé I	73
2.2 Eigenvalue problems for Painlevé II	78

2.3	Asymptotic study of the Painlevé equations . . .	81
3	Nonlinear eigenvalue problems for more complicated differential equations	84
	References	88
Michael Borinsky and Dirk Kreimer		
	Feynman diagrams and their algebraic lattices	91
1	The Hopf algebra of Feynman diagrams	91
2	The lattice of subdiagrams	93
3	The Hopf algebra of decorated lattices	95
4	An application of the Hopf algebra of decorated lattices .	97
5	Properties of the lattices	98
6	The quotient $\tilde{\mathcal{H}}_D^{\text{fg}}$: applications	100
6.1	The additive group and renormalization schemes	101
6.2	A tower of Hopf algebras	102
	References	106
Olivier Bouillot and Jean Ecalle		
	Invariants of identity-tangent diffeomorphisms expanded as series of multitangents and multizetas	109
1	Setting and notations	111
1.1	Introduction	111
1.2	Classical results	112
1.3	Affiliates. Generators and mediators	115
1.4	Brief reminder about resurgent functions	118
1.5	Alien derivations as a tool for uniformisation . .	121
1.6	Medial operators	125
1.7	Resurgence of the iterators and generators	127
1.8	Resurgence of the mediators	129
1.9	Invariants, connectors, collectors	131
1.10	The reverse problem: canonical synthesis	132
2	Multitangents and multizetas.	132
2.1	Mould operations and mould symmetries	133
2.2	Multizetas	135
2.3	Multitangents	138
2.4	Resurgence monomials	143
2.5	The non-standard case ($\rho \neq 0$). Normalisation .	148
2.6	The ramified case ($p > 1$) and the localisation constraints	150
2.7	Meromorphic s -continuation of Seh^s and Teh^s etc.	153
3	Collectors and connectors in terms of f	156
3.1	Operator relations	156

3.2	The direct scheme: from g to \mathfrak{p}	158
3.3	The affiliate-based scheme: from g_{\diamond} to \mathfrak{p}_{\diamond}	159
3.4	Parity separation and affiliate selection	161
3.5	The generator-based scheme: from g_* to \mathfrak{p}_*	161
3.6	The mediator-based scheme: from $g_{\#}, g_{\#\#}$ to $\mathfrak{p}_{\#}, \mathfrak{p}_{\#\#}$	162
3.7	From collectors to connectors	164
3.8	The ramified case ($p > 1$)	166
3.9	Reflexive and unitary diffeomorphisms	167
4	Scalar invariants in terms of f	169
4.1	The invariants A_{ω} as entire functions of f	169
4.2	The case $\rho(f) \neq 0$. Normalisation	170
4.3	The case $p \neq 1$. Ramification	171
4.4	Growth properties of the invariants	171
4.5	Alternative computational strategies	173
4.6	Concluding remarks	175
5	Complement: twisted symmetries and multitangets.	176
5.1	Twisted alien operators	176
5.2	Twisted mould symmetries	177
5.3	Twisted co-products	179
5.4	Twisted multitangets	179
5.5	Affiliates : from function to operator	183
5.6	Main and secondary symmetry types	185
6	Complement: arithmetical vs dynamical monics	188
6.1	Distinguishing Stokes constants from holomorphic invariants	188
6.2	Arithmetical multizetas	189
6.3	Dynamical multizetas	193
6.4	The ramified case (tangency order $p > 1$)	196
7	Complement: convergence issues and phantom dynamics	196
7.1	The scalar invariants	196
7.2	The connectors	202
7.3	The collectors	202
7.4	Groups of invariant-carrying formal diffeos	205
7.5	A glimpse of phantom holomorphic dynamics	208
8	Conclusion	209
8.1	Some historical background	209
8.2	Multitangets and multizetas	210
8.3	Remark about the general composition equation	210
9	Tables	212
9.1	Multitangets: symmetrel, alternal, olternol	212
9.2	Parity properties of alternal and olternol multitangets	213

9.3	The invariants as entire functions of f : the general case	222
9.4	The invariants as entire functions of f : the reflexive case	226
9.5	The invariants as entire functions of f : one-parameter cases	227
10	Synopsis	228
10.1	Diffeos, collectors, connectors, invariants	228
10.2	Affiliates, generators, mediators	229
10.3	Main alien operators	229
10.4	Main moulds	230
10.5	Main results	230
	References	231
 Ricardo Couso-Santamaría		
	The resurgent approach to topological string theory	233
1	Introduction	233
2	Basics of topological strings	237
3	Resurgent approach to topological strings	239
3.1	Main results	242
3.2	Open issues	243
4	Conclusions	246
	References	247
 Gerald V. Dunne and Mithat Ünsal		
	WKB and resurgence in the Mathieu equation	249
1	Introduction	249
1.1	Some Motivation from Physics and Mathematics	249
1.2	Resurgent trans-series in quantum spectral problems	251
2	Basic facts about the Mathieu spectrum	255
2.1	Notation and Scaling	255
2.2	Weak coupling: $N\hbar \ll 1$	256
2.3	Strong Coupling: $N\hbar \gg 1$	258
2.4	Theorems Concerning Band and Gap Widths	260
3	Uniform WKB for the Mathieu equation	261
3.1	Strategy of uniform WKB	261
3.2	Perturbative expansion of the uniform WKB ansatz	263
3.3	Global boundary condition: connecting different minima	265
4	Relating perturbative and non-perturbative sectors	268

4.1	Results of Zinn-Justin and Jentschura	268
4.2	Inversion and a surprise	269
4.3	Implications and two independent confirmations	270
5	All-orders WKB analysis of the Mathieu equation: actions and dual actions	272
5.1	Weak coupling	275
5.2	Strong coupling	278
5.3	Intermediate coupling: instanton condensation near the barrier top	280
5.4	Summary of different behaviors of Mathieu spectrum in different regions	282
6	Path integral interpretation: steepest descents and Lefschetz thimbles	283
7	Conclusion	290
	References	290

Li Guo, Sylvie Paycha and Bin Zhang

	Renormalised conical zeta values	299
1	Introduction	299
2	Generalised Algebraic Birkhoff Factorisation	302
3	A differential coalgebraic structure on lattice cones	305
3.1	Lattice cones	305
3.2	The coalgebra of lattice cones	308
4	Renormalisation on Chen cones	311
5	Renormalised CZVs	314
5.1	Regularisations	315
5.2	Renormalisation	319
6	Comparison of the two renormalisation schemes	322
	References	326

Frédéric Menous, Jean-Christophe Novelli and Jean-Yves Thibon

	Combinatorics of Poincaré's and Schröder's equations	329
1	Introduction	329
2	Notations	333
3	Recursive solution of Poincaré's equation	335
4	A tree-expanded solution	336
5	A binary tree expansion	339
5.1	A bilinear map on Sym	339
5.2	Triduplicial expansion	341
5.3	A bijection between parking quasiribbons and Schröder trees	343

5.4	Triduplicial operations	
	on Schröder pseudocompositions	346
6	Expansion on the ribbon basis	349
7	Schröder's equation for the inverse of h	353
8	A noncommutative mould expansion	354
9	The operad of reduced plane trees	356
	9.1 A free operad	356
	9.2 The group of the operad	357
	9.3 The Hopf algebra of reduced plane trees and its	
	characters	358
10	Noncommutative formal diffeomorphisms	359
	10.1 A group of noncommutative diffeomorphisms . .	359
	10.2 Inversion in G_{ncdiff} and Lagrange inversion . . .	361
	10.3 The conjugacy equation	363
11	Commutative versus noncommutative	364
	11.1 Commutative diffeomorphisms	
	and the Connes-Kreimer algebra	364
	11.2 Relating \mathcal{H}_{CK} and \mathcal{H}_{PT}	366
	11.3 The final diagram	367
12	The Catalan operad	369
13	Appendix: numerical examples	373
	13.1 Warmup: $A = 1$	374
	13.2 The logistic map: $A = -1$	374
	13.3 The Ricker map: $A = \mathbb{E}$	375
	References	375

Preface

The conference “Resurgence, Physics and Numbers” took place in Pisa, at the Centro di Ricerca Matematica Ennio De Giorgi, on May 18–22, 2015. This meeting between mathematicians and theoretical physicists involved in resurgent functions, alien calculus and related combinatorics, with a component on Multiple Zeta Values, enabled an exchange of results in fields which had by that time become very active, and which have seen an outburst of publications since then.

The present volume contains contributions of invited speakers at this conference, reflecting the leading themes illustrated during the workshop. We express our deep gratitude to the staffs of the Scuola Normale Superiore di Pisa and of the CRM Ennio De Giorgi for their dedicated support in the preparation of this meeting; all participants could thus benefit from the wonderful and stimulating atmosphere in these institutions and around Piazza dei Cavalieri. We are also very grateful for the possibility of publishing this volume in the CRM series. We acknowledge with thankfulness the support of the CRM De Giorgi, of the laboratorio Fibonacci, of the ANR project “CARMA” and of the GDR 3340 “Renormalisation” (CNRS).

Pisa, December 2016

Frédéric Fauvet
Dominique Manchon
Stefano Marmi
David Sauzin

Asymptotics, ambiguities and resurgence

Inês Aniceto

Abstract. The appearance of resurgent functions in the context of the perturbative study of observables in physics is now well established. Whether these arise from the related study of non-linear systems or the saddle-point perturbative analysis, one is left with an asymptotic series and the need of a non-perturbative completion, or transseries, which includes different non-perturbative phenomena. The complete understanding of resummation procedures and the resurgence of the non-perturbative phenomena can then lead to a systematic approach to obtain exact results such as strong-weak coupling interpolation, cancellation of ambiguities in the so-called Stokes directions, and more generally the study of analytic properties of the respective transseries solutions. These notes will give a general overview of how to set-up resurgence in simple examples, and how to proceed towards exact analytic results.

Contents	1
1 Introduction and summary	2
2 General concepts and definitions	4
2.1 Transseries, resurgence and discontinuities	7
2.2 Some properties of the alien derivative revisited	14
2.3 Bridge equations	16
3 The simplicity of linear differential equations: the Airy function	18
3.1 Saddle-point analysis	18
3.2 Resurgence and Stokes phenomena	21
3.3 Large-order behaviour and Écalle-Borel-Padé resummation	28
4 Non-linear ODEs and the resurgence of the one-parameter transseries	38
4.1 Alien chain and discontinuities	44
4.2 Large-order relations	49
4.3 Exact results: ambiguity cancellation	51
5 Further directions: multi-parameter transseries, resonance and beyond	57
References	59

1 Introduction and summary

Computing physical observables of a given quantum theory, can often only be performed via perturbation theory in either the weakly or strongly coupled regimes. Such perturbative expansions are however often divergent, with zero radius of convergence, and are defined only as asymptotic series

$$\langle \mathcal{O}(g) \rangle \simeq \sum_{k \geq 0} \mathcal{O}_k g^{-k}. \quad (1.1)$$

whose coefficients are factorially divergent at large order¹

$$\mathcal{O}_k \sim \frac{\Gamma(k + \beta)}{A^{k+\beta}}, \quad k \gg 1. \quad (1.2)$$

It is well known that this divergence is connected to the existence of non-perturbative phenomena, unaccounted for in the perturbative analysis. Resurgence is a mathematical theory which allows us to effectively study this connection, and its consequences. Moreover, it allows us to construct a full non-perturbative solution from perturbative data. First introduced by Écalle in [1–3], modern day resurgence theory has developed in the last three decades into an elegant mathematical tool with a diverse set of applications [4–9].²

Resurgent properties have been observed in a wide range of problems in mathematical physics. They appear for example in solutions of differential and finite difference equations (see *e.g.* the well studied cases of Painlevé I, II and Riccati non-linear differential equations [20–25]). In the contexts of quantum mechanics [26, 27] and quantum field theories [28], non-perturbative phenomena such as instantons [29] and renormalons [30], have long been known to exist beyond perturbation theory. In fact in quantum mechanical problems, it is the existence of asymptotic multi-instanton sectors which allow for a resurgent and unambiguous transseries solution to describe energy eigenvalues [31–33]. Since then, the asymptotic behaviour of perturbation theory and the resurgence behind it, was found in many different examples in physical systems, from quantum mechanics [19, 34–45], to large N gauge theories [23, 24, 46–63], quantum field theories [40, 44, 59, 64–76], and string theory [13, 22–24, 48–51, 77–87].

The aim of this paper is to present a simple, hands-on approach, on the use of resurgence in the study of asymptotic expansions with associated

¹ A, β are numbers encoding the position and type of singularities of the related Borel transform.

² For recent reviews on resurgence, transseries and summability, see [8, 10–19].

non-perturbative phenomena. We will introduce some key ideas behind resurgence theory in Section 2. Concepts such as transseries, Borel resummation, Stokes phenomena and alien calculus will be presented with the help of simple examples, while the respective formal derivations are referenced for the interested reader.

In Sections 3 and 4 we show the tools of resurgence at work in two simple examples: the linear ordinary differential equation (ODE) governing the Airy function [10,49], and the non-linear ODE behind the so-called Müller-Israel-Stuart (MIS) theory [88,89]. Along the way different numerical methods are introduced, including convergence acceleration and resummation. This analysis closely follows the work of [19], together with some results of [42]. The milestones achieved for each example are:

1. Given our asymptotic expansion, we find (or make an educated guess for) the respective transseries solution, with sectors describing both perturbative and non-perturbative phenomena. The tools presented in Section 2 are then used to make predictions of the relations between those different sectors.
2. These predictions can be checked numerically to high precision. In cases where the non-perturbative data is not known, these predictions, together with the assumption that the transseries is resurgent, allow us to construct a full non-perturbative solution from perturbative data.
3. Finally, from the complete resurgent transseries solution, one can perform resummation methods to obtain exact results away from the asymptotic regime. Resurgence theory plays an essential role in deriving these results, such as the cancellation of ambiguities or strong/weak coupling interpolation.

Such linear and non-linear ODEs are the natural starting points to show resurgence at work. Resurgent techniques can also be applied to a much wider range of problems, following the same steps as described above. We finish in Section 5 with a summary of results and a discussion of open problems in mathematical physics, where resurgence can play a key role.

ACKNOWLEDGEMENTS. I would like to thank Romuald Janik and Michał Spaliński for comments and suggestions during a set of lectures I presented at Jagiellonian University in Kraków, in January 2016, based on this work.

2 General concepts and definitions

As a starting point, take the strong coupling regime of some observable $F(z)$, with coupling variable $z \gg 1$. We will further assume that using some procedure of perturbation theory (*e.g.* saddle-point analysis or recursion equation from differential equations) in this regime we obtain an expansion

$$F(z) \simeq \sum_{n=0}^{+\infty} \frac{F_n}{z^{n+1}}. \quad (2.1)$$

which is asymptotic, with zero radius of convergence. Moreover, we will take the large-order behaviour of the coefficients F_n to be growing factorially

$$F_n \sim n! \text{ for } n \gg 1. \quad (2.2)$$

This is a very common problem appearing in the study of observables of interacting theories, for example in QFTs, due to the factorial growth of the number Feynman diagrams at each loop order in perturbation theory [29]. Furthermore, it is often the case that perturbation theory and the associated series of the type (2.1), are the only results one can expect from the study of the observable in question. Given the asymptotic properties of the series, one may wonder how to make sense of the formal power series (2.1): this will be the main question we will address at present. This section follows largely the works [8, 11, 14, 23, 90, 91].

As the preliminary step in our quest, one would like to know how to associate a value to (2.1) for each value of the coupling z . A well known process (see *e.g.* [49]) for asymptotic series is to perform an *optimal truncation*, which leads to very good approximations. Optimal truncation is the truncation of the series to the so-called least term: in the regime $z \gg 1$, the terms of (2.1) start by decreasing very rapidly, and only at some point (the least term) start increasing. In this truncation we want to keep terms such that

$$\frac{|F_n|}{|z|^{n+1}} \ll \frac{|F_{n-1}|}{|z|^n}, \text{ for } n \ll |z| \quad (2.3)$$

In fact we can keep terms such that $\frac{|F_n|}{|F_{n-1}|} \lesssim |z|$ for $n \leq N_{\text{op}}(z)$, thus obtaining an optimally truncated series

$$F_{\text{op}}(z) = \sum_{n=0}^{N_{\text{op}}(z)} \frac{F_n}{z^{n+1}}. \quad (2.4)$$

Note that the least term $N_{\text{op}}(z)$, will depend on the value of the coupling z for which the series (2.1) is being evaluated at. In performing the optimal

truncation, we obtain an extremely accurate approximation of (2.1) and the error can be seen to be

$$|F(z) - F_{\text{op}}(z)| \sim e^{-Az}, \quad (2.5)$$

where A is a characteristic number of the problem in question. This is the first hint of the relation between the asymptotic behaviour of (2.1) and its non-perturbative origins: the error is non-analytic, $e^{-Az} \sim 0$ if one expands around $z \sim \infty$.

One can improve on this error by performing certain resummation procedures to the divergent tail which was left out from the truncation procedure. One such framework to address the asymptotic properties and resummation of the series such as (2.1) is *Borel analysis*. In this framework we introduce the Borel transform, via the following rule

$$\mathcal{B}\left[\frac{1}{z^{\alpha+1}}\right](s) \equiv \frac{s^\alpha}{\Gamma(\alpha+1)}, \quad (2.6)$$

where $\Gamma(\alpha)$ is the gamma function. Performing this transformation to every term of the asymptotic series (2.1), we obtain the Borel transform associated to that series:

$$\mathcal{B}[F](s) = \sum_{k=0}^{+\infty} \frac{F_k}{\Gamma(k+1)} s^k. \quad (2.7)$$

This series is now convergent around the origin in \mathbb{C} , with some non-zero radius of convergence. Note that the rule (2.6) is not well defined for cases where the power of z^{-1} is non-positive (*i.e.* $\alpha \leq -1$). In an asymptotic series for $z \gg 1$ these terms are of finite number and must be excluded from the procedure of Borel analysis. They do not change the asymptotic properties of the series and can be easily re-inserted once the resummation procedure has been performed. The rule (2.6) which leads to the now convergent series (2.7) can be seen more naturally as applying an inverse Laplace transform to each of the terms in (2.1). Due to the divergent nature of the series (2.1), this procedure can only be seen as the inverse Laplace transform of $F(z)$ at a formal level. Nevertheless, given the convergent properties of (2.7) one can study the analytic properties of this second series and sum it around the origin in \mathbb{C} .

The Borel transform $\mathcal{B}[F](s)$ will naturally have singularities (defining its radius of convergence). To study the analytic properties of (2.7) one needs to locate these singularities in the complex s -plane (which we shall also call the *Borel plane*). Within the radius of convergence, the series (2.7) will define an analytic function, which can sometimes be

guessed, but more often will be approximated numerically (as we shall see later). In directions $\arg s = \theta$ where there are no singularities, one may analytically continue this function along the ray $e^{i\theta}\mathbb{R}^+$ and define an inverse Borel transform - or *Borel resummation* of $F(z)$ along θ - by a Laplace transform

$$\mathcal{S}_\theta F(z) = \int_0^{e^{i\theta}\infty} ds \mathcal{B}[F](s) e^{-zs}. \quad (2.8)$$

The function $\mathcal{S}_\theta F(z)$ has the same asymptotic expansion as $F(z)$, and for each z will give a better approximation to the value of the asymptotic series (2.1) than the optimal truncation method (even if the function $\mathcal{B}[F](s)$ is only known as a numerical approximation).

But what happens when $\mathcal{B}[F](s)$ has singularities (poles and/or branch cuts) along a direction θ ? How can we assign a value for $F(z)$ in this case? The Laplace transform (2.8) will be ill defined as we have singularities exactly on the direction of the integration contour. We then need to choose a contour which avoids the singularities. The most natural contours one can choose give rise to the so-called lateral Borel resummations:

$$\mathcal{S}_{\theta\pm} F(z) \equiv \mathcal{S}_{\theta\pm\varepsilon} F(z), \quad \text{for } \varepsilon \sim 0^+. \quad (2.9)$$

Different integration contours give rise to functions with the same asymptotic behaviour but which differ by non-analytic exponentially suppressed terms. Thus choosing different contours gives rise to a non-perturbative ambiguity and it is said that $F(z)$ is non-Borel summable along these singular directions θ .

As a simple example, assume that the first singularity of $\mathcal{B}[F](s)$ along a certain direction θ is at $s = A$, and it is a simple pole

$$\mathcal{B}[F](s)|_{s \simeq A} \sim \frac{1}{s - A}. \quad (2.10)$$

The difference between the two lateral Borel resummations is

$$\mathcal{S}_{\theta+} F(z) - \mathcal{S}_{\theta-} F(z) \propto \oint_{s=A} ds \frac{e^{-zs}}{s - A} = e^{-Az}. \quad (2.11)$$

Once again the non-analytic term e^{-Az} appears from the analysis of the asymptotic behaviour of (2.1), and the characteristic value A shows up as the leading singularity of the Borel transform (2.7).

The existence of different singular directions $\arg s = \theta_i$ on the Borel plane associated to the original series (2.1) leads to a family of sectorial analytic functions $\{\mathcal{S}_\theta F(z)\}$ all with the same asymptotic behaviour,

and which differ by non-analytic terms. In order to understand how to “connect” each of these sectors, one needs to understand the behaviour of the Borel transform around each singularity for all singular directions θ_i , so we can learn how to jump across the direction θ_i and reach a different sector. The singular directions θ_i are called *Stokes lines*. Learning about the behaviour of the Borel transform along Stokes lines will lead to the construction of an unambiguous result for the resummed function, even along these singular directions: a procedure that known as ambiguity cancellation. To perform a thorough and systematic analysis of what happens at Stokes lines we now turn to resurgence, and the realm of simple resurgent functions.

2.1 Transseries, resurgence and discontinuities

The fact that the resummations in the different sectors $\{\mathcal{S}_\theta F\}$ differ by non-perturbative terms hints to the fact that the full solution associated with the observable $F(z)$ should be some non-perturbative completion of the asymptotic series (2.1), into what is called a transseries. Indeed, in the calculation of energies in quantum mechanics, the transseries is an essential step in the cancellation of ambiguities: the non-perturbative terms are given by instanton sectors, and A is the instanton action related to the probability of tunneling between (possibly complex) saddles of the potential (see *e.g.* [26, 27, 32–36, 40, 43, 92]).

A transseries is a formal series expansion both in the original variable $z \gg 1$ and also in the non-analytic terms. We will work with the so-called log-free height-one transseries, where the expansion is on transmonomials $z^\alpha e^{S(z)}$ with $\alpha \in \mathbb{R}$ and $S(z)$ is some particular convergent series (more intricate examples where $S(z)$ is in itself a transseries, with compositions of exponentials and logarithms, can be also studied, see *e.g.* [12]). In its simplest form, the transseries has the form

$$\mathcal{F}(z, \sigma) = \sum_{\ell=0}^{+\infty} \sigma^\ell F^{(\ell)}(z) \in \mathbb{C} \llbracket z^{-1}, \sigma e^{-Az} \rrbracket, \quad (2.12)$$

where $F^{(0)}(z)$ is just the perturbative series (2.1) and

$$F^{(\ell)}(z) = e^{-\ell Az} \Phi_\ell(z), \quad \ell \geq 1, \quad (2.13)$$

with $\Phi_\ell(z)$ generally an asymptotic series as well

$$\Phi_\ell(z) = z^{\beta_\ell} \sum_{k=0}^{+\infty} \frac{F_k^{(\ell)}}{z^k}. \quad (2.14)$$

In most cases of interest, the leading behaviour of the asymptotic series, given by z^{β_ℓ} is of the form $\beta_\ell = -\ell \beta$, and we shall assume this form from now on, unless otherwise stated. The transseries (2.12) is a one-parameter transseries: it appears when one has non-perturbative sectors such as instantons, which are exponentially suppressed with the same associated action A , and where ℓ is the instanton number. Note that from calculations such as (2.11) we know that the sectorial functions will differ by exponentially small terms $e^{-A z}$, but a more careful analysis of these differences would show that (in the case of simple resurgent functions, as defined below) for each suppressed contribution there is an asymptotic expansion associated with it. The parameter σ in (2.12) is the transseries parameter, which for each particular wedge of the complex plane, selects distinct non-perturbative completions to the original series (2.1).

There are extensions of the above transseries (2.12) to include more parameters σ_i . In fact, if a given observable has different non-analytic contributions $e^{-A_i z}$, for $A_i \neq A$ (and typically also different from the multi-instanton contributions already included in the one-parameter case $A_i \neq \ell A$), one should expect a new transseries parameter for each non-analytic term appearing.

An asymptotic expansion $F(z)$ (such as $F(z)$ in (2.1) or any of the $\Phi_\ell(z)$) is said to be a simple resurgent function if its Borel transform only has simple poles or logarithmic branch cuts as singularities. Taking ω as a singularity, the Borel transform around this singularity will be of the form³

$$\mathcal{B}[F](s)|_{s=\omega} \sim \frac{a_\omega}{2\pi i (s - \omega)} + \Psi(s - \omega) \frac{\log(s - \omega)}{2\pi i} + \zeta_{\text{hol}}(s - \omega), \quad (2.16)$$

where $a_\omega \in \mathbb{C}$ and Ψ, ζ_{hol} are analytic around the origin. Moreover $\Psi(s)$ will be related to a function $G_1(z)$ by the inverse Borel transform

$$\Psi(s) = \mathcal{B}[G_1](s). \quad (2.17)$$

³ Many times the Borel transform is not exactly of the shape (2.16), but instead it has square root branch cuts. Nevertheless we will still be in the realm of simple resurgent functions if the $\mathcal{B}[z^\gamma F](z)$ has the behaviour (2.16) where γ is commonly the “degree” of the branch cut. Typically this is related to a factorial growth of the coefficients F_k in (2.1) which differs from the factorial growth “removed” by the Borel transform. For example, assume in (2.1) that $F_n \sim \Gamma(n + 1 - \gamma)$ for some γ when $n \gg 1$. Then $\mathcal{B}[F](s)$ in (2.7) has coefficients which grow as

$$\frac{F_k}{\Gamma(k+1)} \sim \frac{\Gamma(k+1-\gamma)}{\Gamma(k+1)} \neq 1 \quad \text{if } \gamma \neq 0, k \gg 1. \quad (2.15)$$

On the other hand $\mathcal{B}[z^\gamma F](s) = \sum_{k \geq \gamma} F_k s^{k-\gamma} / \Gamma(k+1-\gamma)$ will have the expected behaviour (2.16). For a detailed analysis on this see [19].

Normally the function $G_1(z)$ is also known as a series and requires a resummation procedure as well. A transseries (2.12) will have resurgent properties if the coefficients of different sectors in (2.13) $F_k^{(\ell)}$ and $F_r^{(\ell')}$ will be related for ℓ close to ℓ' . This can be seen directly at the level of the Borel transforms by noticing that the type of relation (2.16) will relate Φ_ℓ to $\Phi_{\ell'}$ in the same way that F and G_1 are related by (2.16) and (2.17). In other words, if we take $F = \Phi_\ell$ for some particular ℓ , and analyse its behaviour on some particular singularity, we will see that the function G_1 in (2.17) will be $\Phi_{\ell'}$ for ℓ close to ℓ' . In fact, the value of ℓ' will directly depend on the singularity we are analysing. These relations can be checked via the so-called large-order relations, which will be exemplified later on.

To highlight how the behaviour (2.16) is related to the non-perturbative jump (2.11), assume that the Borel transform (2.7) has only one singularity $s = \omega_1$ of the type (2.16), in some direction θ of the complex Borel plane (see Figure 2.1). The difference between lateral Borel resummations will be given by the integration over the Hankel contour C_ω around the branch cut starting at ω_1 , as defined on the right of Figure 2.1:

$$\begin{aligned} (\mathcal{S}_{\theta^+} - \mathcal{S}_{\theta^-}) F(z) &= \int_{C_\omega} ds \mathcal{B}[F](s) e^{-sz} \\ &= -a_{\omega_1} e^{-\omega_1 z} + e^{-\omega_1 z} \int_{C_0} \frac{ds}{2\pi i} \Psi(s) \log(s) e^{-sz}. \end{aligned} \quad (2.18)$$

The last integration over C_0 (Hankel contour now centred at the origin) will return the discontinuity across the log cut $(-2\pi i)$ multiplied by the Laplace transform of the function $\Psi(s)$. Given that we have the identification (2.17), this last part is nothing more than the resummation of the function $G_1(z)$. We can write⁴

$$(\mathcal{S}_{\theta^+} - \mathcal{S}_{\theta^-}) F(z) = - (a_{\omega_1} + \mathcal{S}_{\theta^-} G_1(z)) e^{-\omega_1 z} + \dots \quad (2.19)$$

In the \dots we have included the possibility that the Borel transform of $G_1(z)$ would also have a singularity along the same direction θ . If $G_1(z)$ is an analytic function, there are no more contributions and $\mathcal{S}_{\theta^-} G_1(z) = \mathcal{S}_\theta G_1(z)$. But if $\mathcal{B}[G_1](s)$ has a singularity along the direction θ , say at

⁴ If $G_1(z)$ is in itself asymptotic with singularities along direction θ , we need to choose a lateral resummation for $G_1(z)$, which will be directly linked to the choice of the discontinuity for the log branch cut chosen.

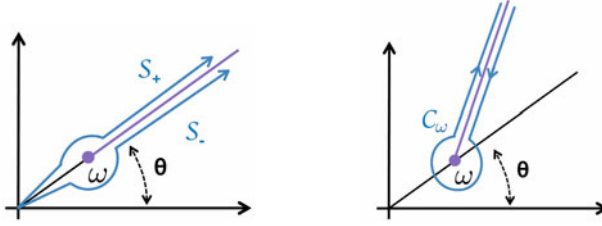


Figure 2.1. On the left: lateral Borel resummation contours around singularity $s = \omega$. On the right: Hankel contour around the branch cut starting at $s = \omega$.

$s = \omega_2$

$$\begin{aligned} \mathcal{B}[G_1](s)|_{s=\omega_2} &\sim \frac{a_{\omega_2}}{2\pi i (s - \omega_2)} \\ &+ \mathcal{B}[G_2](s - \omega_2) \frac{\log(s - \omega_2)}{2\pi i} \\ &+ \text{holomorphic,} \end{aligned} \quad (2.20)$$

then one can expect that this singularity will also contribute to the overall difference between lateral Borel resummations of $F(z)$, and the position of this singularity will naturally be at $s = \omega_1 + \omega_2$ (thus its contribution will be exponentially suppressed by $e^{-(\omega_1 + \omega_2)z}$ in (2.1)). This contribution can in fact be visible if we analyse the Borel transform $\mathcal{B}[F](s)$ at $s = \omega_1 + \omega_2 \equiv \omega$, and it will be of the same form as $\mathcal{B}[G_1](s)|_{s=\omega_2}$ up to an overall constant

$$\begin{aligned} \mathcal{B}[F](s)|_{s=\omega \equiv \omega_1 + \omega_2} &\sim \frac{C_2 a_{\omega_2}}{2\pi i (s - \omega)} \\ &+ C_2 \mathcal{B}[G_2](s - \omega) \frac{\log(s - \omega)}{2\pi i} \\ &+ \text{holomorphic.} \end{aligned} \quad (2.21)$$

To reach this new singularity, coming from $\mathcal{B}[G_1](s)$, there are in general different ways to analytically continue the paths of resummation to avoid the previous singularities (in this case only one), passing these singularities from above or from below. These different paths of analytic continuation to reach each singular point are encoded in the jump of $F(z)$ across the Stokes line, through a weighed average of such paths (see [14, 90]).

The difference between lateral Borel resummations along a Stokes line defines the *discontinuity* of $F(z)$ across that line:

$$(\mathcal{S}_{\theta^+} - \mathcal{S}_{\theta^-}) F(z) \equiv -\mathcal{S}_{\theta^-} \circ \text{Disc}_{\theta} F(z). \quad (2.22)$$

For the example shown above (where each asymptotic expansion $F(z)$ and $G_i(z)$ will only have one independent singularity each in the Stokes direction θ), this discontinuity will be given by the sum of the contributions of all the differences between lateral Borel resummations:

$$\begin{aligned} \text{Disc}_\theta F(z) &= (a_{\omega_1} + G_1(z)) e^{-\omega_1 z} + C_2 (a_{\omega_2} + G_2(z)) e^{-(\omega_1 + \omega_2)z} + \dots \\ &= \sum_{\omega_n \in \text{Sing}_\theta} C_n (a_{\omega_n} + G_n(z)) e^{-\sum_{j=1}^n \omega_j z}. \end{aligned} \quad (2.23)$$

In the above result, $\text{Sing}_\theta = \{\omega_i\}$ is the collection of singularities appearing in all asymptotic expansions in the direction θ . The constants C_n reflect the weighed average of paths that encode the contribution of the singularities of other Borel transforms $\mathcal{B}[G_n](s)$ to the discontinuity of the original asymptotic series $F(z)$, where

$$\begin{aligned} \mathcal{B}[G_i](s)|_{s=\omega_{i+1}} &\sim \frac{a_{\omega_{i+1}}}{2\pi i (s - \omega_{i+1})} \\ &+ \mathcal{B}[G_{i+1}](s - \omega_{i+1}) \frac{\log(s - \omega_{i+1})}{2\pi i} \\ &+ \text{holomorphic}. \end{aligned} \quad (2.24)$$

We have assumed that the singular behaviour of the Borel transform of $F(z)$ at $\omega \equiv \sum_{j=1}^n \omega_j$ (for $n > 1$), originated solely from the behaviour of $\mathcal{B}[G_{n-1}]$ at $s = \omega_n$ (and equivalently for the $G_i(z)$). More generally, the Borel transform of the asymptotic expansion $F(z)$ will have a singular behaviour at $\omega \equiv \sum_{j=1}^n \omega_j$

$$\begin{aligned} \mathcal{B}[F](s)|_{s=\omega \equiv \sum_{j=1}^n \omega_j} &\sim \frac{C_{0,n} a_{\omega_n}}{2\pi i (s - \omega)} \\ &+ C_{0,n} \mathcal{B}[G_n](s - \omega) \frac{\log(s - \omega)}{2\pi i} \\ &+ \text{holomorphic}, \end{aligned} \quad (2.25)$$

where the $C_{0,n}$ can have contributions from the singularities of all the sectors $G_i(z)$, as well as a contribution not associated to any of these. In this case, (2.22) and (2.23) still hold true, but the explicit form of the coefficients $C_n \equiv C_{0,n}$ will be more involved. For the Borel transforms of $G_i(z)$ we also expect the behaviour

$$\begin{aligned} \mathcal{B}[G_i](s)|_{s=\omega \equiv \sum_{j=i+1}^n \omega_j} &\sim \frac{C_{i,n} a_{\omega_n}}{2\pi i (s - \omega)} \\ &+ C_{i,n} \mathcal{B}[G_n](s - \omega) \frac{\log(s - \omega)}{2\pi i} \\ &+ \text{holomorphic}, \end{aligned} \quad (2.26)$$

and an expression similar to (2.23) can be found for their discontinuity.

In the interest of systematically determining the general explicit formulas for the discontinuity across Stokes directions,⁵ we now turn to *alien calculus*. The discontinuous jump across Stokes lines, given by (2.22), naturally defines another operator called the Stokes automorphism $\underline{\mathcal{S}}_\theta$

$$\mathcal{S}_{\theta^+} = \mathcal{S}_{\theta^-} \circ \underline{\mathcal{S}}_\theta = \mathcal{S}_{\theta^-} \circ (\mathbf{1} - \text{Disc}_\theta). \quad (2.27)$$

The Stokes automorphism acts on the set of simple resurgent functions (which forms a subalgebra of $\mathbb{C}[[z^{-1}]]$), and will induce a differentiation operation on the same algebra via exponentiation (see e.g. [90]):⁶

$$\underline{\mathcal{S}}_\theta = \exp \{ \underline{\Delta}_\theta \}. \quad (2.28)$$

The operator $\underline{\Delta}_\theta$ is called a directional differentiation, and can be decomposed into components which depend only on each of the singularities existing in the direction θ . The Stokes automorphism in the direction θ becomes

$$\underline{\mathcal{S}}_\theta = \exp \left\{ \sum_{\omega_i \in \text{Sing}_\theta} e^{-\omega_i z} \Delta_{\omega_i} \right\}. \quad (2.29)$$

These *alien derivatives* Δ_ω are a differentiation (obey Leibnitz rule, as shown below in a simple example) and have the following properties:⁷ for a resurgent function $F(z)$

- if ω is not a singular point in the Borel plane, then $\Delta_\omega F = 0$;
- if ω is the only (or the first) singular point in the direction θ of Borel plane, then (2.16) holds true, and Δ_ω is related to the algebraic structure of the Borel transform at the singular point (shedding the functional structure)

$$\mathcal{S}_\theta (\Delta_\omega F) = -a_\omega - \mathcal{S}_\theta G \quad (2.30)$$

or equivalently $\Delta_\omega F(z) = -a_\omega - G(z)$;

⁵ Each term in (2.23) can be directly determined by the analysis of singularities of Borel transforms for each sector $F(z)$ and $G_i(z)$. Nevertheless, it is extremely valuable to have an approach which uses the information that these are simple resurgent functions, with a set of singularities in each singular direction θ , to systematically construct a general formula for the discontinuity.

⁶ In an equivalent way, the automorphism $T : f(x) \rightarrow f(x+1)$ which defines translations also induces a differentiation via $T = \exp\left(\frac{d}{dx}\right)$, which can be checked by a Taylor expansion of this exponential.

⁷ These properties can be checked by expanding the exponential in (2.29) and taking into consideration the different paths of analytic continuation one can take to reach a given singularity, see e.g. [14].

- if we have a collection of singular points $\omega \in \{\omega_1, \omega_1 + \omega_2, \dots, \dots, \sum_i \omega_i, \dots\}$ on the Borel plane, then for $\omega \equiv \sum_{i=1}^n \omega_i$ the alien derivative Δ_ω will be given by

$$\Delta_\omega F = - \sum_{s=1}^n \frac{1}{s} \sum_{0=m_0 < m_1 < \dots < m_s = n} \prod_{r=0}^{s-1} C_{m_r, m_{r+1}} (a_{\omega_n} + G_n), \quad (2.31)$$

where the $C_{m,n}$ are defined in (2.25) and (2.26).

The exponential factors appearing in (2.29) are an essential part of the construction of the jump across the Stokes line, as they will be responsible for the exponential weights appearing in (2.23). Another definition which will be of importance is the pointed alien derivative

$$\dot{\Delta}_\omega = e^{-\omega z} \Delta_\omega. \quad (2.32)$$

If we expand the exponential in (2.29) we find

$$\begin{aligned} & \mathfrak{S}_\theta F(z) \\ &= F(z) + \sum_{\substack{r \geq 1 \\ \omega_{n_i} \in \text{Sing}_\theta}} \frac{1}{r!} e^{-(\omega_{n_1} + \omega_{n_2} + \dots + \omega_{n_r})z} \Delta_{\omega_{n_1}} \Delta_{\omega_{n_2}} \dots \Delta_{\omega_{n_r}} F(z). \end{aligned} \quad (2.33)$$

The jump of $F(z)$ across the Stokes direction θ is then

$$\begin{aligned} & \mathcal{S}_{\theta^+} F - \mathcal{S}_{\theta^-} F \\ &= \sum_{\substack{r \geq 1 \\ \omega_{n_i} \in \text{Sing}_\theta}} \frac{1}{r!} e^{-(\omega_{n_1} + \omega_{n_2} + \dots + \omega_{n_r})z} \mathcal{S}_{\theta^-} \left(\Delta_{\omega_{n_1}} \Delta_{\omega_{n_2}} \dots \Delta_{\omega_{n_r}} F(z) \right). \end{aligned} \quad (2.34)$$

Take the example given above where $F(z)$ has a singularity in the Borel plane at $s = \omega_1$, each of the higher sectors $G_i(z)$ have also one singularity in the Borel plane at $s = \omega_{i+1}$, with behaviour around the singularities given by (2.16) and (2.24), respectively. We can directly write the non-zero alien derivatives acting on these functions:

$$\Delta_{\omega_1} F(z) = -a_{\omega_1} - G_1(z), \quad \Delta_{\omega_{i+1}} G_i(z) = -a_{\omega_{i+1}} - G_{i+1}(z). \quad (2.35)$$

The set of all singularities appearing in the direction θ is $\text{Sing}_\theta = \{\omega_i, i \in \mathbb{N}\}$. It is not hard to see that the only terms in (2.33) acting

non-trivially on $F(z)$ are

$$\begin{aligned}
 \mathfrak{S}_\theta F(z) &= F(z) + \left(e^{-\omega_1 z} \Delta_{\omega_1} + \frac{1}{2!} e^{-(\omega_1 + \omega_2)z} \Delta_{\omega_2} \Delta_{\omega_1} \right. \\
 &\quad \left. + \frac{1}{3!} e^{-(\omega_1 + \omega_2 + \omega_3)z} \Delta_{\omega_3} \Delta_{\omega_2} \Delta_{\omega_1} + \dots \right) F(z) \quad (2.36) \\
 &= F(z) + \sum_{n \geq 1} \frac{(-1)^n}{n!} e^{-\sum_{i=1}^n \omega_i z} (a_{\omega_n} + G_n(z)).
 \end{aligned}$$

Comparing with (2.23) and taking into consideration (2.27), we find an agreement with the expression found before for the discontinuity of $F(z)$ with the identification of the constants $C_n = \frac{(-1)^n}{n!}$.

2.2 Some properties of the alien derivative revisited

There are two major properties of the alien operator Δ_ω extremely useful in the study of the Stokes phenomena occurring across singular directions: Δ_ω is a differentiation, and the pointed alien derivative $\dot{\Delta}_\omega$ as defined in (2.32) commutes with the natural derivative $[\dot{\Delta}_\omega, \frac{d}{dz}] = 0$. In this subsection we follow [14] and analyse these two properties in more detail.

The alien derivative operator is indeed a differentiation, in the sense that it obeys Leibnitz rule. Let $F(z)$ and $G(z)$ be simple resurgent functions. Then

$$\Delta_\omega (F(z) G(z)) = (\Delta_\omega F)(z) G(z) + F(z) (\Delta_\omega G(z)). \quad (2.37)$$

This can be clearly seen at the level of the respective Borel transforms for simple examples. Start by noting that the product of two simple resurgent functions will correspond to the convolution of their Borel transforms

$$\mathcal{B}[F G](s) = \mathcal{B}[F] * \mathcal{B}[G](s) = \int_0^s d\zeta \mathcal{B}[F](\zeta) \mathcal{B}[G](s - \zeta). \quad (2.38)$$

For simplicity take the case of the Borel transforms being simple poles at $s = \omega$ for both functions F, G :

$$\mathcal{B}[F](s) = \frac{a}{2\pi i (s - \omega)}, \quad \mathcal{B}[G](s) = \frac{b}{2\pi i (s - \omega)}. \quad (2.39)$$

The alien derivatives acting on each of these resurgent functions give non-zero results at $s = \omega$: $\Delta_\omega F(z) = -a$, $\Delta_\omega G(z) = -b$. One can easily

see that a resummation (2.8) of each of these Borel transforms will lead to the relation $\mathcal{S}_\theta F(z) = \frac{a}{b} \mathcal{S}_\theta G(z)$. The Borel transform of the product of the two functions will be:

$$\begin{aligned} \mathcal{B}[F G](s) &= \frac{a b}{(2\pi i)^2} \int_0^s d\xi \frac{1}{\xi - \omega} \frac{1}{s - \xi - \omega} \\ &= \frac{a b}{(2\pi i)^2} \frac{1}{s - 2\omega} \left(\int_0^s d\xi \frac{1}{\xi - \omega} + \int_0^s d\xi \frac{1}{s - \xi - \omega} \right) \\ &= \frac{2 a b}{(2\pi i)^2 (s - 2\omega)} \log \left(1 - \frac{s}{\omega} \right), \end{aligned} \quad (2.40)$$

where we assumed $|s| < |\omega|$. Note the appearance of a new pole at $s = 2\omega$, and a log cut at $s = \omega$. We shall firstly focus on the singular behaviour at $s = \omega$. From the above result we can now read

$$\mathcal{B}[F G](s) = \Psi(s - \omega) \frac{\log(s - \omega)}{2\pi i} + \text{holomorphic}. \quad (2.41)$$

The function

$$\Psi(s) \equiv \mathcal{B}[H](s) = \frac{2 a b}{(2\pi i)(s - \omega)} \quad (2.42)$$

corresponds to the Borel transform of a function $H(z)$, such that the only non-zero alien derivative acting on the product FG is given by $\Delta_\omega(FG)(z) = -H(z)$. Given the Borel transforms of F and G , it is not difficult to note that

$$\Psi(s) = a \mathcal{B}[G](s) + b \mathcal{B}[F](s). \quad (2.43)$$

Consequently for this simple example we have just shown that the operator Δ_ω obeys the Leibnitz rule:

$$\begin{aligned} \Delta_\omega(FG)(z) &= -a G(z) - b F(z) \\ &= \Delta_\omega F(z) G(z) + \Delta_\omega G(z) F(z). \end{aligned} \quad (2.44)$$

One could worry that the new singularity at $s = 2\omega$ for the Borel transform of the product FG would give rise to a new non-zero alien derivative $\Delta_{2\omega}$. Given that neither Borel transforms of F or G have a singularity at this point, one expects that $\Delta_{2\omega}(FG) = 0$, as it is a differentiation. But if one analytically continues (2.40) past the first singularity $s = \omega$ we find that the residue at $s = 2\omega$ is non-zero. This is not an inconsistency however, because the alien derivative can be defined via a combination

of different analytic continuations of the paths of integration avoiding the previous singularities (in our case $s = \omega$).⁸

Another important property of the alien derivative is its commutation relations with the usual derivative $d_z \equiv \frac{d}{dz}$. Firstly note that d_z commutes with the lateral Borel resummations. Using (2.7)

$$\begin{aligned} d_z \mathcal{S}_{\theta^\pm} F(z) &= \int_0^{e^{\pm i\epsilon} \infty} ds \mathcal{B}[F](s) (-s) e^{-sz} \\ &= - \int_0^{e^{\pm i\epsilon} \infty} ds \sum_{k=0}^{+\infty} \frac{F_k s^{k+1}}{\Gamma(k+1)} = \mathcal{S}_{\theta^\pm} (d_z F)(z), \end{aligned} \quad (2.45)$$

and we conclude that $d_z \mathcal{S}_{\theta^\pm} = \mathcal{S}_{\theta^\pm} d_z$. From this result and (2.27) we easily obtain

$$d_z \mathcal{S}_{\theta^+} = d_z \mathcal{S}_{\theta^-} \circ \underline{\mathfrak{S}}_\theta = \mathcal{S}_{\theta^-} \circ \underline{\mathfrak{S}}_\theta d_z \Leftrightarrow \mathcal{S}_{\theta^-} d_z \underline{\mathfrak{S}}_\theta = \mathcal{S}_{\theta^-} \underline{\mathfrak{S}}_\theta d_z, \quad (2.46)$$

from which we see that d_z also commutes with the Stokes automorphism. Now using the definition of the Stokes automorphism in terms of the pointed alien derivatives, $\underline{\mathfrak{S}}_\theta = \exp\left(\sum_{\omega_i \in \text{Sing}_\theta} \dot{\Delta}_{\omega_i}\right)$, we conclude that the pointed alien derivative commutes with the usual derivative

$$\left[\dot{\Delta}_\omega, \frac{d}{dz} \right] = 0. \quad (2.47)$$

With this relation it is now easy to determine the commutation relations of the usual derivative and the regular alien derivative Δ_ω :

$$\left[\Delta_\omega, \frac{d}{dz} \right] = -\omega \Delta_\omega. \quad (2.48)$$

These properties will allow us to find a connection between alien calculus and usual calculus, thus providing a way to determine the action of the alien derivative from the knowledge of the relevant transseries: this comes in the form of a set of equations called *bridge equations*.

2.3 Bridge equations

In the context of non-linear problems in ordinary differential equations, the transseries solution $\mathcal{F}(z, \sigma)$ (we are taking the simplest one-parameter example (2.12)) will obey a particular non-linear ODE in the variable

⁸ Using (2.31), we can write $\Delta_{2\omega}(FG) = -C_{0,2} - \frac{1}{2}C_{0,1}C_{1,2}$, where the constants $C_{i,j}$ can be read from the local behaviour of $\mathcal{B}[FG](s)$ at $s = \omega$ and $s = 2\omega$ ($C_{0,1} = 1$ and $C_{0,2} = -ab$, respectively), as well as of $\Psi(s)$ at $s = \omega$ ($C_{1,2} = 2ab$). We then conclude that $\Delta_{2\omega}(FG) = 0$.

z . Given that the pointed alien derivative commutes with the usual derivative, $[\dot{\Delta}_\omega, d_z] = 0$, and that the transseries depends on two commuting parameters z and σ , $[d_z, d_\sigma] = 0$, one finds that $\dot{\Delta}_\omega F$ and $d_\sigma F$ will obey the same linearised ODE (in variable z).⁹ As these are two complete solutions of the same ODE, it follows that they must be proportional

$$\dot{\Delta}_\omega F = S_\omega(\sigma) \frac{dF}{d\sigma}, \quad (2.49)$$

with the proportionality factor only allowed to depend on the parameter σ via some Taylor expansion:

$$S_\omega(\sigma) = \sum_{k=0}^{+\infty} S_\omega^{(k)} \sigma^k. \quad (2.50)$$

The equations (2.49) are Écalle's *bridge equations*. The coefficients in the expansion of the proportionality factor (2.50) will depend on the specific problem one is solving, *i.e.* the ansatz used for the transseries and the type of singularities in it.¹⁰ The constants $S_\omega^{(k)}$ appearing in (2.50) are the well-known *Stokes coefficients* (or Stokes constants), which encode the Stokes phenomena across the singular Stokes directions. They naturally appear in the analysis of singularities in the Borel plane, as we will see in the examples below. Note that if the transseries has more than one-parameter (more than one singular direction) the bridge equations will reflect this (see for example Section 4 of [23], and [19]).

We shall now turn to some applications, and detail how to use resurgence in different examples of ODEs. In particular we will focus on the construction of transseries, the resurgent analysis of Borel transforms and analytic properties of the transseries solutions (such as varying $z \in \mathbb{C}$, performing strong-weak coupling interpolation and how to deal with the cancellation of ambiguities, see *e.g.* [42, 55, 60]). The first example we will discuss is of a linear ODE: the very well known example of the Airy function.

⁹ This linearised ODE is directly obtained from the original ODE for the transseries $\mathcal{F}(z, \sigma)$.

¹⁰ Given a particular transseries and using the bridge equations, many of these constants will in fact be zero.

3 The simplicity of linear differential equations: the Airy function

The Airy function example has been thoroughly studied from the point of view of resurgence and Stokes phenomena, being the quintessential example of these phenomena. It has been studied from the perspective of saddle-point analysis and hyperasymptotics (see [49,93–95] and references therein), and of resurgence techniques (see *e.g.* [10,49]). Presently, we will provide a brief analysis of the known results, together with the numerical checks and applications which can be performed. This is a very good setting to introduce many of these numerical checks, which can then be generalised to cases with more structure, such as the one studied in the following Section.

The linear ODE describing the Airy function is

$$Z''(\kappa) - \kappa Z(\kappa) = 0, \quad (3.1)$$

whose solutions can be written in integral form as

$$Z_\gamma = \frac{1}{2\pi i} \int_\gamma du e^{-V(u)}, \quad V(u) = -\kappa u + \frac{u^3}{3}. \quad (3.2)$$

The path γ is a contour chosen such that the integral converges. There are two homologically independent contours γ originating two independent solutions of (3.1), usually denoted by Z_{A_i} and Z_{B_i} . A general solution to (3.1) will be a linear combination of these two, forming a (two-parameter) transseries.

Given the integral form of the solution (3.2) we will analyse this problem perturbatively in two ways:

1. Take the solution (3.2) as a zero dimensional path integral and perform saddle-point analysis;
2. Construct a transseries solution and perform resurgent analysis directly from (3.1).

3.1 Saddle-point analysis

In order to construct explicit perturbative solutions of (3.2) as asymptotic expansions, one can perform saddle-point analysis. The saddle-points of the potential in (3.2) are

$$V'(u) = -\kappa + u^2 = 0 \Leftrightarrow u_\pm^* = \pm\sqrt{\kappa}, \quad (3.3)$$

with $V(u_\pm^*) = \mp\frac{2}{3}\kappa^{3/2}$. The leading contribution from each saddle to the exponential in the integrand of (3.2) can be found from the expansion

$$(V''(u_{\pm}^*) = \pm 2\sqrt{\kappa})$$

$$V(u) = V(u_{\pm}^*) + \frac{1}{2}V''(u_{\pm}^*)(u - u_{\pm}^*)^2 \quad (3.4)$$

and will be given by $\exp(-V(u_{\pm}^*))$. The dominant saddle will naturally depend on the argument of κ . For each saddle u^* one can define the steepest descent contour, as the contour of integration γ passing through u^* such that:

- $\text{Im}(V(u) - V(u^*)) = 0, u \in \gamma$;
- $\text{Re}(V(u)) \rightarrow +\infty$ when $u \rightarrow \infty$.

In the set of images of Figure 3.1 the potential is shown normalised to $V(u_-^*)$ (the saddle u_-^* is always at the edge of brown areas and blue areas of the potential). In brown $\text{Re}(V(u) - V(u_-^*)) > 0$ is shown, while the opposite is in blue, for different values of the argument of $\kappa = e^{i\theta}$. We see that in general a single steepest descent contour passes through each saddle: we can choose a particular saddle contribution and determine its asymptotic expansion. However, when

$$\text{Im}(V(u_+^*) - V(u_-^*)) = 0 \Leftrightarrow \text{Im}\kappa^{3/2} = 0 \Rightarrow \arg \kappa = \ell \frac{2\pi}{3}, \ell \in \mathbb{Z}, \quad (3.5)$$

the contour passes through both saddles. In Figure 3.1 this is seen at $\arg \kappa = 0, \frac{2\pi}{3}, \frac{4\pi}{3}$. These lines are *Stokes lines*. As we shall see in more detail below, these are the directions where a subleading (exponentially suppressed) contribution gets picked up and starts contributing to the full solution.

By increasing θ , the once subleading contributions become of the same order of magnitude as the original saddle. This happens in the so-called *anti-Stokes lines*

$$\text{Re}(V(u_+^*) - V(u_-^*)) = 0 \Leftrightarrow \text{Re}\kappa^{3/2} = 0 \Rightarrow \arg \kappa = \frac{\pi}{3} + \ell \frac{2\pi}{3}, \ell \in \mathbb{Z}. \quad (3.6)$$

Both saddles contribute at the same order when $\arg \kappa = \frac{\pi}{3}, \pi, \frac{5\pi}{3}$, as can be seen in Figure 3.1, when both saddles are at intersections between brown and blue areas of the potential. At these points, one will find an oscillatory pattern in the asymptotic behaviour. This is just the Stokes phenomena: in the asymptotic regime, different sectors will have different asymptotic formulae, which describe the same analytic function. These different sectors will be fully captured by the transseries.

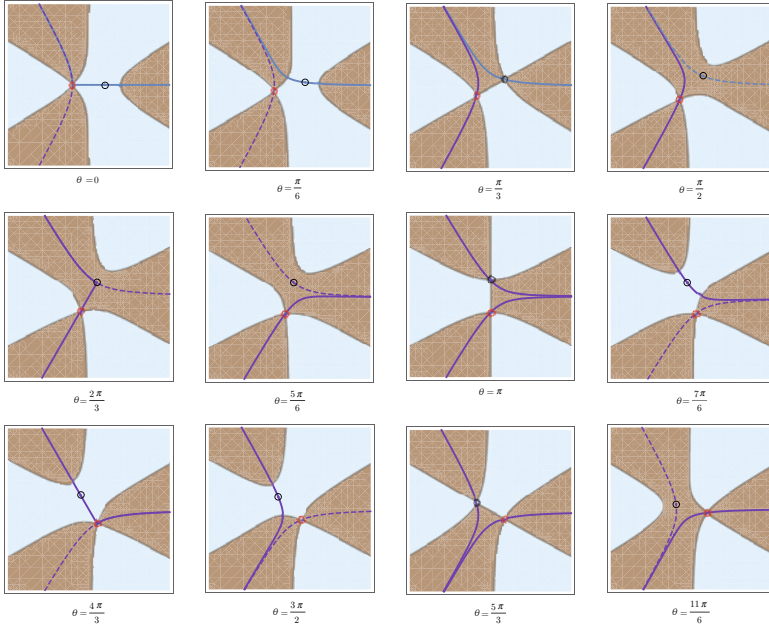


Figure 3.1. Steepest decent contours passing through saddles u_{\pm}^* , for different values of the argument of $\kappa = e^{i\theta}$. Dashed lines correspond to the subleading saddle and solid lines to the leading one. The saddle u_{-}^* , which corresponds to the solution Z_{A_i} , is shown as a red circle, while the saddle u_{+}^* , corresponding to Z_{B_i} is shown as a black circle. At $\theta = 0$ we keep only the contribution of the u_{-}^* saddle, shown in purple (while in blue is the contour corresponding to Z_{B_i} , whose coefficient is set to zero). After crossing a Stokes line, at $\theta = \frac{2\pi}{3}$, the second contour gets picked up (also starts contributing): both are then shown in purple.

The two-parameter transseries solution will be given by a linear combination of the homologically different contour solutions:

$$Z(\kappa, \sigma_1, \sigma_2) = \sigma_1 Z_{A_i}(\kappa) + \sigma_2 Z_{B_i}(\kappa). \quad (3.7)$$

The $Z_{A_i}(\kappa)$ and $Z_{B_i}(\kappa)$ can be determined perturbatively for $\kappa \gg 1$ from an expansion around the respective saddle points u_{-}^* and u_{+}^* . Both expansions will be asymptotic in inverse powers of $z = \kappa^{3/2}$.

For example, let us assume that at the ray $\kappa \in \mathbb{R}^+$ ($\theta = 0$), we start solely with the exponentially decreasing solution $Z_{A_i}(\kappa)$, which corresponds to the usual Airy function $A_i(\kappa)$ (in the first plot of Figure 3.1 we keep the contour in purple). This corresponds to taking $\sigma_1 = 1$ and $\sigma_2 = 0$ in the transseries (3.7). Now rotate the argument of κ , and analyse what happens with the transseries. Analytically continuing the solution,

we find (see Figure 3.1) that at $\theta = \frac{\pi}{3}$ both saddles have the same magnitude, but as we started with only one contour of integration (and have not yet crossed a Stokes line), the second saddle remains invisible. From $\frac{\pi}{3} < \theta < \pi$ the second saddle Z_{B_i} is exponentially suppressed as compared to the leading one Z_{A_i} we have started with.

Let us analyse the behaviour of the contour of integration passing through saddle u_-^* (*i.e.* the one associated with Z_{A_i}) when crossing the Stokes line $\theta = \frac{2\pi}{3}$: from Figure 3.1 one can see that this contour changes directions from $\theta = \frac{\pi}{2}$ to $\theta = \frac{5\pi}{6}$; moreover at $\theta = \frac{5\pi}{6}$ the new contour is a combination of the contour previously associated with u_-^* and the contour passing through the second saddle u_+^* . This is because exactly at the Stokes line $\theta = \frac{2\pi}{3}$ the contour associated with u_-^* passes through both saddles, signalling that from here on one should include both of them, despite the contribution of the second saddle being highly exponentially suppressed (in Figure 3.1 we can see that from this point on both contours are purple, and will contribute to the transseries). In the transseries (3.7) this is seen by a jump in the value of σ_2 , which becomes non-zero at $\theta = \frac{2\pi}{3}$. Note that even though σ_2 has a discrete jump in its value, the total solution (3.7) is analytic at the Stokes line $\theta = \frac{2\pi}{3}$, because the saddle contribution just added, Z_{B_i} is then highly exponentially suppressed. Picking the two saddles at the Stokes line, and analytically continuing the transseries solution to the anti-Stokes line $\theta = \pi$ (where both contributions are of the same magnitude), we will find the known oscillatory pattern of the function $A_i(\kappa)$ when $\kappa \in \mathbb{R}^-$.

This analysis can be extended to the whole complex plane. In fact, the monodromy of the transseries requires a double sheeted Riemann surface, as one will need to rotate $\arg \kappa$ all the way to 4π to obtain the saddles in their original positions (notice in Figure 3.1 that the next plot at $\theta = 2\pi$ would see the two saddles exchange positions as compared to $\theta = 0$).

We will now turn to the resurgent analysis of this problem, where the transseries can be analysed systematically and the jumps in the transseries parameters can be explicitly determined.

3.2 Resurgence and Stokes phenomena

We shall now analyse the Airy problem from the perspective of resurgence, starting from the ODE (3.1). If we take an ansatz of the form $Z(\kappa) = e^{-\frac{1}{2}A\kappa^\alpha} \Phi(\kappa)$ where

$$\Phi(\kappa) \simeq \kappa^\beta \sum_{\ell=0}^{+\infty} a_\ell \kappa^{-\alpha \ell}, \quad (3.8)$$

we easily find from (3.1) that there are two values of A allowed

$$A_{\pm} = \pm A, \quad A = \frac{4}{3}. \quad (3.9)$$

We will also find $\alpha = 3/2$ and $\beta = -1/4$. This information tells us (together with the fact that we are studying a linear ODE) that we will have two independent solutions, each related to one of the saddle points of the previous section.¹¹ The full solution will be a two-parameter transseries given by (3.7) as expected, where

$$\begin{aligned} Z_{\text{Ai}}(\kappa) &= \frac{1}{2\sqrt{\pi}\kappa^{1/4}} e^{-\frac{1}{2}A\kappa^{3/2}} \Phi_{-\frac{1}{2}}(\kappa); \\ Z_{\text{Bi}}(\kappa) &= \frac{1}{2\sqrt{\pi}\kappa^{1/4}} e^{\frac{1}{2}A\kappa^{3/2}} \Phi_{\frac{1}{2}}(\kappa), \end{aligned} \quad (3.10)$$

and

$$\Phi_{\pm\frac{1}{2}}(\kappa) \simeq \sum_{n=0}^{+\infty} a_n^{(\pm 1/2)} \kappa^{-\frac{3}{2}n}, \quad (3.11)$$

with coefficients

$$a_n^{(\pm 1/2)} \equiv \mp (\pm 1)^n a_n, \quad a_n = \frac{1}{2\pi} A^{-n} \frac{\Gamma(n + \frac{5}{6}) \Gamma(n + \frac{1}{6})}{n!}. \quad (3.12)$$

These coefficients can be determined in closed form by putting the above ansatz into the ODE (3.1) and solving the ensuing recursive equations for the a_n .

We can read the position of the Stokes and anti-Stokes lines directly from the exponentials in (3.10). Stokes lines occur at arguments of κ such that these exponentials are as damped (or enhanced) as possible, *i.e.* when $\text{Im}(\frac{A}{2}\kappa^{3/2}) = 0$. The anti-Stokes lines occur when both of these exponentials are of the same order, *i.e.* $\text{Re}(\frac{A}{2}\kappa^{3/2}) = 0$. Summarising, we have

$$\begin{aligned} \text{Stokes lines at} \quad \arg \kappa &= 0, \frac{2\pi}{3}, \frac{4\pi}{3}; \\ \text{anti-Stokes lines at} \quad \arg \kappa &= \frac{\pi}{3}, \pi, \frac{8\pi}{3}. \end{aligned} \quad (3.13)$$

¹¹ Because we are dealing with a linear problem, we have found a finite number of “instanton” sectors, unlike the one-parameter transseries shown in (2.12). The example studied in the next section will deal with a non-linear problem, where the transseries will indeed be of the type (2.12).

Note that the natural variable appearing in Z_{Ai} , Z_{Bi} is $z = \kappa^{3/2} \gg 1$. In this new variable it is easy to see that the Stokes lines will fall at $\arg z = 0, \pi$. Recall that discontinuities occur at Stokes lines (associated to a non-trivial action of the Stokes automorphism $\underline{\mathfrak{S}}_\theta$). In the z variable we have either a discontinuity of the type $\underline{\mathfrak{S}}_0$ or of the type $\underline{\mathfrak{S}}_\pi$. Following the analysis of [42] and recalling that the monodromy of the problem is 4π (discussed again below), we find the following succession of discontinuities in the κ -plane as shown in Figure 3.2 (reproduced from [42]). From here on, unless stated otherwise, we will be using the natural variable z .

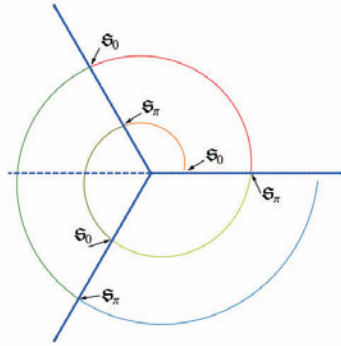


Figure 3.2. Different types of discontinuities $\underline{\mathfrak{S}}_0$ or $\underline{\mathfrak{S}}_\pi$ (as defined for the variable $z = \kappa^{3/2}$) when one moves in the $\arg \kappa$. In solid blue are the 3 Stokes lines in the κ -plane, and the dashed line is $\arg \kappa = \pi$ (an anti-Stokes line). The monodromy is 4π , so we need to go around the complex plane twice to reach the initial point.

Taking another look at the coefficients a_n in (3.12), it is not difficult to check that the series (3.11) are asymptotic. Moreover, the coefficients a_n will have a factorial growth at large order $n \gg 1$, with a subleading exponential growth:

$$\frac{a_{n+1}}{a_n} = \frac{1}{A} \frac{\left(n + \frac{5}{6}\right) \left(n + \frac{1}{6}\right)}{n+1} \sim \frac{n}{A} + \mathcal{O}(n^0). \quad (3.14)$$

The next step is to construct the Borel transform of the asymptotic series $\Phi_{\pm 1/2}(z)$. Given the simplicity of the example at hand, and the fact that we know the coefficients a_n in closed form, we can determine the Borel transforms exactly from rule (2.6): they are just hypergeometric functions (up to residual coefficients $a_0 = 1$ which need to be separately added as

to make use of (2.6) we need to take the expansions (3.11) from $n \geq 1$)

$$\mathcal{B} \left[\check{\Phi}_{\pm 1/2} \right] (s) = -\frac{5}{48} {}_2F_1 \left(\frac{7}{6}, \frac{11}{6}, 2 \left| \pm \frac{s}{A} \right. \right). \quad (3.15)$$

Here, ${}_2F_1(a, b, c|z)$ is a hypergeometric function with a branch cut in the complex z -plane in the positive real axis starting at $z = 1$. The functions $\check{\Phi}_{\pm 1/2}(z)$ are just the original expansions (3.11) with the residual coefficient a_0 removed,

$$\check{\Phi}_{\pm 1/2}(z) = \Phi_{\pm 1/2}(z) \pm a_0. \quad (3.16)$$

Consequently $\mathcal{B} \left[\check{\Phi}_{\pm 1/2} \right] (s)$ have a singularity at $s = \pm A$, respectively. Both Borel transforms have a non-zero radius of convergence at $s = 0$, as expected. The behaviour of the Borel transforms around their respective singularities is:

$$\begin{aligned} \mathcal{B} \left[\check{\Phi}_{1/2} \right] (s) \Big|_{s=A} &= \frac{i}{2\pi i (s - A)} \\ &+ i\mathcal{B} \left[\check{\Phi}_{-1/2} \right] (s - A) \frac{\log(s - A)}{2\pi i} \\ &+ \text{holomorphic}; \\ \mathcal{B} \left[\check{\Phi}_{-1/2} \right] (s) \Big|_{s=-A} &= \frac{i}{2\pi i (s + A)} \\ &+ i\mathcal{B} \left[\check{\Phi}_{1/2} \right] (s + A) \frac{\log(s + A)}{2\pi i} \\ &+ \text{holomorphic}. \end{aligned} \quad (3.17)$$

The effects of resurgence are evident from these expansions: in the singular behaviour of $\mathcal{B} \left[\check{\Phi}_{1/2} \right] (s)$ we can see the *resurgence* of the $\Phi_{-1/2}$ sector through its Borel transform evaluated at $s = 0$, and in the singular behaviour of $\mathcal{B} \left[\check{\Phi}_{-1/2} \right] (s)$ we see the *resurgence* of the sector $\Phi_{1/2}$! It is in fact this appearance of different sectors in the singular behaviour of Borel transforms of every sector that describes the theory of resurgence. The analysis of the resurgent properties of sectors $\Phi_{\pm 1/2}$ shown below closely follows [19].

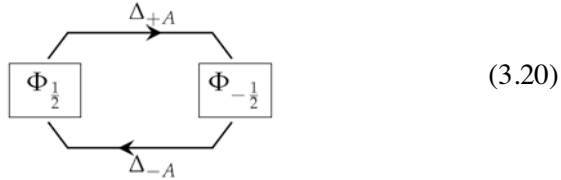
One can now look beyond the functional nature of the singularities and realise that in (3.17) we have in fact the relations between the asymptotic series $\Phi_{\pm 1/2}$, the building blocks of the transseries. From this point of view, we can define a linear operator Δ_ω , where ω is a point in the complex plane, acting on these building blocks Φ_n and returning the structure

encoded in (3.17):¹²

$$\begin{aligned} \Delta_A \Phi_{1/2} &= -i\Phi_{-1/2} \quad ; \quad \Delta_\omega \Phi_{1/2} = 0 \text{ for } \omega \neq A; & (3.19) \\ \Delta_{-A} \Phi_{-1/2} &= -i\Phi_{1/2} \quad ; \quad \Delta_\omega \Phi_{-1/2} = 0 \text{ for } \omega \neq -A. \end{aligned}$$

Thus the Borel transform of $\Phi_{1/2}$ has a singularity at $\omega = A$ given by the Stokes coefficient $S_1 = -i$ multiplying $\Phi_{-1/2}$ (up to the functional structure of the singularity). In the same way $\Phi_{-1/2}$ has a singularity at $\omega = -A$ described by the Stokes coefficient $S_{-1} = -i$ multiplying $\Phi_{1/2}$. In non-singular points ω of the Borel transforms, the operator Δ_ω will return zero. This operator is nothing but the alien derivative introduced in the previous Section, and (3.19) are just the result of the bridge equations (2.49). In here we shall not dwell on how to determine (3.19) directly from the bridge equations, but this can be found in the appendices of [19] for a transseries with a finite number of sectors Φ_n , and in Section 2 of [23] for a one-parameter transseries of the type (2.12).¹³

The algebraic structure of the action of Δ_ω on the building blocks of our transseries (3.7) can be summarised pictorially as shown in [19]



To study the transitions that happen at Stokes lines we have to construct the Stokes automorphism (2.29). For $\theta = 0$ (in the z variable) there is only one possible singularity at $\omega = A$, while for $\theta = \pi$ the only possible singularity is at $\omega = -A$. The Stokes automorphism simplifies to

$$\begin{aligned} \underline{\mathfrak{S}}_0 &= \exp \{ e^{-Az} \Delta_A \} = \sum_{n=0}^{+\infty} (e^{-Az} \Delta_A)^n \frac{1}{n!}; \\ \underline{\mathfrak{S}}_\pi &= \exp \{ e^{Az} \Delta_{-A} \} = \sum_{n=0}^{+\infty} (e^{Az} \Delta_{-A})^n \frac{1}{n!}. \end{aligned} \quad (3.21)$$

¹² The expression for the series $\check{\Phi}_{\pm 1/2}$ includes the pole contribution, e.g.

$$\Delta_A \check{\Phi}_{1/2} = -i \left(1 + \check{\Phi}_{-1/2} \right). \quad (3.18)$$

Nevertheless, this can be easily re-written in terms of the original expansions (3.11) as shown here. Naturally, $\Delta_\omega a_0 = 0$.

¹³ This last case will in fact be reviewed in the next Section.

From (3.19) we find that $(\Delta_A)^2 \Phi_{1/2} = (\Delta_{-A})^2 \Phi_{-1/2} = 0$,¹⁴ so one easily reaches the result:

$$\begin{aligned} \underline{\mathfrak{S}}_0 \Phi_{1/2} &= \Phi_{1/2} - i e^{-Az} \Phi_{-1/2} & ; & \quad \underline{\mathfrak{S}}_\pi \Phi_{1/2} = \Phi_{1/2}; \\ \underline{\mathfrak{S}}_\pi \Phi_{-1/2} &= \Phi_{-1/2} - i e^{Az} \Phi_{1/2} & ; & \quad \underline{\mathfrak{S}}_0 \Phi_{-1/2} = \Phi_{-1/2}. \end{aligned} \quad (3.22)$$

Recall from (2.27) that the Stokes automorphism acting trivially, $\underline{\mathfrak{S}}_\theta \Phi_n = \Phi_n$, corresponds to Φ_n having no discontinuity along the direction θ .

At the level of the functions Z_{A_i} and Z_{B_i} we have

$$\underline{\mathfrak{S}}_\pi Z_{A_i} = Z_{A_i} + S_{-1} Z_{B_i} \quad ; \quad \underline{\mathfrak{S}}_0 Z_{B_i} = Z_{B_i} + S_1 Z_{A_i}; \quad (3.23)$$

with the other two relevant actions being trivial. These two transformations encode all Stokes phenomena across all Stokes lines: the Stokes line in the original variable κ will not lie at $\theta = 0, \pi$ but they will be of the type $\underline{\mathfrak{S}}_0$ or $\underline{\mathfrak{S}}_\pi$, as shown in [42] and reproduced in Figure 3.2. Finally, at the level of the transseries, the Stokes transitions are

$$\begin{aligned} \underline{\mathfrak{S}}_0 Z(z, \sigma_1, \sigma_2) &= Z(z, \sigma_1 + S_1, \sigma_2); \\ \underline{\mathfrak{S}}_\pi Z(z, \sigma_1, \sigma_2) &= Z(z, \sigma_1, \sigma_2 + S_{-1} \sigma_1). \end{aligned} \quad (3.24)$$

As an exercise, we shall now analyse what happens to the resummed transseries solution when we go from the positive real axis in original variable $\kappa \in \mathbb{R}^+$ to the negative real axis $\kappa \in \mathbb{R}^-$ (this analysis closely follows [42]). The general resummed transseries solution at $\arg \kappa = 0^+$ (just above the Stokes line at $\theta = 0$) is

$$S_{0^+} Z(\kappa, \sigma_1, \sigma_2) = \sigma_1 S_{0^+} Z_{A_i}(\kappa) + \sigma_2 S_{0^+} Z_{B_i}(\kappa). \quad (3.25)$$

We will further assume that at $\arg \kappa = 0^+$ we are starting with the solution Z_{A_i} , *i.e.* $\sigma_2 = 0$. Then our initial solution is given by

$$S_{0^+} Z_{\text{initial}}(\kappa) = S_{0^+} Z(\kappa, 1, 0) = S_{0^+} Z_{A_i}(\kappa). \quad (3.26)$$

We now want to analytically continue this solution across the complex κ -plane, keeping $|\kappa|$ fixed, and moving $\arg \kappa$ towards the negative real axis. When $\theta_\kappa \equiv \arg \kappa = \frac{2\pi}{3}$ we reach a Stokes line, which we need to cross. Just before the Stokes line we still have, by analytic continuation,

$$S_{\theta_\kappa^-} Z_{\text{initial}}(\kappa) = S_{\theta_\kappa^-} Z(\kappa, 1, 0) = S_{\theta_\kappa^-} Z_{A_i}(\kappa). \quad (3.27)$$

¹⁴ Combinations such as $\Delta_A \Delta_{-A}$ are not considered as they mix singularities from different singular directions. The Stokes automorphism in each singular direction will only include the singularities in that direction.

This Stokes line at $\theta_\kappa = \frac{2\pi}{3}$ is of the type $\underline{\mathfrak{S}}_\pi$ in (3.24), and we have $\mathcal{S}_{\theta_\kappa^+} Z(\kappa, \sigma_1, \sigma_2) = \mathcal{S}_{\theta_\kappa^-} Z(\kappa, \sigma_1, \sigma_2 + S_{-1}\sigma_1)$. Consequently,

$$\mathcal{S}_{\theta_\kappa^-} Z(\kappa, 1, 0) = \mathcal{S}_{\theta_\kappa^+} Z(\kappa, 1, -S_{-1}), \quad (3.28)$$

and we can write

$$\mathcal{S}_{\theta_\kappa^+} Z_{\text{initial}}(\kappa) = \mathcal{S}_{\theta_\kappa^+} Z(\kappa, 1, -S_{-1}) = \mathcal{S}_{\theta_\kappa^+} Z_{\text{Ai}}(\kappa) - S_{-1} \mathcal{S}_{\theta_\kappa^+} Z_{\text{Bi}}(\kappa). \quad (3.29)$$

Continuing the analytic continuation all the way to $\kappa \in \mathbb{R}^-$, we reach the anti-Stokes line at $\arg \kappa = \pi$, where our solution is now of the form (recall $S_{-1} = -i$)

$$\begin{aligned} \mathcal{S}_\pi Z_{\text{initial}}(\kappa) &= \mathcal{S}_\pi Z(|k| e^{i\pi}, 1, i) \\ &= \mathcal{S}_\pi Z_{\text{Ai}}(|k| e^{i\pi}) + i \mathcal{S}_\pi Z_{\text{Bi}}(|k| e^{i\pi}). \end{aligned} \quad (3.30)$$

This result should reflect the known Airy function $A_i(\kappa)$ in the negative real axis. While in the positive real axis this function was approximated solely by the asymptotic series $Z_{\text{Ai}}(\kappa)$, in the negative real axis the correct oscillatory behaviour of $A_i(\kappa)$ will in fact be the above combination of the two asymptotic series $Z_{\text{Ai}}(\kappa)$ and $Z_{\text{Bi}}(\kappa)$. This will be more concretely shown in the figures of the next Subsection, where we will compare results coming from just the perturbative series $Z_{\text{Ai}}(\kappa)$, the full transseries $Z_{\text{initial}}(\kappa)$ and the exact results for the Airy function $A_i(\kappa)$ for different resummation procedures, keeping $|k|$ fixed and varying $\arg \kappa \in]0, \pi]$.

Summarising the results up to this point:

1. Resurgence techniques provided a direct calculation of the Stokes transitions at every Stokes line (3.24), with the prediction for the discrete jumps the transseries parameters undergo at these lines;
2. Taking into account all Stokes phenomena of the problem, one will arrive at the expected asymptotic oscillatory behaviour at the anti-Stokes line $\theta = \pi$, given by (3.30).

In conclusion, resurgence gives a systematic approach to connect all different asymptotic sectors through the Stokes automorphism (2.27). A non-trivial Stokes automorphism reflects the existence of discontinuities at the level of the asymptotic series Φ_n , the building blocks of the transseries. Nevertheless, the full transseries solution is analytic and will not have discontinuities (or ambiguities, as we shall see in the next Section) even at Stokes lines.

3.3 Large-order behaviour and Écalle-Borel-Padé resummation

At this point, there are two relevant issues which have not been addressed: checking resurgence from approximate Borel transforms and the resummation procedure for the pursuit of exact results. The example of the Airy function (or other linear ODE) is quite simple: we can directly see resurgence at work from the Borel transforms which are known exactly. But in most situations one cannot obtain the Borel transforms exactly, so what are the (numerical) checks one can do which evidence the resurgent properties of the observables? This is the core of the first issue. The second issue focuses on the goal of obtaining exact results and the analytic properties of the transseries away from the asymptotic regime.

The answer to the first question is in the so-called large-order behaviour. For the second question one needs to understand the so-called Écalle-Borel-Padé resummation method.

Given a function $F(z)$ with a discontinuity along some directions $\{\theta_k\}$ in the complex plane, we can use Cauchy's theorem to write

$$\begin{aligned} F(z) &= \frac{1}{2\pi i} \oint_{w=x} dw \frac{F(w)}{w-z} \\ &= - \sum_{\{\theta_k\}} \frac{1}{2\pi i} \int_0^{e^{i\theta_k}\infty} dw \frac{\text{Disc}_{\theta_k} F(w)}{w-z} + \text{contributions at } z=\infty. \end{aligned} \quad (3.31)$$

To recover the second line above one deforms the contour as shown in Figure 3.3. (In this figure it is assumed that there is only one discontinuous direction; in general one needs to deform the contour to avoid all discontinuous directions θ_k .) In most cases of interest, scaling arguments can be used to indicate that there is no contribution around ∞ [27, 96]. The relation (3.31) can be applied to any of the asymptotic series $\Phi_n(z)$. Let us do so for $\Phi_{1/2}$: using variable $x = 1/z \ll 1$ we obtain

$$\Phi_{1/2}(x) = - \frac{1}{2\pi i} \int_0^{+\infty} dw \frac{\text{Disc}_0 \Phi_{1/2}(w)}{w-x}. \quad (3.32)$$



Figure 3.3. Deformation of the contour to circle the discontinuities of a function $F(z)$.

From (2.27) we can write

$$\text{Disc}_0 \Phi_{1/2}(x) = -S_1 e^{-A/x} \Phi_{-1/2}(x) = i e^{-A/x} \Phi_{-1/2}. \quad (3.33)$$

Also taking into account that for $x \ll 1$, $\frac{1}{w-x} = \frac{1}{w} \sum_{\ell=0}^{+\infty} \left(\frac{x}{w}\right)^\ell$ and using the asymptotic expansions (3.11), we can re-write (3.32) as

$$\sum_{n=0}^{+\infty} a_n^{(1/2)} x^n \simeq + \frac{S_1}{2\pi i} \sum_{\ell=0}^{+\infty} x^\ell \int_0^{+\infty} dw e^{-A/w} \sum_{h=0}^{+\infty} a_h^{(-1/2)} w^{h-\ell-1}. \quad (3.34)$$

Comparing equal powers of x , one writes

$$a_n^{(1/2)} \simeq + \frac{S_1}{2\pi i} \sum_{h=0}^{+\infty} a_h^{(-1/2)} \int_0^{+\infty} dw e^{-A/w} w^{h-n-1}, \quad n \gg 1. \quad (3.35)$$

The integral appearing above only converges when $h < n$, and we are taking a sum over all $h \geq 0$. This relation will thus be valid only for large values of order n , making it a *large-order relation*. Performing the formal integration we find

$$\begin{aligned} a_n^{(1/2)} &\simeq + \frac{S_1}{2\pi i} \sum_{h=0}^{+\infty} a_h^{(-1/2)} \frac{\Gamma(n-h)}{A^{n-h}} \\ &\simeq + \frac{S_1}{2\pi i} \frac{\Gamma(n)}{A^n} \sum_{h=0}^{+\infty} a_h^{(-1/2)} A^h \left(\prod_{r=1}^h \frac{1}{n-r} \right), \quad n \gg 1. \end{aligned} \quad (3.36)$$

We have derived the large-order expressions relating the large-order coefficients $a_n^{(1/2)}$ of the asymptotic sector $\Phi_{1/2}$ to the low order ones of the sector $\Phi_{-1/2}$. These expressions also evidenciate the factorial growth of such coefficients, as well as the subleading exponential growth. One can expand this result for large n , and the resulting expansion is once again asymptotic in the variable n . In the example of the Airy function, we have only two asymptotic sectors: one can perform the same analysis starting from the other sector $\Phi_{-1/2}$, obtaining very similar relations. In particular we will see a closure between the two sectors. In the example of the next Section we shall see that the large-order relations for each sector (of an infinite number) will relate its coefficients to the coefficients of all other sectors, with some being more exponentially suppressed than others.

These large-order relations show once again the *resurgence* of one sector in the asymptotic behaviour of another.¹⁵ This derivation offers a prediction (from resurgence) for the large-order behaviour of the coefficients

¹⁵ It is not surprising that it appears as large-order relations, as the asymptotic properties of the series $\Phi_{\pm 1/2}$ are governed by the higher terms (if we removed a finite number of terms from start of the series, we would not change its asymptotic behaviour).

of asymptotic sectors $\Phi_{\pm 1/2}$ (3.36). Naturally, one now asks how can the accuracy of this prediction be checked. It can be done by studying the convergence of $a_n^{(1/2)}$ in (3.36) at large n towards different coefficients on the right-hand side, as we shall see next.

3.3.1 Numerical checks of large-order relations Expanding the right-hand side of (3.36) for large n we find

$$\begin{aligned} a_n^{(1/2)} &\simeq + \frac{S_1}{2\pi i} \frac{\Gamma(n)}{A^n} \left\{ a_0^{(-1/2)} + a_1^{(-1/2)} \frac{A}{n} \right. \\ &\quad \left. + \frac{A}{n^2} \left(a_1^{(-1/2)} + A a_2^{(-1/2)} \right) + \dots \right\} \quad (3.37) \\ &\equiv + \frac{S_1}{2\pi i} \frac{\Gamma(n)}{A^n} \sum_{k=0}^{+\infty} \frac{c_k}{n^k}. \end{aligned}$$

This defines the coefficients c_k , *e.g.* $c_0 = a_0^{(-1/2)} = 1$, $c_1 = a_1^{(-1/2)} A$ and $c_2 = A a_1^{(-1/2)} + A^2 a_2^{(-1/2)}$. We can now plot

$$-\frac{2\pi A^n}{\Gamma(n)} a_n^{(1/2)} \simeq iS_1 c_0 + \mathcal{O}(n^{-1}) \quad (3.38)$$

and check the large n convergence to $iS_1 c_0 = iS_1 a_0^{(-1/2)}$. The best means to perform this check is by using an acceleration method for the convergence, such as Richardson transforms (RT). The method of Richardson extrapolation (see *e.g.* [22, 48]) assumes the existence of a sequence for large n :

$$S(n) \simeq s_0 + \frac{s_1}{n} + \frac{s_2}{n^2} + \dots \quad (3.39)$$

Label the N -Richardson transform for the sequence S converging to its element s_ℓ as $\text{RT}_S(\ell, n, N)$. For $\ell = 0$ (convergence to s_0) the Richardson transform is defined recursively as

$$\left\{ \begin{array}{l} \text{RT}_S(0, n, 0) = S(n); \\ \text{RT}_S(0, n, N) = \text{RT}_S(0, n+1, N-1) \\ \quad + \frac{n}{N} (\text{RT}_S(0, n+1, N-1) - \text{RT}_S(0, n, N-1)), \quad N \geq 1. \end{array} \right. \quad (3.40)$$

It is not hard to see that the N -Richardson transform is effectively cancelling the subleading terms in $S(n)$ up to order n^{-N} , thus resulting in an improved convergence to s_0 . To check any of the higher coefficients s_ℓ , define

$$S_\ell(n) \equiv \left(S(n) - \sum_{r=0}^{\ell-1} \frac{s_r}{n^r} \right) n^\ell \simeq s_\ell + \frac{s_{\ell+1}}{n} + \frac{s_{\ell+2}}{n^2} + \dots, \quad (3.41)$$

together with the related RT

$$\begin{cases} \text{RT}_S(\ell, n, 0) = S_\ell(n); \\ \text{RT}_S(\ell, n, N) = \text{RT}_S(\ell, n+1, N-1) \\ \quad + \frac{n}{N}(\text{RT}_S(\ell, n+1, N-1) - \text{RT}_S(\ell, n, N-1)), \quad N \geq 1. \end{cases} \quad (3.42)$$

Applying the method of RT to the series (3.38) we obtain the convergence shown in Figure 3.4, to the value $iS_1 = 1$. In this figure, the convergence of the original series and of the 5-RT are shown, with estimated error of 10^{-13}

$$\frac{\text{RT}_S(0, 90, 5) - iS_1}{iS_1} \sim 10^{-13}. \quad (3.43)$$

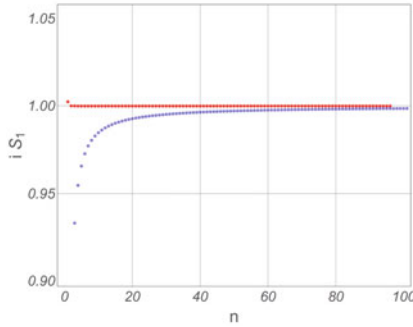


Figure 3.4. Convergence of left-hand side of the large-order relation (3.38) to the leading coefficient $iS_1 = 1$. In blue the values of left-hand side of (3.37) are plotted, and in red the corresponding 5-RT is shown.

One can check these large-order relations numerically even without knowing the value of the Stokes coefficient (which in the majority of the situations needs to be determined numerically from large-order relations such as just discussed). To do so, we analyse instead the convergence of

$$\begin{aligned} \frac{a_{n+1}^{(1/2)}}{a_n^{(1/2)}} \frac{A}{n} &\simeq \frac{\sum_{k=0}^{\infty} \frac{c_k}{(n+1)^k}}{\sum_{k=0}^{\infty} \frac{c_k}{n^k}} \\ &\simeq 1 - \frac{c_1}{c_0} \frac{1}{n^2} + \frac{c_1^2 + c_0 c_1 - 2c_0 c_2}{c_0^2 n^3} + \mathcal{O}(n^{-4}) \\ &\equiv \sum_{k=0}^{\infty} \frac{d_k}{n^k}. \end{aligned} \quad (3.44)$$

The coefficients c_k were determined directly from the expansion (3.37), so (3.44) defines the coefficients d_k , e.g. $d_0 = 1$, $d_1 = 0$, $d_2 = -\frac{c_1}{c_0}$ and

$d_3 = \frac{c_1^2 + c_0 c_1 - 2c_0 c_2}{c_0^2}$. We can apply the method of Richardson transforms to this expansion and show the convergence to any of the coefficients d_k . In Figure 3.5 we show the convergence of the series $\frac{a_{n+1}^{(1/2)}}{a_n^{(1/2)}} A n - d_0 n^2$ to the coefficient $d_2 = \frac{5}{36}$, with estimated error of 10^{-9} (for the 5-RT).

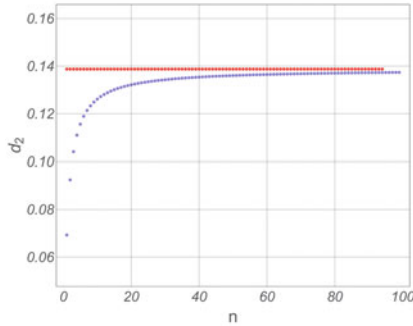


Figure 3.5. Convergence of left-hand side of the large-order relation (3.44) to the coefficient d_2 . In blue the values of $\frac{a_{n+1}^{(1/2)}}{a_n^{(1/2)}} A n - d_0 n^2$ are plotted, and in red the corresponding 5-RT is shown.

Note that for this example, numerical tests such as the ones above are in fact not necessary. The simplicity of this example is reflected in the fact that the resurgent relations between sectors $\Phi_{\pm 1/2}$ close, as pictorially shown in (3.20). Thus using the definitions (3.12) for the large-order relation (3.36) returns the following relation

$$\begin{aligned} \frac{2\pi}{iS_1} &\simeq \frac{\Gamma(n+1)(-1)^n}{\Gamma(n+5/6)\Gamma(n+1/6)} \sum_{h=0}^{+\infty} \\ &\times \frac{\Gamma(n-h)\Gamma(h+5/6)\Gamma(h+1/6)}{\Gamma(h+1)} \xrightarrow{n \rightarrow \infty} 2\pi, \end{aligned} \quad (3.45)$$

where the following property was used:

$$\frac{\Gamma(n+1)(-1)^n \Gamma(n-h)\Gamma(h+5/6)\Gamma(h+1/6)}{\Gamma(n+5/6)\Gamma(n+1/6)\Gamma(h+1)} \xrightarrow{n \rightarrow \infty} \delta_{h,0} 2\pi. \quad (3.46)$$

Now that we have checked the resurgent properties of the transseries (3.7), the following step is to analyse how to calculate resummations and obtain exact results.

3.3.2 Écalle-Borel-Padé resummation and exact results from asymptotic series We have already seen how to perform (very accurate) numer-

ical checks of the resurgent properties of our transseries. The subsequent question one poses is how to retrieve exact analytic results from the asymptotic building blocks of that transseries. We will not focus here on the so-called cancellation of ambiguities (as one of the exact analytic outcomes of resurgence) and leave this discussion for the example in the next Section. Instead, we will now focus on how to obtain analytic transseries results for the Airy function in the complex κ -plane, and how to perform interpolation between the asymptotic regime $\kappa \gg 1$ and κ small. The simplicity of the example at hand, together with the well known and thoroughly studied function $A_i(\kappa)$ allows us to easily compare the results we will obtain from the resummation of the transseries to known exact results.

The two regimes to be studied are:

1. Keep $|\kappa|$ fixed and change $\arg \kappa$ from 0 to π . In doing so, we cross a Stokes line: we start at $\arg \kappa = 0^+$ with just the asymptotic series Z_{Ai} (as done before, by taking $\sigma_1 = 1$ and $\sigma_2 = 0$ in the transseries (3.7)), then after the Stokes line at $\theta = 2\pi/3$ both asymptotic solutions in the transseries will contribute ($\sigma_1 = 1$ still remains, and σ_2 jumps in value by $-S_1$).
2. Once we reach the line $\arg \kappa = \pi$, where we will have the typical oscillatory behaviour of an anti-Stokes line, we keep the $\arg \kappa$ fixed at this value and take $|\kappa|$ from large values to small ones (strong/weak coupling interpolation).

In both regimes, one needs to analyse the resummation of the two asymptotic solutions $\mathcal{S}_\theta Z_{Ai}$ and $\mathcal{S}_\theta Z_{Bi}$ in the transseries (3.7).

At $\arg \kappa = 0^+$ there will only be the asymptotic solution Z_{Ai} . As a first approximation, we can perform optimal truncation (2.4):

$$Z_{Ai-\text{op}}(\kappa) = \frac{1}{2\sqrt{\pi}\kappa^{1/4}} e^{-\frac{1}{2}A\kappa^{3/2}} \sum_{n=0}^{N_{\text{op}}} a_n^{(-1/2)} \kappa^{-3n/2}. \quad (3.47)$$

N_{op} is the highest value of n such that $\left| \frac{a_{n+1}}{a_n} \right| < |\kappa|^{3/2}$, so

$$N_{\text{op}}(\kappa) = \left\lfloor \frac{4}{3} |\kappa|^{3/2} \right\rfloor, \quad (3.48)$$

where $\lfloor \dots \rfloor$ denotes the integer part. Taking for example the value $|k| = 1.7171$, we find $N_{\text{op}} = 3$. Changing $\arg \kappa \in]0, \pi]$ and comparing with known exact results for the Airy function, we find that the optimal truncation of the perturbative series diverges from the expected results after

the Stokes line $\arg \kappa = \frac{2\pi}{3}$. This can be seen on the first plot of Figure 3.6, where the truncated perturbative series (in blue) follows rather closely the exact result (in yellow) up to the Stokes line, after which the two lines diverge.

The next approximation one can do is an optimal truncation at the level of the transseries. The value of N_{op} remains the same, but now

$$Z_{\text{op}}(\kappa) = Z_{\text{Ai-op}}(\kappa) - S_1 \Theta \left(\arg \kappa - \frac{2\pi}{3} \right) Z_{\text{Bi-op}}(\kappa), \quad (3.49)$$

where $Z_{\text{Bi-op}}(\kappa)$ is defined in the same way as $Z_{\text{Ai-op}}(\kappa)$ above, but with the starting point being the asymptotic solution Z_{Bi} . The function $\Theta(x)$ is the usual Heaviside function (with value 1 when $x > 0$ and 0 when $x < 0$), and the truncation of the transseries detailed above is valid for $\arg \kappa \in]0, \pi]$.¹⁶ With the same choice for the value of $|\kappa|$, the comparison of the optimal truncation of the transseries to the exact results is shown on the second plot of Figure 3.6. We now find that the optimal truncation follows the exact result more closely, even after crossing the Stokes line. As a last note, the third plot of Figure 3.6 shows the truncation of the transseries where we kept twice the number of terms as required by optimal truncation (6 instead of 3 for the chosen value of κ): we easily see a poorer approximation to the exact results.

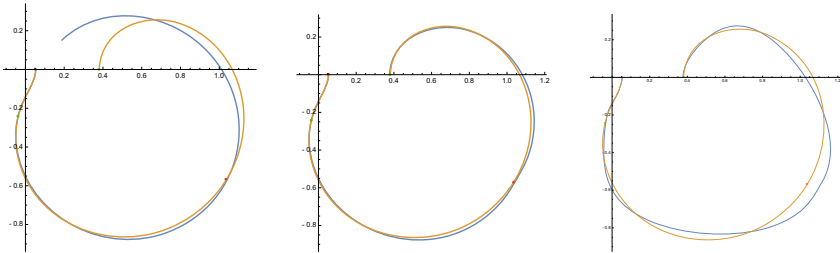


Figure 3.6. Comparison of optimal truncations for the original perturbative series $Z_{\text{Ai}}(\kappa)$ (first plot, in blue), and full transseries solution $Z_{\text{initial}}(\kappa)$ (second plot, in blue) to the exact results of the Airy function $A_i(\kappa)$ (in yellow), for $\kappa = 1.7171e^{i\theta}$, $\theta \in]0, \pi]$. On the third plot, a non-optimal truncation (adding 6 terms instead of the optimal 3) of the transseries solution is shown (in blue) in contrast with the exact solution (in yellow). The red dots correspond to the Stokes lines $\theta = 0, \frac{2\pi}{3}$, while the green dots are the anti-Stokes lines $\theta = \frac{\pi}{3}, \pi$.

¹⁶ This is the case because up to $\arg \kappa = \pi$ we only cross one Stokes line. Once we cross extra Stokes lines, other transseries parameters jump in value, and the expression for the truncated transseries will change.

Finally, one may be interested in going beyond the optimal truncation, in particular how to include the asymptotic information encoded in the higher terms of the series after N_{op} . This can be done by performing a resummation (inverse Borel transform) for the Borel transforms of every sector of the transseries, in this example $\mathcal{B}[\Phi_{\pm 1/2}](s)$. For the simple case at hand these are known as analytic functions (3.15). However, such is not the general situation: the Borel transforms of the asymptotic sectors of a transseries, $\mathcal{B}[\Phi_n](s)$, are usually known as convergent series, and often we only know a finite number of terms in those series. In these cases, before performing the resummation, one needs to approximate the finite number of terms of the Borel transform to an analytic function. One of the preferred methods to do so is the *method of Padé approximants*: the Padé approximant of the first N elements of a convergent series such as $\mathcal{B}[\Phi_n](s)$ gives the approximated function as a ratio of two polynomials (for the diagonal approximant case, which is commonly used, these two polynomials are of the same order $N/2$). As the method is being applied to Borel transforms, one calls the resulting object Borel-Padé approximant. For the case of diagonal Padé approximants, we have the form

$$\text{BP}_N[\Phi_n](s) = \frac{P_{N/2}[\Phi_n](s)}{Q_{N/2}[\Phi_n](s)}, \quad (3.50)$$

with $P_{N/2}$, $Q_{N/2}$ being two polynomials of order $N/2$. A major advantage of this method of approximation is that the zeros of the polynomial in the denominator, $Q_{N/2}[\Phi_n]$, reflect the singularities of the Borel transform: the poles will condense in certain directions indicating branch cuts in the Borel plane.

Looking back at our example, let us expand the Borel transforms $\mathcal{B}[\Phi_{\pm 1/2}](s)$ in (3.15) around $s = 0$, and keep terms up to power s^N with $N = 60$. We then determine the respective diagonal Borel-Padé approximants $\text{BP}_{60}[\Phi_{\pm 1/2}](s)$, and analyse the position of the poles for each case. This can be found in Figure 3.7. Analysing this figure we find (as expected) that $\mathcal{B}[\Phi_{-1/2}](s)$ has a condensation of poles starting at $s = -A$, indicating a branch cut starting at that point, while $\mathcal{B}[\Phi_{1/2}](s)$ has poles condensing into a cut starting at $s = A$.

Once we have the approximate function for the Borel transforms $\text{BP}_N[\Phi_n](s)$, we can perform the resummation procedure, – the inverse Borel transform (2.8) – thus retrieving an approximate value for the resummation of these sectors:

$$\mathcal{S}_\theta^{(N)}\Phi_n(z) = \int_0^{e^{i\theta}\infty} ds \text{BP}_N[\Phi_n](s) e^{-zs}. \quad (3.51)$$

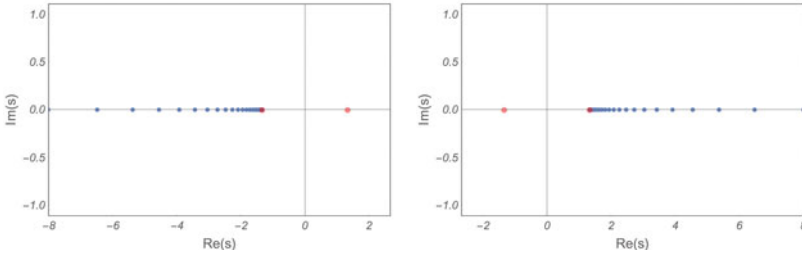


Figure 3.7. Poles of the Borel-Padé approximants $\text{BP}_{60}[\Phi_{-1/2}]$ (left) and $\text{BP}_{60}[\Phi_{1/2}]$ (right). In red are shown the singularities in the Borel plane, at $s = \pm A$.

When the direction θ is singular, *i.e.* a Stokes line, instead of the regular resummation we need to perform the lateral Borel resummations (2.9). The result $\mathcal{S}_\theta^{(N)}\Phi_n(z)$ is called the Écalle-Borel-Padé resummation for the asymptotic series $\Phi_n(z)$. In principle we need to perform this resummation to all sectors of the transseries, but in effect one needs only to do so for the first (least exponentially suppressed) sectors to obtain very accurate results in all the complex plane z . The more resummed sectors we add at every value z , the more accurate the result will be. We shall see this at the level of cancellation of ambiguities in the example of the next Section.

For our current example, we will keep only $N = 10$ terms of the expansions of the Borel transforms $\mathcal{B}[\Phi_{\pm 1/2}](s)$ in (3.15) around $s = 0$. We then determine the corresponding diagonal Borel-Padé approximants $\text{BP}_{10}[\Phi_{\pm 1/2}](s)$, and finally calculate the resummed values $\mathcal{S}_\theta^{(10)}\Phi_{\pm 1/2}(\kappa)$ where $\kappa = z^{-2/3} = |\kappa|e^{i\theta}$ as before. The resummed transseries for $\arg \kappa = \theta \in]0, \pi[$ can again be written with the help of the Heaviside function as

$$\mathcal{S}_\theta^{(10)}Z(\kappa) = \mathcal{S}_\theta^{(10)}Z_{\text{Ai}}(\kappa) - S_1 \Theta\left(\arg \kappa - \frac{2\pi}{3}\right) \mathcal{S}_\theta^{(10)}Z_{\text{Bi}}(\kappa), \quad (3.52)$$

with

$$\mathcal{S}_\theta^{(10)}Z_{\text{Ai}}(\kappa) = \frac{1}{2\sqrt{\pi}\kappa^{1/4}} e^{-\frac{1}{2}A\kappa^{3/2}} \mathcal{S}_\theta^{(10)}\Phi_{-\frac{1}{2}}(\kappa) \quad (3.53)$$

and equivalently for $\mathcal{S}_\theta^{(10)}Z_{\text{Bi}}(\kappa)$ using (3.10).

We first assume $|\kappa| = 1.7171$ and take θ to vary in the interval $]0, \pi[$, in increments of $\frac{\pi}{100}$. This gives rise to the the first plot in Figure 3.8: the blue line shows the expected exact results; the yellow line shows the optimal truncation of the perturbative series; the optimally truncated

transseries is shown in dashed purple; the red dots exactly following the blue line are the numerical resummations $\mathcal{S}_\theta^{(10)} \Phi_{\pm 1/2}(\kappa)$ for the different values of $\arg \kappa$. We can see that with just 10 terms in the expansion of the Borel transforms, the numerical resummations result is a better approximation than the optimal truncation. The resummation of the transseries can be taken all around the complex κ -plane, and the analytic properties of the full solution can then be analysed at any κ . In particular, if we keep $\arg \kappa = \pi$ fixed, we can analyse the oscillatory behaviour of the resummed solution along this anti-Stokes line by changing $|\kappa|$ from the large asymptotic regime to small values. This analysis is shown in the second plot of Figure 3.8: the resummed transseries (in red) follows the expected exact results (in blue) all the way to very small coupling $|\kappa|$, while the optimally truncated transseries (dashed purple) diverges for small values of $|\kappa|$ and the optimal truncation of $Z_{A_i}(\kappa)$ (in yellow) does not follow the exact results for any $|\kappa|$ as expected.

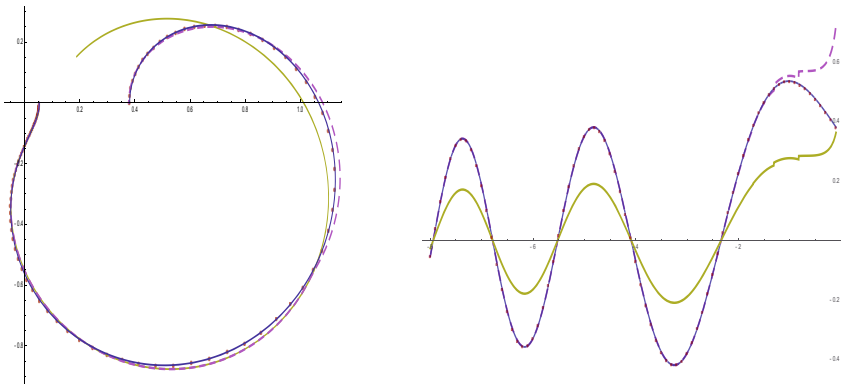


Figure 3.8. Comparison between different approximations to the value of the function $Ai(\kappa)$. The exact results are shown in blue; in yellow is the optimal truncation of $Z_{A_i}(\kappa)$; in dashed purple is shown the optimal truncation of the transseries (3.49); the red dots show the Écalle-Borel-Padé resummation of the transseries (3.52). The first plot corresponds to keeping $|\kappa| = 1.7171$ and changing $\arg \kappa \in]0, \pi]$. The second plot keeps $\arg \kappa = \pi$ fixed and changes $|\kappa|$.

With this we finish the analysis of the transseries solution to the Airy differential equation (3.1). The asymptotic solutions found for this ODE at $\kappa \gg 1$ allowed us to build a full transseries solution, with resurgent properties which can be systematically used to analyse the Stokes phenomena associated with this example. From resurgence and alien calculus we learned how to cross singular directions (Stokes lines) and reach any value of the complex coupling κ . This procedure, together with the numerical resummation of results presented, enables the study of the full transseries solution in the whole complex plane. Hence, results beyond

the asymptotic regime such as analytic properties of the transseries and strong/weak coupling interpolation can be easily achieved.

In the next Section we turn to a more complex example, where we will have an infinite number of asymptotic sectors in the transseries. The employment of resurgent techniques in that case will be much more important as it gives a fast and systematic approach to obtain resummed results from the asymptotics.

4 Non-linear ODEs and the resurgence of the one-parameter transseries

As an example of a first-order non-linear ODE, we will now turn to the differential equation controlling the hydrodynamic series of the Müller-Israel-Stuart (MIS) theory [88,89]. This model has recently been studied in the light of resurgence [56,62,63], and we review here some of the key aspects, in particular the subject of ambiguity cancellations. The respective differential equation is a first-order non-linear ODE for a function $f(w)$ (encoding the dependence of temperature with respect to proper time, see *e.g.* [63] for more details and derivation), given by¹⁷

$$C_{\tau\Pi} f f' + 4C_{\tau\Pi} f^2 + \left(w - \frac{16C_{\tau\Pi}}{3} \right) f - \frac{4C_{\eta}}{9} + \frac{16C_{\tau\Pi}}{9} - \frac{2w}{3} = 0. \quad (4.1)$$

The coefficients $C_{\tau\Pi}, C_{\eta}$ appearing in this equation are dimensionless constants which are known from the so-called fluid-gravity duality to be¹⁸

$$C_{\tau\Pi} = \frac{2 - \log 2}{2\pi}, \quad C_{\eta} = \frac{1}{4\pi}. \quad (4.2)$$

The asymptotic regime we intend to study via resurgence is the case of $w \gg 1$. If we take an ansatz of the type $\Phi_0 = \sum_{m=0}^{+\infty} a_m^{(0)} w^{-m}$ and plug it into (4.1), we can easily find a recursion relation for the $a_m^{(0)}$:

$$\begin{aligned} a_0^{(0)} &= 2/3; \\ a_1^{(0)} &= 4 \frac{C_{\eta}}{9}; \\ a_{k+1}^{(0)} &= C_{\tau\Pi} \left(\frac{16}{3} a_k^{(0)} - \sum_{n=0}^k (4-n) a_{k-n}^{(0)} a_n^{(0)} \right), \quad k > 1. \end{aligned} \quad (4.3)$$

¹⁷ Here one uses the notation $f', f'',$ etc to denote first, second and higher derivatives, respectively.

¹⁸ In MIS theory another coefficient appears C_{λ_1} , which was currently set to zero, see [63].

From these relations we can determine the first few coefficients $a_k^{(0)}$ and see that these grow factorially, with a subleading exponential growth

$$a_k^{(0)} \sim \frac{\Gamma(k)}{A^k}, \quad k \gg 1, \quad \text{where } A \approx \frac{3}{2C_{\tau\Pi}}. \quad (4.4)$$

In the same manner as in [63], we can find reproduced in Figure 4.1 the plot of the weighted coefficients $a_k^{(0)} \frac{2\pi A^{k+\beta}}{\Gamma(k+\beta)}$, together with the respective Richardson transforms 2-RT and 5-RT.¹⁹ We can indeed confirm the expected growth for the coefficients $a_m^{(0)}$, from the convergence in this figure to a constant (the identification of this constant with a Stokes coefficient will be discussed at a later stage). This hints to the existence of exponentially suppressed “instanton” sectors with action $A = \frac{3}{2C_{\tau\Pi}}$. Assume an ansatz of the form

$$F^{(\ell)}(w) = e^{-\ell A w} \Phi_\ell(w), \quad \Phi_\ell(w) = w^{\beta_\ell} \sum_{k=0}^{+\infty} a_k^{(\ell)} w^{-k}. \quad (4.5)$$

Plugging this into (4.1) we find

$$A = \frac{3}{2C_{\tau\Pi}}; \quad \beta_\ell \equiv -\ell\beta = -\ell \frac{C_\eta}{C_{\tau\Pi}}. \quad (4.6)$$

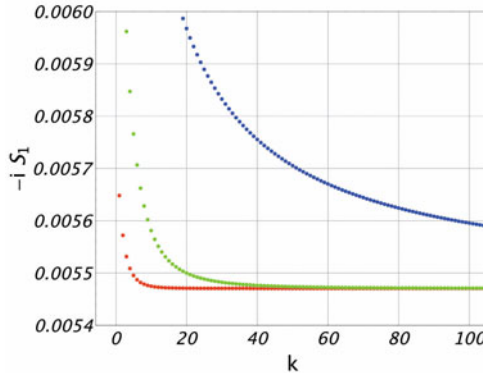


Figure 4.1. Plot of the weighted coefficients $a_k^{(0)} \frac{2\pi A^{k+\beta}}{\Gamma(k+\beta)}$ given in (4.3) and the corresponding 2-RT (green) and 5-RT (red), showing the convergence to the Stokes coefficient iS_1 .

¹⁹ The particular weight used will be justified in the subsection dealing with the large-order behaviours predicted by resurgence. In here β is given by $-C_\eta/C_{\tau\Pi}$.

Thus all the sectors $F^{(\ell)}(w)$ with $\ell \geq 0$ are then allowed as part of a general solution to (4.1), the *transseries*

$$\mathcal{F}(w, \sigma) = \sum_{n=0}^{+\infty} \sigma^n F^{(n)}(w). \quad (4.7)$$

The transseries (4.7) has to obey the non-linear ODE (4.1): this requirement will lead to linearised equations obeyed by the asymptotic sectors $\Phi_\ell(w)$ for $\ell \geq 1$; only $\Phi_0(w)$ obeys the original non-linear differential equation. Indeed equating equal powers of σ^n and of $e^{-\ell Aw}$, we find that Φ_0 obeys (4.1) and Φ_ℓ , $\ell \geq 1$ obey

$$\begin{aligned} C_{\tau\Pi} \sum_{m=0}^{\ell} \left(\Phi'_m - m A \Phi_m \right) \Phi_{\ell-m} + 4C_{\tau\Pi} \sum_{m=0}^{\ell} \Phi_m \Phi_{\ell-m} \\ + \left(w - \frac{16C_{\tau\Pi}}{3} \right) \Phi_\ell = 0. \end{aligned} \quad (4.8)$$

From these equations one obtains the recursion equations relating the coefficients $a_k^{(\ell)}$ to the lower coefficients $a_k^{(m)}$ for $m < \ell$. We do not find a closed form expression for the coefficients anymore, but can determine these up to any order or accuracy. Doing so we can verify numerically (in the same way as was done for the $a_m^{(0)}$) that all grow factorially: every sector Φ_ℓ is asymptotic. To understand the asymptotic behaviour of the sectors Φ_ℓ and to resum these, we need to analyse their respective Borel transforms. There is no closed form expression for the coefficients, thus we cannot determine the Borel transforms in an exact form. Still, we can determine a set of coefficients, say N , and approximate the Borel transform via a Padé approximant of order N (which we will generally choose to be diagonal), defined in (3.50). As explained for the Airy function example, given the Padé approximant, we can study the singular structure of the Borel transform by determining the zeros of the polynomial in the denominator and observing any condensation of poles. For the Borel transform of sector Φ_0 this is shown in Figure 4.2. We can see in the real line the condensation of poles into a cut starting at the initial value $A \equiv \frac{3}{2C_{\tau\Pi}}$. Any other cuts, starting in the positive real axis at more distant points from the origin, will be overshadowed by the leading one in the numerical checks.

The same analysis can be done for every asymptotic sector Φ_ℓ with $\ell \geq 1$. Doing so will show that both Φ_0 and Φ_1 will have singularities only in the positive real axis, with cuts starting at $s = A \equiv \frac{3}{2C_{\tau\Pi}}$ (the plot of the poles of Borel-Padé for the asymptotic sector Φ_1 will be exactly the same as the one in Figure 4.2). Nevertheless performing an analysis

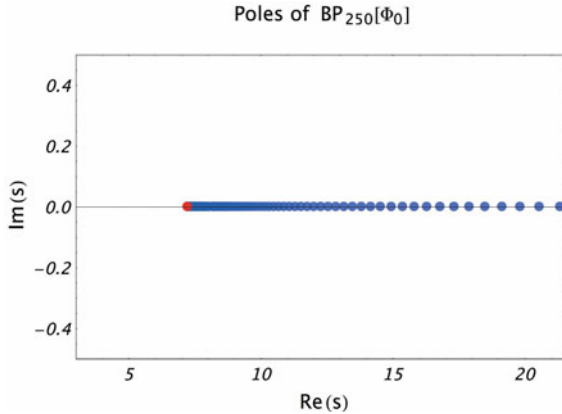


Figure 4.2. In blue, the poles (in the Borel s -plane) of the Borel-Padé of order $N = 250$ for the sector $\Phi_0(w)$, $\text{BP}_{250}[\Phi_0](s)$, are shown. In red the value of the non-perturbative “instanton” action $A = \frac{3}{2C_{\tau\pi}}$ is shown.

of the poles of the Borel-Padé for any of the sectors Φ_2 and higher will show a condensation of poles not only in the positive real axis starting at $s = A$, but also in the negative real axis starting at $s = -A$! This means that the Borel transform of these sectors will have at least two cuts, starting at these points (see [62] for further plots and behaviours). The use of “at least” is related to the fact that numerically any other cuts starting at further distances from the origin are on top of each other, thus being indistinguishable. This behaviour is naturally expected from the shape of the transseries (4.7). The singularities associated with the Borel-Padé for each asymptotic sector as expected from the shape of the transseries (4.7) can be found in Figure 4.3. In this figure, the sector being analysed is shown in blue, the possible cuts expected to appear (numerically) in the positive real axis of the Borel plane are shown in red, while the ones appearing in the negative real axis of the Borel plane are shown in green. Note that there is no cut associated with the perturbative sector Φ_0 , as this would correspond to having an action $A = 0$ as a solution in the transseries (to see examples where this is the case, see [19]). From Figure 4.3 we conclude:

- The singularities in the $\text{BP}_N[\Phi_0](s)$ will appear at positions $s = \ell A$, $\ell \geq 1$ (positive real axis), with contributions coming from sectors Φ_ℓ , respectively. This means that we expect the asymptotic sector $\Phi_0(w)$ to have a discontinuity in the direction $\arg w = 0$ (positive real axis);
- The $\text{BP}_N[\Phi_1](s)$ will also have singularities starting at $s = \ell A$, $\ell \geq 1$ (positive real axis), but now they are related to sectors $\Phi_{\ell+1}$. There are

no singular cuts in the negative real axis, as there is no cut associated with Φ_0 (there is no action $A = 0$). $\Phi_1(w)$ will only have a discontinuity in the positive real axis, $\arg w = 0$;

- Starting at the $\text{BP}_N[\Phi_2](s)$, there will be singularities in both the positive and negative directions of the real axis: in the positive real axis we can expect singular contributions at $s = \ell A$, $\ell \geq 1$, coming from sectors $\Phi_{\ell+2}$, respectively; in the negative real axis we have one singular cut starting at $s = -A$, related to the sector Φ_1 . The asymptotic sector $\Phi_2(w)$ will have two discontinuities, in both the positive real direction, $\arg w = 0$, and the negative one, $\arg w = \pi$;
- Finally the last sector shown in Figure 4.3 is the expected cuts for $\text{BP}_N[\Phi_3](s)$. The singular behaviour for this case is: singularities in the positive real axis at $s = \ell A$, $\ell \geq 1$ (respectively associated with sectors $\Phi_{\ell+3}$); singularities in the negative real axis at $s = -A$ (associated with Φ_2) and $s = -2A$ (associated with Φ_1). Sector $\Phi_3(w)$ will again have two discontinuities at $\arg w = 0, \pi$.

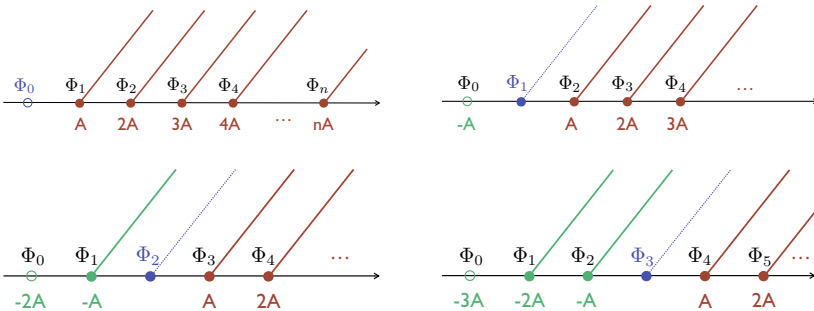


Figure 4.3. Expected cuts appearing in the numerical analysis of the Borel-Padé of sectors Φ_ℓ , $\ell = 0, 1, 2, 3$. The sector being analysed is shown in blue, the expected cuts appearing in the positive real axis (and their positions) are shown in red, and the cuts appearing in the negative real axis are shown in green. Note that the cuts are shown going to infinity in a direction other than the real line, in order to highlight where they start. Numerically, however, these cuts will all be on top of each other, on the real axis.

One can write the expected behaviour near the singularities of the Borel transforms for any sector $\Phi_n(w)$:²⁰

$$\mathcal{B}[\Phi_n](s)|_{s=kA} \simeq h(\{S_r\}) \mathcal{B}[\Phi_{n+k}](s - kA) \frac{\log(s - kA)}{2\pi i}, \quad (4.9)$$

$$k > -n, k \neq 0.$$

²⁰ In [56] a different behaviour for the Borel transforms was found, related to the removal of a different factorial growth. See footnote 3 on page 8 for more information.

This is in fact the predicted behaviour coming from the form of the one-parameter transseries (4.7): near any singularity $s = kA$ of $\mathcal{B}[\Phi_n](s)$, the sector Φ_{n+k} *resurges* through its Borel transform, up to a proportionality factor $h(\{S_r\})$. This proportionality factor is a function of the Stokes coefficients S_r , with $r \in \{1, 2, \dots, k\}$ if $k > 0$, and $r \in \{-1, -2, \dots, -k\}$ if $k < 0$. Abstracting oneself from the functional form of the Borel transform and keeping only the algebraic form of the relations (4.9), we can define the alien derivative as introduced in Section 2:

$$\Delta_{kA} \Phi_n = (n+k) S_k \Phi_{n+k}, \quad k \leq 1, k \neq 0, \quad (4.10)$$

and $\Delta_\omega \Phi_n = 0$ for all other non-singular points $\omega \in \mathbb{C}$. These are once again the so-called bridge equations, linking alien calculus with ordinary calculus.²¹

This result can be derived systematically from the original bridge equations (2.49) and (2.50) introduced in Section 2 for the case of the one-parameter transseries, and can also be found in Section 2 of [23]. Before moving forward in our example let us briefly summarise how this derivation works. Start from the general bridge equations for a one-parameter transseries (2.49), with expansion (2.50). Plugging the one-parameter transseries (4.7) (with sectors defined in (4.5)) into (2.49), we obtain from the left-hand side (recall that $\dot{\Delta}_{kA} = e^{-kAw} \Delta_{kA}$)

$$\dot{\Delta}_{kA} \mathcal{F}(w, \sigma) = \sum_{n=0}^{+\infty} \sigma^n e^{-(n+k)Aw} \Delta_{kA} \Phi_n, \quad (4.11)$$

while from the right-hand side we find

$$S_{kA}(\sigma) \frac{\partial \mathcal{F}(w, \sigma)}{\partial \sigma} = \sum_{r=0}^{+\infty} S_k^{(r)} \sum_{m=0}^{+\infty} \sigma^{r+m-1} e^{-mA w} \Phi_m. \quad (4.12)$$

Comparing equal powers of the exponential e^{-Aw} and of σ on both sides one obtains restrictions to the constants $S_k^{(r)}$ and to the alien derivative acting on Φ_n . It is not difficult to see that $k \leq 1$ (and $k \neq 0$ as by construction there is no singularity at the origin of the Borel plane), and that $r = 1 - k$. Thus for each $k \leq 1$ the allowed expansion (2.50) reduces to

$$S_{kA}(\sigma) = S_k^{(1-k)} \sigma^{1-k} \equiv S_k \sigma^{1-k}, \quad k \leq 1. \quad (4.13)$$

From this, we easily see that the only non-zero alien derivatives acting of each sector Φ_n will be the ones read from the behaviour of the Borel transforms (4.10).

²¹ Note that Φ_n is only defined for $n \geq 0$; if $n+k < 0$ for any k , we have $\Delta_{kA} \Phi_n = 0$.

4.1 Alien chain and discontinuities

We can summarise the algebraic structure of (4.10) pictorially as the one-parameter alien chain of [19], reproduced in Figure 4.4. The $k \leq 1$ restriction of (4.10) means that only Δ_A is non-zero in the positive real axis ($\theta = 0$ direction). Equivalently, the singularities at $s = (k + 1)A$, $k \geq 1$, for each $\mathcal{B}[\Phi_n](s)$ are directly related to the singularity at $s = A$ of all $\mathcal{B}[\Phi_{n+\ell}](s)$ with $1 \geq \ell \leq k$. We can see this directly in Figure 4.4: to move forward in the chain (from left to right) we can only act with Δ_{+A} , so that to connect two sectors Φ_m and Φ_ℓ with $\ell > m$ we need to act with the alien derivative $\ell - m$ times. In the negative real axis we have singularities at $s = -kA$, $k = 1, \dots, n$ (a finite number of them, always stopping at Φ_0), so to get from Φ_ℓ to Φ_m we need to act with N alien derivatives $\Delta_{-n_i A}$ in sequence, $\Delta_{-n_1 A} \Delta_{-n_2 A} \cdots \Delta_{-n_N A}$, such that $\sum_{i=1}^N n_i = \ell - m$. Therefore, moving in the negative real direction one can have many different paths, which are shown in Figure 4.4: any left-moving paths are allowed with any combination of “instanton” sectors Φ_k with $m < k < \ell$ as middle nodes. As an example, we have 4 possible paths to connect Φ_4 to Φ_1 :

- act with $(\Delta_{-A})^3$: black links $\Phi_4 \rightarrow \Phi_3 \rightarrow \Phi_2 \rightarrow \Phi_1$;
- act with Δ_{-A} followed by Δ_{-2A} , *i.e.* $\Delta_{-2A} \Delta_{-A}$: black link $\Phi_4 \rightarrow \Phi_3$, then blue link $\Phi_3 \rightarrow \Phi_1$;
- act with Δ_{-2A} followed by Δ_{-A} , *i.e.* $\Delta_{-A} \Delta_{-2A}$: blue link $\Phi_4 \rightarrow \Phi_2$, then black link $\Phi_2 \rightarrow \Phi_1$;
- act with Δ_{-3A} : red link $\Phi_4 \rightarrow \Phi_1$.

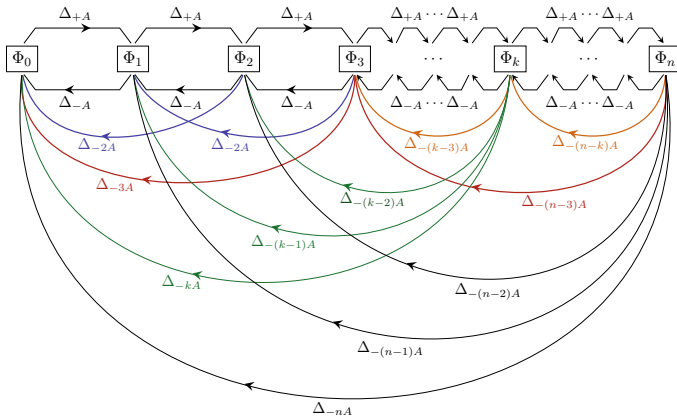


Figure 4.4. The *alien chain* (reproduction from [19]): pictorial representation of the allowed actions of the alien derivative on the instanton sectors Φ_k . Different colours encode different actions.

The chain of motions in Figure 4.4 only shows the allowed steps but not the proportionality constants, or weights, that come associated with each step (each action of an alien derivative). Using (4.10) the chain can be re-drawn as in Figure 4.5 (also reproduced from [19]). For the example given above, $\Phi_4 \rightarrow \Phi_1$, the weights associated to each possible path are

- $(\Delta_{-A})^3 \Phi_4 = 3S_{-1} \times 2S_{-1} \times S_{-1} \Phi_1 = 6(S_{-1})^3 \Phi_1$;
- $\Delta_{-2A} \Delta_{-A} \Phi_4 = 3S_{-1} \times S_{-2} \Phi_1$;
- $\Delta_{-A} \Delta_{-2A} \Phi_4 = 2S_{-2} \times S_{-1} \Phi_1$;
- $\Delta_{-3A} \Phi_4 = S_{-3} \Phi_1$.

Note that action of two different alien derivatives does not commute (the middle steps will be different). In this example we can easily see that $\Delta_{-2A} \Delta_{-A} \neq \Delta_{-A} \Delta_{-2A}$. This will be true in general: Δ_{nA} and Δ_{mA} will not commute. From (4.10) one can determine their commutation relations to be:

$$[\Delta_{-nA}, \Delta_{-mA}] \Phi_\ell = S_{-m} S_{-n} (n - m)(\ell - n - m) \Phi_{\ell - n - m}. \quad (4.14)$$

If we define operators formally as $L_n = \frac{1}{S_{-n}} \Delta_{-nA}$, one can easily see that these obey the commutation relations of a Virasoro algebra for $n \geq 1$ (see [19] for a more detailed discussion on the algebra associated to the alien derivative operators).

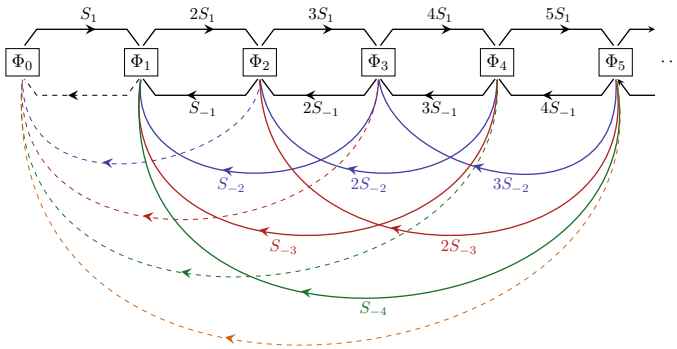


Figure 4.5. The *alien chain* revisited (reproduction from [19]): pictorial representation of the action of alien derivatives on the first 5 asymptotic sectors, Φ_k , $k = 0, \dots, 5$ in terms of weights of steps (a step is a single arrow), as given by the bridge equations (4.10). The action of Δ_{+A} , Δ_{-A} is shown by black links, with arrows pointing to the right or left, respectively. The action of Δ_{-2A} , Δ_{-3A} , Δ_{-4A} , Δ_{-5A} are shown by blue, red, green and orange links, respectively. The dashed links refer to when the action of the alien derivative is zero. The weight of each step is written next to the arrow.

In order to describe the algebraic structure behind the bridge equations (4.10), we closely follow [19] and introduce some elements needed to

describe the motions in the alien chain:

- *Step* \mathcal{S} : any single link connecting two nodes

$$\mathcal{S} = \overset{\curvearrowright}{\longrightarrow} \quad (4.15)$$

- *Weight of step* $w(\mathcal{S})$: product of Stokes coefficients and numerical factors associated with the step, given by (4.10). These weights are shown for each step in Figure 4.5. For a step connecting nodes Φ_m and Φ_k :

$$w(\mathcal{S}(m \rightarrow k)) = k S_{k-m}. \quad (4.16)$$

- *Path* \mathcal{P} : trajectory connecting two nodes Φ_m to Φ_k , composed by any number of steps

$$\mathcal{P} = \mathcal{S}_1 \cup \mathcal{S}_2 \cup \dots \cup \mathcal{S}_\ell, = \boxed{\Phi_m} \overset{\curvearrowright}{\longrightarrow} \dots \overset{\curvearrowright}{\longrightarrow} \boxed{\Phi_k} \quad (4.17)$$

- *Length of path* $\ell(\mathcal{P})$: number of steps in path \mathcal{P} (each step has length one)

$$\ell(\mathcal{P}) = \#\{\mathcal{S}_i \in \mathcal{P}\}. \quad (4.18)$$

- *Weight of path* $w(\mathcal{P})$: product of the weights of all steps $\mathcal{S}_i \in \mathcal{P}$

$$w(\mathcal{P}) = \prod_{i=1}^{\ell(\mathcal{P})} w(\mathcal{S}_i). \quad (4.19)$$

- *Combinatoric factor of path* $\text{CF}(\mathcal{P})$: division by permutations of $\{\mathcal{S}_i \in \mathcal{P}\}$

$$\text{CF}(\mathcal{P}) = \frac{1}{(\ell(\mathcal{P}))!}. \quad (4.20)$$

To fully describe Stokes phenomena, once the action of the alien derivatives is understood one needs to determine the Stokes automorphisms (or equivalently the discontinuities) along the singular Stokes directions. For the problem at hand, the Stokes lines are at $\theta = 0$ (for all sectors Φ_n , $n \geq 0$) and at $\theta = \pi$ (for sectors Φ_n , $n \geq 2$). Recalling the definition of the Stokes automorphism (2.29), and the non-zero alien derivatives acting in each singular direction (4.10), we can write

$$\begin{aligned} \underline{\mathfrak{S}}_0 \Phi_n(w) &= \exp\{e^{-Aw} \Delta_A\} \Phi_n; \\ \underline{\mathfrak{S}}_\pi \Phi_n(w) &= \exp\left\{\sum_{k=1}^n e^{kAw} \Delta_{-kA}\right\} \Phi_n. \end{aligned} \quad (4.21)$$

We shall now show two particular examples of the above expressions. Let us write the first terms of $\underline{\mathfrak{S}}_0 \Phi_2(w)$, obtained from expanding the exponential:

$$\begin{aligned} \underline{\mathfrak{S}}_0 \Phi_2(w) &= \Phi_2 + \left\{ e^{-Aw} \Delta_A + \frac{1}{2!} e^{-2Aw} (\Delta_A)^2 + \frac{1}{3!} (\Delta_A)^3 + \dots \right\} \Phi_2 \\ &= \Phi_2 + 3S_1 e^{-Aw} \Phi_3 + \frac{12}{2!} (S_1)^2 e^{-2Aw} \Phi_4 \\ &\quad + \frac{60}{3!} (S_1)^3 e^{-3Aw} \Phi_5 + \dots \end{aligned} \quad (4.22)$$

The Stokes automorphism $\underline{\mathfrak{S}}_0$ connects the sector Φ_2 to all other higher sectors Φ_m , $m > 2$, with some weight. For example for the connection $\Phi_2 \rightarrow \Phi_4$ the weight appearing above is the product of the non-analytic factor e^{-2Aw} and a statistical part given by (looking at Figure 4.5): one path \mathcal{P} of length $\ell(\mathcal{P}) = 2$ (2 steps of black links), weight $w(\mathcal{P}) = 12(S_1)^2$ and a combinatoric factor $\text{CF}(\mathcal{P}) = \frac{1}{2!}$.

In fact, it is very easy to generalise these results and obtain a closed-form expression for the Stokes automorphism in the direction $\theta = 0$. Due to having only Δ_A acting in this direction, by expanding the exponential and using (4.10) we find

$$\begin{aligned} \underline{\mathfrak{S}}_0 \Phi_n(w) &= \sum_{k=0}^{+\infty} \frac{1}{k!} e^{-kAw} (\Delta_A)^k \Phi_n(w) \\ &= \sum_{k=0}^{+\infty} e^{-kAw} (S_1)^k \frac{(n+k)!}{n!k!} \Phi_{n+k}(w). \end{aligned} \quad (4.23)$$

We now turn to the calculation of $\underline{\mathfrak{S}}_\pi \Phi_4(w)$. Expanding the exponential:

$$\begin{aligned} \underline{\mathfrak{S}}_\pi \Phi_4(w) &= \Phi_4 + \left\{ \sum_{k=1}^4 e^{kAw} \Delta_{-kA} + \frac{1}{2!} \left(\sum_{k=1}^4 e^{kAw} \Delta_{-kA} \right)^2 \right. \\ &\quad \left. + \frac{1}{3!} \left(\sum_{k=1}^4 e^{kAw} \Delta_{-kA} \right)^3 + \dots \right\} \Phi_4 \\ &= \Phi_4 + 3S_{-1} e^{Aw} \Phi_3 + \left(2S_{-2} + \frac{6}{2!} (S_{-1})^2 \right) e^{2Aw} \Phi_2 + \\ &\quad + \left(S_{-3} + \frac{5}{2!} S_{-1} S_{-2} + \frac{1}{3!} (S_{-1})^3 \right) e^{3Aw} \Phi_1. \end{aligned} \quad (4.24)$$

The Stokes automorphism $\underline{\mathcal{S}}_\pi$ connects the sector Φ_4 to all lower sectors Φ_m , $m < 4$, which are of finite number, with some weight.²² Looking at the particular connection $\Phi_4 \rightarrow \Phi_2$, the weight associated is the product of the non-analytic factor e^{2Aw} and a statistical factor coming from two paths (see Figure 4.5 once again): path \mathcal{P}_1 (one step, blue link) with length $\ell(\mathcal{P}_1) = 1$, weight $w(\mathcal{P}_1) = 2S_{-2}$ and combinatoric factor $\text{CF}(\mathcal{P}_1) = 1$; path \mathcal{P}_2 (two steps, black links) with $\ell(\mathcal{P}_2) = 2$, $w(\mathcal{P}_2) = 6(S_{-1})^2$ and $\text{CF}(\mathcal{P}_2) = \frac{1}{2!}$. A closed form expression for the Stokes automorphism in the direction $\theta = \pi$ has been derived in [23], but its expression is intricate due to several possible Stokes coefficients S_{-k} appearing, and we will not reproduce it here (see Section 2 of [23] for the expression and derivation).

This pattern of determining the contributions to the Stokes automorphisms was summarised in [19] as the following statement for the discontinuities (2.27)

Disc₀ Φ_n in positive real line: sum over all paths linking nodes to the right $\Phi_{m>n}$.

Disc _{π} Φ_n in negative real line: sum over paths linking nodes to the left $\Phi_{m<n}$.

Each term in these sums ($\Phi_n \rightarrow \Phi_m$) is decomposed into two factors:

- Non-analytic factor, dictated solely by beginning and end nodes:

$$-e^{-(m-n)A/x} \Phi_m.$$

- Statistical factor, sum over all allowed paths linking the two nodes $\mathcal{P}(n \rightarrow m)$, as in Figure 4.5:

$$\text{SF}_{(n \rightarrow m)} \equiv \sum_{\mathcal{P}(n \rightarrow m)} \frac{w(\mathcal{P})}{\ell(\mathcal{P})}.$$

These discontinuities, or Stokes automorphisms, encode all jumps the transseries parameter σ goes through at Stokes lines, and define all the resurgent properties of the transseries. Nevertheless, we have not yet addressed how to check that the transseries has indeed resurgent properties, or how to determine the Stokes coefficients appearing in the bridge equa-

²² Note that the weight associated to reaching sector Φ_0 is in fact zero.

tions (4.10) (and consequently in the weights of paths as defined above). This can be achieved via the large-order relations.

4.2 Large-order relations

To perform tests of the asymptotic behaviour of the sectors Φ_n and check whether the predictions given by resurgence are correct, we need to determine the large-order relations using Cauchy's theorem (in much the same way as was shown in the example of the previous Section). We have seen that the sectors Φ_n will generally have two Stokes lines, at $\theta = 0, \pi$ (the only exceptions are Φ_0, Φ_1 , which have only one Stokes line at $\theta = 0$). Taking $F(x) = \Phi_n(x)$ (and assuming $x = 1/w$) for some asymptotic sector, Cauchy's theorem (3.31) can be written as

$$F(x) = -\frac{1}{2\pi i} \int_0^{+\infty} dw \frac{\text{Disc}_0 F(w)}{w-x} - \frac{1}{2\pi i} \int_0^{-\infty} dw \frac{\text{Disc}_\pi F(w)}{w-x}. \quad (4.25)$$

For the specific case of the perturbative series Φ_0 in (4.5), and following the same procedure as was done in Section 3.3, we now find for large order $k \gg 1$ (general large-order relations for the coefficients of higher sectors were derived in [23])

$$a_k^{(0)} \simeq \sum_{m=1}^{+\infty} \frac{(S_1)^m \Gamma(k+m\beta)}{2\pi i (mA)^{k+m\beta}} \sum_{h=0}^{+\infty} a_h^{(m)} (mA)^h \frac{\Gamma(k+m\beta-h)}{\Gamma(k+m\beta)}, \quad k \gg 1 \quad (4.26)$$

$$\simeq S_1 \frac{\Gamma(k+\beta)}{2\pi i A^{k+\beta}} \left(a_0^{(1)} + a_1^{(1)} \frac{A}{k} + \frac{A^2 a_2^{(1)} - (\beta-1) A a_1^{(1)}}{k^2} + \dots \right) + \quad (4.27)$$

$$+ (S_1)^2 \frac{\Gamma(k+2\beta)}{2\pi i (2A)^{k+2\beta}} \left(a_0^{(2)} + a_1^{(2)} \frac{2A}{k} + \frac{4A^2 a_2^{(1)} - 2A(\beta-1) a_1^{(1)}}{k^2} + \dots \right) + \mathcal{O}(3^{-k}). \quad (4.28)$$

To obtain the second and third lines, (4.27) and (4.28), we simply expanded the first two terms of the sum in m for large order k . The leading behaviour at large order is given in line (4.27), while (4.28) is exponentially suppressed as 2^{-k} (all the other terms of the sum in m are more suppressed). Here, each line is an asymptotic expansion in $k \gg 1$. By plotting the coefficients $a_k^{(0)} \frac{2\pi A^{k+\beta}}{\Gamma(k+\beta)}$ and related Richardson transforms, we can see that for large order $k \gg 1$ these should converge to the Stokes coefficient $-iS_1 a_0^{(1)} = -iS_1$. This is exactly what is shown in Figure 4.1,

and provides a direct numerical calculation of the Stokes coefficient S_1 , which value is estimated to be (with error 10^{-13})

$$S_1 = 0.00547029853i. \quad (4.29)$$

We have thus used the leading behaviour (4.27) predicted by resurgence to determine the value of the Stokes coefficient S_1 . But we still need to make further consistency checks of the predictions made by resurgence on the large-order behaviour of sectors Φ_n . The easiest check to perform is of the subleading $1/k$ behaviour in (4.27): start by defining the ratio of coefficients as done in [63]

$$R_k \equiv \frac{a_{k+1}^{(0)}}{a_k^{(0)}} \frac{A}{k}, \quad (4.30)$$

with leading large-order behaviour given by

$$R_k \simeq \sum_{\ell=0}^{+\infty} \frac{c_\ell}{k^\ell}, \quad c_0 = 1, \quad c_1 = \beta, \quad c_2 = -A \frac{a_1^{(1)}}{a_0^{(1)}}, \quad \dots \quad (4.31)$$

The coefficients c_ℓ predicted by resurgence can be directly read from the behaviour in (4.27), once the ratio of coefficients $a_k^{(0)}$ is taken. We can check the convergence of R_k to the predicted coefficients c_ℓ (as was done in [63]) by plotting the following

$$\tilde{R}_k(\ell) \equiv \left(R_k - \sum_{r=0}^{\ell-1} \frac{c_r}{k^r} \right) k^\ell \simeq c_\ell + \mathcal{O}(k^{-1}). \quad (4.32)$$

In Figure 4.6 we plot $\tilde{R}_k(2)$ and the related Richardson transforms, in order to see the convergence to the predicted value $c_2 = -2.44197298$ (determined directly from the recursion equations coming from (4.1)). We see that there is a rapid convergence to the predicted value, with error 10^{-10} . One can also check higher predicted coefficients c_ℓ , thus verifying the large-order behaviour predicted by resurgence for the perturbative sector Φ_0 .

To further verify the predicted large-order behaviour predicted by resurgence, we can also check the subleading (exponentially suppressed) terms in (4.28). To do so, we need to perform a resummation of the leading behaviour in (4.27) and subtract it from the original $a_k^{(0)}$. In doing so we can reach the exponentially suppressed terms in 2^{-k} and check the predictions in (4.28). As the series in k^{-1} appearing in line (4.27) is

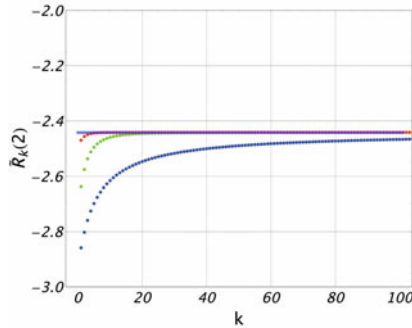


Figure 4.6. Convergence of the large-order behaviour of the ratio (4.30) to the coefficient c_2 (whose predicted value is shown in light blue). The original values for the coefficients \tilde{R}_k are shown in blue, and in green and red are the corresponding 2-RT and 5-RT.

asymptotic, the resummation procedure can be performed via the Borel-Padé method reviewed in the previous Section. This Borel-Padé resummation in the order parameter k has some subtleties²³ which go beyond the scope of this review, but are treated in detail in [19, 23].

Once convinced from the large-order checks that the transseries has resurgent properties, we can now address the study of exact results.

4.3 Exact results: ambiguity cancellation

The transseries (4.7) is the full solution to our differential equation (4.1). Even though it is written as a formal sum of asymptotic expansions around $w \gg 1$, it should include all analytic properties at every point of the complex w -plane. In particular it should provide a way of determining the solution at $\arg w = 0$, and allow us to perform strong-weak coupling interpolation (that is, from the strong coupling regime $w \gg 1$ that we started from, we ought to be able to reach the small coupling $w \lesssim 1$ regime via numerical resummation):

1. The analytic properties of the transseries reflect its behaviour over all the complex plane. Nevertheless, in many cases we are interested in how these properties collapse for the line $w \in \mathbb{R}^+$, *i.e.* for positive real coupling. In the case of MIS theory, this line ($\arg w = 0$) is a Stokes line, so using methods such as Écalle-Borel-Padé resummation

²³ In general one needs to determine lateral resummations in order to avoid poles in the integration along the positive real axis (recall that the order parameter is real and positive), and this introduces typically an exponentially suppressed error which is then cancelled by the next order in the large-order relations.

lead to non-perturbative ambiguities: due to the singularities along this direction, we can only define the lateral resummations $\mathcal{S}_{0\pm} F(w)$. In fact, this is not the whole story: knowing the Stokes automorphism across this Stokes line allows us to determine an unambiguous result even when $\arg w = 0$;

2. Once the problem of cancelling any non-perturbative ambiguities along the positive real line is solved, the method of Écalle-Borel-Padé resummation will provide a way of determining exact results beyond the regime $w \gg 1$. To do so, we will need to include increasingly higher non-perturbative “instanton” sectors Φ_n , leading to better results and allowing us to reach “weaker” coupling values. Moreover, one can go beyond the line $w \in \mathbb{R}^+$, into any direction on the complex w -plane by analytic continuation.

In summary, from the Stokes automorphism across the Stokes line $w \in \mathbb{R}^+$, we can write an unambiguous solution along this particular line. One can then reach any other (non-singular) directions by simple analytic continuation of the resummation procedure. In this Subsection, we will focus on the procedure of cancellation of non-perturbative ambiguities.

From the resummation procedure, we find a non-perturbative ambiguity along the Stokes line $\arg w = 0$, since the lateral resummations of each sector Φ_ℓ will return different values

$$(\mathcal{S}_{0+} - \mathcal{S}_{0-}) \Phi_\ell(w) \neq 0. \quad (4.33)$$

This difference is exponentially small, and moreover, for an ODE with real coefficients such as (4.1), where all the coefficients $a_k^{(\ell)}$ are real, this difference will be pure imaginary [42]. However, each of these sectors is only part of the full transseries solution (4.7). For a general complex parameter σ , having (4.33) for every sector of the transseries will result in

$$(\mathcal{S}_{0+} - \mathcal{S}_{0-}) \mathcal{F}(w, \sigma) \neq 0. \quad (4.34)$$

What we will see next is that there is a proper choice of the transseries parameter $\sigma = \sigma_0$ which will allow us to cancel this difference, *at the level of the transseries*. This will be achieved by a particular resummation prescription, called *median resummation* (see e.g. [8, 42]). Cancelling this ambiguity corresponds to cancelling the pure imaginary difference between the lateral resummations, and reaching a final result which is real.

Re-write the lateral resummations as $\mathcal{S}_{0\pm} = \frac{1}{2}(\mathcal{S}_{0+} + \mathcal{S}_{0-}) \pm \frac{1}{2}(\mathcal{S}_{0+} - \mathcal{S}_{0-})$. As was mentioned, this separation corresponds to taking the real

and imaginary contributions from the lateral resummations. The imaginary ambiguity of a sector $F^{(\ell)} = e^{-\ell Aw} \Phi_\ell(w)$ of the transseries (4.7) is defined as

$$\mathbb{I}mF^{(\ell)} \equiv \frac{1}{2i} (\mathcal{S}_{0^+} - \mathcal{S}_{0^-}) F^{(\ell)}, \quad (4.35)$$

while the real contribution of this sector to the lateral resummations is

$$\mathbb{R}eF^{(\ell)} \equiv \frac{1}{2} (\mathcal{S}_{0^+} + \mathcal{S}_{0^-}) F^{(\ell)}. \quad (4.36)$$

It is straightforward to write the lateral resummations as

$$\mathcal{S}_{0^\pm} F^{(\ell)} = \mathbb{R}eF^{(\ell)} \pm i \mathbb{I}mF^{(\ell)}. \quad (4.37)$$

Each of these sectors will contribute with its own imaginary ambiguity (and real part) to the transseries solution. All these contributions, together with a proper choice of the transseries parameter σ , will allow us to have an ambiguity-free, real transseries. Looking at the last expression we could be tempted to start from the perturbative series $F^{(0)}(w)$ and keep only the real contribution as the final unambiguous result (thus effectively eliminating the imaginary part). However, this will not be the full real, unambiguous solution to our problem: we know that it is the transseries (4.7) which describes the full solution to the problem (4.1), and we would find discrepancies if we were to compare the result coming from just the perturbative series to some numerical calculation of the solution to (4.1).

This is where resurgence plays a major role: we know that the lateral resummations are linked via the Stokes automorphism (2.27). Applied to each sector $F^{(\ell)}$ we write

$$2i \mathbb{I}mF^{(\ell)} = -\mathcal{S}_{0^-} \circ (\mathbf{1} - \underline{\mathcal{S}}_0) F^{(\ell)}, \quad (4.38)$$

where $\underline{\mathcal{S}}_0 F^{(\ell)}$ is known from the previous Subsection, determined with the help of alien calculus. For the direction $\arg w = 0$ one has a simple closed form expression for the Stokes automorphism (4.23). From this we can write

$$2i \mathbb{I}mF^{(\ell)} = \sum_{k=1}^{+\infty} (\mathcal{S}_1)^k \binom{\ell+k}{\ell} \mathcal{S}_{0^-} F^{(\ell+k)}, \quad (4.39)$$

where $\binom{k}{\ell} \equiv \frac{(k)!}{\ell!(k-\ell)!}$. This expression relates the imaginary ambiguity of any sector $F^{(\ell)}$ to the lateral resummation $\mathcal{S}_{0^-} F^{(m)}$ of all higher sectors $m > \ell$. On the other hand this lateral resummation can be rewritten in terms of its real part contribution and its imaginary ambiguity

by using (4.37). We can iteratively re-write each imaginary contribution in terms of the real and imaginary contributions of higher sectors, and finally obtain an expression for the imaginary ambiguity of sector $F^{(\ell)}$ only in terms of the real contributions. This was derived in [42] (Appendix B) and we transcribe the result:

$$2i \Im F^{(\ell)} = \sum_{k=1}^{+\infty} \binom{\ell+k}{\ell} \Omega(k) (S_1)^k \Re F^{(\ell+k)}, \quad (4.40)$$

$$\Omega(k) = \sum_{r=1}^k \sum_{s=1}^r \binom{r}{s} (-1)^{s+1} \frac{s^k}{2^{r-1}}.$$

Note that this relation between the imaginary ambiguity of any sector and the real contributions of higher sectors is intimately related to the fact that we have a one-parameter resurgent transseries. If the transseries solution was not resurgent, we would not be able to derive these relations; if the transseries had more than one transseries parameter, one would have to re-derive similar relations (see [42] for a more in depth discussion).

We are now ready to see how to cancel the imaginary ambiguity for the transseries solution. Our goal is to iteratively construct a real solution to our problem. From a lateral resummation of the transseries solution (4.7), we define (in the same way as done for each of its sectors)

$$S_{0+} \mathcal{F}(w, \sigma) = \Re \mathcal{F}(w, \sigma) + i \Im \mathcal{F}(w, \sigma), \quad (4.41)$$

where

$$\Re \mathcal{F}(w, \sigma) = \sum_{\ell=0}^{+\infty} \Re \sigma^\ell \Re F^{(\ell)}(w) - \Im \sigma^\ell \Im F^{(\ell)}(w); \quad (4.42)$$

$$\Im \mathcal{F}(w, \sigma) = \sum_{\ell=0}^{+\infty} \Im \sigma^\ell \Re F^{(\ell)}(w) + \Re \sigma^\ell \Im F^{(\ell)}(w). \quad (4.43)$$

The transseries solution will be real and unambiguous if one can find a value of $\sigma = \sigma_0$ such that $\Im \mathcal{F}(w, \sigma_0) = 0$. To solve this condition, we analyse the first few terms of $\Im \mathcal{F}(w, \sigma)$ ($\sigma = \sigma_R + i\sigma_I$ is the decomposition of the transseries parameter into real and imaginary parts):

$$\begin{aligned} \Im \mathcal{F}(w, \sigma) &= \Im F^{(0)} + \sigma_I \Re F^{(1)} + \sigma_R \Im F^{(1)} + 2\sigma_R \sigma_I \Re F^{(2)} \\ &\quad + (\sigma_R^2 - \sigma_I^2) \Im F^{(2)} + (3\sigma_R^2 \sigma_I - \sigma_I^3) \Re F^{(3)} \\ &\quad + (\sigma_R^3 - 3\sigma_R \sigma_I^2) \Im F^{(3)} + \dots \end{aligned} \quad (4.44)$$

We know from (4.40) that the imaginary part of the each resummed sector can be re-written via resurgence in terms of the real parts of higher (more

exponentially suppressed sectors. One can do exactly this iteratively for each term in the above expression. We start by re-writing the imaginary ambiguity for the perturbative sector, $\mathbb{I}mF^{(0)}$ using the formula (4.40):

$$\mathbb{I}mF^{(0)} = -\frac{i}{2}S_1\mathbb{R}eF^{(1)} + \frac{i}{4}(S_1)^3\mathbb{R}eF^{(3)} - \frac{i}{2}(S_1)^5\mathbb{R}eF^{(5)} + \dots \quad (4.45)$$

As a result, (4.44) becomes

$$\begin{aligned} \mathbb{I}m\mathcal{F}(w, \sigma) &= \left(\sigma_I - \frac{i}{2}S_1\right)\mathbb{R}eF^{(1)} + \sigma_R\mathbb{I}mF^{(1)} \\ &\quad + 2\sigma_R\sigma_I\mathbb{R}eF^{(2)} + (\sigma_R^2 - \sigma_I^2)\mathbb{I}mF^{(2)} \\ &\quad + \left(3\sigma_R^2\sigma_I - \sigma_I^3 + \frac{i}{4}(S_1)^3\right)\mathbb{R}eF^{(3)} \\ &\quad + (\sigma_R^3 - 3\sigma_R\sigma_I^2)\mathbb{I}mF^{(3)} + \dots \end{aligned} \quad (4.46)$$

Noticing that the contribution from $\mathbb{I}mF^{(1)}$ will be proportional to $\mathbb{R}eF^{(\ell)}$, with $\ell > 1$ (and all other contributions will be of even higher order), the cancellation at the level of $\mathbb{R}eF^{(1)}$ requires (recall that S_1 is a pure imaginary number)

$$i\sigma_I = -\frac{S_1}{2}. \quad (4.47)$$

Let us perform a consistency check of this result by checking the cancellations at the next order. To do so, re-write $\mathbb{I}mF^{(1)}$ using (4.40):

$$\mathbb{I}mF^{(1)} = -iS_1\mathbb{R}eF^{(2)} + i(S_1)^3\mathbb{R}eF^{(4)} + \dots \quad (4.48)$$

Plugging this into $\mathbb{I}m\mathcal{F}(w, \sigma)$ results in

$$\begin{aligned} \mathbb{I}m\mathcal{F}(w, \sigma) &= \left(\sigma_I - \frac{i}{2}S_1\right)\mathbb{R}eF^{(1)} + \sigma_R(2\sigma_I - iS_1)\mathbb{R}eF^{(2)} \\ &\quad + (\sigma_R^2 - \sigma_I^2)\mathbb{I}mF^{(2)} \\ &\quad + \left(3\sigma_R^2\sigma_I - \sigma_I^3 + \frac{i}{4}(S_1)^3\right)\mathbb{R}eF^{(3)} \\ &\quad + (\sigma_R^3 - 3\sigma_R\sigma_I^2)\mathbb{I}mF^{(3)} + \dots \end{aligned} \quad (4.49)$$

Once again, $\mathbb{I}mF^{(2)}$ will have contributions proportional to higher terms $\mathbb{R}eF^{(\ell)}$, $\ell > 2$. Thus, the coefficients multiplying $\mathbb{R}eF^{(1)}$ and $\mathbb{R}eF^{(2)}$ need to (separately) vanish. We can easily see that these do vanish provided (4.47) is satisfied. To check the next order one would have to

re-write $\mathbb{I}mF^{(2)}$ using (4.40), and check what happened at the order of $\mathbb{R}eF^{(3)}$. One finds that indeed (4.47) cancels the imaginary ambiguity of the transseries at every order. It should be noted that only the imaginary part of transseries parameter is fixed by this argument, with the real part still a free parameter to be fixed via some initial conditions for the ODE (4.1).

The final, unambiguous solution along the positive real axis is given by

$$F_{\mathbb{R}}(w, \sigma_R) = \mathcal{S}_{0+} \mathcal{F}(w, \sigma_R + i\sigma_I) = \mathcal{S}_{0+} \mathcal{F}\left(w, \sigma_R - \frac{S_1}{2}\right), \quad \sigma_R \in \mathbb{R}. \quad (4.50)$$

If one started from the perturbative series $F^{(0)}(w)$ alone, kept its real part and used resurgence (*i.e.* (4.40)) to cancel its imaginary contribution, we would reach the above result for $\sigma_R = 0$:

$$F_{\mathbb{R}}(w, 0) = \mathcal{S}_{0+} \mathcal{F}\left(w, -\frac{S_1}{2}\right). \quad (4.51)$$

The unambiguous real transseries given in (4.50) is an exact result, as it requires the full transseries (with the asymptotic sectors weighted by the Stokes coefficient) to cancel the ambiguities coming from each sector. Given a choice of σ_R , one can use the transseries solution (4.50) defined in the positive real axis and analytically continue it to the whole complex w -plane, including to small values of w . This was performed in [56], and compared to a numerical solution of the differential equation (4.1): for small values of w the authors showed that the real transseries solution obtained above correctly converged to the expected attractor solution (after the decay of nonhydrodynamic modes), once a proper choice of σ_R was made.

To conclude this discussion, note that we can see this ambiguity cancellation numerically from the lateral resummations of the transseries sectors. Looking back at (4.44), we have

$$\mathbb{I}m\mathcal{F}\left(w, -\frac{S_1}{2}\right) = \mathbb{I}mF^{(0)} + \frac{iS_1}{2}\mathbb{R}eF^{(1)} + \dots \quad (4.52)$$

From (4.40) we expect that $\mathbb{I}mF^{(0)}$ will be of the order of $\mathbb{R}eF^{(1)} \sim e^{-Aw}$, and that the two terms given above should cancel up to order of $F^{(2)} \sim e^{-2Aw}$. In Figure 4.7 this cancellation is shown for different values of $w \in \mathbb{R}^+$. The exponential order of the $y_0 = -\log \mathbb{I}mF^{(0)}(w)$ is shown in blue, while the exponential order of $y_1 = -\log(\mathbb{I}mF^{(0)} + \frac{iS_1}{2}\mathbb{R}eF^{(1)})$ is shown in purple. We see that the imaginary contributions become notably

smaller, and that indeed the choice of the transseries parameter cancels these contributions up to the next order $\sim e^{-2Aw}$ (for example see that when $w = 3$, $y_0 \sim 25$ and $y_1 \sim 47$). To determine the real and imaginary parts of sectors $F^{(0)}$ and $F^{(1)}$ we performed numerical lateral resummations \mathcal{S}_{0+} of these sectors for different values of $w \in \mathbb{R}^+$, and used the relation (4.37).²⁴

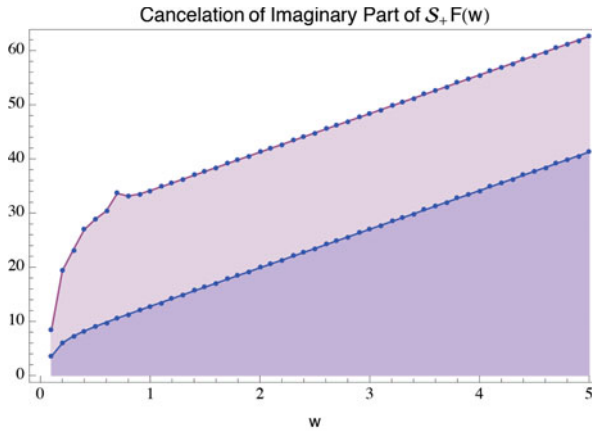


Figure 4.7. Exponential order of the imaginary part of leading terms in the unambiguous transseries solution $-\log \mathbb{I}m \mathcal{F}(w, \sigma_0)$. In blue the leading imaginary part coming from the resummation of the perturbative series is shown, while in purple the cancellation of this imaginary contribution with the one coming from the “one-instanton” sector is shown, resulting in a greatly suppressed imaginary part.

5 Further directions: multi-parameter transseries, resonance and beyond

In this review we focused on some simple examples of resurgent transseries solutions for ordinary differential equations: a linear ODE (Airy function) and a first-order non-linear ODE (MIS model). After introducing the basic concepts of resurgence and alien calculus, we developed the two examples to show how to use of resurgence to make predictions for the perturbative and non-perturbative asymptotic series of their transseries solutions. These predictions can be thoroughly checked

²⁴ Note the rapid decrease of the imaginary part of the transseries in Figure 4.7 when we take both terms in (4.52), for small values of w , while for $w > 1$ the decrease stabilises. One can expect this decrease not to stabilise but to be increase once the asymptotic regime $w \gg 1$ is reached, as was seen in [23, 60]. However, the limiting factor in the present case is the accuracy in the calculation of the Stokes coefficient (4.29).

numerically to high accuracy, using the Richardson extrapolation acceleration method, and resummation methods such as Écalle-Borel-Padé.

The tools (both analytic and numerical) presented in this paper can be widely used to study any observable thought to have resurgent properties. This analysis proceeds as follows:

- compute the observable via perturbation theory, and study the asymptotic behaviour of the perturbative expansion;
- identify the expected non-perturbative objects relevant to that observable (whether they are instantons, renormalons or other non-perturbative semi-classical contributions);
- incorporate both perturbative and non-perturbative results into a transseries ansatz;
- from the theory of resurgence, make predictions for large-order behaviour of the transseries sectors, and numerically check these predictions against perturbative/non-perturbative data; alternatively use the predictions to obtain non-perturbative data from the perturbative series;²⁵
- use Écalle-Borel-Padé resummation to resum the transseries, study Stokes phenomena and obtain exact results such as strong/weak coupling interpolation (see *e.g.* [44,55,60,71]) and cancellation of ambiguities (recent applications are *e.g.* [56,60,61]).

The general case of non-linear ODEs provides a natural setting to use these tools (see *e.g.* [5,6] for more general results). Nevertheless, their use has been recently extended to observables governed by finite-difference equations (*e.g.* string equation for free energies of matrix models [23,55]), or implicitly defined via some set of partial differential equations (*e.g.* holomorphic anomaly equations in the context of topological strings [82,84,97], exact quantisation conditions and uniform WKB in the context of quantum mechanics [43,98]) or integral equations (*e.g.* the so-called BES equation in the context of gauge-gravity duality [60,61]).

Recently, we have started to understand the resurgent properties of a wide range of problems in mathematical physics. These include observables in quantum field theories [66–68,99,100] and supersymmetric gauge theories [44,54,101–103]. These problems are often challenging, due to the lack of equations dictating the behaviour of the observables, or difficulty in performing perturbation theory around non-perturbative saddles. For this reason, the resurgence predictions for non-perturbative

²⁵ This is particularly important in situations where the equations governing the behaviour of the observable are unknown, and we can only have access to the perturbative results.

phenomena can greatly help complete any information missing in the transseries solution.

The relation between resurgence and the saddle point analysis of the Airy function, as presented in Section 3, is a toy example of that between the so-called Picard-Lefschetz theory and resurgence for finite dimensional exponential type integrals (see *e.g.* [104, 105]). It is of great interest to understand how general this relation is, in particular for infinite dimensional path integrals. This open problem has been the focus of recent research (see [16] and references therein).

The non-linear ODE studied in this paper required a one-parameter transseries ansatz: we had only one type of non-perturbative contributions, *i.e.* only one “instanton” action A . However, in general there can be different non-perturbative objects, with different actions $A_i \in \mathbb{C}$. These require a multi-parameter transseries ansatz (generally one parameter for each independent A_i). Moreover, if some of these actions are collinear such that $nA_i + mA_j = 0$, for $n, m \in \mathbb{N}$, a phenomenon called resonance can occur. The transseries ansatz often needs to be extended to lift the resonant behaviour, with the inclusion of other non-perturbative trans-monomials such as $\log z$. Examples of multi-parameter transseries and resonance have been studied in [19, 23], but a more general approach of resurgence to multi-parameter transseries is of great interest for a wide range of applications (including most of the open problems previously mentioned).

On a more conceptual note, further directions of research on resurgence theory, relevant to the study of physical observables, include: the computation of Stokes coefficients via general methods such as integrability properties [25]; the study of higher order Stokes phenomenon [106]; the analysis of Stokes phenomena for observables depending on two or more parameters; the study of the algebraic structure of alien derivative operators for multi-parameter transseries [19].

References

- [1] J. ÉCALLE, “Les fonctions résurgentes”, Vol. 1, Algèbres de fonctions résurgentes, Publ. Math. Orsay, 81-05, 1981, 248 pp.
- [2] J. ÉCALLE, “Les fonctions résurgentes”, Vol. 2, Les fonctions résurgentes appliquées à l’itératio, Publ. Math. Orsay, 81-06, 1981, 283 pp.

- [3] J. ÉCALLE, “Les fonctions résurgentes”, Vol. 3, L'équation du pont et la classification analytique des objets locaux, Publ. Math. Orsay, 85-05, 1985, 585 pp.
- [4] B. CANDELPERGHER, J. NOSMAS and F. PHAM, *Premiers pas en calcul étranger*, Ann. Inst. Fourier **43** (1993), 201.
- [5] O. COSTIN, *Exponential asymptotics, transseries, and generalized Borel summation for analytic, nonlinear, rank-one systems of ordinary differential equations*, Internat. Math. Res. Notices **8** (1995), 377. [arXiv:math.CA/0608414]
- [6] O. COSTIN, *On Borel summation and Stokes phenomena for rank-1 nonlinear systems of ordinary differential equations*, Duke Math. J. **93** (1998), 289–344. [arXiv:math.CA/0608408]
- [7] J. P. BOYD, *The Devil's invention: asymptotic, superasymptotic and hyperasymptotic series*, Acta Appl. Math. **56** (1999), 1.
- [8] E. DELABAERE and F. PHAM, *Resurgent methods in semi-classical asymptotics*, Ann. Inst. Henri Poincaré **71** (1999), 1.
- [9] T. SEARA and D. SAUZIN, *Resumació de Borel i teoria de la ressurgència*, Butl. Soc. Catalana Mat. **18** (2003), 131.
- [10] E. DELABAERE, *Effective resummation methods for an implicit resurgent function*. [arXiv:math-ph/0602026]
- [11] D. SAUZIN, *Resurgent functions and splitting problems*, RIMS Kokyuroku **1493** (2006), 48–117. [arXiv:0706.0137]
- [12] G. A. EDGAR, *Transseries for beginners*, Real Anal. Exchange **35** (2009), 253. [arXiv:0801.4877]
- [13] M. MARIÑO, *Lectures on non-perturbative effects in large N Gauge theories, matrix models and mtrings*, Fortsch. Phys. **62** (2014), 455–540. [arXiv:1206.6272]
- [14] D. SAUZIN, *Introduction to 1-summability and Resurgence*, In: “Divergent Series, Summability and Resurgence I, Monodromy and Resurgence, Part II”, Lecture Notes in Mathematics, Vol. 2153, Springer, Heidelberg, 2016, 121–293. [arXiv:1405.0356]
- [15] D. DORIGONI, *An introduction to resurgence, trans-series and alien calculus*. [arXiv:1411.3585]
- [16] G. V. DUNNE and M. ÜNSAL, *What is QFT? Resurgent trans-series, Lefschetz thimbles, and new exact saddles*, In: “Proceedings, 33rd International Symposium on Lattice Field Theory (Lattice 2015)”, 2015. [arXiv:1511.05977]
- [17] M. MARIÑO, “Instantons and Large N : An Introduction to Non-Perturbative Methods in Quantum Field Theory”, Cambridge University Press, 2015.

- [18] G. V. DUNNE and M. ÜNSAL, *New methods in QFT and QCD: from large- N orbifold equivalence to bions and resurgence*. [arXiv:1601.03414]
- [19] I. ANICETO, G. BAŞAR and R. SCHIAPPA, *A primer on resurgent transseries and their asymptotics*, upcoming (2017).
- [20] A. OLDE DAALHUIS, *Hyperasymptotics for nonlinear ODEs I. A Riccati equation*, Proceedings of the Royal Society of London **A461** (2005), 2503–2520.
- [21] A. OLDE DAALHUIS, *Hyperasymptotics for nonlinear ODEs II. The first Painlevé equation and a second-order Riccati equation*, Proceedings of the Royal Society of London A: Mathematical, Physical and Engineering Sciences **A461** (2005), no. 2062, 3005–3021.
- [22] S. GAROUFALIDIS, A. ITS, A. KAPAEV and M. MARIÑO, *Asymptotics of the instantons of Painlevé I*, Int. Math. Res. Notices **2012** (2012), 561. [arXiv:1002.3634]
- [23] I. ANICETO, R. SCHIAPPA and M. VONK, *The resurgence of instantons in string theory*, Commun. Num. Theor. Phys. **6** (2012), 339. [arXiv:1106.5922]
- [24] R. SCHIAPPA and R. VAZ, *The resurgence of instantons: multi-cut Stokes phases and the Painlevé II equation*, Commun. Math. Phys. **330** (2014), 655–721. [arXiv:1302.5138]
- [25] O. COSTIN, R. D. COSTIN and M. HUANG, *A direct method to find Stokes multipliers in closed form for P_1 and more general integrable systems*, Trans. Amer. Math. Soc. (2012). [arXiv:1205.0775]
- [26] C. M. BENDER and T. T. WU, *Anharmonic oscillator*, Phys. Rev. **184** (1969), 1231.
- [27] C. M. BENDER and T. WU, *Anharmonic oscillator 2: a study of perturbation theory in large order*, Phys. Rev. **D7** (1973), 1620.
- [28] F. DYSON, *Divergence of perturbation theory in quantum electrodynamics*, Phys. Rev. **85** (1952), 631–632.
- [29] J. ZINN-JUSTIN, *Perturbation series at large orders in quantum mechanics and field theories: application to the problem of resummation*, Phys. Rept. **70** (1981), 109.
- [30] M. BENEKE, *Renormalons*, Phys. Rept. **317** (1999), 1. [arXiv:hep-ph/9807443]
- [31] E. BOGOMOLNY, *Calculation of instanton—anti—instanton contributions in quantum mechanics*, Phys. Lett. **B91** (1980), 431.
- [32] J. ZINN-JUSTIN, *Multi - instanton contributions in quantum mechanics*, Nucl. Phys. **B192** (1981), 125–140.

- [33] J. ZINN-JUSTIN, *Multi - instanton contributions in quantum mechanics. 2*, Nucl. Phys. **B218** (1983), 333–348.
[http://dx.doi.org/10.1016/0550-3213\(83\)90369-3](http://dx.doi.org/10.1016/0550-3213(83)90369-3)
- [34] J. ZINN-JUSTIN, *From multi-instantons to exact results*, Ann. Inst. Fourier **53** (2003) 1259.
- [35] J. Zinn-Justin and U. D. Jentschura, *Multi-instantons and exact results I: conjectures, WKB expansions, and instanton interactions*, Annals Phys. **313** (2004), 197.
<http://arXiv.org/abs/quant-ph/0501136> arXiv:quant-ph/0501136
- [36] J. ZINN-JUSTIN and U. D. JENTSCHURA, *Multi-instantons and exact results II: specific cases, higher-order effects, and numerical calculations*, Annals Phys. **313** (2004), 269. [arXiv:quant-ph/0501137]
- [37] U. D. JENTSCHURA and J. ZINN-JUSTIN, *Instantons in quantum mechanics and resurgent expansions*, Phys. Lett. **B596** (2004), 138. [arXiv:hep-ph/0405279]
- [38] U. D. JENTSCHURA, A. SURZHYKOV and J. ZINN-JUSTIN, *Multi-instantons and exact results. III: unification of even and odd anharmonic oscillators*, Annals Phys. **325** (2010), 1135–1172.
- [39] U. D. JENTSCHURA and J. ZINN-JUSTIN, *Multi-instantons and exact results. IV: path integral formalism*, Annals Phys. **326** (2011) 2186–2242.
- [40] G. V. DUNNE and M. ÜNSAL, *Generating nonperturbative physics from perturbation theory*, Phys. Rev. **D89** (2014), no. 4, 041701. [arXiv:1306.4405]
- [41] G. BAŞAR, G. V. DUNNE and M. ÜNSAL, *Resurgence Theory, Ghost-instantons, and Analytic Continuation of Path Integrals*, JHEP **10** (2013), 041. [arXiv:1308.1108]
- [42] I. ANICETO and R. SCHIAPPA, *Nonperturbative ambiguities and the reality of resurgent transseries*, Commun. Math. Phys. **335** (2015), no. 1, 183–245. [arXiv:1308.1115]
- [43] G. V. DUNNE and M. ÜNSAL, *Uniform WKB, Multi-Instantons, and Resurgent Trans-Series*, Phys. Rev. **D89** (2014), no. 10, 105009. [arXiv:1401.5202]
- [44] G. BAŞAR and G. V. DUNNE, *Resurgence and the Nekrasov-Shatashvili limit: connecting weak and strong coupling in the Mathieu and Lamé systems*, JHEP **1502** (2015), 160. [arXiv:1501.05671]
- [45] T. MISUMI, M. NITTA and N. SAKAI, *Resurgence in sine-Gordon quantum mechanics: exact agreement between multi-instantons and uniform WKB*, JHEP **09** (2015), 157. [arXiv:1507.00408]
- [46] F. DAVID, *Phases of the large N matrix model and nonperturbative effects in 2-d gravity*, Nucl. Phys. **B348** (1991), 507–524.

- [47] F. DAVID, *Nonperturbative effects in matrix models and vacua of two-dimensional gravity*, Phys. Lett. **B302** (1993), 403–410. [arXiv:hep-th/9212106]
- [48] M. MARIÑO, R. SCHIAPPA and M. WEISS, *Nonperturbative effects and the large-order behavior of matrix models and topological strings*, Commun. Num. Theor. Phys. **2** (2008), 349. [arXiv:0711.1954]
- [49] M. MARIÑO, *Nonperturbative effects and nonperturbative definitions in matrix models and topological strings*, JHEP **0812** (2008), 114. [arXiv:0805.3033]
- [50] M. MARIÑO, R. SCHIAPPA and M. WEISS, *Multi-instantons and multi-cuts*, J. Math. Phys. **50** (2009), 052301. [arXiv:0809.2619]
- [51] S. PASQUETTI and R. SCHIAPPA, *Borel and Stokes nonperturbative phenomena in topological string theory and $c = 1$ matrix models*, Annales Henri Poincaré **11** (2010), 351. [arXiv:0907.4082]
- [52] M. MARIÑO, S. PASQUETTI and P. PUTROV, *Large N duality beyond the genus expansion*, JHEP **07** (2010), 074. [arXiv:0911.4692]
- [53] J. G. RUSSO, *A note on perturbation series in supersymmetric gauge theories*, JHEP **1206** (2012), 038. [arXiv:1203.5061]
- [54] I. ANICETO, J. G. RUSSO and R. SCHIAPPA, *Resurgent analysis of localizable observables in supersymmetric gauge theories*, JHEP **1503** (2015), 172. [arXiv:1410.5834]
- [55] R. COUSO-SANTAMARÍA, R. SCHIAPPA and R. VAZ, *Finite N from resurgent large N* , Annals Phys. **356** (2015), 1–28. [arXiv:1501.01007]
- [56] M. P. HELLER and M. SPALIŃSKI, *Hydrodynamics beyond the gradient expansion: resurgence and resummation*, Phys. Rev. Lett. **115** (2015), no. 7, 072501. [arXiv:1503.07514]
- [57] M. HONDA and D. P. JATKAR, *Interpolating function and Stokes phenomena*. [arXiv:1504.02276]
- [58] A.-K. KASHANI-POOR and J. TROOST, *Pure $N=2$ super Yang-Mills and exact WKB*. [arXiv:1504.08324]
- [59] G. V. DUNNE and M. ÜNSAL, *Resurgence and dynamics of $O(N)$ and Grassmannian sigma models*. [arXiv:1505.07803]
- [60] I. ANICETO, *The Resurgence of the cusp anomalous dimension*, J. Phys. **A49** (2016), 065403. [arXiv:1506.03388]
- [61] D. DORIGONI and Y. HATSUDA, *Resurgence of the cusp anomalous dimension*, JHEP **09** (2015), 138. [arXiv:1506.03763]
- [62] G. BAŞAR and G. V. DUNNE, *Hydrodynamics, resurgence and trans-asymptotics*. [arXiv:1509.05046]
- [63] I. ANICETO and M. SPALIŃSKI, *Resurgence in extended hydrodynamics*, Phys. Rev. **D93** (2016), 085008. [arXiv:1511.06358]

- [64] M. STINGL, *Field theory amplitudes as resurgent functions*. [arXiv:hep-ph/0207349]
- [65] P. ARGYRES and M. ÜNSAL, *A semiclassical realization of infrared renormalons*, Phys. Rev. Lett. **109** (2012), 121601. [arXiv:1204.1661]
- [66] P. C. ARGYRES and M. ÜNSAL, *The semi-classical expansion and resurgence in gauge theories: new perturbative, instanton, bion, and renormalon effects*, JHEP **1208** (2012), 063. [arXiv:1206.1890]
- [67] G. V. DUNNE and M. ÜNSAL, *Resurgence and trans-series in quantum field theory: the $\mathbb{C}\mathbb{P}^{N-1}$ model*, JHEP **1211** (2012), 170. [arXiv:1210.2423]
- [68] G. V. DUNNE and M. ÜNSAL, *Continuity and resurgence: towards a continuum definition of the $\mathbb{C}\mathbb{P}^{N-1}$ model*, Phys. Rev. **D87** (2013), 025015. [arXiv:1210.3646]
- [69] A. CHERMAN, D. DORIGONI, G. V. DUNNE and M. ÜNSAL, *Resurgence in quantum field theory: nonperturbative effects in the principal chiral model*, Phys.Rev.Lett. **112** (2014), 021601. [arXiv:1308.0127]
- [70] A. CHERMAN, D. DORIGONI and M. ÜNSAL, *Decoding perturbation theory using resurgence: Stokes phenomena, new saddle points and Lefschetz thimbles*. [arXiv:1403.1277]
- [71] A. CHERMAN, P. KOROTEEV and M. ÜNSAL, *Resurgence and holomorphy: from weak to strong coupling*, J. Math. Phys. **56** (2015), no. 5, 053505. [arXiv:1410.0388]
- [72] M. P. BELLON and P. J. CLAVIER, *A Schwinger-Dyson equation in the Borel plane: singularities of the solution*, Lett. Math. Phys. **105** (2015), no. 6, 795–825.
- [73] M. SHIFMAN, *Resurgence, operator product expansion, and remarks on renormalons in supersymmetric Yang-Mills theory*, J. Exp. Theor.Phys. **120** (2015), no. 3, 386–398. [arXiv:1411.4004]
- [74] G. V. DUNNE, M. SHIFMAN and M. ÜNSAL, *Infrared renormalons versus operator product expansions in supersymmetric and related Gauge theories*, Phys. Rev. Lett. **114** (2015), no. 19, 191601. [arXiv:1502.06680]
- [75] A. BEHTASH, E. POPPITZ, T. SULEJMANPASIC and M. ÜNSAL, *The curious incident of multi-instantons and the necessity of Lefschetz thimbles*, JHEP **11** (2015), 175. [arXiv:1507.04063]
- [76] L. KLACZYNSKI, *Resurgent transseries & Dyson-Schwinger equations*. [arXiv:1601.04140]
- [77] M. MARIÑO, *Open string amplitudes and large-order behavior in topological string theory*, JHEP **0803** (2008), 060. [arXiv:hep-th/0612127]

- [78] B. EYNARD and M. MARIÑO, *A Holomorphic and background independent partition function for matrix models and topological strings*, J. Geom. Phys. **61** (2011), 1181–1202. [arXiv:0810.4273]
- [79] S. GAROUFALIDIS and M. MARIÑO, *Universality and asymptotics of graph counting problems in nonorientable surfaces*. [arXiv:0812.1195]
- [80] A. KLEMM, M. MARIÑO and M. RAUCH, *Direct integration and non-perturbative effects in matrix models*, JHEP **1010** (2010), 004. [arXiv:1002.3846]
- [81] N. DRUKKER, M. MARIÑO and P. PUTROV, *Nonperturbative aspects of ABJM theory*, JHEP **1111** (2011), 141. [arXiv:1103.4844]
- [82] R. COUSO-SANTAMARÍA, J. D. EDELSTEIN, R. SCHIAPPA and M. VONK, *Resurgent transseries and the holomorphic anomaly*, Annales Henri Poincaré, in press (2013). [arXiv:1308.1695]
- [83] A. GRASSI, M. MARIÑO and S. ZAKANY, *Resumming the string perturbation series*, JHEP **1505** (2015), 038. [arXiv:1405.4214]
- [84] R. COUSO-SANTAMARÍA, J. D. EDELSTEIN, R. SCHIAPPA and M. VONK, *Resurgent transseries and the holomorphic anomaly: nonperturbative closed strings in local \mathbb{CP}^2* , Commun. Math. Phys. **338** (2015), no. 1, 285–346. [arXiv:1407.4821]
- [85] M. VONK, *Resurgence and topological strings*. [arXiv:1502.05711]
- [86] Y. HATSUDA and K. OKUYAMA, *Resummations and non-perturbative corrections*. [arXiv:1505.07460]
- [87] R. COUSO-SANTAMARÍA, *Universality of the topological string at large radius and NS-brane resurgence*. [arXiv:1507.04013]
- [88] I. MULLER, *Zum Paradoxon der Wärmeleitungstheorie*, Z.Phys. **198** (1967), 329–344.
- [89] W. ISRAEL and J. STEWART, *Transient relativistic thermodynamics and kinetic theory*, Annals Phys. **118** (1979), 341–372.
- [90] E. DELABAERE, *Introduction to the Écalle theory*, In: “Computer Algebra and Differential Equations”, E. Tournier, (ed.), Cambridge University Press, 1994, 59–102.
- [91] O. COSTIN, “Asymptotics and Borel Summability”, Monographs and Surveys in Pure and Applied Mathematics, Chapman and Hall/CRC, 2008.
- [92] J. ZINN-JUSTIN, *Instantons in quantum mechanics: numerical evidence for a conjecture*, J. Math. Phys. **25** (1984), 549.
- [93] M. V. BERRY and C. J. HOWLS, *Hyperasymptotics*, Proc. R. Soc. London **A430** (1990), 653–668.
- [94] M. V. BERRY and C. J. HOWLS, *Hyperasymptotics for integrals with saddles*, Proc. R. Soc. London **A434** (1991), 657.

- [95] M. V. BERRY, “Asymptotics, Superasymptotics, Hyperasymptotics...” Asymptotics beyond all orders, Plenum, New York, 1991.
- [96] J. C. COLLINS and D. E. SOPER, *Large order expansion in perturbation theory*, Annals Phys. **112** (1978), 209–234.
- [97] R. COUSO-SANTAMARÍA, R. SCHIAPPA and R. VAZ, *On asymptotics and resurgent structures of enumerative Gromov-Witten invariants*. [arXiv:1605.07473]
- [98] G. V. DUNNE and M. ÜNSAL, *WKB and resurgence in the Mathieu equation*. [arXiv:1603.04924]
- [99] T. MISUMI, M. NITTA and N. SAKAI, *Non-BPS exact solutions and their relation to bions in $\mathbb{C}P^{N-1}$ models*, JHEP **05** (2016), 057. [arXiv:1604.00839]
- [100] T. FUJIMORI, S. KAMATA, T. MISUMI, M. NITTA and N. SAKAI, *Non-perturbative contributions from complexified solutions in $\mathbb{C}P^{N-1}$ models*. [arXiv:1607.04205]
- [101] M. P. HELLER, R. A. JANIK and P. WITASZCZYK, *Hydrodynamic gradient expansion in Gauge theory plasmas*, Phys.Rev.Lett. **110** (2013), no. 21, 211602. [arXiv:1302.0697]
- [102] S. GUKOV, M. MARIÑO and P. PUTROV, *Resurgence in complex Chern-Simons theory*. [arXiv:1605.07615]
- [103] S. DEMULDER, D. DORIGONI and D. C. THOMPSON, *Resurgence in η -deformed principal chiral models*, JHEP **07** (2016), 088. [arXiv:1604.07851]
- [104] F. PHAM, *Vanishing homologies and the n variable saddle-point method*, Proc. Sympos. Pure Math. **40** (1983), 319.
- [105] E. DELABAERE and C. J. HOWLS, *Global asymptotics for multiple integrals with boundaries*, Duke Math. J. **112** (2002), 199–264.
- [106] C. J. HOWLS, P. J. LANGMAN and A. B. O. DAALHUIS, *On the higher-order Stokes phenomenon*, Proc. R. Soc. London **A460** (2004), 2285.

Nonlinear eigenvalue problems

Carl M. Bender, Javad Komijani and Qing-hai Wang

Abstract. This paper begins with a review of earlier work on extending the notion of an eigenvalue problem for a linear differential equation to an eigenvalue problem for a nonlinear differential equation. In previous work it was argued that in the nonlinear context a separatrix plays the role of an eigenfunction and the initial conditions that spawn the separatrix play the role of an eigenvalue. Previously discussed nonlinear differential equations that have discrete eigenvalue structure include the first-order equation $y' = \cos(\pi xy)$ and the Painlevé transcendents P-I and P-II. In new work it is shown here that the concept of a nonlinear eigenvalue problem extends to huge classes of nonlinear differential equations. Numerical and analytical results on the eigenvalue behavior for some of these new differential equations are presented.

1 Introduction

Eigenvalue problems for linear second-order differential equations are well understood. For example, consider the Sturm-Liouville eigenvalue problem [1] for the time-independent Schrödinger equation

$$-y''(x) + V(x)y(x) = Ey(x), \quad (1.1)$$

where E is the eigenvalue and $y(x)$ is the eigenfunction. The eigenfunction $y(x)$ is required to satisfy homogeneous boundary conditions. For rising potentials $V(x)$ these boundary conditions are often imposed at $\pm\infty$:

$$y(-\infty) = 0, \quad y(\infty) = 0.$$

Variational methods [2] may be used to find accurate approximations to the low-lying eigenvalues, and semiclassical (WKB) techniques [3] may be used to find accurate approximations to the large eigenvalues. The leading WKB approximation to the n th eigenvalue E_n is given by the implicit phase-integral condition

$$\int_{x_L}^{x_R} dx \sqrt{E_n - V(x)} \sim \left(n + \frac{1}{2}\right) \pi \quad (n \gg 1), \quad (1.2)$$

where $x = x_L$ and $x = x_R$ are turning points satisfying the algebraic equation $V(x) = E_n$. Typically, the semiclassical (high-energy) approximation to E_n has the form

$$E_n \sim ab^n \quad (n \gg 1),$$

where the numbers a and b are determined by the condition (1.2). For instance, the semiclassical approximation to the eigenvalues of the harmonic oscillator $V(x) = x^2$ is

$$E_n \sim 2n \quad (n \gg 1),$$

and the semiclassical approximation to the eigenvalues of the anharmonic oscillator $V(x) = x^4$ is

$$E_n \sim [3\Gamma(3/4)\sqrt{\pi}/\Gamma(1/4)]^{4/3} n^{4/3} \quad (n \gg 1).$$

The solutions to the linear eigenvalue problem (1.1) have several characteristic qualitative features. Let us assume that the potential $V(x)$ has a single minimum and rises as $x \rightarrow \pm\infty$, like the potentials x^2 and x^4 . Then, the eigenfunctions exhibit distinct behaviors in each of five regions of x . When $x > x_R$ and when $x < x_L$, the eigenfunctions $y_n(x)$ decay exponentially as $|x| \rightarrow \infty$; these are the *classically forbidden* regions. However, when $x_L < x < x_R$, the eigenfunctions are oscillatory and $y_n(x)$ has exactly n nodes; this is the *classically allowed* region. When x is near x_L and x_R , there is an abrupt transition between exponentially decreasing and oscillatory behavior. This transition is universally described by the Airy function $\text{Ai}(x)$. Furthermore, the eigenfunctions exhibit an unstable behavior in the following sense. If the parameter E in (1.1) is not an eigenvalue, there are two linearly independent solutions to this equation; one solution grows exponentially as $x \rightarrow \infty$ and decays exponentially as $x \rightarrow -\infty$ while the linearly independent solution grows exponentially as $x \rightarrow -\infty$ and decays exponentially as $x \rightarrow \infty$. However, if E is an eigenvalue, a solution that is linearly independent of the eigenfunction grows exponentially as $x \rightarrow \pm\infty$. Thus, an infinitesimal change in E away from an eigenvalue causes the solution to (1.1) to lose the property of square integrability. We emphasize that there is an abrupt change in the character of the solution to (1.1) as E moves away from an eigenvalue.

We show in this paper that nonlinear differential equations can have eigenfunction-like solutions whose behaviors are strongly analogous to the behaviors of eigenfunctions for linear eigenvalue problems. This idea was originally proposed and investigated in Reference [4]. Specifically, it

was proposed that *a nonlinear differential equation may have a discrete set of critical initial conditions that give rise to unstable separatrix solutions*. We interpret these special initial conditions as *eigenvalues* and the unstable separatrices that emerge from these critical initial conditions as the corresponding *eigenfunctions*. Our ultimate objective is to find the large- n (semiclassical) asymptotic behavior of the n th eigenvalue by using both numerical and analytic techniques.

A simple-looking first-order nonlinear differential equation that exhibits eigenfunction and eigenvalue behavior is

$$y'(x) = \cos[\pi x y(x)] \quad (1.3)$$

subject to the initial condition $y(0) = E$. The initial value E plays the role of an eigenvalue. Solutions to this equation for various initial conditions E are plotted in Figure 1.1.

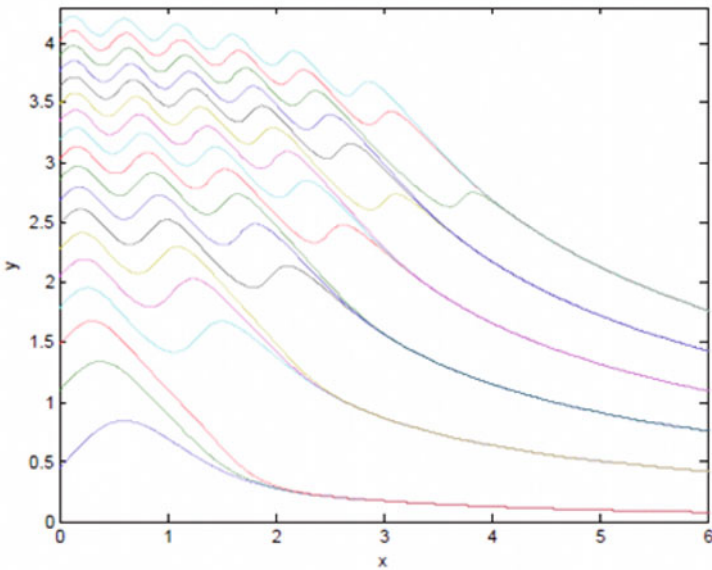


Figure 1.1. Numerical solutions $y(x)$ to (1.3) for $0 \leq x \leq 6$ with initial conditions $y(0)$ ranging from 0 to 4.2. The solutions initially oscillate but abruptly change their character and become smoothly and monotonically decaying. In the decaying regime the solutions merge into discrete quantized bundles. The bundles decay like $1/x$ as $x \rightarrow \infty$.

Figure 1.1 shows that solutions to the initial-value problem (1.3) have n maxima before vanishing like $1/t$ as $t \rightarrow \infty$. As the initial condition $y(0)$ increases past the special critical value E_n , the number of maxima changes from n to $n + 1$. At these critical values the solution $y(t)$ to (1.3)

is an unstable separatrix curve. We understand this instability as follows: If $y(0)$ lies infinitesimally below E_n the solution merges with a bundle of stable solutions all having n maxima, and when $y(0)$ is infinitesimally above E_n the solution merges with a bundle of stable solutions all having $n+1$ maxima. The separatrix curves are displayed in Figure 1.2 as dashed curves.

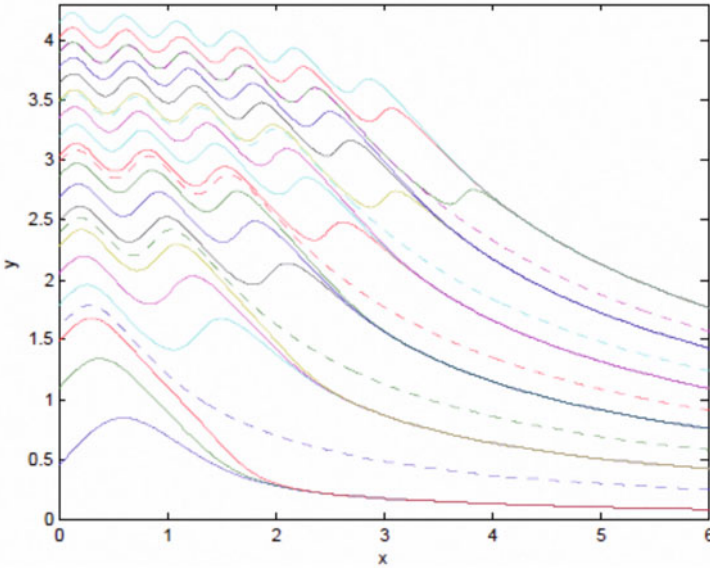


Figure 1.2. Same as in Figure 1.1 except that the separatrix (eigenfunction) solutions (dashed lines) to (1.3) are shown. The separatrix solutions begin at the eigenvalues $E_1 = 1.6026$, $E_2 = 2.3884$, $E_3 = 2.9767$, $E_4 = 3.4675$, and $E_5 = 3.8975$. The separatrices are unstable; if the initial condition $y(0)$ lies infinitesimally below (above) the eigenvalue, the solution rapidly diverges away from the separatrix and merges with the bundle of solutions below (above) the separatrix.

It is evident that the nonlinear eigenvalue problem illustrated in Figures 1.1 and 1.2 is qualitatively similar to the linear eigenvalue problem (1.1) for the time-independent Schrödinger equation. First, the separatrices are unstable with respect to a small change in the eigenvalue E_n ; if $y(0) = E_n$ is increased or decreased slightly, $y(x)$ abruptly jumps from the asymptotic bundle of solutions on one side of the separatrix to the asymptotic bundle on the other side of the separatrix. Furthermore, the eigenfunctions (separatrix curves) corresponding to the n th eigenvalue (the initial condition E_n) exhibit n oscillations in the “classically allowed” region before decreasing monotonically to 0 in the “classically forbidden” region. We can see in Figures 1.1 and 1.2 that this change

from oscillatory to decaying behavior occurs over a narrow “turning-point” region.

There is no known exact formula for the n th eigenvalue E_n . Lacking such a formula, the challenge is to determine the asymptotic behavior of the critical values E_n for large n . It was shown in Reference [4] that for large n the nonlinear-differential-equation problem (1.3) reduces to a *linear* one-dimensional random-walk problem. This random-walk problem was solved exactly and it was thereby established analytically that the n th eigenvalue grows like an^b for large n :

$$E_n \sim 2^{5/6} \sqrt{n} \quad (n \rightarrow \infty). \quad (1.4)$$

Kerr subsequently found an alternative derivation of this remarkable semiclassical (high-energy) solution to this asymptotics problem and verified (1.4) [5]. [The numerical constant $a = 2^{5/6}$ and the exponent $b = 1/2$ are surprising because there is no hint of such numbers in the differential equation (1.3).]

The purpose of this paper is to demonstrate that there is a huge class of *second-order* nonlinear-differential-equation eigenvalue problems having discrete eigenvalues. It was shown in Refs. [4, 6] that nonlinear eigenvalue problems could be posed for the first two Painlevé transcendents. These eigenvalue problems and their solutions are summarized in Section 2. The Painlevé equations have the special property that their solutions only have *movable* (or *spontaneous*) singularities that are poles; there are no other kinds of movable singularities, such as branch points. Thus, the solutions to these differential equations are *meromorphic* (they only live on a one-sheeted Riemann surface). Consequently, such solutions are relatively easy to study by using both numerical and asymptotic analysis. The large-eigenvalue behaviors of these equations can be found asymptotically by linearizing the eigenvalue problems. Specifically, for large n the nonlinear eigenvalues are approximated by the eigenvalues of a *linear* Schrödinger eigenvalue problem and the Hamiltonian for this problem belongs to the class of \mathcal{PT} -symmetric non-Hermitian Hamiltonians [7].

In Reference [6] it was proposed that one might extend the study of nonlinear-differential-equation eigenvalue problems beyond the Painlevé transcendents to more complicated differential equations such as the Thomas-Fermi equation $y''(x) = [y(x)]^{3/2}x^{1/2}$. Indeed, the standard physical solution to this equation, which satisfies the boundary conditions $y(0) = 1$ and $y(+\infty) = 0$, is an eigenfunction solution. Like the solutions to (1.3), $y(x)$ vanishes algebraically (specifically, like $144x^{-3}$) as $x \rightarrow \infty$. This is an unstable separatrix solution and the specific value

of $y'(0)$ that gives rise to this solution is an eigenvalue. If $y'(0)$ is larger than the critical value of $y'(0)$, the function $y(x)$ becomes singular at some point $x = a$ and blows up like $400a(x - a)^{-4}$ as $x \rightarrow a$; if $y'(0)$ is less than the critical value, the function $y(x)$ crosses 0 and becomes complex. Unfortunately, the movable singularity at $x = a$ is a *logarithmic branch-point* singularity [this is verified by expanding $y(x)$ to high order (sixteenth order!) in powers of $(x - a)$] and therefore the solutions to this equation live on a Riemann surface having infinitely many sheets. Consequently, this equation is difficult to analyze and it is hard to find additional separatrix solutions.

Fortunately, we have found infinite numbers of nonlinear differential equations whose movable singularities are just algebraic branch points, and these equations, which are discussed in Section 3 are quite tractable. It is most satisfying that the features of these new kinds of nonlinear-differential-eigenvalue problems are qualitatively very similar to those of the Painlevé equations, which are described in Section 2.

2 Nonlinear eigenvalue problems for Painlevé I and II

The Painlevé transcendents are six second-order nonlinear differential equations whose movable (spontaneous) singularities are poles (and not branch points, essential singularities, or other kinds of singularities). Many papers and books have been written on these beautiful differential equations [8–15] and these equations arise often in mathematical physics [16–23].

This section considers the first and second Painlevé transcendents, referred to here as P-I and P-II. The initial-value problem (IVP) for the P-I differential equation is

$$y''(t) = 6[y(t)]^2 + t, \quad y(0) = c, \quad y'(0) = b \quad (2.1)$$

and the IVP for P-II (in which we have set an arbitrary additive constant to 0) is

$$y''(t) = 2[y(t)]^3 + ty(t), \quad y(0) = c, \quad y'(0) = b. \quad (2.2)$$

In this section we show that for the fixed initial condition $y(0) = 0$ there is a discrete set of initial slopes $y'(0) = b_n$ that give rise to unstable separatrix solutions. Analogously, for a fixed initial slope $y'(0) = 0$, there is a discrete set of initial values $y(0) = c_n$ that give rise to separatrix solutions. For Painlevé I the large- n asymptotic behavior of the eigenvalues b_n is

$$b_n \sim B_1 n^{3/5} \quad (n \rightarrow \infty) \quad (2.3)$$

and that of the eigenvalues c_n is

$$c_n \sim C_I n^{2/5} \quad (n \rightarrow \infty). \quad (2.4)$$

For Painlevé II the large- n asymptotic behavior of the eigenvalues b_n is

$$b_n \sim B_{II} n^{2/3} \quad (n \rightarrow \infty) \quad (2.5)$$

and that of the eigenvalues c_n is

$$c_n \sim C_{II} n^{1/3} \quad (n \rightarrow \infty). \quad (2.6)$$

The coefficients B_I , C_I , B_{II} , and C_{II} in these asymptotic behaviors can be determined analytically as well as numerically. The analytical calculation of these constants for P-I and P-II is done by reducing the nonlinear equations to the linear eigenvalue problems for the cubic and quartic \mathcal{PT} -symmetric Hamiltonians $H = \frac{1}{2}p^2 + 2ix^3$ and $H = \frac{1}{2}p^2 - \frac{1}{2}x^4$ [6].

2.1 Eigenvalue problems for Painlevé I

In Reference [24] there is a brief asymptotic study of the first Painlevé transcendent (2.1). It is easy to see that there are two possible asymptotic behaviors of the solution to this differential equation as $t \rightarrow -\infty$; the solutions to the P-I equation can approach either $+\sqrt{-t/6}$ or $-\sqrt{-t/6}$. An elementary asymptotic analysis shows that if the solution $y(t)$ approaches $-\sqrt{-t/6}$, the solution oscillates *stably* about this curve with gradually decreasing amplitude. On the other hand, while the curve $+\sqrt{-t/6}$ is another possible asymptotic behavior, this behavior is *unstable* and nearby solutions tend to veer away from it. The eigenfunction solutions to the first Painlevé transcendent are those solutions that *do* approach the curve $+\sqrt{-t/6}$ as $t \rightarrow -\infty$. These separatrix solutions resemble the eigenfunctions of conventional quantum mechanics in that they exhibit n oscillations before settling down to this asymptotic behavior. However, because the P-I equation is nonlinear, these oscillations are unbounded; the n th eigenfunction passes through $[n/2]$ double poles where it blows up, and only then does it smoothly approach the curve $+\sqrt{-t/6}$. (The symbol $[n/2]$ means greatest integer in $n/2$.)

Let us discuss in greater detail the numerical solutions to the initial-value problem for the P-I equation (1.1) for $t < 0$. To find these solutions we use Runge-Kutta to integrate down the negative-real axis. When we approach a double pole and the solution becomes large and positive, we estimate the location of the pole and integrate along a semicircle in the complex- t plane around the pole. We then continue integrating down the negative-real axis. We choose the fixed initial value $y(0) = 0$ and allow

the initial slope $y'(0) = b$ to have increasingly positive values. (We only present results for positive initial slope; the behavior for negative initial slope is analogous.) We have found that the particular choice of $y(0)$ is not crucial; for *any* fixed $y(0)$ the large- n leading asymptotic behavior of the initial-slope eigenvalues b_n is the same.

We find that above the critical value $b_1 = 1.851854034$ (the first eigenvalue) there is a continuous interval of b for which $y(t)$ first has a minimum and then has an infinite sequence of double poles (see Figure 2.1, left panel). However, if b increases past the next critical value $b_2 = 3.004031103$ (the second eigenvalue), the character of the solutions changes abruptly and $y(t)$ oscillates stably about $-\sqrt{-t/6}$ (Figure 2.1, right panel). When b exceeds the critical value $b_3 = 3.905175320$ (the third eigenvalue), the solutions again exhibit an infinite sequence of poles (Figure 2.2, left panel). When b increases past the fourth critical value $b_4 = 4.683412410$ (fourth eigenvalue), the solutions once again oscillate stably about $-\sqrt{-t/6}$ (Figure 2.2, right panel). Our numerical analysis indicates that there is an infinite sequence of critical points (eigenvalues) at which the P-I solutions alternate between infinite sequences of double poles and stable oscillation about $-\sqrt{-t/6}$.

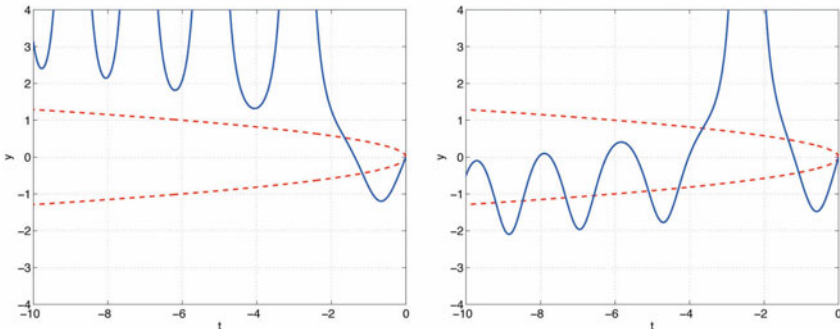


Figure 2.1. Typical behavior of solutions to the first Painlevé transcendent $y(t)$ for the initial conditions $y(0) = 0$ and $b = y'(0)$. In the left panel $b = 2.504031103$, which lies between the eigenvalues $b_1 = 1.851854034$ and $b_2 = 3.004031103$. In the right panel $b = 3.504031103$, which lies between the eigenvalues $b_2 = 3.004031103$ and $b_3 = 3.905175320$. The dashed curves are $y = \pm\sqrt{-t/6}$. In the left panel the solution $y(t)$ has an infinite sequence of double poles and in the right panel the solution oscillates stably about $-\sqrt{-t/6}$.

The separatrix (eigenfunction) solutions that arise when $y'(0)$ is an eigenvalue have a completely different (and unstable) character from those in Figures 2.1 and 2.2. These special solutions exhibit a *finite* number $[n/2]$ of double poles (analogous to the oscillatory behavior of quantum-mechanical bound-state eigenfunctions in the classically allowed region

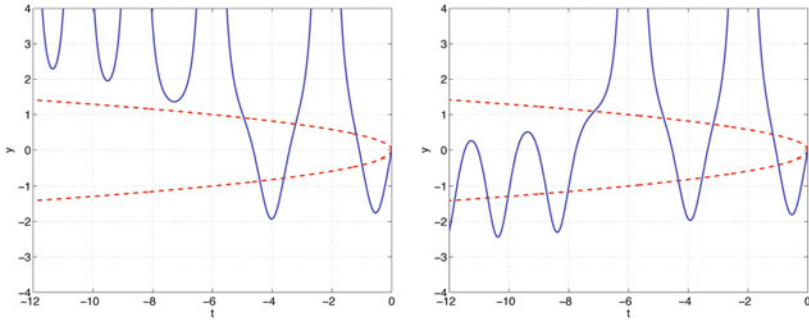


Figure 2.2. Solutions to the P-I equation (1.1) for $y(0) = 0$ and $b = y'(0)$. Left panel: $b = 4.583412410$, which lies between the eigenvalues $b_3 = 3.905175320$ and $b_4 = 4.6834124103$. Right panel: $b = 4.783412410$, which lies between the eigenvalues $b_4 = 4.683412410$ and $b_5 = 5.383086722$.

of a potential well) and then exhibit a turning-point-like transition in which the poles abruptly cease and $y(t)$ exponentially decays towards the limiting curve $+\sqrt{-t/6}$. The solutions arising from the first and second critical points b_1 and b_2 are shown in Figure 2.3, those arising from the third and fourth critical points b_3 and b_4 are shown in Figure 2.4, and those arising from the tenth and eleventh critical points b_{10} and b_{11} are shown in Figure 2.5. The critical points are analogous to eigenvalues because they give rise to *unstable* separatrix solutions; if $y'(0)$ changes by an infinitesimal amount above or below a critical value, the character of the solutions changes abruptly and the solutions exhibit the two possible kinds of generic behaviors shown in Figures 2.1 and 2.2.

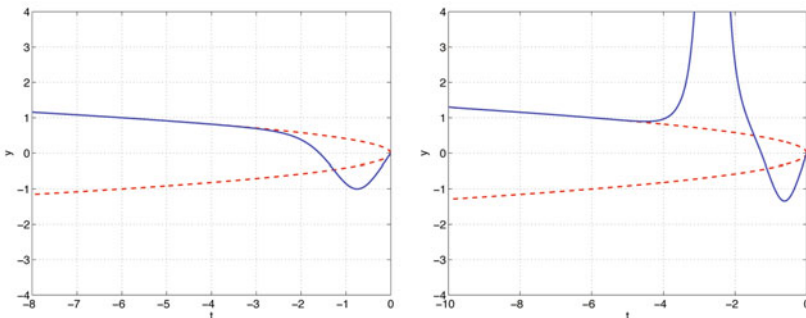


Figure 2.3. First two separatrix solutions (eigenfunctions) of Painlevé I with initial condition $y(0) = 0$. Left panel: $y'(0) = b_1 = 1.851854034$; right panel: $y'(0) = b_2 = 3.004031103$. The dashed curves are $y = \pm\sqrt{-t/6}$.

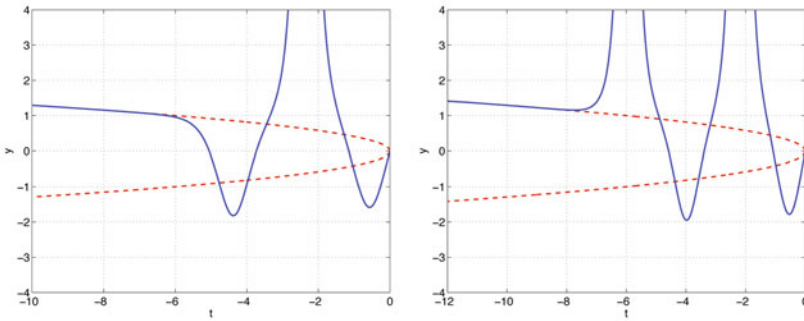


Figure 2.4. Third and fourth eigenfunctions of Painlevé I with initial condition $y(0) = 0$. Left panel: $y'(0) = b_3 = 3.905175320$; right panel: $y'(0) = b_4 = 4.683412410$.

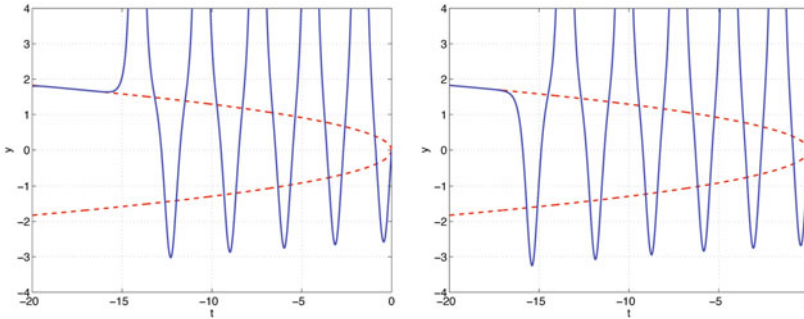


Figure 2.5. Tenth and eleventh eigenfunctions of Painlevé I with initial condition $y(0) = 0$. Left panel: $y'(0) = b_{10} = 8.244932302$; right panel: $y'(0) = b_{11} = 8.738330156$. Note that as n increases, the eigenfunctions pass through more and more double poles before exhibiting a turning-point-like transition and approaching the limiting curve $+\sqrt{-t}/6$ exponentially rapidly. This behavior is analogous to that of the eigenfunctions of a time-independent Schrödinger equation for a particle in a potential well; the higher-energy eigenfunctions exhibit more and more oscillations in the classically allowed region before entering the classically forbidden region, where they decay exponentially.

In Reference [6] the constant B_1 was determined numerically with great accuracy by applying fifth-order Richardson extrapolation to the first eleven eigenvalues. The value of B_1 in (2.3) was found to an accuracy of one part in nine decimal places:

$$B_1 = 2.09214674\underline{4}. \quad (2.7)$$

On the basis of the numerical analysis, one can say with confidence that the underlined digit lies in the range from 3 to 5, so the determination of B_1 is accurate to one part in 2×10^8 .

If the initial slope is held fixed at $y'(0) = 0$ and the initial value $y(0) = c$ is allowed to become increasingly negative, a new sequence of negative eigenvalues c_n appears for which the solutions resemble the eigenfunction separatrix solutions in Figures 2.3–2.5. The first four eigenfunctions are plotted in Figures 2.6 and 2.7.

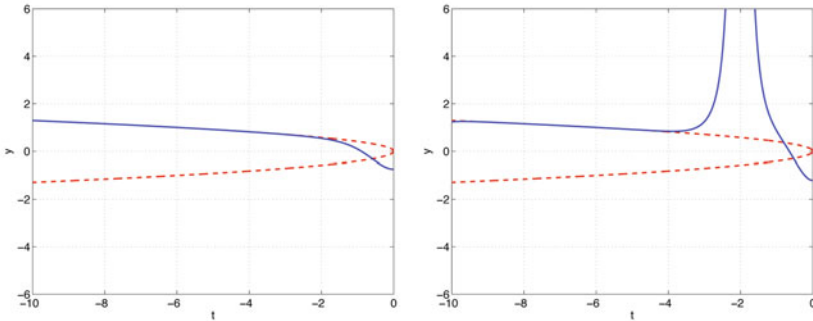


Figure 2.6. First two separatrix solutions (eigenfunctions) of Painlevé I with fixed initial slope $y'(0) = 0$. Left panel: $y(0) = c_1 = -0.7401954236$; right panel: $y(0) = c_2 = -1.206703845$. The dashed curves are $y = \pm\sqrt{-t/6}$.

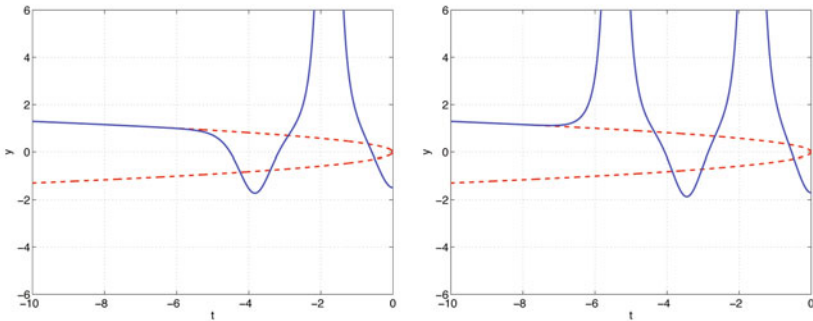


Figure 2.7. Third and fourth eigenfunctions of Painlevé I with initial slope $y'(0) = 0$. Left panel: $y(0) = c_3 = -1.484375587$; right panel: $y(0) = c_4 = -1.69951765$.

Fourth-order Richardson extrapolation applied to the first 15 eigenvalues, reveals that for large n the sequence of initial-value eigenvalues c_n is asymptotic to $C_1 n^{2/5}$, where the numerical value of the constant C_1 in (2.4) is [6]

$$C_1 = -1.0304844. \quad (2.8)$$

The last digit is accurate to an error of ± 1 and thus C_1 is determined to an accuracy of one part in 10^7 .

2.2 Eigenvalue problems for Painlevé II

For P-II, a straightforward asymptotic analysis shows that as $t \rightarrow -\infty$, there are three possible asymptotic behaviors for solutions $y(t)$: $y(t)$ either oscillates stably about the negative axis or it approaches the curves $\pm\sqrt{-t/2}$; both of these asymptotic behaviors are unstable. If we numerically integrate (2.2), we see that when t becomes large and negative, a typical solution to the P-II initial-value problem either oscillates about the negative axis or passes through an infinite sequence of simple poles. The special eigenfunction solutions pass through only a finite number of poles and then approach either the positive or the negative branches of the square-root curves. These eigenfunctions obey the boundary conditions $y(0) = 0$ and $y'(0) = \pm b$. [Because P-II is symmetric under $y \rightarrow -y$, there are two sets of eigenfunctions, one for each sign of $y'(0)$.] The P-II equation is particularly interesting because as $t \rightarrow +\infty$, the behavior $y \rightarrow 0$ becomes *unstable*. Thus, there are new kinds of eigenfunctions for positive t . We have found eigenfunctions that satisfy $y'(0) = 0$ and $y(0) = c$ and we examine the positive- c eigenfunctions numerically.

As in the case of P-I, if we choose $y(0) = 0$, there are critical values $y'(0) = b_n$ at which the solutions $y(t)$ to P-II change their character. Figures 2.8 and 2.9 show the solutions to the P-II equation for the initial condition $y(0) = 0$ and $y'(0) = b$ for $b_1 < b < b_2$, $b_2 < b < b_3$, $b_3 < b < b_4$, and $b_4 < b < b_5$. In these figures the behavior of the solution alternates between having an infinite sequence of simple poles and oscillating stably about $y(t) = 0$. However, when $y'(0) = b$ is at a critical value (eigenvalue) b_n , the solution $y(t)$ passes through a *finite* number $[n/2]$ of simple poles and then approaches either $+\sqrt{-t/2}$ or $-\sqrt{-t/2}$. These eigenfunctions (separatrices) are plotted in Figures 2.10, 2.11, and 2.12 for $n = (1, 2)$, $(3, 4)$, and $(20, 21)$.

The eigenfunctions in Figures 2.10, 2.11, and 2.12 alternate between approaching the upper-unstable branch $+\sqrt{-t/2}$ or the lower-unstable branch $-\sqrt{-t/2}$. Thus, there are actually two sequences of eigenvalues, one for even n and one for odd n . Using Richardson extrapolation, we find that the sequences of eigenvalues b_{2n} and b_{2n+1} have the same asymptotic behavior

$$b_{2n} \sim b_{2n+1} \sim B_{\text{II}} n^{2/3} \quad (n \rightarrow \infty). \quad (2.9)$$

Our numerical calculations reveal that the value of B_{II} in (2.5) is [6]

$$B_{\text{II}} = 1.862412\text{\underline{8}}. \quad (2.10)$$

The numerical data for P-II are noisier than those for P-I, and fourth-order Richardson extrapolation gives the underlined eighth digit as 8 ± 2 .

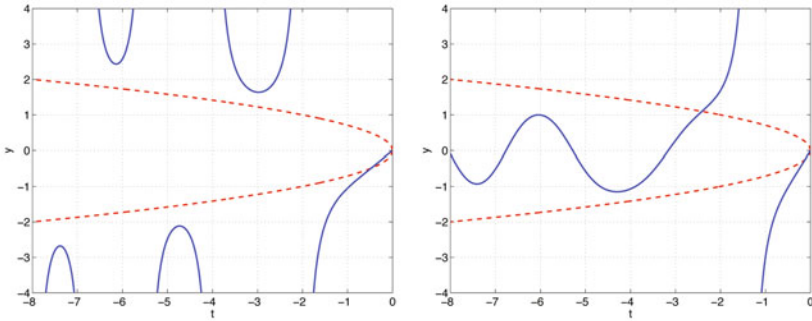


Figure 2.8. Typical behavior of solutions to the second Painlevé transcendent for the initial conditions $y(0) = 0$ and $b = y'(0)$. In the left panel $b = 1.028605106$, which lies between the eigenvalues $b_1 = 0.5950825526$ and $b_2 = 1.528605106$. In the right panel $b = 2.028605106$, which lies between the eigenvalues $b_2 = 1.528605106$ and $b_3 = 2.155132869$. In the left panel the solution $y(t)$ has an infinite sequence of simple poles and in the right panel the solution oscillates stably about $-\sqrt{t/6}$. The dashed curves are the functions $\pm\sqrt{-t/2}$.

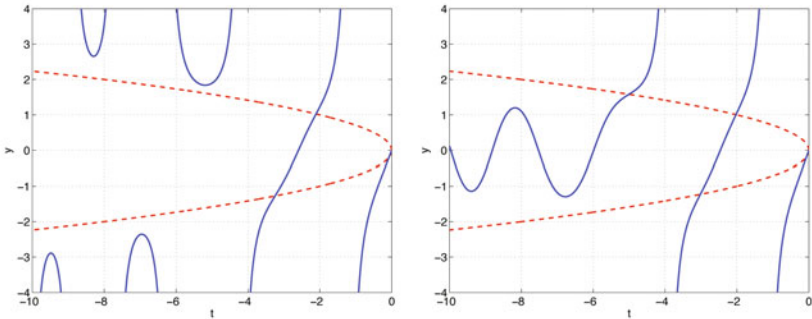


Figure 2.9. Solutions to the P-II equation (1.2) for $y(0) = 0$ and $b = y'(0)$. Left panel: $b = 2.600745985$, which lies between the eigenvalues $b_3 = 2.155132869$ and $b_4 = 2.700745985$. Right panel: $b = 2.800745985$, which lies between the eigenvalues $b_4 = 2.700745985$ and $b_5 = 3.195127590$.

Next, we consider the *positive- t* solutions to P-II for vanishing initial slope and positive initial condition for $t \geq 0$. As $t \rightarrow +\infty$ (not $-\infty$), the n th eigenfunction passes through n simple poles before it approaches zero monotonically. Fourth-order Richardson verifies (2.6) and determines that for large n , $c_n \sim C_{\text{II}} n^{1/3}$ [6], where

$$C_{\text{II}} = 1.21581165. \quad (2.11)$$

The last digit 5 has an uncertainty of ± 1 .

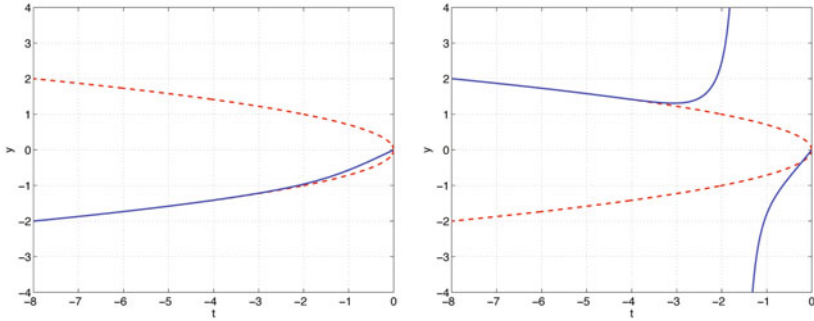


Figure 2.10. First two separatrix solutions (eigenfunctions) of Painlevé II with initial condition $y(0) = 0$. Left panel: $y'(0) = b_1 = 0.5950825526$; right panel: $y'(0) = b_2 = 1.528605106$. The dashed curves are $\pm\sqrt{-t/2}$.

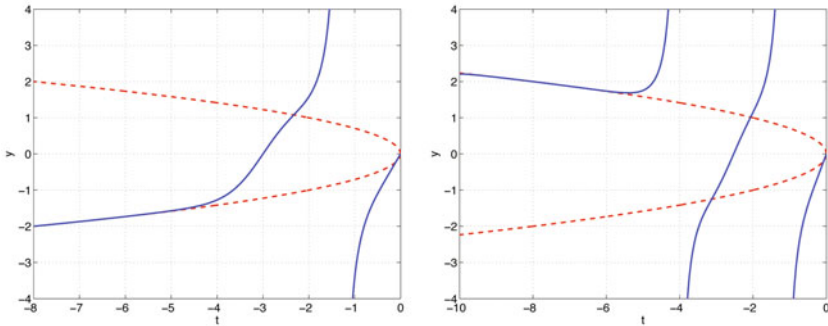


Figure 2.11. Third and fourth eigenfunctions of Painlevé II with initial condition $y(0) = 0$. Left panel: $y'(0) = b_3 = 2.155132869$; right panel: $y'(0) = b_4 = 2.700745985$.

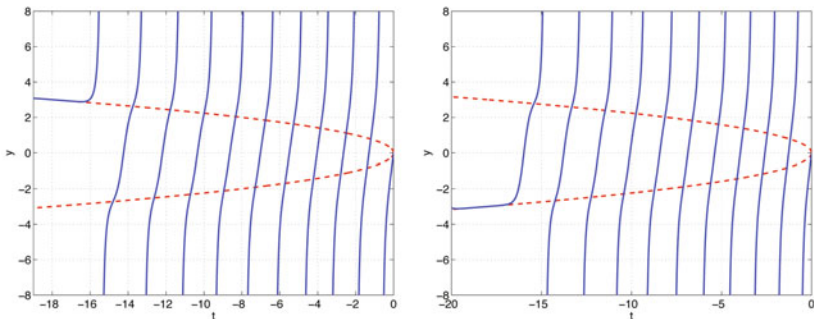


Figure 2.12. The twentieth and twenty-first eigenfunctions of Painlevé II with initial condition $y(0) = 0$. Left panel: $y'(0) = b_{20} = 8.499476190$; right panel: $y'(0) = b_{21} = 8.787666814$.

2.3 Asymptotic study of the Painlevé equations

In Reference [6] heuristic asymptotic techniques were proposed to obtain analytic expressions for the constants B_I and C_I for P-I and B_{II} and C_{II} for P-II. If we multiply the Painlevé-I equation in (2.1) by $y'(t)$ and integrate from $t = 0$ to $t = x$, we get

$$H \equiv \frac{1}{2}[y'(x)]^2 - 2[y(x)]^3 = \frac{1}{2}[y'(0)]^2 - 2[y(0)]^3 + I(x), \quad (2.12)$$

where $I(x) = \int_0^x dt ty'(t)$. The path of integration is the same as that used to calculate $y(t)$ numerically; the path follows the negative-real axis until it gets near a pole, at which point it makes a semicircular loop in the complex- t plane to avoid the pole.

We calculate $I(x)$ for large-negative x in the classically allowed region (before the poles abruptly cease at the turning point) and find that on the real- x axis, as $n \rightarrow \infty$, $I(x)$ fluctuates and becomes small compared with H . This is not surprising because $I(x)$ receives many positive and negative contributions from the poles. We can see from the definition of $I(x)$ that $I(x)$ vanishes when $y'(x)$ vanishes. Near the points where $y'(x)$ vanishes, we verify numerically that $I(x)$ is small compared with $-2[y(x)]^3$. Far from these points $y(x)$ becomes large, but so does $I(x)$. However, $-2[y(x)]^3$ blows up like a sixth-order pole and $I(x)$ blows up like a second-order pole. These asymptotic estimates are difficult to verify analytically, but numerical analysis confirms these results. These estimates are valid when x is large and negative but only in the classically allowed region and not as $x \rightarrow -\infty$.

By examining $I(x)$ as $x \rightarrow -\infty$, we can see a signal of an eigenvalue; as $y'(0) = b$ passes an eigenvalue, $I(x)$ goes from having positive to negative (or negative to positive) fluctuations, but at an eigenvalue $I(x)$ is smooth and does not fluctuate. For large n we treat the fluctuating quantity $I(x)$ as small and we interpret H as a time-independent quantum-mechanical Hamiltonian. [The isomonodromic properties of H when $I(x)$ is not neglected were studied in Reference [13].]

To support these observations regarding the behavior of $I(x)$ on the real axis, we have done extremely detailed numerical studies of the distribution of poles and the behavior of P-I in the complex- x plane. This gives a much clearer and cleaner picture of the behavior of $I(x)$ for large x . We find that along the lines $x = re^{\pm i\pi/4}$, where r is real, the function $I(x)$ rapidly approaches 0 as $r \rightarrow \infty$. This provides strong evidence that the large- n (semiclassical) behavior of the eigenvalues is determined by solving the *linear* time-independent quantum-mechanical eigenvalue problem $\hat{H}\psi = E\psi$, where $\hat{H} = \frac{1}{2}\hat{p}^2 - 2\hat{x}^3$ along these lines in the complex- x plane. To find these eigenvalues we simply rotate \hat{H} into the

complex plane by 45° [25] and obtain the well-studied \mathcal{PT} -symmetric Hamiltonian [7]

$$\hat{H} = \frac{1}{2}\hat{p}^2 + 2i\hat{x}^3. \quad (2.13)$$

The large eigenvalues of this Hamiltonian can be found by using the complex WKB techniques discussed in Reference [7]. For the general class of \mathcal{PT} -symmetric Hamiltonians $\hat{H} = \frac{1}{2}\hat{p}^2 + g\hat{x}^2 (i\hat{x})^\epsilon$ ($\epsilon \geq 0$), the WKB approximation to the n th eigenvalue ($n \gg 1$) is given by

$$E_n \sim \frac{1}{2}(2g)^{2/(4+\epsilon)} \left[\frac{\Gamma\left(\frac{3}{2} + \frac{1}{\epsilon+2}\right) \sqrt{\pi} n}{\sin\left(\frac{\pi}{\epsilon+2}\right) \Gamma\left(1 + \frac{1}{\epsilon+2}\right)} \right]^{(2\epsilon+4)/(\epsilon+4)}. \quad (2.14)$$

For H in (2.13) we take $g = 2$ and $\epsilon = 1$ and obtain the asymptotic behavior

$$E_n \sim 2 \left[\sqrt{3\pi} \Gamma\left(\frac{11}{6}\right) n / \Gamma\left(\frac{1}{3}\right) \right]^{6/5} \quad (n \rightarrow \infty). \quad (2.15)$$

The Hamiltonian \hat{H} in (2.13) is time independent, so we evaluate H in (2.12) for fixed $y(0)$ and large $y'(0) = b_n$ and obtain the result that

$$b_n \sim \sqrt{2E_n} = B_I n^{3/5} \quad (n \rightarrow \infty), \quad (2.16)$$

which verifies (2.3). We read off the analytic value of the constant B_I :

$$B_I = 2 \left[\sqrt{3\pi} \Gamma\left(\frac{11}{6}\right) / \Gamma\left(\frac{1}{3}\right) \right]^{3/5}, \quad (2.17)$$

which agrees with the numerical result in (2.7). Also, if we take the initial slope $y'(0)$ to vanish and take the initial condition $y(0) = c_n$ to be large, we obtain an analytic expression for C_I ,

$$C_I = - \left[\sqrt{3\pi} \Gamma\left(\frac{11}{6}\right) / \Gamma\left(\frac{1}{3}\right) \right]^{2/5}, \quad (2.18)$$

which verifies the numerical result in (2.8). *We emphasize that these analytic results are in precise agreement with our numerical work on the large- n behavior of the eigenvalues.*

To obtain analytic expressions for B_{II} in (2.10) and C_{II} in (2.11), we follow the same procedure as for P-I. We multiply the P-II equation by $y'(t)$ and integrate from $t = 0$ to $t = x$, where x is in the turning-point region (where the simple poles stop). The result is

$$H \equiv \frac{1}{2}[y'(x)]^2 - \frac{1}{2}[y(x)]^4 = \frac{1}{2}[y'(0)]^2 - \frac{1}{2}[y(0)]^4 + I(x), \quad (2.19)$$

where $I(x) = \int_0^x dt ty(t)y'(t)$. The path of integration is the same as that used to calculate P-II numerically; it follows the negative-real axis until it gets near a simple pole, at which point it makes a loop in the complex- t plane to avoid the pole. As before, we argue that along this path the integrand of $I(x)$ is oscillatory and that because of cancellations we may neglect $I(x)$ when n is large.

We treat H as the \mathcal{PT} -symmetric quantum-mechanical Hamiltonian

$$\hat{H} = \frac{1}{2}\hat{p}^2 - \frac{1}{2}\hat{x}^4 \quad (2.20)$$

and we use (2.14) with $g = 1/2$ and $\epsilon = 2$ to obtain

$$E_n \sim \frac{1}{2} \left[3n\sqrt{2\pi}\Gamma\left(\frac{3}{4}\right) / \Gamma\left(\frac{1}{4}\right) \right]^{4/3} \quad (2.21)$$

for the large eigenvalues of \hat{H} . We then calculate the eigenvalues b_n by using

$$\sqrt{2E_n} \sim \left[3n\sqrt{2\pi}\Gamma\left(\frac{3}{4}\right) / \Gamma\left(\frac{1}{4}\right) \right]^{2/3} \quad (n \rightarrow \infty). \quad (2.22)$$

This formula allows us to identify the value of B_{II} :

$$B_{II} = \left[3\sqrt{2\pi}\Gamma\left(\frac{3}{4}\right) / \Gamma\left(\frac{1}{4}\right) \right]^{2/3}. \quad (2.23)$$

This result agrees with the numerical determination in (2.10).

To calculate C_{II} we note that the initial value $y(0)$ is positive. However, if we neglect $I(x)$ and assume a vanishing initial slope, we see that the right side of (2.19) is negative. Thus, as we did for the cubic Hamiltonian $\frac{1}{2}\hat{p}^2 - 2\hat{x}^3$, we perform a complex rotation of the coupling constant to convert the quartic Hamiltonian to the form

$$\hat{H} = \frac{1}{2}\hat{p}^2 + \frac{1}{2}\hat{x}^4. \quad (2.24)$$

In this case we obtain the conventional Hermitian quartic-anharmonic-oscillator Hamiltonian, which does not belong to the class of \mathcal{PT} -symmetric Hamiltonians $\hat{H} = \frac{1}{2}\hat{p}^2 + g\hat{x}^2(i\hat{x})^\epsilon$. The WKB calculation mentioned earlier in Section 1 gives the large-eigenvalue approximation

$$E_n \sim \left[3n\sqrt{\pi}\Gamma\left(\frac{3}{4}\right) / \Gamma\left(\frac{1}{4}\right) \right]^{4/3} \quad (n \rightarrow \infty) \quad (2.25)$$

from which one can read off the value of C_{II} :

$$C_{II} = \left[3\sqrt{\pi}\Gamma\left(\frac{3}{4}\right) / \Gamma\left(\frac{1}{4}\right) \right]^{1/3}, \quad (2.26)$$

which agrees with the numerical result in (2.11).

3 Nonlinear eigenvalue problems for more complicated differential equations

In this section we introduce a new infinite class of nonlinear-differential-equation eigenvalue problems of the form

$$y''(x) = \frac{2M+2}{(M-1)^2} [y(x)]^M + x[y(x)]^N, \quad (3.1)$$

where M and N are integers. We refer to the equations in this class as $SP(M, N)$ (SP stands for super-Painlevé). These equations are a natural generalization of the first two Painlevé equations; P-I in (2.1) is $SP(2, 0)$ and P-II in (2.2) is $SP(3, 1)$. These equations become particularly interesting nonlinear eigenvalue problems when N is less than $M - 1$. We consider this special class of equations because their solutions appear not to have logarithmic movable singularities.

To understand the behaviors of solutions to these equations, let us first recall how P-I works. It is clear that the solution to P-I can become singular at an arbitrary point $x = A$ and that the leading asymptotic approximation to such a solution is

$$y(x) \sim \frac{1}{(x-A)^2} \quad (x \rightarrow A).$$

However, it is not obvious that the singularity at $x = A$ is a pole. To verify that this singularity is indeed a pole it is necessary to show that an expansion around $x = A$ is a Laurent series. To do this we substitute

$$y(x) = \frac{1}{(x-A)^2} \left[1 + \sum_{n=1}^{\infty} a_n (x-A)^n \right] \quad (3.2)$$

into (2.1) and collect powers of $(x - A)$. If we solve recursively for the coefficients a_n , we find that the first five coefficients are $a_1 = 0$, $a_2 = 0$, $a_3 = 0$, $a_4 = -A/10$, and $a_5 = -1/6$. However, the key result is that a_6 is *undetermined* and thus is *arbitrary*. Since the series expansion for $y(x)$ contains *two arbitrary constants*, A and a_6 , it follows that this series is the most general solution to the P-I equation. To complete the argument one must show that the series expansion for $y(x)$ converges when $|x - A|$ is sufficiently small. This establishes that the expansion (3.2) is a Laurent series and verifies that the solutions to P-I are meromorphic.

To see what changes if we alter the P-I equation slightly, let us replace the term x by $x + x^2$. Now, if we seek a solution of the form (3.2), we find that while the first five coefficients remain unchanged, a contradictory equation arises in the next order; the only way to resolve this contradiction is to include a new term of the form $b_6(x - A)^6 \log(x - A)$. Now,

the coefficient a_6 remains arbitrary and b_6 is determined. However, six orders later a new contradiction arises and requires that we insert a new logarithmic term of the form $c_{12}(x - A)^{12}[\log(x - A)]^2$. New logarithmic singularities continue to appear every six orders. This shows that the solutions to the equation have movable singularities that are not second-order poles; rather they are a complicated superposition of logarithms. Thus, the solutions are not meromorphic and they live on a Riemann surface having an infinite number of sheets.

The analysis above generalizes straightforwardly to the solutions to the $SP(M, N)$ equation. It is easy to see that solutions to this equation can become singular at a point $x = A$ and that these singular solutions have the leading asymptotic behavior

$$y(x) \sim (x - A)^{-2/(M-1)} \quad (x \rightarrow A). \quad (3.3)$$

For simplicity, we study solutions that remain real on both sides of this singularity, so hereafter we will assume that M is an *even* integer or $(M - 1)/2$ is an odd integer. We seek an asymptotic expansion of $y(x)$ about the point $x = A$ of the form

$$y(x) = (x - A)^{-2/(M-1)} \left[1 + \sum_{n=1}^{\infty} a_n (x - A)^{1/(M-1)} \right].$$

(This expansion is actually correct for both even and odd M ; for odd M half of the terms vanish.) If we substitute this expansion into the $SP(M, N)$ equation and compare like powers of $x - A$ to determine the coefficients, we find that the a_n are uniquely determined up to $n = 2(M + 1)$ for even M and $n = M + 1$ for odd M . However, so long as N is less than $M - 1$, at this value of n the coefficient a_n is *arbitrary*. It is crucial that if $N \geq M - 1$, the a_n term contains logarithmic terms.

As an example, let us consider $SP(4, 0)$. For this case the first seven coefficients vanish $a_1 = a_2 = a_3 = a_4 = a_5 = a_6 = a_7 = 0$ and the next two coefficients are $a_8 = -9A/22$ and $a_9 = 0$. Next, we find that a_{10} is *not determined and thus is arbitrary*. The next few coefficients are $a_{11} = 9/14$, $a_{12} = a_{13} = a_{14} = a_{15} = 0$, $a_{16} = 405A^2/4598$, $a_{17} = 0$. From here on the coefficients begin to depend on the choice of a_{10} : $a_{18} = -45Aa_{10}/154$, $a_{19} = -135A/847$, $a_{20} = 6a_{10}^2/23$, $a_{21} = 45a_{10}/154$, and so on. Clearly, we have found the general solution because the series contains two arbitrary constants, namely A and a_{10} . Furthermore, while we do not present a proof here, numerical analysis shows that the coefficients in the series have only geometric growth for large n , so the radius of convergence of the series is nonzero.

Of course, the series (3.3) is not a Laurent series because it contains fractional powers of $(x - A)$. However, our analysis shows that the solutions to the class of equations $\text{SP}(M, N)$ have only algebraic singularities, and because M is chosen to be even, we may seek solutions that are entirely real. In particular, we can seek eigenfunction (separatrix) solutions that are real.

Solutions to the $\text{SP}(M, N)$ equation have one or two possible real asymptotic behaviors as $x \rightarrow -\infty$:

$$y(x) \sim \pm \left[-\frac{(M-1)^2 x}{2M+2} \right]^{1/(M-N)}.$$

(There are two possible asymptotic curves when $M - N$ is even but only one when $M - N$ is odd.) As in the P-I case, the upper curve is unstable and the lower curve is stable. Thus, the discrete eigenfunction (separatrix) solutions that we seek approach the upper curve. For brevity, we only consider here the eigenfunction solutions for which $y(0) = 0$. The eigenvalues E_n are the initial values of the slope $y'(0)$ that give rise to solutions that approach the upper curve. For example, for $M = 4$ and $N = 2$, the first eight eigenvalues are 2.4240, 4.5364, 6.2471, 7.7792, 9.1960, 10.5292, 11.7973, 13.0127. The eigenfunctions associated with the 31st, 52nd, and 77th eigenvalues are plotted in Figures 3.1, 3.2, and 3.3.

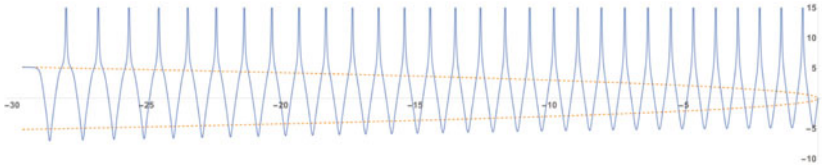


Figure 3.1. Eigenfunction $n = 31$ for the $\text{SP}(4, 2)$ equation. Note that the eigenfunction solution is not bounded; at each of the peaks it blows up like $(x - A)^{-2/3}$. The dashed lines are the asymptotic curves $\pm\sqrt{-9x/10}$. Note the strong similarity to the eigenfunctions shown in the right panels of Figures 2.3 and 2.4 and the left panel of Figure 2.5.

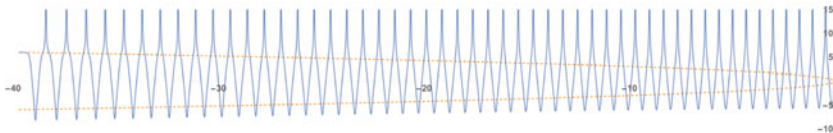


Figure 3.2. Eigenfunction $n = 52$ for the $\text{SP}(4, 2)$ equation. The dashed lines are the curves $\pm\sqrt{-9x/10}$.

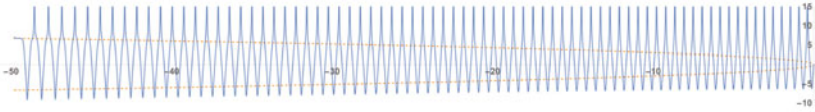


Figure 3.3. Eigenfunction $n = 77$ for the SP(4, 2) equation.

An analysis like that used to obtain (2.12) shows that if it is valid to neglect the function $I(x)$, we can replace the SP(M , N) equation by a simpler equation generated by the *linear* Hamiltonian

$$\hat{H} = \frac{1}{2}\hat{p}^2 + \frac{2}{(M-1)^2}\hat{x}^{M+1}.$$

We need only solve the linear eigenvalue problem associated with this Hamiltonian. Note that in this approximation the term containing the parameter N has completely dropped out.

From the WKB formula (1.2) we determine that for large n , the n th eigenvalue of \hat{H} grows like $n^{(2M+2)/(M+3)}$ as $n \rightarrow \infty$. Thus, the n th separatrix eigenvalue $y'(0)$ grows like

$$y'(0) \sim n^{(M+1)/(M+3)} \quad (n \rightarrow \infty). \quad (3.4)$$

From our preliminary numerical studies we find that (3.4) holds in some (but not all!) cases. For the case $M = 4$ we expect the large- n behavior $n^{5/7}$ and for $M = 6$ we expect the behavior $n^{7/9}$. For $M = 4$ and $N = 2$ and for $M = 6$ and $N = 4$ this is exactly what we find. Specifically, we find that when $M = 4$, there are no eigenfunctions for $N = 0$, a full set of eigenfunctions qualitatively identical to those shown in Figures 2.3-2.5 for $N = 1$, and a half-set of eigenfunctions qualitatively identical to those shown in the right panels of Figures 2.3 and 2.4 and the left panel of Figure 2.5 when $N = 2$. For the case $N = 2$ the eigenvalues grow like $n^{5/7}$. However, when $N = 1$, the eigenvalues grow slightly less rapidly; the n th eigenvalue grows like an^b , where $a = 2.04$ and $b = 0.56$.

When, $M = 6$, there is a half-set of eigenfunctions when $N = 0$ and no eigenfunctions when $N = 1$. However, when $N = 2$, $N = 3$, and $N = 4$, there are full sets of eigenfunctions. For the case $N = 4$ the eigenvalues grow like $n^{7/9}$, but when $N < 4$, the eigenvalues grow slightly less rapidly. Interestingly, it is the *largest* value of N that gives an eigenspectrum whose asymptotic behavior is determined by a linear approximation in which the y^N term in the nonlinear equation can be neglected! Evidently, for smaller values of N , the y^N term cannot be neglected. Specifically, when $N = 0$, the n th eigenvalue grows like $2.43n^{0.41}$; when $N = 2$, the n th eigenvalue grows like $2.55n^{0.54}$; when

$N = 3$, the n th eigenvalue grows like $1.69n^{0.65}$. However, when $N = 4$, the n th eigenvalue grows like $3.06n^{7/9}$.

We have shown in this paper that there is a huge, rich, and remarkable class of nonlinear-differential-equation eigenvalue problems for which there exists an infinite discrete set of eigenvalues. These differential equations are generalizations of the Painlevé transcendents. In full generality, the differential equations resulting from extending P-I and P-II have the form

$$y''(x) = \frac{2M + 2}{(M - 1)^2} [y(x)]^M + xP(y) + Q(y),$$

where $P(y)$ and $Q(y)$ are polynomials in $y(x)$ of degree less than $M - 1$. Clearly, there are additional general classes of nonlinear eigenvalue problems that result from generalizing the other Painlevé transcendents. These new kinds of problems deserve much intensive further analysis.

References

- [1] For a general reference on Sturm-Liouville theory see Wikipedia https://en.wikipedia.org/wiki/Sturm-Liouville_theory.
- [2] For a general reference on the Rayleigh-Ritz method see Wikipedia https://en.wikipedia.org/wiki/Rayleigh-Ritz_method.
- [3] C. M. BENDER and S. A. ORSZAG, “Advanced Mathematical Methods for Scientists and Engineers”, McGraw Hill, New York, 1978, chap. 10.
- [4] C. M. BENDER, A. FRING and J. KOMIJANI, *J. Phys. A: Math. Theor.* **47** (2014), 235204.
- [5] O. S. KERR, *J. Phys. A: Math. Theor.* **47** (2014), 368001.
- [6] C. M. BENDER and J. KOMIJANI, *J. Phys. A: Math. Theor.* **48** (2015), 475202.
- [7] C. M. BENDER and S. BOETTCHE, *Phys. Rev. Lett.* **80** 5246 (1998), 5243.
- [8] E. L. INCE, “Ordinary Differential Equations”, Dover, New York, 1956, J. W. MILES, *Proc. Royal Soc. London A* **361** (1978), 277; P. HOLMES and D. SPENCE, *Quart. J. Mech. Appl. Math.* **37** (1984), 525; S. P. HASTINGS and J. B. MCLEOD, “Classical Methods in Ordinary Differential Equations: With applications to boundary value problems”, Graduate Studies in Math., Vol. 129, American Mathematical Society, 2011.
- [9] A detailed study of the asymptotic behavior of the Painlevé transcendents may be found in M. JIMBO and T. MIWA, *Physica D* **2** (1981), 407.

- [10] Separatrix behavior of the first Painlevé transcendent is mentioned briefly in A. A. KAPAEV, *Differential Equations* **24** (1989), 1107; see also A. A. KAPAEV, *CRM Proc. Lect. Notes* **32** (2002), 157.
- [11] P. A. CLARKSON, *J. Comp. Appl. Math.* **153** (2003), 127.
- [12] D. MASEORO, “Essays on the Painlevé First Equation and the Cubic Oscillator”, PhD Thesis, SISSA (2010).
- [13] T. KAWAI and Y. TAKEI, “Algebraic Analysis of Singular Perturbation Theory”, American Mathematical Society, New York, 2005.
- [14] O. COSTIN, R. D. COSTIN and M. HUANG, *Tronquée solutions of the Painlevé equation P_1* (2013), unpublished.
- [15] A. S. FOKAS, A. R. ITS, A. A. KAPAEV and V. Y. NOVOKSHONOV, “Painlevé Transcendents: The Riemann-Hilbert Approach”, American Mathematical Society, New York, 2006.
- [16] The spin-spin correlation function for the two-dimensional Ising model for temperatures near T_c is described by P-III. See T. T. WU, B. M. MCCOY, C. A. TRACY and E. BAROUCH, *Phys. Rev. B* **13** (1976), 316.
- [17] For all temperatures the diagonal correlation function for the Ising model in two dimensions $\langle \sigma_{0,0} \sigma_{N,N} \rangle$ is given in terms of P-VI. See M. JIMBO and T. MIWA, *Proc. Jap. Acad.* **56A** (1980), 405 and **57A** (1981), 347.
- [18] E. BRÉZIN and V. A. KAZAKOV, *Phys. Lett. B* **236** (1990), 144.
- [19] M. DOUGLAS and S. SHENKER, *Nucl. Phys. B* **335** (1990), 635.
- [20] D. GROSS and A. MIGDAL, *Nucl. Phys. B* **340** (1990), 333.
- [21] G. MOORE, *Comm. Math. Phys.* **133** (1990), 261.
- [22] G. MOORE, *Prog. Theor. Phys. Suppl.* **102** (1990), 255.
- [23] A. S. FOKAS, A. R. ITS and A. V. KITAEV, *Comm. Math. Phys.* **147** (1992), 395.
- [24] See Reference [3], Chap. 4.
- [25] See W. P. REINHARDT, *Ann. Rev. Phys. Chem.* **33** (1982), 223 for a review of complex rotation of coordinates.

Feynman diagrams and their algebraic lattices

Michael Borinsky and Dirk Kreimer

Abstract. We present the lattice structure of Feynman diagram renormalization in physical QFTs from the viewpoint of Dyson–Schwinger–Equations and the core Hopf algebra of Feynman diagrams. The lattice structure encapsulates the nestedness of diagrams. This structure can be used to give explicit expressions for the counterterms in zero-dimensional QFTs using the lattice-Moebius function. Different applications for the tadpole-free quotient, in which all appearing elements correspond to semimodular lattices, are discussed.

1 The Hopf algebra of Feynman diagrams

Following [11] the BPHZ renormalization algorithm to obtain finite amplitudes in quantum field theory (QFT) shows that Feynman diagrams act as generators of a Hopf algebra $\mathcal{H}_D^{\text{fg}}$. Elaborate expositions of this Hopf algebra exist [19].

The coproduct of the Hopf algebra of Feynman diagrams on a renormalizable QFT takes the form

$$\begin{aligned} \mathcal{H}_D^{\text{fg}} &\rightarrow \mathcal{H}_D^{\text{fg}} \otimes \mathcal{H}_D^{\text{fg}} \\ \Delta : \Gamma &\mapsto \sum_{\gamma \in \mathcal{P}_D^{\text{s.d.}}(\Gamma)} \gamma \otimes \Gamma/\gamma \end{aligned} \tag{1.1}$$

($\gamma = \emptyset, \gamma = \Gamma$ allowed) where Γ/γ is the contracted diagram which is obtained by shrinking all edges of γ in Γ to a point and

$$\mathcal{P}_D^{\text{s.d.}}(\Gamma) := \left\{ \gamma \subset \Gamma \text{ such that } \gamma = \prod_i \gamma_i, \gamma_i \in \mathcal{P}_{\text{PI}}(\Gamma) \text{ and } \omega_D(\gamma_i) \leq 0 \right\}, \tag{1.2}$$

is the set of *superficially divergent subdiagrams* or s.d. subdiagrams. $\omega_D(\Gamma)$ denotes the power counting superficial degree of divergence of

the diagram Γ in D dimensional spacetime in the sense of Weinberg's Theorem [24]. These are subdiagrams of Γ whose connected components are superficially divergent 1PI diagrams. Applying an evaluation of graphs by renormalized Feynman rules $\Phi_R : \mathcal{H}_D^{\text{fg}} \rightarrow \mathbb{C}$, a specific Feynman diagram will always map to a unique power in \hbar , $\hbar^{h_1(\Gamma)}$.

For renormalized Feynman rules the task is to produce for each graph providing an unrenormalized integrand (a form on the de Rham side) and a domain of integration (the Betti side) a well-defined period by pairing those two sides. There are two avenues to proceed to obtain renormalized Feynman rules: one can either introduce a regulator ϵ say (dimensional regularization being a prominent choice with spacetime dimension $D = 4 - \epsilon$) and work with unrenormalized Feynman rules $\Phi(\epsilon)$ depending on the regulator ϵ , or one renormalizes the integrand first avoiding a regulator altogether. In the former case, the pairing gives a Laurent series with poles of finite order in ϵ . The degree of the pole is bounded by the coradical degree of the Feynman graph under consideration. Adding correction terms as dictated by the Hopf algebra provides an expression for which the regulator can be removed, $\epsilon \rightarrow 0$. In the latter case, the integrand is relegated to correction terms -again dictated by the Hopf algebra- which amount to sequences of blow-ups with the length of the sequence bounded by the coradical degree [9, 10, 16]. The nature of the coradical degree and its systematic study using the lattice structure of Feynman diagrams will be described in what follows.

Using the reduced coproduct, $\tilde{\Delta} = \Delta - \mathbb{I} \otimes \text{id} - \text{id} \otimes \mathbb{I}$, the coradical degree of an element $h \in \mathcal{H}_D^{\text{fg}}$ is the minimal number $d =: \text{cor}(h)$ such that

$$\underbrace{(\text{id}^{\otimes(d-1)} \otimes \tilde{\Delta}) \circ \dots \circ (\text{id} \otimes \tilde{\Delta}) \circ \tilde{\Delta}}_{d\text{-times}} h = 0. \quad (1.3)$$

The coradical degree of a Feynman diagram is a measure for the 'nestedness' of Feynman diagrams. For instance, a Feynman diagram of coradical degree 1 has no subdivergences. Such a diagram is a primitive element of the Hopf algebra $\mathcal{H}_D^{\text{fg}}$. A diagram with a single subdivergence has coradical degree 2 and a diagram with a subdivergence, which has itself a subdivergence, coradical degree 3 and so on.

But what is the coradical degree if we have to deal with overlapping divergences? Of course, every diagram will have a well defined ϵ expansion even if it is not accessible by explicit calculation, but is there a combinatorial description that enables us to analyze the coradical degree directly? The answer can be found in the lattice structure of Feynman diagrams.


ACKNOWLEDGEMENTS. DK thanks the Alexander von Humboldt Foundation and the BMBF for support by an Alexander von Humboldt Professorship. It is a pleasure for both authors to thank David Broadhurst, Spencer Bloch, Dominique Manchon and Karen Yeats for helpful discussions. We also thank Frédéric Fauvet for organizing the workshop *Resurgence, Physics and Numbers*, Centro de Giorgi, Pisa, May 2015, and hospitality there.

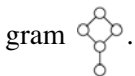
2 The lattice of subdiagrams

It is obvious that $\mathcal{P}_D^{\text{s.d.}}(\Gamma)$ is a poset ordered by inclusion. The statement that a subdiagram γ_1 covers γ_2 in $\mathcal{P}_D^{\text{s.d.}}(\Gamma)$ is equivalent to the statement that γ_1/γ_2 is primitive.

The Hasse diagram of a s.d. diagram Γ can be constructed by the following procedure:

- (i) Draw the diagram and find all the maximal forests $\gamma_i \in \mathcal{P}_D^{\text{s.d.}}(\Gamma)$ such that Γ/γ_i is primitive.
- (ii) Draw the diagrams γ_i under Γ and draw lines from Γ to the γ_i .
- (iii) Subsequently, determine all the maximal forests μ_i of the γ_i and draw them under the γ_i .
- (iv) Draw a line from γ_i to μ_i if $\mu_i \subset \gamma_i$.
- (v) Repeat this until only primitive diagrams are left.
- (vi) Then draw lines from the primitive subdiagrams to an additional \emptyset -diagram underneath them.
- (vii) In the end, replace diagrams by vertices.

Example 2.1. For instance, the set of superficially divergent subdiagrams for $D = 4$ of the diagram,  can be represented as the Hasse diagram



The motivation to search for more properties of these posets came from the work of Berghoff [1], who studied the posets of subdivergences in the context of Epstein-Glaser renormalization and discovered that the posets of diagrams with only logarithmic divergent subdivergences are distributive lattices. The lattice nature of the set of subdivergencies of Feynman diagrams has also been discussed in [12].

An important observation to make is that the set of superficially divergent subdiagrams $\mathcal{P}_D^{\text{s.d.}}(\Gamma)$ of a diagram Γ is a lattice for a big class of QFTs. For convenience, we repeat the definition of a lattice here:

Definition 2.2 (Lattice). A lattice is a poset L for which an unique least upper bound (*join*) and an unique greatest lower bound (*meet*) exists for any combination of two elements in L . The join of two elements $x, y \in L$

is denoted as $x \vee y$ and the meet as $x \wedge y$. Every lattice has a unique greatest element denoted as $\hat{1}$ and a unique smallest element $\hat{0}$. Every interval of a lattice is also a lattice.

In many QFTs, $\mathcal{P}^{\text{s.d.}}(\Gamma)$ is a lattice for every s.d. diagram Γ [7]. The union of two subdiagrams will play the role of the join.

Definition 2.3 (Join-meet-renormalizable quantum field theory).

A renormalizable QFT is called join-meet-renormalizable if $\mathcal{P}_D^{\text{s.d.}}(\Gamma)$, ordered by inclusion, is a lattice for every s.d. Feynman diagram Γ .

It turns out to be a sufficient requirement on the set $\mathcal{P}_D^{\text{s.d.}}(\Gamma)$ to be a lattice that it is closed under taking unions of subdiagrams.

Theorem 2.4. *A renormalizable QFT is join-meet-renormalizable if $\mathcal{P}_D^{\text{s.d.}}(\Gamma)$ is closed under taking unions for all s.d. diagrams $\Gamma: \gamma_1, \gamma_2 \in \mathcal{P}_D^{\text{s.d.}}(\Gamma) \Rightarrow \gamma_1 \cup \gamma_2 \in \mathcal{P}_D^{\text{s.d.}}(\Gamma)$ for all s.d. diagrams Γ .*

Proof. $\mathcal{P}_D^{\text{s.d.}}(\Gamma)$ is ordered by inclusion $\gamma_1 \leq \gamma_2 \Leftrightarrow \gamma_1 \subset \gamma_2$. The join is given by taking the union of diagrams: $\gamma_1 \vee \gamma_2 := \gamma_1 \cup \gamma_2$. $\mathcal{P}_D^{\text{s.d.}}(\Gamma)$ has a unique greatest element $\hat{1} := \Gamma$ and a unique smallest element $\hat{0} := \emptyset$. Therefore $\mathcal{P}_D^{\text{s.d.}}(\Gamma)$ is a lattice [21, Prop. 3.3.1]. The unique meet is given by the formula, $\gamma_1 \wedge \gamma_2 := \bigcup_{\mu \leq \gamma_1 \text{ and } \mu \leq \gamma_2} \mu$. □

Not every Feynman diagram fulfills this requirement. A counterexample of a Feynman diagram of ϕ^6 -theory in 3 dimensions where $\mathcal{P}_D^{\text{s.d.}}(\Gamma)$ is not a lattice is given in figure 2.1b.



Figure 2.1. Counter-example for a renormalizable but not join-meet-renormalizable QFT: ϕ^6 -theory in 3 dimensions. (a) Example of a diagram where $\mathcal{P}_3^{\text{s.d.}}(\Gamma)$ is not a lattice. (b) The corresponding non-lattice poset. Trivial vertex multiplicities were omitted.

On the other hand, there is a large class of join-meet-renormalizable quantum field theories which includes the standard model as established by the following theorem:

Theorem 2.5 ([7, Corr. 2]). *All renormalizable QFTs with only four-or-less-valent vertices are join-meet-renormalizable.*

The proof follows from combinatorial properties of the underlying graphs. This is a surprising result. Lattices are very well studied objects in combinatorics. It is worthwhile to search for more properties which the lattices in physical QFTs carry. But first, we will explore how the Hopf algebra and the lattice structure fit together.

3 The Hopf algebra of decorated lattices

It is well known that lattices and posets can be equipped with Hopf algebra structures [20]. The Hopf algebra structure applicable in the present case is the following decorated version of an incidence Hopf algebra:

Definition 3.1 (Hopf algebra of decorated posets). Let \mathcal{D} be the set of tuples (P, ν) , where P is a finite poset with a unique lower bound $\hat{0}$ and a unique upper bound $\hat{1}$ and a strictly order preserving map $\nu : P \rightarrow \mathbb{N}_0$ with $\nu(\hat{0}) = 0$. One can think of \mathcal{D} as the set of bounded posets augmented by a strictly order preserving decoration. An equivalence relation is set up on \mathcal{D} by relating $(P_1, \nu_1) \sim (P_2, \nu_2)$ if there is an isomorphism $j : P_1 \rightarrow P_2$, which respects the decoration ν : $\nu_1 = \nu_2 \circ j$.

Let \mathcal{H}^P be the \mathbb{Q} -algebra generated by all the elements in the quotient \mathcal{P} / \sim with the commutative multiplication:

$$m_{\mathcal{H}^P} : \begin{array}{ccc} \mathcal{H}^P \otimes \mathcal{H}^P & \rightarrow & \mathcal{H}^P, \\ (P_1, \nu_1) \otimes (P_2, \nu_2) & \mapsto & (P_1 \times P_2, \nu_1 + \nu_2), \end{array} \quad (3.1)$$

which takes the Cartesian product of the two posets and adds the decorations ν . The sum of the two functions ν_1 and ν_2 is to be interpreted in the sense: $(\nu_1 + \nu_2)(x, y) = \nu_1(x) + \nu_2(y)$. The singleton poset $P = \{\hat{0}\}$ with $\hat{0} = \hat{1}$ and the trivial decoration $\nu(\hat{0}) = 0$ serves as a multiplicative unit: $u(1) = \mathbb{1}_{\mathcal{H}^P} := (\{\hat{0}\}, \hat{0} \mapsto 0)$.

Equipped with the coproduct,

$$\Delta_{\mathcal{H}^P} : \begin{array}{ccc} \mathcal{H}^P & \rightarrow & \mathcal{H}^P \otimes \mathcal{H}^P, \\ (P, \nu) & \mapsto & \sum_{x \in P} ([\hat{0}, x], \nu) \otimes ([x, \hat{1}], \nu - \nu(x)), \end{array} \quad (3.2)$$

where $(\nu - \nu(x))(y) = \nu(y) - \nu(x)$ and the counit ϵ which vanishes on every generator except $\mathbb{1}_{\mathcal{H}^P}$, the algebra \mathcal{H}^P becomes a counital coalgebra.

This algebra and coalgebra is in fact a Hopf algebra [7] which augments the corresponding incidence Hopf algebra by a decoration. The decoration is needed to capture at least the simplest invariant of a diagram: The loop number.

Having defined the Hopf algebra, we can set up a Hopf algebra morphism from $\mathcal{H}_D^{\text{fg}}$ to \mathcal{H}^P :

Theorem 3.2 ([7, Thm. 3]). *Let $v(\gamma) = h_1(\gamma)$. The map,*

$$\begin{aligned} \chi_D : \quad \mathcal{H}_D^{\text{fg}} &\quad \rightarrow \quad \mathcal{H}^P, \\ \Gamma &\quad \mapsto \quad (\mathcal{P}_D^{\text{s.d.}}(\Gamma), \nu), \end{aligned} \tag{3.3}$$

which assigns to every diagram, its poset of s.d. subdiagrams decorated by the loop number of the subdiagram, is a Hopf algebra morphism.

Because of the special structure of $\mathcal{P}_D^{\text{s.d.}}(\Gamma)$ in join-meet-renormalizable theories, it is reasonable to define,

$$\mathcal{H}_D^{\text{fg,L}} := \text{im } \chi_D \tag{3.4}$$

and it follows immediately that:

Corollary 3.3. *In a join-meet-renormalizable QFT, $\mathcal{H}_D^{\text{fg,L}} \subset \mathcal{H}^L \subset \mathcal{H}^P$, where \mathcal{H}^L is the subspace of \mathcal{H}^P which is generated by all elements (L, ν) , where L is a lattice. In other words: In a join-meet-renormalizable QFT, χ_D maps s.d. diagrams and products of them to decorated lattices.*

Example 3.4. For any primitive 1PI diagram, i.e. $\Gamma \in \ker \tilde{\Delta}$,

$$\chi_D(\Gamma) = (\mathcal{P}_D^{\text{s.d.}}(\Gamma), \nu) = \begin{array}{c} \textcircled{L} \\ | \\ \textcircled{0} \end{array}, \tag{3.5}$$

where the vertices in the Hasse diagram are decorated by the value of ν and $L = h_1(\Gamma)$ is the loop number of the primitive diagram.

The coproduct of $\chi_D(\Gamma)$ in \mathcal{H}^P can be calculated using equation (3.2):

$$\Delta_{\mathcal{H}^P} \begin{array}{c} \textcircled{L} \\ | \\ \textcircled{0} \end{array} = \begin{array}{c} \textcircled{L} \\ | \\ \textcircled{0} \end{array} \otimes \mathbb{I} + \mathbb{I} \otimes \begin{array}{c} \textcircled{L} \\ | \\ \textcircled{0} \end{array}. \tag{3.6}$$

As expected, these decorated posets are also primitive in \mathcal{H}^P .

Example 3.5. For the diagram $\times \textcircled{\text{fish}} \times \in \mathcal{H}_4^{\text{fg}}$, χ_D gives the decorated poset,

$$\chi_D \left(\times \textcircled{\text{fish}} \times \right) = \begin{array}{c} \textcircled{3} \\ / \quad \backslash \\ \textcircled{2} \quad \textcircled{2} \\ | \\ \textcircled{1} \\ | \\ \textcircled{0} \end{array} \tag{3.7}$$

of which the reduced coproduct in \mathcal{H}^P can be calculated,

$$\tilde{\Delta}_{\mathcal{H}^P} \begin{array}{c} \textcircled{3} \\ \textcircled{2} \quad \textcircled{2} \\ \textcircled{1} \\ \textcircled{0} \end{array} = 2 \begin{array}{c} \textcircled{2} \\ \textcircled{1} \\ \textcircled{0} \end{array} \otimes \begin{array}{c} \textcircled{1} \\ \textcircled{0} \end{array} + \begin{array}{c} \textcircled{1} \\ \textcircled{0} \end{array} \otimes \begin{array}{c} \textcircled{2} \\ \textcircled{1} \\ \textcircled{0} \end{array}. \quad (3.8)$$

This can be compared to the coproduct calculation,

$$\tilde{\Delta}_4 \begin{array}{c} \diagup \quad \diagdown \\ \diagdown \quad \diagup \end{array} = 2 \begin{array}{c} \diagup \\ \diagdown \end{array} \otimes \begin{array}{c} \diagdown \\ \diagup \end{array} + \begin{array}{c} \diagdown \\ \diagup \end{array} \otimes \begin{array}{c} \diagup \\ \diagdown \end{array} \quad (3.9)$$

and the fact that χ_D is a Hopf algebra morphism is verified after computing the decorated poset of each subdiagram of $\begin{array}{c} \diagup \quad \diagdown \\ \diagdown \quad \diagup \end{array}$ and comparing the previous two equations:

$$\tilde{\Delta}_4 \begin{array}{c} \diagup \quad \diagdown \\ \diagdown \quad \diagup \end{array} = 2 \begin{array}{c} \diagup \\ \diagdown \end{array} \otimes \begin{array}{c} \diagdown \\ \diagup \end{array} + \begin{array}{c} \diagdown \\ \diagup \end{array} \otimes \begin{array}{c} \diagup \\ \diagdown \end{array} \quad (3.10)$$

4 An application of the Hopf algebra of decorated lattices

Some calculations are easily performed in the Hopf algebra of decorated lattices, but hard do on the Feynman diagram counterpart. One example is the evaluation of the counterterm in zero-dimensional QFTs, where the Feynman rules map every diagram to a constant. The counterterm map in a zero-dimensional field theory takes the form

$$S_D^R := \phi \circ S_D, \quad (4.1)$$

where ϕ are the Feynman rules, which map Γ to $\hbar^{h_1(\Gamma)}$ and S_D is the antipode on $\mathcal{H}_D^{\text{fg}}$.

Using the fact that χ_D is a Hopf algebra morphism it can be shown that

Proposition 4.1 ([7, Corr. 5]).

$$S_D^R(\Gamma) = \hbar^{h_1(\Gamma)} \mu_{\mathcal{P}_D^{\text{s.d.}}(\Gamma)}(\hat{0}, \hat{1}) \quad (4.2)$$

on the Hopf algebra of Feynman diagrams with $\hat{0} = \emptyset$ and $\hat{1} = \Gamma$, the lower and upper bound of $\mathcal{P}_D^{\text{s.d.}}(\Gamma)$, where S_D^R is the counterterm map in zero-dimensional field theory and μ_L the Moebius function of the lattice L . The Moebius function is defined as,

$$\mu_P(x, y) = \begin{cases} 1, & \text{if } x = y \\ - \sum_{x \leq z < y} \mu_P(x, z) & \text{if } x < y. \end{cases} \quad (4.3)$$

for a poset P and $x, y \in P$.

The calculation of the Moebius function is in general much easier than the calculation of the antipode in formula (4.1). This statement can also be used to deduce generating functions for the weighted number of primitive diagrams in QFTs as was done for ϕ^4 and Yang-Mills in terms of the counter terms in [7]. In a future publication, these ideas will be used to enumerate the weighted number of primitive diagrams for these theories explicitly [8].

5 Properties of the lattices

Having established a connection between the Hopf algebra of Feynman diagrams and the lattices, we can ask what the lattices tell us about the coradical degree of the diagrams. It is easily seen from the definition of the coproducts in \mathcal{H}^L and \mathcal{H}^{fg} that the length of the longest ‘chain’, a path from top of the Hasse diagram to the bottom, is the coradical degree of the Feynman diagram. If all complete chains have the same length, this number is called the rank of the poset or lattice and the poset or lattice is called ranked or graded.

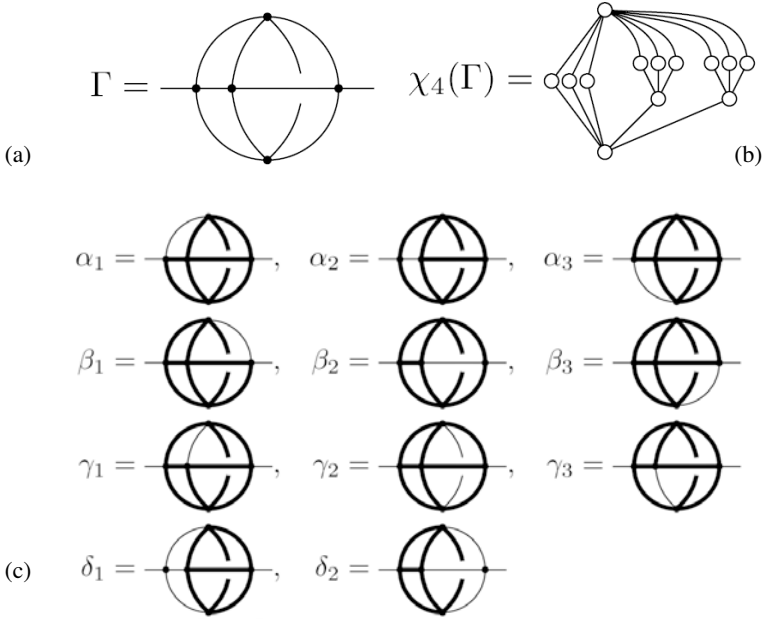
A chain of the poset $\mathcal{P}_D^{\text{s.d.}}(\Gamma)$ corresponds to a *forest* of the diagram in the scope of the BPHZ algorithm. The statement that the poset $\mathcal{P}_D^{\text{s.d.}}(\Gamma)$ is graded implies that all complete forests of the diagram have the same cardinality. Furthermore, it means that the coradical filtration is in fact a graduation of the Hopf algebra of Feynman diagrams [7].

Not all join-meet-renormalizable theories have this property for every Feynman diagram. For instance, in ϕ^4 -theory in 4-dimensional space-time, the diagram depicted in figure 5.1 with its subdiagrams in figure 5.1 appears. The corresponding lattice, shown in figure 5.1, is not graded. Therefore, the corresponding Hopf algebra $\mathcal{H}_D^{\text{fg,L}}$ is also not graded by the length of the maximal chains of the lattices.

The appearance of these diagrams with non-graded lattices is characteristic for theories with four-valent vertices. In theories with only three-or-less-valent vertices all lattices are graded:

Theorem 5.1 ([7, Thm. 4]). *In a renormalizable QFT with only three-or-less-valent vertices:*

- $\mathcal{P}_D^{\text{s.d.}}(\Gamma)$ is a graded lattice for every propagator, vertex-type diagram or disjoint unions of both;
- $\mathcal{H}_D^{\text{fg,L}}$ is bigraded by $v(\hat{1})$ and the length of the maximal chains of the lattices, which coincides with the coradical degree in $\mathcal{H}_D^{\text{fg,L}}$;
- $\mathcal{H}_D^{\text{fg}}$ is bigraded by $h_1(\Gamma)$ and the coradical degree of Γ ;
- Every complete forest of Γ has the same length.



with the complete forests $\emptyset \subset \delta_1 \subset \alpha_i \subset \Gamma, \emptyset \subset \delta_2 \subset \beta_i \subset \Gamma$ and $\emptyset \subset \gamma_i \subset \Gamma$.

Figure 5.1. Counter example of a lattice, which appears in join-meet-renormalizable QFTs with four-valent vertices and is not graded. (a) Example of a diagram where $\mathcal{P}_4^{\text{s.d.}}(\Gamma)$ forms a non-graded lattice. (b) The Hasse diagram of the corresponding non-graded lattice, where the decoration was omitted. (c) The non-trivial superficially divergent subdiagrams and the complete forests which can be formed out of them..

In theories with four-valent vertices, we can also enforce the disappearance of all non-graded lattices by working in a renormalization scheme where *tadpole*-diagrams vanish. Tadpoles are diagrams which can be separated in two connected components by the removal of a single vertex such that one connected component does not contain any external legs of the initial diagram. Tadpole diagrams are also called snail or seagull diagrams.

If we use such a renormalization scheme, we can define a Hopf ideal I generated by all tadpole diagrams of the initial Hopf algebra $\mathcal{H}_D^{\text{fg}}$ and form the quotient $\tilde{\mathcal{H}}_D^{\text{fg}} := \mathcal{H}_D^{\text{fg}}/I$. Instead of working with $\mathcal{H}_D^{\text{fg}}$ the quotient $\tilde{\mathcal{H}}_D^{\text{fg}}$ can be used without changing any results, because the Feynman rules vanish on the ideal I by requirement. In this quotient, the lattices corresponding to the Feynman diagrams behave in a similar way as for theories with only three valent vertices!

Theorem 5.2 ([7, Thm. 5]). *In a renormalizable QFT with only four-or-less-valent vertices:*

- $\widetilde{\mathcal{P}}_D^{\text{s.d.}}(\Gamma)$ is a graded lattice for every propagator, vertex-type diagram or disjoint unions of both;
- $\mathcal{H}_D^{\text{fg,L}}/\chi_D(I)$ is bigraded by $v(\hat{1})$ and the length of the maximal chains of the lattices, which coincides with the coradical degree in $\mathcal{H}_D^{\text{fg,L}}$;
- $\widetilde{\mathcal{H}}_D^{\text{fg}} := \mathcal{H}_D^{\text{fg}}/I$ is bigraded by $h_1(\Gamma)$ and the coradical degree of Γ ;
- Every complete forest of Γ , which does not result in a tadpole upon contraction, has the same length.

Where $\widetilde{\mathcal{P}}_D^{\text{s.d.}}(\Gamma)$ is the set of s.d. subdiagrams γ of Γ which do not yield tadpole diagrams upon contraction Γ/γ .

6 The quotient $\widetilde{\mathcal{H}}_D^{\text{fg}}$: applications

Kinematic renormalization schemes $\Phi_R : \widetilde{\mathcal{H}}_D^{\text{fg}} \rightarrow \mathbb{C}$ cover renormalization schemes which allow for well-defined asymptotic states and hence are natural from a physicists viewpoint. Such schemes evaluate tadpole graphs to zero and hence are naturally defined for the above quotient $\widetilde{\mathcal{H}}_D^{\text{fg}}$ as $\Phi_R(I) = 0$.

Evaluating graphs by renormalized Feynman rules in such schemes leads to periods which have a motivic interpretation [2, 3, 9]. We discuss some of such schemes most crucial aspects. We closely follow [10] in this section. As usual we concentrate on scalar field theory which is generic for the whole situation.

As we saw already amplitudes in quantum field theory can be written as a function of a chosen scale variable $L = \ln(S/\mu^2)$ chosen such that it only vanishes when all external momenta vanish. We take S to be a suitable linear combination of scalar products $q_i \cdot q_j$ of external momenta and squared masses m_e^2 . Dimensionless scattering angles Θ are defined accordingly as ratios $q_i \cdot q_j/S$ and m_e^2/S .

In these variables, amplitudes can be calculated as a perturbation expansion in terms of Feynman graphs Γ as $\sum_{\Gamma} \Phi_R(\Gamma)$. Here, the renormalized Feynman rules Φ_R are expressed in terms of such angle and scale variables, and the graphs Γ are chosen in our quotient Hopf algebra $\widetilde{\mathcal{H}}_D^{\text{fg}}$.

For any choice of angle and scale variables, Φ_R is in the group $\text{Spec}_{\mathbb{C}}(\widetilde{\mathcal{H}}_D^{\text{fg}})$, and the restriction of this group to maps which originate from evaluation of graphs by Feynman rules defines a sub-group $G_{\text{Feyn}} := \text{Spec}_{\text{Feyn}}(\widetilde{\mathcal{H}}_D^{\text{fg}}) \subset \text{Spec}_{\mathbb{C}}(\widetilde{\mathcal{H}}_D^{\text{fg}})$.

Such a chosen decomposition of the variables reflects itself then in a chosen decomposition of the group G_{Feyn} into two subgroups $G_{\text{o.s.}}$, maps

dependent on only one scale (o.s.) and G_{fin} , maps dependent only on the angles. Elements $\Phi \in G_{\text{o.s.}}$ are of the form

$$\Phi(\Gamma) = \sum_{j=1}^{\text{cor}(\Gamma)} p_j L^j, \quad (6.1)$$

where the coefficients p_j are periods in the sense of algebraic geometry and are independent of the angles $\{\Theta\}$, with the coradical degree $\text{cor}(\Gamma)$ giving the bound.

Still following [10], we allow for renormalization conditions which are defined by kinematic constraints on Green-functions: we demand that such Green functions, regarded as functions of S and $\{\Theta\}$, vanish (up to a specified order) at a reference point (in $S, \{\Theta\}$ -space) given by $S_0, \{\Theta_0\}$. We implement these constraints graph by graph. Hence renormalized Green functions as well as renormalized Feynman rules become functions of S, S_0, Θ, Θ_0 . Here, Θ, Θ_0 stand for the whole set of angles in the Feynman rules, with Θ_0 specifying the renormalization point. Note that minimal subtraction is not included in our set-up, renormalized Feynman rules in that scheme do not vanish on the ideal I defined by tadpole graphs.

Elements $\Phi_{\text{fin}} \in G_{\text{fin}}$ are of the form

$$\Phi_{\text{fin}}(\Gamma) = c_0^\Gamma(\Theta), \quad (6.2)$$

with $c_0^\Gamma(\Theta)$ an L -independent function of the angles.

We hence obtain the decomposition of G_{Feyn} as a map $\Phi^R \mapsto (\Phi_{\text{fin}}, \Phi_{\text{o.s.}})$, which proceeds then by a twisted conjugation:

$$G_{\text{Feyn}} \ni \Phi_R(S, S_0, \Theta, \Theta_0) = \Phi_{\text{fin}}^{-1}(\Theta_0) \star \Phi_{\text{o.s.}}(S, S_0) \star \Phi_{\text{fin}}(\Theta), \quad (6.3)$$

with $\Phi_{\text{fin}}(\Theta_0), \Phi_{\text{fin}}(\Theta) \in G_{\text{fin}}$ and $\Phi_{\text{o.s.}}(S, S_0) \in G_{\text{o.s.}}$. The group law \star and inversion $^{-1}$ are defined through the Hopf algebra underlying G_{Feyn} .

6.1 The additive group and renormalization schemes

The most striking aspect of kinematic renormalization schemes is that they allow for an intimate connection between the additive group \mathbb{G}_a and $\text{Spec}(\tilde{\mathcal{H}}_D^{\text{fg}})$. We have $\forall h \in \tilde{\mathcal{H}}_D^{\text{fg}}$ [4, 10]

$$\Phi_R^L(h) = \Phi_R^{L_1+L_2} = m \circ (\Phi_R^{L_1} \otimes \Phi_R^{L_2}) \circ \Delta(h) = \Phi_R^{L_1} \star \Phi_R^{L_2}, \quad L = L_1 + L_2. \quad (6.4)$$

Here, $L = \ln S/\mu^2$ defines the scale relative to a renormalization scale μ . $\Phi_R^L : \tilde{\mathcal{H}}_D^{\text{fg}} \rightarrow \mathbb{C}$ are renormalized Feynman rules, and $\Phi_R^L(\Gamma) \equiv$

$\Phi_R^L(\Gamma)(\{\Theta, \Theta_0\})$ is a function also of angles $\{\Theta\}$ and $\{\Theta_0\}$ (the latter for the renormalization point).

Note that to derive Equation (6.4) and therefore the renormalization group in the context of the quotient Hopf algebra $\tilde{\mathcal{H}}_D^{\text{fg}}$ only combinatorial properties of graphs and graph polynomials are needed [4, 10]. There is an intimate connection to the representation theory of the additive group \mathbb{G}_a and Tannaka categories of Feynman graphs hiding between this set-up which is studied elsewhere [6].

6.2 A tower of Hopf algebras

The quotient Hopf algebra $\tilde{\mathcal{H}}_D^{\text{fg}}$ is actually part of a tower of Hopf algebras which was defined in [17], which we follow closely here. We start with the quotient $\tilde{\mathcal{H}}_\infty^{\text{fg}}$ of the core Hopf algebra $\mathcal{H}_\infty^{\text{fg}}$ [15] of Feynman graphs, in which every union of 1PI subdiagrams is superficially divergent, by I , $\tilde{\mathcal{H}}_\infty^{\text{fg}} = \mathcal{H}_\infty^{\text{fg}}/I$.

$\mathcal{H}_\infty^{\text{fg}}$ contains the renormalization Hopf algebra $\tilde{\mathcal{H}}_D^{\text{fg}}$ itself as a quotient Hopf algebra [15, 17] and similarly $\tilde{\mathcal{H}}_\infty^{\text{fg}}$ contains $\tilde{\mathcal{H}}_D^{\text{fg}}$.

For the structure of Green functions with respect to the Hopf algebra $\tilde{\mathcal{H}}_D^{\text{fg}}$ we write $G^r(\{Q\}, \{M\}, \{g\}; R)$ for a generic Green function, where

- r indicates the residue under consideration and we write $|r|$ for its number of external legs. Amongst all possible residues, there is a set of residues provided by the free propagators and vertices of the theory. We write \mathcal{R} for this set. It is in one-to-one correspondence with field monomials in a Lagrangian approach to field theory. The set of all residues is denoted by $\mathcal{A} = \mathcal{F} \cup \mathcal{R}$, which defines \mathcal{F} as those residues only present through quantum corrections.
- $\{Q\}$ is the set of external momenta q_e subject to the condition $\sum_{e \in r} q_e = 0$, where the sum is over the external half edges of r .
- $\{M\}$ is the set of masses in the theory.
- $\{g\}$ is the set of coupling constants specifying the theory. Below, we proceed for the case of a single coupling constant g , the general case posing no principal new problems.
- R indicates a chosen kinematic renormalization scheme.

We also note that a generic Green function $G^r(\{Q\}, \{M\}, \{g\}; R)$ has an expansion into scalar functions

$$G^r(\{Q\}, \{M\}, \{g\}; R) = \sum_{t(r) \in S(r)} t(r) G_{t(r)}^r(\{Q\}, \{M\}, \{g\}; R). \quad (6.5)$$

In terms of mass dimensions ($[m^2] = 2$) we have $\mathbb{N}_0 \ni [t(r)] \geq 0$ and $[G_{t(r)}^r(\{Q\}, \{M\}, \{g\}; R)] = 0$.

Here, $S(r)$ is a basis set of Lorentz covariants $t(r)$ in accordance with the quantum numbers specifying the residue r . For each $t(r) \in S(r)$, there is a projector $P^{t(r)}$ onto this form factor.

For $r \in \mathcal{R}$, we can write

$$G^r(\{Q\}, \{M\}, \{g\}; R) = \Phi(r)G_{\Phi(r)}^r(\{Q\}, \{M\}, \{g\}; R) + R^r(\{Q\}, \{M\}, \{g\}; R), \quad (6.6)$$

where $R^r(\{Q\}, \{M\}, \{g\}; R)$ sums up all form factors $t(r)$ but it only contributes through quantum corrections. Φ are the unrenormalized Feynman rules. Applied on the residue r , they evaluate to the tree-level amplitude $\Phi(r)$ for the vertex or edge associated to the residue r .

Each $G^r(\{Q\}, \{M\}, \{g\}; R)$ can be obtained by the evaluation of a series of 1PI graphs

$$X^r(g) = \mathbb{I} - \sum_{\text{res}(\Gamma)=r} g^{|\Gamma|} \frac{\Gamma}{\text{Sym}(\Gamma)}, \quad \forall r \in \mathcal{R}, \quad |r| = 2, \quad (6.7)$$

$$X^r(g) = \mathbb{I} + \sum_{\text{res}(\Gamma)=r} g^{|\Gamma|} \frac{\Gamma}{\text{Sym}(\Gamma)}, \quad \forall r \in \mathcal{R}, \quad |r| > 2, \quad (6.8)$$

$$X^r(g) = \sum_{\text{res}(\Gamma)=r} g^{|\Gamma|} \frac{\Gamma}{\text{Sym}(\Gamma)}, \quad \forall r \notin \mathcal{R}, \quad (6.9)$$

where we take the minus sign for $|r| = 2$ and the plus sign for $|r| > 2$. Furthermore, the notation $\text{res}(\Gamma) = r$ indicates a sum over graphs with external leg structure in accordance with r .

We write Φ, Φ_R for the unrenormalized and renormalized Feynman rules regarded as a map: $\tilde{\mathcal{H}}_D^{\text{fg}} \rightarrow \mathbb{C}$ from the Hopf algebra to \mathbb{C} .

We have

$$G_{t(r)}^r(\{Q\}, \{M\}, \{g\}; R) = \Phi_R^{t(r)}(X^r(g))(\{Q\}, \{M\}, \{g\}; R), \quad (6.10)$$

where each non-empty graph is evaluated by the renormalized Feynman rules

$$\Phi_R^{t(r)}(\Gamma) := (\text{id} - R) \circ m \circ (S_R^\Phi \otimes P^{t(r)} \Phi P) \circ \Delta(\Gamma) \quad (6.11)$$

$$S_R^\Phi(\Gamma) := -R \circ m \circ (S_R^\Phi \otimes \Phi P) \circ \Delta(\Gamma) \quad (6.12)$$

and $\Phi_R^{t(r)}(\mathbb{I}) = 1$, and P the projection into the augmentation ideal of $\tilde{\mathcal{H}}_D^{\text{fg}}$, $P^{t(r)}$ the projector on the form factor $t(r)$ and R the renormalization map.

It is in the evaluation Equation (6.11) that the coproduct of the renormalization Hopf algebra appears. Combining the combinatorial Dyson–Schwinger equations (see [14] for a recent overview of such equations) Equations (6.7, 6.8, 6.9) with Feynman rules and with the renormalization group Equation (6.4) turns them into ordinary non-linear differential equations studied in [22,23] which determine the physics behind quantum field theory.

The above sum over all graphs simplifies when one takes the Hochschild cohomology of the (renormalization) Hopf algebra into account:

$$X^r(g) = \delta_{r,\mathcal{R}} \mathbb{I} \pm \sum_{\substack{\Gamma \text{ 1PI} \\ \text{res}(\Gamma)=r \\ \tilde{\Delta}(\Gamma)=0}} \frac{1}{\text{Sym}(\Gamma)} g^{|\Gamma|} B_+^\Gamma(X^r(g) Q(g)), \quad (6.13)$$

(− sign for $|r| = 2$, + sign for $|r| > 2$, $\delta_{r,\mathcal{R}} = 1$ for $r \in \mathcal{R}$, 0 else) with $Q(g)$ being the formal series of graphs assigned to an invariant charge of the coupling g :

$$Q^r(g) := \left[\frac{X^r}{\prod_{e \in r} \sqrt{X^e}} \right]^{\frac{1}{|r|-2}}. \quad (6.14)$$

The existence of a unique invariant charge depends on the existence of suitable coideals. Although we can define an invariant charge for every residue $r \in \mathcal{R}$ with $|r| > 2$, the Slavnov-Taylor-Identities guaranty that upon evaluation with a counter-term map, they will all give the same renormalized charge. We can therefore drop the index r and write $Q = Q^r$. B_+^γ are *grafting operators* which are Hochschild cocycles, and the above combinatorial Dyson–Schwinger equations can be formulated in any quotient Hopf algebra. More on such equations can be found in [13, 14,17, 18,25].

The existence of the equation above indicates immediately that there is a natural Hopf algebra homomorphism η from the Hopf algebra of rooted trees \mathcal{H}^{rt} by the universal property. Together with the Hopf algebra morphism χ_D to the Hopf algebra of decorated lattices, we have the following relationships:

$$\mathcal{H}^{\text{rt}} \xrightarrow{\eta} \mathcal{H}_D^{\text{fg}} \xrightarrow{\chi_D} \mathcal{H}_D^{\text{fg,L}} \quad (6.15)$$

The relationships of these different Hopf algebras especially the morphism given by $\eta \circ \chi_D : \mathcal{H}^{\text{rt}} \rightarrow \mathcal{H}_D^{\text{fg,L}}$, will be subject of a future work.

Summarizing, there is a projective system of quotient Hopf algebras (all of them can be obtained by taking the quotient with respect to I)

$$\tilde{\mathcal{H}}_4^{\text{fg}} \leftarrow \tilde{\mathcal{H}}_6^{\text{fg}} \dots \leftarrow \tilde{\mathcal{H}}_{2n}^{\text{fg}} \leftarrow \dots \leftarrow \tilde{\mathcal{H}}_{\text{core}}^{\text{fg}} = \tilde{\mathcal{H}}_\infty^{\text{fg}}, \quad (6.16)$$

obtained by restricting the coproduct to sums over graphs which are superficially divergent in

$$D = 4, 6, \dots, 2n, \dots, \infty$$

dimensions.

We can make this explicit by including the spacetime into the notation for the coproduct:

$$\begin{aligned} \mathcal{H}_D^{\text{fg}} &\rightarrow \mathcal{H}_D^{\text{fg}} \otimes \mathcal{H}_D^{\text{fg}} \\ \Delta_D : \Gamma &\mapsto \sum_{\gamma \in \mathcal{P}_D^{\text{s.d.}}(\Gamma)} \gamma \otimes \Gamma/\gamma. \end{aligned} \quad (6.17)$$

Most striking is the connection to the additive group \mathbb{G}_a which establishes itself here as announced previously. We have

$$X^r = \mathbb{I} \pm \sum_{j \geq 1} h_j^r. \quad (6.18)$$

It follows from the above that the representation of \mathbb{G}_a on the subvector-space ${}^*\tilde{\mathcal{H}}_D^{\text{fg}}$ spanned by such generators h_i^r of the sub-Hopf algebras (Foissy [13] discusses the appearance of such sub-Hopf algebras in great detail) defined by a combinatorial DSE has the form $L \rightarrow \exp LN^r$ where N^r is a lower triangular matrix for each residue r . More on this and the resulting Tannakian structure of Feynman graphs will be given in [6].

Let us conclude with two remarks which follow from this set-up.

Remark 6.1. Investigating the Cutkosky rules [5] we can write fix-point equations for cut graphs and therefore fix-point equations for imaginary part of Green functions. Indeed, following [5], all algebraic structures needed to study the analytic properties of amplitudes can be formulated in $\tilde{\mathcal{H}}_D^{\text{fg}}$, as tadpole graphs do not allow for non-trivial variations in external momenta as there is no momentum flow through them.

The 1-cocycles B_+^γ which run a Green function can then be decomposed according to the complete k -particle cuts of γ to obtain recursive equations for Green functions and their imaginary parts. Details will be given in future work (see also [5], in particular lemma (3) in that reference).

Remark 6.2. In the quotient $\tilde{\mathcal{H}}_D^{\text{fg}}$ together with its accompanying combinatorial Dyson–Schwinger equations all renormalization group effects come from a soft logarithmic breaking of conformal invariance as there are no quadratic divergences left for kinematic renormalization schemes.

Accordingly, Dyson–Schwinger equations are determined by kinematical boundary conditions, and the equations themselves describe the dimensionless quantum corrections to dimensionful tree-level amplitudes.

Fine-tuning or hierarchy problems are hence spurious. They are a typical consequence of using either a dimensionful regulator and/or renormalization schemes not in accordance with the equations of motion.

References

- [1] M. BERGHOFF, *Wonderful compactifications in quantum field theory*, Commun. Num. Theor. Phys. **09** (2015), 477–547.
- [2] S. BLOCH, “Motives Associated to Graphs”, Takagi Lectures, Kyoto, November, 2006.
- [3] S. BLOCH, H. ESNAULT and D. KREIMER, *On Motives associated to graph polynomials*, Commun. Math. Phys. **267** (2006), 181–225.
- [4] S. BLOCH and D. KREIMER, *Feynman amplitudes and Landau singularities for 1-loop graphs*, Commun. Num. Theor. Phys. **4** (2010), 709–753.
- [5] S. BLOCH and D. KREIMER, “Cutkosky Rules and Outer Space”, 2015.
- [6] S. BLOCH, D. KREIMER and K. YEATS, *On Feynman graphs and Tannakian Categories*, in preparation.
- [7] M. BORINSKY, *Algebraic lattices in qft renormalization*, Letters in Mathematical Physics **106** (2016), 879–911.
- [8] M. BORINSKY, *Renormalized asymptotic enumeration of Feynman diagrams*, <https://arxiv.org/abs/1703.00840>
- [9] F. BROWN, “Lectures on Renormalization”, Bingen Spring School, 2013.
- [10] F. BROWN and D. KREIMER, *Angles, scales and parametric renormalization*, Lett. Math. Phys. **103** (2013), 933–1007.
- [11] A. CONNES and D. KREIMER, *Renormalization in quantum field theory and the Riemann–Hilbert problem i: The Hopf algebra structure of graphs and the main theorem*, Communications in Mathematical Physics **210**(2000), 249–273.
- [12] H. FIGUEROA and JOSÉ M GRACIA-BONDIA, *Combinatorial Hopf algebras in quantum field theory i*, *Reviews in Mathematical Physics*, 17(08):881–976, 2005.
- [13] L. FOISSY, *Multigraded Dyson-Schwinger systems*, 2015.
- [14] J. KOCK, *Polynomial functors and combinatorial Dyson-Schwinger equations*, 2015.
- [15] D. KREIMER, *The core Hopf algebra*, Clay Math. Proc. **11** (2010), 313–322.

- [16] D. KREIMER, *Quantum fields, periods and algebraic geometry*, Contemporary Mathematics (2015), 648.
- [17] D. KREIMER and W. D. VAN SUIJLEKOM, *Recursive relations in the core Hopf algebra*, Nucl. Phys. B **820** (2009), 682–693.
- [18] O. KRUEGER and D. KREIMER, *Filtrations in Dyson-Schwinger equations: Next-to^j-leading log expansions systematically*, Annals Phys. **360** (2015), 293–340.
- [19] D. MANCHON, *Hopf algebras, from basics to applications to renormalization*, arXiv preprint math/0408405, 2004.
- [20] W. R. SCHMITT, *Incidence hopf algebras* Journal of Pure and Applied Algebra **96** (3) (1994), 299 – 330.
- [21] R. P. STANLEY, “Enumerative Combinatorics”, Vol. 1, volume 49 of 1997.
- [22] G. VAN BAALEN, D. KREIMER, D. UMINSKY and K. YEATS, *The QED beta-function from global solutions to Dyson-Schwinger equations*, Annals Phys. **324** (2009), 205–219.
- [23] G. VAN BAALEN, D. KREIMER, D. UMINSKY and K. YEATS, *The QCD beta-function from global solutions to Dyson-Schwinger equations*, Annals Phys. **325** (2010), 300–324.
- [24] S. WEINBERG, *High-energy behavior in quantum field theory*, Phys. Rev. **118** (1960), 838–849.
- [25] K. A. YEATS, “Growth Estimates for Dyson-Schwinger Equations”, PhD thesis, 2008.

Invariants of identity-tangent diffeomorphisms expanded as series of multitangents and multizetas

Olivier Bouillot and Jean Ecalle

Abstract. We return to the subject of local, identity-tangent diffeomorphisms f of \mathbb{C} and their analytic invariants $A_\omega(f)$, under the complementary viewpoints of effective computation and explicit expansions. The latter rely on two basic ingredients: the so-called multizetas (transcendental numbers) and multitangents (transcendental functions), with resurgence monomials and their monics providing the link between the two. We also stress the difference between the collectors (pre-invariant but of one piece) and the connectors (invariant but mutually unrelated).

Much attention has been paid to streamlining the nomenclature and notations. On the analysis side, resurgence theory rules the show. On the algebraic or combinatorial side, mould theory brings order and structure into the profusion of objects. Along the way, the paper introduces quite a few novel notions: new alien operators, new forms of resurgence, new symmetry types for moulds. It also broaches the subject of ‘phantom dynamics’ (dealing with formal diffeos that nonetheless possess invariants $A_\omega(f)$) and culminates in the comparison of arithmetical and dynamical monics, a distinction that reflects the dual nature of the $A_\omega(f)$ as Stokes constants and holomorphic invariants.

Contents	109
1 Setting and notations	111
1.1 Introduction	111
1.2 Classical results	112
1.3 Affiliates. Generators and mediators	115
1.4 Brief reminder about resurgent functions	118
1.5 Alien derivations as a tool for uniformisation	121
1.6 Medial operators	125
1.7 Resurgence of the iterators and generators	127
1.8 Resurgence of the mediators	129
1.9 Invariants, connectors, collectors	131
1.10 The reverse problem: canonical synthesis	132
2 Multitangents and multizetas.	132
2.1 Mould operations and mould symmetries	133
2.2 Multizetas	135
2.3 Multitangents	138
2.4 Resurgence monomials	143

2.5	The non-standard case ($\rho \neq 0$). Normalisation . . .	148
2.6	The ramified case ($p > 1$) and the localisation constraints	150
2.7	Meromorphic s -continuation of Seh^s and Teh^s etc.	153
3	Collectors and connectors in terms of f	156
3.1	Operator relations	156
3.2	The direct scheme: from g to \mathfrak{p}	158
3.3	The affiliate-based scheme: from g_\diamond to \mathfrak{p}_\diamond	159
3.4	Parity separation and affiliate selection	161
3.5	The generator-based scheme: from g_* to \mathfrak{p}_*	161
3.6	The mediator-based scheme: from $g_{\#}$, $g_{\#\#}$ to $\mathfrak{p}_{\#}$, $\mathfrak{p}_{\#\#}$	162
3.7	From collectors to connectors	164
3.8	The ramified case ($p > 1$)	166
3.9	Reflexive and unitary diffeomorphisms	167
4	Scalar invariants in terms of f	169
4.1	The invariants A_ω as entire functions of f	169
4.2	The case $\rho(f) \neq 0$. Normalisation	170
4.3	The case $p \neq 1$. Ramification	171
4.4	Growth properties of the invariants	171
4.5	Alternative computational strategies	173
4.6	Concluding remarks	175
5	Complement: twisted symmetries and multitangents.	176
5.1	Twisted alien operators	176
5.2	Twisted mould symmetries	177
5.3	Twisted co-products	179
5.4	Twisted multitangents	179
5.5	Affiliates : from function to operator	183
5.6	Main and secondary symmetry types	185
6	Complement: arithmetical vs dynamical monics	188
6.1	Distinguishing Stokes constants from holomorphic invariants	188
6.2	Arithmetical multizetas	189
6.3	Dynamical multizetas	193
6.4	The ramified case (tangency order $p > 1$)	196
7	Complement: convergence issues and phantom dynamics	196
7.1	The scalar invariants	196
7.2	The connectors	202
7.3	The collectors	202
7.4	Groups of invariant-carrying formal diffeos	205
7.5	A glimpse of phantom holomorphic dynamics	208
8	Conclusion	209
8.1	Some historical background	209

8.2	Multitangents and multizetas	210
8.3	Remark about the general composition equation .	210
9	Tables	212
9.1	Multitangents: symmetrel, alternel, olternol . . .	212
9.2	Parity properties of alternel and olternol multitangents	213
9.3	The invariants as entire functions of f : the general case	222
9.4	The invariants as entire functions of f : the reflexive case	226
9.5	The invariants as entire functions of f : one-parameter cases	227
10	Synopsis	228
10.1	Diffeos, collectors, connectors, invariants	228
10.2	Affiliates, generators, mediators	229
10.3	Main alien operators	229
10.4	Main moulds	230
10.5	Main results	230
	References	231

1 Setting and notations

1.1 Introduction

The holomorphic invariants of identity-tangent diffeomorphisms are a long-established subject. Awareness of their existence is as old as the hills. It goes back at least 120 years, to Fatou's geometric treatment [11]. The sharper-edged resurgent treatment, which yields a wealth of information denied to the geometric approach, is not exactly new either: it was laid out in full in [4] and [5], in the late seventies.

What is sorely lacking, however, is a realisation that these invariants can be accurately described and explicitly calculated. Indeed, the prevailing (if seldom clearly stated) opinion in the holomorphic dynamics community appears to be that *they cannot*. With a view to correcting this misapprehension, we posted in 2012 a short paper¹ that showed otherwise. Though it contained little that was strictly new (in the main, it restated results already extant in decades-old papers like [3] or [5], and referred for the computational programs to a recent PhD thesis [1]),

¹ *Invariants of identity-tangent diffeomorphisms: explicit formulae and effective computation*. The paper with the appended tables can be accessed online on
< http://www.math.u-psud.fr/~ecalle/fichiersweb/WEB_iden_tang_0.pdf >.

such feedback as we received convinced us that these questions were still dimly understood, and in need of a more thorough exposition.

So, with something of a sinking heart, we set about re-revisiting the whole subject. Since we were at it, however, and given that *ter repetita non placent*, we felt that we might just as well insert some new material. These extras include:

- (1) a procedure for the ‘uniformisation’ of convolution products and powers in the Borel plane, leading to optimal bounds;
- (2) a new class of alien operators, the *medial operators* Δ_ω^\sharp and $\Delta_\omega^{\sharp\sharp}$, which do not obey the Leibniz rule but make up for it by having a simpler definition and being easier to evaluate;
- (3) the notion of *affiliates* of a diffeomorphism f , defined via the corresponding substitution operators F and their images $\gamma(F-1)$ under an analytic γ ;
- (4) a new class of mouldian *symmetry types*, of proven usefulness, and the rather intriguing combinatorics that goes with them;
- (5) special classes of *multizetas* and *multitangents* well-suited for expressing the invariants $A_\omega(f)$ and bringing out their parity properties;
- (6) the distinction between the semi-invariant *collectors*, which carry the multitangents, and the exactly invariant *connectors*, which carry the multizetas;
- (7) the distinction between the full *arithmetical constraints* on the multizetas and the weaker *dynamical constraints*, which are responsible for *making the invariants invariant*;
- (8) the complications specific to the *ramified case* (for diffeos f of tangency order $p \geq 2$), which call for new monics related to, yet distinct from, the rational-indexed multizetas;
- (9) the subject of *phantom dynamics* which deals with groups of formal diffeos that nonetheless possess holomorphic invariants and for which many of the key notions familiar from holomorphic dynamics (sectorial models, connectors, Fourier analysis, etc) still make sense, albeit in a new setting, with *acceleration operators* replacing Laplace integration.

1.2 Classical results

We shall be concerned here with *local² identity-tangent diffeomorphisms* of \mathbb{C} , or *diffeos* for short, with the fixed-point located at ∞ for technical

² *I.e. analytic germs of–*

convenience:

$$f : z \mapsto z + \sum_{1 \leq s} f_s z^{1-s} \quad f_s \in \mathbb{C}. \quad (1.1)$$

Unless f be the identity map, we can always subject it to an analytic (respectively formal) conjugation $f \mapsto f_1 = h \circ f \circ h^{-1}$, followed if necessary by an elementary ramification $(f_1(z^{1/p}))^p$, so as to give f the following *prepared* (respectively *normal*) form:

$$f_{\text{prep}} : z \mapsto z + 1 - \rho z^{-1} + \sum_{2 < s_0 \leq s} f_{[s]} z^{1-s} \quad \left(s \in \frac{1}{p} \mathbb{N}^* \right) \quad (1.2)$$

$$f_{\text{norm}} : z \mapsto z + 1 - \rho z^{-1} \quad (1.3)$$

where s_0 may be chosen as large as one wishes.³

The *tangency order* p and *iteration residue* ρ are the only *formal invariants* of identity-tangent diffeos. But our diffeos also possess countably many (independent) scalar *analytic invariants*, also known as *holomorphic invariants*,⁴ which are best defined as the Fourier coefficients of the so-called *connectors*.⁵ The connectors are pairs of germs of 1-periodic analytic mappings $\pi = (\pi_{\text{no}}, \pi_{\text{so}})$ defined on the upper/lower half-planes $\pm \Im(z) \gg 1$. There are p such pairs, corresponding to the p -fold ramification of z in (1.2). Here, *no* and *so* stand for *north* and *south*, i.e. the upper and lower half-planes.

We shall throughout prioritise the *standard case* $p = 1$, $\rho = 0$, i.e. focus on diffeos of the form:

$$f := l \circ g \text{ with } l := z \mapsto z + 1 \text{ and } g : z \mapsto z + \sum_{3 \leq s} g_s z^{1-s} \quad (1.4)$$

and merely sketch the changes required to cover the general case.

Any standard f possesses two well-defined, mutually inverse so-called *iterators*, to wit f_{\pm}^* (direct iterator) and ${}^*f_{\pm}$ (reciprocal iterator), defined

³ After ‘preparation’, the diffeo acquires new coefficients denoted $f_{[s]}$ for distinctiveness.

⁴ *Analytic invariants* means invariant relative to analytic changes of z -coordinate, whereas *holomorphic invariant* points to the holomorphic dependence of $A_{\omega}(f)$ in f – in contradistinction to cases like that of diffeos with Liouvillian multipliers λ . Such diffeos do possess non-trivial *analytic invariants*, but none with holomorphic dependence on f .

⁵ In the context of identity-tangent diffeos, the connectors are sometimes referred to as *horn maps*, but the former notion is more general: in resurgent analysis (see Section 1.2 *infra*) the connectors are the operators that take us from one sectorial model to the next.

on U-shaped domains⁶ by the limits:

$$f_{\pm}^*(z) = \lim_{k \rightarrow \pm\infty} l^{-k} \circ f^k \quad ; \quad {}^*f_{\pm}(z) = \lim_{k \rightarrow \pm\infty} f^{-k} \circ l^k. \quad (1.5)$$

The connectors $\pi^{\pm 1}$, with their northern and southern components, are then defined on $\pm\mathfrak{S}(z) \gg 1$ by:

$$\pi := f_+^* \circ {}^*f_- \quad ; \quad \pi^{-1} := f_-^* \circ {}^*f_+. \quad (1.6)$$

For reasons that will soon become apparent, we must also consider the infinitesimal generators f_* and π_* of f and π . These are formal, generically divergent power respectively Fourier series. Of course, π_* is not constructed directly from π , but via its northern and southern components. We thus have the three pairs:

$$\pi := (\pi_{\text{no}}, \pi_{\text{so}}) \quad ; \quad \pi^{-1} := (\pi_{\text{no}}^{-1}, \pi_{\text{so}}^{-1}) \quad ; \quad \pi_* := (\pi_{*\text{no}}, \pi_{*\text{so}}) \quad (1.7)$$

along with the relations

$$f(z) = \exp(f_*(z) \partial_z) \cdot z \quad \left(f_* \partial_z f^* \equiv 1 \right) \quad (1.8)$$

$$\pi_{\text{no}}^{\pm 1}(z) = \exp(\pm \pi_{*\text{no}}(z) \partial_z) \cdot z \quad (1.9)$$

$$\pi_{\text{so}}^{\pm 1}(z) = \exp(\pm \pi_{*\text{so}}(z) \partial_z) \cdot z. \quad (1.10)$$

In (1.8) f^* and *f denote of course the *formal iterators*, i.e. the power series solutions of the equations

$$f^* \circ f = l \circ f^* \quad \text{with} \quad f^*(z) = z + o(1) \quad (1.11)$$

$$f \circ {}^*f = {}^*f \circ l \quad \text{with} \quad {}^*f(z) = z + o(1) \quad (1.12)$$

normalised by the condition of carrying no constant term. Anticipating on the sequel, here is how the scalar invariants can be read off the Fourier expansions of the connectors:

$$\pi_{\text{no}}(z) = z + \sum_{\omega \in \Omega^-} A_{\omega}^+ e^{-\omega z} \quad ; \quad \pi_{\text{so}}(z) = z + \sum_{\omega \in \Omega^+} A_{\omega}^- e^{-\omega z} \quad (1.13)$$

$$\pi_{\text{no}}^{-1}(z) = z + \sum_{\omega \in \Omega^-} A_{\omega}^- e^{-\omega z} \quad ; \quad \pi_{\text{so}}^{-1}(z) = z + \sum_{\omega \in \Omega^+} A_{\omega}^+ e^{-\omega z} \quad (1.14)$$

$$\pi_{*\text{no}}(z) = +2\pi i \sum_{\omega \in \Omega^-} A_{\omega} e^{-\omega z} \quad ; \quad \pi_{*\text{so}}(z) = -2\pi i \sum_{\omega \in \Omega^+} A_{\omega} e^{-\omega z}. \quad (1.15)$$

⁶ f_+^* and ${}^*f_+$ are defined on a west-north-south domain, while f_-^* and ${}^*f_-$ are defined on an east-north-south domain.

Pay attention to the altered position of \pm in 1.13 and 1.14; the reasons for this apparent incoherence shall become clear in due course. The indices ω run through $\Omega := 2\pi i\mathbb{Z}^*$ or $\Omega^\pm := \pm 2\pi i\mathbb{N}^*$, and each of the three systems

$$\{A_\omega^+, \omega \in \Omega\} \quad , \quad \{A_\omega^-, \omega \in \Omega\} \quad , \quad \{A_\omega, \omega \in \Omega\} \quad (1.16)$$

constitutes a *free* and *complete* system of analytic invariants.⁷

1.3 Affiliates. Generators and mediators

General affiliates. To each identity-tangent germ f and each power series $\gamma(t) = t + \sum \gamma_r t^{r+1}$ we associate the so-called γ -affiliate f_\diamond along with an infinite-order differential operator F_\diamond . The correspondence $(f, F) \mapsto (f_\diamond, F_\diamond)$ goes like this:

$$f \mapsto f_\diamond := F_\diamond \cdot z \quad ; \quad F \mapsto F_\diamond := \gamma(F - 1). \quad (1.17)$$

For a general γ , the operator F_\diamond has a non-elementary coproduct:

$$\text{cop}(F_\diamond) := F_\diamond \oplus 1 + 1 \oplus F_\diamond + \sum_{1 \leq p, q} \gamma^{[p, q]} (F_\diamond)^p \oplus (F_\diamond)^q. \quad (1.18)$$

As a consequence, the straightforward germ-to-operator correspondence:

$$f \mapsto F = 1 + \sum_{1 \leq n} \underline{(f)}^n \frac{\partial^n}{n!} \quad (\underline{(f)}(z) := f(z) - z) \quad (1.19)$$

assumes a more intricate form for the affiliates:

$$f_\diamond \mapsto F_\diamond = f_\diamond \partial + \sum_{2 \leq r} \sum_{1 \leq n_1, 2 \leq n_r} \diamond^{n_1, \dots, n_r} (f_\diamond)^{n_1} \frac{\partial^{n_1}}{n_1!} \dots (f_\diamond)^{n_r} \frac{\partial^{n_r}}{n_r!}. \quad (1.20)$$

Special affiliates: generators and mediators. The structure coefficients $\gamma^{[p, q]}$ and $\diamond^{n_1, \dots, n_r}$ shall be investigated in Section 5-1, Section 5-2 and Section 5-4, but they assume a particularly simple form for three special types of affiliates:

- (i) the infinitesimal *generator* (f_*, F_*) with $\gamma(t) = \log(1 + t)$;
- (ii) the main *mediator* (f_\sharp, F_\sharp) with $\gamma(t) = 2 \frac{(1+t)-1}{(1+t)+1} = \frac{t}{1+\frac{1}{2}t}$;
- (iii) the second *mediator* $(f_{\sharp\sharp}, F_{\sharp\sharp})$ with $\gamma(t) = \frac{(1+t)^2-1}{(1+t)^2+1} = \frac{t+\frac{1}{2}t^2}{1+t+\frac{1}{2}t^2}$.

⁷ With the minor qualifier that, under a conjugation by a shift h of the form $l^\alpha(z) := z + \alpha$, the periodic germs π^\pm also undergo conjugation by the same shift, with obvious repercussions for their Fourier coefficients.

The *generators* we have already mentioned. For them, the co-product and the germ-to-operator correspondence reduce to

$$\text{cop}(F_*) = F_* \otimes 1 + 1 \otimes F_* \quad , \quad f \mapsto F_* = f_* \partial . \quad (1.21)$$

For the *mediators*, the formulae, while still relatively simple, become more interesting

$$\begin{aligned} \text{cop}(F_{\sharp}) &= F_{\sharp} \otimes 1 + 1 \otimes F_{\sharp} \\ &\quad + \sum_{1 \leq n} \left(-\frac{1}{4}\right)^n \left(F_{\sharp}^{n+1} \otimes F_{\sharp}^n + F_{\sharp}^n \otimes F_{\sharp}^{n+1}\right) \end{aligned} \quad (1.22)$$

$$\begin{aligned} \text{cop}(F_{\#\#}) &= F_{\#\#} \otimes 1 + 1 \otimes F_{\#\#} \\ &\quad + \sum_{1 \leq n} (-1)^n \left(F_{\#\#}^{n+1} \otimes F_{\#\#}^n + F_{\#\#}^n \oplus F_{\#\#}^{n+1}\right) . \end{aligned} \quad (1.23)$$

Relating F and $F_{\sharp}, F_{\#\#}$. As operators, the mediators F_{\sharp} and $F_{\#\#}$ admit three distinct types of expansions, each with its own merits and drawbacks:

$$F_{\sharp} = 2 \frac{F - 1}{F + 1} = 2 C_{\sharp} D_{\sharp}^{-1} = 2 D_{[\sharp]}^{-1} C_{[\sharp]} \quad (1.24)$$

$$F_{\#\#} = \frac{F - F^{-1}}{F + F^{-1}} = C_{\#\#} D_{\#\#}^{-1} = D_{[\#\#]}^{-1} C_{[\#\#]} . \quad (1.25)$$

The operators $C_{\sharp}, D_{\sharp}, C_{\#\#}, D_{\#\#}$ are defined as follows:

$$\begin{aligned} C_{\sharp} &= \sum_{1 \leq n}^{n \text{ odd}} 2^{-n} f_{\sharp}^n \frac{\partial^n}{n!} \quad || \quad C_{\sharp} : \varphi(z) \mapsto \frac{1}{2}(\varphi(z + \frac{1}{2} f_{\sharp}(z)) - \varphi(z - \frac{1}{2} f_{\sharp}(z))) \\ D_{\sharp} &= 1 + \sum_{1 \leq n}^{n \text{ even}} 2^{-n} f_{\sharp}^n \frac{\partial^n}{n!} \quad || \quad C_{\sharp} : \varphi(z) \mapsto \frac{1}{2}(\varphi(z + \frac{1}{2} f_{\sharp}(z)) + \varphi(z - \frac{1}{2} f_{\sharp}(z))) \\ C_{\#\#} &= \sum_{1 \leq n}^{n \text{ odd}} f_{\#\#}^n \frac{\partial^n}{n!} \quad || \quad C_{\#\#} : \varphi(z) \mapsto \frac{1}{2}(\varphi(z + f_{\#\#}(z)) - \varphi(z - f_{\#\#}(z))) \\ D_{\#\#} &= 1 + \sum_{1 \leq n}^{n \text{ even}} f_{\#\#}^n \frac{\partial^n}{n!} \quad || \quad C_{\#\#} : \varphi(z) \mapsto \frac{1}{2}(\varphi(z + f_{\#\#}(z)) + \varphi(z - f_{\#\#}(z))) . \end{aligned}$$

The operators $C_{[\sharp]}, D_{[\sharp]}, C_{[\#\#]}, D_{[\#\#]}$ are defined in exactly the same way, but relative to inputs $f_{[\sharp]}, f_{[\#\#]}$ with $f_{\sharp}(z) \sim f_{\#\#}(z) \sim f_{[\sharp]}(z) \sim f_{[\#\#]}(z) \sim f(z) - z$. As operators acting on formal germs, D_{\sharp}^{-1} and $D_{\#\#}^{-1}$ have to be expanded in the predictable way, leading to formulae such as:

$$f_{\#} \mapsto F_{\#} = f_{\#} \partial + \sum_{\substack{1 \leq r \\ (n_1 \text{ odd} \\ n_2, \dots, n_r \text{ even})}} (-1)^{r-1} 2^{1-\sum n_i} f_{\#}^{n_1} \frac{\partial^{n_1}}{n_1!} f_{\#}^{n_2} \frac{\partial^{n_2}}{n_2!} \dots f_{\#}^{n_r} \frac{\partial^{n_r}}{n_r!} \quad (1.26)$$

$$f_{\#\#} \mapsto F_{\#\#} = f_{\#\#} \partial + \sum_{\substack{1 \leq r \\ (n_1 \text{ odd} \\ n_2, \dots, n_r \text{ even})}} (-1)^{r-1} f_{\#\#}^{n_1} \frac{\partial^{n_1}}{n_1!} f_{\#\#}^{n_2} \frac{\partial^{n_2}}{n_2!} \dots f_{\#\#}^{n_r} \frac{\partial^{n_r}}{n_r!}. \quad (1.27)$$

Let us focus on the *second* mediator $F_{\#\#}$, to avoid the nuisance of the factors $(1/2)^n$. Its first expansion $F_{\#\#} = \frac{F-F^{-1}}{F+F^{-1}}$ is wholly unproblematic, with a commuting numerator and denominator, and simply reflects the definition of $F_{\#\#}$. The *existence* of parallel expansions $C_{\#\#} D_{\#\#}^{-1}$ and $D_{\#\#}^{-1} C_{\#\#}$ follows, to put it briefly, from the fact that the operators

$$C_{\#\#} \text{ and } C_{[\#\#]}, \quad D_{\#\#} \text{ and } D_{[\#\#]}, \quad D_{\#\#}^{-1} \text{ and } D_{[\#\#]}^{-1}, \quad C_{\#\#} D_{\#\#}^{-1} \text{ and } D_{\#\#}^{-1} C_{\#\#}$$

verify exactly the same types of co-product as, respectively, the operators

$$\sinh(\partial) \quad , \quad \cosh(\partial) \quad , \quad \cosh(\partial)^{-1} \quad , \quad \tanh(\partial)$$

and from the fact that $\tanh(\partial)$ has precisely a co-product of type (1.23). But since numerators and denominators no longer commute, we should expect the inputs $f_{\#\#}$ and $f_{[\#\#]}$ to differ, in a way that remains to elucidate.

For the moment, let us observe that, of the latter two expansions, $F_{\#\#} = C_{\#\#} D_{\#\#}^{-1}$ is the more useful, since it allows us to express the *operatorial* mediator $F_{\#\#}$ directly in terms of the germ $f_{\#\#} := F_{\#\#}.z$. But the other expansion, namely $F_{\#\#} = D_{\#\#}^{-1} C_{\#\#}$, has its merits too, since it relies on a germ $f_{[\#\#]}$ which, as we shall see in a moment, is ‘closer’ than $f_{\#\#}$ to the original f and, unlike $f_{\#\#}$, converges whenever f does. It is also more economical than the first expansion $F_{\#\#} = \frac{F-F^{-1}}{F+F^{-1}}$, in the sense of concentrating all the odd or even terms respectively in the numerator and denominator.

Relating $f_{\#}$, $f_{\#\#}$ to f . Equating the first two expansions of the mediators, we get

$$(F + 1) C_{\#} D_{\#}^{-1} = F - 1 \quad \text{an} \quad (F^2 + 1) C_{\#\#} D_{\#\#}^{-1} = F^2 - 1.$$

Letting these operators act on z , we find the sought-for relations

$$f_{\#}(f(z)) + f_{\#}(z) = f(z) - z \quad (1.28)$$

$$f_{\#\#}(f(z)) + f_{\#\#}(f^{-1}(z)) = f(z) - f^{-1}(z). \quad (1.29)$$

Relating $f_{[\sharp]}$, $f_{[\sharp\sharp]}$ to f . Inverting the definition-based expansion of the mediators, we get successively

$$\begin{aligned} F - 1 &= (1 - (1/2)F_{\sharp})^{-1}F_{\sharp} \text{ and } F^2 - 1 = 2(1 - F_{\sharp\sharp})^{-1}F_{\sharp\sharp} \\ (1 - (1/2)F_{\sharp})(F - 1) &= F_{\sharp} \text{ and } (1 - F_{\sharp\sharp})(F^2 - 1) = 2F_{\sharp\sharp} \\ (1 - \mathcal{D}_{[\sharp]}^{-1}\mathcal{C}_{[\sharp]})(F - 1) &= 2\mathcal{D}_{[\sharp]}^{-1}\mathcal{C}_{[\sharp]} \text{ and } (1 - \mathcal{D}_{[\sharp\sharp]}^{-1}\mathcal{C}_{[\sharp\sharp]})(F^2 - 1) = 2\mathcal{D}_{[\sharp\sharp]}^{-1}\mathcal{C}_{[\sharp\sharp]} \\ (\mathcal{D}_{[\sharp]} - \mathcal{C}_{[\sharp]})F &= (\mathcal{D}_{[\sharp]} + \mathcal{C}_{[\sharp]}) \text{ and } (\mathcal{D}_{[\sharp\sharp]} - \mathcal{C}_{[\sharp\sharp]})F^2 = (\mathcal{D}_{[\sharp\sharp]} + \mathcal{C}_{[\sharp\sharp]}). \end{aligned}$$

Finally, letting the operators act on z , we get:

$$f\left(z - \frac{1}{2}f_{[\sharp]}\right) = z + \frac{1}{2}f_{[\sharp]} \quad (1.30)$$

$$f^{\circ 2}(z - f_{[\sharp\sharp]}) = z + f_{[\sharp\sharp]}. \quad (1.31)$$

This implies, first, that the germs $z \mapsto z - \frac{1}{2}f_{[\sharp]}$ and $z \mapsto z - f_{[\sharp\sharp]}$ are respectively reciprocal to the germs $z \mapsto \frac{1}{2}(z + f(z))$ and $z \mapsto \frac{1}{2}(z + f^{\circ 2}(z))$ and, second, that $f_{[\sharp]}$ and $f_{[\sharp\sharp]}$ are convergent if and only if f is.

Relating f_{\sharp} , $f_{\sharp\sharp}$ and $f_{[\sharp]}$, $f_{[\sharp\sharp]}$. Post-composing the identities (1.28)-(1.29) by the germs $z - (1/2)f_{[\sharp]}(z)$ or $z - f_{[\sharp\sharp]}(z)$ and using (1.30)-(1.31) to eliminate f , we find:

$$2f_{[\sharp]}(z) = f_{\sharp}\left(z + \frac{1}{2}f_{[\sharp]}(z)\right) + f_{\sharp}\left(z - \frac{1}{2}f_{[\sharp]}(z)\right) \quad (1.32)$$

$$2f_{[\sharp\sharp]}(z) = f_{\sharp\sharp}(z + f_{[\sharp\sharp]}(z)) + f_{\sharp\sharp}(z - f_{[\sharp\sharp]}(z)). \quad (1.33)$$

After some non-commutative manipulations on differential operators and their generating series, this yields:

$$f_{[\sharp]} = f_{\sharp} + \sum_{1 \leq s} \sum_{1 \leq m_i} \frac{(\sum 2m_i)! 4^{-\sum m_i}}{s!(1-s+\sum 2m_i)!} f_{\sharp}^{1-s+2\sum m_i} \prod_{1 \leq i \leq s} f_{\sharp}^{(2m_i)} \quad (1.34)$$

$$f_{[\sharp\sharp]} = f_{\sharp\sharp} + \sum_{1 \leq s} \sum_{1 \leq m_i} \frac{(\sum 2m_i)!}{s!(1-s+\sum 2m_i)!} f_{\sharp\sharp}^{1-s+2\sum m_i} \prod_{1 \leq i \leq s} f_{\sharp\sharp}^{(2m_i)} \quad (1.35)$$

1.4 Brief reminder about resurgent functions

We will have to be content here with a very sketchy presentation. The algebra of *resurgent fonctions* admits three different realisations or models:

- (i) the *formal model*, consisting of formal power series $\tilde{\varphi}(z)$ in z^{-1} or of more general *transseries*;⁸
- (ii) the *convolutive model*, consisting of microfunctions⁹ at $\zeta = 0$, whose *majors* $\check{\varphi}(\zeta)$ are defined at the origin only and constraint-free but whose *minors* $\hat{\varphi}(\zeta)$ have the property of endless continuation¹⁰ and exponential growth;¹¹
- (iii) the *geometric model(s)*, consisting of analytic germs $\varphi_\theta(z)$ defined on sectorial neighbourhoods of ∞ of bisectrix $\arg(z^{-1}) = \theta$ and aperture at least π .

The natural algebra product in the z -models (i) and (iii) is of course multiplication. In the ζ -model (ii) it is convolution, defined first *locally*¹² by

$$(\hat{\varphi}_1 * \hat{\varphi}_2)(\zeta) := \int_0^\zeta \hat{\varphi}_1(\zeta_1) \hat{\varphi}_2(\zeta - \zeta_1) d\zeta_1 \quad (\zeta \sim 0) \quad (1.36)$$

and then *in the large* by analytic continuation.

In practice, one starts with elements $\tilde{\varphi}$ of model (i) obtained as formal solutions of differential or functional equations, and the aim is to resum them, *i.e.* to go to model (iii). Generally speaking, this is possible only over the detour through model (ii), with the *formal Borel transform* \mathcal{B}

$$z^{-\sigma} \mapsto \frac{\zeta^{\sigma-1}}{\Gamma(\sigma)} \quad ; \quad (\partial_\sigma)^n z^{-\sigma} \mapsto (\partial_\sigma)^n \frac{\zeta^{\sigma-1}}{\Gamma(\sigma)} \quad ; \quad \text{etc} \quad (1.37)$$

taking us from (i) to (ii), and the *polarised Laplace transform* \mathcal{L}_θ

$$\varphi_\theta(z) = \int_{\arg(\zeta)=\theta} \hat{\varphi}(\zeta) e^{-\zeta z} d\zeta \quad (1.38)$$

taking us from (ii) to (iii).

⁸ The tilda stands for ‘formal’, but will be omitted in contexts where everything is formal.

⁹ *I.e.* minor-major pairs $(\hat{\varphi}(\zeta), \check{\varphi}(\zeta))$. The *majors* are defined up to regular germs at the origin, and the *minors* are related to them under $2\pi i$ $\hat{\varphi}(\zeta) \equiv \check{\varphi}(\zeta e^{-\pi i}) - \check{\varphi}(\zeta e^{+\pi i})$ for $\zeta \sim 0$. In the present paper, we shall almost entirely dispense with majors, since we shall mostly be dealing with so-called *integrable* microfunctions, whose minors carry the complete information.

¹⁰ Laterally along any *finite and finitely punctured* broken lines.

¹¹ *I.e.* at most exponential, along *infinite but finitely punctured broken lines*, with a suitable uniformity condition.

¹² When the *minors* $\hat{\varphi}$ are not integrable at the origin, one must modify the definition and draw in the *majors* $\check{\varphi}$. Convolution is then defined on loop integrals that avoid the origin.

The most outstanding feature of the resurgence algebras is the existence on them of a rich array of so-called *alien operators* Δ_ω and Δ_ω^\pm , with indices ω running through $\mathbb{C}_\bullet := \widehat{\mathbb{C}} - \{0\}$. These operators act on all three models¹³, but are first defined in the convolutive model, where they have the effect of measuring the singularities of the (often highly ramified) minors $\widehat{\varphi}$ at or rather *over* ω . Here is how they act:

$$(\widehat{\Delta}_\omega \widehat{\varphi})(\zeta) := \sum_{\epsilon_1, \dots, \epsilon_r} \frac{\epsilon_r}{2\pi i} \lambda_{\epsilon_1, \dots, \epsilon_{r-1}} \widehat{\varphi}^{(\epsilon_1 \dots \epsilon_r)}_{(\omega_1 \dots \omega_r)}(\omega + \zeta) \quad (1.39)$$

$$(\widehat{\Delta}_\omega^\pm \widehat{\varphi})(\zeta) := \sum_{\epsilon_1, \dots, \epsilon_r} \pm \epsilon_r \lambda_{\epsilon_1, \dots, \epsilon_{r-1}}^\pm \widehat{\varphi}^{(\epsilon_1 \dots \epsilon_r)}_{(\omega_1 \dots \omega_r)}(\omega + \zeta) \quad (1.40)$$

with $\omega_r = \omega$, with signs $\epsilon_j \in \{+, -\}$, with weights $\lambda_\epsilon, \lambda_\epsilon^+, \lambda_\epsilon^-$ defined by

$$\lambda_{\epsilon_1, \dots, \epsilon_{r-1}} := \frac{p! q!}{r!} \quad \text{with} \quad p := \sum_{\epsilon_i = +} 1, \quad q := \sum_{\epsilon_i = -} 1 \quad (1.41)$$

$$\begin{aligned} \lambda_{\epsilon_1, \dots, \epsilon_{r-1}}^\epsilon &:= 1 \quad \text{if} \quad \epsilon_1 = \dots = \epsilon_{r-1} = \epsilon & (1.42) \\ &:= 0 \quad \text{otherwise} \end{aligned}$$

and with $\widehat{\varphi}^{(\epsilon_1 \dots \epsilon_r)}_{(\omega_1 \dots \omega_r)}(\omega + \zeta)$ denoting the analytic continuation of $\widehat{\varphi}$ from ζ to $\omega + \zeta$ under right (respectively left) circumvention of each intervening singularity ω_j if $\epsilon_j = +$ (respectively $\epsilon_j = -$). We start of course with a point ζ close enough to 0 on the axis $arg(\zeta) = arg(\omega)$, and extend the definition in the large by analytic continuation. The operators $\widehat{\Delta}_\omega$ and their pull-backs Δ_ω in the formal model are *derivations*. This means that in the convolutive or formal models the Leibniz identities hold:

$$\widehat{\Delta}_\omega(\widehat{\varphi}_1 * \widehat{\varphi}_2) = \widehat{\Delta}_\omega(\widehat{\varphi}_1) * \widehat{\varphi}_2 + \widehat{\varphi}_1 * \widehat{\Delta}_\omega(\widehat{\varphi}_2) \quad (1.43)$$

$$\Delta_\omega(\widetilde{\varphi}_1 \cdot \widetilde{\varphi}_2) = \Delta_\omega(\widetilde{\varphi}_1) \cdot \widetilde{\varphi}_2 + \widetilde{\varphi}_1 \cdot \Delta_\omega(\widetilde{\varphi}_2) \quad (1.44)$$

When working in any one of the multiplicative models (formal or geometric), it is often convenient to phase-shift the alien operators, and to set:

$$\mathbf{\Delta}_\omega := e^{-\omega z} \Delta_\omega \quad ([\partial_z, \mathbf{\Delta}_\omega] \equiv 0) \quad (1.45)$$

$$\mathbf{\Delta}_\omega^\pm := e^{-\omega z} \Delta_\omega^\pm \quad ([\partial_z, \mathbf{\Delta}_\omega^\pm] \equiv 0) \quad (1.46)$$

The gain here is that the new operators commute with ∂_z . These phase-shifted operators are also the natural ingredients of the *axial operators*

¹³ With the same symbols doing service in all three, since no confusion is possible.

\mathcal{D}_θ and \mathcal{D}_θ^\pm :

$$\mathcal{D}_\theta = \sum_{\arg(\omega)=\theta} \Delta_\omega \quad (1.47)$$

$$\mathcal{D}_\theta^\pm = 1 + \sum_{\arg(\omega)=\theta} \Delta_\omega^\pm = \exp(\pm 2\pi i \mathcal{D}_\theta) \quad (1.48)$$

which are the key to the *axis-crossing* identities :

$$\varphi_{\theta-\epsilon} = (\mathcal{D}_\theta^+ \varphi)_{\theta+\epsilon} \quad ; \quad (\Phi \cdot \mathcal{D}_\theta^+)_{\theta-\epsilon} = (\mathcal{D}_\theta^+ \cdot \Phi)_{\theta+\epsilon} \quad (1.49)$$

$$\varphi_{\theta+\epsilon} = (\mathcal{D}_\theta^- \varphi)_{\theta-\epsilon} \quad ; \quad (\Phi \cdot \mathcal{D}_\theta^-)_{\theta-\epsilon} = (\mathcal{D}_\theta^- \cdot \Phi)_{\theta+\epsilon} \quad (1.50)$$

that connect two sectorial germs $\varphi_{\theta-\epsilon}$ and $\varphi_{\theta+\epsilon}$ relative to Laplace integration right and left of any given singularity-carrying axis θ in the ζ -plane.¹⁴

1.5 Alien derivations as a tool for uniformisation

Convolution domains. A Riemann surface \mathcal{R} is said to be *unobstructed* if, for any point ζ on it, the set S_ζ of all singular points *seen* or *half-seen* from ζ has a discrete projection S_ζ on \mathbb{C} .

A ramified analytic germ $\widehat{\varphi}(\zeta)$ at the origin 0_\bullet of \mathbb{C}_\bullet is said to be *endlessly continuable* if under analytic continuation it extends to an *unobstructed* Riemann surface.

Endlessly continuable germs are stable under convolution.

A *convolution domain* is an unobstructed Riemann surface $\underline{\mathcal{R}}$ for which the space $Hol(\underline{\mathcal{R}})$ of all holomorphic functions on $\underline{\mathcal{R}}$ is closed under convolution.

Any unobstructed Riemann surface \mathcal{R} can, in a unique way, through the adjunction of a suitable set of singular points, be turned into a minimally ramified convolution domain $\underline{\mathcal{R}}$ – the so-called convolution completion, or stabilisation, of \mathcal{R} .

Fine convolution domains. We shall introduce a notion of *fine* Riemann surface and *fine* convolution domain which is hardly restrictive (all resurgent functions encountered in practice have Borel transforms that naturally extend to *fine* surfaces) and has the merit of greatly facilitating the proofs of all the statements to follow in this section.¹⁵

¹⁴ In (1.43), (1.44), φ denotes any *resurgent function* and Φ any *resurgent operator* (such as multiplication or postcomposition by a resurgent function etc).

¹⁵ Let us stress that *fineness* is by no means necessary for the statements in question to hold. It simply makes life easier and costs nothing.

For any $\rho > 0$ and $\theta_1 < \theta_2$ in \mathbb{R} , let $\mathcal{D}_{\rho, \theta_1, \theta_2}^\pm$ denote the sets of all alien operators Δ of the form:

$$\mathcal{D}_{\rho, \theta_1, \theta_2}^+ := \left\{ \Delta = \Delta_{\omega_r}^+ \dots \Delta_{\omega_1}^+ ; \sum |\omega_i| \leq \rho, \theta_1 \leq \arg \omega_r \leq \dots \leq \arg \omega_1 \leq \theta_2 \right\}$$

$$\mathcal{D}_{\rho, \theta_1, \theta_2}^- := \left\{ \Delta = \Delta_{\omega_r}^- \dots \Delta_{\omega_1}^- ; \sum |\omega_i| \leq \rho, \theta_1 \leq \arg \omega_1 \leq \dots \leq \arg \omega_r \leq \theta_2 \right\}.$$

Note that the number r of factors in the decomposition of Δ is not bounded.

Let us say that an (unobstructed) Riemann surface \mathcal{R} is *fine* if, for any $(\rho, \theta_1, \theta_2)$, the number of operators Δ in $\mathcal{D}_{\rho, \theta_1, \theta_2}^\pm$ such that $\Delta.Hol(\mathcal{R}) \neq \emptyset$ is finite. This amounts to an extremely weak condition on the distribution of \mathcal{R} 's ramification points.

Any fine Riemann surface \mathcal{R} can, in a unique way, through the adjunction of a suitable set of singular points, be turned into a minimally ramified fine convolution domain $\underline{\mathcal{R}}$ – the completion, or stabilisation, of \mathcal{R} .

Atomic alien operators. Any ramification point η of a fine convolution domain $\underline{\mathcal{R}}$ is connected with the origin 0_\bullet by a well-defined *taut broken line* Γ_η or TT-path, which in turn can be uniquely represented by a sequence $(\omega_1, \dots, \omega_r)$ whose elements $\omega_i \in \mathbb{C}_\bullet$ represent the successive intervals of Γ_η . Inequalities of the form

$$0 < \pi(2n - 1) < \arg \omega_{i+1} - \arg \omega_i < \pi(2n + 1)$$

respectively $-\pi(2n + 1) < \arg \omega_{i+1} - \arg \omega_i < -\pi(2n - 1) < 0$

signal that Γ_η makes n positive (respectively negative) turns round its i^{th} summit. Between any two aligned¹⁶ ω_i, ω_{i+1} we must insert a sign $\epsilon_i \in \{+, -\}$ to indicate whether Γ_η circumvents the i^{th} ‘summit’ to the right or to the left.

To each ramification point η of a fine convolution domain $\underline{\mathcal{R}}$ there also correspond two ‘ramified shifts’ S_η^+, S_η^- and an alien operator \widehat{D}_η .

Each S_η^\pm is defined locally, near 0_\bullet . In projection on \mathbb{C} , it amounts to an ordinary $\dot{\eta}$ -shift but it takes 0_\bullet to the end-point of Γ_η in such a way as to map the small intervals issuing from 0_\bullet in the direction $\arg \omega \mp \pi$ onto the small interval of same length that ends the broken line Γ_η .

The atomic alien operators \widehat{D}_η (so-called because they measure *the* singularity at the end-point of Γ_η rather than a *superposition* of singularities,

¹⁶ *I.e.* when $\arg \omega_i = \arg \omega_{i+1}$.

as the alien derivations do) are then defined by:

$$\begin{aligned} \widehat{D}_\eta &: \text{Hol}(\underline{\mathcal{R}}) \rightarrow \text{Hol}(\underline{\mathcal{R}}_\eta) \\ \widehat{D}_\eta \widehat{\varphi}(\zeta) &:= \widehat{\varphi}(S_\eta^+(\zeta)) - \widehat{\varphi}(S_\eta^-(\zeta)) \end{aligned} \quad (1.51)$$

first for ζ near 0_\bullet , and then continued in the large, on a fine convolution domain $\underline{\mathcal{R}}_\eta$ that may, and often is, *more* (never *less*) ramified than $\underline{\mathcal{R}}$.

There is a natural order \prec on the ramification set $\underline{\mathcal{R}}_{ram}$ of any fine convolution domain $\underline{\mathcal{R}}$, along with a natural co-product on its atomic operators:

$$\widehat{D}_\eta(\widehat{\varphi}_1 * \widehat{\varphi}_2) \equiv \sum_{\eta_1, \eta_2 \prec \eta} H_\eta^{\eta_1, \eta_2} (R^{P_\eta^{\eta_1, \eta_2}} \widehat{D}_{\eta_1} \widehat{\varphi}_1) * (R^{Q_\eta^{\eta_1, \eta_2}} \widehat{D}_{\eta_2} \widehat{\varphi}_2) \quad (1.52)$$

(i) with R denoting the one-turn rotation operator round 0_\bullet ,

(ii) with a sum $\sum_{\eta_1, \eta_2 \prec \eta}$ that is always finite,

(iii) with integers $H_\eta^{\eta_1, \eta_2}$, $P_\eta^{\eta_1, \eta_2}$, $Q_\eta^{\eta_1, \eta_2}$ that reflect the self-intersection pattern of the broken line Γ_η .

The structure tensor $H_\eta^{\eta_1, \eta_2}$ turns $\mathcal{C}(\underline{\mathcal{R}}_{ram})$ into a commutative algebra with its own discretised convolution

$$(h_1 * h_2)(\eta) := \sum_{\eta_1, \eta_2 \prec \eta} H_\eta^{\eta_1, \eta_2} h_1(\eta_1) h_2(\eta_2) \quad (h_1, h_2 \in \mathcal{C}(\underline{\mathcal{R}}_{ram})) \quad (1.53)$$

The convolution algebra $\mathcal{C}(\underline{\mathcal{R}}_{ram})$ may be viewed as the discrete scaffolding of the convolution algebra $\text{Hol}(\underline{\mathcal{R}})$. In fact, $\mathcal{C}(\underline{\mathcal{R}}_{ram})$ is isomorphic to the quotient¹⁷ $\text{Hol}_{polar}(\underline{\mathcal{R}})/\text{Hol}_{subpolar}(\underline{\mathcal{R}})$.

Uniformisation of convolution products or powers. Similar formulae (of which there exist several variants) hold for ordinary points ζ of $\underline{\mathcal{R}}$.

The following variant involves the standard alien derivations and has the advantage of uniqueness:

$$\widehat{\varphi}(\zeta) \equiv \sum_s K_{\zeta_s}^\zeta \widehat{\varphi}(\zeta_s) + \sum_r \sum_{\omega_i} \sum_s (2\pi i)^r K_{\zeta_s, \omega}^\zeta \widehat{\Delta}_{\omega_r} \dots \widehat{\Delta}_{\omega_1} \widehat{\varphi}(\zeta_{s, \omega}) \quad (1.54)$$

¹⁷ A function $\widehat{\varphi}$ in $\text{Hol}(\underline{\mathcal{R}})$ is said to be of *polar* respectively *subpolar* type if it behaves like $\frac{h(\eta)}{2\pi i(\zeta - \eta)} + o(\frac{1}{(\zeta - \eta)})$ respectively $o(\frac{1}{(\zeta - \eta)})$ in the ramified vicinity of any given $\eta \in \underline{\mathcal{R}}_{ram}$. The space $\text{Hol}_{polar}(\underline{\mathcal{R}})$ is clearly closed under convolution, with $\text{Hol}_{subpolar}(\underline{\mathcal{R}})$ as an ideal.

with a finite number of points ζ_s (respectively $\zeta_{s,\omega}$) located over $\dot{\zeta}$ (respectively $\dot{\zeta} - \sum \dot{\omega}_i$) but lying within the holomorphy star of $\widehat{\varphi}$ (respectively $\widehat{\Delta}_{\omega_r} \dots \widehat{\Delta}_{\omega_1} \widehat{\varphi}$), and with entire (respectively rational) structure coefficients $K_{\zeta_s}^\zeta$ (respectively $K_{\zeta_{s,\omega}}^\zeta$).

Here is a second variant that relies on the operators $\widehat{\Delta}_\omega^+$ and $\widehat{\Delta}_\omega^-$ of (1.40). It is not unique, but can always be adjusted so as to involve only entire coefficients $H_{\zeta_s}^\zeta$ and $H_{\zeta_{s,\omega,\epsilon}}^\zeta$.

$$\widehat{\varphi}(\zeta) \equiv \sum_s H_{\zeta_s}^\zeta \widehat{\varphi}(\zeta_s) + \sum_r \sum_{\omega_i, \epsilon_i} \sum_s H_{\zeta_{s,\omega,\epsilon}}^\zeta \widehat{\Delta}_{\omega_r}^{\epsilon_r} \dots \widehat{\Delta}_{\omega_1}^{\epsilon_1} \widehat{\varphi}(\zeta_{s,\omega,\epsilon}) \quad (1.55)$$

Both variants reduce the evaluation of any convolution product or power, at any given point ζ of $\underline{\mathcal{R}}$, on any Riemann sheet, however distant from 0_\bullet , to a finite number of convolution integrals to be calculated on straight intervals joining 0_\bullet to points ζ_i or $\zeta_{i,\omega}$, $\zeta_{i,\omega,\epsilon}$ that lie on the main Riemann sheet.

For instance, if we apply (1.54) to the evaluation of the convolution power $\widehat{\varphi}^{*n}(\zeta)$, for any $\zeta \in \underline{\mathcal{R}}$, any $\widehat{\varphi} \in \text{Hol}(\underline{\mathcal{R}})$, and $n \rightarrow \infty$, we find that everything reduces to finitely many terms of the form

$$\widehat{\Delta}_\omega \widehat{\varphi}^{*n}(\zeta_{s,\omega}) = \sum_{\substack{1 \leq k \leq r \\ \omega \in \text{sha}(\omega^1, \dots, \omega^k)}} \frac{n!}{k!(n-k)!} (\widehat{\varphi}^{*(n-k)} * \widehat{\Delta}_{\omega^1} \widehat{\varphi} * \dots * \widehat{\Delta}_{\omega^k} \widehat{\varphi})(\zeta_{s,\omega}) \quad (1.56)$$

with s and k bounded, so that in the end the asymptotics is dominated by trite convolution integrals $\widehat{\varphi}^{*(n-k)}(\zeta_{s,\omega})$ evaluated on simple intervals $(0_\bullet, \zeta_{s,\omega}]$ safely located within the main Riemann sheet (or its boundary).

This *uniformising virtue* of alien derivations (by which we mean their power to reduce complicated operations on ramified, multivalued functions to simple operations on their, and their alien derivatives', uniform restrictions to the holomorphy star) is one of the main justifications (though not the topmost) of alien calculus.

Remark. Alongside the *TT-paths*¹⁸ that connect any $\zeta \in \underline{\mathcal{R}}$ to the origin 0_\bullet , we must also consider two classes of more convolution-friendly, but also more complex paths: the wildly contorted *SS-paths*¹⁹ and the even more intricate *ZZ-paths*²⁰. The SS-paths are useful for establishing the

¹⁸ "Taut broken lines".

¹⁹ "Self-symmetrical and self-symmetrically shrinkable paths".

²⁰ "Self-symmetrical, self-symmetrically shrinkable, and self-replicating paths".

stability under convolution of *endless continuability*, and the ZZ-paths for illustrating the formulae (1.52)-(1.56).

Where these paths fail miserably, though, is in providing decent estimates for convolution products or powers on far-flung Riemann sheets. For the convolution powers²¹, SS-path considerations lead to asymptotically correct estimates

$$|\widehat{\varphi}^{*n}(\zeta)| \leq c_0(\zeta) \frac{c_1(\zeta)^n}{n!} \quad (c_0(\zeta), c_1(\zeta) > 0).$$

However, for points $\zeta \in \mathcal{R}$ whose TT-path has k summits, the bounds derivable in this way (especially c_0) become hopelessly suboptimal as k increases. Even for values as small as $k = 20$, c_0 can fall off the mark by something like a factor 10^{10} .

The convolution domains $\mathcal{R} := \widetilde{\mathbb{C} - \Omega}$ with Ω a lattice. For any discrete lattice $\Omega = \tau_1\mathbb{Z}$ or $\tau_1\mathbb{Z} + \tau_2\mathbb{Z}$ ($\tau_i \in \mathbb{C}^*$, $\Im(\tau_1/\tau_2) \neq 0$), the surface $\mathcal{R} := \widetilde{\mathbb{C} - \Omega}$ is an – obviously *fine* – convolution domain with a particularly simple structure: its ramified shifts S_η^\pm form a group which contains the one-turn rotation R and is generated by just two elements (whether Ω is one- or two-dimensional!). There is even an elementary algorithm for finding all the \prec -antecedents of any ramification point $\eta \in \mathcal{R}_{ram}$, as well as all the structure coefficients featuring in (1.52) and (1.54). This applies in particular for the surface $\mathcal{R} := \widetilde{\mathbb{C} - 2\pi i\mathbb{Z}}$, which is the natural surface of practically all the resurgent functions to appear in this investigation.

1.6 Medial operators

Their definition resembles that of the alien derivations

$$(\widehat{\Delta}_\omega^\# \widehat{\varphi})(\zeta) := \sum_{\epsilon_1, \dots, \epsilon_r} \frac{\epsilon_r}{2\pi i} \lambda_{\epsilon_1, \dots, \epsilon_{r-1}}^\# \widehat{\varphi}^{(\epsilon_1 \dots \epsilon_r)}(\omega + \zeta) \quad (1.57)$$

$$(\widehat{\Delta}_\omega^{\#\#} \widehat{\varphi})(\zeta) := \sum_{\epsilon_1, \dots, \epsilon_r} \frac{\epsilon_r}{2\pi i} \lambda_{\epsilon_1, \dots, \epsilon_{r-1}}^{\#\#} \widehat{\varphi}^{(\epsilon_1 \dots \epsilon_r)}(\omega + \zeta) \quad (1.58)$$

with $\omega_r = \omega$ and the usual signs $\epsilon_j \in \{+, -\}$ but with simpler weights $\lambda_\epsilon^\#, \lambda_\epsilon^{\#\#}$, still independent of the intervals ω_j :

$$\lambda_{\epsilon_1, \dots, \epsilon_{r-1}}^\# = \lambda_\#^{[p, q]} := 2^{-p-q} = 2^{1-r} \quad (1.59)$$

$$\lambda_{\epsilon_1, \dots, \epsilon_{r-1}}^{\#\#} = \lambda_{\#\#}^{[p, q]} := \varrho(p - q) 2^{-int(\frac{p+q+1}{2})} \quad (1.60)$$

²¹ Of a function $\widehat{\varphi}(\zeta)$ regular at 0_\bullet .

As usual, p and q denote the numbers of $+$ and $-$ signs in $\{\epsilon_1, \dots, \epsilon_{r-1}\}$. As for the elementary factor $\varrho(p - q) \equiv \varrho(q - p)$, it assumes only three values, $0, 1, -1$, and displays a remarkable 8-periodicity :

$$\varrho(k+8) \equiv \varrho(k) \quad , \quad \varrho : [0, 1, 2, 3, 4, 5, 6, 7] \mapsto [1, 1, 0, -1, -1, -1, 0, 1] \quad (1.61)$$

Like the earlier weights λ_ϵ in (1.41) attached to the standard alien derivations, the new weights $\lambda_\epsilon^\sharp, \lambda_\epsilon^{\sharp\sharp}$ add up to 1:

$$\sum_{\epsilon_i \in \{+, -\}} \lambda_{\epsilon_1, \dots, \epsilon_{r-1}} = \sum_{\epsilon_i \in \{+, -\}} \lambda_{\epsilon_1^\sharp, \dots, \epsilon_{r-1}^\sharp} = \sum_{\epsilon_i \in \{+, -\}} \lambda_{\epsilon_1^{\sharp\sharp}, \dots, \epsilon_{r-1}^{\sharp\sharp}} = 1 \quad (\forall r)$$

The simplest way to express the relations between the new operators and the classical ones is via the generating series:

$$\mathcal{D}^\sharp = \sum_{\arg(\omega)=0} \Delta_\omega^\sharp \quad , \quad \mathcal{D}^{\sharp\sharp} = \sum_{\arg(\omega)=0} \Delta_\omega^{\sharp\sharp} \quad (1.62)$$

The relations read:

$$\mathcal{D}^\sharp = \frac{1}{\pi} \tan(\pi \mathcal{D}) = \frac{1}{\pi i} \frac{\mathcal{D}^+ - 1}{\mathcal{D}^+ + 1} = \frac{1}{\pi i} \frac{1 - \mathcal{D}^-}{1 + \mathcal{D}^-} \quad (1.63)$$

$$\mathcal{D}^{\sharp\sharp} = \frac{1}{2\pi} \tan(2\pi \mathcal{D}) = \frac{1}{2\pi i} \frac{\mathcal{D}^+ - \mathcal{D}^-}{\mathcal{D}^+ + \mathcal{D}^-} \quad (1.64)$$

As pointed out at the outset, the new operators are neither derivations nor automorphisms. They possess co-products *sui generis* which, once again, are best expressed in terms of the generating series:

$$\begin{aligned} \mathcal{D}^\sharp &\mapsto \mathcal{D}^\sharp \otimes \mathbf{1} + \mathbf{1} \otimes \mathcal{D}^\sharp \\ &\quad + \sum_{1 \leq n} (\pi)^{2n} \left[(\mathcal{D}^\sharp)^{n+1} \otimes (\mathcal{D}^\sharp)^n + (\mathcal{D}^\sharp)^n \otimes (\mathcal{D}^\sharp)^{n+1} \right] \\ \mathcal{D}^{\sharp\sharp} &\mapsto \mathcal{D}^{\sharp\sharp} \otimes \mathbf{1} + \mathbf{1} \otimes \mathcal{D}^{\sharp\sharp} \\ &\quad + \sum_{1 \leq n} (2\pi)^{2n} \left[(\mathcal{D}^{\sharp\sharp})^{n+1} \otimes (\mathcal{D}^{\sharp\sharp})^n + (\mathcal{D}^{\sharp\sharp})^n \otimes (\mathcal{D}^{\sharp\sharp})^{n+1} \right] \end{aligned}$$

Short proofs. The quickest way to prove all the above relations at one go is to start with the axis $\arg \zeta = 0$ punctured over \mathbb{N} . Denoting σ and τ the non-commuting “shifts” that take ζ small (with $\arg \zeta = 0$) to $\zeta + 1$ after circumventing the point at 1 respectively to the right or to the left (and then extending the action of σ and τ in the large), we find that

$$\mathcal{D}^+ = (1 - \tau)(1 - \sigma)^{-1} \quad , \quad \mathcal{D}^- = (1 - \sigma)(1 - \tau)^{-1} \quad (1.65)$$

Next, proceeding backwards, we define $\Delta_\omega^\sharp, \Delta_\omega^{\sharp\sharp}$ via (1.62) in terms of $\mathcal{D}^\sharp, \mathcal{D}^{\sharp\sharp}$; then $\mathcal{D}^\sharp, \mathcal{D}^{\sharp\sharp}$ via (1.63)-(1.64) in terms of \mathcal{D}^\pm ; then \mathcal{D}^\pm via (1.65) in terms of the elementary shifts σ, τ . After some rather easy calculations in the non-commutative variables σ, τ , we find the expressions (1.59), (1.60) for the weights $\lambda_\omega^\sharp, \lambda_\omega^{\sharp\sharp}$, though at first only for the case when $\{\omega_1, \omega_2, \omega_3 \dots\} = \{1, 2, 3 \dots\}$. But we clearly have

$$\sum_{\epsilon_{i_0}=\pm} \lambda_{\epsilon_1, \dots, \epsilon_{r-1}}^\sharp = \lambda_{\epsilon_1, \dots, [\epsilon_{i_0}], \dots, \epsilon_{r-1}}^\sharp,$$

$$\sum_{\epsilon_{i_0}=\pm} \lambda_{\epsilon_1, \dots, \epsilon_{r-1}}^{\sharp\sharp} = \lambda_{\epsilon_1, \dots, [\epsilon_{i_0}], \dots, \epsilon_{r-1}}^{\sharp\sharp} \quad (\forall i_0 < r)$$

with the notation $[\epsilon_{i_0}]$ signaling the omission of ϵ_{i_0} . It follows that the weights $\lambda_\omega^\sharp, \lambda_\omega^{\sharp\sharp}$ retain their expression (1.59),(1.60) for all sequences $\{\omega_i\}$ over \mathbb{N} and, in fact, over \mathbb{R}^+ .

1.7 Resurgence of the iterators and generators

The iterator f^* and *f , characterised by the relations (1.11)-(1.12), and the (infinitesimal) generator f_* , characterised by the relation (1.8), verify the following resurgence equations

$$\Delta_\omega {}^*f(z) = +A_\omega \partial_z {}^*f(z) \quad (\forall \omega \in \Omega) \quad (1.66)$$

$$\Delta_\omega f^*(z) = -A_\omega e^{-\omega(f^*(z)-z)} \quad (\forall \omega \in \Omega) \quad (1.67)$$

$$\Delta_\omega f_*(z) = -\omega A_\omega f_*(z) e^{-\omega(f^*(z)-z)} \quad (1.68)$$

with the very same scalar coefficients A_ω as in (1.15). For all values of ω not in Ω , the alien derivatives are $\equiv 0$. If we now introduce the differential operators:

$$\mathbb{A}_\omega := A_\omega e^{-\omega z} \partial_z \quad (\forall \omega \in \Omega) \quad (1.69)$$

the resurgence equations assume the form of the Bridge equation:²²

$$\Delta_\omega {}^*f(z) = +\mathbb{A}_\omega {}^*f(z) \quad (1.70)$$

$$\Delta_\omega f^*(z) = -(\mathbb{A}_\omega \cdot z) \circ f^*(z). \quad (1.71)$$

²² So-called because it relates *ordinary* and *alien* derivatives of one and the same resurgent function. The Bridge equation has in fact much wider applications, and extends, in one form or another, to practically all *resonant* local objects, of which *identity-tangent diffeos* are but a special case. An entire book [6] has been devoted to the subject.

When expressed in terms of the substitution operators F^* and $*F$ associated with $*f$, f^* , the Bridge equation takes an even more pleasant form

$$[\Delta_\omega, F^*] = -F^* \mathbb{A}_\omega \quad (F^* \varphi := \varphi \circ f^*) \quad (1.72)$$

$$[\Delta_\omega, *F] = +\mathbb{A}_\omega *F \quad (*F \varphi := \varphi \circ *f). \quad (1.73)$$

Likewise, with the (operatorial) generator $F_* := f_* \partial = F^* \cdot \partial \cdot F^*$, we get:

$$[\Delta_\omega, F_*] = F^* [\partial, \mathbb{A}_\omega] *F. \quad (1.74)$$

But whichever variant we may care to consider, the commutation identities $[\Delta_{\omega_1}, \mathbb{A}_{\omega_2}] = 0$ make it easy to iterate the above resurgence equations. Thus from (1.70) we straightaway derive

$$\Delta_{\omega_r} \dots \Delta_{\omega_1} *f(z) = \mathbb{A}_{\omega_1} \dots \mathbb{A}_{\omega_r} *f(z) \quad (\text{order reversion!}). \quad (1.75)$$

As a consequence, the effect on $*f$ and f^* of the alien operators Δ_ω^\pm and of the axial operators \mathcal{D}_θ is easy to calculate. It is best written in terms of the substitution operators $*F$ and F^* associated with $*f$, f^* , and results in the so-called *axial* Bridge equation:

$$\mathcal{A}_\theta = \mathcal{D}_\theta - *F \mathcal{D}_\theta F^* \quad (1.76)$$

$$\mathcal{A}_\theta^+ = \mathcal{D}_\theta^+ *F \mathcal{D}_\theta^- F^* = *F \mathcal{D}_\theta^- F^* \mathcal{D}_\theta^+ \quad (1.77)$$

$$\mathcal{A}_\theta^- = \mathcal{D}_\theta^- *F \mathcal{D}_\theta^+ F^* = *F \mathcal{D}_\theta^+ F^* \mathcal{D}_\theta^-. \quad (1.78)$$

The axial Bridge equation²³ involves differential (respectively substitution) operators \mathcal{A}_θ (respectively \mathcal{A}_θ^\pm):

$$\mathcal{A}_\theta = \sum_{\arg(\omega)=\theta} \mathbb{A}_\omega \quad (1.79)$$

$$\mathcal{A}_\theta^\pm = 1 + \sum_{\arg(\omega)=\theta} \mathbb{A}_\omega^\pm = \exp(\pm 2\pi i \mathcal{A}_\theta) \quad (1.80)$$

that are simply related to the differential (respectively substitution) operators Π_* (respectively Π^\pm) associated with the connectors of Section 1.1:

$$\Pi_{no} := \mathcal{A}_{-\frac{\pi}{2}}^+ \quad ; \quad \Pi_{so} := \mathcal{A}_{+\frac{\pi}{2}}^- \quad (1.81)$$

$$\Pi_{no}^{-1} := \mathcal{A}_{-\frac{\pi}{2}}^- \quad ; \quad \Pi_{so}^{-1} := \mathcal{A}_{+\frac{\pi}{2}}^+ \quad (1.82)$$

$$\Pi_{*no} := +2\pi i \mathcal{A}_{-\frac{\pi}{2}} \quad ; \quad \Pi_{*so} := -2\pi i \mathcal{A}_{+\frac{\pi}{2}}. \quad (1.83)$$

²³ We say *Bridge equation* in the singular since (1.77) and (1.78) are merely exponential variants of (1.76). The commutation of the three automorphisms $\mathcal{A}_\theta^\pm, \mathcal{D}_\theta^\pm, *F \mathcal{D}_\theta^\mp F^*$ is itself a consequence of the commutation of the three derivations $\mathbb{A}_\theta, \mathcal{D}_\theta, *F \mathcal{D}_\theta F^*$.

The first identity (1.81) results from applying the direct axis-crossing formula (1.49) with $\theta = -\frac{\pi}{2}$ and $\varphi = {}^*f$ or $\Phi = {}^*F$, since ${}^*f_{\theta\pm\epsilon} = {}^*f_{\pm}$. The second identity (1.81) results from applying the inverse axis-crossing formula (1.50) with $\theta = +\frac{\pi}{2}$ and $\varphi = {}^*f$ or $\Phi = {}^*F$, since in that case ${}^*f_{\theta\pm\epsilon} = {}^*f_{\mp}$ (inversion!). The identities (1.82) and (1.82) immediately follow.

Direct access to the generators and mediators of π . Consider now the mediators $\pi_{\sharp}, \pi_{\sharp\sharp}$ of the connector π , with their northern/southern components and their formal Fourier expansions. They run parallel to those (see (1.68)) of the infinitesimal generator π_* :

$$\pi_{\sharp,\text{no}}(z) = +2\pi i \sum_{\omega \in \Omega^-} A_{\omega}^{\sharp} e^{-\omega z} ; \pi_{\sharp,\text{so}}(z) = -2\pi i \sum_{\omega \in \Omega^+} A_{\omega}^{\sharp} e^{-\omega z} \quad (1.84)$$

$$\pi_{\sharp\sharp,\text{no}}(z) = +2\pi i \sum_{\omega \in \Omega^-} A_{\omega}^{\sharp\sharp} e^{-\omega z} ; \pi_{\sharp\sharp,\text{so}}(z) = -2\pi i \sum_{\omega \in \Omega^+} A_{\omega}^{\sharp\sharp} e^{-\omega z} \quad (1.85)$$

Based on (1.67) and (1.57)-(1.58), we see that we can access the Fourier coefficients of $\pi_*, \pi_{\sharp}, \pi_{\sharp\sharp}$, or indeed those of the general affiliate π_{\diamond} , *directly* from one and the same resurgent function, namely f^* :

$$\begin{aligned} \Delta_{\omega} f^* &= -A_{\omega} e^{-\omega f^*}, \\ \Delta_{\omega}^{\sharp} f^* &= -A_{\omega}^{\sharp} e^{-\omega f^*}, \\ \Delta_{\omega}^{\sharp\sharp} f^* &= -A_{\omega}^{\sharp\sharp} e^{-\omega f^*} \end{aligned} \quad (1.86)$$

without bothering about the corresponding affiliates of f , *i.e.* $f_*, f_{\sharp}, f_{\sharp\sharp}, f_{\diamond}$. Though it is true, as we shall aver in the next section, that $f_{\sharp}, f_{\sharp\sharp}$ etc. verify their own interesting resurgence equations with a mixture of invariant and non-invariant resurgence constants from which, after some sifting, all the Fourier coefficients $A_{\omega}^{\sharp}, A_{\omega}^{\sharp\sharp}$ etc. can be reconstructed, the fact remains that the f -affiliates have no particular closeness to the corresponding π -affiliates.

1.8 Resurgence of the mediators

The relations (1.28)-(1.29), which may be viewed as perturbed difference equations, determine f_{\sharp} and $f_{\sharp\sharp}$ in terms of f . A standard argu-

ment shows that $f_{\sharp}(z)$ and $f_{\sharp\sharp}(z)$ are resurgent in z , with first-order alien derivatives verifying the homogeneous equation:

$$(\Delta_{\omega_0} f_{\sharp}) \circ f + \Delta_{\omega_0} f_{\sharp} = 0 \quad (\forall \omega_0 \in \pi i \mathbb{Z} - 2\pi i \mathbb{Z}) \quad (1.87)$$

$$(\Delta_{\omega_0} f_{\sharp\sharp}) \circ f^{\circ 2} + \Delta_{\omega_0} f_{\sharp\sharp} = 0 \quad (\forall \omega_0 \in \frac{1}{2} \pi i \mathbb{Z} - \pi i \mathbb{Z}) \quad (1.88)$$

whose general solution are of the form

$$\Delta_{\omega_0} f_{\sharp} = \underline{A}_{\omega_0} e^{-\omega_0 f^*} \quad (\forall \omega_0 \in \pi i \mathbb{Z} - 2\pi i \mathbb{Z}) \quad (1.89)$$

$$\Delta_{\omega_0} f_{\sharp\sharp} = \underline{\underline{A}}_{\omega_0} e^{-\omega_0 f^*} \quad \left(\forall \omega_0 \in \frac{1}{2} \pi i \mathbb{Z} - \pi i \mathbb{Z} \right) \quad (1.90)$$

with resurgent constants \underline{A}_{ω_0} and $\underline{\underline{A}}_{\omega_0}$ unrelated to the invariants $A_{\omega}(f)$. In fact, \underline{A}_{ω_0} and $\underline{\underline{A}}_{\omega_0}$ are not invariant under analytic changes of z -coordinates and, unlike the invariants $A_{\omega}(f)$, they involve *coloured multizetas* as their transcendental ingredients, as we shall see in Section 3.6. But the mediators' alien derivatives of second (and higher) order obviously depend only on the iterator f^* and involve no new resurgent constants other than the invariants A_{ω} :

$$\Delta_{\omega_1} \Delta_{\omega_0} f_{\sharp} = \omega_0 \underline{A}_{\omega_0} A_{\omega_1} e^{-(\omega_0 + \omega_1) f^*} \quad (\forall \omega_1 \in 2\pi i \mathbb{Z}) \quad (1.91)$$

$$\Delta_{\omega_1} \Delta_{\omega_0} f_{\sharp\sharp} = \omega_0 \underline{\underline{A}}_{\omega_0} A_{\omega_1} e^{-(\omega_0 + \omega_1) f^*} \quad (\forall \omega_1 \in 2\pi i \mathbb{Z}) \quad (1.92)$$

Both systems still hold if we replace $f_{\sharp}(z) := F_{\sharp}.z$ and $f_{\sharp\sharp}(z) := F_{\sharp\sharp}.z$ by $\Phi_{\sharp}(z) := F_{\sharp}.\phi(z)$ and $\Phi_{\sharp\sharp}(z) := F_{\sharp\sharp}.\phi(z)$ for any convergent ϕ , except that the first resurgent constants \underline{A}_{ω_0} and $\underline{\underline{A}}_{\omega_0}$ now depend on ϕ (while the A_{ω_1} depend on f alone). It would thus be possible to recover the invariants of f from any such Φ_{\sharp} or $\Phi_{\sharp\sharp}$, barring the highly exceptional (but not impossible) case when all *initial* resurgent constants \underline{A}_{ω_0} or $\underline{\underline{A}}_{\omega_0}$ vanish.

This state of affairs is fairly typical for the general affiliates: whenever γ is meromorphic with actual poles, the affiliate $f_{\diamond}(z) := \gamma(F-1).z$ of f verifies resurgent equations that involve, alongside the invariants A_{ω} of f , non-invariant constants like \underline{A}_{ω_0} and $\underline{\underline{A}}_{\omega_0}$.

1.9 Invariants, connectors, collectors

Let us survey in one table some of the main objects introduced so far or yet to come.

<i>diffeo</i>	<i>collectors</i>	<i>connectors</i>	<i>invariants</i>
g_{\sharp}	$\xrightarrow{3'_{\sharp}} p_{\sharp} \xrightarrow{3''_{\sharp}} \mathfrak{sp}_{\sharp} \xrightarrow{3'''_{\sharp}}$	$\pi_{\sharp} = (\pi_{\sharp \text{no}}, \pi_{\sharp \text{so}}) \xrightarrow{3''''_{\sharp}}$	$\{A_{\omega}^{\sharp}\}$
$\uparrow 2_{\sharp}$	$\downarrow 4_{\sharp}$	$\downarrow 5_{\sharp \text{no}} \quad \downarrow 5_{\sharp \text{so}}$	$\downarrow 6_{\sharp}$
$f = l \circ g \xrightarrow{1'}$	$p^{\pm} \xrightarrow{1''} \mathfrak{sp}^{\pm} \xrightarrow{1'''}$	$\pi^{\pm} = (\pi_{\text{no}}^{\pm}, \pi_{\text{so}}^{\pm}) \xrightarrow{1''''}$	$\{A_{\omega}^{\pm}\}$
$\downarrow 2_{*}$	$\uparrow 4_{*}$	$\uparrow 5_{* \text{no}} \quad \uparrow 5_{* \text{so}}$	$\uparrow 6_{*}$
g_{*}	$\xrightarrow{3'_{*}} p_{*} \xrightarrow{3''_{*}} \mathfrak{sp}_{*} \xrightarrow{3'''_{*}}$	$\pi_{*} = (\pi_{* \text{no}}, \pi_{* \text{so}}) \xrightarrow{3''''_{*}}$	$\{A_{\omega}\}$

The middle row carries the objects of direct interest to us, while the upper and lower rows carry their two main affiliates (the first mediator and the infinitesimal generator), which are more in the nature of auxiliary constructs.

The first, third and fourth columns carry objects already familiar to us. The second column, however, carries novel, highly interesting objects, the *collectors*, which are very close in a sense to the *connectors*, yet should be, for the sake of conceptual cleanness, clearly held apart. The *collectors* may assume four distinct forms:

- (i) formal series of multitangents, noted p ;
- (ii) formal series of monotangents, also noted p ;
- (iii) formal Laurent series of z^{-1} , noted \mathfrak{lp}
- (iv) the singular part, noted \mathfrak{sp} , of these Laurent series.

One goes from (i) to (ii) by multitangent reduction as in Section 2.3 ; and from (ii) to (iv) by the change $Te^{s_1} \mapsto z^{-s_1}$.

In any of these incarnations, the collectors are but a step removed from the invariants. Yet they are not invariant themselves: they depend on the z -chart in which the diffeo f is taken. Another difference is that whereas the collectors π^{\pm} are convergent Fourier series, the collectors p^{\pm} are condemned to remain formal power series in the countably many coefficients f_n of f . But this is perfectly all right, since the function of the collectors is precisely to carry, in conveniently compact form, all the information about the f -dependence of the connector π and, ultimately, of the invariants A_{ω} .

One last remark is in order here: although we are basically interested in the objects of the middle row, and more specifically in getting from f to the invariants $\{A_\omega^\pm\}$, we shall see that the most advantageous route is not the straight path through the arrows $1, 1', 1'', 1''''$, but any of the roundabout paths that start with 2_* or $2_\#$: these indirect routes are much more economical in terms of calculations and also more respectful of the underlying symmetries and parities.

1.10 The reverse problem: canonical synthesis

It can be shown that any convergent pair $\pi = (\pi_{\text{no}}, \pi_{\text{so}})$ is the connector pair of some standard diffeo $f = l \circ g$. This raises the problem of *synthesis*: how to reconstitute a germ f with a prescribed set of (admissible) invariants? And how to select a canonical f among all possible choices? A semi-canonical synthesis was sketched in [5] and a fully canonical one was constructed in [9]. The latter depends on a single parameter c whose real part must be chosen large enough.²⁴ The construction produces a canonical $f_c := {}^*f_c \circ l \circ f_c^*$ from its iterator f_c^* , which in turn is explicitly given, in operator form, by the formula

$$F_c^* := 1 + \sum_r \sum_{\omega_i \in \Omega} (-1)^r \mathcal{U}e_c^{\omega_1, \omega_2, \dots, \omega_r}(z) \mathbb{A}_{\omega_r} \dots \mathbb{A}_{\omega_2} \mathbb{A}_{\omega_1} \quad (1.93)$$

with a careful re-arrangement of the terms²⁵ necessary to ensure convergence. The two ingredients in (1.93) are the invariants \mathbb{A}_ω taken in operator form (1.69), and some special resurgence monomials $\mathcal{U}e_c^\omega(z)$ defined by

$$\mathcal{U}e_c^\omega(z) := e^{\|\omega\|z + c^2\|\bar{\omega}\|z^{-1}} \text{SPA} \int_0^\infty \frac{e^{-\sum(\omega_i t_i + c^2 \bar{\omega}_i t_i^{-1})}}{(t_r - t_{r-1}) \dots (t_2 - t_1)(t_1 - z)} dt_1 \dots dt_r \quad (1.94)$$

where SPA denotes a suitable average of all the 2^{r-1} possible integration multipaths that reflect the 2^{r-1} manners in which the variables t_j may circumvent each other on their way from 0 to ∞ .

2 Multitangents and multizetas.

The *multitangents* and *multizetas*, being the transcendental ingredient in the analytical expression of the invariants of identity-tangent diffeos²⁶,

²⁴ Synthesis cannot be *absolute*, i.e. parameter-free.

²⁵ Known as arborification-coarborification.

²⁶ And of much else – they are almost coextensive with the whole field of difference equations.

deserve a short excursus. But we must begin with a brief reminder about *moulds*, which are the proper tool for handling multi-indexed objects of whatever description.

2.1 Mould operations and mould symmetries

Main mould operations. Moulds are functions of finite sequences $\omega = (\omega_1, \dots, \omega_r)$ of any length $r \geq 0$, noted as right-upper indices and rendered, as mute variables, by a plain bold dot \bullet . Moulds can be *multiplied* and *composed*:

$$C^\bullet = A^\bullet \times B^\bullet \iff C^\omega = \sum_{\omega' \omega'' = \omega} A^{\omega'} B^{\omega''} \quad (2.1)$$

$$C^\bullet = A^\bullet \circ B^\bullet \iff C^\omega = \sum_{\omega^1 \dots \omega^s = \omega} A^{|\omega^1|, \dots, |\omega^s|} B^{\omega^s} \dots B^{\omega^1} \quad (\omega^i \neq \emptyset)$$

with all the predictable relations, including

$$(A^\bullet \times B^\bullet) \circ C^\bullet = (A^\bullet \circ C^\bullet) \times (B^\bullet \circ C^\bullet).$$

The units for multiplication or composition are the moulds $\mathbf{1}^\bullet$, Id^\bullet respectively defined by:

$$\mathbf{1}^\beta := 1 \quad ; \quad \mathbf{1}^{\omega_1, \dots, \omega_r} := 0 \quad \text{if } r \neq 0 \quad (2.2)$$

$$Id^{\omega_1} := 1 \quad ; \quad Id^{\omega_1, \dots, \omega_r} := 0 \quad \text{if } r \neq 1 \quad (2.3)$$

There exist scores of other mould operations, unary or binary. They are far too numerous to be assigned distinct symbols. So we resort to short letter combinations instead – even, retroactively, for mould multiplication and composition, which for clarity are often noted $mu(M_1^\bullet, M_2^\bullet)$ and $ko(M_1^\bullet, M_2^\bullet)$ instead of $M_1^\bullet \times M_2^\bullet$ and $M_1^\bullet \circ M_2^\bullet$. The corresponding Lie brackets are noted $lu(M_1^\bullet, M_2^\bullet)$ and $lo(M_1^\bullet, M_2^\bullet)$.

The multiplicative inverse of a mould M^\bullet is usually noted muM^\bullet . It exists if and only if $M^\beta \neq 0$.

The composition inverse of a mould M^\bullet is usually noted koM^\bullet . It exists if and only if $M^\beta = 0$ and $M^{\omega_1} \neq 0 \forall \omega_1$.

A mould M^\bullet is said to be of *constant type* if M^ω depends only on the length $r := r(\omega)$ of the sequence ω , i.e. if $M^\omega := m_r$. Such moulds may conveniently be noted $m(Id^\bullet)$ with $m(t) := \sum m_r t^r$. Multiplying or composing constant-type moulds M^\bullet reduces to multiplying or composing the underlying power series $m(t)$.

Main mould symmetries. Most moulds tend to fall into one or the other of four symmetry classes or types:

$$\begin{aligned}
 M^\bullet \text{symmetral (respectively alternel)} &\Leftrightarrow \\
 &\Leftrightarrow \sum_{\omega \in \text{sha}(\omega', \omega'')} M^\omega = M^{\omega'} M^{\omega''} \text{ (respectively } 0) \\
 M^\bullet \text{symmetrel (respectively alternel)} &\Leftrightarrow \\
 &\Leftrightarrow \sum_{\omega \in \text{she}(\omega', \omega'')} M^\omega = M^{\omega'} M^{\omega''} \text{ (respectively } 0).
 \end{aligned}$$

Here, $\text{sha}(\omega', \omega'')$ (respectively $\text{she}(\omega', \omega'')$) denotes the set of all sequences ω deducible from ω' and ω'' under plain (respectively contracting²⁷) shufflings. The main symmetry-types get exchanged under pre- or post-composition by special constant-type moulds. Thus

$$\text{symmetral}^\bullet = \exp(\text{Id}^\bullet) \circ \text{alternel}^\bullet, \quad \text{alternel}^\bullet = \text{alternel} \circ \log(\mathbf{1}^\bullet + \text{Id}^\bullet)$$

$$\text{symmetrel}^\bullet - \mathbf{1}^\bullet = \text{eternel}^\bullet = (\exp(\text{Id}^\bullet) - \mathbf{1}^\bullet) \circ \text{alternel}^\bullet \circ \log(\mathbf{1}^\bullet + \text{Id}^\bullet).$$

Hairsplitting though it may seem, the distinction between *symmetrel* and *eternel* should be maintained throughout: *symmetral* or *symmetrel* moulds are stable under multiplication, whereas *alternel* and *eternel* moulds are stable under composition. Likewise, *alternel* and *alternel* moulds are stable under the Lie bracket lu .

Pre- respectively post-composition of *alternel* moulds by $c^{-1} \tanh(c \text{Id}^\bullet)$ respectively $c^{-1} \text{arctanh}(c \text{Id}^\bullet)$ (chiefly for $c = 1, 1/2, i, i/2$) generates new symmetry types, signalled by one or two “o” vowels in their name. Though second in importance and frequency of occurrence to the four main symmetry types, these new exotic types are of more than marginal importance, especially in this investigation. They will repeatedly occur in connection with the *mediators*, the *medial* alien operators, and the multi-tangents To^\bullet, Too^\bullet .

Moulds of *symmetral*, *symmetrel*, or c -*symmetrol*²⁸ type generate three multiplicative groups and their multiplicative inverses are given by simple

²⁷ *I.e.* allowing order-compatible, pairwise contactions $(\omega'_i, \omega''_j) \mapsto \omega'_i + \omega''_j$ of elements from the parent sequences.

²⁸ *I.e.* moulds of type $\text{symmetral}^\bullet \circ (c^{-1} \tanh(c \text{Id}^\bullet))$ or $\text{symmetrel}^\bullet \circ (\frac{\text{Id}^\bullet}{\mathbf{1}^\bullet - \frac{1}{2} \text{Id}^\bullet})$ if $c = \frac{1}{2}$.

involution formulae:

$$\text{muS}^\bullet = \text{anti.S}^\bullet \circ (-Id^\bullet) \quad \text{if } S^\bullet \in \text{symmetrel} \quad (2.4)$$

$$\text{muS}^\bullet = \text{anti.S}^\bullet \circ \left(-\frac{Id^\bullet}{\mathbf{1}^\bullet + Id^\bullet}\right) \quad \text{if } S^\bullet \in \text{symmetrel} \quad (2.5)$$

$$\text{muS}^\bullet = \text{anti.S}^\bullet \circ (-Id^\bullet) \quad \text{if } S^\bullet \in \text{c-symmetrol} \quad (2.6)$$

with $\text{anti } S^{\omega_1, \dots, \omega_r} := S^{\omega_r, \dots, \omega_1}$.

Main moulds relevant to our investigation.

<i>symmetrel</i>	<i>symmetrol</i>	<i>symmetrol</i>		
ze^\bullet	za^\bullet	zo^\bullet	<i>scalar-valued</i>	<i>(multizetas)</i>
$\tilde{Se}^\bullet(z)$	$\tilde{Sa}^\bullet(z)$	$\tilde{So}^\bullet(z)$	<i>resurgent-valued</i>	<i>(resur. monomials)</i>
$Te^\bullet(z)$	$Ta^\bullet(z)$	$To^\bullet(z)$	<i>meromorphic-va.</i>	<i>(multitangents)</i>
<i>eternel</i>	<i>altornal</i>	<i>olternol</i>		
$Tee^\bullet(z)$	$Taa^\bullet(z)$	$Too^\bullet(z)$	<i>meromorphic-va.</i>	<i>(multitangents)</i>
Tee_ω^\bullet	Taa_ω^\bullet	Too_ω^\bullet	<i>scalar-valued</i>	<i>(multizeta sums)</i>

2.2 Multizetas

In this subsection, all indices s_i are in \mathbb{N}^* and, to preempt divergence, we (provisionally) assume $s_1 \neq 1$ for multizetas and $s_1, s_r \neq 1$ for multitangents.

We first consider three multizeta-valued moulds, ze^\bullet , za^\bullet and zo^\bullet :

$$ze^{s_1, \dots, s_r} := \sum_{n_1 > \dots > n_r > 0} n_1^{-s_1} \dots n_r^{-s_r} \quad (2.7)$$

$$za^{s_1, \dots, s_r} := \sum_{n_1 \geq \dots \geq n_r > 0} n_1^{-s_1} \dots n_r^{-s_r} \prod \frac{1}{r_j!} \quad (2.8)$$

$$zo^{s_1, \dots, s_r} := \sum_{n_1 \geq \dots \geq n_r > 0} n_1^{-s_1} \dots n_r^{-s_r} \prod 2^{1-r_j} \quad (2.9)$$

If the monomial $\prod n_i^{-s_i}$ in (2.8) or (2.9) involves t clusters of r_1, \dots, r_t identical integers n_i ($1 \leq t \leq r$), the multiplicity corrections have to be defined accordingly, as $\prod 1/r_j!$ or $\prod 2^{1-r_j}$. Clearly

$$za^\bullet = ze^\bullet \circ (\exp(Id^\bullet) - \mathbf{1}^\bullet) \quad (2.10)$$

$$zo^\bullet = ze^\bullet \circ \left(\frac{Id^\bullet}{\mathbf{1}^\bullet - \frac{1}{2} Id^\bullet}\right) = za^\bullet \circ \left(2 \operatorname{arctanh}\left(\frac{1}{2} Id^\bullet\right)\right) \quad (2.11)$$

The moulds ze^\bullet and za^\bullet are obviously *symmetrel* and *symmetrol*, while zo^\bullet falls into a subaltern symmetry type: *symmetrol* (see Section 5.1).

Fast computation of the multizetas. Our two guiding concerns here are: replacing the sluggish rate of convergence of the series (2.7), (2.8), (2.9) by a *geometric rate* of convergence and making manifest the multizetas' hidden *parity* properties.

Let trunze_n^\bullet be the *truncated* multizetas, defined as in (2.7) but with summation over $n \geq n_1 > \dots > n_r > 0$, and let remze_n^\bullet be the *remainder* multizetas, defined again as in (2.7) but with summation over $+\infty \geq n_1 > \dots > n_r > n$. Let trunza_n^\bullet , trunzo_n^\bullet and remza_n^\bullet , remzo_n^\bullet be similarly defined. The symmetry types are preserved, so too are the relations (2.10)-(2.11), and we have obvious mould factorisations

$$\text{ze}^\bullet = \text{remze}_n^\bullet \times \text{trunze}_n^\bullet \tag{2.12}$$

$$\text{za}^\bullet = \text{remza}_n^\bullet \times \text{trunza}_n^\bullet \tag{2.13}$$

$$\text{zo}^\bullet = \text{remzo}_n^\bullet \times \text{trunzo}_n^\bullet. \tag{2.14}$$

Using the elementary difference equations (in n) verified by remze_n^\bullet , we find for that mould a divergent but Borel resummable (and resurgent) asymptotic expansion asremze_n^\bullet , in decreasing powers of n , of the form:

$$\begin{aligned} \text{asremze}^{s_1, \dots, s_r} &= \frac{e^\partial}{1 - e^\partial} n^{-s_r} \frac{e^\partial}{1 - e^\partial} n^{-s_{r-1}} \dots \frac{e^\partial}{1 - e^\partial} n^{-s_1} \tag{2.15} \\ &= \frac{1}{n^{s_1 + \dots + s_r - r}} \prod_{1 \leq i \leq r} \frac{1}{s_1 + \dots + s_i - i} + o\left(\frac{1}{n^{s_1 + \dots + s_r - r}}\right). \end{aligned}$$

Here $\partial := \partial_n$ and each operator $\frac{e^\partial}{1 - e^\partial} = -\partial^{-1} - \frac{1}{2} - \frac{1}{12} \partial + \dots$ in (2.15) acts on everything standing to its right. The last two asymptotic series factor into:

$$\text{asremza}_n^\bullet = \underline{\text{asremza}}_n^\bullet \times \left(\frac{2}{\mathbf{1}^\bullet + e^{I_n^\bullet}} \right) \tag{2.16}$$

$$\text{asremzo}_n^\bullet = \underline{\text{asremzo}}_n^\bullet \times \left(\frac{I_n^\bullet}{\mathbf{1}^\bullet - \frac{1}{2} I_n^\bullet} \right) \tag{2.17}$$

with elementary right factors involving the moulds I_n^\bullet and $K_n^\bullet = 2(\mathbf{1}^\bullet + e^{I_n^\bullet})^{-1}$

$$I_n^{s_1, \dots, s_r} = 0 \quad \text{if } r \neq 1 \quad \text{and} \quad I_n^{s_1} := n^{-s_1}, \quad I_n^\emptyset := 0 \tag{2.18}$$

$$K_n^{s_1, \dots, s_r} = \kappa_r n^{-(s_1 + \dots + s_r)} \quad \text{with} \quad \frac{2}{1 + e^t} =: \sum \kappa_r t^r \tag{2.19}$$

and with non elementary but essentially (up to an elementary power of n) *even* left factors of the form

$$\underline{\text{asremza}}_n^{s_1, \dots, s_r} \quad \text{and} \quad \underline{\text{asremzo}}_n^{s_1, \dots, s_r} \in n^{r - (s_1 + \dots + s_r)} \mathbb{C}[[n^{-2}]]. \tag{2.20}$$

There is, however, a significant difference between the two factorisations. Whereas we can see, by post-composing (2.15) by $Id^\bullet \times (\mathbf{1}^\bullet - Id^\bullet)^{-1}$, that $\underline{asremzo}^\bullet$ is given by a simple induction:

$$\underline{asremzo}^{s_1, \dots, s_r} = H(\partial) n^{-s_r} H(\partial) n^{-s_{r-1}} \dots H(\partial) n^{-s_1} \quad (2.21)$$

with $H(\partial) := \frac{e^\partial}{1-e^\partial} + \frac{1}{2} = -\frac{1}{2} \coth(\frac{1}{2}\partial)$, no such induction holds for $\underline{asremza}^\bullet$. That mould admits only indirect definitions, like:

$$\underline{asremza}^\bullet = \underline{asremzo}^\bullet \circ \left(2 \tanh\left(\frac{1}{2} Id^\bullet\right) \right) \quad (2.22)$$

or

$$\underline{asremza}^{s_1, \dots, s_r} = \left[\mathcal{S}A^{d_1, \dots, d_r} \cdot \prod_{1 \leq i \leq r} n_i^{-s_i} \right]_{n_i=n} \quad (2.23)$$

with

$$\mathcal{S}A^\bullet := \left(\mathcal{S}\mathcal{E}^\bullet \times (\mathbf{1}^\bullet + Id^\bullet) \right) \circ \left(\exp(Id^\bullet) - \mathbf{1}^\bullet \right) \quad (2.24)$$

and with the important symmetrel mould $\mathcal{S}\mathcal{E}^\bullet$:

$$\mathcal{S}\mathcal{E}^{d_1, \dots, d_r} := \prod_{1 \leq i \leq r} \frac{e^{d_1 + \dots + d_i}}{1 - e^{d_1 + \dots + d_i}} \quad (2.25)$$

The first definition (2.22) results directly from (2.11) restricted to the remainders. The second definition calls for some explanations. Here, each d_i denotes the operator ∂_{n_i} that acts on n_i alone. On the right-hand side of (2.23), we let the operator $\mathcal{S}A^d$ act on the product $\prod n_i^{-s_i}$ and then set $n_i := n$. To establish (2.23), we observe that (2.15) may be written

$$\underline{asremze}^{s_1, \dots, s_r} = \left[\mathcal{S}\mathcal{E}^{d_1, \dots, d_r} \cdot \prod_{1 \leq i \leq r} n_i^{-s_i} \right]_{n_i=n} \quad (2.26)$$

and we then use the relation $\underline{asremza}^\bullet = \underline{asremze}^\bullet \circ (\exp(Id^\bullet) - \mathbf{1}^\bullet)$ that results from restricting (2.10) to the remainders. The interesting point about (2.23) is that it relates the *parity* property (2.20) of $\underline{asremza}^\bullet$ to the following *parity* property of $\mathcal{S}\mathcal{E}^\bullet$

$$\text{neg.}\mathcal{S}\mathcal{E}^\bullet = \left(\mathcal{S}\mathcal{E}^\bullet \times (\mathbf{1}^\bullet + Id^\bullet) \right) \circ \left(-\frac{Id^\bullet}{\mathbf{1}^\bullet + Id^\bullet} \right) \quad (2.27)$$

and to the formula for its multiplicative inverse $\text{mu}\mathcal{S}\mathcal{E}^\bullet$:

$$\text{mu}\mathcal{S}\mathcal{E}^\bullet = e^{|\bullet|} \text{anti.}\text{neg.}\mathcal{S}\mathcal{E}^\bullet \quad (2.28)$$

with

$$|(s_1, \dots, s_r)| = \sum s_i, \quad \text{neg.}\mathcal{S}^{s_1, \dots, s_r} := S^{-s_1, \dots, -s_r}, \quad \text{anti.}\mathcal{S}^{s_1, \dots, s_r} := S^{s_r, \dots, s_1}$$

Acceleration of the convergence . When we calculate ze^\bullet according to formula (2.12) by taking the exact value of the truncated factor $trunze_n^\bullet$ and calculating the remainder factor $remze_n^\bullet$ from its asymptotic expansion (2.15) cut off at the least term, we get an excellent approximation, with an error that decreases roughly like $\exp(-2\pi n)$ as the truncation order n increases. The same applies to za^\bullet and zo^\bullet : the truncated factors $trunza^\bullet$ and $trunzo^\bullet$ may have more summands than $trunze^\bullet$, but this is more than offset by the parity simplifications in the remainder factors $remza^\bullet$ and especially $remzo^\bullet$.

We may note that this method remains valid, and retains its high efficiency, for general complex values of the weights s_i , *even when the inequalities $\Re(s_1 + \dots + s_i) > i$ that guarantee the convergence of (2.7)-(2.9) no longer hold.*

Quadratic constraints. The symmetrelity of ze^\bullet , or the strictly equivalent symmetries of za^\bullet and zo^\bullet , do not exhaust the set of algebraic constraints on the multizetas: there exists another set of constraints, of ‘equal strength’, based on a radically different, essentially discrete²⁹ encoding: see Section 6.2.

2.3 Multitangents

The multizetas enter invariant analysis *indirectly*, as scalars attached to elementary periodic meromorphic functions – the so-called *multitangents*.

Here are the main multitangent-valued moulds with their symmetry types:

$$\begin{array}{ccccc}
 \text{Te}^\bullet & \xrightarrow{1} & \text{Ta}^\bullet & \xrightarrow{2} & \text{To}^\bullet & \text{symmetrel} & \xrightarrow{1} & \text{symmetral} & \xrightarrow{2} & \text{symmetrol} \\
 \downarrow 3 & & \downarrow 4 & & \downarrow 5 & & \downarrow 3 & & \downarrow 4 & & \downarrow 5 \\
 \text{Tee}^\bullet & \xrightarrow{1} & \text{Taa}^\bullet & \xrightarrow{2} & \text{Too}^\bullet & \text{eternel} & \xrightarrow{1} & \text{altern} & \xrightarrow{2} & \text{olternol}
 \end{array}$$

The two upper moulds are defined directly by³⁰

$$\text{Te}^{s_1, \dots, s_r}(z) := \sum_{n_1 > \dots > n_r} (n_1 + z)^{-s_1} \dots (n_r + z)^{-s_r} \tag{2.29}$$

$$\text{Ta}^{s_1, \dots, s_r}(z) := \sum_{n_1 \geq \dots \geq n_r} (n_1 + z)^{-s_1} \dots (n_r + z)^{-s_r} \prod \frac{1}{r_i!} \tag{2.30}$$

$$\text{To}^{s_1, \dots, s_r}(z) := \sum_{n_1 \geq \dots \geq n_r} (n_1 + z)^{-s_1} \dots (n_r + z)^{-s_r} \prod 2^{1-r_i} \tag{2.31}$$

²⁹ Unlike the s_i -encoding, which of course extends to the complex field.

³⁰ With the same r_j in (2.30) as in (2.8).

and the two lower moulds are derived from them through a suitable pre-composition. Thus:

$$Te^\bullet = see \quad (2.29) \quad Tee^\bullet = Te^\bullet - \mathbf{1}^\bullet \quad (Te - Tee)$$

$$Ta^\bullet = Te^\bullet \circ (e^{Id^\bullet} - \mathbf{1}^\bullet) \quad Taa^\bullet = \log(\mathbf{1}^\bullet + Id^\bullet) \circ Ta^\bullet \circ (e^{Id^\bullet} - \mathbf{1}^\bullet) \quad (Ta - Taa)$$

$$To^\bullet = Te^\bullet \circ \left(\frac{Id^\bullet}{\mathbf{1}^\bullet - \frac{1}{2} Id^\bullet}\right) \quad Too^\bullet = \left(\frac{Id^\bullet}{\mathbf{1}^\bullet + \frac{1}{2} Id^\bullet}\right) \circ Te^\bullet \circ \left(\frac{Id^\bullet}{\mathbf{1}^\bullet - \frac{1}{2} Id^\bullet}\right) \quad (To - Too)$$

In the sequel, we shall also require the inverses of Te^\bullet , Ta^\bullet , To^\bullet for mould multiplication. In view of (2.4)-(2.6), we get

$$\text{muTe}^{s_1, \dots, s_r}(z) = \sum_{n_1 \leq \dots \leq n_r} (-1)^r (n_1 + z)^{-s_1} \dots (n_r + z)^{-s_r} \quad (2.32)$$

$$\text{muTa}^{s_1, \dots, s_r}(z) = \sum_{n_1 \leq \dots \leq n_r} (-1)^r (n_1 + z)^{-s_1} \dots (n_r + z)^{-s_r} \prod \frac{1}{r_i!} \quad (2.33)$$

$$\text{muTo}^{s_1, \dots, s_r}(z) = \sum_{n_1 \leq \dots \leq n_r} (-1)^r (n_1 + z)^{-s_1} \dots (n_r + z)^{-s_r} \prod n^{1-r_i} \quad (2.34)$$

with an order reversal in the summation rule, and large inequalities in place of the strict inequalities in (2.29)-(2.31).

Parity aspects. All six types of multitangents obviously verify

$$T^{s_1, \dots, s_r}(-z) \equiv (-1)^{s_1 + \dots + s_r} T^{s_r, \dots, s_1}(z) \quad (\forall T \in \{Te, Ta, To \text{ etc.}\}). \quad (2.35)$$

In the case of Taa^\bullet and Too^\bullet , however, due to alternality/olternolity we have an additional relation

$$Taa^{s_r, \dots, s_1}(z) \equiv (-1)^{r-1} Taa^{s_1, \dots, s_r}(z) \quad (2.36)$$

$$Too^{s_r, \dots, s_1}(z) \equiv (-1)^{r-1} Too^{s_1, \dots, s_r}(z). \quad (2.37)$$

Combining (2.35) and (2.36)-(2.37) we get the crucial *parity separation* property, which sets Taa^\bullet , Too^\bullet apart from $Te^\bullet \approx Tee^\bullet$:

$$Taa^{s_1, \dots, s_r}(-z) \equiv (-1)^{1 + \sum d_i} Taa^{s_1, \dots, s_r}(z) \quad \text{with } d_i := s_i - 1 \quad (2.38)$$

$$Too^{s_1, \dots, s_r}(-z) \equiv (-1)^{1 + \sum d_i} Too^{s_1, \dots, s_r}(z) \quad \text{with } d_i := s_i - 1 \quad (2.39)$$

Multitangents in terms of monotangents and multizetas. Multitangents are entirely determined by their polar parts at the entire points $z = n$. By calculating, based on the expansion (2.29), the Laurent expansion of $Te^s(z)$ at such points, and then retaining only the polar part, we find that $Te^s(z)$ can be expressed as a finite sum of elementary monotangents

$Te^{s_1}(z) = \sum_{n_1} (n_1 + z)^{-s_1}$, also known as Eisenstein series. Here is the formula:³¹

$$Te^{s_1, \dots, s_r}(z) = \sum_{\sigma=2}^{\sup(s_i)} teze_{i, \sigma_i}^{s_1, \dots, s_r} Te^\sigma(z) = \sum_{i=1}^r \sum_{\sigma_i=2}^{s_i} teze_{i, \sigma_i}^{s_1, \dots, s_r} Te^{\sigma_i}(z) \quad (2.40)$$

with

$$\begin{aligned} teze_{i, \sigma_i}^{s_1, \dots, s_r} &= \\ &= \sum_{\substack{\sum \sigma_k = \sum s_k \\ \sigma_i \leq s_i \\ s_j \leq \sigma_j (j \neq i)}} ze^{\sigma_1, \dots, \sigma_{i-1}} ze^{\sigma_r, \dots, \sigma_{i+1}} \prod_{j=1}^{i-1} (-1)^{\sigma_j} \prod_{1 \leq j \leq r}^{j \neq i} \frac{(-1)^{s_j} (\sigma_j - 1)!}{(\sigma_j - s_j)! (s_j - 1)!} \end{aligned}$$

or more symmetrically

$$\begin{aligned} teze_{i, \sigma_i}^{s_1, \dots, s_r} &= \\ &= \sum_{\substack{\sum \sigma_k = \sum s_k \\ \sigma_i \leq s_i \\ s_j \leq \sigma_j (j \neq i)}} ze^{\sigma_1, \dots, \sigma_{i-1}} (-1)^{s_i - \sigma_i} vize^{\sigma_{i+1}, \dots, \sigma_r} \prod_{1 \leq j \leq r}^{j \neq i} \frac{(\sigma_j - 1)!}{(\sigma_j - s_j)! (s_j - 1)!} \\ vize^{s_1, \dots, s_r} &= (-1)^{s_1 + \dots + s_r} ze^{s_r, \dots, s_1}. \end{aligned} \quad (2.41)$$

The leading monotangent $Te^1(z) = \frac{\pi}{\tan(\pi z)}$ generates all others under differentiation, and admits the following northern and southern expansions:

$$Te_{no}^1(z) = -\pi i - 2\pi i \sum_{0 < n} e^{+2\pi i n z} \quad \text{if } \Im(z) > 0 \quad (2.42)$$

$$Te_{so}^1(z) = +\pi i + 2\pi i \sum_{0 < n} e^{-2\pi i n z} \quad \text{if } \Im(z) < 0. \quad (2.43)$$

Since $Te^{s_1}(z) = \frac{(-1)^{s_1-1}}{(s_1-1)!} \partial_z^{s_1-1} Te^1(z)$, this yields

$$Te^{s_1}(z) = \sum_{\omega \in \Omega^\mp} Te_\omega^{s_1} e^{-\omega z} \quad \text{on each half-plane } \pm \Im(z) > 0 \quad (2.44)$$

with

$$Te_\omega^{s_1} = \text{sign}(\Im(\omega)) 2\pi i \frac{\omega^{s_1-1}}{(s_1-1)!} \quad \text{and} \quad \Omega^\mp = 2\pi i \mathbb{Z}^\mp. \quad (2.45)$$

³¹ For a more compact expression, based on generating series, see Section 6.3.

All the above amounts to a simple procedure for calculating the Fourier expansions, north and south, of the four classes of multitangents. The three classes $Te^\bullet \approx Te^\bullet$, Taa^\bullet , Too^\bullet shall be of direct concern to us:

$$Te_{no}^\bullet(z) = \sum_{\omega \in \Omega^-} Tee_\omega^\bullet e^{-\omega z} \quad ; \quad Tee_{so}^\bullet(z) = \sum_{\omega \in \Omega^+} Tee_\omega^\bullet e^{-\omega z} \quad (2.46)$$

$$Taa_{no}^\bullet(z) = \sum_{\omega \in \Omega^-} Taa_\omega^\bullet e^{-\omega z} \quad ; \quad Taa_{so}^\bullet(z) = \sum_{\omega \in \Omega^+} Taa_\omega^\bullet e^{-\omega z} \quad (2.47)$$

$$Too_{no}^\bullet(z) = \sum_{\omega \in \Omega^-} Too_\omega^\bullet e^{-\omega z} \quad ; \quad Too_{so}^\bullet(z) = \sum_{\omega \in \Omega^+} Too_\omega^\bullet e^{-\omega z} \quad (2.48)$$

Localisation constraints. When dealing with a product of multitangents Te^s , we may perform the operations of *reduction* (of multitangents into sums of monotangents) and *symmetrel linearisation* in either order. If we then identify the multizeta superpositions in front of each monotangent, we get to the so-called reduction constraints:

$$\begin{aligned} Te^{s^1}(z) \cdot Te^{s^2}(z) &\xrightarrow{\text{reduction}} \left(\sum \tau_{s_1}^{s^1} Te^{s_1}(z) \right) \cdot \left(\sum \tau_{s_2}^{s^2} Te^{s_2}(z) \right) \\ &\downarrow \text{linearisation} \qquad \qquad \qquad \downarrow \text{linearisation} \\ \sum \epsilon_{s_3}^{s^1, s^2} Te^{s^3}(z) &\xrightarrow{\text{reduction}} \sum \epsilon_{s_3}^{s^1, s^2} \tau_{s_3}^{s^3} Te^{s_3}(z) = \sum \tau_{s_1}^{s^1} \tau_{s_2}^{s^2} \epsilon_{s_3}^{s^1, s^2} Te^{s_3}(z). \end{aligned}$$

Here, the $\epsilon_{s^k}^{s^i, s^j}$ are elementary, integer-valued coefficients and the expressions $\tau_{s_j}^{s^i}$ are finite, homogeneous sums of multizetas of total weight $\|s^i\| - s_i - 1$.

If, instead of *reduction*, we use *localisation* (replacing each multitangent by its two-sided Laurent expansion at $z = 0$), we get the so-called localisation constraints:

$$\begin{aligned} Te^{s^1}(z) \cdot Te^{s^2}(z) &\xrightarrow{\text{localisation}} \left(\sum \theta_{n_1}^{s^1} z^{n_1} \right) \cdot \left(\sum \theta_{n_2}^{s^2} z^{n_2} \right) \\ &\downarrow \text{linearisation} \qquad \qquad \qquad \downarrow \text{linearisation} \\ \sum \epsilon_{s_3}^{s^1, s^2} Te^{s^3}(z) &\xrightarrow{\text{localisation}} \sum \epsilon_{s_3}^{s^1, s^2} \theta_{n_3}^{s^3} z^{n_3} = \sum \theta_{n_1}^{s^1} \theta_{n_2}^{s^2} z^{n_1+n_2} \end{aligned}$$

with expressions $\theta_{n_j}^{s^i}$ that are again finite, homogeneous sums of multizetas of total weight $\|s^i\| + n_j$.

Though more numerous, the localisation constraints are actually equivalent to the reduction constraints, but they extend more smoothly to the ramified case, *i.e.* to the case of multitangents and multizetas that carry fractional indices s_i . In any case, the localisation constraints are *not* a consequence of the symmetrelness of Te^\bullet .

The multitangents Taa^\bullet and Too^\bullet in terms of $Tee^\bullet \approx Te^\bullet$. Applying to Too^\bullet a beautiful formula (see (5.16)-(5.17) in Section 5.4) that holds for multitangents Te^\bullet_\diamond of any symmetry type and gives their explicit linearisation into sums of symmetrel multitangents Te^\bullet , we find:

$$Too^{s_1, \dots, s_r}(z) = \sum_{\sigma \in \mathfrak{S}_r} \sum_{2 \leq i \leq r} \sum_{(\mathcal{I}_1, \dots, \mathcal{I}_i)^{\# \sigma}}_{r_1 + \dots + r_i = r} (-1)^{q(\sigma)} 2^{1-r} Te^{s_{\sigma, r_1}, \dots, s_{\sigma, r_i}}(z) \quad (2.49)$$

with $s_{\sigma, j} := \sum_{k \in \mathcal{I}_j} s_\sigma(k)$ and $q(\sigma) := \#\{k \mid k < r, \sigma^{-1}(k) > \sigma^{-1}(k+1)\}$

The summation is over all permutations σ of r elements and, for each σ , over all partitions of $[1, \dots, r]$ into intervals \mathcal{I}_i of r_i elements, whereby we demand that the partition $(\mathcal{I}_1, \dots, \mathcal{I}_r)$ be ‘orthogonal’ to σ , i.e. such that

- (i) on any given \mathcal{I}_j the permutation σ assumes no two consecutive values;
- (ii) σ increases on each interval \mathcal{I}_j .

In other words, we should have $\{k, k+1\} \in \mathcal{I}_j \Rightarrow \{\sigma(k+1) - \sigma(k) \geq 2\}$. The orthogonality condition proper is (i). The condition (ii) is there simply to ensure that any given summand $Te^{s_{\sigma, r_1}, \dots, s_{\sigma, r_i}}$ is counted only once. Lastly, $q(\sigma)$ measures the incompatibility of the natural order $<$ on $[1, \dots, r]$ with the σ -induced order $\{i <_\sigma j\} \Leftrightarrow \{\sigma(i) < \sigma(j)\}$. Indeed, if j is not $<_\sigma$ -maximal and j^+ denotes the $<_\sigma$ -successor of j , we have $q(\sigma) = \#\{j; j > j^+\}$.

When applied to Taa^\bullet , the general formula (5.16)-(5.17) produces a similar expansion, but with more numerous Te^\bullet -summands and, in front of each of them, rational coefficients whose numerators possess no simple multiplicative structure.³² They may be calculated, though, by applying the universal formula (5.17).

Remark. Taa^\bullet better than Te^\bullet and Too^\bullet better than Taa^\bullet .

Actually, a systematic comparison would show that, of all types Te^\bullet_\diamond of multitangents that possess the desirable parity property (2.38)-(2.39), Taa^\bullet and especially Too^\bullet are the simplest choices, not only where Te^\bullet -linearisation is concerned, but in most other respects.

Taa^\bullet and Too^\bullet even compare favourably with Te^\bullet , which in any case does not verify the parity property(2.38)-(2.39). Taa^\bullet and Too^\bullet may lack

³² Although, for r small, they seem to be all equal to 1. This, however, is deceptive.

a simple direct definition like that of Te^\bullet , but after reduction to monotan-
gents, it is Taa^\bullet and especially Too^\bullet , not Te^\bullet , that give rise, by and large,
to the simpler expansions³³, as shown by the Tables of Section 9.

2.4 Resurgence monomials

There exists an alternative, *resurgent* approach to multitangent reduc-
tion. In the convergent (*i.e.* $s_1, s_r \neq 1$) and non-ramified (*i.e.* $s_j \in \mathbb{N}^*$
rather than \mathbb{Q}^*) case, it hardly improves on the above procedure (see Sec-
tion 2.3) but in the general case, especially when we go over to fractional
indices s_j , the resurgent approach becomes the more flexible of the two
methods and even, in a sense, the only practical one. For clarity, though,
we first keep our two simplifying assumptions – no divergence³⁴ and no
ramification³⁵ – to sketch this alternative method.

Multizetaic monomials in the formal model. We shall set about construct-
ing three elementary resurgent-valued moulds³⁶ $\tilde{S}e^\bullet(z)$, $\tilde{S}a^\bullet(z)$, $\tilde{S}o^\bullet(z)$,
beginning with the *formal model*. We start with the symmetrel monomi-
als $\tilde{S}e^s(z)$. They are defined by:

$$\tilde{S}e^\bullet(z) = \frac{e^{\partial_z}}{(1 - e^{\partial_z})} \left(\tilde{S}e^\bullet(z) \times J^\bullet(z) \right) \tag{2.50}$$

with an elementary mould $J^\bullet(z)$:

$$J^\emptyset(z) := 0 \quad ; \quad J^{s_1}(z) := z^{-s_1} \quad ; \quad J^{s_1, \dots, s_r}(z) := 0 \quad (\forall r \geq 2). \tag{2.51}$$

Together with the conditions $\tilde{S}e^\emptyset(z) = 1$, $\tilde{S}e^{s_1, \dots, s_r}(\infty) = 0$ ($\forall r \geq 1$) the
induction (2.50) uniquely defines each $\tilde{S}e^s(z)$ as a constant-free, formal
power series in z^{-1} . The companions monomials $\tilde{S}a^\bullet(z)$, $\tilde{S}o^\bullet(z)$ are then
defined in the usual way, by post-composition:

$$\tilde{S}a^\bullet(z) := \tilde{S}e^\bullet(z) \circ (\exp(Id^\bullet - \mathbf{1}^\bullet)) \tag{2.52}$$

$$\tilde{S}o^\bullet(z) := \tilde{S}e^\bullet(z) \circ \left(\frac{Id^\bullet}{\mathbf{1}^\bullet - \frac{1}{2} Id^\bullet} \right). \tag{2.53}$$

³³ Especially after the symmetrel linearisation of the multizetas occuring as scalar coefficients in these expansions.

³⁴ *I.e.* $s_1 > 1$

³⁵ *I.e.* $s_i \in \mathbb{N}^*$

³⁶ They must be distinguished from the similar moulds $asremze_n^\bullet, asremza_n^\bullet, asremzo_n^\bullet$, because the emphasis here will be on the convolutive model and the associated monics.

Multizetaic monomials in the convolutive model. In the *convolutive model* the induction becomes

$$\widehat{\text{Se}}^{s_1, \dots, s_r}(\zeta) = \frac{e^{-\zeta}}{(1 - e^{-\zeta})} \int_0^\zeta \widehat{\text{Se}}^{s_1, \dots, s_{r-1}}(\zeta - \zeta_r) \frac{\zeta_r^{s_r - 1}}{\Gamma(s_r)} d\zeta_r \quad (2.54)$$

Multizetaic monomials in the sectorial model. Lastly, in the *sectorial* or '*geometric*' models + and - (*east* and *west*), corresponding to Laplace integration along the axes $\arg(\zeta) = 0$ and $\arg(\zeta) = \pi$, we get

$$\text{Se}_+^{s_1, \dots, s_r}(z) = \sum_{0 < n_r < \dots < n_1} (n_1 + z)^{-s_1} \dots (n_r + z)^{-s_r} \quad (2.55)$$

$$\text{Se}_-^{s_1, \dots, s_r}(z) = \sum_{n_1 \leq \dots \leq n_r \leq 0} (-1)^r (n_1 + z)^{-s_1} \dots (n_r + z)^{-s_r} \quad (2.56)$$

$$\text{muSe}_+^{s_1, \dots, s_r}(z) = \sum_{0 < n_1 \leq \dots \leq n_r} (-1)^r (n_1 + z)^{-s_1} \dots (n_r + z)^{-s_r} \quad (2.57)$$

$$\text{muSe}_-^{s_1, \dots, s_r}(z) = \sum_{n_r < \dots < n_1 \leq 0} (n_1 + z)^{-s_1} \dots (n_r + z)^{-s_r} \quad (2.58)$$

For $S^\bullet = Sa^\bullet$ or So^\bullet and multiplicity corrections $\chi(r_i) = 1/r_i!$ or 2^{1-r_i} , these expansions become respectively

$$S_+^{s_1, \dots, s_r}(z) = \sum_{0 < n_r \leq \dots \leq n_1} (n_1 + z)^{-s_1} \dots (n_r + z)^{-s_r} \chi(r_i) \quad (2.59)$$

$$S_-^{s_1, \dots, s_r}(z) = \sum_{n_1 \leq \dots \leq n_r \leq 0} (-1)^r (n_1 + z)^{-s_1} \dots (n_r + z)^{-s_r} \chi(r_i) \quad (2.60)$$

$$\text{muS}_+^{s_1, \dots, s_r}(z) = \sum_{0 < n_1 \leq \dots \leq n_r} (-1)^r (n_1 + z)^{-s_1} \dots (n_r + z)^{-s_r} \chi(r_i) \quad (2.61)$$

$$\text{muS}_-^{s_1, \dots, s_r}(z) = \sum_{n_r \leq \dots \leq n_1 \leq 0} (n_1 + z)^{-s_1} \dots (n_r + z)^{-s_r} \chi(r_i) \quad (2.62)$$

Multizetaic monics. From the structure of the induction (2.50), one infers directly (without calculation) that our monomials verify resurgence

equations of the form³⁷

$$\Delta_{\omega}^{+} \text{Se}^{\bullet}(z) = \text{Tee}_{\omega}^{\bullet} \times \text{Se}^{\bullet}(z) \quad (\forall \omega \in \Omega^{+} = 2\pi i\mathbb{Z}^{+}) \quad (2.63)$$

$$\Delta_{\omega}^{-} \text{Se}^{\bullet}(z) = \text{Tee}_{\omega}^{\bullet} \times \text{Se}^{\bullet}(z) \quad (\forall \omega \in \Omega^{-} = 2\pi i\mathbb{Z}^{-}) \quad (2.64)$$

$$+2\pi i \Delta_{\omega} \text{Sa}^{\bullet}(z) = \text{Taa}_{\omega}^{\bullet} \times \text{Sa}^{\bullet}(z) \quad (\forall \omega \in \Omega^{+} = 2\pi i\mathbb{Z}^{+}) \quad (2.65)$$

$$-2\pi i \Delta_{\omega} \text{Sa}^{\bullet}(z) = \text{Taa}_{\omega}^{\bullet} \times \text{Sa}^{\bullet}(z) \quad (\forall \omega \in \Omega^{-} = 2\pi i\mathbb{Z}^{-}) \quad (2.66)$$

$$+2\pi i \Delta_{\omega}^{\sharp} \text{So}^{\bullet}(z) = \text{Too}_{\omega}^{\bullet} \times \text{So}^{\bullet}(z) \quad (\forall \omega \in \Omega^{+} = 2\pi i\mathbb{Z}^{+}) \quad (2.67)$$

$$-2\pi i \Delta_{\omega}^{\sharp} \text{So}^{\bullet}(z) = \text{Too}_{\omega}^{\bullet} \times \text{So}^{\bullet}(z) \quad (\forall \omega \in \Omega^{-} = 2\pi i\mathbb{Z}^{-}) \quad (2.68)$$

with scalar-valued moulds $\text{Tee}_{\omega}^{\bullet}$, $\text{Taa}_{\omega}^{\bullet}$, $\text{Too}_{\omega}^{\bullet}$, whose symmetry types follow from their construction.³⁸ These three moulds, for the moment, need not bear any relation to their namesakes in Section 2.3, but we shall show that they actually coincide with them.

Writing down the axis-crossing identity (1.49) with (2.12) and $\theta = +\frac{\pi}{2}$ and the reverse identity (1.50) with (2.13) and $\theta = -\frac{\pi}{2}$, and minding the fact that

$$\text{Se}_{\frac{\pi}{2} \pm \epsilon}^{\bullet} = \text{Se}_{\mp}^{\bullet} \quad (\textit{inversion!}) \quad ; \quad \text{Se}_{-\frac{\pi}{2} \pm \epsilon}^{\bullet} = \text{Se}_{\pm}^{\bullet} \quad (\textit{no inversion!})$$

we find respectively

$$\text{Te}_{\text{so}}^{\bullet}(z) \times \text{Se}_{-, \text{so}}^{\bullet}(z) = \text{Se}_{+, \text{so}}^{\bullet}(z) \quad \textit{with} \quad \text{Te}_{\text{so}}^{\bullet}(z) = \sum_{\omega \in \Omega^{+}} \text{Te}_{\omega}^{\bullet} e^{-\omega z} \quad (2.69)$$

$$\text{Te}_{\text{no}}^{\bullet}(z) \times \text{Se}_{-, \text{no}}^{\bullet}(z) = \text{Se}_{+, \text{no}}^{\bullet}(z) \quad \textit{with} \quad \text{Te}_{\text{no}}^{\bullet}(z) = \sum_{\omega \in \Omega^{-}} \text{Te}_{\omega}^{\bullet} e^{-\omega z} \quad (2.70)$$

Thus, whether looking “north” or “south”, we arrive at the elementary identity

$$\text{Te}^{\bullet}(z) = \text{Se}_{+}^{\bullet}(z) \times \text{muSe}_{-}^{\bullet}(z) \quad (2.71)$$

which of course can also be directly derived from the definitions (2.29) paired with (2.59)-(2.62). But we get an interesting extra – namely, that the moulds $\text{Tee}_{\omega}^{\bullet}$ of (2.63) and (2.64) coincide with those defined in the preceding subsection. If we now interpret the resurgence equations (2.63)-(2.68) in the convolutive model, we get an alternative expression

³⁷ We drop the tilde for simplicity.

³⁸ $\text{Taa}_{\omega}^{\bullet}$ is eternal, while $\sum \text{Tee}_{\omega}^{\bullet} e^{-\omega z}$ (respectively $\sum \text{Too}_{\omega}^{\bullet} e^{-\omega z}$) is eternal (respectively olternol).

of Tee_ω^\bullet , Taa_ω^\bullet , Too_ω^\bullet as finite integrals in the ζ -plane, which translate, after some work, into fast-convergent power series. This will stand us in good stead in the *divergent* and above all in the *ramified* cases. But we must first devote a short aside to the question of parity.

Parity aspects. There is something slightly incongruous about the formulae (2.65)-(2.68): they express the monics Taa_ω^\bullet , Too_ω^\bullet , which separate parity, in terms of monomials $Sa^\bullet(z)$, $So^\bullet(z)$, which do not. To remove this blemish, let us replace them by parity-separating monomials $\underline{Sa}^\bullet(z)$, $\underline{So}^\bullet(z)$:

$$\tilde{S}a^\bullet(z) = \tilde{\underline{S}}a^\bullet(z) \times 2(\mathbf{1}^\bullet + e^{J^\bullet(z)})^{-1} \quad (2.72)$$

$$\tilde{S}o^\bullet(z) = \tilde{\underline{S}}o^\bullet(z) \times (\mathbf{1}^\bullet - \frac{1}{2}J^\bullet(z)) \quad (2.73)$$

with $J^{s_1}(z) := z^{-s_1}$ and $J^{s_1, \dots, s_r}(z) := 0$ if $r \neq 1$.

In the case of $\tilde{\underline{S}}o^\bullet$, we get the bonus of a simple induction

$$\tilde{\underline{S}}o^\bullet(z) := H(\partial) \left(\tilde{\underline{S}}o^\bullet(z) \times J^\bullet(z) \right) \quad \text{with} \quad (2.74)$$

$$H(\partial) := \frac{e^\partial}{1 - e^\partial} + \frac{1}{2} = \frac{1}{2} \frac{1 + e^\partial}{1 - e^\partial} = -\frac{1}{2} \cotan\left(\frac{\partial}{2}\right). \quad (2.75)$$

Since the right factors in (2.72)-(2.73) are convergent, the new monomials verify the same resurgence equations as the old ones, with the same resurgence constants:

$$\pm 2\pi i \Delta_\omega \underline{S}a^\bullet(z) = Taa_\omega^\bullet \times \underline{S}a^\bullet(z) \quad (\forall \omega \in \Omega^\pm = 2\pi i \mathbb{Z}^\pm) \quad (2.76)$$

$$\pm 2\pi i \Delta_\omega \underline{S}o^\bullet(z) = Taa_\omega^\bullet \times \underline{S}o^\bullet(z) \quad (\forall \omega \in \Omega^\pm = 2\pi i \mathbb{Z}^\pm). \quad (2.77)$$

Remark. Our new monomials may separate parity and generate the required monics, but they no longer belong to the clear-cut symmetry types *symmetral/symmetrol*, a fact that is reflected in the unusual form of their multiplicative inverses:

$$\text{mu}\tilde{\underline{S}}a^\bullet(z) = \left(\cosh(J^\bullet(z)) \right)^{-2} \times \text{anti}.\tilde{\underline{S}}a^\bullet(z) \circ (-Id^\bullet) \quad (2.78)$$

$$\text{mu}\tilde{\underline{S}}o^\bullet(z) = \left(\mathbf{1}^\bullet - \frac{1}{4}J^\bullet(z) \times J^\bullet(z) \right) \times \text{anti}.\tilde{\underline{S}}o^\bullet(z) \circ (-Id^\bullet) \quad (2.79)$$

If we now ask for monomials that separate parity *and* possess the exact symmetries *and* produce the right monics, we can have that, too, by

setting:

$$\text{var}\tilde{\text{Se}}^\bullet(z) := \tilde{\text{Se}}^\bullet(z) \times (\mathbf{1}^\bullet + J^\bullet(z))^{\frac{1}{2}}$$

$$\text{var}\tilde{\text{Sa}}^\bullet(z) := \tilde{\text{Se}}^\bullet(z) \times \left(2 \tanh \left(\frac{1}{2} J^\bullet(z) \right) \right) = \tilde{\text{Sa}}^\bullet(z) \times \cosh(J^\bullet(z))^{-1}$$

$$\text{var}\tilde{\text{So}}^\bullet(z) := \tilde{\text{Se}}^\bullet(z) \times \left(\frac{J^\bullet(z)}{\mathbf{1}^\bullet - \frac{1}{2} J^\bullet(z)} \right) = \tilde{\text{So}}^\bullet(z) \times \left(\mathbf{1}^\bullet - \frac{1}{2} J^\bullet(z) \times J^\bullet(z) \right)^{\frac{1}{2}}.$$

These variants still verify the resurgence equations (2.76)-(2.77). Moreover:

$$\text{varSe}_+^{s_1, \dots, s_r}(-z) \equiv (-1)^{s_1 + \dots + s_r} \text{varSe}_-^{s_r, \dots, s_1}(-z) \text{ and } \text{varSe}^\bullet \text{ symmetrel}$$

$$\text{varSa}_+^{s_1, \dots, s_r}(-z) \equiv (-1)^{s_1 + \dots + s_r} \text{varSa}_-^{s_r, \dots, s_1}(-z) \text{ and } \text{varSa}^\bullet \text{ symmetral}$$

$$\text{varSo}_+^{s_1, \dots, s_r}(-z) \equiv (-1)^{s_1 + \dots + s_r} \text{varSo}_-^{s_r, \dots, s_1}(-z) \text{ and } \text{varSo}^\bullet \text{ symmetrol}$$

Polylogarithmic monomials. We recall the inductive definition of the polylogarithmic monomials $\tilde{\mathcal{V}}^\bullet(z)$ (symmetral) and monics V^\bullet (alternal), whose proper province is the study of singular, resurgence-inducing ODEs:

$$-(\partial_z + \omega_1 + \dots + \omega_r) \tilde{\mathcal{V}}^{\omega_1, \dots, \omega_r}(z) = \tilde{\mathcal{V}}^{\omega_1, \dots, \omega_{r-1}}(z) z^{-1} \quad (2.80)$$

$$\Delta_{\omega_0} \tilde{\mathcal{V}}^{\omega_1, \dots, \omega_r}(z) = \sum_{\omega_1 + \dots + \omega_i = \omega_0} V^{\omega_1, \dots, \omega_i} \tilde{\mathcal{V}}^{\omega_{i+1}, \dots, \omega_r}(z) \quad (2.81)$$

We also require the (apparently) more general monomials $\mathcal{V}_{\mathcal{H}}^\bullet(z)$, defined by a similar induction:

$$-(\partial_z + \|\bullet\|) \tilde{\mathcal{V}}_{\mathcal{H}}^\bullet(z) = \tilde{\mathcal{V}}_{\mathcal{H}}^\bullet(z) \times \mathcal{H}^\bullet(z) \quad (\mathcal{H}^\bullet(z) \in z^{-1} \mathbb{C}\{z^{-1}\}) \quad (2.82)$$

relative to any *alternal* mould $\mathcal{H}^\bullet(z)$ with values in the ring of convergent power series of z^{-1} (without constant term). Modulo convergent series of z^{-1} , the mould $\tilde{\mathcal{V}}_{\mathcal{H}}^\bullet(z)$ actually reduces to $\tilde{\mathcal{V}}^\bullet(z)$, thanks to the formula:

$$\tilde{\mathcal{V}}_{\mathcal{H}}^\bullet(z) = (\tilde{\mathcal{V}}^\bullet(z) \circ L_{\mathcal{H}}^\bullet) \times \mathcal{L}_{\mathcal{H}}^\bullet(z) \text{ with } L_{\mathcal{H}}^\bullet \in \mathbb{C}, \mathcal{L}_{\mathcal{H}}^\bullet(z) \in z^{-1} \mathbb{C}\{z^{-1}\} \quad (2.83)$$

with an alternal, scalar-valued mould $L_{\mathcal{H}}^\bullet$ and a symmetral, convergent-valued mould $\mathcal{L}_{\mathcal{H}}^\bullet(z)$. Both $L_{\mathcal{H}}^\bullet$ and $\mathcal{L}_{\mathcal{H}}^\bullet(z)$ are defined by the joint induction:

$$L_{\mathcal{H}}^\omega = \sum_{\omega^1 \omega^2 = \omega}^{\omega^2 \neq \emptyset} (\widehat{\mathcal{L}}_H^{\omega^1} * \widehat{\mathcal{H}}^{\omega^2})(|\omega|) - \sum_{\omega^1 \omega^2 = \omega}^{\omega^1, \omega^2 \neq \emptyset} L_{\mathcal{H}}^{\omega^1} \cdot (1 * \widehat{\mathcal{L}}_H^{\omega^2})(|\omega|) \quad (2.84)$$

$$-(\partial_z + \|\bullet\|) \mathcal{L}_{\mathcal{H}}^\bullet(z) = \mathcal{L}_{\mathcal{H}}^\bullet(z) \times \mathcal{H}^\bullet(z) - z^{-1} L_{\mathcal{H}}^\bullet \times \mathcal{L}_{\mathcal{H}}^\bullet(z). \quad (2.85)$$

The first relation, (2.84), expresses the constant $L_{\mathcal{H}}^{\omega}$ in terms of earlier (shorter) mould components. The second relation, (2.85), when interpreted in the convolutive model, says that $(\zeta - |\omega|)\widehat{\mathcal{L}}_{\mathcal{H}}^{\omega}(\zeta)$ is equal to an entire function $\widehat{\mathcal{E}}^{\omega}(\zeta)$ which, due to (2.84), vanishes for $\zeta = |\omega|$. So $\widehat{\mathcal{L}}_{\mathcal{H}}^{\omega}(\zeta)$, too, is an entire function with at most exponential growth, and that makes $\mathcal{L}_{\mathcal{H}}^{\omega}(z)$ a convergent power series of z^{-1} . The resurgence constants $V_{\mathcal{H}}^{\bullet}$ associated with $\widetilde{\mathcal{V}}_{\mathcal{H}}^{\bullet}(z)$ also reduce to the polylogarithmic monics V^{\bullet} , since $\widetilde{\mathcal{V}}_{\mathcal{H}}^{\omega}(z)$, owing to (2.83), verifies the following resurgence equations:

$$\Delta_{\omega_0} \widetilde{\mathcal{V}}_{\mathcal{H}}^{\omega_1, \dots, \omega_r}(z) = \sum_{\omega_1 + \dots + \omega_i = \omega_0} V_{\mathcal{H}}^{\omega_1, \dots, \omega_i} \widetilde{\mathcal{V}}_{\mathcal{H}}^{\omega_{i+1}, \dots, \omega_r}(z) \quad (2.86)$$

with $V_{\mathcal{H}}^{\bullet} = V^{\bullet} \circ L_{\mathcal{H}}^{\bullet}$

Multizetaic monomials in terms of polylogarithmic monomials. From what precedes and from the decomposition

$$\frac{e^{-\zeta}}{1 - e^{-\zeta}} + \frac{1}{2} = H(-\zeta) = \sum_{|\omega| \leq \rho} \frac{1}{\zeta + \omega} + H_{\rho}(-\zeta) \quad (\forall \rho > 0) \quad (2.87)$$

we can see that, for $|\zeta|, |\omega| < \rho$, the monomials $\widehat{\mathcal{S}}^s(\zeta), \widehat{\mathcal{S}}a^s(\zeta), \widehat{\mathcal{S}}o^s(\zeta)$, and the monics $Tee_{\omega}^s, Taa_{\omega}^s, Too_{\omega}^s$ that go with them, can be expressed as finite sums of three ingredients:

- (i) classical monomials $\widehat{\mathcal{V}}^{\omega}(\zeta)$ and monics $V^{\omega}(\zeta)$ indexed by sequences ω that are ρ -small, *i.e.* such that $|\omega^1| \leq \rho, |\omega^2| \leq \rho$ for all factorisation $\omega = \omega^1 \cdot \omega^2$;
- (ii) functions of type $\widehat{\mathcal{L}}_{\mathcal{H}}^{\omega}(\zeta)$ which, though not entire, are holomorphic on the disk $|\zeta| \leq \rho$;
- (iii) the companion monics $L_{\mathcal{H}}^{\omega}$.

Altogether, this results in an effective procedure for calculating the monics $Tee_{\omega}^s, Taa_{\omega}^s, Too_{\omega}^s$, with a guaranteed geometric rate of convergence which, moreover, can be arbitrarily improved by taking ρ large (albeit at the cost of increasing the number of summands).

2.5 The non-standard case ($\rho \neq 0$). Normalisation

If we now drop the condition that ensured convergence, namely $s_1, s_r \neq 1$, and yet insist on retaining all properties and symmetries of our moulds, we must do two things to our infinite series: *truncate* them and *correct*

them. Concretely, we must set

$$\begin{aligned} \text{Te}^\bullet(z) &:= \lim_{k \rightarrow \infty} \text{Te}_k^\bullet(z) &:= \lim_{k \rightarrow \infty} \text{mucoSe}_k^\bullet \times \text{doTe}_k^\bullet(z) \times \text{coSe}_k^\bullet \\ \text{Se}_\pm^\bullet(z) &:= \lim_{k \rightarrow \infty} \text{Se}_{k,\pm}^\bullet(z) &:= \lim_{k \rightarrow \infty} \text{mucoSe}_k^\bullet \times \text{doSe}_{k,\pm}^\bullet(z) \\ \text{muSe}_\pm^\bullet(z) &:= \lim_{k \rightarrow \infty} \text{muSe}_{k,\pm}^\bullet(z) &:= \lim_{k \rightarrow \infty} \text{mudoSe}_{k,\pm}^\bullet(z) \times \text{coSe}_k^\bullet. \end{aligned}$$

Here, the symmetrel *dominant* factors Te^\bullet , $\text{doSe}_{k,\pm}^\bullet$, $\text{mudoSe}_{k,\pm}^\bullet$ are defined as in (2.29) and (2.55)-(2.58) but with sums truncated at $\pm k$ instead of $\pm\infty$. Thus

$$\text{doTe}_k^{s_1, \dots, s_r}(z) := \sum_{-k \leq n_r < \dots < n_1 \leq k} (n_r + z)^{-s_r} \dots (n_1 + z)^{-s_1} \quad (\forall s_i). \quad (2.88)$$

As for the symmetrel, z -constant *corrective* factors $\text{coSe}_{k\pm}^\bullet$ and $\text{invcoSe}_{k\pm}^\bullet$, their definition reduces to

$$\text{coSe}_k^{s_1, \dots, s_r} := \frac{(c + \log k)^r}{r!} \quad \text{if } (s_1, \dots, s_r) = (1, \dots, 1) \quad (2.89)$$

$$\text{mucoSe}_k^{s_1, \dots, s_r} := \frac{(-c - \log k)^r}{r!} \quad \text{if } (s_1, \dots, s_r) = (1, \dots, 1) \quad (2.90)$$

$$\text{coSe}_k^{s_1, \dots, s_r} = \text{mucoSe}_k^{s_1, \dots, s_r} := 0 \quad \text{if } (s_1, \dots, s_r) \neq (1, \dots, 1). \quad (2.91)$$

In the formal model, the resurgent-valued moulds $\tilde{\text{Se}}^\bullet$ and $\text{mu}\tilde{\text{Se}}^\bullet$ are still uniquely defined by the induction (2.50) together with the condition

$$\tilde{\text{Se}}^s(z), \text{mu}\tilde{\text{Se}}^s(z) \in \mathbb{Q}[[z^{-1}]] \otimes \mathbb{Q}[(c + \log z)] \dot{-} \mathbb{Q} \quad (\forall s \neq \emptyset). \quad (2.92)$$

The normalising condition, in other words, is that $\tilde{\text{Se}}^s(z)$ and $\text{mu}\tilde{\text{Se}}^s(z)$, as formal series in z^{-1} and polynomials in the bloc $(c + \log z)$, should have no constant term.

In the sectorial models, the c -normalisation implies:

$$\text{Se}_\pm^{\overbrace{1, \dots, 1}^{r \text{ times}}}(0) = \frac{(\gamma - c)^r}{r!} \quad ; \quad \text{muSe}_\pm^{\overbrace{1, \dots, 1}^{r \text{ times}}}(0) = \frac{(c - \gamma)^r}{r!} \quad (2.93)$$

with

$$\gamma = \lim_{k \rightarrow \infty} \left(1 + \frac{1}{2} + \dots + \frac{1}{k} - \log k \right) = 0.577215\dots = \text{Euler constant}. \quad (2.94)$$

For multitangents, we may still formally apply the procedure (2.40)-(2.41) of Section 2.3 to reduce them into combinations of monotangents

and multizetas, but this time we are liable to get formally divergent multizetas. The c -normalisation then amounts to setting $\zeta(1) = ze^1 := \gamma - c$ and to adopting for all divergent multizetas³⁹ the unique *symmetrel extension* compatible with that initial choice.⁴⁰

There are two natural choices for the normalisation constant c :

(i) Either we set $c = 0$, in which case we eschew γ in the formal model but at the cost of introducing it in the convolutive and sectorial models. It also complicates the definition of the multitangents and multizetas, since it forces us to set $ze^1 = \gamma$, which however is not entirely unnatural, in view of the formula

$$\sigma \Gamma(\sigma) = \exp \left(-\gamma \sigma + \sum_{2 \leq n} (-1)^n \frac{\zeta(n)}{n} \sigma^n \right) \tag{2.95}$$

(ii) Or we set $c = \gamma$, which forcibly introduces γ into the formal model but rids us of it everywhere else, including in the definition of multitangents and multizetas, since it amounts to setting $ze^1 = 0$. This shall be our preferred choice.

2.6 The ramified case ($p > 1$) and the localisation constraints

For diffeos f of tangency order $p > 1$, the prepared form (1.2) becomes a power series of $z^{-1/p}$. This inevitably leads to moulds whose indices s_i (the *weights*) are no longer in \mathbb{N}^* but in $p^{-1}\mathbb{N}^*$ or even, in some instances, in $p^{-1}\mathbb{Z}^*$.

Most results, starting with the symmetry relations, carry over to that case, but with three significant changes:

- (i) The *finite* reduction of multitangents into monotangents and multizetas breaks down,
- (ii) The Fourier coefficients $Tee_\omega^s, Taa_\omega^s, Too_\omega^s$, which are the *direct* ingredients of the invariants $A_\omega(f)$, cease to be expressible as finite sums of multizetas (even ramified ones).
- (iii) The formulae (2.40)-(2.41) still make formal sense but lead to expansions which are not only infinite but also divergent. When properly re-summed, they yield the correct expressions, but from the point of view of calculational expediency, this approach is worthless. Of course, straightforward Fourier analysis in the upper and

³⁹ *I.e.* for all multizetas with initial index $s_1 = 1$.

⁴⁰ Thus $ze^{1,1} := -\frac{1}{2}ze^2 + \frac{1}{2}(\gamma - c)^2$, $ze^{1,2} := -ze^{2,1} - ze^3 + (\gamma - c)ze^2$ etc. There exist simple formulae for calculating the symmetrel extension of all multizetas relative to any given choice of ze^1 .

lower halves of the z -plane would yield the coefficients Tee_ω^s , Taa_ω^s , Too_ω^s , but not in the form of nice convergent series, and again at great cost.

The resurgence approach of Section 2.4 and Section 2-5, on the other hand, survives ramification without any modification. When pursued to the end, this approach even leads to some sort of functional equation for multizetas, that is to say, to something vaguely resembling the classical relation between $\zeta(s)$ and $\zeta(1-s)$.

However, the presence of ramifications makes it advisable to rotate our multitangents and monomials, so that we may handle functions which (as far as the index symmetries permit) assume real values on the main real half-axis. Thus, instead of Te^\bullet , \tilde{Se}^\bullet etc, we shall consider:

$$\text{Teh}^{s_1, \dots, s_r}(z) := \left(\frac{1}{i}\right)^{s_1 + \dots + s_r} \text{Te}^{s_1, \dots, s_r}\left(\frac{z}{i}\right) \quad (2.96)$$

$$\tilde{\text{Seh}}^{s_1, \dots, s_r}(z) := \left(\frac{1}{i}\right)^{s_1 + \dots + s_r} \tilde{\text{Se}}^{s_1, \dots, s_r}\left(\frac{z}{i}\right). \quad (2.97)$$

No finite reduction to monotangents. If we consider the equation (2.63) for $r=1$ but with s_1 in \mathbb{Q}^+ and interpret it correctly in the Borel plane, we see that the familiar formula (2.45) for the Fourier coefficients of monotangents transposes (taking the $\pi/2$ -rotation into account) to the fractional case:

$$\text{Teh}^{s_1}(z) = \sum_{\omega \in 2\pi\mathbb{N}} \text{Teh}_\omega^{s_1} \quad \text{with} \quad \text{Teh}_\omega^{s_1} = 2\pi \frac{\omega^{s_1-1}}{\Gamma(s_1)}. \quad (2.98)$$

So the product⁴¹ $\text{Teh}^{s_1} \text{Teh}^{s_2} \equiv \text{Teh}^{s_1, s_2} + \text{Teh}^{s_2, s_1} + \text{Teh}^{s_1+s_2}$ has Fourier coefficients of the form

$$\text{Teh}_\omega^{s_1, s_2} + \text{Teh}_\omega^{s_2, s_1} + \text{Teh}_\omega^{s_1+s_2} = \frac{(2\pi)^{s_1+s_2}}{\Gamma(s_1)\Gamma(s_2)} \sum_{n_1+n_2=n}^{\omega=2\pi n} n_1^{s_1-1} n_2^{s_2-1} \quad (2.99)$$

and this makes it obvious that Teh^{s_1, s_2} and Teh^{s_2, s_1} cannot simultaneously be finite sums of monotangents Teh^s .

⁴¹ Since symmetrelity survives ramification.

SingTeh[•] still determines *Teh*[•] but in a completely new way. For $n \rightarrow +\infty$, the right-hand side of (2.99) can be shown to possess a divergent but n -resurgent and Borel resummable asymptotic expansion of the form $n^{s_1+s_2-1} \sum c_s n^{-s}$ ($s \in \mathbb{Q}^+$).

More generally, by adapting the argument leading to (2.40), one can easily calculate the ramified Laurent series of any multitangent *Teh*^s:

$$\text{Teh}^s(z) = \text{SingTeh}^s(z) + \text{RegTeh}^s(z) = \sum_{\nu \in \mathbb{N}} \theta_\nu^s z^\nu + \sum_{\nu \in \mathbb{Q}-\mathbb{N}} \theta_\nu^s z^\nu \quad (2.100)$$

with its multizetaic coefficients θ_ν^s . As in the non-ramified case, *Teh*^s is still completely determined by its singular part *SingTeh*^s. We may even, if we so wish, derive from the singular part of (2.100) a formal reduction of *Teh*^s into monotangents:

$$\text{Teh}^s(z) = \sum_{\sigma \in \mathbb{Q}-\mathbb{N}}^{-\infty < \sigma \leq |s|} \tau_\sigma^s \text{Teh}^\sigma(z) \quad \text{with} \quad \tau_\sigma^s := \theta_{-\sigma}^s \quad (2.101)$$

but the series defined in this way will be, generally speaking, everywhere divergent, even if we take care to correctly define, as in (2.108) *infra*, the monotangents *Teh*^{s₁}(z) with index $s_1 \in (1, -\infty)$. If we now attempt to calculate the Fourier coefficient of a general multitangent:

$$\text{Teh}^{s_1, \dots, s_r}(z) =: \sum_{\omega \in 2\pi\mathbb{N}^*} \text{Teh}_\omega^{s_1, \dots, s_r} e^{-\omega z} \quad (2.102)$$

by identifying the Fourier coefficients on both sides of (2.101) and taking (2.98) into account:

$$\begin{aligned} \text{Teh}_\omega^s &= \sum_{\sigma \in \mathbb{Q}-\mathbb{N}}^{-\infty < \sigma \leq |s|} \tau_\sigma^s \text{Teh}_\omega^\sigma = 2\pi \sum_{\sigma \in \mathbb{Q}-\mathbb{N}}^{-\infty < \sigma \leq |s|} \tau_\sigma^s \frac{\omega^{\sigma-1}}{\Gamma(\sigma)} \\ &= -2 \sum_{\substack{-|s| < \nu < +\infty \\ -\nu \in \mathbb{Q}-\mathbb{N}}} \theta_\nu^s \Gamma(1+\nu) \sin(\pi\nu) \omega^{-\nu-1} \end{aligned} \quad (2.103)$$

what we get on the right-hand side is again a divergent expansion, which is ω -resurgent and Borel resummable. But Borel resummation in the present instance amounts to calculating the following loop integral:

$$\text{Teh}_\omega^{s_1, \dots, s_r} = \frac{1}{i} \oint_{-\infty-\epsilon i}^{-\infty+\epsilon i} \text{Teh}^{s_1, \dots, s_r}(z) e^{\omega z} dz \quad (2.104)$$

$$= \frac{1}{i} \oint_{-\infty-\epsilon i}^{-\infty+\epsilon i} \text{SingTeh}^{s_1, \dots, s_r}(z) e^{\omega z} dz \quad (2.105)$$

with an integration path connecting $-\infty - \epsilon i$ to $-\infty + \epsilon i$ and having as its middle part a small half-circle $\{|z| = \epsilon, \Re z > 0\}$ centered at the origin 0 , and located in the *main* positive half-plane. This is indeed the proper procedure for retrieving the Fourier coefficients of $Teh^s(z)$ from the singular part $SingTeh^s(z)$.

The ramified localisation constraints. Defining the formal multitangent-to-monotangent reduction as in (2.101), we get the *reduction constraints*:

$$\begin{array}{ccc} Teh^{s^1}(z).Teh^{s^2}(z) & \xrightarrow{\text{reduction}} & (\sum \tau_{s_1}^{s^1} Teh^{s^1}(z)).(\sum \tau_{s_2}^{s^2} Teh^{s^2}(z)) \\ \downarrow \text{linearisation} & & \downarrow \text{linearisation} \\ \sum \epsilon_{s_3}^{s^1, s^2} Teh^{s^3}(z) & \xrightarrow{\text{reduction}} & \sum \epsilon_{s_3}^{s^1, s^2} \tau_{s_3}^{s^3} Teh^{s^3}(z) = \sum \tau_{s_1}^{s^1} \tau_{s_2}^{s^2} \epsilon_{s_3}^{s_1, s_2} Teh^{s^3}(z) \end{array}$$

with elementary, integer-valued coefficients $\epsilon_{s^i, s^j}^{s^k}$ and coefficients $\tau_{s^i}^{s^j}$ that are finite, homogeneous sums of multizetas of total weight $\|s^i\| - s_i - 1$. Although the multitangent expansions diverge, by equating (in the right-lower corner) the coefficients in front of each $Teh^{s^3}(z)$ we get a system of finite relations between multizetas.

Using instead the (locally convergent) expansions at $z = 0$, we get the *localisation constraints*, which are only seemingly more general than the reduction constraints:

$$\begin{array}{ccc} Teh^{s^1}(z).Teh^{s^2}(z) & \xrightarrow{\text{localisation}} & (\sum \theta_{v_1}^{s^1} z^{v_1}).(\sum \theta_{v_2}^{s^2} z^{v_2}) \\ \downarrow \text{linearisation} & & \downarrow \text{linearisation} \\ \sum \epsilon_{s_3}^{s^1, s^2} Teh^{s^3}(z) & \xrightarrow{\text{localisation}} & \sum \epsilon_{s_3}^{s^1, s^2} \theta_{v_3}^{s^3} z^{v_3} = \sum \theta_{v_1}^{s^1} \theta_{v_2}^{s^2} z^{v_1+v_2} \end{array}$$

Here, the coefficients $\theta_{n_j}^{s^i}$ are finite, homogeneous sums of multizetas of total weight $\|s^i\| + n_j$.

Lastly, for the Fourier coefficients Teh_{ω}^{\bullet} (these monics, we recall, are the direct ingredients of the holomorphic invariants $A_{\omega}(f)$) we get the following system of constraints:

$$\begin{array}{ccc} Teh^{s^1}(z).Teh^{s^2}(z) & \xrightarrow{\text{Fourier}} & (\sum Teh_{\omega_1}^{s^1} e^{-\omega_1 z}).(\sum Teh_{\omega_2}^{s^2} e^{-\omega_2 z}) \\ \downarrow \text{linearisation} & & \downarrow \text{linearisation} \\ \sum \epsilon_{s_3}^{s^1, s^2} Teh^{s^3}(z) & \xrightarrow{\text{Fourier}} & \sum \epsilon_{s_3}^{s^1, s^2} Teh_{\omega_3}^{s^3} e^{-\omega_3 z} = \sum Teh_{\omega_1}^{s^1} Teh_{\omega_2}^{s^2} e^{-(\omega_1+\omega_2)z}. \end{array}$$

2.7 Meromorphic s -continuation of Seh^s and Teh^s etc.

The whole subject of s -continuation, being simply incidental to our investigation, shall receive only a sketchy treatment.

Meromorphic s -continuation of the multizetas ze^s . There exist various ways of proving the existence of a meromorphic continuation of ze^{s_1, \dots, s_r} to the whole of \mathbb{C}^r , with a singularity locus confined to the hyperplanes $\cup_{i,n} \{s_1 + \dots + s_i \in i - n\}$ ($n \in \mathbb{N}$). One of them relies on the convergent expansions

$$\begin{aligned}
 ze^{s_1, \dots, s_i, \dots, s_r} &= - \sum_{k_i \geq 1} \frac{\Gamma(k_i + s_i)}{(k_i + 1)! \Gamma(s_i)} ze^{s_1, \dots, s_i + k_i, \dots, s_r} \\
 &\quad + \frac{1}{s_i - 1} ze^{s_1, \dots, s_i + s_{i+1} - 1, \dots, s_r} \\
 &\quad - \sum_{k_i \geq -1} \frac{\Gamma(k_i + s_i)}{(k_i + 1)! \Gamma(s_i)} ze^{s_1, \dots, s_{i-1} + s_i + k_i, \dots, s_r}
 \end{aligned}
 \tag{2.106}$$

valid for $1 < i < r$, and with slight modifications for $i = 1$ or $i = r$ as well. The expansion (2.107) in turn results from plugging the identity

$$n_i^{-s_i} = \sum_{k_i \geq 0} \frac{\Gamma(k_i + s_i)}{k_i! \Gamma(s_i)} (1 + n_i)^{-s_i - k_i}$$

into the definition of $ze^{s_1, \dots, s_i, \dots, s_r}$ or rather $ze^{s_1, \dots, s_i - 1, \dots, s_r}$.

Similar expansions hold for za^s and zo^s , of course, but here the parity properties have the effect of ‘halving’ the number of hyperplanes in the singularity locus.

The multiresidues at singular points $s \in \mathbb{Z}^r$ are simple combinations of convergent multizetas with indices $s' \in \mathbb{N}^{r'}$. The more negative components s_i in s , the smaller the depths r' of the convergent multizetas contributing to the multiresidues.

Meromorphic s -continuation of the multitangents $Teh^s(z)$. The s -continuation of multitangents proceeds on the same lines as that of multizetas. The main difference is the persistence, for multitangents, of convergent ‘polar’ expansions that rely on convergence-restoring corrections $[\dots]_K^{-s}$. For any integer K we set:

$$\begin{aligned}
 [z \pm i n]_K^{-s} &= \sum_{0 \leq k \leq K} (\pm i)^k e^{\mp \frac{1}{2} \pi i s} \frac{\Gamma(k + s)}{k! \Gamma(s)} n^{-s-k} z^k \quad (0 < n, 0 < \Re z) \\
 [z]_K^{-s} &= \sum_{0 \leq k \leq K} 2 (\pm i)^k \cos\left(\frac{1}{2} \pi i s\right) \frac{\Gamma(k + s)}{k! \Gamma(s)} \zeta(s + k) z^k.
 \end{aligned}
 \tag{2.107}$$

For $s \in \mathbb{C} - \mathbb{Z}^-$, the monotangents admit ‘polar’ expansions of the form

$$Teh^s(z) = \sum_{n \in \mathbb{Z}} \left((z + i n)^{-s} - [z \pm i n]_K^{-s} \right) \quad (\Re(s) + K > 2) \tag{2.108}$$

There exist exact analogues for the multizetas.

Meromorphic s -continuation of the monomials $Seh^s(z)$. In the convolutive model (hence in the other models as well), the s -continuation of the monomials $Seh^s(z)$ presents no difficulty, and provides an alternative approach to the s -continuation of the multizetas and multizetas, since the latter can be derived from the monomials $Seh^s(z)$.

The closest thing to a reflection equation for multizetas. Let us start for orientation with depth one, *i.e.* with ordinary zetas. Calculating the Laurent expansion of $Teh^s(z)$ at $z = 0$, and assuming $\Re(s) > 1$, we find:

$$Teh^s(z) := z^{-s} + 2 \zeta(s) \cos\left(\frac{\pi}{2}s\right) + o(1). \tag{2.109}$$

Due to (2.108), this also extends to all regular values of s , with the only difference that when $\Re(s) < 0$ the term z^{-s} is absorbed by $o(1)$. On the other hand, starting from the Fourier expansion of $Teh^s(z)$ and assuming $\Re(s) < 0, s \notin -\mathbb{N}$, we find

$$Teh^s(z) := 2\pi \sum_{0 < n} \frac{(2\pi n)^{s-1}}{\Gamma(s)} e^{-2\pi n z} = (2\pi)^s \frac{\zeta(1-s)}{\Gamma(s)} + o(1). \tag{2.110}$$

Comparing (2.109) and (2.110) for $\Re(s) < 0$, we recover the classical reflection equation for the Riemann zeta function:

$$\begin{aligned} 2 \zeta(s) \cos\left(\frac{\pi}{2}s\right) &= (2\pi)^s \frac{\zeta(1-s)}{\Gamma(s)} \\ \iff \zeta(s) &= 2^s \pi^{s-1} \sin\left(\frac{\pi}{2}s\right) \Gamma(1-s) \zeta(1-s). \end{aligned}$$

To find out if something of that reflection equation survives at depth $r \geq 2$, let us fix a sequence $\mathbf{s} = (s_1, \dots, s_r)$ with $\Re(s_i) < 0$ and all partial sums $s_1 + \dots + s_i, s_i + \dots + s_r$ not in \mathbb{Z} , and let us exploit the commutative diagram:

$$\begin{array}{ccc} Teh^{\mathbf{s}}(z) & \xrightarrow{\text{reduction}} & \text{sing}Teh^{\mathbf{s}}(z) \\ & \searrow & \downarrow \\ & & \text{reg}Teh^{\mathbf{s}}(z). \end{array}$$

The leading term of the Laurent expansion of $Teh^{\mathbf{s}}(z)$ at $z = 0$ is:

$$Teh^{\mathbf{s}}(z) = \sum_{\substack{s' s'' = \mathbf{s}}} e^{\frac{\pi i}{2}(|s''| - |s'|)} z e^{s'} \text{vize}^{s''} + o(1) \tag{2.111}$$

with $vize^{s_1, \dots, s_r} := ze^{s_r, \dots, s_1}$. As for the purely singular part $\sum c_s z^{-s}$ of that same Laurent expansion, it yields the formal, infinite, monotangential expansion $\sum c_s Teh^s(z)$ of $Teh^s(z)$:

$$Teh^s(z) \stackrel{\text{formally}}{=} \sum_{\substack{0 \leq n_i \in \mathbb{N} \\ \underline{s}^i s_i \bar{s}^i = s}} Teh^{s_i - n_i}(z) Ze^{\underline{s}^i, n_i, \bar{s}^i}. \quad (2.112)$$

The scalars $Ze^{\underline{s}^i, n_i, \bar{s}^i}$ are here finite, homogeneous superposition of multizetas of total weight $n_i - |\underline{s}^i| - |\bar{s}^i| = n_i + s_i - |s|$. All monotangents $Teh^{s_i - n_i}(z)$ having indices of negative real part, they tend to known constants as z goes to 0:

$$Teh^s(z) \stackrel{\text{formally}}{=} \sum_{\substack{0 \leq n_i \in \mathbb{N} \\ \underline{s}^i s_i \bar{s}^i = s}} (2\pi)^{s_i - n_i} \frac{\zeta(1 + n_i - s_i)}{\Gamma(s_i - n_i)} Ze^{\underline{s}^i, n_i, \bar{s}^i} + o(1). \quad (2.113)$$

Finally, formally equating (2.111) and (2.113), we get:

$$\sum_{s' s'' = s} e^{\frac{\pi i}{2} (|s''| - |s'|)} ze^{s'} vize^{s''} \approx \sum_{\substack{0 \leq n_i \in \mathbb{N} \\ \underline{s}^i s_i \bar{s}^i = s}} (2\pi)^{s_i - n_i} \frac{\zeta(1 + n_i - s_i)}{\Gamma(s_i - n_i)} Ze^{\underline{s}^i, n_i, \bar{s}^i}. \quad (2.114)$$

The finitely many multizetas on the left-hand side all carry indices with *negative* real parts, and two of them (ze^s and $vize^s$) are exactly of depth r . On the right-hand side, all but a finite number of multizetas carry indices with *positive* real parts, and all are of depth $< r$.

This, sadly, is the closest thing we can get, with this approach, to a reflection identity for multizetas. Note that the expansion on the right-hand side of (2.114) is divergent, but Borel resummable when viewed as a series in negative powers of the ‘variable’ $t := 2\pi$.

Ultimately, the obstruction to finding a satisfactory reflection formula is the non-existence of a multivariate, symmetrel Poisson formula. The fact is that the Fourier transform of the symmetrel Poisson distribution De^\bullet

$$De^{x_1, \dots, x_r} := \sum_{-\infty < n_1 < \dots < n_r < +\infty} \delta(x_1 - n_1) \dots \delta(x_r - n_r) \quad (\delta = \text{Dirac}) \quad (2.115)$$

not only differs from De^\bullet , but is not even an atomic distribution.

3 Collectors and connectors in terms of f

3.1 Operator relations

We begin with identity-tangent germs f in the standard class $(p, \rho) = (1, 0)$, *i.e.* of the form $f = l \circ g$, with the unit shift $l(z) = z+1$ and a germ

$g(z) = z + \underline{g}(z) = z + \mathcal{O}(z^{-2})$ which may be viewed as a perturbation. This is an invitation to expand everything (collectors, connectors, invariants) in series with a 1-linear, 2-linear, etc, part in \underline{g} or, more conveniently, in the corresponding operator $\underline{G} := G - 1$.

The iterator f^* is characterised by the germ identities $f^* = l^{-1} \circ f^* \circ f \equiv l^{-1} \circ f^* \circ l \circ g$ which in order-reversing operator notation⁴² read:

$$F^* = G F_{:1}^* \quad \text{with} \quad F_{:1}^* := L F^* L^{-1}. \tag{3.1}$$

To solve (3.1) while respecting the symmetry between f, g and f^{-1}, g^{-1} , we take as our basic ‘infinitesimals’ the following operators

$$\underline{G}_{:n}^+ := L^n \cdot (G - 1) \cdot L^{-n} \quad (n_i \in \mathbb{Z}) \tag{3.2}$$

$$\underline{G}_{:n}^- := L^n \cdot (G^{-1} - 1) \cdot L^{-n} \quad (n_i \in \mathbb{Z}). \tag{3.3}$$

With the notations of Section 1.2, this leads straightaway to simple formal expansions for the iterators

$$F_+^* = 1 + \sum_{1 \leq r} \sum_{0 \leq n_r < \dots < n_1} \underline{G}_{:n_r}^+ \dots \underline{G}_{:n_1}^+ \quad (n_i \in \mathbb{Z}) \tag{3.4}$$

$$F_-^* = 1 + \sum_{1 \leq r} \sum_{n_1 < \dots < n_r < 0} \underline{G}_{:n_r}^- \dots \underline{G}_{:n_1}^- \quad (n_i \in \mathbb{Z}) \tag{3.5}$$

$${}^*F_+ = 1 + \sum_{1 \leq r} \sum_{0 \leq n_1 < \dots < n_r} \underline{G}_{:n_r}^- \dots \underline{G}_{:n_1}^- \quad (n_i \in \mathbb{Z}) \tag{3.6}$$

$${}^*F_- = 1 + \sum_{1 \leq r} \sum_{n_r < \dots < n_1 < 0} \underline{G}_{:n_r}^+ \dots \underline{G}_{:n_1}^+ \quad (n_i \in \mathbb{Z}). \tag{3.7}$$

These formulae, in turn, combine to produce new expansions which, depending on how we analyse them (- whether in terms of multitanents or Fourier series -) shall yield the collectors \mathfrak{P} or the connectors Π in operator form:

$$\mathfrak{P}^+ \approx \Pi^+ := {}^*F_- \cdot F_+^* = 1 + \sum_{1 \leq r} \sum_{n_r < \dots < n_1} \underline{G}_{:n_r}^+ \dots \underline{G}_{:n_1}^+ \quad (n_i \in \mathbb{Z}) \tag{3.8}$$

$$\mathfrak{P}^- \approx \Pi^- := {}^*F_+ \cdot F_-^* = 1 + \sum_{1 \leq r} \sum_{n_1 < \dots < n_r} \underline{G}_{:n_r}^- \dots \underline{G}_{:n_1}^- \quad (n_i \in \mathbb{Z}). \tag{3.9}$$

For standard diffeos f , the above expansions for $F^*, {}^*F$ (respectively $\Pi^{\pm 1}$) are easily shown to *converge* when they are made to act on test

⁴² To diffeos $f, g \dots$ we associate the operators $F, G \dots$ of postcomposition by $f, g \dots$

functions that are defined on suitably extended U-shaped domains (respectively on suitably distant half-planes $|\Im(z)| \gg 1$). See Section 7.2. *But at this stage we do not have to worry about convergence: we shall provisionnaly (up to Section 6 inclusively) regard our connectors and collectors as generating functions that carry, in conveniently compact form, the various k-linear contributions⁴³. Each k-linear contribution unproblematically converges, and for the moment this is all we require.*

The real challenge is to extract from these expansions (- first in the standard, then in the general case -) *theoretically appealing, analytically transparent, and computationally manageable* expressions for (in that order) the *collectors, connectors, and invariants*.

3.2 The direct scheme: from g to p

To break down the expansions (3.8)-(3.9) into sums of multitanagents, we require scalar coefficients Γ_{\pm}^n that can be collectively defined by the generating function:

$$\left[\underline{G}_{:c^{-1}}^{\pm} \cdots \underline{G}_{:c^{-1} \cdot z}^{\pm} \right]_{z=0} =: \sum \Gamma_{\pm}^{n_1, \dots, n_r} c_1^{n_1} \dots c_r^{n_r} \tag{3.10}$$

with
$$\underline{G}_{:c^{-1}}^{\pm} = \sum_{1 \leq k} \frac{1}{k!} (g^{\pm 1}(z + c^{-1}) - (z + c^{-1}))^k \partial_z^k. \tag{3.11}$$

The collectors then read:

$$p^+(z) = z + \sum_{1 \leq r} \sum_{n_i} \Gamma_+^{n_1, \dots, n_r} \text{Te}^{n_1, \dots, n_r}(z) \tag{3.12}$$

$$p^-(z) = z + \sum_{1 \leq r} \sum_{n_i} \Gamma_-^{n_r, \dots, n_1} \text{Te}^{n_1, \dots, n_r}(z) \tag{3.13}$$

with an order reversal between (3.10) and (3.12) that reflects the order reversal between (3.8) and (3.9).

Let us give an alternative, more analytical expansion. We first set

$$\frac{1}{n!} (g(z) - z)^n =: \sum_{2n \leq s} g_{n,s}^+ z^{-s+1} \quad , \quad \frac{1}{n!} (g^{-1}(z) - z)^n =: \sum_{2n \leq s} g_{n,s}^- z^{-s+1}$$

Next, to account for the action of the *derivation* operators ∂_z implicit in the definition of the *substitution* operators $\underline{G}_{:n}^{\pm}$, we require integers δ_{\bullet}

⁴³ k-linear, that is, in the ‘perturbation’ g or its coefficients g_n

defined by⁴⁴

$$\sum_{\sum(n_i-l_i)=1} \delta_{n_1, \dots, n_r}^{l_1, \dots, l_r} x_1^{l_1} \dots x_r^{l_r} \equiv x_1^{n_2} (x_1+x_2)^{n_3} \dots (x_1+\dots+x_{r-1})^{n_r} \quad (3.14)$$

Letting the operators on both sides of (3.8) respectively (3.9) act on the test function z , and collecting all r -linear summands, we find the sought-after expansions for the collectors p^\pm :

$$p^+(z) \equiv \sum_{1 \leq r} \sum_{\substack{0 \leq l_i \\ 1 \leq n_i}}^{n_i+l_i \leq s_i} (-1)^{n-1} \delta_{n_1, \dots, n_r}^{l_1, \dots, l_r} \text{Te}^{s_1, \dots, s_r}(z) \prod_{1 \leq i \leq r} \frac{(s_i-1)! g_{n_i, s_i-l_i+1}^+}{(s_i-l_i-1)!} \quad (3.15)$$

$$p^-(z) \equiv \sum_{1 \leq r} \sum_{\substack{0 \leq l_i \\ 1 \leq n_i}}^{n_i+l_i \leq s_i} (-1)^{n-1} \delta_{n_1, \dots, n_r}^{l_1, \dots, l_r} \text{Te}^{s_r, \dots, s_1}(z) \prod_{1 \leq i \leq r} \frac{(s_i-1)! g_{n_i, s_i-l_i+1}^-}{(s_i-l_i-1)!} \quad (3.16)$$

with $n := n_1 + \dots + n_r$.

3.3 The affiliate-based scheme: from g_\diamond to p_\diamond

We shall now express the general affiliate p_\diamond of p in terms of the corresponding affiliate g_\diamond of g – not so much for the sake of p_\diamond , but to prepare for the specialisations g_* (generator) and $g_\sharp, g_{\sharp\sharp}$ (mediators), and to show what is so special about these three cases.

The first step is to take our stand on the trivial affiliate - p itself - and to observe that after re-indexation, (3.8) may be re-written as

$$\underline{\Pi}^+ = \sum_{1 \leq r} \sum_{n_i \in \mathbb{Z}} \mathfrak{D}^{n_1, \dots, n_r} \underline{G}_{n_1}^+ \dots \underline{G}_{n_r}^+ \quad (3.17)$$

with $\underline{\Pi}^+ := \Pi^+ - 1$, $\underline{G}^+ := G^+ - 1$, $\underline{G}_n^+ := L^n \underline{G}^+ L^{-n}$ and with an elementary ‘ordering mould’ \mathfrak{D}^\bullet , clearly of symmetrel type:

$$\mathfrak{D}^{n_1} := 1, \quad \mathfrak{D}^{n_1, \dots, n_r} := 1 \quad \text{if } n_1 < \dots < n_r \quad \text{resp.} := 0 \text{ otherwise.} \quad (3.18)$$

Let us show that for any $\gamma(t) = t + \sum \gamma_r t^{r+1}$, an expansion exactly analogous to (3.17) holds for the corresponding affiliates

$$\Pi_\diamond = \sum_{1 \leq r} \sum_{n_i \in \mathbb{Z}} \mathfrak{D}_\diamond^{n_1, \dots, n_r} G_{\diamond; n_1} \dots G_{\diamond; n_r} \quad (3.19)$$

⁴⁴ For $r = 1$, one should of course take $\delta_1^0 := 1$ and $\delta_{n_1}^{l_1} := 0$ if $\binom{l_1}{n_1} \neq \binom{0}{1}$. The presence of n_1, x_r on the left-hand side and their absence on the right-hand side is no oversight. It simply implies that $\delta_{n_1, \dots, n_r}^{l_1, \dots, l_r} = 0$ when $n_1 \neq 1$ or $l_r \neq 0$. If one finds (3.14) confusing, one should think of it as $\sum \delta_{1, n_2, \dots, n_{r-1}, n_r}^{l_1, l_2, \dots, l_{r-1}, 0} x_1^{l_1} \dots x_{r-1}^{l_{r-1}} \equiv x_1^{n_2} (x_1+x_2)^{n_3} \dots (x_1+\dots+x_{r-1})^{n_r}$.

with

$$\begin{aligned} \mathbf{\Pi}_\diamond &:= \gamma(\underline{\mathbf{\Pi}}) = \gamma(\mathbf{\Pi} - 1) , \\ G_\diamond &:= \gamma(\underline{G}) = \gamma(G - 1) , \\ G_{\diamond;n} &:= L^n . G_\diamond . L^{-n} \end{aligned}$$

and with a suitable variant $\mathfrak{D}_\diamond^\bullet$ of the ordering mould \mathfrak{D}^\bullet :

$$\mathfrak{D}_\diamond^\bullet := \gamma(Id^\bullet) \circ \mathfrak{D}^\bullet \circ \gamma^{-1}(Id^\bullet)$$

$\mathfrak{D}_\diamond^\bullet$ is derived from \mathfrak{D}^\bullet by ordinary pre-composition by $\gamma(Id^\bullet)$ and *modified post-composition* by $\gamma^{-1}(Id^\bullet)$. See (3.20) below. The order in which these two operations are performed does not matter. The formula for \circ -composition is patterned on the formula (2.1) for \circ -composition:

$$C^\bullet = A^\bullet \circ B^\bullet \iff C^\omega = \sum_{\omega^1 \dots \omega^s = \omega}^{\omega^i \text{ monoindicial}} A^{(\omega^1), \dots, (\omega^s)} B^{\omega^1} \dots B^{\omega^s} \quad (3.20)$$

except that the sum on the right-hand side of (3.20) extends only to those factorisations of ω that involve *mono-indicial* factor sequences ω^i , *i.e.* factor sequences consisting each of *one* index ω_i repeated r_i times. And $\langle \omega^i \rangle := (\omega_i)$ denotes that same factor sequence collapsed to its one index. Thus we get:

$$\begin{aligned} C^{3,3,3,5} &= A^{3,3,3,5} B^3 B^3 B^3 B^5 + A^{3,3,5} B^{3,3} B^3 B^5 \\ &\quad + A^{3,3,5} B^3 B^{3,3} B^5 + A^{3,5} B^{3,3,3} B^5 . \end{aligned}$$

The last missing items are the multitangents Tee_\diamond^\bullet and the corresponding structure coefficients. The former are defined by:

$$Tee_\diamond^\bullet = \gamma(Id^\bullet) \circ Tee^\bullet \circ \delta(Id^\bullet) \quad (\gamma \circ \delta = id) \quad (3.21)$$

The latter are given by the generating series:

$$\left[G_{\diamond, c_r^{-1}} \dots G_{\diamond, c_1^{-1}} . z \right]_{z=0} =: \sum \Gamma_\diamond^{n_1, \dots, n_r} c_1^{n_1} \dots c_r^{n_r} \quad (3.22)$$

where $G_{\diamond, c^{-1}}$ denotes the translated γ -affiliate of G :

$$G_{\diamond, c^{-1}} := \sum_{1 \leq r} \sum_{1 \leq n_i} \diamond^{n_1, \dots, n_r} g_\diamond^{n_1}(z + c^{-1}) \frac{\partial^{n_1}}{n_1!} \dots g_\diamond^{n_r}(z + c^{-1}) \frac{\partial^{n_r}}{n_r!} . \quad (3.23)$$

See Section 1.3 and Section 3.2 and recall that $\diamond^1 = 1$ and $\diamond^{n_1, \dots, n_r} = 0$ if $1 < r$ and $n_r = 1$. We are now in a position to expand p_\diamond in series of multitangents Tee_\diamond :

$$p_\diamond(z) = z + \sum_{1 \leq r} \sum_{n_i} \Gamma_\diamond^{n_1, \dots, n_r} Tee_\diamond^{n_1, \dots, n_r}(z) \quad (3.24)$$

Short proof: One should compare step by step the derivation of (3.24) with that of the expansion (3.8) for \mathfrak{p}^+ . The key point here is that changing from operators to multitangents changes \circ to \bullet . Indeed, in a sum of the form

$$\sum_{n_i \in \mathbb{Z}} C^{n_1, \dots, n_r} (z + n_1)^{-\sigma_1} \dots (z + n_r)^{-\sigma_r} \quad \text{with} \quad C^\bullet := A^\bullet \circ B^\bullet \quad (3.25)$$

any contribution to C^n of the form $A^{(n^1), \dots, (n^t)} B^{n^1} \dots B^{n^t}$, with monoindicial factor sequences \mathbf{n}^k consisting of identical indices n_k , will contract to

$$\prod_{1 \leq k \leq t} \prod_{n_i \in \mathbf{n}^k} (z + n_i)^{-s_i} = \prod_{1 \leq k \leq t} (z + n_k)^{-\sum_{n_i \in \mathbf{n}^k} s_i} \quad (3.26)$$

3.4 Parity separation and affiliate selection

The relative complexity of g_\diamond counts for nothing. What matters is

- (i) to get Tee_\diamond^\bullet and the corresponding expansions for \mathfrak{p} as simple as possible;
- (ii) to pick parity-respecting affiliates: $(g^{-1})_\diamond \equiv -g_\diamond$, $(\mathfrak{p}^{-1})_\diamond \equiv -\mathfrak{p}_\diamond$.

We already know three parity-respecting affiliates:

$$\gamma_0(t) = \log(1 + t) \quad (\text{infinitesimal generator}), \quad (3.27)$$

$$\gamma_1(t) = \frac{t}{1 + \frac{1}{2}t}, \quad (\text{first mediator}) \quad (3.28)$$

$$\gamma_2(t) = \frac{(1+t)^2 - 1}{(1+t)^2 + 1} \quad (\text{second mediator}) \quad (3.29)$$

and the general parity-respecting affiliate obviously corresponds to functions of the form $\gamma = h_i \circ \gamma_i$ ($0 \leq i \leq 2$) with h_i odd. So the task now is to select one of those γ so as to optimise Tee_\diamond^\bullet and in particular to make the formulae for their symmetrical Te^\bullet -linearisation as simple as possible. But we have already suggested in Section 2.3 and we shall show more conclusively in Section 5.4 that there exist no simpler choices than $\gamma_0, \gamma_1, \gamma_2$, with γ_1 topping the list, and γ_0 coming second. So we shall focus here on these three choices.

3.5 The generator-based scheme: from g_* to \mathfrak{p}_*

Here, the structure coefficients Γ_*^n are given by the series:

$$\left[g_*(z + c_r^{-1}) \partial \dots g_*(z + c_1^{-1}) \partial . z \right]_{z=0} =: \sum \Gamma_*^{n_1, \dots, n_r} c_1^{n_1} \dots c_r^{n_r} \quad (3.30)$$

The corresponding expansion for \mathfrak{p}_* reads:

$$\mathfrak{p}_*(z) = \sum_{1 \leq r} \sum_{n_i} \Gamma_*^{n_1, \dots, n_r} \text{Taa}^{n_1, \dots, n_r}(z) \quad (3.31)$$

Like with Γ_{\pm}^\bullet , one may prefer more analytical variants. These rely on integers δ^\bullet and δ_1^\bullet much simpler than the δ_\bullet^\bullet of Section 3.2

$$\sum_{l_i \geq 0, \sum l_i = r-1} \delta^{l_1, \dots, l_r} x_1^{l_1} \dots x_r^{l_r} \equiv x_1 \cdot (x_1 + x_2) \dots (x_1 + \dots + x_{r-1}) \quad (3.32)$$

$$\sum_{l_i \geq 0, \sum l_i = r} \delta_1^{l_1, \dots, l_r} x_1^{l_1} \dots x_r^{l_r} \equiv x_1 \cdot (x_1 + x_2) \dots (x_1 + \dots + x_r) \quad (3.33)$$

and of course on the coefficients g_{*s} of $g_* : g_*(z) = \sum_{2 \leq s} g_{*s} z^{1-s}$.

The corresponding expansion for \mathfrak{p}_* and \mathfrak{p}'_* read:

$$\mathfrak{p}_*(z) = \sum_{1 \leq r} (-1)^{r-1} \sum_{0 \leq l_i < s_i} \delta^{l_1, \dots, l_r} \text{Taa}^{s_1, \dots, s_r}(z) \prod_{1 \leq i \leq r} \frac{(s_i - 1)! g_{*s_i - l_i + 1}}{(s_i - l_i - 1)!} \quad (3.34)$$

$$\mathfrak{p}'_*(z) = \sum_{1 \leq r} (-1)^r \sum_{0 \leq l_i < s_i} \delta_1^{l_1, \dots, l_r} \text{Taa}^{s_1, \dots, s_r}(z) \prod_{1 \leq i \leq r} \frac{(s_i - 1)! g_{*s_i - l_i + 1}}{(s_i - l_i - 1)!} \quad (3.35)$$

The second expansion is formally more appealing in that its multitan-gents Taa^\bullet have exactly the same total weight $\sum s_j$ as the accompanying coefficient clusters. We may note that while it would be possible (though rather pointless) to produce similar expansions for all derivatives $\mathfrak{p}_*^{(n)}$, nothing analogous exists for the indefinite integrals \mathfrak{p}_* , $\mathfrak{p}_* \dots$

3.6 The mediator-based scheme: from $g_\sharp, g_{\sharp\sharp}$ to $\mathfrak{p}_\sharp, \mathfrak{p}_{\sharp\sharp}$

The relevant structure coefficients Γ_\sharp are defined in the usual way

$$\left[G_{\sharp, c^{-1}} \dots G_{\sharp, c^{-1}} \cdot z \right]_{z=0} =: \sum \Gamma_\sharp^{n_1, \dots, n_r} c_1^{n_1} \dots c_r^{n_r} \quad (3.36)$$

using the translates of the mediator in operator form:

$$G_{\sharp, c^{-1}} := 2 \left(\sum_{1 \leq n \text{ odd}} \frac{(g_\sharp(z+c^{-1}))^n}{2^n n!} \partial^n \right) \left(\sum_{0 \leq n \text{ even}} \frac{(g_\sharp(z+c^{-1}))^n}{2^n n!} \partial^n \right)^{-1}. \quad (3.37)$$

The corresponding expansion for the collector involves Too^\bullet and reads:

$$p_\sharp(z) = \sum_{1 \leq r} \sum_{n_i} \Gamma_\sharp^{n_1, \dots, n_r} \text{Too}^{n_1, \dots, n_r}(z) \quad (3.38)$$

Appearance of coloured multitanents and multizetas. Although, as pointed out in Section 1.8, the resurgence properties of the mediators f_{\sharp} and g_{\sharp} are completely unrelated (both have distinct critical times and distinct resurgence constants) and have no bearing on the object of interest to us, namely p_{\sharp} , a few complements about the very specific resurgence regimen of mediators, quite different from that of infinitesimal generators but fairly typical for the behaviour of general affiliates, may not be superfluous. The actual resurgence equations were obtained in Section 1.8. Here, we shall focus on the nature of their resurgence constants \underline{A}_{ω} and \underline{A}_{ω} .

The definition of the (first) mediator leads formally to an expansion

$$F_{\sharp} = 2 - 4(1 + L + \underline{G}L)^{-1} \tag{3.39}$$

$$= 2 - 4(1+L)^{-1} - 4(1+L)^{-1} \sum_{1 \leq r} (-1)^r (\underline{G}L(1+L)^{-1})^r \tag{3.40}$$

valid in the formal model and, after the proper transpositions, in the convolutive model. In the right sectorial model this becomes:

$$F_{\sharp,+} = 2 - 4 \sum_{0 \leq n_0} L^{n_0} - 4 \sum_{0 \leq n_r < \dots < n_1 < n_0}^{0 \leq r} (-1)^{r+n_0} \underline{G}_{:n_r} \dots \underline{G}_{:n_1} L^{n_0}. \tag{3.41}$$

Note that, due to the rightmost factor L^{n_0} , this expansion is only superficially similar to the expansion (3.4) of F_{+}^* . However, applying both sides of (3.41) to z and using

$$L(1+L)^{-1} \cdot z = \frac{1}{2}z + \frac{1}{4}, \quad \underline{G}_{:n_1}L(1+L)^{-1} \cdot z = \frac{1}{2}\underline{G}_{:n_1} \cdot z$$

we get for $f_{\sharp,+}$ an expansion much closer in outward shape to that of $f_{+}^*(z)$:

$$f_{\sharp,+}(z) = 1 - 2 \sum_{0 \leq n_r < \dots < n_1}^{1 \leq r} (-1)^{r+n_1} \underline{G}_{:n_r} \dots \underline{G}_{:n_1} \cdot z. \tag{3.42}$$

Mind the change $(-1)^{r+n_0} \rightarrow (-1)^{r+n_1}$ from (3.41) to (3.42), which is correct. If we now consider the limit $\Lambda_{\sharp}(z) := \lim_{n \rightarrow +\infty} f_{\sharp,+}(z - n)$, we obtain for $\Lambda_{\sharp}(z)$ a formal expansion

$$\Lambda_{\sharp}(z) = -2 \sum_{-\infty \leq n_r < \dots < n_1 < +\infty}^{1 \leq r} (-1)^{r+n_1} \underline{G}_{:n_r} \dots \underline{G}_{:n_1} \cdot z \tag{3.43}$$

which, like the expansion (3.8) of $\Pi^+(z)$ and for much the same reasons, is going to converge in the half-planes $|\Im z| > y$ for y large enough, and

whose Fourier coefficient are going to give the resurgence constants of $f_{\#}$. (See Section 1.8). That said, the main difference with (3.8) is not so much the presence of a factor $(-1)^r$ in (3.43), but of the factor $(-1)^{n_1}$, which will be responsible for introducing *bi-coloured* multitangents and *bi-coloured* multizetas: see (6.2) and take $\epsilon_j \in \frac{1}{2}\mathbb{Z}_1/\mathbb{Z}$.

The picture for the second mediator $f_{\#\#}$ would be quite similar, leading to $\Lambda_{\#\#}(z) := \lim_{n \rightarrow +\infty} f_{\#\#,+}(z - n)$ and a periodic expansion

$$\Lambda_{\#\#}(z) = - \sum_{-\infty \leq n_r < \dots < n_1 < +\infty}^{1 \leq r} (-1)^{r+n_1} \underline{GG}_{,n_r} \dots \underline{GG}_{,n_1} \cdot z \tag{3.44}$$

with $\underline{GG}_{,n} := L^n \cdot (G \cdot G - 1) \cdot L^{-n}$. In any case, we see that while $\Lambda_{\#}$ and $\Lambda_{\#\#}$ bear some resemblance to Π^+ , they are completely unrelated to $p_{\#}$ and $p_{\#\#}$.

3.7 From collectors to connectors

The dichotomy collector/connector. The various objects p_{\diamond} constructed so far in this section have to be simultaneously examined under the viewpoint of their f - and z -dependence.

They depend on a germ $f = l \circ g$ that moves freely within the formal class $(p, \rho) = (1, 0)$. As such, they are to begin with nothing more than formal power series in the coefficients g_s of g or, equivalently, the coefficients $g_{\diamond,s}$ of its affiliates g_{\diamond} :

$$p_{\diamond}(z) = \sum_{1 \leq r} \sum_{s_i, n_i}^{s_i < s_{i+1}} \prod_{1 \leq i \leq r} (g_{\diamond, s_i})^{n_i} T_{\diamond}^{(n_1, \dots, n_r)}(z). \tag{3.45}$$

As functions of z , however, our objects may be viewed

- (i) either as *collectors* (and noted p_{\diamond}), *i.e.* as global meromorphic functions defined on the whole of \mathbb{C} with all their poles on \mathbb{Z} and with well defined expansions as finite sums of multitangents or, after reduction, as sums of monotangents with multizeta coefficients;
- (ii) or as *connectors* (and noted π_{\diamond}), *i.e.* as pairs of 1-periodic functions defined in the upper or lower half-plane and possessing their own distinct Fourier expansions there.

So far, the distinction between *collectors* and *connectors* may appear tenuous, but it acquires all its significance when, ceasing to regard the f -dependence as formal, we focus on individual, convergent germs $f = l \circ g$ and try to associate with them global z -functions (impossible) or pairs of periodic z -germs (possible).

To that end, let us consider the s -truncations $trunc_s.p_\diamond(z)$ obtained by retaining in (3.45) the sole terms of global weight⁴⁵ $\sum n_i s_i \leq s$. Notice that weight-truncation is intrinsic, in the sense that, in any given z -chart⁴⁶, it stays the same whether we choose the natural coefficient system $\{g_s, s \geq 3\}$ or any affiliate-based system $\{g_{\diamond,s}, s \geq 3\}$.

Divergence of the collectors. When $s \rightarrow +\infty$, $trunc_s.p_\diamond(z)$ does not tend to a global function, irrespective of the choice of affiliation \diamond . Moreover, even after finite reduction to monotangents, $trunc_s.p_\diamond(z)$ does not converge to an infinite sum (even a formal one) of monotangents. This may seem surprising, because:

- (*) reducing $trunc_s.p_\diamond(z)$ to a series of montangents $\sum_{0 < \sigma} a_{s,\sigma}^\diamond Te^\sigma(z)$ is the same as taking the negative part $\sum_{0 < \sigma} a_{s,\sigma}^\diamond z^{-\sigma}$ of the Laurent expansion at $z = 0$ of $trunc_s.p_\diamond(z)$;
- (**) the Borel transform $\sum_{0 < \sigma} a_{s,\sigma}^\diamond \zeta^{\sigma-1}/(\sigma - 1)!$ of that negative part, when evaluated at the points $\zeta = 2\pi in$, yields precisely the Fourier coefficients of the truncated connectors $trunc_s.\pi_\diamond(z)$ — and these Fourier coefficients, as we shall see in a moment, *do converge* when $s \rightarrow \infty$.

We shall have more to say about this apparent paradox and the reasons behind it in Section 7, but for the moment let us observe that the only meaning that can be attached to the limit $\lim_{s \rightarrow \infty} trunc_s.p_\diamond(z)$ is the formal series (3.45) with its individual clusters $\prod_i g_{\diamond,s_i}^{n_i} T_s^{(n)}(z)$ kept separate.

Convergence of the connectors.

(*) **From p to $\pi = (\pi_{no}, \pi_{so})$:**

As s goes to ∞ and for K_\pm large enough, $trunc_s.\pi(z) - z$ tends uniformly to a 1-periodic limit $\pi_{no}(z) - z$ (respectively $\pi_{so}(z) - z$) on the upper or ‘northern’ half-plane $\Im z > K_+$ (respectively on the lower or ‘southern’ half-plane $\Im z < -K_-$).

(**) **From p_\diamond to $\pi_\diamond = (\pi_{\diamond,no}, \pi_{\diamond,so})$:**

The affiliate $\pi_\diamond(z)$ of π being of the form $\gamma(\Pi - 1).z$, the n^{th} Fourier coefficient of its northern or southern component is a polynomial in the first n

⁴⁵ The ‘weight’ in question is that of the coefficient clusters. But the weight of the accompanying multitangents (or, after reduction, of the multizeta-monotangent combinations) differs from the first only by one unit.

⁴⁶ But the weight truncation is of course dependent on the choice of z -chart.

Fourier coefficients of π_{no} or π_{so} . So, as $s \rightarrow \infty$, the (convergent) Fourier series $\text{trunc}_s \cdot \pi_{\diamond, \text{no}}$ and $\text{trunc}_s \cdot \pi_{\diamond, \text{so}}$ converge (coefficient-wise)⁴⁷, to two formal Fourier series $\pi_{\diamond, \text{no}}$ and $\pi_{\diamond, \text{so}}$. These are generally divergent, but usually (and definitely so in the case of the generators π_* or mediators $\pi_{\#}$, $\pi_{\#\#}$) resurgent and Borel-resummable, with respect to some critical time of the form $z' := \exp(\pm n\pi iz)$. In any case their Fourier coefficients are well-defined, and this is all that matters to us at the moment.

More on the dichotomy collector/connector. Despite being very close to the *connectors*, the *collectors* differ from them in two fundamental respects: they are *not invariant* and they are *of one piece*.

The *non-invariance* is fairly obvious when \mathfrak{p} is taken in its *natural* multitangent expansion, but even after monotangent reduction (when at all it exists), \mathfrak{p} still remains non-invariant. Indeed, even when a formal limit $\sum_{s \in \mathbb{N}} Te^s(z)$ exists (it sometimes does, though very exceptionally) as the truncation goes to infinity, the ‘Borel transform’ $\sum_{s \in \mathbb{N}} \zeta^{s-1}/(s-1)!$ assumes invariant values only when restricted to the set $2\pi\mathbb{Z}^*$.

As for being *of one piece*, this is a property not so much of the collectors as of their constituent multitangents or monotangents, which are meromorphic over the whole of \mathbb{C} , in complete contrast to the connectors, whose northern and southern components are usually completely unrelated: each one may a priori be *anything*.

3.8 The ramified case ($p > 1$)

Everything carries over to the general case, when f ranges though a general formal class (p, ρ) . But when $p > 1$, we must take f to a prepared form $f = f_{\text{norm}} \circ g$ (see (1.2)) with a ramified perturbation $g(z) = z + \sum g_s z^{1-s}$ and with fractional indexation: $s \in p^{-1}\mathbb{N}^*$.

The *connectors* are of course still invariant, but even more ‘fragmented’ than usual: there are now $2p$ of them – p northern and p southern ones. Each of these $2p$ periodic germs is unrelated to the others and may a priori be anything.

As for the *collectors*, as formal objects they are still *of one piece*, but things get more tangled when we regard the truncations $\text{trunc}_s \cdot \mathfrak{p}_{\diamond}(z)$ or the individual clusters $T_s^{(n)}(z)$ in the ramified equivalent of (3.45) as *global functions* on $(\mathbb{C} - 2\pi i\mathbb{Z})_p$ (the p -ramified covering of $\mathbb{C} - 2\pi i\mathbb{Z}$). The thing is that we can no longer go from one upper-plane determination to the two neighbouring lower-plane determination by simply cross-

⁴⁷ Recall that s -truncation is independent of \diamond .

ing the real axis between two consecutive singularities n and $n + 1$: by so doing, one would get a wrong determination, dependent on n , and not even periodic.

3.9 Reflexive and unitary diffeomorphisms

In this section, we find it convenient to switch from the s - or *weight*-indexation $g(z) = z + \sum g_s z^{1-s}$ to the d - or *degree*-indexation $g(z) = z + \sum g_{1+d} z^{-d}$.

In Section 3.4 we observed that in the expansion (3.34) of p_* , coefficient clusters $\prod g_{*1+d_i}$ of even (respectively odd) total degree $\sum d_i$ accompany multitanents Taa^\bullet that are even functions with real Fourier coefficients (respectively odd functions with purely imaginary Fourier coefficients). As a consequence, there is no simple condition on the coefficients g_{*1+d_i} of g_* capable of ensuring that p_* be *odd*, whereas three elementary conditions may ensure that it be *even*, namely:

- (i) all coefficients g_{*1+d_i} of odd degree d_i vanish and those of even degree are real;
- (ii) all coefficients g_{*1+d_i} of even degree d_i vanish and those of odd degree are purely imaginary;
- (iii) all coefficients g_{*1+d_i} of even degree d_i are real and those of odd degree are purely imaginary.

No special significance attaches to case (ii), but the cases (i) and (iii) present interesting stability properties, with collectors and connectors inheriting the nature of f . This is an incentive for singling out the following three types of diffeos f whose inverses f^{-1} either coincide with, or are analytically conjugate to, the image of f under an elementary involution:

$$\begin{aligned} \text{reflexive} : \check{f} &= f^{-1} \quad || \quad \text{weakly reflexive} : \check{f} \stackrel{\text{an. cj.}}{\sim} f^{-1} \\ \text{unitary} : \bar{f} &= f^{-1} \quad || \quad \text{weakly unitary} : \bar{f} \stackrel{\text{an. cj.}}{\sim} f^{-1} \\ \text{counitary} : \check{\check{f}} &= f^{-1} \quad || \quad \text{weakly counitary} : \check{\check{f}} \stackrel{\text{an. cj.}}{\sim} f^{-1}. \end{aligned}$$

Here, \bar{f} denotes the complex conjugate of f , and $\check{f} := \sigma \circ f \circ \sigma$ with $\sigma(z) \equiv -z$. Conjugation by τ , with $\tau(z) \equiv iz$, clearly exchanges *unitary* and *counitary*, so that *weakly unitary* is equivalent to *weakly counitary*. Though *unitariness* seems a more natural notion, we shall work here with *counitariness*, which is better adapted to the correspondance $f \mapsto \pi$ and enables us to take f in standard form $f = l \circ g$.

P₁: f is reflexive iff the power series f_* respectively f^* are *even* respectively *odd*, in which case $f_{*\pm}(-z) \equiv f_{*\mp}(z)$ and $f_{\pm}^*(-z) \equiv -f_{\mp}^*(z)$.

Likewise, f is counitary iff the power series f_* respectively f^* are of the form $f_{*re} \circ \tau$ respectively $\tau^{-1} \circ f_{re}^* \circ \tau$ with real f_{*re}, f_{re}^* , in which case $f_{*\pm}(-z) \equiv f_{*\mp}(z)$ and $\bar{f}_{\pm}^*(-z) \equiv -f_{\mp}^*(z)$.

P₂: If a standard f is reflexive respectively counitary, then its conjugate $l^{+\frac{1}{2}} \circ f \circ l^{-\frac{1}{2}}$ is of the standard form $f = l \circ g$ with reflexive respectively counitary factors l and $g := l^{-\frac{1}{2}} \circ f \circ l^{-\frac{1}{2}}$.

P₃: If f is (weakly or strictly) reflexive respectively counitary, then its connector π is (strictly) reflexive respectively counitary. This is geometrically obvious, from the relations **P₁** injected into the definition (1.6), but the remarkable fact is that the analytical procedure (3.34) also respects this conservation of reflexivity or counitariness at every single step. Thus, if we apply it to the decomposition $f = l \circ g$ (as in **P₂**) of a reflexive f , we have to do with an *even* infinitesimal generator g_* that carries only coefficients g_{*1+d} of *even* degree d , and (3.34) automatically produces an *even* p_* . The diffeo g itself is of mixed parity, but its coefficients of g_{*1+d} of *odd* degree are fully determined by the earlier coefficients of *even* degree, and can thus be used in place of the g_{*1+d} . Either way, for reflexive diffeos the calculation of the invariants is a much more pleasant affair than for general diffeos, due to the drastic reduction in the mass of coefficients and (provided f be real) to the realness of p_* and π_* .

P₄: Conversely, any reflexive respectively counitary π is the invariant of some reflexive respectively counitary f . This follows from the *canonical synthesis* (see Section 1.4) which, for c real and large enough, automatically produces diffeos f_c of the required type.⁴⁸

P₅: (Reinhard Schäfke). The product or quotient of two reflexive (respectively unitary) diffeomorphisms is obviously conjugate to a reflexive (respectively unitary) diffeomorphism, but the converse is also true: any weakly reflexive (respectively unitary) f can, for any consecutive integers n_j , be represented as a quotient of two strictly reflexive (respectively unitary) diffeos f_j :

$$f := f_1 \circ f_2^{-1} \quad \text{with}$$

$$f(z) := z + 1 + o(1), \quad f_j(z) := z + n_j + o(1), \quad n_1 - n_2 = 1$$

⁴⁸ As pointed out to us by Reinhard Schäfke, this can also be deduced from the bifactorisation of f in **P₅** below, provided we admit the existence of a pre-image f for any given π , which fact again follows from the canonical synthesis, but may also be established more directly.

and that too with explicit factors f_j :

$$f \text{ weakly reflexive} \quad || \quad f \text{ weakly counitary}$$

$$f_j := (*f) \circ l^{n_j} \circ \sigma \circ (f^*) \circ \sigma \quad || \quad f_j := (*f) \circ l^{n_j} \circ \sigma \circ (\bar{f}^*) \circ \sigma \quad (3.46)$$

$$= f^{n_j} \circ (*f) \circ \sigma \circ (f^*) \circ \sigma \quad || \quad = f^{n_j} \circ (*f) \circ \sigma \circ (\bar{f}^*) \circ \sigma \quad (3.47)$$

$$= f^{n_j} \circ h^{-1} \circ \sigma \circ h \circ \sigma \quad || \quad = f^{n_j} \circ h^{-1} \circ \sigma \circ \bar{h} \circ \sigma \quad (3.48)$$

Indeed, the equivalent definitions (3.46), (3.47), (3.48) make it clear, respectively:

- that f_1, f_2 are reflexive (respectively counitary);
- that $f = f_1 \circ f_2^{-1}$;
- that f_1, f_2 are analytic.⁴⁹

P₆: Piecing together all the above, we see that the commutative, non-associative⁵⁰ operation mix_c :

$$mix_c : (\pi_1, \pi_2) \mapsto \pi := \pi_{f_{1,c} \circ f_{2,c}} = \pi_{f_{2,c} \circ f_{1,c}} \quad (3.49)$$

(where $f_{j,c}$ stands for the c -canonical pre-image of π_j) respects reflexivity and counitariness.

4 Scalar invariants in terms of f

4.1 The invariants A_ω as entire functions of f

Let π_ω^\pm and $\pi_{\diamond,\omega}$ be the Fourier coefficients of the *connectors*, as defined in Section 3.5 by weight-wise truncation of the *collectors* and passage to the limit:

$$\text{If } +\Im(z) \gg 1: \pi^{\pm 1}(z) = z + \sum_{\omega \in \Omega^-} \pi_\omega^\pm e^{-\omega z}; \quad \pi_\diamond(z) = \sum_{\omega \in \Omega^-} \pi_{\diamond,\omega} e^{-\omega z} \quad (4.1)$$

$$\text{If } -\Im(z) \gg 1: \pi^{\pm 1}(z) = z + \sum_{\omega \in \Omega^+} \pi_\omega^\pm e^{-\omega z}; \quad \pi_\diamond(z) = \sum_{\omega \in \Omega^+} \pi_{\diamond,\omega} e^{-\omega z} \quad (4.2)$$

The Fourier series for $\pi^\pm(z) - z$ are convergent, whereas those for $\pi_\diamond(z), \pi_*, \pi_\#$ etc are (usually) merely formal. But this makes no difference to

⁴⁹ The analytic h in (3.48) conjugates the weakly reflexive/counitary f with a strictly reflexive/counitary f_0 , i.e. $h \circ f = f_0 \circ h$. By definition, such a pair h, f_0 exists. We may note in passing that the factorisation $f = f_1 \circ f_2^{-1}$ would still hold for complex (in the reflexive case) or real (in the unitary case) values of n_j , but in that case the above formulae break down (f_1, f_2 are no longer analytic) and we must take recourse to another, more involved construction.

⁵⁰ $mix_c(\pi_1, \pi_2)$ is doubly germinal: for a given (π_1, π_2) , it is defined for c large enough, and for a given c , it is defined for (π_1, π_2) close enough to (id, id) .

the Fourier coefficients, which are always given by *convergent* series:

$$\pi_\omega^\pm = z + \sum_{1 \leq r} \sum_{n_i} \Gamma_\pm^{n_1, \dots, n_r} \text{Tee}_\omega^{n_1, \dots, n_r} \tag{4.3}$$

$$\pi_{*\omega} = \sum_{1 \leq r} \sum_{n_i} \Gamma_*^{n_1, \dots, n_r} \text{Taa}_\omega^{n_1, \dots, n_r} \tag{4.4}$$

$$\pi_{\sharp\omega} = \sum_{1 \leq r} \sum_{n_i} \Gamma_\sharp^{n_1, \dots, n_r} \text{Too}_\omega^{n_1, \dots, n_r} \tag{4.5}$$

with the g -dependence implicit in the coefficients $\Gamma_\pm, \Gamma_*, \Gamma_\sharp$ as defined in (3.10), (3.30), (3.36), or explicit in the definitions (3.14), (3.32).

However, the need to define the alien operators Δ_ω^\pm and Δ_ω in uniform manner for all ω clashes with the need to associate within one and the same pair $(\pi_{\text{no}}, \pi_{\text{so}})$ respectively $(\pi_{\text{no}}^{-1}, \pi_{\text{so}}^{-1})$ northern and southern components originating from the same collector p or p^{-1} . This clash leads to a regrettable but unavoidable disharmony in the correspondance between the invariants A_ω^\pm and A_ω , as defined from the resurgence equations, and the Fourier coefficients of the connectors, as derived from the collectors. This correspondance takes the form:

$$\begin{aligned} \forall \omega \in \Omega^- : A_\omega^+ &= \pi_\omega^+ ; A_\omega^- &= \pi_\omega^- ; +2\pi i A_\omega &= \pi_{*\omega} \\ \forall \omega \in \Omega^+ : A_\omega^- &= \pi_\omega^+ ; A_\omega^+ &= \pi_\omega^- ; -2\pi i A_\omega &= \pi_{*\omega} \end{aligned}$$

Remark. Nature of the convergence

- (i) The convergence in (4.3) is completely unproblematic – absolute with respect to the contributions attached to individual clusters $\prod_i (g_{s_i})^{n_i}$
- (ii) We also have absolute, cluster-wise convergence in (4.4) and (4.5) provided we take the precaution of switching from the coefficient systems $\{g_{*,s}\}$ or $\{g_{\sharp,s}\}$ back to the natural system $\{g_s\}$.
- (iii) But we can also dispense with that change if we take the precaution of collecting in (4.4) or (4.5) all terms (in finite number) of total weight s , and then of summing all s -contributions. But summing separately the contributions attached to the clusters $\prod_i (g_{*,s_i})^{n_i}$ or $\prod_i (g_{\sharp,s_i})^{n_i}$ would not do.

4.2 The case $\rho(f) \neq 0$. Normalisation

For diffeos of the form $f(z) = z + 1 - \rho z^{-1} + \mathcal{O}(z^{-2})$ with a non-vanishing ‘iterative residue’ ρ , the defining relation (1.5) for the right and left iterators must be changed to

$$f_\pm^*(z) = \lim_{k \rightarrow \pm\infty} f^k(z) - k \pm \rho (c + \log |k|) \tag{4.6}$$

with the normalisation constant c as in Section 2.5. In the formal model, this leads to

$$\tilde{f}^*(z) = z + \rho(c + \log z) + o(z^{-1}). \quad (4.7)$$

That apart, nothing changes and all the previous results and formulae still hold, including the explicit expansions (3.12)-(3.13) and (4.3), provided we set $ze^1 := \gamma - c$ and normalise all multizetas and multitanents accordingly. As mentioned in Section 2.6, the recommended choice is $c = \gamma$, since it amounts to setting $ze^1 := 0$.

4.3 The case $p \neq 1$. Ramification

Here again, the transition is straightforward. The ‘prepared’ form (1.2) for the diffeo now carries fractional exponents $s \in p^{-1}\mathbb{N}^*$. As a consequence, the multiplicative z -plane and the convolutive ζ -plane are now p -ramified, and so is the index set Ω , which is embedded in the ζ -plane. We still have one single collector \mathfrak{p} respectively \mathfrak{p}_* , \mathfrak{p}_{\ddagger} etc, *ramified yet of one piece*, but p distinct pairs of connectors, $\pi = (\pi_{\text{no}}, \pi_{\text{so}})$ respectively $\pi_* = (\pi_{*\text{no}}, \pi_{*\text{so}})$ or $\pi_{\ddagger} = (\pi_{\ddagger\text{no}}, \pi_{\ddagger\text{so}})$ etc, separately *unramified* and mutually *unrelated*. The invariants π_{ω}^{\pm} respectively $\pi_{*\omega}$, $\pi_{\ddagger\omega}$ are still given by the familiar formulae (4.3), (4.4), (4.5) but with Fourier coefficients Tee_{ω}^s respectively Taa_{ω}^s , Too_{ω}^s etc that are best calculated by resurgent analysis, as in Section 2.7, and are no longer finite sums of multizetas, even of ramified ones.

The transition to the most general case, with (ρ, p) any element of $(\mathbb{C}, \mathbb{N}^*)$, follows on exactly the same lines, and merely combines the partial adjustments of the present and preceding subsections.

4.4 Growth properties of the invariants

Growth in ω for a given analytic f : For a diffeo f in prepared form (1.2), any majorisation of its coefficients easily translates into a majorisation of its invariants:

$$\left\{ |f_{[s]}| \leq c_0 c_1^s \right\} \implies \left\{ |A_{\omega}^{\pm}| \leq C_0 C_1^{|\omega|} \right\}. \quad (4.8)$$

Rough estimates of (C_0, C_1) in terms of (c_0, c_1) were given in [5] and sharper ones in [1]. These results can be derived from a geometric analysis in the z -plane or from a resurgent analysis in the ζ -plane. Things change, though, when we go over to the Gevrey case.

Growth in ω for a given f of Gevrey class: Formal diffeos f (in prepared form) of Gevrey class τ are easily shown to be stable under formal conjugations (also in prepared form) of the same Gevrey class. For $0 < \tau$,

the Gevrey class is non-analytic, and Gevrey conjugacy turns out to be strictly stronger than formal conjugacy if and only if $\tau < 1$. This implies, for $0 < \tau < 1$, the existence of Gevrey conjugation invariants. These, however, can no longer be defined in the z -plane, since f is purely formal and has no geometric realisation there. In the ζ -plane, though, the Borel transforms of the iterators *f and f^* still exist (again, assuming $\tau < 1$); still extend to uniform analytic functions on $\mathbb{C} - 2\pi i \mathbb{Z}$; still verify the familiar resurgence equations (1.66)-(1.67); and still unambiguously define invariants A_ω^\pm and A_ω , which are still given by the explicit expansions (4.3)-(4.4). The only difference lies in the faster than exponential growth of $\hat{f}^*(\zeta)$ and ${}^*\hat{f}(\zeta)$ as $|\zeta| \rightarrow \infty$, and in the faster than exponential growth of A_ω^\pm as $|\omega| \rightarrow \infty$. More precisely, for $0 < \tau < 1$, the earlier implication (4.8) becomes⁵¹:

$$\{ |f_{[s]}| \leq c_0 c_1^s s^{\tau s} \} \implies \{ |A_\omega^\pm| \leq C_0 C_1^{|\omega|} \exp(C_2 |\omega|^{\frac{1}{1-\tau}}) \} \quad (4.9)$$

Growth in f for a given ω . We may now fix ω and ask how $A_\omega^+(f)$, $A_\omega^-(f)$, $A_\omega(f)$ behave as functions of f or, to simplify, as entire functions of any given coefficient $f_{[s]}$ ($s \geq 2$) relative to a prepared form (1.2). Unlike with the ω -growth, there is little difference here between A_ω^\pm and A_ω .

- (i) If $s > 2$, all three entire functions $A_\omega^+(f_{[s]})$, $A_\omega^-(f_{[s]})$, $A_\omega(f_{[s]})$ have at most exponential growth in $|f_{[s]}|^{\frac{1}{s-1}}$.
- (ii) If $s = 2$, the corresponding coefficient coincides up to sign with the iterative residue (*i.e.* $f_{[2]} = -\rho$), and the entire functions $A_\omega^+(\rho)$, $A_\omega^-(\rho)$, $A_\omega(\rho)$ have at most exponential growth in $|\rho \log \rho|$. The result appears to be sharp.⁵²

These results are almost “special cases” of the following statement: at any given point ζ_0 on $\mathbb{C} - \Omega$, the Borel transform of the direct iterator assumes a value $\hat{f}^*(\zeta_0)$ which, as an entire function of $f_{[s]}$, is exactly of exponential type in $|f_{[s]}|^{\frac{1}{s-1}}$. This applies even for $s = 2$. The difference between the cases $s \neq 2$ and $s = 2$ makes itself felt only when we move ζ_0 to some point ω_0 located over Ω , to investigate the leading singularity there and infer from it the value of the invariants. When $\rho = 0$, the leading singularity in question is a simple pole $a_{\omega_0}(\zeta - \omega_0)^{-1}$, but when

⁵¹ For details, see [5, page 424]

⁵² See the argument in [2, Section 8].

$\rho \neq 0$ it is of the form $a_{\omega_0}(\zeta - \omega_0)^{\rho \omega_0 - 1} / \Gamma(\rho \omega_0)$ and can be quite violent if ρ has an imaginary part.

We shall take up these growth and convergence issues more systematically in Section 7.

4.5 Alternative computational strategies

Direct Fourier analysis in the multiplicative plane. The method amounts to calculating the limit:⁵³

$$A_{\omega}^{\mp \epsilon(\omega)} = \pi_{\omega}^{\pm} = \lim_{k \rightarrow \pm \infty} \int_{z_0}^{1+z_0} \left(l^{-k} \circ f^{2k} \circ l^{-k}(z) - z \right) e^{\omega z} dz \quad (4.10)$$

with $\epsilon(\omega) := \text{sign}(\Im(\omega))$. Although the parenthesised part of the integrand converges to $\pi^{\pm}(z) - z$ for $|\Im(z)|$ large enough, the above scheme, even after optimisation in the choice of z_0 , is computationally costly (integral instead of series) and inefficient (arithmetical convergence) as well as theoretically opaque (it sheds no light on the internal structure of the invariants as functions of f). But it has the merit of being almost insensitive to the choice of ω , unlike the next method.

(ii) Asymptotic coefficient analysis in the formal model. The method starts with the inductive calculation of the first N coefficients of the direct iterator $f^*(z)$ from its functional equation (1.11). One then switches to the Borel transform $\hat{f}^*(\zeta)$ and uses the method of *coefficient asymptotics*⁵⁴ to derive the form of the two singularities⁵⁵ closest to the origin (they are located over $\pm 2\pi i$). When applied to a parameter-free diffeo f with proper optimising precautions, the method is superbly efficient for computing $A_{\pm 2\pi i}$, even for diffeos f that are ‘large’, *i.e.* distant from the identity. Thus, with N taken in the region of 200 or 300, one typically gets $A_{\pm 2\pi i}$ with 100 exact digits or more, in less than half an hour of Maple time.

The method works less well, however, for $\omega_0 = 2\pi i n$ with $n > 1$. One must then start with a conformal mapping $\zeta \mapsto \zeta' = h(\zeta)$ of $\mathcal{R} = \mathbb{C} - 2\pi i \mathbb{Z}$ that keeps 0_{\bullet} fixed and takes the points $+\omega_0^{\text{main}}$ and $-\omega_0^{\text{main}}$

⁵³ If $\rho(f) \neq 0$, the shift l^{-k} should of course be replaced by $l^{-k+(c+\log k)\rho}$, with $c = \gamma$ as recommended choice for the normalisation constant c . See Section 2.6.

⁵⁴ For a brief exposition of the method, see for ex. the section Section 2.3 of *Power Series with sum-product Taylor coefficients and their resurgence algebra*, J. Ecalle and S. Sharma, Ed. Scuola Normale Superiore, Pisa, 2011.

⁵⁵ Or of the 2 p closest singularities when $p(f) \neq 0$.

closer to the origin than all other points $\pm\omega^{\text{main}}$, with ω^{main} denoting *the* ramification point of \mathcal{R} over ω that abuts the *main* real half-plane. One can then apply the method of coefficient asymptotics in the ζ' -plane, with the Taylor series $\widehat{f}^*(h^{-1}(\zeta'))$ in place of the series $\widehat{f}^*(\zeta)$, to calculate $A_{\omega_0}^+$ and $A_{-\omega_0}^-$.

(iii) Resurgent analysis in the Poincaré plane. That method also is based on the resurgence equation (1.67) verified by the direct iterator f^* . But instead of interpreting that resurgence equation, as usual, in the highly ramified ζ -plane, one performs a conformal transform $\zeta \rightarrow \xi$ derived from the classical modular function λ :

$$\zeta = q(\xi) := -\log(1 - \lambda(\xi)) = -\log \lambda \left(-\frac{1}{\xi} \right) = 16 \sum_{n \text{ odd}} q_n e^{2\pi i \xi} \quad (4.11)$$

$$q_n := \sum_{d|n} \frac{1}{d} = \frac{1}{n} \sum_{d|n} d \quad (4.12)$$

That comformal transform does three things:

(*) it maps the Riemann surface $\mathcal{R} := \mathbb{C} - \widetilde{2\pi i \mathbb{Z}}$ of the ζ variable uniformly onto the Poincaré half-plane $\Im(\xi) > 0$;

(**) it changes the power series $\widehat{f}^*(\zeta)$ with finite radius of convergence into a Fourier series $\widehat{f}^*(q(\xi))$ that converges on the entire Poincaré half-plane.

(***) it turns the alien operators into finite superpositions of post-composition operators – more precisely, post-composition by simple homographies $h_{\omega,j}^\pm$ or $h_{\omega,j}^\mp$ with entire coefficients:

$$\Delta_\omega^\pm \widehat{\varphi}(\xi) := \widehat{\varphi} \circ h_{\omega,1}^\pm(\xi) - \widehat{\varphi} \circ h_{\omega,2}^\pm(\xi) \quad (4.13)$$

$$\Delta_\omega \widehat{\varphi}(\xi) := \sum_{1 \leq j \leq 2^r} m_{\omega,j} \widehat{\varphi} \circ h_{\omega,j}(\xi) \quad \left(r := \left\lfloor \frac{\omega}{2\pi i} \right\rfloor, m_{\omega,j} \in \mathbb{Q} \right) \quad (4.14)$$

The method is efficient enough for small values of ω , but as $r := \left\lfloor \frac{\omega}{2\pi i} \right\rfloor$ increases, the distances

$$H^\pm(\omega) := \max_{\Im(\xi) > 0} \inf \{ \Im(\xi), \Im(h_{\omega,1}^\mp(\xi)), \Im(h_{\omega,2}^\mp(\xi)) \} \quad (4.15)$$

$$H(\omega) := \max_{\Im(\xi) > 0} \inf \{ \Im(\xi), \Im(h_{\omega,1}(\xi)), \dots, \Im(h_{\omega,2^r}(\xi)) \} \quad (4.16)$$

rapidly decrease to zero, making it necessary to evaluate our Fourier series for $\widehat{f}^*(q(\xi))$ close to the boundary of their domain of convergence, *i.e.* the real axis, which of course is computationally costly.

(iv) **Explicit multizetaic expansions.** This method, to which the present paper is devoted, has the advantage of explicitness and theoretical transparency, expressing as it does the invariants in terms of universal transcendental constants (the multizetas) and of the diffeo's Taylor coefficients. It has the further advantage of handling large values of ω almost as efficiently as small ones. But the method's chief drawback would seem to be this: it involves expansions which converge very fast (faster than geometrically) once they reach 'cruising speed', but which often take a damn long time to reach that speed. This is the case, not so much for ω large, but for f large, *i.e.* for diffeos too distant from *id*.

4.6 Concluding remarks

(i) The invariants as autark functions.

Local, analytic, resonant vector fields X ranging through a *fixed* formal conjugacy class, possess holomorphic invariants A_ω which are *autark* functions of X , that is to say, of any given *free*⁵⁶ Taylor coefficient of X . Autark functions, very informally, are entire functions whose asymptotic behaviour in every sector of exponential increase or decrease admits a complete description, with dominant exponential terms accompanied by divergent-resurgent power series, which in turn verify a *closed* system of resurgence equations. Whether the invariants A_ω of diffeos are autark, too, seems likely but is yet unproved. Be that as it may, one would like to fully understand the asymptotic behaviour of A_ω as f grows, or as any given coefficient or parameter in f grows, since for very 'large' diffeos f the *direct* computation of the invariants would in any case be very costly.

(ii) Formal multizetas: dynamical vs arithmetical variants.

There exist several distinct but most probably equivalent notions of *arithmetical formal multizetas*, like the multizeta symbols subject to the two systems of so-called *quadratic multizeta relations*, or again to the *pentagonal, hexagonal and digonal relations*. But there also exists a demonstrably distinct and *weaker* notion of *dynamical formal multizetas* (and *multitangents*), by which we mean any system \mathbb{S} of scalar-valued multizeta symbols (respectively function-valued multitangent symbols) that, when inserted into the expansions (4.3) (respectively (3.15)) guarantees, first, the convergence of these expansions, and, second, the invariance of the A_ω (respectively π) so produced. This immediately suggests a pro-

⁵⁶ *I.e.* of each coefficient that may freely vary without causing X to leave its formal conjugacy class.

gramme: to repeat for the dynamical multizetas what has been successfully done for their arithmetical counterparts, in particular to construct *explicit, complete and canonical systems of irreducibles*.

(iii) Abstract invariants.

Let $\{\mathbb{S}A_\omega, \omega \in \Omega\}$ be the system of ‘abstract’ invariants induced by a system \mathbb{S} of dynamical multizetas as above. Since the system of natural invariants $\{A_\omega, \omega \in \Omega\}$ is complete, there necessarily exist conversion formulae of the form:

$$\mathbb{S}A_{\omega_0} = \sum_{1 \leq r} \sum_{\omega_1 + \dots + \omega_r = \omega_0} H_{\mathbb{S}}^{\omega_1, \dots, \omega_r} A_{\omega_1} \dots A_{\omega_r} \tag{4.17}$$

that respect the basic ω -gradation and carry interesting ‘universal’ structure constants $H_{\mathbb{S}}$. These constants ought to be of particular significance in the case of the system \mathbb{S}_0 of ‘rational’ dynamical multizetas which is analogous, on the dynamical side, to the canonical system of ‘rational’⁵⁷ multizetas on the arithmetical side.

5 Complement: twisted symmetries and multitangents.

The aim of this section is twofold:

- (i) to review in a systematic and orderly fashion the combinatorial lemmas relevant to this investigation
- (ii) to examine the most general *symmetry types* and the structure coefficients attached to them — less for their own sake than for showing how exceptional and deserving of attention the dozen or so *special symmetry types* are.

5.1 Twisted alien operators

Let $\gamma(t) = \sum_{0 \leq r} \gamma_r t^{r+1}$ and consider the alien operator

$$\mathcal{D}^\diamond := \gamma(\mathcal{D}^+ - 1) = \gamma(e^{2\pi i \mathcal{D}} - 1) \tag{5.1}$$

The ω -components of \mathcal{D}^\diamond are of the form:

$$\mathcal{D}^\diamond = \sum_{\arg(\omega)=0} \Delta_\omega^\diamond = \sum_{\arg(\omega)=0} e^{-\omega \cdot z} \Delta_\omega^\diamond \tag{5.2}$$

$$(\widehat{\Delta}_\omega^\diamond \hat{\varphi})(\zeta) := \sum_{\epsilon_1, \dots, \epsilon_r} \frac{\epsilon_r}{2\pi i} \lambda_{\epsilon_1, \dots, \epsilon_{r-1}}^\diamond \hat{\varphi}^{\left(\begin{smallmatrix} \epsilon_1 & \dots & \epsilon_r \\ \omega_1 & \dots & \epsilon_r \end{smallmatrix}\right)}(\omega + \zeta). \tag{5.3}$$

⁵⁷ They become rational, of course, only after a homogeneous rescaling that amounts to setting $\pi := 1$.

Like with the λ -coefficients of the already familiar operators Δ_ω , Δ_ω^\pm , Δ_ω^\sharp , $\Delta_\omega^{\sharp\sharp}$, the coefficients $\lambda_{\epsilon_1, \dots, \epsilon_{r-1}}^\diamond$ that describe the action of Δ_ω^\diamond depend only on the *crossing pattern*, i.e. on the number p, q of plus and minus signs in the sequence $\{\epsilon_i\}$. But in this case they are given by:

$$\lambda_{\epsilon_1, \dots, \epsilon_{r-1}}^\diamond = \lambda_{\diamond}^{[p,q]} = (-1)^q \sum_{0 \leq k \leq p} \frac{p!}{(p-k)! k!} \gamma_{q+k}. \tag{5.4}$$

For $\gamma(t) = \frac{t}{1+t/2}$ or $\gamma(t) = \frac{(1+t)^2-1}{(1+t)^2+1}$, we recover the structure coefficients $\lambda_{\sharp}^{[p,q]}$, $\lambda_{\sharp\sharp}^{[p,q]}$ for the alien operators Δ_ω^\sharp and $\Delta_\omega^{\sharp\sharp}$ introduced in Section 1.6.

$$\lambda_{\sharp}^{[p,q]} = 2^{-p-q} \quad , \quad \lambda_{\sharp\sharp}^{[p,q]} = \varrho(p-q) 2^{-int(\frac{p+q+1}{2})}$$

where ϱ is the even function from $\mathbb{Z}/8\mathbb{Z}$ to \mathbb{Z} verifying $\varrho(k+4) = -\varrho(k)$ and $\varrho(0) = \varrho(\pm 1) = 1$. Since $\varrho(2) = -\varrho(2+4) = -\varrho(-2) = -\varrho(2)$, it follows that $\varrho(\pm 2) = 0$.

Short proof: After checking that the λ -coefficients of \mathcal{D}^\diamond inherit from those of \mathcal{D}^+ the crucial property of depending solely on the crossing pattern (p, q) , we are left with the simple task of considering the case of p initial right-crossings followed by q final left crossings. As in Section 1.6 we begin with the situation when all singularities are located over \mathbb{N} . Next we define the non-commuting elementary shifts σ, τ as in Section 1.6, then use the expansion

$$\begin{aligned} \mathcal{D}^+ - 1 &= (1 - \tau)(1 - \sigma)^{-1} - 1 = (\sigma - \tau)(1 - \sigma)^{-1} \\ &= \left(\sigma - \tau \right) \left(1 + \sum_{1 \leq p} \sigma^p \right) \end{aligned}$$

and in each power $(\mathcal{D}^+ - 1)^r$ collect the terms that contribute to $(\sigma - \tau)\tau^q\sigma^p$.

5.2 Twisted mould symmetries

Given any two power series without constant term

$$\alpha(t) = \sum_{0 \leq r} \alpha_r t^{1+r} \quad , \quad \beta(t) = \sum_{0 \leq r} \beta_r t^{1+r} \quad (\alpha_0 \neq 0, \beta_0 \neq 0)$$

we denote by $\alpha(Id^\bullet)$, $\beta(Id^\bullet)$, or simply α^\bullet , β^\bullet the moulds whose length-0 components vanish and whose length- r components are equal to

$$\alpha^{\omega_1} \equiv \alpha_0 \quad , \quad \alpha^{\omega_1, \dots, \omega_r} \equiv \alpha_{r-1} \quad , \quad \beta^{\omega_1} \equiv \beta_0 \quad , \quad \beta^{\omega_1, \dots, \omega_r} \equiv \beta_{r-1}$$

irrespective of the actual values of ω_i . We then define coefficients $\alpha^{p,q}$ and $\beta_{p,q}$ by setting

$$\sum \alpha^{p,q} t_1^p t_2^q := \alpha(\alpha^{-1}(t_1) + \alpha^{-1}(t_2)) \quad (5.5)$$

$$\sum \beta_{p,q} t_1^p t_2^q := \beta^{-1}(\beta(t_1) + \beta(t_2)). \quad (5.6)$$

If $M^\bullet \in \alpha^\bullet \circ \text{alternat}^\bullet$, then for any two sequences $\omega', \omega'' \neq \emptyset$:

$$\sum_{\substack{1 \leq p, 1 \leq q \\ (\omega'^1 \dots \omega'^p = \omega' \\ \omega''^1 \dots \omega''^q = \omega'')}} \alpha^{p,q} M^{\omega^1} \dots M^{\omega'^p} M^{\omega''^1} \dots M^{\omega''^q} \equiv \sum_{\omega \in \text{sha}(\omega', \omega'')} M^\omega. \quad (5.7)$$

If $M^\bullet \in \text{alternat}^\bullet \circ \beta^\bullet$, then for any two sequences $\omega', \omega'' \neq \emptyset$:

$$0 \equiv \sum_{\omega \in \text{sha}_{p,q}(\omega', \omega'')} \beta_{p,q} M^\omega. \quad (5.8)$$

If $M^\bullet \in \alpha^\bullet \circ \text{alternat}^\bullet \circ \beta^\bullet$, then for any two sequences $\omega', \omega'' \neq \emptyset$:

$$\sum_{\substack{1 \leq p, 1 \leq q \\ (\omega'^1 \dots \omega'^p = \omega' \\ \omega''^1 \dots \omega''^q = \omega'')}} \alpha^{p,q} M^{\omega^1} \dots M^{\omega'^p} M^{\omega''^1} \dots M^{\omega''^q} \equiv \sum_{\omega \in \text{sha}_{p,q}(\omega', \omega'')} \beta_{p,q} M^\omega. \quad (5.9)$$

An important sub-case is when α, β are reciprocal, for it corresponds to a symmetry type $\alpha^\bullet \circ \text{alternat}^\bullet \circ \beta^\bullet$ stable under mould-composition and leads to identical coefficients $\alpha^{p,q} = \beta_{p,q}$ on both sides of (5.9).

It is often preferable to take *eternel* rather than *alternat* as a standard of reference. Since

$$\text{eternel}^\bullet = (\exp(\text{Id}^\bullet) - 1^\bullet) \circ \text{alternat}^\bullet \circ \log(1^\bullet + \text{Id}^\bullet) \quad (5.10)$$

we see at once that moulds respectively of type

$$\text{eternel}^\bullet \circ \delta^\bullet, \quad \gamma^\bullet \circ \text{eternel}^\bullet, \quad \gamma^\bullet \circ \text{eternel}^\bullet \circ \delta^\bullet$$

still verify identities of the form (5.7), (5.8), (5.9), but with new coefficients $\gamma^{[p,q]}$, $\delta_{[p,q]}$, defined by

$$\sum \gamma^{[p,q]} t_1^p t_2^q := \gamma(\gamma^{-1}(t_1) + \gamma^{-1}(t_2) + \gamma^{-1}(t_1) \gamma^{-1}(t_2)) \quad (5.11)$$

$$\sum \delta_{[p,q]} t_1^p t_2^q := \delta^{-1}(\delta(t_1) + \delta(t_2) + \delta(t_1) \delta(t_2)) \quad (5.12)$$

in place of $\alpha_{p,q}, \beta^{p,q}$. Indeed, in view of (5.10), (5.11)-(5.12) results from (5.5)-(5.6) under the change $\alpha(t) = \gamma(e^t - 1)$, $\beta(t) = \log(1 + \delta(t))$

5.3 Twisted co-products

As useful as the statements of Section 5.2 are the dual statements:

(i) If $\theta_\diamond = \alpha(\theta_*)$ with $\text{cop}(\theta_*) = 1 \oplus \theta_* + \theta_* \oplus 1$, then

$$\text{cop}(\theta_\diamond) = 1 \oplus \theta_\diamond + \theta_\diamond \oplus 1 + \sum_{1 \leq p, q} \alpha^{p, q} (\theta_\diamond)^p \oplus (\theta_\diamond)^q. \quad (5.13)$$

(ii) If $\theta_\diamond = \gamma(\theta)$ with $\text{cop}(\theta) = 1 \oplus \theta + \theta \oplus 1 + \theta \oplus \theta$, then

$$\text{cop}(\theta_\diamond) = 1 \oplus \theta_\diamond + \theta_\diamond \oplus 1 + \sum_{1 \leq p, q} \gamma^{[p, q]} (\theta_\diamond)^p \oplus (\theta_\diamond)^q. \quad (5.14)$$

5.4 Twisted multitangents

Let $\gamma(t) = \sum_{0 \leq r} \gamma_r t^{r+1}$ and $\delta(t) = \sum_{0 \leq r} \delta_r t^{r+1}$ as usual⁵⁸ and let

$$\text{Te}_{\gamma, \delta}^\bullet := \gamma(\text{Id}^\bullet) \circ (\text{Te}^\bullet - 1^\bullet) \circ \delta(\text{Id}^\bullet) = \gamma(\text{Id}^\bullet) \circ \text{Tee}^\bullet \circ \delta(\text{Id}^\bullet). \quad (5.15)$$

Linearisation lemma: *The twisted multitangents $\text{Te}_{\gamma, \delta}^\bullet(z)$ can be uniquely expanded into sums of symmetrel multitangents $\text{Te}^\bullet(z)$*

$$\text{Te}_{\gamma, \delta}^{n_1, \dots, n_r}(z) = \sum_{1 \leq s \leq r} \sum_{1 \leq r_i}^{r_1 + \dots + r_s = r} \sum_{\sigma \in \mathfrak{S}_{r_1, \dots, r_s}} H_\sigma^{r_1, \dots, r_s} \text{Te}^{n_{\sigma, 1}, \dots, n_{\sigma, s}}(z) \quad (5.16)$$

with universal coefficients $H_\sigma^r = H_{[p, q]}^{r*}$ defined as follows

$$\begin{aligned} H^{r_1, \dots, r_s}(\sigma) &= H_{[p, q]}^{r_1^*, \dots, r_s^*} \\ &= \sum_{k=0}^{r-s^*} \left[\sum_{l=0}^p \gamma_{k+q+l} \frac{p!}{(p-l)! l!} \right] \left[\frac{\nabla^k}{k!} (\delta_{r_1^*-1} \dots \delta_{r_s^*-1}) \right]. \end{aligned} \quad (5.17)$$

(i) The sum (5.16) ranges over all ordered sequences (r_1, \dots, r_s) and all permutations σ in $\mathfrak{S}_{r_1, \dots, r_s}$, i.e. all σ that *increase* on each of the intervals I_{r_k} of the partition

$$\mathcal{I}_{r_1} \sqcup \dots \sqcup \mathcal{I}_{r_s} = [1, \dots, r] \in \mathbb{Z} \quad (\text{card}(\mathcal{I}_{r_i}) = r_i).$$

(ii) The indices of $\text{Te}^\bullet(z)$ on the right-hand side of (5.16) are given by

$$n_{\sigma, i} = \sum_{j \in \mathcal{I}_{r_i}} n_{\sigma(j)} \quad \forall i \in [1, s].$$

⁵⁸ For the moment, we assume neither $\gamma \circ \delta = \text{id}$ nor $\gamma_0 \neq 0, \delta_0 \neq 0$.

(iii) $\mathcal{I}_{r_1^*} \sqcup \cdots \sqcup \mathcal{I}_{r_{s^*}^*}$ denotes the *minimal* sub-partition of $\mathcal{I}_{r_1} \sqcup \cdots \sqcup \mathcal{I}_{r_s}$ such that σ increases *without gaps* on each $\mathcal{I}_{r_k^*}$, *i.e.* such that

$$\sigma(j) - \sigma(i) \equiv j - i \quad \forall i, j \in \mathcal{I}_{r_k^*} \quad , \quad \forall k \in [1, s^*].$$

(iv) There exist two full orders $<$ and $<_\sigma$ on the set $\{\mathcal{I}_{r_1^*}, \dots, \mathcal{I}_{r_{s^*}^*}\}$:

$$\begin{aligned} \{\mathcal{I}_{r_k^*} < \mathcal{I}_{r_l^*}\} &\Leftrightarrow i < j & \forall (i, j) \in (\mathcal{I}_{r_k^*}, \mathcal{I}_{r_l^*}) &\Leftrightarrow k < l \\ \{\mathcal{I}_{r_k^*} <_\sigma \mathcal{I}_{r_l^*}\} &\Leftrightarrow \sigma(i) < \sigma(j) & \forall (i, j) \in (\mathcal{I}_{r_k^*}, \mathcal{I}_{r_l^*}). \end{aligned}$$

For each $k \leq s^*$ the immediate $<_\sigma$ -successor of $\mathcal{I}_{r_k^*}$ is noted $\mathcal{I}_{r_{k^+}^*}$ (when it exists, *i.e.* when $\mathcal{I}_{r_k^*}$ is not $<_\sigma$ -maximal). The integer p (respectively q) so defined

$$p := \sum_{k < k^+} 1 \quad , \quad q := \sum_{k > k^+} 1 \quad (p + q \equiv s^* - 1)$$

measures the compatibility (respectively incompatibility) of $<$ and $<_\sigma$.

(v) ∇ denotes the *derivation* on $\mathbb{Q}[\delta_0, \delta_1, \delta_2 \dots]$ characterised by

$$\nabla \delta_0 := 0, \quad \nabla \delta_1 := (\delta_0)^2, \quad \nabla \delta_2 := 2 \delta_0 \delta_1, \dots, \quad \nabla \delta_r := \sum_{r'=0}^{r-1} \delta_{r'} \delta_{r-1-r'}.$$

It readily follows that

$$\frac{\nabla^r}{r!} \delta_r \equiv (\delta_0)^{r+1} \quad , \quad \frac{\nabla^l}{l!} \delta_r \equiv 0 \quad \text{iff } r < l.$$

Remark 1. When k takes either of its extreme values 0 or $r - s^*$, the formula (5.17) gives for $H_{[p,q]}^{r^*}$ two γ -dependent parts respectively of the form

$$\begin{aligned} (*) & \gamma_q + \cdots + \gamma_{p+q} \\ (**) & \gamma_{q+r-s^*} + \cdots + \gamma_{p+q+r-s^*} = \gamma_{r-1-p} + \cdots + \gamma_{r-1} \end{aligned}$$

while the δ -dependent parts reduce to

$$\begin{aligned} (*) & \frac{\nabla^0}{0!} \prod_i \delta_{r_i^*-1} = \prod_i \delta_{r_i^*-1} \\ (**) & \frac{\nabla^{r-s^*}}{(r-s^*)!} \prod_i \delta_{r_i^*-1} = \prod_i \left(\frac{\nabla^{r_i^*-1}}{(r_i^*-1)!} \delta_{r_i^*-1} \right) = \prod_i (\delta_0)^{r_i^*} = (\delta_0)^r \end{aligned}$$

As a consequence of (**), $H_{[p,q]}^{r^*}$ always contains the term $\gamma_{r-1}(\delta_0)^r$ among its summands.

Remark 2. Exchanging two adjacent intervals $\mathcal{I}_{r_i^*}$ and $\mathcal{I}_{r_{i+1}^*}$ with *non-adjacent* images⁵⁹ $\sigma(\mathcal{I}_{r_i^*})$ and $\sigma(\mathcal{I}_{r_{i+1}^*})$ leaves the pair (p, q) unchanged. On the other hand, once (p, q) has been determined in function of σ and the ordered sequence r^* , the order in r^* no longer counts for the determination of $H_{\gamma,\delta}^{r^*}(p, q)$. For a given depth r , therefore, the maximum number of distinct values assumed by $H_{\gamma,\delta}^{r^*}(p, q)$ cannot exceed $\sum_{k=1}^r k p(r, k)$, with $p(r, k)$ denoting the number of k -multiple partitions of r .

Example. Let us calculate the coefficients of $Te^{n_1, n_3+n_4, n_2+n_6+n_7}$ in the expansion (5.16) of $Te_{\gamma,\delta}^{n_1, \dots, n_6}$. Starting from a partition $r = (1, 2, 3)$ with $s = 3$ we arrive at the refined partition $r^* = (1, 2, 1, 2)$ with $s^* = 4$. Applying (5.17) and the rules for handling ∇ , we successively find:

$$\begin{aligned} H_{[2,1]}^{1,2,1,2} &= \sum_{k=0}^2 (\gamma_{1+k} + 2\gamma_{2+k} + \gamma_{3+k}) \frac{\nabla^k}{k!} (\delta_0 \delta_1 \delta_0 \delta_1) \\ &= +(\gamma_1 + 2\gamma_2 + \gamma_3) (\delta_0^2 \delta_1^2) \\ &\quad +(\gamma_2 + 2\gamma_3 + \gamma_4) (2\delta_0^4 \delta_1) \\ &\quad +(\gamma_3 + 2\gamma_4 + \gamma_5) (\delta_0^6). \end{aligned}$$

We would find exactly the same coefficient for $Te^{n_1, n_3+n_4, n_2, n_6+n_7}$ and for $Te^{n_1, n_3+n_4, n_6+n_7, n_2}$, in agreement with the observation of Remark 2 above.

Special cases. If we now assume that $\gamma \circ \delta = id$, we find few noteworthy simplications, apart from the automatic vanishing of the coefficient $H_{[r-1,0]}^r$ that stands in front of the lone ‘monotangent’ $Te^{|n|}$ in the Te^\bullet -expansion (5.16) of Te^n . For real simplications, we must turn to the multi-tangents $Te_{\#c}^\bullet = Te_{\gamma_c, \delta_c}^\bullet$ with homographic driving series $\gamma_c(t) = \frac{t}{1+ct}$ and $\delta_c(t) = \frac{t}{1-ct}$. In that case, a simple calculation shows that in the expansion (5.16) of $Te_{\gamma_c, \delta_c}^n$ the only surviving terms $Te^{n_{\sigma,1}, \dots, n_{\sigma,s}}$ are those whose indices $n_{\sigma,k}$ carry no sums $n_i + n_{i+1}$ of consecutive terms. This implies that the only non-zero coefficients $H_{\gamma_c, \delta_c}^{r^*}(p, q)$ correspond to reduced sequences r^* with all multiplicities $r_i^* \equiv 1$, so that $s = r$. Moreover, even these surviving $H_{[p,q]}^{r^*}$ turn out to be extremely simple:

$$H_{[p,q]}^{1, \dots, 1} = (1 - c)^p (-c)^q. \tag{5.18}$$

⁵⁹ This of course is possible only if $\mathcal{I}_{r_i^*}$ and $\mathcal{I}_{r_{i+1}^*}$ do not stem from one and the same \mathcal{I}_k .

When $c = 1/2$, we recover the formula (2.49) for the Te^\bullet -expansion of the olternol multitangents Too^\bullet .

The family

$$\gamma(t) := \frac{1(1+t)^{2c} - 1}{c(1+t)^{2c} + 1}, \quad \delta(t) := \left(\frac{1+ct}{1-ct}\right)^{\frac{1}{2c}} - 1 \quad (5.19)$$

does not lead to simple results, except of course in the case $c = 1/2$, where it coincides with (5.18), and in the case $c = 1$, where all coefficients $H_{\gamma_c, \delta_c}^{r^*}(p, q)$ turn out to be simple products of Catalan numbers times a negative power of 2 and an appropriate sign in front. Here is the precise statement:

8-periodicity of $H_{[p,q]}^{r^*}$. For γ, δ of the form

$$\gamma(t) := \frac{t + \frac{1}{2}t^2}{1 + t + \frac{1}{2}t^2}, \quad \delta(t) := \left(\frac{1+t}{1-t}\right)^{\frac{1}{2}} - 1 \quad (5.20)$$

we have

$$H_{[p,q]}^{r_1^*, \dots, r_s^*} = \rho_*(s_u - s_e + 2p) 2^{\text{int}(s/2)} \prod_{1 \leq i \leq s} \kappa(r_i^*) \quad (5.21)$$

$$= \rho(2s_u + p - q) 2^{\text{int}(s/2)} \prod_{1 \leq i \leq s} \kappa(r_i^*) \quad (5.22)$$

with

$$s_u := \sum_{r_i^*=1} 1, s_e := \sum_{r_i^* \text{ even} \geq 2} 1, s_o := \sum_{r_i^* \text{ odd} \geq 3} 1 \quad (1+p+q \equiv s_u + s_o + s_e)$$

$$\text{int}(s) = \text{integer part of } s \quad (5.23)$$

$$\rho_*(m) : \mathbb{Z}/8\mathbb{Z} \rightarrow \mathbb{Z}, [0, 1, 2, 3, 4, 5, 6, 7] \mapsto [-1, 2, -1, 0, 1, -2, 1, 0] \quad (5.24)$$

$$\rho(m) : \mathbb{Z}/8\mathbb{Z} \rightarrow \mathbb{Z}, [0, 1, 2, 3, 4, 5, 6, 7] \mapsto [0, -1, 2, -1, 0, 1, -2, 1] \quad (5.25)$$

$$\kappa(1) := 1/2, \kappa(2n) := \frac{1}{2^{2n}} \frac{(2n-2)!}{n!(n-1)!}, \kappa(2n+1) := 0 \quad \forall n > 1. \quad (5.26)$$

Due to (5.26), $H_{[p,q]}^{r^*}$ vanishes unless none of the indices r_i^* is odd ≥ 3 . Moreover, when all r_i^* are either 1 or even, after division by elementary factors (- powers of 2 and Catalan numbers -) we get an expression h :

$$h(p, q, s_u, s_e) := H_{[p,q]}^{r_1^*, \dots, r_s^*} 2^{-\text{int}(s/2)} \prod_i (1/\kappa(r_i^*)) \quad (5.27)$$

$$= \rho(2s_u + p - q) \quad (5.28)$$

$$= \rho_*(s_u - s_e + 2p) = \rho_*(3s_u + s_e - 2q - 2) \quad (5.29)$$

which turns out, quite unexpectedly, to be 8-periodic in the order-compatibility coefficients p, q and the multiplicities s_u, s_e .

5.5 Affiliates : from function to operator

We have the choice between relating an affiliate F_{\diamond} to F itself or to its infinitesimal generator F_* :

$$F_{\diamond} := \gamma(F - 1) = \alpha(F_*) \quad (F_* := \log(F)). \quad (5.30)$$

This implies handling two distinct systems of coefficients:

$$\alpha(t) = t + \sum_{1 \leq r} \alpha_r t^{r+1}, \quad \gamma(t) = t + \sum_{1 \leq r} \gamma_r t^{r+1}, \quad (\gamma(t) = \alpha(\log(1+t))). \quad (5.31)$$

The choice impacts the analytic expression of the correspondence $f_{\diamond} \mapsto F_{\diamond}$:

$$F_{\diamond} \mapsto f_{\diamond} = F_{\diamond} \cdot z \quad (5.32)$$

$$f_{\diamond} \mapsto F_{\diamond} = \sum_{1 \leq r} \sum_{1 \leq n_i} \diamond_{n_1, \dots, n_r} \left(f_{\diamond}^{n_1} \frac{\partial^{n_1}}{z^{n_1!}} \right) \dots \left(f_{\diamond}^{n_r} \frac{\partial^{n_r}}{z^{n_r!}} \right) \quad (n_r > 1 \text{ if } r > 1). \quad (5.33)$$

Although F_{\diamond} is usually derived from F rather than F_* , the structure coefficients $\diamond_{n_1, \dots, n_r}$ are simpler to express in terms of the coefficients α_n than in terms of γ_n : in the former case, the sums involve fewer terms $\prod \alpha_{m_j}$ due to the homogeneity constraints $\sum n_i = \sum m_j$. The simplest way to ensure (5.32) is to set $\diamond_1 = 1$ and to impose that all other coefficients $\diamond_{n_1, \dots, n_r}$ ending with $n_r = 1$ should vanish. This, however, is not enough to enforce the uniqueness of the expansion (5.33), due to the existence, for n large enough, of universal identities of the form

$$0 \equiv \sum_{n_1 + \dots + n_r = n} c_{n_1, \dots, n_r} \left(f_{\diamond}^{n_1} \frac{\partial^{n_1}}{z^{n_1!}} \right) \dots \left(f_{\diamond}^{n_r} \frac{\partial^{n_r}}{z^{n_r!}} \right) \quad (c_{n_1, \dots, n_r} \in \mathbb{Z}). \quad (5.34)$$

The latitude in the choice of the structure coefficients being $2^{r-2} - par(r)$ for $r > 1$ ($par =$ partition number), it is clear that even imposing a natural condition⁶⁰ like

$$\left\{ \alpha_n = \frac{1}{(n+1)!} \quad \forall n \right\} \implies \left\{ \diamond^{n_1} = 1 \quad \forall n_1, \quad \diamond^{n_1, \dots, n_r} = 0 \quad \forall r \geq 2 \right\} \quad (5.35)$$

is not enough to restore uniqueness. In fact, we know of no *simple* condition that does. In any case, here is a natural choice for the first structure

⁶⁰ Natural indeed, since this choice of α leads to the fonction $f_{\diamond}(z) = f(z) - z$ and to the operator $F_{\diamond} = F - 1 = \sum_{1 \leq n} f_{\diamond}^n \frac{\partial^n}{n!}$.

coefficients:

$$\begin{aligned}
 \diamond^1 &= 1 \\
 \diamond^2 &= 2\alpha_1 \\
 \diamond^3 &= -3\alpha_2 + 6\alpha_1^2 \\
 \diamond^{1,2} &= 3\alpha_2 - 2\alpha_1^2 \\
 \diamond^4 &= 4\alpha_3 - 20\alpha_1\alpha_2 + 20\alpha_1^3 \\
 \diamond^{1,3} &= -7\alpha_3 + 20\alpha_1\alpha_2 - 11\alpha_1^3 \\
 \diamond^{2,2} &= 2\alpha_3 + 2\alpha_1\alpha_2 - 2\alpha_1^3 \\
 \diamond^{1,1,2} &= 3\alpha_3 - 6\alpha_1\alpha_2 + 3\alpha_1^3 \\
 \\
 \diamond^5 &= -5\alpha_4 + 30\alpha_1\alpha_3 + 15\alpha_2^2 - 105\alpha_1^2\alpha_2 + 70\alpha_1^4 \\
 \diamond^{1,4} &= 21\alpha_4 - \frac{366}{5}\alpha_1\alpha_3 - \frac{171}{5}\alpha_2^2 + \frac{789}{5}\alpha_1^2\alpha_2 - \frac{342}{5}\alpha_1^4 \\
 \diamond^{2,3} &= -28\alpha_4 + \frac{348}{5}\alpha_1\alpha_3 + \frac{168}{5}\alpha_2^2 - \frac{552}{5}\alpha_1^2\alpha_2 + \frac{196}{5}\alpha_1^4 \\
 \diamond^{3,2} &= 9\alpha_4 - \frac{114}{5}\alpha_1\alpha_3 - \frac{99}{5}\alpha_2^2 + \frac{321}{5}\alpha_1^2\alpha_2 - \frac{138}{5}\alpha_1^4 \\
 \diamond^{1,1,3} &= 0 \\
 \diamond^{1,2,2} &= -\alpha_4 + \frac{86}{5}\alpha_1\alpha_3 + \frac{51}{5}\alpha_2^2 - \frac{229}{5}\alpha_1^2\alpha_2 + \frac{102}{5}\alpha_1^4 \\
 \diamond^{2,1,2} &= +4\alpha_1\alpha_3 - 8\alpha_1^2\alpha_2 + 4\alpha_1^4 \\
 \diamond^{1,1,1,2} &= 4\alpha_4 - \frac{64}{5}\alpha_1\alpha_3 - \frac{24}{5}\alpha_2^2 + \frac{116}{5}\alpha_1^2\alpha_2 - \frac{48}{5}\alpha_1^4.
 \end{aligned}$$

Remarkably enough, for index sums $|\mathbf{n}| \geq 5$, a fair number of structure coefficients $\diamond^{\mathbf{n}}$ are always $= 0$, irrespective of α and despite having a last index $n_r \neq 1$. Here are the first unconditionally vanishing coefficients:

$$\begin{aligned}
 |\mathbf{n}|=5 &: \diamond^{1,1,3} \\
 |\mathbf{n}|=6 &: \diamond^{2,4}, \diamond^{3,1,2}, \diamond^{1,1,1,3}, \diamond^{1,1,1,1,2} \\
 |\mathbf{n}|=7 &: \diamond^{2,5}, \diamond^{1,3,3}, \diamond^{1,1,1,4}, \diamond^{1,1,2,3}, \diamond^{1,2,1,3}, \diamond^{2,1,1,3}, \diamond^{2,1,2,2}, \diamond^{1,1,1,1,3}, \\
 &\quad \diamond^{1,1,1,2,2}, \diamond^{1,1,2,1,2}, \diamond^{1,2,1,1,2}, \diamond^{2,1,1,1,2}, \diamond^{1,1,1,1,1,2}.
 \end{aligned}$$

Here again, the case

$$\alpha(t) = \frac{1}{c} \tanh(ct) \quad , \quad \gamma(t) = \frac{1}{c} \frac{(1+t)^{2c} - 1}{(1+t)^{2c} + 1} \quad (5.36)$$

stands out for simplicity. It makes it possible to choose a system of structure coefficients which are all $\equiv 0$ except those of the form:

$$\diamond^{2m_1-1, 2m_2, 2m_3, \dots, 2m_r} = (-1)^{r-1} c^{-2+2\sum m_i} \quad (\forall r, \forall m_i \geq 1). \quad (5.37)$$

When $c = \frac{1}{2}$ we recover the earlier formula (1.26) for the mediator.

5.6 Main and secondary symmetry types

Let us stand back and take stock. Alongside the four ubiquitous symmetry types:

$$\begin{aligned}
 \mathit{alternel}^\bullet &= \mathit{basic\ symmetry\ type} \\
 \mathit{symmetral}^\bullet &= (\exp Id^\bullet) \circ \mathit{alternel}^\bullet \\
 \mathit{alternel}^\bullet &= \mathit{alternel}^\bullet \circ \log(1^\bullet + Id^\bullet) \\
 \mathit{symmetrel}^\bullet &= (\exp Id^\bullet) \circ \mathit{alternel}^\bullet \circ \log(1^\bullet + Id^\bullet)
 \end{aligned}$$

we have a number of special symmetry types, of secondary but non-negligible importance:

$$\begin{aligned}
 \mathit{olternal}^\bullet &= \alpha(Id^\bullet) \circ \mathit{alternel}^\bullet \\
 &= \gamma(Id^\bullet) \circ (\mathit{symmetral}^\bullet - 1^\bullet) \\
 \mathit{alternol}^\bullet &= \mathit{alternel}^\bullet \circ \beta(Id^\bullet) \\
 &= \mathit{alternel}^\bullet \circ \delta(Id^\bullet) \\
 \mathit{olternol}^\bullet &= \alpha(Id^\bullet) \circ \mathit{alternel}^\bullet \circ \beta(Id^\bullet) \\
 &= \gamma(Id^\bullet) \circ (\mathit{symmetrel}^\bullet - 1^\bullet) \circ \delta(Id^\bullet) \\
 \mathit{symmetrol}^\bullet &= \mathit{symmetral}^\bullet \circ \beta(Id^\bullet) \\
 &= \mathit{symmetrel}^\bullet \circ \delta(Id^\bullet).
 \end{aligned}$$

Choice 1. The most common choice for the quartet $(\alpha, \beta, \gamma, \delta)$ is

$$\alpha(t) := 2 \tanh\left(\frac{1}{2}t\right), \quad \beta(t) := 2 \operatorname{arctanh}\left(\frac{1}{2}t\right) \quad (5.38)$$

$$\gamma(t) := \frac{t}{1 + \frac{1}{2}t}, \quad \delta(t) := \frac{t}{1 - \frac{1}{2}t}. \quad (5.39)$$

The corresponding structure constants are:

$$\begin{aligned}
 \lambda^{[p,q]} &= 2^{-p-q} \\
 \gamma^{[p,q]} &= \left(-\frac{1}{4}\right)^{\inf(p,q)} \text{ if } |p-q|=1 \quad (\text{resp. } 0 \text{ otherwise}) \\
 \diamond^{n_1, \dots, n_r} &= (-1)^{r-1} 2^{1-\sum n_i} \text{ if } r, n_1 \text{ odd}, n_2, \dots, n_r \text{ even} \quad (\text{resp. } 0 \text{ otherwise}) \\
 H_{[p,q]}^{r_1^*, \dots, r_s^*} &= (-1)^q \left(\frac{1}{4}\right)^{s-1} \text{ if } r_1^* = \dots = r_s^* = 1 \quad (\text{resp. } 0 \text{ otherwise}).
 \end{aligned}$$

Choice 2. More rarely we take

$$\alpha(t) := \tanh(t) \quad , \quad \beta(t) := \operatorname{arctanh}(t) \tag{5.40}$$

$$\gamma(t) := \frac{t + \frac{1}{2}t^2}{1 + t + \frac{1}{2}t^2} \quad , \quad \delta(t) := \left(\frac{1+t}{1-t}\right)^{\frac{1}{2}} - 1. \tag{5.41}$$

This choice leads to marginally less simple structure coefficients:

$$\begin{aligned} \lambda^{[p,q]} &= \varrho(p-q) 2^{-\operatorname{int}(\frac{p+q+1}{2})} \\ \gamma^{[p,q]} &= (-1)^{\operatorname{inf}(p,q)} \text{ if } |p-q| = 1 \quad (\text{resp. } 0 \text{ otherwise}) \\ \diamond^{n_1, \dots, n_r} &= (-1)^{r-1} \text{ if } r, n_1 \text{ odd, } n_2, \dots, n_r \text{ even } (\text{resp. } 0 \text{ otherwise}) \\ H_{[p,q]}^{r_1^*, \dots, r_s^*} &= \rho(2s_u + p - q) 2^{\operatorname{int}(s/2)} \prod_{1 \leq i \leq s} \kappa(r_i^*) \quad (\text{resp. } 0 \text{ if } s_0 \neq 0) \end{aligned}$$

with $s_u, s_o, s_e, \rho, \varrho, \kappa$ as in (5.24)-(5.26). In particular:

$$\rho : \mathbb{Z}/8\mathbb{Z} \rightarrow \mathbb{Z} \quad , \quad [0, 1, 2, 3, 4, 5, 6, 7] \mapsto [0, -1, 2, -1, 0, 1, -2, 1]$$

$$\varrho : \mathbb{Z}/8\mathbb{Z} \rightarrow \mathbb{Z} \quad , \quad [0, 1, 2, 3, 4, 5, 6, 7] \mapsto [1, 1, 0, -1, -1, -1, 0, 1]$$

ρ is odd and ϱ even but both change signs under 4-shifts

$$\rho(k+4) \equiv -\rho(k) \quad , \quad \varrho(k+4) \equiv -\varrho(k).$$

Choice 3. If $c \notin \{\pm 1, \pm i, \pm \frac{1}{2}, \pm \frac{i}{2}\}$ the one-parameter family

$$\alpha_c(t) := \frac{1}{c} \tanh(ct) \quad , \quad \beta_c(t) := \frac{1}{c} \operatorname{arctanh}(ct) \tag{5.42}$$

$$\gamma_c(t) := \frac{1(1+t)^{2c} - 1}{c(1+t)^{2c} + 1} \quad , \quad \delta_c(t) := \left(\frac{1+ct}{1-ct}\right)^{\frac{1}{2c}} - 1. \tag{5.43}$$

makes only $\gamma^{[p,q]}$ and \diamond^\bullet simple:

$$\begin{aligned} \lambda^{[p,q]} &= \text{no simple multiplicative structure} \\ \gamma^{[p,q]} &= (-c^2)^{\operatorname{inf}(p,q)} \text{ if } |p-q| = 1 \quad , \quad (\text{else } = 0) \\ \diamond^{n_1, \dots, n_r} &= (-1)^{r-1} c^{-1+\sum n_i} \text{ if } r, n_1 \text{ odd, } n_2, \dots, n_r \text{ even } (\text{else } = 0) \\ H_{[p,q]}^{r_1^*, \dots, r_s^*} &= \text{no simple multiplicative structure.} \end{aligned}$$

Choice 4. The homographic quartet:

$$\underline{\alpha}_c(t) := \frac{(e^t - 1)}{1 + c(e^t - 1)} \quad , \quad \underline{\beta}_c(t) := \frac{t}{1 - ct} \tag{5.44}$$

$$\underline{\gamma}_c(t) := \frac{t}{1 + ct} \quad , \quad \underline{\delta}_c(t) := \frac{t}{1 - ct} \tag{5.45}$$

predictably leads to simpler structure coefficients:

$$\begin{aligned} \lambda^{[p,q]} &= c^q (1 - c)^p \\ \gamma^{[p,q]} &= 0 \quad \text{if } |p - q| \geq 2 \\ \gamma^{[p,p]} &= (1 - 2c) c^{p-1} (c - 1)^{p-1} \\ \gamma^{[p,p+1]} &= \gamma_c^{[p+1,p]} = c^p (c - 1)^p \\ \diamond^{n_1, \dots, n_r} &= \text{no simple multiplicative structure} \end{aligned}$$

$$H_{[p,q]}^{r_1^*, \dots, r_s^*} = (-c)^q (1 - c)^p \text{ if } r_1^* = \dots = r_s^* = 1 \text{ (resp. } 0 \text{ otherwise).}$$

General case. Lastly, for arbitrary but mutually reciprocal (γ, δ) , the formulae read

$$\begin{aligned} \lambda^{[p,q]} &= (-1)^q \sum_{0 \leq k \leq p} \frac{p!}{(p-k)! k!} \gamma_{q+k} \\ \gamma^{[p,q]} &: \text{generated by } \gamma(\delta(t_1) + \delta(t_2) + \delta(t_1)\delta(t_2)) = \sum \gamma^{[p,q]} t_1^p t_2^q \\ \diamond^{n_1, \dots, n_r} &: \text{multiple competing expressions.} \end{aligned}$$

$$H_{[p,q]}^{r_1^*, \dots, r_s^*} = \sum_{k=0}^{r-s^*} \left[\sum_{l=0}^p \gamma_{k+q+l} \frac{p!}{(p-l)! l!} \right] \left[\frac{\nabla^k}{k!} (\delta_{r_1^*-1} \dots \delta_{r_s^*-1}) \right]$$

In conclusion, of all secondary symmetry types, the simplest (and most frequently occurring in practice) is the one at the intersection of the two one-parameter families: $\gamma = \gamma_{\frac{1}{2}} = \underline{\gamma}_{\frac{1}{2}}$, $\delta = \delta_{\frac{1}{2}} = \underline{\delta}_{\frac{1}{2}}$.

Remark 1. Consider the \mathbb{N} -indexed mould har^\bullet defined by the induction

$$|\bullet| \text{ har}^\bullet = \text{har}^\bullet \times Id^\bullet \times \text{har}^\bullet \text{ (resp. } = 0 \text{) if } r(\bullet) \text{ odd (resp. even)}$$

or more explicitly

$$\text{har}^{n_1} = \frac{1}{n_1} \tag{5.46}$$

$$\text{har}^{n_1, \dots, n_r} := 0 \quad \forall r \text{ even} \quad (\text{in particular } \text{har}^\emptyset := 0) \tag{5.47}$$

$$\text{har}^{n_1, \dots, n_r} := \frac{1}{n_1 + \dots + n_r} \sum_{1 < i < r} \text{har}^{n_1, \dots, n_{i-1}} \text{har}^{n_{i+1}, \dots, n_r} \quad (\forall r \text{ odd } \geq 3) \tag{5.48}$$

har^\bullet is the simplest example of a i -olternal mould. It occurs naturally in the study of some special trigonometric flexion algebras.⁶¹ Its inverse $kohar^\bullet$ under mould composition is even more elementary:

$$\text{kohar}^{n_1, \dots, n_{2r}} \equiv 0 \quad , \quad \text{kohar}^{n_1, \dots, n_{2r+1}} \equiv (-1)^r n_r \tag{5.49}$$

$kohar^\bullet$ is the simplest instance of a i -alternol mould.

⁶¹ Cf. [10, page 177].

Remark 2. There is an important operator \mathfrak{S} , also acting on a trigonometric flexion algebra⁶², that happens to verify a co-symmetrol co-product.⁶³

Remark 3. There seems to exist no simple notion of *bracket* (anti-commutative and rational in its two arguments) for mediators and consequently no proper equivalent of the Campbell-Hausdorff formula for expressing $(F.G)_{\sharp}$ in terms of F_{\sharp} and G_{\sharp} , other than the obvious expansion that relies on the coefficients $\gamma^{[\bullet]}$ defined by the series in the non-commutative variables t_1, t_2 :

$$\sum \gamma^{[[p_1, q_1, \dots, p_r, q_r]]} t_1^{p_1} t_2^{q_1} \dots t_1^{p_r} t_2^{q_r} := \gamma(\gamma^{-1}(t_1) + \gamma^{-1}(t_2) + \gamma^{-1}(t_1)\gamma^{-1}(t_2))$$

with $p_1, q_r \geq 0$ and all other $p_i, q_i \geq 1$.

6 Complement: arithmetical vs dynamical monics

6.1 Distinguishing Stokes constants from holomorphic invariants

The scalars $A_{\omega}(f)$ may be viewed

- (i) as Stokes constants;
- (ii) as holomorphic invariants.

In their first capacity, they govern the Stokes transitions and are rigidly determined. So too are the (presumably transcendental) monics — the multizetas — which enter their expansions. We speak accordingly of *rigid* or *arithmetical monics*.

There is more latitude, however, when we look upon the scalars $A_{\omega}(f)$ as holomorphic invariants and retain only those multizeta properties which are directly responsible for their invariance. We speak in that case of *dynamical monics*.

Both types of monics verify various types of relations, some infinite, some finite-algebraic. When viewed as subject only to their various systems of algebraic relations over \mathbb{Q} , our monics (whether rigid-arithmetical or dynamical) become *formal monics*. As such, they possess their own system of independent generators, the so-called *irreducibles*. Being subject to laxer constraints, the *dynamical irreducibles* should be expected to be, and in fact are, more ‘numerous’ than the *rigid-arithmetical irreducibles*.⁶⁴

⁶² Cf. [10, (11.42)-(11.43)].

⁶³ Cf. [10, (11.47)].

⁶⁴ Though of course any complete system of irreducibles, of either sort, has to be countably infinite.

6.2 Arithmetical multizetas

The two classical systems of algebraic (quadratic) constraints. Either system of constraints is best expressed as a specific multiplication rule relative to a specific encoding.

In the *first* or α -*encoding*, the multizetas are given by polylogarithmic integrals:

$$\text{wa}_*^{\alpha_1, \dots, \alpha_l} := (-1)^{l_0} \int_0^1 \frac{dt_1}{(\alpha_1 - t_1)} \cdots \int_0^{t_3} \frac{dt_2}{(\alpha_2 - t_2)} \int_0^{t_2} \frac{dt_1}{(\alpha_1 - t_1)} \quad (6.1)$$

with indices α_j that are either 0 or unit roots, and $l_0 := \sum_{\alpha_i=0} 1$.

In the *second* or (ϵ_s) -*encoding*, the multizetas are expressed as “harmonic sums”:

$$\text{ze}_*^{\binom{\epsilon_1 \dots \epsilon_r}{s_1 \dots s_r}} := \sum_{n_1 > \dots > n_r > 0} n_1^{-s_1} \dots n_r^{-s_r} e_1^{-n_1} \dots e_r^{-n_r} \quad (6.2)$$

with $s_j \in \mathbb{N}^*$ and unit roots $e_j := \exp(2\pi i \epsilon_j)$ of ‘logarithms’ $\epsilon_j \in \mathbb{Q}/\mathbb{Z}$.

The stars $*$ means that the integrals or sums are provisionally assumed to be convergent or semi-convergent: for wa_*^α this means that $\alpha_1 \neq 0$ and $\alpha_l \neq 1$, and for $\text{ze}_*^{\binom{\epsilon}{s}}$ this means that $\binom{\epsilon_1}{s_1} \neq \binom{0}{1}$ i.e. $\binom{\epsilon_1}{s_1} \neq \binom{1}{1}$.

The corresponding moulds wa_*^\bullet and ze_*^\bullet turn out to be respectively *symmetral* and *symmetrel*:⁶⁵

$$\text{wa}_*^{\alpha^1} \text{wa}_*^{\alpha^2} = \sum_{\alpha \in \text{sha}(\alpha^1, \alpha^2)} \text{wa}_*^\alpha \quad \forall \alpha^1, \forall \alpha^2 \quad (6.3)$$

$$\text{ze}_*^{\binom{\epsilon^1}{s^1}} \text{ze}_*^{\binom{\epsilon^2}{s^2}} = \sum_{\binom{\epsilon}{s} \in \text{she}\left(\binom{\epsilon^1}{s^1}, \binom{\epsilon^2}{s^2}\right)} \text{ze}_*^{\binom{\epsilon}{s}} \quad \forall \binom{\epsilon^1}{s^1}, \forall \binom{\epsilon^2}{s^2}. \quad (6.4)$$

These are the so-called *quadratic relations*, which express *multizeta dimorphism*. As for the conversion rule, it reads:⁶⁶

$$\text{wa}_*^{e_1, 0^{[s_1-1]}, \dots, e_r, 0^{[s_r-1]}} := \text{ze}_*^{\binom{\epsilon_r, \epsilon_{r-1:r}, \dots, \epsilon_{1:2}}{s_r, s_{r-1}, \dots, s_1}} \quad (6.5)$$

$$\text{ze}_*^{\binom{\epsilon_1, \epsilon_2, \dots, \epsilon_r}{s_1, s_2, \dots, s_r}} =: \text{wa}_*^{e_1 \dots e_r, 0^{[s_r-1]}, \dots, e_1 e_2, 0^{[s_2-1]}, e_1, 0^{[s_1-1]}} \quad (6.6)$$

with $0^{[k]}$ denoting a subsequence of k zeros.

⁶⁵ As usual, $\text{sha}(\omega', \omega'')$ denotes the set of all simple shufflings of the sequences ω', ω'' , whereas in $\text{she}(\omega', \omega'')$ we allow (any number of) order-compatible contractions $\omega'_i + \omega''_j$.

⁶⁶ With the usual shorthand for differences: $\epsilon_{i:j} := \epsilon_i - \epsilon_j$.

There happen to be unique extensions $wa_*^\bullet \rightarrow wa^\bullet$ and $ze_*^\bullet \rightarrow ze^\bullet$ that cover the divergent cases and keep our moulds symmetrical or symmetrel while conforming to the ‘initial conditions’ $wa^0 = wa^1 = 0$ and $ze^{(0)} = 0$. As we shall see in a moment, however, the divergent case calls for a slight modification of the conversion rules (6.5)-(6.6).

Arithmetical multizeta irreducibles. The \mathbb{Q} -ring $\mathbb{Z}\mathbb{E}$ of *formal multizetas*, i.e. the \mathbb{Q} -ring generated by the symbols wa^α and $ze^{(\xi)}$ subject only to the conversion rule (6.5)-(6.6) and the quadratic relations⁶⁷ (6.3)-(6.4), is known to be a polynomial ring, freely generated by a countable number of so-called *irreducibles*.

Generating series. As borne out by past experience, it is advisable, for most intents and purposes, to switch from the scalar multizetas wa^\bullet and ze^\bullet to the generating series Zag^\bullet and Zig^\bullet :

$$Zag \binom{u_1 \dots u_r}{\epsilon_1 \dots \epsilon_r} := \sum_{1 \leq s_j} wa^{e_1, 0^{[s_1-1]}, \dots, e_r, 0^{[s_r-1]}} u_1^{s_1-1} u_{1,2}^{s_2-1} \dots u_{1\dots r}^{s_r-1} \quad (6.7)$$

$$Zig \binom{\epsilon_1 \dots \epsilon_r}{v_1 \dots v_r} := \sum_{1 \leq s_j} ze \binom{\epsilon_1 \dots \epsilon_r}{s_1 \dots s_r} v_1^{s_1-1} \dots v_r^{s_r-1} \quad (6.8)$$

The bimould⁶⁸ Zag^\bullet is *symmetrel*, just as wa^\bullet was, while the bimould Zig^\bullet has its own symmetry type: *symmetril*. The *symmetrility* relations are patterned on the *symmetrelity* relations, but with the additive contractions $w_i + w_j$ replaced by ‘polar’ contractions $\widehat{w_i, w_j}$, according to the rules:

$$\begin{aligned} S \binom{\widehat{u_i, u_j}}{v_i, v_j} &= S \binom{u_i + u_j}{v_i} P(v_i - v_j) \\ &+ S \binom{u_i + u_j}{v_j} P(v_j - v_i). \end{aligned} \quad (6.9)$$

⁶⁷ Though yet unproven, it is generally assumed (and backed by massive numerical evidence) that the two systems of quadratic relations imply all other (known or yet to be discovered) algebraic relations between multizetas.

⁶⁸ What turns Zag^\bullet , Zig^\bullet into *bimoulds* is not so much their two-tier indexation $w_i = \binom{u_i}{v_i}$ but rather the fact that the u_i ’s and v_i ’s interact in a very special way, through so-called *flexions*, which allow only the addition of (several consecutive) u_i ’s and the subtraction of (two not necessarily consecutive) v_i ’s with conservation of $\sum u_i v_i$.

Here $P(t) := 1/t$. In (6.9) the dots may themselves contain any number of additional contractions $\widehat{w_k, w_l}$. Thus:

$$\begin{aligned} S\left(\begin{matrix} \dots \widehat{u_i, u_j} \dots \dots \widehat{u_k, u_l} \dots \dots \\ \dots v_i, v_j \dots \dots v_k, v_l \dots \dots \end{matrix}\right) &= +S\left(\begin{matrix} \dots u_i+u_j \dots \dots u_k+u_l \dots \dots \\ \dots v_i \dots \dots v_k \dots \dots \end{matrix}\right) P(v_i-v_j) P(v_k-v_l) \\ &+ S\left(\begin{matrix} \dots u_i+u_j \dots \dots u_k+u_l \dots \dots \\ \dots v_j \dots \dots v_k \dots \dots \end{matrix}\right) P(v_j-v_i) P(v_k-v_l) \\ &+ S\left(\begin{matrix} \dots u_i+u_j \dots \dots u_k+u_l \dots \dots \\ \dots v_i \dots \dots v_l \dots \dots \end{matrix}\right) P(v_i-v_j) P(v_l-v_k) \\ &+ S\left(\begin{matrix} \dots u_i+u_j \dots \dots u_k+u_l \dots \dots \\ \dots v_j \dots \dots v_l \dots \dots \end{matrix}\right) P(v_j-v_i) P(v_l-v_k) \end{aligned}$$

A typical symmetrility relation reads:

$$\begin{aligned} S^{w_1, w_2} S^{w_3, w_4} &= +S^{w_1, w_2, w_3, w_4} + S^{w_1, w_3, w_2, w_4} + S^{w_3, w_1, w_2, w_4} + S^{w_1, w_3, w_4, w_2} \\ &+ S^{w_3, w_1, w_4, w_2} + S^{w_3, w_4, w_1, w_2} + S^{\widehat{w_1, w_3, w_2, w_4}} + S^{\widehat{w_1, w_3, w_4, w_2}} \\ &+ S^{w_1, \widehat{w_2, w_3, w_4}} + S^{w_3, \widehat{w_1, w_4, w_2}} + S^{w_1, w_3, \widehat{w_2, w_4}} + S^{w_1, w_3, \widehat{w_2, w_4}} \\ &+ S^{\widehat{w_1, w_3, w_2, w_4}}. \end{aligned}$$

Summing up, not only do we have an exact equivalence between the old and new symmetries:

$$\{\text{wa}^\bullet \text{ symmetrality}\} \iff \{\text{Zag}^\bullet \text{ symmetrality}\} \tag{6.10}$$

$$\{\text{ze}^\bullet \text{ symmetrality}\} \iff \{\text{Zig}^\bullet \text{ symmetrality}\} \tag{6.11}$$

but the old conversion rule for scalar multizetas⁶⁹ becomes:

$$\text{Zig}^\bullet = \text{Mini}^\bullet \times \text{swap}(\text{Zag}^\bullet) \tag{6.12}$$

$$(\iff \text{swap}(\text{Zig}^\bullet) = \text{Zag}^\bullet \times \text{Mana}^\bullet). \tag{6.13}$$

Here, *swap* is the basic involution of the flexion structure:

$$(\text{swap}.S)\left(\begin{matrix} u_1 \dots u_r \\ v_1 \dots v_r \end{matrix}\right) := S\left(\begin{matrix} v'_r \dots v'_1 \\ u'_r \dots u'_1 \end{matrix}\right) \tag{6.14}$$

with $u'_i := u_1 + \dots + u_i$ and $v'_i := v_i - v_{i+1}$ if $i < r$ respectively $v'_r := v_r$.

As for *Mana*[•] and *Mini*[•] := *swap.Mana*[•], they are elementary bi-moulds whose only non-vanishing components are those carrying only zeros in the lower (respectively upper) index row:

$$\text{Mana}\left(\begin{matrix} u_1 \dots u_r \\ 0 \dots 0 \end{matrix}\right) \equiv \text{Mini}\left(\begin{matrix} 0 \dots 0 \\ v_1 \dots v_r \end{matrix}\right) \equiv \text{mono}_r. \tag{6.15}$$

⁶⁹ Namely the rules (6.5)-(6.6) suitably modified to cover the *divergent* case.

They can be expressed in terms of monozetas:

$$1 + \sum_{r \geq 2} \text{mono}_r t^r := \exp \left(\sum_{s \geq 2} (-1)^{s-1} \zeta(s) \frac{t^s}{s} \right) \quad (6.16)$$

Even-odd separation. The natural environment of Zag^\bullet is the group $GARI$, central to flexion theory. Its complicated product $gari$ is highly non-linear in its second factor. Nonetheless Zag^\bullet admits remarkable factorisations in $GARI$:

$$Zag^\bullet := gari(Zag_I^\bullet, Zag_{II}^\bullet, Zag_{III}^\bullet) = gari(Zag_{ev}^\bullet, Zag_{odd}^\bullet) \quad (6.17)$$

$$Zag_{ev}^\bullet := gari(Zag_I^\bullet, Zag_{II}^\bullet) \quad (6.18)$$

$$Zag_{odd}^\bullet := Zag_{III}^\bullet \quad (6.19)$$

where the various factors, like Zag^\bullet itself, possess a double symmetry: $Zag_{ev}^\bullet, Zag_{odd}^\bullet$ etc are *symmetril*, while the swapees $Zig_{ev}^\bullet, Zig_{odd}^\bullet$ etc are *symmetril*. The ‘even’ and ‘odd’ factors Zag_{ev}^\bullet and Zag_{odd}^\bullet are characterized by their behaviour under the involutions *neg, pari*:

$$(\text{neg}S) \binom{u_1 \dots u_r}{v_1 \dots v_r} := S \binom{-u_1 \dots -u_r}{-v_1 \dots -v_r}; (\text{pari}S) \binom{u_1 \dots u_r}{v_1 \dots v_r} := (-1)^r S \binom{u_1 \dots u_r}{v_1 \dots v_r} \quad (6.20)$$

and under *invgari*, i.e. the taking of the *gari*-inverse:

$$\text{neg.pari.Zag}_{ev}^\bullet = Zag_{ev}^\bullet \quad (6.21)$$

$$\text{neg.pari.Zag}_{odd}^\bullet = \text{invgari.Zag}_{odd}^\bullet \quad (6.22)$$

$$gari(Zag_{odd}^\bullet, Zag_{odd}^\bullet) = gari(\text{neg.pari.invgari.Zag}^\bullet, Zag^\bullet). \quad (6.23)$$

Since all elements of $GARI$ have one well-defined square-root,⁷⁰ the last identity (6.23) readily yields Zag_{odd}^\bullet . Separating the last factor from the first two is thus an easy matter (assuming the flexion machinery). Separating Zag_I^\bullet from Zag_{II}^\bullet is easy too, unless we insist on doing this in a ‘canonical’ way.

Here is the significance of these Zag^\bullet -factors in terms of multizeta irreducibles.⁷¹ For simplicity, we consider only the case of ordinary or ‘colourless’ multizetas:

- (i) The factor Zag_I^\bullet carries only powers of the special irreducibe $\zeta(2) = \pi^2/6$, of weight 2.

⁷⁰ Apply *expari*. $\frac{1}{2}$.*logari*.

⁷¹ Recall that the weight s , length (or depth) r , and degree d are related by $s = r + d$.

- (ii) The factor Zag_{II}^\bullet carries only irreducibles of even weight $s \geq 4$ and even *depth*, along with their products.
- (iii) The factor Zag_{III}^\bullet carries only irreducibles of odd weight $s \geq 3$ and odd *depth*, along with their products.

The even-multizeta / odd-multizeta irreducibles. The even/odd factorisation (6.17) of Zag^\bullet leads to a canonical decomposition $\mathbb{Z}\mathbb{E} = \mathbb{Z}\mathbb{E}_{\text{ev}} \oplus \mathbb{Z}\mathbb{E}_{\text{odd}}$ of the \mathbb{Q} -ring of multizetas into a direct sum of two sub-rings, each with its own irreducibles. These *even-irreducibles* and *odd-irreducibles* will lead in Section 9 to simpler expansions for the holomorphic invariants $A_\omega(f)$. Mark in passing the importance of the hyphenation: a system of, say, odd-irreducibles is not simply a system of irreducibles with odd weight and odd depth; it must also consist of elements in $\mathbb{Z}\mathbb{E}_{\text{odd}}$, *i.e.* of elements generated by the scalar coefficients of Zag_{odd}^\bullet .

The even-multitangents $Te_{\text{ev}}^\bullet(z)$. For any multitangent $Te^s(z)$ of monotangential expansion $Te^s(z) = \sum z e_\sigma^s Te^\sigma(z)$ we set $Te_{\text{ev}}^s(z) = \sum ev(z e_\sigma^s) Te^\sigma(z)$, with *ev* the natural projection of $\mathbb{Z}\mathbb{E}$ onto $\mathbb{Z}\mathbb{E}_{\text{ev}}$. Since the multiplication of monotangents involves only rational powers of π^2 , *i.e.* elements of $\mathbb{Z}\mathbb{E}_{\text{ev}}$, the *even-multitangents* $Te_{\text{ev}}^s(z)$ are stable under multiplication, and their multiplication stays commutative.

6.3 Dynamical multizetas

If we review those multizeta properties on which our expansions of the invariants $A_\omega(f)$ effectively relied, we find three systems of ‘dynamical constraints’:

- (i) the *symmetrelness constraints*: $ze^{s'} ze^{s''} = \sum_{s \in \text{she}(s', s'')} ze^s$, which are none other than the *second quadratic relations* (6.4).
- (ii) the *localisation constraints* (see Section 2.3) which take into account the commutation of two operations on multitangents – multiplication and localisation⁷² – and derive from this fact finite multizetas relations much weaker than the *first quadratic relations*.
- (iii) the *shift constraints* (non-algebraic, see Section 2.7) which, for any $i \leq r$, expand $ze^{s_1, \dots, s_i, \dots, s_r}$ as a convergent series of:
 - (*) all s_i -translates $ze^{s_1, \dots, s_i + k_i, \dots, s_r}$ of depth r and shift $k_i \geq 1$;
 - (**) some multizetas of depth $< r$.

⁷² *I.e.* taking the Laurent expansion of a multitangent at $z = 0$.

Although the shift constraints (iii) are the ones most directly responsible for the invariance of the $A_\omega(f)$, they are not finite. So we shall concentrate on the algebraic constraints (i)-(ii).

Algebraic dynamical constraints. We begin by introducing the *coloured* symmetrel multitangent mould $Te^\bullet(z)$ and the bimould $Tig^\bullet(z)$ formed from the generating series of multitangents. The definitions are transparently patterned on those of ze^\bullet and Zig^\bullet :

$$Te^{(\epsilon_1 \dots \epsilon_r)}_{(s_1 \dots s_r)}(z) := \sum_{+\infty > n_1 > \dots > n_r > -\infty} \prod_{i=1}^{i=r} \left(e_i^{-n_i} (n_i + z)^{-s_i} \right) \tag{6.24}$$

$$Tig^{(\epsilon_1 \dots \epsilon_r)}_{(v_1 \dots v_r)}(z) := \sum_{s_i \geq 1} Te^{(\epsilon_1 \dots \epsilon_r)}_{(s_1 \dots s_r)}(z) v_1^{s_1-1} \dots v_r^{s_r-1}. \tag{6.25}$$

Clearly $\{Tig^\bullet \text{ symmetril}\} \Leftrightarrow \{Te^\bullet \text{ symmetrel}\} \Rightarrow \{ze^\bullet \text{ symmetrel}\}$.

To see now how the localisation constraints compare with the *first quadratic relations* (6.3), we must express the multitangents in terms of multizetas, in two distinct ways that reflect (at the level of the generating series $Tig^\bullet(z)$ and Zig^\bullet) the two paths in the corresponding commutative diagram of Section 2.3. We find:

$$\begin{aligned} Tig^w(z) &= \sum_{w=w^+w^-} Zig^{w^+}(z) viZig^{w^-}(z) - \sum_{w=w^+w_0w^-} Zig^{w^+}(z) Pi^{w_0}(z) viZig^{w^-}(z) \\ Tig^w(z) &= Rig^w - \sum_{w=w^+w_0w^-} Zig^{w^+} Qii^{[w_0]}(z) viZig^{w^-}. \end{aligned} \tag{6.26}$$

The ingredient Pi , Qii , Rig^\bullet in the above formulae are defined as follows:

$$Pi^{(\epsilon_1)}_{(v_1)} := \frac{1}{v_1}, \quad Qii^{(\epsilon_1)}_{(v_1)} := \sum_{n_1 \in \mathbb{Z}} \frac{e^{-2\pi i n_1 \epsilon_1}}{n_1 + v_1} \quad \forall \epsilon_1 \tag{6.27}$$

$$Pi^{(\epsilon_1 \dots \epsilon_r)}_{(v_1 \dots v_r)} := 0, \quad Qii^{(\epsilon_1 \dots \epsilon_r)}_{(v_1 \dots v_r)} := 0 \quad \forall r \neq 1 \tag{6.28}$$

$$Rig^{w_1, \dots, w_r} := 0 \quad \text{for } r = 0 \text{ or } r \text{ odd} \tag{6.29}$$

$$Rig^{w_1, \dots, w_r} := \frac{(\pi i)^r}{r!} \delta(\epsilon_1) \dots \delta(\epsilon_r) \quad \text{for } r \text{ even } > 0 \tag{6.30}$$

with δ denoting as usual the discrete dirac⁷³ and $viZig^\bullet := neg.pari.anti.Zig^\bullet$. Lastly, the bimoulds $Pi^\bullet(z)$, $Qii^\bullet(z)$, $Zig^\bullet(z)$, $viZig^\bullet(z)$ are derived from Pi^\bullet , Qii^\bullet , Zig^\bullet , $viZig^\bullet$ by changing v_i into $v_i - z$ ($\forall i$).

⁷³ $\delta(0) := 1$ and $\delta(t) := 0$ for $t \neq 0$.

Dynamical multizeta irreducibles. Finding a system of irreducibles relative to the sole symmetrality constraints on multizetas (*‘second quadratic relations’*) is very easy.⁷⁴ So let us examine instead the full (algebraic) dynamical constraints (i.e. *symmetrality* plus *‘localisation’*) and show that we can derive from them a simple algorithm for *expressing every (colourless) multizeta of odd degree and depth ≥ 2 as a finite sum, with rational coefficients, of multizetas of even degree.*⁷⁵ By equating our *uninflected* and *inflected* expressions of $\text{Zig}^w(z)$ and then setting $z = 0$, we get the remarkable identity:

$$\begin{aligned} & \sum_{w=w^+w^-} \text{Zig}^{w^+} \text{viZig}^{w^-} - \sum_{w=w^+w_0w^-} \text{Zig}^{w^+} \text{Pi}^{w_0} \text{viZig}^{w^-} \\ &= \text{Rig}^w - \sum_{w=w^+w_0w^-} \text{Zig}^{w^+} \text{Qii}^{\lceil w_0 \rceil} \text{viZig}^{\lfloor w^- \rfloor} \quad (\forall w) \end{aligned} \quad (6.31)$$

with factor sequences w^\pm that can be \emptyset , and with the usual flexion conventions.⁷⁶ As a consequence, (6.31) is of the form:

$$\text{Zig}^{w_1, \dots, w_r} + (-1)^r \text{Zig}^{-w_r, \dots, -w_1} = \text{“shorter terms”}. \quad (6.32)$$

But Zig^\bullet is symmetril and therefore *mantir*-invariant⁷⁷, which again yields an identity of the form:

$$\text{Zig}^{-w_1, \dots, -w_r} + (-1)^r \text{Zig}^{-w_r, \dots, -w_1} = \text{“shorter terms”}. \quad (6.33)$$

If we now take ‘colourless’ indices w_i , i.e. indices $w_i := \binom{0}{v_i}$, then subtract (6.32) from (6.33), and calculate therein the coefficient of $\prod v_i^{s_i-1}$, we find:

$$(1 - (-1)^d) z^{\binom{0 \dots 0}{s_1 \dots s_r}} = \text{“shorter terms”} \quad \left(d := -r + \sum s_i \right) \quad (6.34)$$

with quite explicit ‘shorter terms’.

⁷⁴ For the uncoloured multizetas, it amounts to constructing a basis (the Lyndon basis will do, or any other) on the Lie algebra freely generated by the symbols e_s with $s \in \mathbb{N}^*$.

⁷⁵ Recall that the degree $d := s - r$ of a multizeta is defined as its total weight s minus its length (or depth) r .

⁷⁶ One goes from w_0 to $\lceil w_0 \rceil$ by changing the upper index ϵ_0 to $\lvert \epsilon^+ \rvert + \epsilon_0 + \lvert \epsilon^- \rvert$, and from w^+ (respectively w^-) to $w^{\lceil \cdot \rceil}$ (respectively $w^{\lfloor \cdot \rfloor}$) by changing the lower indices v_i to $v_i - v_0$.

⁷⁷ *Mantir* is a non-linear involution on bimoonds, whose definition is given in [10, pages 67-69]. But all we need to know here is that *mantir.S* $^\bullet = -\text{pari.anti.S}^\bullet + \text{shorter terms}$.

The dynamical constraints on multizetas thus provide us with a very effective algorithm for the *reduction* (to simpler multizetas) of all *un-coloured* multizetas $\zeta(s_1, \dots, s_r)$ of depth $r \geq 2$ and *odd* degree $d := \sum_i (s_i - 1)$. We may note that, at depth $r = 1$, the monozetas of odd degree are precisely the $\zeta(s)$ of even weight s . These are of course commensurate with $\pi^s = (6\zeta(2))^{s/2}$, but this is a consequence of the *rigid-arithmetical* constraints, *not* of the *dynamical* ones!

6.4 The ramified case (tangency order $p > 1$)

Another striking difference between the (algebraic) dynamical constraints and the (algebraic) arithmetical ones makes itself felt when we go over to the ramified situation, for diffeos f of tangency order $p \geq 2$ and multizetas with indices $s_i \in p^{-1}\mathbb{N}^*$.

The *dynamical constraints* on the multizetas⁷⁸ carry over almost unchanged: the symmetrality of ze^\bullet survives, of course, and so do the finite localisation constraints (although the finite reduction of multitan-gents into monotangents breaks down), as shown in Section 2.3.

On the other hand, it is not only the symmetrality of wa^\bullet — the first leg of the *arithmetical constraints* — that cannot survive ramification: the very definition of the mould wa^\bullet and the conversion rules (6.5)-(6.6) cease to make sense, since these rules would equate the *entire* lengths of 0-sequences in α with the *fractional* weights s_i in s .

7 Complement: convergence issues and phantom dynamics

7.1 The scalar invariants

Although convergence issues are by no means central to this investigation — the analytical expressions of the invariants $A_\omega(f)$ in terms of f is — there seems to be a lot of muddled thinking about these questions, with some authors insisting on seeing difficulties where there are none. So a short section entirely devoted to the subject may not be superfluous, even if it entails some repetitions and leads us, now and then, to state the obvious.

Scalar invariant attached to convergent diffeos f . There are two ways of establishing the existence of the scalar invariants as entire functions of

⁷⁸ Recall, though, that in the ramified case the monics Te_ω^s take the place of the multizetas as direct transcendental ingredient of the invariants $A_\omega(f)$, and these Te_ω^s are no longer finite superpositions of multizetas.

f (i.e. of $\{f_n\}$) when f ranges through a formal class $\mathbb{G}^{p,\rho}$ of identity-tangent diffeomorphisms. Briefly restated in the terminology of this paper, they are:

- (i) The quite old and very elementary *geometric approach*. It constructs the iterators f_{\pm}^* and ${}^*f_{\pm}$ in the z -plane; derives from them the connectors π^{\pm} ; then subjects the 1-periodic germs $\pi^{\pm}(z) - z$ to Fourier analysis; and arrives directly at the invariants $A_{\omega}^{\pm}(f)$.
- (ii) The more informative *resurgent approach*, less ancient but already four decades old. It focuses on the formal iterator $\tilde{f}^*(z)$; forms its Borel transform $\hat{f}^*(\zeta)$; readily finds its resurgence locus $2\pi i\mathbb{Z}$; then, based solely on the functional equation $f^* \circ f = 1 + f^*$, it immediately infers the form of the resurgence equations. Lastly, depending on which alien operators it applies to $\hat{f}^*(\zeta)$, it directly reaches all systems of invariants, whether $\{A_{\omega}^{\pm}(f)\}$ or $\{A_{\omega}(f)\}$ or $\{A_{\omega}^{\sharp}(f)\}$ etc, plus a wealth of information about them.

Having once establish the existence of the invariants $A_{\omega}(f)$ as entire functions of f , the only task left is to find their Taylor expansion in the countably many coefficients f_n – or rather g_n if $f = l \circ g$:

$$A_{\omega}(f) = \sum_r \sum_{n_i, s_i} H_{\omega}^{\binom{n_1 \dots n_r}{s_1 \dots s_r}} \prod_i (g_{s_i})^{n_i} \tag{7.1}$$

Series like (4.3) do just that, since their mode of derivation exactly mimics the parallel constructions of the invariants according to the geometric and resurgent methods. *And the shape of the expansion (7.1) once found, its convergence is guaranteed beforehand by the mere fact of $A_{\omega}(f)$ being an entire function of f . We do not have to bother about majorising the coefficients $H_{\omega}^{\binom{n}{s}}$ to prove the convergence of (7.1). It is exactly the other way round: it is by directly establishing bounds on the growth of $A_{\omega}(f)$ as a function of f or $\{g_n\}$ (as in the next subsection) that we can most easily derive bounds on the coefficients $H^{\binom{n}{s}}$.*

f -growth of the scalar invariants. This is yet another context where the d -indexation (degree-based) is preferable to the s -indexation (weight-based), for reasons spelled out in *Remark 3* at the end of this paragraph. So let us consider a diffeo $f = l \circ g$ in the standard class $(p, \rho) = (1, 0)$, with $\underline{g}(z) := g(z) - z = \sum_{2 \leq d} g_{1+d} z^{-d}$. The iterator f^* , or rather its

essential part $\underline{\tilde{f}}(z) := \tilde{f}(z) - z$, is given in the formal model by

$$\begin{aligned} \underline{\tilde{f}}^*(z) &= \sum_{1 \leq r} \left[\frac{e^\partial}{1 - e^\partial} \cdot \sum_{1 \leq k_r} (\underline{g}(z))^{k_r} \frac{\partial^{k_r}}{k_r!} \right] \cdots \left[\frac{e^\partial}{1 - e^\partial} \cdot \sum_{1 \leq k_1} (\underline{g}(z))^{k_1} \frac{\partial^{k_1}}{k_1!} \right] \cdot z \quad (7.2) \\ &= \underline{g}(z) + \sum_{2 \leq r} \left[\frac{e^\partial}{1 - e^\partial} \cdot \sum_{1 \leq k_r} (\underline{g}(z))^{k_r} \frac{\partial^{k_r}}{k_r!} \right] \cdots \left[\frac{e^\partial}{1 - e^\partial} \cdot \sum_{1 \leq k_2} (\underline{g}(z))^{k_2} \frac{\partial^{k_2}}{k_2!} \right] \cdot \underline{g}(z). \end{aligned}$$

In the convolution model, this translates to an everywhere⁷⁹ convergent series

$$\widehat{f}^*(\zeta) = \widehat{g}(\zeta) + \sum_{1 \leq n} \widehat{W}^n \widehat{g}(\zeta) \quad (7.3)$$

with the mixed (multiplication-convolution) operators \widehat{K} acting thus:

$$(\widehat{W} \widehat{\varphi})(\zeta) := \frac{e^{-\zeta}}{1 - e^{-\zeta}} \cdot \sum_{1 \leq k} \left[(\widehat{g})^{*k}(\zeta) \right] *_\zeta \left[\frac{(-\zeta)^k}{k!} \widehat{\varphi}(\zeta) \right]. \quad (7.4)$$

A product of two consecutive operators \widehat{W} involves a series of middle terms of the form

$$\widehat{W} \cdot \widehat{W} = (\dots) \cdot \left(\sum_{1 \leq k} \frac{(-\zeta)^k}{k!} \frac{e^{-\zeta}}{1 - e^{-\zeta}} \right) \cdot (\dots) \quad (7.5)$$

with bounds

$$\left| \frac{(-\zeta)^k}{k!} \frac{e^{-\zeta}}{1 - e^{-\zeta}} \right| \leq c_\epsilon \frac{|\zeta|^{k-1}}{(k-1)!} (1 + |\zeta|) \quad (\forall \zeta \in K_\epsilon, c_\epsilon^\pm > 0) \quad (7.6)$$

uniformly valid on the K_ϵ

$$K_\epsilon := \{ \zeta \in \mathbb{C}, \text{dist}(\zeta, 2\pi i \mathbb{Z}^*) \geq \epsilon \}. \quad (7.7)$$

$$K_\epsilon := \{ \zeta \in \mathcal{R}, \text{dist}(\zeta, \widetilde{\mathcal{R}_{ram} - 0_\bullet}) \geq \epsilon \} \quad \text{with } \mathcal{R} = \mathbb{C} - \widetilde{2\pi i \mathbb{Z}}. \quad (7.8)$$

Note that K_ϵ (respectively K_ϵ) contains a neighbourhood of the origin 0 (resp 0_\bullet). Using the expansion (7.4)-(7.5), the bounds (7.6), and the estimates

$$|(\widehat{g})^{*k}(\zeta)| < \gamma_0 \exp(\gamma_1 |\zeta|) |\zeta|^{2k-1} / (2k-1)! \quad (7.9)$$

⁷⁹ *I.e.* at all points ζ not located *over* the singularity locus $2\pi i \mathbb{Z}$.

tedious but elementary calculations⁸⁰ lead to optimal⁸¹ estimates of type:

$$|\widehat{f}(\zeta)| < c_{0,d}(\zeta) \exp\left(c_d(\zeta) |g_{1+d}|^{\frac{1}{d}}\right) \quad (2 \leq d) \quad (7.10)$$

$$< c_{0,D}(\zeta) \exp\left(\sum_{d \in D} c_{d,D}(\zeta) |g_{1+d}|^{\frac{1}{d}}\right) \quad (D \text{ finite } \subset \{2, 3, \dots\}) \quad (7.11)$$

$$< c_{0,\infty}(\zeta) \exp\left(c_\infty(\zeta) \sup_d |g_{1+d}|^{\frac{1}{d}}\right) \quad (7.12)$$

for any ζ on the convolution domain $\mathcal{R} := \mathbb{C} - \widetilde{2\pi i\mathbb{Z}}$. The main point to observe is that all the terms $\widehat{W}^n \widehat{g}(\zeta)$ in (7.3) can be calculated inductively as convolution integrals of the form

$$\frac{e^{-\zeta}}{1 - e^{-\zeta}} \int_0^\zeta (\widehat{g})^{*k}(\zeta - \zeta_1) \widehat{\varphi}_{n,k}(\zeta_1) d\zeta_1 \quad (7.13)$$

with a first convolution factor $(\widehat{g})^{*k}(\zeta - \zeta_1)$ that is uniform on \mathbb{C} with the bounds (7.9) and a second factor that is uniform on \mathcal{R} and easily bounded (by induction) on any \mathcal{K}_ϵ . To continue the induction, it is enough to calculate the integral on a ζ_1 -path confined within the largest \mathcal{K}_ϵ that contains ζ , without worrying about $\zeta - \zeta_1$.

To derive from the estimates (7.10)-(7.12) analogous estimates for the invariants A_ω^+ , we write the resurgence equations $\Delta_\omega^\pm \widehat{f}^*(z) = -A_\omega^\pm \exp(-\omega \widehat{f}^*(z))$. In the Borel plane this becomes⁸²

$$\begin{aligned} \widehat{f}^*(\zeta'_\pm) - \widehat{f}^*(\zeta''_\pm) &= A_\omega^+ \cdot \widehat{f}^*(\zeta) \text{ with} \\ \widetilde{f}^*(z) &= e^{-\omega \widetilde{f}^*(z)} - 1 \sim -\omega g_{s_0} \cdot z^{1-s_0} \end{aligned} \quad (7.14)$$

with ζ close to 0_\bullet on the main Riemann sheet and ζ'_\pm, ζ''_\pm both over $\dot{\zeta} + \omega$ but on two consecutive Riemann sheets. Since $\widehat{f}^*(\zeta) \sim -\omega g_{s_0} \zeta^{s_0-2} / (s_0 - 2)!$ for ζ close to 0_\bullet , there exists for each value of the variable coefficient g_{1+d} at least one point $\zeta = \zeta(g_{1+d})$ on the circle $|\zeta| = 1$ where

⁸⁰ Even if one were to retain only the part of the operators \widehat{W} that correspond to $k = 1$, the (much simpler) calculations would already show that the estimates (7.10)-(7.12) cannot be improved upon. Taking all k -parts into account does not alter the shape of the estimates, due to the bounds (7.9).

⁸¹ *Optimal* as long as we consider the absolute values $|g_{1+d}|^{1/d}$. But one might improve on (7.10) by finding the indicatrix of exponential growth in $|g_{1+d}|^{1/d}$.

⁸² Since the first term “1” in $\exp(-\omega \widehat{f}^*(z)) = 1 + \dots$ contributes nothing to the minors.

$|\widehat{f}_\omega^*(\zeta)| = |\omega g_{s_0}/(s_0-1)!|$. Considering the identity (7.14) for this particular ζ and its images ζ'_\pm and ζ''_\pm and using (7.10), we get (7.15) for A_ω^+ , as well as (7.16) and (7.17) by a similar argument. The analogous estimates for $A_\omega, A_\omega^\sharp, A_\omega^{\sharp\sharp}$ etc. follow in view of the bipolynomial correspondance between any two systems of invariants.

$$|A_\omega^\pm|, |A_\omega|, |A_\omega^\sharp|, |A_\omega^{\sharp\sharp}| \text{ etc.} < c_{0,d}(\omega) \exp\left(c_d(\omega) |g_{1+d}|^{\frac{1}{d}}\right) \quad (\forall \omega, d \geq 2) \tag{7.15}$$

$$< c_{0,D}(\omega) \exp\left(\sum_{d \in D} c_{d,D}(\omega) |g_{1+d}|^{\frac{1}{d}}\right) \quad (D \text{ finite}) \tag{7.16}$$

$$< c_{0,\infty}(\omega) \exp\left(c_\infty(\omega) \sup_d |g_{1+d}|^{\frac{1}{d}}\right) \tag{7.17}$$

Remark 1. The case of the iteration residue ρ . If we now let $f = l \circ g$ range through all classes $(1, \rho)$ by taking $g(z) = -\rho z^{-1} + \mathcal{O}(z^{-1})$, and ask about the asymptotics in ρ , we would get the wrong result by simply setting $g_2 = -\rho$ in the estimate (7.15). The correct estimate is rather:

$$|A_\omega^\pm|, |A_\omega|, |A_\omega^\sharp|, |A_\omega^{\sharp\sharp}| \text{ etc.} < c_{0,1}(\omega) \exp(c_1(\omega) |\rho \log |\rho||) \quad (\forall \omega). \tag{7.18}$$

The reason is *not* the change from (7.9) to the weaker estimates:

$$|\widehat{g}^{*k}(\zeta)| < \gamma_0 \exp(\gamma_1 |\zeta|) |\zeta|^{k-1}/(k-1)! \tag{7.19}$$

The real reason is that we now have $\widehat{f}^*(z) = \rho \log z + \underline{\widehat{f}}^*(z)$ and

$$\widetilde{f}_\omega^*(z) = z^{-\omega\rho} \exp(-\omega \underline{\widetilde{f}}_\omega^*(z)) = z^{-\omega\rho} \underline{\underline{f}}_\omega^*(z) \tag{7.20}$$

so that (7.14) presently becomes⁸³

$$\underline{\widehat{f}}^*(\zeta') - \underline{\widehat{f}}^*(\zeta'') = A_\omega^+ \cdot \frac{\zeta^{\omega\rho-1}}{\Gamma(\omega\rho)} *_\zeta \underline{\underline{f}}_\omega^*(\zeta) \tag{7.21}$$

Remark 2. ‘Uniformisation’. Due to the ‘uniformisation’ formula (1.54) or (1.55), we see that for any $\zeta \in \mathcal{R}$ (but not above the imaginary axis), $\underline{\widehat{f}}^*(\zeta)$ reduces to a finite sum

$$\underline{\widehat{f}}^*(\zeta) = a_0 \underline{\widehat{f}}^*(\zeta) + \sum_{\omega \in 2\pi i \mathbb{Z}^*} a_\omega \underline{\widehat{f}}_\omega^*(\zeta - \omega) \tag{7.22}$$

⁸³ At least when $-\omega\rho \notin \mathbb{N}$. When $-\omega\rho \in \mathbb{N}$, the positive z -powers in $z^{-\omega\rho} \underline{\underline{f}}_\omega^*(z)$ should be neglected, as contributing nothing to the minors in the Borel plane.

- (i) with \widehat{f}_ω^* as in (7.20)
- (ii) with coefficients a_0, a_ω polynomial in the A_ω
- (iii) with ζ the projection of $\zeta \in \mathcal{R}$ onto the main Riemann sheet.

Remark 3. Weight-based vs degree-based indexation. While the s -indexation $f(z) = z + \sum f_s z^{1-s}$ is well-adapted to germ composition, the d -indexation $\sum f_{\{d\}} z^{-d}$ is better suited to germ conjugation and, consequently, to studying the asymptotics of $A_\omega(f)$. Indeed, take a diffeo f in the standard class and fix $2 \leq d \leq d'$. There clearly exists a unique diffeo h of the form $h(z) := z + \sum_{d-1 \leq n \leq d'-1} h_{\{n\}} z^{-n}$ that conjugates f to ${}^{\text{var}}f$ so as to remove the coefficient $f_{\{d\}}$ while keeping all other coefficients between d and d' unchanged:

$$\begin{aligned} f(z) := z + 1 + \sum_{2 \leq d} f_{\{n\}} z^{-n} &\rightarrow {}^{\text{var}}f(z) := (h \circ f \circ h^{-1})(z) \\ &= z + 1 + \sum_{2 \leq d} {}^{\text{var}}f_{\{n\}} z^{-n} \end{aligned}$$

On top of the defining condition (i), the h -conjugation verifies (ii)-(iii):

- (i) ${}^{\text{var}}f_{\{d\}} = 0$ if $n \leq d'$, and ${}^{\text{var}}f_{\{n\}} = f_{\{n\}}$ with $n \neq d$;
- (ii) if $d' < n$, ${}^{\text{var}}f_{\{n\}}$ is a polynomial in $f_{\{2\}}, f_{\{3\}}, \dots, f_{\{n\}}$ involving only ‘subhomogeneous’ monomials of form $\prod_i (f_{\{n_i\}})^{m_i}$ with $n_1 m_1 + \dots + n_r m_r \leq n$;
- (iii) if $d|n$ and $d' < n$, the monomial $(f_{\{d\}})^{n/d}$ is effectively present, with a nonzero rational coefficient, in the expression of ${}^{\text{var}}f_{\{n\}}$.

Since $A_\omega(f) = A_\omega({}^{\text{var}}f)$, we see that the additional properties (ii)-(iii) are perfectly coherent with the asymptotic estimates (7.10)-(7.15).

ω -growth of the scalar invariants. Fixing $f = l \circ g$ and $\epsilon_0 < \pi$, using the relations (7.3), and calculating the successive integrals in (7.4) on ζ_1 -paths contained in \mathcal{K}_{ϵ_0} , one easily arrives at exponential estimates

$$|A_\omega^\pm| < \gamma_0^\pm \exp(\gamma_1^\pm |\omega|) \quad (\forall \omega \in 2\pi\mathbb{Z}^*, \gamma_0^\pm, \gamma_1^\pm > 0) \quad (7.23)$$

with constants $\gamma_0^\pm, \gamma_1^\pm$ that depend only on the growth of $\widehat{g}(\zeta)$ in the vertical stripes $|\Re(\zeta)| < \epsilon$. This, however, does not apply to the other systems of invariants, like $A_\omega, A_\omega^\#, A_\omega^{\#\#}$ etc, which, being the coefficients of generically divergent but resummable Fourier series (see below), generically possess exponential growth in $|\omega| \cdot \log |\omega|$ rather than $|\omega|$.

7.2 The connectors

For $f = l \circ g$ fixed and convergent, only the connectors $\pi^\pm(z)$ with Fourier coefficients A_ω^\pm have guaranteed convergence in some bi-domain $|\Im(z)| > y$. But as shown in Section 1.7, and 1.8, most other connectors $\pi_\diamond(z)$ are merely resurgent and Borel resummable, each with a definite critical time $z_0 := \exp(\mp 2\pi i z)$, where n_0 is the index of the first non-vanishing invariant. This is definitely the case with the connectors $\pi_*(z)$, $\pi_{\#}(z)$, $\pi_{\#\#}(z)$.

7.3 The collectors

As already pointed out, collectors can be classified under two viewpoints:

- (i) *type*: there is $\mathfrak{p}(z)$ itself and its various affiliates $\mathfrak{p}_\diamond(z)$ — generators, mediators etc,
- (ii) *nature*: we can consider their natural multitangent expansions; or their reduced monotangent expansions; or their local Laurent expansions at $z = 0$.

Now, as long as the collectors are viewed as generating series in the coefficients g_n , as in Section 3, the question of their convergence does not arise — the coefficients of each bloc is always convergent, and this is all that matters from the perspective of this paper. But we may also ask, gratuitously so to speak: given a fixed convergent germ f , which impersonations of the collectors do converge, and in what sense?

From what we already know about the connectors, the question makes sense only for $\mathfrak{p}(z)$ itself, not for its affiliates. And $\mathfrak{p}(z)$, as we shall see, *converges only in its natural multitangent presentation*.⁸⁴

Convergence of the multitangential collectors $\mathfrak{p}(z)$. The convergence of the connectors π as scalar germs can be established in any number of ways (*e.g.* from the estimates (7.23)) and it implies the convergence of the associated substitution operators Π . However, in order to ease the transition to the collectors \mathfrak{p} and \mathfrak{P} , we need to look more closely at these operators Π and *their constituent parts*.

Set $\Pi := \Pi^+$, $G := G^+$, $G_{,n} := L^n \cdot G \cdot L^{-n}$ consider the (for the moment, formal) operator Π as given by (3.8) and replace its bifactorisation $\Pi = {}^*F_- \cdot F_+^*$ by the trifactorisation

$$\Pi = \Pi_{L,n} \cdot \Pi_{M,n} \cdot \Pi_{R,n} \quad (n \text{ large}) \quad (7.24)$$

⁸⁴ Natural means that we take the $\mathcal{T}e^\bullet$ -expansions as they naturally result from the series (3.12) in Section 3 and resort, at most, to symmetrel linearisation.

with L, M, R standing for *left, middle, right* and with the truncated expansions

$$\Pi_{R,n} := 1 + \sum_{1 \leq r} \sum_{n \leq n_r < \dots < n_1} \underline{G}_{:n_r}^+ \dots \underline{G}_{:n_1}^+ = L^n \cdot F_+^* \cdot L^{-n} \quad (7.25)$$

$$\Pi_{M,n} := 1 + \sum_{1 \leq 2n} \sum_{-n \leq n_r < \dots < n_1 < n} \underline{G}_{:n_r}^+ \dots \underline{G}_{:n_1}^+ = G_{:(-n)} \dots G_{:(n-1)} \quad (7.26)$$

$$\Pi_{L,n} := 1 + \sum_{1 \leq r} \sum_{n_r < \dots < n_1 < -n} \underline{G}_{:n_r}^+ \dots \underline{G}_{:n_1}^+ = L^{-n} \cdot {}^*F_- \cdot L^n. \quad (7.27)$$

For any two open sets $\mathcal{D}_1, \mathcal{D}_2$ of \mathbb{C} , bounded or not, connected or not, but with $\overline{\mathcal{D}}_2 \subset \mathcal{D}_1$, and any operator H , we set

$$\|H\|_{\mathcal{D}_1, \mathcal{D}_2} := \sup_{\|\varphi\|_{\mathcal{D}_1} \leq 1} \|H\varphi\|_{\mathcal{D}_2} \quad \text{and} \quad \|H\|_{\mathcal{D}} := \|H\|_{\mathcal{D}, \mathcal{D}^*} \quad (7.28)$$

where \mathcal{D}^* denotes the set of all points in \mathcal{D} whose distance from the boundary of \mathcal{D} is more than 1.

For any ϵ we can find $n \in \mathbb{N}$ and $y \in \mathbb{R}^+$ large enough to ensure

$$\|\Pi_{R,n} - 1\|_{\mathcal{D}_R} \leq \epsilon \quad \forall \mathcal{D}_R \subset \{z, \Re z \geq -6\} \quad (7.29)$$

$$\|\Pi_{M,n} - 1\|_{\mathcal{D}_M} \leq \epsilon \quad \forall \mathcal{D}_M \subset \{z, |\Im z| \geq y\} \quad (7.30)$$

$$\|\Pi_{L,n} - 1\|_{\mathcal{D}_L} \leq \epsilon \quad \forall \mathcal{D}_L \subset \{z, \Re z \leq +6\} \quad (7.31)$$

and therefore

$$\|\Pi - 1\|_{\mathcal{D}} \leq 4\epsilon \quad \forall \mathcal{D} \subset \{z, |\Re z| \leq 3, |\Im z| \geq y + 3\}. \quad (7.32)$$

Moreover, one can show that the statement would still hold (for a slightly larger choice of n, y) if, instead of considering the norm $\|\Pi - 1\|_{\mathcal{D}}$, we were to consider the larger norms:

$$\|\Pi - 1\|_{\mathcal{D}}^{\mathcal{S}} = \sum \|H \binom{n}{s}\|_{\mathcal{D}} \prod |g_{s_i}|^{n_i} \quad \text{with} \quad \Pi - 1 = \sum H \binom{n}{s} \prod (g_{s_i})^{n_i}$$

relative to any *natural* expansion \mathcal{S} of $\Pi - 1$ as a series of monomials $\prod (g_{s_i})^{n_i}$. But expanding Π in this way is tantamount to viewing it as the *collector* \mathfrak{P} with its natural multitangent expansion (relative to the system Te^\bullet). Of course, the multitangential \mathfrak{P} and \mathfrak{p} converge *separately* on the two half-planes $|\Im(z)| > y$, but in that sense, *qua* convergent objects, already cease to be of one piece.

Divergence of the monotangential collectors $p(z)$. By multiplying the Laurent expansions of $Te^{s_1}(z)$ and $Te^{s_2}(z)$ at $z = 0$ and then retaining only the z -negative powers in the product, we get the multiplication rule for (integer-indexed) monotangents:

$$Te^{s_1}(z)Te^{s_2}(z) = Te^{s_1+s_2}(z) + \sum_{2 \leq s_3 < \max(s_1, s_2)} te_{s_3}^{s_1, s_2} Te^{s_3}(z) \quad (s_1, s_2 \in N^*) \quad (7.33)$$

with

$$te_{s_3}^{s_1, s_2} = [1 + (-1)^{s_1+s_2-s_3}] \zeta(s_1 + s_2 - s_3) \\ \times \left[\frac{(-1)_+^{s_1-s_3} (s_1 + s_2 - s_3)!}{(s_1 - s_3)!(s_2 - 1)!} + \frac{(-1)_+^{s_2-s_3} (s_1 + s_2 - s_3)!}{(s_2 - s_3)!(s_1 - 1)!} \right] \quad (7.34)$$

and $(-1)_+^s := (-1)^s$ if $s > 0$ respectively $(-1)_+^s := 0$ if $s \leq 0$. Now, if the monotangential expansions for p^+ and p^- always existed, since $p^+ \circ p^- = id$, going from the one to the other would involve multiplying many infinite sums of the form

$$\left(\sum_{s_1 \text{ even}} a_{s_1} Te^{s_1}(z) \right) \left(\sum_{s_2 \text{ even}} b_{s_2} Te^{s_2}(z) \right) \mapsto \left(\sum_{s_3 \text{ even}} c_{s_3} Te^{s_3}(z) \right) \quad (7.35)$$

with series $\sum a_{s_1} z^{-s_1}$ and $\sum b_{s_2} z^{-s_2}$ whose convergence radii might be small, since the convergence radius of the underlying series $g(z)$ may be anything. But the coefficient c_{s_3} on the right-hand side of (7.35) are given by

$$c_{s_3} = \sum_{s_3=s_1+s_2} a_{s_1} b_{s_2} + \sum_{s_3 < \max(s_1, s_2)} a_{s_1} b_{s_2} te_{s_3}^{s_1, s_2} \quad (7.36)$$

with a second sum that diverges if, for instance, all a_{s_1} and b_{s_2} are positive with $\lim |a_{s_1}|^{\frac{1}{s_1}} = a > 0$, $\lim |b_{s_2}|^{\frac{1}{s_2}} = b > 0$ and $2ab > 1$. In that case, the coefficients c_{s_3} are not even defined.

So it would be more accurate to say that the monotangential collectors, rather than diverging, *generally do not even exist*: they cannot be defined, not even as formal series. What exists but fails to converge as $s \rightarrow +\infty$ is the *weight-truncated, monotangential collectors*⁸⁵ $trunc_{s_0} p^\pm(z)$ (see Section 3.7).

⁸⁵ They exist unproblematically as *finite* sums, whether in multi- or monotangential form.

7.4 Groups of invariant-carrying formal diffeos

One of the many advantages of the resurgent approach to the study of holomorphic invariants is that it extends effortlessly to many subgroups \mathbb{G}_χ of the group \mathbb{G} of all *formal* identity-tangent diffeos. Typically, these groups \mathbb{G}_χ are defined by a growth condition on the coefficients f_s of their elements that is

- (i) stable under composition and reciprocation⁸⁶;
- (ii) stringent enough to ensure that formal conjugacy (in \mathbb{G}) does not imply actual conjugacy (in \mathbb{G}_χ).

This implies the existence on these groups \mathbb{G}_χ of non-formal invariants, and immediately raises the question of their description/calculation.

If we put aside a few pathological instances⁸⁷, all such groups \mathbb{G}_χ consist of elements \tilde{f} whose Borel transforms $\tilde{f}(\zeta)$ extend to well-defined entire functions (albeit with supra-exponential growth), with iterators \tilde{f}^* , ${}^*\tilde{f}$ that verify the familiar resurgence equations and produce complete systems of holomorphic invariants $A_\omega(\tilde{f})$, exactly as on the analytic group \mathbb{G}_0 .

Before taking a closer look at some examples of ‘invariant-carrying’ groups \mathbb{G}_χ , let us state a few useful lemmas.

Given a system $\{a_n, n \in \mathbb{C}\}$ with a geometric or slightly faster-than-geometric rate of growth, and a number $\omega_0 \in \mathbb{C}^*$, we set $b_m := \sum_n \frac{\omega_0 m^n}{n!} a_n$. Using the rough estimates $\log^+ |b_m| \sim \sup_n \log^+ |\frac{\omega_0 m^n}{n!} a_n|$, we easily infer the growth rate of $\log |b_m|$ from that of $\log |a_m|$ in these four important cases:

$$\{\log^+ |a_n| = \mathcal{O}(n)\} \implies \{\log^+ |b_m| = \mathcal{O}(m)\} \quad (7.37)$$

$$\{\log^+ |a_n| = \mathcal{O}(n \log_k n)\} \implies \{\log^+ |b_m| = \mathcal{O}(m \log_{k-1} m)\} \quad (7.38)$$

$$\left\{ \log^+ |a_n| = \mathcal{O}\left(n \frac{\log n}{\log_k n}\right) \right\} \implies \left\{ \log^+ |b_m| = \mathcal{O}\left(m \exp\left(\frac{\log m}{\log_k m}\right)\right) \right\} \quad (7.39)$$

$$\left\{ \limsup \frac{\log^+ |a_n|}{n \log n} \leq \tau < 1 \right\} \implies \left\{ \limsup \frac{\log^+ |b_m|}{m^{1/(1-\tau)}} \leq 1 \right\}. \quad (7.40)$$

Here, $\log^+ x := \log x$ if $1 < x$ (respectively $:= 0$ if $0 \leq x \leq 1$). As we can see, the actual value of ω_0 is immaterial.

⁸⁶ I.e. the taking of the composition inverse.

⁸⁷ Corresponding to wildly irregular (‘oscillating’ in some sense) growth conditions χ .

Moreover, if we set

$$b(w) = w + \sum b_m e^{-m\omega_0 w} \tag{7.41}$$

$$c(z) = z + \sum c_m z^{1-m} = \exp\left(-\omega_0 b\left(\frac{1}{\omega_0}\right) \log\left(\frac{1}{z}\right)\right) \tag{7.42}$$

the Taylor coefficients c_m are, in all four instances (7.37)-(7.40), subject to exactly the same growth constraints as the Fourier coefficients b_m .

Lastly, it is an easy matter to check that each of the growth conditions listed in (7.37)-(7.40) is stable under composition and reciprocation, and thus defines a group \mathbb{G}_χ .

The analytic subgroup \mathbb{G}_0 . There is no need to return to the group \mathbb{G}_0 and its invariants, except to emphasise a remarkable feature: any germ $f \neq id$ in \mathbb{G}_0 has $2p$ connectors which, after a rescaling of type (7.42), produce $2p$ new germs $f_{(i_1)}$ still in \mathbb{G}_0 . Each one of these $f_{(i_1)}$ produces $2p_{i_1}$ new germs $f_{(i_1, i_2)}$, each of which in turn produces $2p_{i_1, i_2}$ germs $f_{(i_1, i_2, i_3)}$, and so on indefinitely⁸⁸, without ever leaving the group \mathbb{G}_0 . This infinite self-replication property of \mathbb{G}_0 is more than a curiosity: it has practical implications.⁸⁹ It also raises the question: is self-replication an exclusive feature of \mathbb{G}_0 , or does it extend to other invariant-carrying groups \mathbb{G}_χ ? It does, as we shall see, provided the growth condition χ is *extremely* close to geometric growth (which ensures analyticity).

The near-analytic, self-replicating subgroup \mathbb{G}_{0+} . The implication (7.38) being optimal, on the group $\mathbb{G}_{[k]}$ consisting of all f (let us drop the clumsy tilda) whose coefficients verify

$$\lim_{n \rightarrow +\infty} \frac{\log^+ |f_n|}{n \log_k n} = 0 \tag{7.43}$$

the mapping⁹⁰ $f \mapsto resc.\pi$ is from $\mathbb{G}_{[k]}$ to $\mathbb{G}_{[k-1]} \subset \mathbb{G}_{[k]}$. So it is only the limit or intersection

$$\mathbb{G}_{0+} := \lim_k \mathbb{G}_{[k]} = \bigcap_k \mathbb{G}_{[k]} \tag{7.44}$$

⁸⁸ For the process to stop, at a certain stage all $f_{(i_1, \dots, i_r)}$ would have to be *id*, which of course almost never happens.

⁸⁹ *E.g.*, in fractal analysis (see [12]) and in resummation theory: it played a part in the original proof of Dulac's conjecture about the non-accumulation of limit-cycles, prior to the introduction of *well-behaved* convolution averages (see [7]).

⁹⁰ *resc.* π is the connector π *rescaled* so as to become an element of \mathbb{G} .

that possess the property of self-replication. To realise how close \mathbb{G}_{0+} is to \mathbb{G}_0 , we may note that verifying (7.43) for any k is a far more severe condition than verifying the Denjoy quasi-analyticity conditions. Expressed in terms of Taylor coefficients, these read:

$$|g_n|^{\frac{1}{n}} \leq \mathcal{O}(\log_1 n \log_2 n \dots \log_{k-1} n) \tag{7.45}$$

for some given k . That merely implies

$$\log^+ |f_n| \leq n (\log_2 n + \dots + \log_k n + o(\log_k n)) \tag{7.46}$$

which is much weaker than (7.43), let alone (7.44). This is not to say, of course, that \mathbb{G}_{0+} consists only of quasi-analytic germs, since a smooth function f must verify a Denjoy condition on a whole interval to qualify as quasi-analytic.⁹¹

The maximal subgroup \mathbb{G}_{0++} . Consider the Gevrey subgroups of \mathbb{G} defined by the growth conditions

$$\mathbb{G}_{[[\tau]]} := \left\{ f ; \limsup_{n \rightarrow +\infty} \frac{\log^+ |f_n|}{n \log n} \leq \tau \right\}. \tag{7.47}$$

For all elements f in $\mathbb{G}_{[[\tau]]}$ of tangency order $p = 1$ to have everywhere convergent Borel transforms, τ has to be < 1 , in which case these f possess invariants whose growth pattern is bounded by the b_m -estimates of (7.40). Elements f of tangency order $p > 1$, however, must first be brought to a prepared form $(f(z^{1/p}))^p$, which belongs to $\mathbb{G}_{[[p\tau]]}$, or rather to the ramified equivalent of $\mathbb{G}_{[[p\tau]]}$. So the largest group whose elements all possess holomorphic invariants is the intersection \mathbb{G}_{0++} of all these Gevrey groups:

$$\mathbb{G}_{0++} := \left\{ f ; \lim_{n \rightarrow +\infty} \frac{\log^+ |f_n|}{n \log n} = 0 \right\} \tag{7.48}$$

Elements of \mathbb{G}_{0++} have connectors which are usually not in \mathbb{G}_{0++} . since their coefficients are subject only to the very weak growth constraints

$$\log^+ \log^+ |c_r| = o(r \log r) \tag{7.49}$$

⁹¹ Growth conditions at *one* point never suffice to ensure the existence of a quasi-analytic ‘continuation’ on a neighbourhood of that point. In fact, when the coefficients are all > 0 and with faster than geometric growth, the ‘continuation’ never exists.

This results from the optimal implication (7.39) or rather from its – still valid – extension to the case where \log_k is replaced on both sides by any regular⁹² germ \mathcal{L} with ultra-slow growth.

7.5 A glimpse of phantom holomorphic dynamics

Let us for definiteness consider the “near-analytic” group \mathbb{G}_{0+} . It has much more in common with its analytic prototype \mathbb{G}_0 than the existence of non-trivial (*i.e.* non-formal) conjugacy classes characterisable by holomorphic invariants $A_\omega(f)$. The notion of *polarised sectorial model* too has its equivalent, but with *acceleration operators* taking the place of Laplace integration. Indeed, for any slow acceleration $z \rightarrow z_\dagger$ with

$$\frac{z_\dagger}{z} \rightarrow +\infty \quad \text{but} \quad \frac{\log z_\dagger}{\log z} \rightarrow 1 \quad \text{e.g.} \quad z = \mathfrak{F}(z_\dagger) := \frac{z_\dagger}{\log z_\dagger} \quad (7.50)$$

the acceleration integrals $\zeta \rightarrow \zeta_\dagger$

$$\widehat{f}_{\dagger,\pm}^*(\zeta_\dagger) = \int_0^{(1\pm\epsilon)i\infty} C_{\mathfrak{F}}(\zeta_\dagger, \zeta) \widehat{f}^*(\zeta) \quad (7.51)$$

$${}^*\widehat{f}_{\dagger,\pm}(\zeta_\dagger) = \int_0^{(1\pm\epsilon)i\infty} C_{\mathfrak{F}}(\zeta_\dagger, \zeta) {}^*\widehat{f}(\zeta) \quad (7.52)$$

turns the non-polarised iterators $\widehat{f}^*, {}^*\widehat{f}$ into polarised iterators $\widehat{f}_{\dagger,\pm}^*, {}^*\widehat{f}_{\dagger,\pm}$ defined and regular in sectors $\mathcal{S}_{\dagger,\pm}$ of the ζ_\dagger -plane. Moreover, on the intersection $\mathcal{S}_{\dagger,+} \cap \mathcal{S}_{\dagger,-}$, which contains a southern half-plane $\{\Im \zeta_\dagger < -y\}$, these polarised iterators can be subjected to the operation $\widehat{\circ}$ (which transposes the ordinary composition \circ to the Borel planes⁹³) to produce an object $\widehat{\pi}_{\dagger,\text{so}}(\zeta_\dagger)$ that will be the exact counterpart of a connector’s southern component $\pi_{\text{so}}(z)$ for an ordinary analytic germs f in \mathbb{G}_0 .

One may even perform Fourier analysis on $\widehat{\pi}_{\dagger,\text{so}}(\zeta_\dagger)$ and $\widehat{\pi}_{\dagger,\text{no}}(\zeta_\dagger)$ in the ζ_\dagger -plane⁹⁴ to calculate the invariants $A_\omega(f)$. This procedure (inefficient but perfectly workable) would essentially differ from the (efficient) resurgent analysis in the ζ -plane. It would exactly mirror the (moderately efficient – see Section 4.5) Fourier analysis performed on ordinary connectors $\pi_{\text{so}}(z), \pi_{\text{no}}(z)$ in the multiplicative z -plane.

⁹² “Regular” in the sense of verifying the *universal asymptotics of slow-growing germs*. See *e.g.* [7, 8]. For instance, we may take \mathcal{L} to be any transfinite exponential of \log , again in the sense of [7, 8].

⁹³ $(\widehat{\circ} \widehat{f})(\zeta) := \widehat{\varphi}(\zeta) + \sum_{1 \leq k} \frac{1}{k!} (\widehat{f})^{*k}(\zeta) *_{\zeta} \left((-\zeta)^k \widehat{\varphi}(\zeta) \right)$ with $\underline{f}(z) = f(z) - z$.

⁹⁴ There is no contradiction here: the exponentials $e^{\pm\omega z}$ have no image in the ζ -plane, but they have one in the ζ_\dagger -plane, since $e^{\pm\omega z} = e^{\pm\omega \mathfrak{F}(z_\dagger)}$ is strictly sub-exponential in z_\dagger .

For any f in \mathbb{G}_{0+} , the mapping $\widehat{\varphi} \mapsto \widehat{\varphi} \widehat{\circ} \widehat{f}$ is an algebra isomorphism (relative to the convolution product), just as the substitution operators are (relative to ordinary multiplication). Another aspect of “phantom holomorphic dynamics” (in non-polarised and polarised Borel planes) is the notion of invariant subspaces or *fuzzy orbits*, which in a sense fill the role of *orbits* in the (here non-existent) multiplicative plane. But the subject is still in its infancy, and we had better stop here.

8 Conclusion

8.1 Some historical background

(i) Identity-tangent diffeos in holomorphic dynamics.

The iteration of one-dimensional analytic mappings – whether local or global; identity-tangent or not – has a long history going back a century or more. Fatou, for one, knew about the analytic classes of identity-tangent diffeos and had formed a clear, geometry-based idea of their invariants. The subject then went into something of a hibernation until the advent of high-power computation, which brought about an explosive revival of holomorphic dynamics, one- and many-dimensional. For the specific subject of analytic invariants, however, the main impetus for renewal came from an unexpected quarter: resurgent analysis.

(ii) Identity-tangent diffeos and resurgent analysis.

The fact is that identity-tangent diffeos possess generically divergent but always resurgent iterators and fractional iterates, with an interesting, non-linear pattern of resurgence or self-reproduction at the singular points in the Borel plane, and it was in the process of sorting out these phenomena that resurgence theory was born, and later applied to general local objects and much else. In a sense, this involved a retreat from dynamics proper, since it meant focusing on the Borel plane, where the key dynamic notions of trajectory, fixed point etc admit no simple interpretation. For the invariants A_ω , however, the shift in focus brought a definite advantage, since in the Borel plane these invariants are automatically *localised* and *isolated* (they appear as coefficients of the leading singularities over the point ω) whereas in the multiplicative plane they are *diffuse* and *intertwined* (they make themselves felt only collectively and indirectly, via Stokes phenomena and the like, and the only way to isolate them is by Fourier analysis of type (4.10), which is but a half-hearted way of doing what Borel analysis does neatly and efficiently). This applies not just to identity-tangent diffeos, but to a huge range of local objects and equations. It also works in both directions: in that of “*analysis*”, *i.e.* calculating and investigating the invariants of a given object; and in that of “*synthesis*”, *i.e.* prescribing an admissible system of ‘invariants’ and

then constructing an object of which they are the actual invariants. And it has to be said that in both directions resurgence theory performs rather better than geometry. It leads in particular to a privileged or “canonical” synthesis, a notion which eludes geometry.

8.2 Multitangents and multizetas

(iii) Identity-tangent diffeos and the resuscitation of multizetas.

Multizetas (of depth 2, to be precise) were first considered by Euler as an isolated curiosity, and later fell into a protracted oblivion for want of applications. They resurfaced only in the late 1970s and early 1980s in [3–5], precisely in the context of holomorphic dynamics and identity-tangent diffeos, as *the* transcendental ingredient in the make-up of their invariants. Ten years later, the multizetas started cropping up in half a dozen, largely unconnected contexts: braid groups and knot theory; Feynman diagrams; Galois theory; mixed Tate motives; arithmetical dimorphism; ARI/GARI and the flexion structure, etc. At the moment, all these strands are in the process of merging or at least cross-fertilising, and constitute a vibrant field of research.

(iv) Identity-tangent diffeos and the actual computation of their invariants.

The sections of [5] devoted to the invariants of identity-tangent diffeos were written with no computational applications in mind, and no attempt was made to optimise the calculational procedures. On the contrary, the PhD thesis [1], which revisits the subject 30 years on, lays its main emphasis on these neglected aspects and provides effective Maple programmes for the computations of the invariants; it also offers copious asides on the algebraic aspects of multitangents, which largely, but not exactly, mirror those of multizetas.

8.3 Remark about the general composition equation

The equations verified by the iterators and iteration roots of identity-tangent diffeos are extremely special cases of the general composition equation:

$$f^{om_r} \circ g_r \circ \dots \circ f^{om_2} \circ g_2 \circ f^{om_1} \circ g_1 = id \quad (8.1)$$

with f unknown, $m_i \in \mathbb{Z}$ and $g_i(z) = z + \tau_i + \mathcal{O}(z^{-1})$. The general solution⁹⁵ of (8.1) is also generally divergent but always resurgent

⁹⁵ It is *unique* under the genericity assumption $\sum m_i \neq 0$.

and resumable.⁹⁶ The subject is investigated in Section 11 and 12 of a preprint accessible on the author’s homepage.⁹⁷

The critical set Ω (containing the indices ω of all *active* alien derivations Δ_ω) is often huge: it usually consists of all finite combinations $-\lambda_{j_0} + \sum n_j \lambda_i$ ($n_j > 0$) spanned by the (countably many) roots of some exponential polynomial constructed from the data m_i and τ_i . We may adjust these data m_i, τ_i so as to ensure $\Omega = 2\pi i\mathbb{Z}$, for example by considering composition equations of the form

$$f \circ g_r \circ \dots \circ f \circ g_2 \circ f \circ g_1 = id \tag{8.2}$$

with $g_1(z) = z + 1 + \mathcal{O}(z^{-2})$, $g_i(z) = z + \mathcal{O}(z^{-2})$ ($i \geq 2$). But even then the complete formal solution remains extremely complex, and still depends non-linearly on a countable infinity of parameters u_j :

$$\tilde{f}(z, u) = \tilde{f}(z) + \sum \mathbf{u}^n e^{\omega z} \tilde{f}_n(z) \quad (\mathbf{u}^n = \prod u_j^{n_j}). \tag{8.3}$$

The bridge equation reads $\mathbf{\Delta}_\omega \tilde{f}(z, u) = \mathbb{A}_\omega \tilde{f}(z, u)$ with operators \mathbb{A}_ω that are hardly less complex:

$$\mathbb{A}_\omega = \sum_{\langle n, j \rangle - j = k} u_{j_1}^{n_{j_1}} \dots u_{j_r}^{n_{j_r}} A_{\omega, \mathbf{n}}^j \partial_{u_j} \quad (\dot{\omega} = 2\pi i k, k \in \mathbb{Z} - r\mathbb{Z}). \tag{8.4}$$

However, a drastic simplification occurs in the case $r = 2$:

$$\mathbb{A}_\omega = 2\pi i A_\omega \sum_{k \in \mathbb{Z}^*} (j+k) u_{j+k} \partial_{u_j} \quad (\dot{\omega} = 2\pi i k, k \in \mathbb{Z} - 2\mathbb{Z}). \tag{8.5}$$

Instead of depending on a huge set of unrelated resurgence constants $A_{\omega, \mathbf{n}}^j$, with $\omega \in 2\pi i\mathbb{Z}^*$ but an index \mathbf{n} running through all finite parts of \mathbb{Z} , the operators \mathbb{A}_ω now depend on an incomparably smaller set of resurgence constants A_ω , with $\omega \in 2\pi i\mathbb{Z}^*$.

The reason is of course that in the case $r = 2$, the composition equation reduces to an iteration equation - to the taking of a ‘square root’:

$$f \circ g_2 \circ f \circ g_1 = id \iff (f \circ g_2) \circ (f \circ g_2) = g_1^{-1} \circ g_2. \tag{8.6}$$

This huge complexity gap between the case $r \geq 3$ and $r = 2$ is reminiscent of the equally dramatic simplification that takes place with first order singular ODE’s of ‘Euler type’ :

$$\partial_z Y = Y + \sum_{-1 \leq n \leq n_0} b_n(z) Y^{1+n} \quad (b_n(z) \in z^{-1}\mathbb{C}\{z^{-1}\}). \tag{8.7}$$

⁹⁶ The critical time too is unique under the same genericity assumption $\sum m_i \neq 0$.

⁹⁷ *The Natural Growth Scale*.

In the general case ($2 \leq n_0 \leq \infty$), we get a resurgent formal solution $\tilde{f}(z, u)$ in $\mathbb{C}[[z^{-1}, u z^\tau e^z]]$, a critical set $\Omega = \{-1\} \cup \mathbb{N}^*$, and an infinite series of independent invariants $\mathbb{A}_n = A_\omega u^{n+1} \partial_u$ with indices $n \in \{-1, 1, 2, 3, \dots\}$, whereas in the case $n_0 = 1$, the equation (8.7) becomes an ODE of Riccati type; the critical set Ω reduces to $\{-1, 1\}$; and we are left with just two independent invariants $\mathbb{A}_{-1}, \mathbb{A}_1$.

9 Tables

9.1 Multitangents: symmetrel, alternal, olternol

We express Taa^\bullet and Too^\bullet in terms of $Te^\bullet \approx Tee^\bullet$ according to the linearisation lemma of Section 5.4, using throughout the shorthand $n_{i,j,\dots}$ for $n_i + n_j + \dots$.

Table 1: Comparing $Te^\bullet \sim Tee^\bullet, Taa^\bullet, Too^\bullet$.

$$Taa^{n_1} = Too^{n_1} = Te^{n_1} \quad , \quad Taa^{n_1, n_2} = Too^{n_1, n_2} = \frac{1}{2} Te^{n_1, n_2} - \frac{1}{2} Te^{n_2, n_1}$$

$$\begin{aligned} 6 Taa^{n_1, n_2, n_3} &= 2 Te^{n_1, n_2, n_3} - Te^{n_1, n_3, n_2} - Te^{n_2, n_1, n_3} - Te^{n_2, n_3, n_1} - Te^{n_3, n_1, n_2} \\ &\quad + 2 Te^{n_3, n_2, n_1} - Te^{n_1 + n_3, n_2} + \frac{1}{2} Te^{n_1, n_2, 3} + \frac{1}{2} Te^{n_1, 2, n_3} + \frac{1}{2} Te^{n_3, n_1, 2} \\ &\quad + \frac{1}{2} Te^{n_2, 3, n_1} - Te^{n_2, n_1, 3} \end{aligned}$$

$$\begin{aligned} 4 Too^{n_1, n_2, n_3} &= Te^{n_1, n_2, n_3} - Te^{n_1, n_3, n_2} - Te^{n_2, n_1, n_3} - Te^{n_2, n_3, n_1} - Te^{n_3, n_1, n_2} \\ &\quad + Te^{n_3, n_2, n_1} - Te^{n_1, 3, n_2} - Te^{n_2, n_1, 3} \end{aligned}$$

$$12 Taa^{n_1, n_2, n_3, n_4} =$$

$$\begin{aligned} &3 Te^{n_1, n_2, n_3, n_4} - Te^{n_1, n_2, n_4, n_3} - Te^{n_1, n_3, n_2, n_4} - Te^{n_1, n_3, n_4, n_2} - Te^{n_1, n_4, n_2, n_3} \\ &+ Te^{n_1, n_4, n_3, n_2} - Te^{n_2, n_1, n_3, n_4} + Te^{n_2, n_1, n_4, n_3} - Te^{n_2, n_3, n_1, n_4} - Te^{n_2, n_3, n_4, n_1} \\ &+ Te^{n_2, n_4, n_1, n_3} + Te^{n_2, n_4, n_3, n_1} - Te^{n_3, n_1, n_2, n_4} - Te^{n_3, n_1, n_4, n_2} + Te^{n_3, n_2, n_1, n_4} \\ &+ Te^{n_3, n_2, n_4, n_1} - Te^{n_4, n_1, n_2, n_3} + Te^{n_4, n_1, n_3, n_2} + Te^{n_4, n_2, n_1, n_3} + Te^{n_4, n_2, n_3, n_1} \\ &+ Te^{n_4, n_3, n_1, n_2} - 3 Te^{n_4, n_3, n_2, n_1} + Te^{n_1, n_2, n_3, 4} - Te^{n_1, n_3, n_2, 4} - Te^{n_2, n_3, n_1, 4} \\ &+ Te^{n_2, n_4, n_1, 3} - Te^{n_3, n_1, n_2, 4} + Te^{n_3, n_2, n_1, 4} + Te^{n_4, n_2, n_1, 3} - Te^{n_4, n_3, n_1, 2} \\ &+ Te^{n_1, n_2, 3, n_4} - Te^{n_1, n_2, 4, n_3} - Te^{n_2, n_1, 3, n_4} + Te^{n_2, n_1, 4, n_3} - Te^{n_3, n_1, 4, n_2} \\ &+ Te^{n_3, n_2, 4, n_1} + Te^{n_4, n_1, 3, n_2} - Te^{n_4, n_2, 3, n_1} + Te^{n_1, 2, n_3, n_4} - Te^{n_1, 3, n_2, n_4} \\ &- Te^{n_1, 3, n_4, n_2} + Te^{n_2, 4, n_1, n_3} + Te^{n_2, 4, n_3, n_1} - Te^{n_1, 4, n_2, n_3} + Te^{n_1, 4, n_3, n_2} \\ &- Te^{n_3, 4, n_2, n_1} + \frac{1}{2} Te^{n_1, 2, n_3, 4} - Te^{n_1, 3, n_2, 4} + Te^{n_2, 4, n_1, 3} - \frac{1}{2} Te^{n_3, 4, n_1, 2} \end{aligned}$$

$$\begin{aligned}
& 8 \text{Too}^{n_1, n_2, n_3, n_4} = \\
& + \text{Te}^{n_1, n_2, n_3, n_4} - \text{Te}^{n_1, n_2, n_4, n_3} - \text{Te}^{n_1, n_3, n_2, n_4} - \text{Te}^{n_1, n_3, n_4, n_2} - \text{Te}^{n_1, n_4, n_2, n_3} \\
& + \text{Te}^{n_1, n_4, n_3, n_2} - \text{Te}^{n_2, n_1, n_3, n_4} + \text{Te}^{n_2, n_1, n_4, n_3} - \text{Te}^{n_2, n_3, n_1, n_4} - \text{Te}^{n_2, n_3, n_4, n_1} \\
& + \text{Te}^{n_2, n_4, n_1, n_3} + \text{Te}^{n_2, n_4, n_3, n_1} - \text{Te}^{n_3, n_1, n_2, n_4} - \text{Te}^{n_3, n_1, n_4, n_2} + \text{Te}^{n_3, n_2, n_1, n_4} \\
& + \text{Te}^{n_3, n_2, n_4, n_1} - \text{Te}^{n_3, n_4, n_1, n_2} + \text{Te}^{n_3, n_4, n_2, n_1} - \text{Te}^{n_4, n_1, n_2, n_3} + \text{Te}^{n_4, n_1, n_3, n_2} \\
& + \text{Te}^{n_4, n_2, n_1, n_3} + \text{Te}^{n_4, n_2, n_3, n_1} + \text{Te}^{n_4, n_3, n_1, n_2} - \text{Te}^{n_4, n_3, n_2, n_1} - \text{Te}^{n_1, 3, n_2, n_4} \\
& - \text{Te}^{n_1, 3, n_4, n_2} - \text{Te}^{n_2, n_1, 3, n_4} + \text{Te}^{n_4, n_1, 3, n_2} + \text{Te}^{n_2, n_4, n_1, 3} + \text{Te}^{n_4, n_2, n_1, 3} \\
& + \text{Te}^{n_2, 4, n_1, n_3} + \text{Te}^{n_2, 4, n_3, n_1} - \text{Te}^{n_1, n_2, 4, n_3} + \text{Te}^{n_3, n_2, 4, n_1} - \text{Te}^{n_1, n_3, n_2, 4} \\
& - \text{Te}^{n_3, n_1, n_2, 4} - \text{Te}^{n_1, 4, n_2, n_3} + \text{Te}^{n_1, 4, n_3, n_2} + \text{Te}^{n_2, n_1, 4, n_3} - \text{Te}^{n_3, n_1, 4, n_2} \\
& - \text{Te}^{n_2, n_3, n_1, 4} + \text{Te}^{n_3, n_2, n_1, 4} + \text{Te}^{n_2, 4, n_1, 3} - \text{Te}^{n_1, 3, n_2, 4}
\end{aligned}$$

$$\text{Taa}^{n_1, \dots, n_5} = 540 \text{Te}^\bullet\text{-summands} , \text{Too}^{n_1, \dots, n_5} = 308 \text{Te}^\bullet\text{-summands}$$

$$\text{Taa}^{n_1, \dots, n_6} = 3688 \text{Te}^\bullet\text{-summands} , \text{Too}^{n_1, \dots, n_6} = 2612 \text{Te}^\bullet\text{-summands}$$

$$\text{Taa}^{n_1, \dots, n_7} = 47292 \text{Te}^\bullet\text{-summands} , \text{Too}^{n_1, \dots, n_7} = 25988 \text{Te}^\bullet\text{-summands}$$

9.2 Parity properties of alternal and olternol multitangents

We begin by comparing the number of summands in the monotangent reductions $red_1(\text{Te}^\bullet)$ and $red_1(\text{Taa}^\bullet)$ (respectively $red_2(\text{Te}^\bullet)$ and $red_2(\text{Taa}^\bullet)$) of Te^\bullet and Taa^\bullet before (respectively after) symmetrel linearisation of the resulting multizetas. N.B. A further reduction $red_3(\text{Te}^\bullet)$ and $red_3(\text{Taa}^\bullet)$, corresponding to a complete decomposition of the multizeta into *arithmetical irreducibles*, would yield even fewer summands.

The triplets $[N_1, N_2, N_3]$ of Table 2 are defined as follows. N_1 is the number of summands after reduction into a sum of monotangents Te^{n_i} and symmetrel multizeta coefficients ze^\bullet . N_2 and N_3 represent the number of summands left after taking multizeta dimorphy into account and expressing everything in terms of *multizeta irreducibles* – either plain irreducibles from Zig^\bullet or even-odd irreducibles from $\text{Zig}_{ev}^\bullet, \text{Zig}_{odd}^\bullet$. See Section 6.2, Section 6.3. Note that N_2 is about the same as N_1 , but that N_3 is much smaller.⁹⁸

⁹⁸ Of course, unlike N_1 , which has absolute significance, N_2 and N_3 depend on the particular system of irreducibles chosen for the reduction. There exist privileged systems, but we cannot go into that here. But whatever system we choose, the *average values* N_3 will always be much smaller than that N_2 .

Table 2.

$(n_1, \dots, n_r) \parallel$	$\#(\text{Te}^\bullet) \mid$	$\#(\text{Taa}^\bullet) \mid$	$\#(\text{Too}^\bullet)$
$(2, 7, 4) \parallel$	47, 45, 17 \mid	28, 26, 8 \mid	15, 15, 5
$(5, 2, 2, 4) \parallel$	40, 39, 21 \mid	37, 37, 13 \mid	30, 30, 11
$(5, 3, 3, 4, 2) \parallel$	210, 209, 69 \mid	294, 289, 38 \mid	212, 207, 32
$(3, 1, 2, 3, 4, 2) \parallel$	455, 455, 33 \mid	491, 488, 30 \mid	382, 382, 26
$(2, 1, 2, 1, 2, 2, 3) \parallel$	220, 203, 15 \mid	659, 578, 15 \mid	631, 567, 12

.....

Table 2 bis : Here are the even-irreducibles and odd-irreducibles to appear in the sequel, with their expression in terms of ordinary irreducibles.

$$\begin{aligned} \zeta_{6,2}^{\text{ev}} &= \zeta_{6,2} - 3\zeta_5\zeta_3 \\ \zeta_{8,2}^{\text{ev}} &= \zeta_{8,2} - 4\zeta_7\zeta_3 - 2\zeta_5^2 \\ \zeta_{10,2}^{\text{ev}} &= \zeta_{10,2} - 5\zeta_3\zeta_9 - 5\zeta_7\zeta_5 \\ \zeta_{8,1,2}^{\text{odd}} &= \zeta_{8,1,2} + \zeta_{6,2}\zeta_3 - 3\zeta_5\zeta_3^2 - \frac{27}{2}\zeta_9\zeta_2 - \frac{13}{10}\zeta_7\zeta_2^2 - \frac{44}{105}\zeta_2^3\zeta_5 + \frac{72}{175}\zeta_3\zeta_2^4 \\ \zeta_{9,3,1}^{\text{odd}} &= \zeta_{9,3,1} + 82\zeta_{11}\zeta_2 + \frac{193}{10}\zeta_9\zeta_2^2 + \frac{8}{55}\zeta_3\zeta_2^5 + \frac{226}{35}\zeta_7\zeta_2^3 + \frac{288}{175}\zeta_5\zeta_2^4 \\ \zeta_{10,2,1}^{\text{odd}} &= \zeta_{10,2,1} - 28\zeta_{11}\zeta_2 - \frac{41}{5}\zeta_9\zeta_2^2 - \frac{36}{25}\zeta_5\zeta_2^4 - \frac{124}{35}\zeta_7\zeta_2^3 - \frac{208}{385}\zeta_3\zeta_2^5 \end{aligned}$$

.....

The following twelve examples of multitangent reduction (of type red_2) are meant to cover all situations. They illustrate the phenomenon of *parity separation* in Taa^\bullet and Too^\bullet , and its absence in $\text{Te}^\bullet \approx \text{Tee}^\bullet$. The last examples involve irreducibles of depth 2 and 3.

Table 3: $Te^{2,7,3}(z)$ has no definite parity in z .

$$Te^{2,7,3}(z) = \sum_{2 \leq m \leq 7} teze_m^{2,7,3} Te^m(z)$$

$$teze_1^{2,7,3} = 10ze^{5,6} + 10ze^{6,5} + 35ze^{8,3} + 56ze^{3,8} - 10ze^{11} - 21ze^{4,7} - 27ze^{7,4} - 28ze^{9,2} = 0$$

$$teze_2^{2,7,3} = 35ze^{3,7} + 36ze^{7,3} + 48ze^{5,5} - 6ze^{10} - 21ze^{8,2} - 28ze^{2,8} - 45ze^{4,6} - 45ze^{6,4} = \frac{7}{2}\zeta_{8,2}^{ev} + 56\zeta_7\zeta_3 + 35\zeta_5^2 - \frac{2296}{275}\zeta_2^5$$

$$teze_3^{2,7,3} = 15ze^{3,6} + 15ze^{6,3} - 6ze^9 - 6ze^{4,5} - 6ze^{5,4} - 14ze^{2,7} - 15ze^{7,2} = \frac{35}{2}\zeta_9 + \frac{104}{35}\zeta_3\zeta_2^3 - 21\zeta_7\zeta_2 - 4\zeta_5\zeta_2^2$$

$$teze_4^{2,7,3} = 16ze^{3,5} + 16ze^{5,3} - 3ze^8 - 10ze^{2,6} - 10ze^{6,2} - 18ze^{4,4} = 16\zeta_5\zeta_3 - \frac{652}{175}\zeta_2^4$$

$$teze_5^{2,7,3} = 3ze^{3,4} + 3ze^{4,3} - 3ze^7 - 6ze^{2,5} - 6ze^{5,2} = \frac{6}{5}\zeta_3\zeta_2^2 - 6\zeta_5\zeta_2$$

$$teze_6^{2,7,3} = 4ze^{3,3} - ze^6 - 3ze^{2,4} - 3ze^{4,2} = 2\zeta_3^2 - \frac{6}{5}\zeta_2^3$$

$$teze_7^{2,7,3} = -ze^5 - ze^{2,3} - ze^{3,2} = -\zeta_3\zeta_2$$

.....

Table 4: $Taa^{2,7,3}(z)$ is even in z since $2+7+3-3$ is odd.

$$Taa^{2,7,3}(z) = \sum_{2 \leq m \text{ even} \leq 10} taaze_m^{2,7,3} Te^m(z)$$

$$taaze_2^{2,7,3} = 35ze^{3,7} + 36ze^{7,3} + 48ze^{5,5} + \frac{373}{6}ze^{10} - \frac{28}{3}ze^{2,8} - \frac{7}{3}ze^{8,2} - 15ze^{4,6} - 15ze^{6,4} = 35\zeta_5^2 + 56\zeta_7\zeta_3 + \frac{7}{2}\zeta_{8,2}^{ev} - \frac{392}{275}\zeta_2^5$$

$$taaze_4^{2,7,3} = 16ze^{3,5} + 16ze^{5,3} + \frac{29}{3}ze^8 - \frac{10}{3}ze^{2,6} - 6ze^{4,4} - \frac{10}{3}ze^{6,2} = 16\zeta_5\zeta_3 - \frac{652}{525}\zeta_2^4$$

$$taaze_6^{2,7,3} = 4ze^{3,3} + \frac{1}{6}ze^6 - ze^{2,4} - ze^{4,2} = 2\zeta_3^2 - \frac{62}{105}\zeta_2^3$$

$$taaze_8^{2,7,3} = 0$$

$$taaze_{10}^{2,7,3} = \frac{1}{6}ze^2 = \frac{1}{6}\zeta_2$$

.....

Table 5: $Too^{2,7,3}(z)$ is even in z since $2+7+3-3$ is odd.

$$\begin{aligned} Too^{2,7,3}(z) &= \sum_{2 \leq m \text{ even} \leq 6} tooze_m^{2,7,3} Te^m(z) \\ tooze_2^{2,7,3} &= 7ze^{8,2} + 35ze^{3,7} + 36ze^{7,3} + 48ze^{5,5} + 105ze^{10} \\ &= 35\zeta_5^2 + 56\zeta_7\zeta_3 + 7/2\zeta_{8,2}^{ev} + \frac{152}{55}\zeta_2^5 \\ tooze_4^{2,7,3} &= 16ze^{3,5} + 16ze^{5,3} + \frac{39}{2}ze^8 = +16\zeta_5\zeta_3 + \frac{12}{25}\zeta_2^4 \\ tooze_6^{2,7,3} &= 2ze^6 + 4ze^{3,3} = 2\zeta_3^2 \end{aligned}$$

.....

Table 6: $Te^{2,7,4}(z)$ has no definite parity in z .

$$\begin{aligned} Te^{2,7,4}(z) &= \sum_{2 \leq m \leq 7} teze_m^{2,7,4} Te^m(z) \\ teze_1^{2,7,4} &= 30ze^{12} + 84ze^{4,8} + 84ze^{10,2} + 100ze^{6,6} + 112ze^{8,4} - 104ze^{7,5} \\ &\quad - 112ze^{5,7} - 112ze^{9,3} - 168ze^{3,9} = 0 \\ teze_3^{2,7,4} &= 14ze^{10} + 28ze^{2,8} + 35ze^{8,2} + 35ze^{4,6} + 35ze^{6,4} - 32ze^{5,5} \\ &\quad - 40ze^{7,3} - 42ze^{3,7} = \frac{992}{175}\zeta_2^5 - 8\zeta_5^2 - 28\zeta_7\zeta_3 \\ teze_4^{2,7,4} &= 8ze^9 + 8ze^{4,5} + 8ze^{5,4} + 20ze^{7,2} + 21ze^{2,7} - 20ze^{3,6} - 20ze^{6,3} \\ &= 14\zeta_7\zeta_2 + \frac{8}{5}\zeta_5\zeta_2^2 + \frac{35}{2}\zeta_9 - \frac{176}{35}\zeta_3\zeta_2^3 \\ teze_5^{2,7,4} &= 5ze^8 + 6ze^{4,4} + 10ze^{2,6} + 10ze^{6,2} - 8ze^{3,5} - 8ze^{5,3} \\ &= \frac{484}{175}\zeta_2^4 - 8\zeta_5\zeta_3 \\ teze_6^{2,7,4} &= 2ze^7 + 4ze^{2,5} + 4ze^{5,2} - 2ze^{3,4} - 2ze^{4,3} = 4\zeta_5\zeta_2 - \frac{4}{5}\zeta_3\zeta_2^2 \\ teze_7^{2,7,4} &= ze^6 + ze^{2,4} + ze^{4,2} = \frac{2}{5}\zeta_2^3 \end{aligned}$$

.....

Table 7: $Taa^{2,7,4}(z)$ is odd in z since $2+7+4-3$ is even.

$$\begin{aligned}
 Taa^{2,7,4}(z) &= \sum_{2 \leq m \text{ odd} \leq 11} taaze_m^{2,7,4} Te^m(z) \\
 taaze_1^{2,7,4} &= 28ze^{4,8} + 36ze^{12} + 56ze^{8,4} + 84ze^{10,2} + \frac{100}{3}ze^{6,6} - 104ze^{7,5} \\
 &\quad - 112ze^{5,7} - 112ze^{9,3} - 168ze^{3,9} = 0 \\
 taaze_3^{2,7,4} &= 11ze^{10} + \frac{28}{3}ze^{2,8} + \frac{35}{3}ze^{4,6} + \frac{35}{3}ze^{6,4} + \frac{49}{3}ze^{8,2} - 32ze^{5,5} \\
 &\quad - 40ze^{7,3} - 42ze^{3,7} = \frac{24352}{5775}\zeta_2^5 - 8\zeta_5^2 - 28\zeta_7\zeta_3 \\
 taaze_5^{2,7,4} &= 2ze^{4,4} + \frac{10}{3}ze^{2,6} + \frac{10}{3}ze^{6,2} + \frac{17}{3}ze^8 - 8ze^{3,5} - 8ze^{5,3} \\
 &= \frac{1156}{525}\zeta_2^4 - 8\zeta_5\zeta_3 \\
 taaze_7^{2,7,4} &= \frac{1}{3}ze^{2,4} + \frac{1}{3}ze^{4,2} + \frac{17}{6}ze^6 = \frac{74}{105}\zeta_2^3 \\
 taaze_9^{2,7,4} &= \frac{2}{3}ze^4 = \frac{4}{15}\zeta_2^2 \\
 taaze_{11}^{2,7,4} &= \frac{1}{6}ze^2 = \frac{1}{6}\zeta_2
 \end{aligned}$$

.....

Table 8: $Too^{2,7,4}(z)$ is odd in z since $2+7+4-3$ is even.

$$\begin{aligned}
 Too^{2,7,4}(z) &= \sum_{3 \leq m \text{ odd} \leq 5} tooze_m^{2,7,4} Te^m(z) \\
 tooze_1^{2,7,4} &= 39ze^{12} + 28ze^{8,4} + 84ze^{10,2} - 104ze^{7,5} - 112ze^{5,7} - 112ze^{9,3} \\
 &\quad - 168ze^{3,9} = 0 \\
 tooze_3^{2,7,4} &= 7ze^{8,2} - \frac{23}{2}ze^{10} - 32ze^{5,5} - 40ze^{7,3} - 42ze^{3,7} \\
 &= \frac{96}{55}\zeta_2^5 - 8\zeta_5^2 - 28\zeta_7\zeta_3 \\
 tooze_5^{2,7,4} &= -8ze^{3,5} - 8ze^{5,3} - \frac{9}{2}ze^8 = \frac{12}{25}\zeta_2^4 - 8\zeta_5\zeta_3
 \end{aligned}$$

.....

Table 9: $Te^{5,3,3,4}(z)$ has no definite parity in z .

$$Te^{5,3,3,4}(z) = \sum_{2 \leq m \leq 5} teze_m^{5,3,3,4} Te^m(z)$$

$$\begin{aligned} teze_1^{5,3,3,4} &= 6ze^{10,4} + 12ze^{5,9} + 15ze^{7,7} + 12ze^{5,5,4} + 15ze^{7,4,3} + 15ze^{4,7,3} \\ &\quad + 30ze^{6,5,3} + 30ze^{5,6,3} + 30ze^{5,4,5} + 30ze^{4,5,5} + 30ze^{7,3,4} \\ &\quad + 60ze^{4,6,4} + 60ze^{5,3,6} + 45ze^{4,4,6} + 90ze^{6,4,4} - 15ze^{6,8} \\ &= -6ze^{4,10} = 0 \end{aligned}$$

$$\begin{aligned} teze_2^{5,3,3,4} &= 2ze^{4,9} + 10ze^{4,6,3} + 12ze^{4,5,4} + 15ze^{4,4,5} + 15ze^{4,3,6} + 30ze^{5,3,5} \\ &\quad + 30ze^{5,5,3} + 35ze^{7,3,3} + 36ze^{5,4,4} + 40ze^{6,3,4} + 45ze^{6,4,3} - 3ze^{5,8} \\ &\quad - 5ze^{6,7} - 6ze^{9,4} = \frac{240}{7} \zeta_7 \zeta_2^3 - 72 \zeta_9 \zeta_2^2 - 175 \zeta_{6,2}^{ev} \zeta_5 - 775 \zeta_5^2 \zeta_3 \\ &\quad - 600 \zeta_7 \zeta_3^2 - 200 \zeta_{9,3,1}^{odd} - 700 \zeta_{10,2,1}^{odd} - \frac{71900}{3} \zeta_{13} - \frac{3198}{35} \zeta_5 \zeta_2^4 \end{aligned}$$

$$\begin{aligned} teze_3^{5,3,3,4} &= ze^{5,7} + 5ze^{6,3,3} + 5ze^{4,3,5} + 6ze^{4,5,3} + 9ze^{5,4,3} + 10ze^{5,3,4} \\ &\quad + 9ze^{4,4,4} - ze^{4,8} = 14 \zeta_{6,2}^{ev} \zeta_2^2 + 14 \zeta_5 \zeta_3 \zeta_2^2 + 15 \zeta_{10,2}^{ev} + 45 \zeta_9 \zeta_3 \\ &\quad + 55 \zeta_7 \zeta_5 + \frac{10576684}{875875} \zeta_2^6 - 50 \zeta_5^2 \zeta_2 \end{aligned}$$

$$\begin{aligned} teze_4^{5,3,3,4} &= 3ze^{4,3,4} + 3ze^{4,4,3} + 5ze^{5,3,3} = \frac{35}{2} \zeta_5 \zeta_3^2 + \frac{35}{4} \zeta_{8,1,2}^{odd} + \frac{72}{5} \zeta_7 \zeta_2^2 \\ &\quad + \frac{29893}{96} \zeta_{11} - 45 \zeta_9 \zeta_2 - \frac{80}{7} \zeta_5 \zeta_2^3 \end{aligned}$$

$$teze_5^{5,3,3,4} = ze^{4,3,3} = 10 \zeta_5 \zeta_3 \zeta_2 + 7 \zeta_7 \zeta_3 + \frac{12932}{1925} \zeta_2^5 + \frac{7}{2} \zeta_{8,2}^{ev} + 10 \zeta_{6,2}^{ev} \zeta_2 - \frac{45}{2} \zeta_5^2$$

.....

Table 10: $Taa^{5,3,3,4}(z)$ is even in z since $5+3+3+4-4$ is odd.

$$\begin{aligned}
 Taa^{5,3,3,4}(z) &= \sum_{2 \leq m \text{ even} \leq 8} taaze_m^{5,3,3,4} Te^m(z) \\
 taaze_2^{5,3,3,4} &= 5ze^{4,3,6} + 22ze^{5,8} + 30ze^{5,5,3} + 30ze^{5,3,5} + 35ze^{7,3,3} + \frac{25}{3}ze^{6,4,3} \\
 &\quad + \frac{40}{3}ze^{6,3,4} + \frac{184}{3}ze^{9,4} + \frac{295}{3}ze^{6,7} + \frac{260}{3}ze^{7,6} + \frac{323}{3}ze^{4,9} \\
 &\quad + \frac{291}{2}ze^{13} - 16ze^{5,4,4} - 24ze^{4,5,4} - 5ze^{4,4,5} - 40ze^{8,5} \\
 &\quad - \frac{35}{3}ze^{10,3} - \frac{80}{3}ze^{4,6,3} = -175\zeta_{6,2}^{ev}\zeta_5 - 200\zeta_{9,3,1}^{odd} - 700\zeta_{10,2,1}^{odd} \\
 &\quad - 600\zeta_7\zeta_3^2 - 775\zeta_5^2\zeta_3 - \frac{3102}{35}\zeta_5\zeta_2^4 - \frac{71614}{3}\zeta_{13} \\
 taaze_4^{5,3,3,4} &= ze^{4,3,4} + 35ze^{4,7} + \frac{41}{2}ze^{7,4} + \frac{55}{6}ze^{5,6} + \frac{155}{6}ze^{11} - \frac{29}{3}ze^{8,3} \\
 &\quad + 5ze^{5,3,3} - ze^{4,4,3} = \frac{35}{4}\zeta_{8,1,2}^{odd} + \frac{35}{2}\zeta_5\zeta_3^2 + \frac{8967}{32}\zeta_{11} - \frac{124}{21}\zeta_5\zeta_3^3 \\
 taaze_6^{5,3,3,4} &= \frac{8}{3}ze^{5,4} + \frac{25}{6}ze^{4,5} + \frac{13}{6}ze^9 - \frac{5}{2}ze^{6,3} = \frac{14}{3}\zeta_5\zeta_2^2 - \frac{21}{2}\zeta_9 \\
 taaze_8^{5,3,3,4} &= -\frac{1}{6}ze^{4,3} - \frac{1}{12}ze^7 = \frac{5}{3}\zeta_2\zeta_5 - \frac{35}{12}\zeta_7
 \end{aligned}$$

.....

Table 11: $Too^{5,3,3,4}(z)$ is even in z since $5+3+3+4-4$ is odd.

$$\begin{aligned}
 Too^{5,3,3,4}(z) &= \sum_{2 \leq m \text{ even} \leq 6} tooze_m^{5,3,3,4} Te^m(z) \\
 tooze_2^{5,3,3,4} &= 5ze^{10,3} + 30ze^{5,3,5} + 30ze^{5,5,3} + 35ze^{7,3,3} + 60ze^{8,5} + 138ze^{4,9} \\
 &\quad + 147ze^{9,4} + 170ze^{6,7} + \frac{123}{2}ze^{5,8} + \frac{385}{2}ze^{7,6} + \frac{861}{2}ze^{13} \\
 &\quad - 42ze^{5,4,4} - 42ze^{4,5,4} - 15ze^{4,4,5} - 10ze^{6,4,3} - 45ze^{4,6,3} \\
 &= -775\zeta_3\zeta_5^2 - 200\zeta_{9,3,1}^{odd} - 700\zeta_{10,2,1}^{odd} - 175\zeta_{6,2}^{ev}\zeta_5 - \frac{306}{5}\zeta_5\zeta_2^4 \\
 &\quad - 600\zeta_7\zeta_3^2 - \frac{285455}{12}\zeta_{13} \\
 tooze_4^{5,3,3,4} &= ze^{8,3} + 25ze^{6,5} + 51ze^{4,7} + \frac{55}{2}ze^{5,6} + \frac{105}{2}ze^{7,4} + \frac{315}{4}ze^{11} \\
 &\quad + 5ze^{5,3,3} - 3ze^{4,4,3} = \frac{35}{4}\zeta_{8,1,2}^{odd} + \frac{29629}{96}\zeta_{11} + \frac{35}{2}\zeta_5\zeta_3^2 \\
 tooze_6^{5,3,3,4} &= \frac{15}{2}ze^{5,4} + \frac{15}{2}ze^{4,5} + \frac{15}{2}ze^9 = 3\zeta_5\zeta_2^2
 \end{aligned}$$

.....

Table 12: $Te^{5,2,3,4}(z)$ has no definite parity in z .

$$Te^{5,2,3,4}(z) = \sum_{2 \leq m \leq 5} teze_m^{5,2,3,4} Te^m(z)$$

$$\begin{aligned} teze_1^{5,2,3,4} = & ze^{5,8} + 2ze^{4,9} + 3ze^{10,3} + 5ze^{11,2} + 15ze^{7,6} - 10ze^{6,7} - 5ze^{4,6,3} \\ & - 15ze^{4,4,5} - 35ze^{8,3,2} - 35ze^{8,2,3} - 42ze^{5,4,4} - 18ze^{4,5,4} \\ & - 30ze^{7,2,4} - 40ze^{5,3,5} - 45ze^{7,4,2} - 50ze^{6,3,4} - 50ze^{5,6,2} \\ & - 50ze^{6,2,5} - 60ze^{6,4,3} - 70ze^{7,3,3} - 70ze^{6,5,2} - 76ze^{5,5,3} = 0 \end{aligned}$$

$$\begin{aligned} teze_2^{5,2,3,4} = & 2ze^{5,7} + 10ze^{6,2,4} + 10ze^{5,2,5} + 15ze^{7,2,3} - ze^{4,8} - ze^{10,2} - 5ze^{6,6} \\ & - 3ze^{9,3} - 5ze^{4,3,5} - 8ze^{5,3,4} - 9ze^{4,4,4} - 10ze^{6,3,3} - 15ze^{4,5,3} \\ & - 15ze^{4,6,2} - 16ze^{5,5,2} - 20ze^{7,3,2} - 24ze^{5,4,3} - 35ze^{6,4,2} \\ = & 16\zeta_{6,2}^{ev} \zeta_2^2 + 35\zeta_7 \zeta_5 + 100\zeta_5^2 \zeta_2 + 105\zeta_9 \zeta_3 - 35\zeta_{10,2}^{ev} - 16\zeta_3^2 \zeta_3^2 \\ & - \frac{12462448}{525525} \zeta_2^6 \end{aligned}$$

$$\begin{aligned} teze_3^{5,2,3,4} = & ze^{5,6} + ze^{9,2} - 2ze^{5,2,4} - 3ze^{4,3,4} - 5ze^{6,2,3} - 5ze^{4,5,2} - 6ze^{4,4,3} \\ & - 10ze^{6,3,2} - 10ze^{5,3,3} - 11ze^{5,4,2} = 8\zeta_5 \zeta_2^3 + 60\zeta_{6,2}^{ev} \zeta_3 \\ & + \frac{4136}{175} \zeta_3 \zeta_2^4 - 30\zeta_5 \zeta_3^2 - 40\zeta_{8,1,2}^{odd} - \frac{112}{5} \zeta_7 \zeta_2^2 - \frac{3040}{3} \zeta_{11} \end{aligned}$$

$$\begin{aligned} teze_4^{5,2,3,4} = & ze^{5,2,3} - 2ze^{4,3,3} - 3ze^{4,4,2} - 4ze^{5,3,2} = 10\zeta_{6,2}^{ev} \zeta_2 + \frac{21}{2} \zeta_7 \zeta_3 \\ & + \frac{105}{4} \zeta_5^2 - 4\zeta_3^2 \zeta_2^2 - \frac{63}{4} \zeta_{8,2}^{ev} - \frac{1696}{275} \zeta_2^5 \end{aligned}$$

$$teze_5^{5,2,3,4} = -Ze^{4,3,2} = 7\zeta_5 \zeta_2^2 + \frac{53}{36} \zeta_9 + \frac{64}{105} \zeta_3 \zeta_2^3 - 14\zeta_7 \zeta_2 - \frac{2}{3} \zeta_3^3$$

.....

Table 13: $Taa^{5,2,3,4}(z)$ is odd in z since $5+2+3+4-4$ is even.

$$\begin{aligned}
 Taa^{5,2,3,4}(z) &= \sum_{3 \leq m \text{ odd} \leq 9} taaze_m^{5,2,3,4} Te^m(z) \\
 taaze_1^{5,2,3,4} &= 5ze^{4,4,5} + 10ze^{4,3,6} + 18ze^{5,4,4} + 22ze^{4,5,4} + 30ze^{7,2,4} \\
 &\quad + 15ze^{7,4,2} + 20ze^{2,5,6} + 30ze^{2,7,4} + 30ze^{4,7,2} + 40ze^{5,2,6} \\
 &\quad + \frac{70}{3}ze^{2,8,3} + \frac{100}{3}ze^{2,6,5} + \frac{145}{3}ze^{4,6,3} + \frac{8}{3}ze^{10,3} + \frac{80}{3}ze^{7,6} \\
 &\quad + \frac{176}{3}ze^{4,9} + \frac{238}{3}ze^{9,4} - 10ze^{5,6,2} - \frac{5}{3}ze^{11,2} - \frac{5}{3}ze^{2,11} \\
 &\quad - \frac{11}{6}ze^{13} - \frac{20}{3}ze^{6,4,3} - \frac{20}{3}ze^{6,3,4} - 40ze^{5,3,5} - 70ze^{7,3,3} \\
 &\quad - 76ze^{5,5,3} - \frac{35}{3}ze^{8,3,2} - \frac{35}{3}ze^{8,2,3} - \frac{50}{3}ze^{6,5,2} - \frac{50}{3}ze^{6,2,5} \\
 &\quad - \frac{70}{3}ze^{6,7} - \frac{115}{3}ze^{8,5} - \frac{200}{3}ze^{5,8} = 0 \\
 taaze_3^{5,2,3,4} &= Ze^{4,3,4} + 2ze^{4,4,3} + 4ze^{2,5,4} + \frac{43}{3}ze^{8,3} + \frac{1}{3}ze^{4,5,2} + \frac{10}{3}ze^{2,6,3} \\
 &\quad + \frac{22}{3}ze^{5,2,4} + \frac{7}{6}ze^{7,4} - 26ze^{2,9} - 10ze^{5,3,3} - \frac{5}{3}ze^{5,4,2} - \frac{5}{3}ze^{6,2,3} \\
 &\quad - \frac{10}{3}ze^{6,3,2} - \frac{10}{3}ze^{2,3,6} - \frac{28}{3}ze^{9,2} - \frac{37}{3}ze^{4,7} - \frac{44}{3}ze^{5,6} \\
 &\quad - \frac{65}{6}ze^{6,5} - \frac{169}{6}ze^{11} \\
 &= 60\zeta_{6,2}^{ev}\zeta_3 + \frac{15112}{525}\zeta_3\zeta_2^4 - \frac{16}{3}\zeta_5\zeta_2^3 - 40\zeta_{8,1,2}^{odd} - 30\zeta_5\zeta_3^2 - 1105\zeta_{11} \\
 taaze_5^{5,2,3,4} &= 5ze^{6,3} - 6ze^{4,5} - 12ze^{2,7} - \frac{1}{3}ze^{4,3,2} - \frac{2}{3}ze^{2,3,4} - \frac{13}{3}ze^{7,2} \\
 &\quad - \frac{14}{3}ze^{5,4} - \frac{32}{3}ze^9 = \frac{152}{35}\zeta_3\zeta_2^3 - \frac{1}{3}\zeta_5\zeta_2^2 - \frac{2}{3}\zeta_3^3 - \frac{1447}{36}\zeta_9 \\
 taaze_7^{5,2,3,4} &= \frac{5}{6}ze^{4,3} - \frac{10}{3}ze^{2,5} - \frac{11}{6}ze^7 - \frac{7}{6}ze^{5,2} = \frac{26}{15}\zeta_3\zeta_2^2 - \frac{5}{6}\zeta_5\zeta_2 - \frac{49}{6}\zeta_7 \\
 taaze_9^{5,2,3,4} &= -\frac{1}{6}ze^5 - \frac{1}{3}ze^{2,3} = \frac{2}{3}\zeta_3\zeta_2 - \frac{5}{3}\zeta_5
 \end{aligned}$$

.....

Table 14: $Too^{5,2,3,4}(z)$ is odd in z since $5 + 2 + 3 + 4 - 4$ is even.

$$\begin{aligned} Too^{5,2,3,4}(z) &= \sum_{3 \leq m \text{ odd} \leq 9} tooze_m^{5,2,3,4} Te^m(z) \\ tooze_1^{5,2,3,4} &= 10ze^{6,5,2} + 10ze^{5,6,2} + 15ze^{4,4,5} + 15ze^{4,3,6} + 15ze^{6,3,4} \\ &\quad + 20ze^{6,4,3} + 30ze^{2,5,6} + 35ze^{2,8,3} + 42ze^{4,5,4} + 45ze^{4,7,2} \\ &\quad + 45ze^{7,4,2} + 45ze^{2,7,4} + 48ze^{5,4,4} + 50ze^{2,6,5} + 60ze^{7,2,4} \\ &\quad + 60ze^{5,2,6} + 75ze^{4,6,3} + 30ze^{8,5} + 40ze^{6,7} + 87ze^{4,9} + 95ze^{7,6} \\ &\quad + 126ze^{9,4} + \frac{47}{2}ze^{10,3} - \frac{5}{2}ze^{5,8} - 5ze^{11,2} - \frac{5}{2}ze^{2,11} - \frac{17}{2}ze^{13} \\ &\quad - 40ze^{5,3,5} - 70ze^{7,3,3} - 76ze^{5,5,3} = 0 \\ tooze_3^{5,2,3,4} &= 3ze^{7,4} + 18ze^{8,3} + 3ze^{4,3,4} + 3ze^{5,4,2} + 3ze^{4,5,2} + 5ze^{2,6,3} \\ &\quad + 6ze^{2,5,4} + 6ze^{4,4,3} + 12ze^{5,2,4} - 5ze^{2,3,6} - 10ze^{5,3,3} - 5ze^{5,6} \\ &\quad - 15ze^{4,7} - 25ze^{9,2} - 39ze^{2,9} - \frac{175}{4}ze^{11} \\ &= 60\zeta_{6,2}^{ev}\zeta_3 + \frac{712}{25}\zeta_3\zeta_2^4 - 30\zeta_5\zeta_3^2 - 40\zeta_{8,1,2}^{odd} - \frac{104}{7}\zeta_5\zeta_2^3 - \frac{12985}{12}\zeta_{11} \\ tooze_5^{5,2,3,4} &= \frac{15}{2}ze^{6,3} - ze^{2,3,4} - 5ze^{5,4} - 18ze^{2,7} - 10ze^{7,2} - \frac{15}{2}ze^{4,5} - \frac{65}{4}ze^9 \\ &= 484/105\zeta_3\zeta_2^3 - 8\zeta_5\zeta_2^2 - \frac{2}{3}\zeta_3^3 - \frac{268}{9}\zeta_9 \\ tooze_7^{5,2,3,4} &= \frac{3}{2}ze^{4,3} - 2ze^{5,2} - 5ze^{2,5} - \frac{11}{4}ze^7 = -5\zeta_5\zeta_2 - \frac{21}{4}\zeta_7 + \frac{12}{5}\zeta_3\zeta_2^2 \\ tooze_9^{5,2,3,4} &= -\frac{1}{4}ze^5 - \frac{1}{2}ze^{2,3} = \zeta_3\zeta_2 - \frac{5}{2}\zeta_5 \end{aligned}$$

9.3 The invariants as entire functions of f : the general case

We write down, up to weight 10 inclusively, the expansions of the collectors p , p_* , $p_\#$ in terms of the g , g_* , $g_\#$. We assume $p(f) = 1$ but impose no restriction on $\rho(f) \equiv -g_2$. In these and all further examples, we order the terms according to their total weight and, within a given total weight, we start with the lowest monotangents.

Table 15: $\mathfrak{p} = id + \sum \mathfrak{P}_s$ up to weight 10 with $f = l \circ g$, $g(z) = z + \sum_{2 \leq s} g_s z^{1-s}$.

$$\begin{aligned}
\mathfrak{P}_2 &= \mathbf{Te}^1 g_2, \mathfrak{P}_3 = \mathbf{Te}^2 g_3, \mathfrak{P}_4 = \mathbf{Te}^3 g_4, \mathfrak{P}_5 = \mathbf{Te}^4 g_5, \\
\mathfrak{P}_6 &= \mathbf{Te}^2 [3\zeta_3 g_2^3 + 6\zeta_3 g_4 g_2 - 6\zeta_3 g_3^2] + \mathbf{Te}^3 [2\zeta_2 g_4 g_2 - 2\zeta_2 g_3^2] + \mathbf{Te}^5 g_6, \\
\mathfrak{P}_7 &= \mathbf{Te}^3 [6\zeta_3 g_2^2 g_3 + 6\zeta_3 g_5 g_2 - 6\zeta_3 g_4 g_3] + \mathbf{Te}^4 [3\zeta_2 g_5 g_2 - 3\zeta_2 g_4 g_3] + \mathbf{Te}^6 g_7, \\
\mathfrak{P}_8 &= \mathbf{Te}^2 [10\zeta_5 g_2^4 + 10\zeta_5 g_6 g_2 + 30\zeta_5 g_4^2 - 40\zeta_5 g_5 g_3 + 50\zeta_5 g_4 g_2^2 - 50\zeta_5 g_2 g_3^2 [\\
&\quad + \mathbf{Te}^3 [\frac{4}{5}\zeta_2^2 g_6 g_2 + \frac{12}{5}\zeta_2^2 g_4^2 + \frac{16}{5}\zeta_2^2 g_4 g_2^2 - \frac{2}{5}\zeta_2^2 g_2^4 - \frac{16}{5}\zeta_2^2 g_2 g_3^2 \\
&\quad - \frac{16}{5}\zeta_2^2 g_5 g_3] + \mathbf{Te}^4 [\zeta_3 g_2 g_3^2 + 3\zeta_3 g_4^2 + 7\zeta_3 g_6 g_2 + 8\zeta_3 g_4 g_2^2 - 10\zeta_3 g_5 g_3] \\
&\quad + \mathbf{Te}^5 [4\zeta_2 g_6 g_2 - 4\zeta_2 g_5 g_3] + \mathbf{Te}^7 g_8, \\
\mathfrak{P}_9 &= \mathbf{Te}^2 [\frac{16}{7}\zeta_2^3 g_5 g_2^2 + \frac{32}{7}\zeta_2^3 g_3^3 - \frac{48}{7}\zeta_2^3 g_4 g_3 g_2 + 18\zeta_3^2 g_5 g_2^2 + 36\zeta_3^2 g_3^3 \\
&\quad - 54\zeta_3^2 g_4 g_3 g_2] + \mathbf{Te}^3 [10\zeta_5 g_2 g_7 + 20\zeta_5 g_2^3 g_3 + 20\zeta_5 g_5 g_4 + 35\zeta_5 g_5 g_2^2 \\
&\quad - 5\zeta_5 g_4 g_3 g_2 - 30\zeta_5 g_3^3 - 30\zeta_5 g_6 g_3 + 12\zeta_3 \zeta_2 g_5 g_2^2 + 24\zeta_3 \zeta_2 g_3^3 \\
&\quad - 36\zeta_3 \zeta_2 g_4 g_2 g_3] + \mathbf{Te}^4 [\frac{6}{5}\zeta_2^2 g_2 g_7 + \frac{12}{5}\zeta_2^2 g_5 g_4 + \frac{21}{5}\zeta_2^2 g_3^3 + \frac{69}{10}\zeta_2^2 g_5 g_2^2 \\
&\quad - \frac{6}{5}\zeta_2^2 g_3 g_2^3 - \frac{18}{5}\zeta_2^2 g_6 g_3 - \frac{111}{10}\zeta_2^2 g_4 g_3 g_2] + \mathbf{Te}^5 [2\zeta_3 g_4 g_3 g_2 + 4\zeta_3 g_5 g_4 \\
&\quad + 8\zeta_3 g_7 g_2 + 10\zeta_3 g_5 g_2^2 - 12\zeta_3 g_6 g_3] + \mathbf{Te}^6 [5\zeta(2) g_2 g_7 - 5\zeta(2) g_6 g_3] \\
&\quad + \mathbf{Te}^8 g_9, \\
\mathfrak{P}_{10} &= \mathbf{Te}^2 [14\zeta_7 g_2 g_8 + \frac{77}{2}\zeta_7 g_2^5 + 147\zeta_7 g_6 g_2^2 + 210\zeta_7 g_6 g_4 + 322\zeta_7 g_4 g_2^3 \\
&\quad + 441\zeta_7 g_4^2 g_2 - 84\zeta_7 g_3 g_7 - 140\zeta_7 g_5^2 - 322\zeta_7 g_3^2 g_2^2 - 588\zeta_7 g_5 g_3 g_2] \\
&\quad + \mathbf{Te}^3 [9\zeta_3^2 g_2^5 + 21\zeta_3^2 g_6 g_2^2 + 33\zeta_3^2 g_4 g_2^3 + 36\zeta_3^2 g_4 g_3^2 - 9\zeta_3^2 g_4 g_2^2 - 33\zeta_3^2 g_3^2 g_2^2 \\
&\quad - 48\zeta_3^2 g_5 g_3 g_2 + \frac{16}{35}\zeta_2^3 g_8 g_2 + \frac{32}{7}\zeta_2^3 g_4 g_2^2 + \frac{48}{7}\zeta_2^3 g_6 g_4 + \frac{32}{105}\zeta_2^3 g_4 g_3^2 \\
&\quad + \frac{248}{35}\zeta_2^3 g_4^2 g_2 + \frac{568}{105}\zeta_2^3 g_6 g_2^2 - \frac{32}{7}\zeta_2^3 g_5^2 - \frac{32}{105}\zeta_2^3 g_3^2 g_2^2 - \frac{244}{105}\zeta_2^3 g_2^5 \\
&\quad - \frac{256}{15}\zeta_2^3 g_5 g_3 g_2 - \frac{96}{35}\zeta_2^3 g_3 g_7] + \mathbf{Te}^4 [\zeta_5 g_2^5 + \frac{1}{2}\zeta_5 g_3^2 g_2^2 + 11\zeta_5 g_8 g_2 \\
&\quad + 45\zeta_5 g_6 g_4 + \frac{59}{2}\zeta_5 g_4 g_2^3 + \frac{81}{2}\zeta_5 g_6 g_2^2 + \frac{123}{2}\zeta_5 g_4^2 g_2 - 20\zeta_5 g_5^2 - 36\zeta_5 g_7 g_3 \\
&\quad - 45\zeta_5 g_4 g_2^2 - 57\zeta_5 g_5 g_3 g_2 + 15\zeta_3 \zeta_2 g_4 g_2^2 + 21\zeta_3 \zeta_2 g_6 g_2^2 + 36\zeta_3 \zeta_2 g_4 g_2^2 \\
&\quad - 9\zeta_3 \zeta_2 g_4^2 g_2 - 15\zeta_3 \zeta_2 g_3^2 g_2^2 - 48\zeta_3 \zeta_2 g_5 g_3 g_2] + \mathbf{Te}^5 [\frac{8}{5}\zeta_2^2 g_8 g_2 + \frac{24}{5}\zeta_2^2 g_6 g_4 \\
&\quad + \frac{42}{5}\zeta_2^2 g_4 g_2^3 + \frac{58}{5}\zeta_2^2 g_6 g_2^2 - \frac{6}{5}\zeta_2^2 g_4 g_2^3 - \frac{6}{5}\zeta_2^2 g_3^2 g_2^2 - \frac{6}{5}\zeta_2^2 g_4^2 g_2 - \frac{8}{5}\zeta_2^2 g_5^2 \\
&\quad - \frac{24}{5}\zeta_2^2 g_7 g_3 - \frac{94}{5}\zeta_2^2 g_5 g_3 g_2] + \mathbf{Te}^6 [\zeta_3 g_4^2 g_2 + 2\zeta_3 g_5 g_3 g_2 + 5\zeta_3 g_6 g_4 \\
&\quad + 9\zeta_3 g_8 g_2 + 12\zeta_3 g_6 g_2^2 - 14\zeta_3 g_7 g_3] + \mathbf{Te}^7 [6\zeta_2 g_8 g_2 - 6\zeta_2 g_7 g_3] + \mathbf{Te}^9 g_{10}
\end{aligned}$$

Table 16: $\mathfrak{p}_* = \sum \mathfrak{P}_{*s}$ up to weight 10 with $f = l \circ g$, $g_*(z) = \sum_{2 \leq s} g_{*s} z^{1-s}$.

$$\begin{aligned}
\mathfrak{P}_{*2} &= \mathbf{Te}^1 g_{*2}, \mathfrak{P}_{*3} = \mathbf{Te}^2 g_{*3}, \mathfrak{P}_{*4} = \mathbf{Te}^3 g_{*4}, \mathfrak{P}_{*5} = \mathbf{Te}^4 g_{*5}, \\
\mathfrak{P}_{*6} &= \mathbf{Te}^2 [6\zeta_3 g_{*2} g_{*4} - 6\zeta_3 g_{*3}^2] + \mathbf{Te}^5 [g_{*6}] \\
\mathfrak{P}_{*7} &= \mathbf{Te}^3 [6\zeta_3 g_{*2} g_{*5} - 6\zeta_3 g_{*3} g_{*4}] + \mathbf{Te}^6 [g_{*7}] \\
\mathfrak{P}_{*8} &= \mathbf{Te}^2 [30\zeta_5 g_{*4}^2 - \frac{5}{2}\zeta_5 g_{*2}^4 + 10\zeta_5 g_{*2} g_{*6} - 40\zeta_5 g_{*3} g_{*5}] \\
&\quad \mathbf{Te}^3 [\frac{4}{3}\zeta_2^2 g_{*2} g_{*3}^2 - \frac{4}{3}\zeta_2^2 g_{*2}^2 g_{*4}] + \mathbf{Te}^4 [3\zeta_3 g_{*4}^2 + \frac{1}{4}\zeta_3 g_{*2}^4 - 10\zeta_3 g_{*3} g_{*5} \\
&\quad + 7\zeta_3 g_{*2} g_{*6}] + \mathbf{Te}^5 [-\frac{2}{3}\zeta_2 g_{*2} g_{*3}^2 + \frac{2}{3}\zeta_2 g_{*2}^2 g_{*4}] + \mathbf{Te}^7 [g_{*8}] \\
\mathfrak{P}_{*9} &= \mathbf{Te}^2 [36\zeta(3)^2 g_{*3}^3 - \frac{32}{5}\zeta_2^3 g_{*3}^3 + 18\zeta_3^2 g_{*5} g_{*2}^2 + \frac{48}{5}\zeta_2^3 g_{*2} g_{*3} g_{*4} \\
&\quad - 54\zeta_3^2 g_{*2} g_{*3} g_{*4} - \frac{16}{5}\zeta_2^3 g_{*5} g_{*2}^2] + \mathbf{Te}^3 [20\zeta_5 g_{*4} g_{*5} + 10\zeta_5 g_{*2} g_{*6} \\
&\quad - 30\zeta_5 g_{*3} g_{*6} - 5\zeta_5 g_{*2}^3 g_{*3}] + \mathbf{Te}^4 [-\frac{1}{5}\zeta_2^2 g_{*3}^3 - \frac{21}{10}\zeta_2^2 g_{*2}^2 g_{*5} \\
&\quad + \frac{23}{10}\zeta_2^2 g_{*2} g_{*3} g_{*4}] + \mathbf{Te}^5 [8\zeta_3 g_{*2} g_{*7} - 12\zeta_3 g_{*3} g_{*6} + 4\zeta_3 g_{*4} g_{*5} \\
&\quad + \zeta_3 g_{*2}^3 g_{*3}] + \mathbf{Te}^6 [\frac{3}{2}\zeta_2 g_{*2}^2 g_{*5} - \frac{1}{3}\zeta_2 g_{*3}^3 - \frac{7}{6}\zeta_2 g_{*2} g_{*3} g_{*4}] + \mathbf{Te}^8 [g_{*9}] \\
\mathfrak{P}_{*10} &= \mathbf{Te}^2 [210\zeta_7 g_{*4} g_{*6} - 140\zeta_7 g_{*5}^2 - 84\zeta_7 g_{*3} g_{*7} + 14\zeta_7 g_{*2} g_{*8}] \\
&\quad - \frac{133}{3}\zeta_7 g_{*2}^3 g_{*4} + \frac{133}{3}\zeta_7 g_{*2}^2 g_{*3}^2] + \mathbf{Te}^3 [36\zeta_3^2 g_{*3}^2 g_{*4} - 9\zeta_3^2 g_{*2} g_{*4}^2 \\
&\quad + 21\zeta_3^2 g_{*2}^2 g_{*6} + \frac{3}{4}\zeta_3^2 g_{*2}^5 - \frac{32}{5}\zeta_2^3 g_{*3}^2 g_{*4} - \frac{64}{15}\zeta_2^3 g_{*2}^2 g_{*6} \\
&\quad + \frac{32}{3}\zeta_2^3 g_{*2} g_{*3} g_{*5} - 48\zeta_3^2 g_{*2} g_{*3} g_{*5}] + \mathbf{Te}^4 [45\zeta_5 g_{*4} g_{*6} - 20\zeta_5 g_{*5}^2 \\
&\quad - 36\zeta_5 g_{*3} g_{*7} + 11\zeta_5 g_{*2} g_{*8} - \frac{10}{3}\zeta_5 g_{*2}^3 g_{*4} - \frac{25}{6}\zeta_5 g_{*2}^2 g_{*3}^2] \\
&\quad + \mathbf{Te}^5 [\frac{10}{3}\zeta_2^2 g_{*2} g_{*3} g_{*5} - \frac{2}{5}\zeta_2^2 g_{*3}^2 g_{*4} - \frac{44}{15}\zeta_2^2 g_{*2}^2 g_{*6}] + \mathbf{Te}^6 [9\zeta_3 g_{*2} g_{*8} \\
&\quad - 14\zeta_3 g_{*3} g_{*7} + 5\zeta_3 g_{*4} g_{*6} + \frac{1}{2}\zeta(3) g_{*2}^2 g_{*3}^2 + 2\zeta_3 g_{*2}^3 g_{*4}] \\
&\quad + \mathbf{Te}^7 [\frac{8}{3}\zeta_2 g_{*2}^2 g_{*6} - \frac{5}{3}\zeta_2 g_{*2} g_{*3} g_{*5} - \zeta_2 g_{*3}^2 g_{*4}] + \mathbf{Te}^9 [g_{*10}]
\end{aligned}$$

Table 17: $\mathfrak{p}_{\#} = \sum \mathfrak{P}_{\#s}$ up to weight 10 with
 $f = l \circ g$, $g_{\#}(z) = \sum_{2 \leq s} g_{\#s} z^{1-s}$.

$$\begin{aligned}
\mathfrak{P}_{\#2} &= \mathbf{Te}^1 g_{\#2}, \mathfrak{P}_{\#3} = \mathbf{Te}^2 g_{\#3}, \mathfrak{P}_{\#4} = \mathbf{Te}^3 g_{\#4}, \mathfrak{P}_{\#5} = \mathbf{Te}^4 g_{\#5}, \\
\mathfrak{P}_{\#6} &= \mathbf{Te}^2 [\mathbf{Te}^5 g_{\#6} + 6\zeta_3 g_{\#4} g_{\#2} - 6\zeta_3 g_{\#3}^2] + \mathbf{Te}^3 \zeta_2 g_{\#2}^3 \\
\mathfrak{P}_{\#7} &= \mathbf{Te}^3 [6\zeta_3 g_{\#5} g_{\#2} - 6\zeta_3 g_{\#4} g_{\#3}] + \mathbf{Te}^4 \zeta_2^3 g_{\#3} g_{\#2}^2 + \mathbf{Te}^6 g_{\#7} \\
\mathfrak{P}_{\#8} &= \mathbf{Te}^2 [10\zeta_5 g_{\#6} g_{\#2} + 30\zeta_5 g_{\#4}^2 - 40\zeta_5 g_{\#5} g_{\#3}] \\
&\quad + \mathbf{Te}^3 \left[\frac{8}{5} \zeta_2^2 g_{\#3}^2 g_{\#2} - \frac{8}{5} \zeta_2^2 g_{\#4} g_{\#2}^2 \right] \\
&\quad + \mathbf{Te}^4 [3\zeta_3 g_{\#4}^2 + 2\zeta_3 g_{\#2}^4 - 10\zeta_3 g_{\#5} g_{\#3} + 7\zeta_3 g_{\#6} g_{\#2}] \\
&\quad + \mathbf{Te}^5 [5\zeta_2 g_{\#4} g_{\#2}^2 - 2\zeta_2 g_{\#3}^2 g_{\#2}] + \mathbf{Te}^7 g_{\#8} \\
\mathfrak{P}_{\#9} &= \mathbf{Te}^2 [18\zeta_3^2 g_{\#5} g_{\#2}^2 + 36\zeta_3^2 g_{\#3}^3 - 54\zeta_3^2 g_{\#4} g_{\#3} g_{\#2} + \frac{624}{35} \zeta_2^3 g_{\#4} g_{\#3} g_{\#2} \\
&\quad - \frac{208}{35} \zeta_2^3 g_{\#5} g_{\#2}^2 - \frac{416}{35} \zeta_2^3 g_{\#3}^3] + \mathbf{Te}^3 [10\zeta_5 g_{\#7} g_{\#2} + 20\zeta_5 g_{\#5} g_{\#4} \\
&\quad - 30\zeta_5 g_{\#6} g_{\#3}] + \mathbf{Te}^4 \left[\frac{87}{10} \zeta_2^2 g_{\#4} g_{\#3} g_{\#2} - \frac{9}{2} \zeta_2^2 g_{\#5} g_{\#2}^2 - \frac{21}{5} \zeta_2^2 g_{\#3}^3 \right] \\
&\quad + \mathbf{Te}^5 [8\zeta_3 g_{\#3} g_{\#2}^3 + 8\zeta_3 g_{\#7} g_{\#2} + 4\zeta_3 g_{\#5} g_{\#4} - 12\zeta_3 g_{\#6} g_{\#3}] \\
&\quad + \mathbf{Te}^6 \left[\frac{17}{2} \zeta_2 g_{\#5} g_{\#2}^2 - \frac{1}{2} \zeta_2 g_{\#4} g_{\#3} g_{\#2} - 3\zeta_2 g_{\#3}^3 \right] + \mathbf{Te}^8 g_{\#9} \\
\mathfrak{P}_{\#10} &= \mathbf{Te}^2 [14\zeta_7 g_{\#8} g_{\#2} + 35\zeta_7 g_{\#2}^3 g_{\#4} + 210\zeta_7 g_{\#6} g_{\#4} - 84\zeta_7 g_{\#7} g_{\#3} \\
&\quad - 35\zeta_7 g_{\#3}^2 g_{\#2}^2 - 140\zeta_7 g_{\#5}^2] + \mathbf{Te}^3 \left[\frac{224}{15} \zeta_2^3 g_{\#5} g_{\#3} g_{\#2} + \frac{128}{35} \zeta_2^3 g_{\#4}^2 g_{\#2} \right. \\
&\quad - \frac{704}{105} \zeta_2^3 g_{\#6} g_{\#2}^2 - \frac{416}{35} \zeta_2^3 g_{\#4} g_{\#3}^2 - \frac{176}{105} \zeta_2^3 g_{\#2}^5 + 6\zeta_2^3 g_{\#2}^5 + 21\zeta_2^3 g_{\#6} g_{\#2}^2 \\
&\quad + 36\zeta_3^2 g_{\#4} g_{\#3}^2 - 9\zeta_3^2 g_{\#4}^2 g_{\#2} - 48\zeta_3^2 g_{\#5} g_{\#3} g_{\#2}] + \mathbf{Te}^4 [11\zeta_5 g_{\#8} g_{\#2} \\
&\quad + 29\zeta_5 g_{\#4} g_{\#2}^3 + 45\zeta_5 g_{\#6} g_{\#4} - 36\zeta_5 g_{\#7} g_{\#3} - 29\zeta_5 g_{\#3}^2 g_{\#2}^2 - 20\zeta_5 g_{\#5}^2 \\
&\quad + 9\zeta_2 \zeta_3 g_{\#4} g_{\#2}^3 - 9\zeta_2 \zeta_3 g_{\#3}^2 g_{\#2}^2] + \mathbf{Te}^5 \left[\frac{9}{4} \zeta_2^2 g_{\#2}^5 + \frac{42}{5} \zeta_2^2 g_{\#5} g_{\#3} g_{\#2} \right. \\
&\quad + \frac{33}{5} \zeta_2^2 g_{\#4}^2 g_{\#2} - \frac{33}{5} \zeta_2^2 g_{\#6} g_{\#2}^2 - \frac{42}{5} \zeta_2^2 g_{\#4} g_{\#3}^2] + \mathbf{Te}^6 [+ 5\zeta_3 g_{\#6} g_{\#4} \\
&\quad + 7\zeta_3 g_{\#3}^2 g_{\#2}^2 + 9\zeta_3 g_{\#8} g_{\#2} + 13\zeta_3 g_{\#4} g_{\#2}^3 - 14\zeta_3 g_{\#7} g_{\#3}] \\
&\quad + \mathbf{Te}^7 [13\zeta_2 g_{\#6} g_{\#2}^2 + \frac{9}{2} \zeta_2 g_{\#4} g_{\#2}^2 - \frac{1}{2} \zeta_2 g_{\#2}^5 - 9\zeta_2 g_{\#4} g_{\#3}^2 - \zeta_2 g_{\#5} g_{\#3} g_{\#2}] \\
&\quad + \mathbf{Te}^9 g_{\#10}
\end{aligned}$$

9.4 The invariants as entire functions of f : the reflexive case

As in Table 16, we write down the expansion of the collector \mathfrak{p}_* in terms of g_* , but this time for a reflexive f . Recall that a standard f is reflexive iff $f(-f(-z)) \equiv z$, in which case its conjugate $l^{1/2} \circ f \circ f^{-1/2}$ is of the form $l \circ g$ with g also reflexive. See Section 3.9. Reflexivity automatically implies $\rho(f) \equiv -g_{*2} \equiv 0$. There being fewer coefficients g_{*s} , we reach weight 13.

Example 18: \mathfrak{p}_* up to weight 13 for $f = l \circ g$ with

$$g_*(z) = \sum_{1 \leq d} g_{*1+2d} z^{-2d}.$$

$$\begin{aligned} \mathfrak{P}_{*3} &= \mathbf{Te}^2 g_{*3}, \mathfrak{P}_{*5} = \mathbf{Te}^4 g_{*5}, \mathfrak{P}_{*6} = \mathbf{Te}^2[-6\zeta_3 g_{*3}^2], \mathfrak{P}_{*7} = \mathbf{Te}^6 g_{*7}, \\ \mathfrak{P}_{*8} &= \mathbf{Te}^2[-40\zeta_5 g_{*5} g_{*3}] + \mathbf{Te}^4[-10\zeta_3 g_{*5} g_{*3}], \\ \mathfrak{P}_{*9} &= \mathbf{Te}^2[36\zeta_3^2 g_{*3}^3 - \frac{32}{5}\zeta_2^3 g_{*3}^3] + \mathbf{Te}^4[-\frac{1}{5}\zeta_2^2 g_{*3}^3] + \mathbf{Te}^6[-\frac{1}{3}\zeta_2 g_{*3}^3] \\ &\quad + \mathbf{Te}^8[g_{*9}], \\ \mathfrak{P}_{*10} &= \mathbf{Te}^2[-84\zeta_7 g_{*7} g_{*3} - 140\zeta_7 g_{*5}^2] + \mathbf{Te}^4[-36\zeta_5 g_{*7} g_{*3} - 20\zeta_5 g_{*5}^2] \\ &\quad + \mathbf{Te}^6[-14\zeta_3 g_{*7} g_{*3}] \\ \mathfrak{P}_{*11} &= \mathbf{Te}^2[560\zeta_5 \zeta_3 g_{*5} g_{*3}^2 - \frac{15648}{175}\zeta_2^4 g_{*5} g_{*3}^2 - 80\zeta_{6,2}^{\text{ev}} g_{*5} g_{*3}^2] \\ &\quad + \mathbf{Te}^4[80\zeta_3^2 g_{*5} g_{*3}^2 - \frac{272}{21}\zeta_2^3 g_{*5} g_{*3}^2] + \mathbf{Te}^6[-\frac{34}{15}\zeta_2^2 g_{*5} g_{*3}^2] \\ &\quad + \mathbf{Te}^8[-\frac{5}{3}\zeta_2 g_{*5} g_{*3}^2] + \mathbf{Te}^{10} g_{*11}, \\ \mathfrak{P}_{*12} &= \mathbf{Te}^2[\frac{576}{5}\zeta_3 \zeta_2^3 g_{*3}^4 - 216\zeta_3^3 g_{*3}^4 - 144\zeta_9 g_{*9} g_{*3} - 210\zeta_9 g_{*3}^4 - 1008\zeta_9 g_{*7} g_{*5}] \\ &\quad + \mathbf{Te}^4[\frac{18}{5}\zeta_3 \zeta_2^2 g_{*3}^4 + 14\zeta_7 g_{*3}^4 - 210\zeta_7 g_{*7} g_{*5} - 78\zeta_7 g_{*3} g_{*9}] \\ &\quad + \mathbf{Te}^6[6\zeta_3 \zeta_2 g_{*3}^4 - \frac{10}{3}\zeta_5 g_{*3}^4 - 28\zeta_5 g_{*7} g_{*5} - 44\zeta_5 g_{*9} g_{*3}] \\ &\quad + \mathbf{Te}^8[-18\zeta_3 g_{*9} g_{*3}], \\ \mathfrak{P}_{*13} &= \mathbf{Te}^2[720\zeta_5^2 g_{*7} g_{*3}^2 + 1200\zeta_5^2 g_{*5} g_{*3}^2 + 1344\zeta_7 \zeta_3 g_{*7} g_{*3}^2 \\ &\quad + 2240\zeta_7 \zeta_3 g_{*5} g_{*3}^2 - 168\zeta_{8,2}^{\text{ev}} g_{*7} g_{*3}^2 - 280\zeta_{8,2}^{\text{ev}} g_{*5} g_{*3}^2 - \frac{125056}{385}\zeta_2^5 g_{*5} g_{*3}^2 \\ &\quad - \frac{375168}{1925}\zeta_2^5 g_{*7} g_{*3}^2] + \mathbf{Te}^4[100\zeta_{6,2}^{\text{ev}} g_{*5} g_{*3}^2 + 500\zeta_5 \zeta_3 g_{*5} g_{*3}^2 \\ &\quad + 540\zeta_5 \zeta_3 g_{*7} g_{*3}^2 + \frac{6544}{525}\zeta_2^4 g_{*5} g_{*3}^2 - \frac{23824}{175}\zeta_2^4 g_{*7} g_{*3}^2 - 180\zeta_{6,2}^{\text{ev}} g_{*7} g_{*3}^2] \\ &\quad + \mathbf{Te}^6[140\zeta_3^2 g_{*7} g_{*3}^2 + \frac{88}{21}\zeta_2^3 g_{*5} g_{*3}^2 - \frac{3064}{105}\zeta_2^3 g_{*7} g_{*3}^2] + \mathbf{Te}^8[\frac{8}{15}\zeta_2^2 g_{*5} g_{*3}^2 \\ &\quad - \frac{39}{5}\zeta_2^2 g_{*7} g_{*3}^2] + \mathbf{Te}^{10}[-4\zeta_2 g_{*7} g_{*3}^2 - \frac{2}{3}\zeta_2 g_{*5} g_{*3}^2] + \mathbf{Te}^{12} g_{*13} \end{aligned}$$

9.5 The invariants as entire functions of f : one-parameter cases

Table 19: \mathfrak{p}_* up to weight 12 for $f = l \circ g$ with $g(z) = z + g_2 z^{-1}$.

$$\begin{aligned}
 \mathfrak{P}_2 &= g_2 \mathbf{Te}^2, \mathfrak{P}_4=0, \mathfrak{P}_6=g_2^3 \mathbf{Te}^2[3\zeta_3], \\
 \mathfrak{P}_8 &= g_2^4 \left(\mathbf{Te}^2[10\zeta_5] + \mathbf{Te}^3 \left[-\frac{2}{5} \zeta_2^2 \right] \right), \\
 \mathfrak{P}_{10} &= g_2^5 \left(\mathbf{Te}^2 \left[\frac{77}{2} \zeta_7 \right] + \mathbf{Te}^3 \left[9\zeta_3^2 - \frac{244}{105} \zeta_2^3 \right] + \mathbf{Te}^4 \zeta_5 \right), \\
 \mathfrak{P}_{12} &= g_2^6 \left(\mathbf{Te}^2[151\zeta_9] + \mathbf{Te}^3 \left[3\zeta_{6,2}^{\text{ev}} + 63\zeta_3\zeta_5 - \frac{878}{105} \zeta_2^4 \right] \right. \\
 &\quad \left. + \mathbf{Te}^4 \left[10\zeta_7 + 3\zeta_2\zeta_5 - \frac{18}{5} \zeta_2^2 \zeta_3 \right] + \mathbf{Te}^5 \left[-\frac{8}{35} \zeta_2^3 \right] \right), \\
 \mathfrak{P}_{14} &= g_2^7 \left(\mathbf{Te}^2 \left[\frac{16}{7} \zeta_2^3 \zeta_5 + 18\zeta_3^2 \zeta_5 + 9\zeta_{8,1,2}^{\text{odd}} + \frac{19343}{24} \zeta_{11} \right] \right. \\
 &\quad \left. + \mathbf{Te}^3 \left[15\zeta_{8,2}^{\text{ev}} + 6\zeta_{6,2}^{\text{ev}} \zeta_2 + 261\zeta_7 \zeta_3 - \frac{5972}{231} \zeta_2^5 + \frac{235}{2} \zeta_5^2 + 6\zeta_5 \zeta_3 \zeta_2 \right] \right. \\
 &\quad \left. + \mathbf{Te}^4 \left[+27\zeta_3^3 + \frac{5027}{72} \zeta_9 + 30\zeta_7 \zeta_2 - \frac{51}{10} \zeta_2^2 \zeta_5 - \frac{732}{35} \zeta_3 \zeta_2^3 \right] \right. \\
 &\quad \left. + \mathbf{Te}^5 \left[11\zeta_3 \zeta_5 - \zeta_{6,2}^{\text{ev}} - \frac{508}{175} \zeta_2^4 \right] + \mathbf{Te}^6[\zeta_7] \right)
 \end{aligned}$$

Table 20: \mathfrak{p}_* up to weight 12 for $f = l \circ g$ with $g(z) = z \left[1 + 2g_{*2} z^{-2} \right]^{\frac{1}{2}}$.

$$\begin{aligned}
 \mathfrak{P}_{*2} &= g_{*2} \mathbf{Te}^1, \mathfrak{P}_{*4}=0, \mathfrak{P}_{*6}=0, \\
 \mathfrak{P}_{*8} &= g_{*2}^4 \left(\mathbf{Te}^2 \left[-\frac{5}{2} \zeta_5 \right] + \mathbf{Te}^4 \left[\frac{1}{4} \zeta_3 \right] \right) \\
 \mathfrak{P}_{*10} &= g_{*2}^5 \mathbf{Te}^3 \left[\frac{3}{4} \zeta_3^2 \right] \\
 \mathfrak{P}_{*12} &= g_{*2}^6 \left(\mathbf{Te}^2 \left[\frac{3}{2} \zeta_3^3 + \frac{47}{6} \zeta_9 - \frac{4}{5} \zeta_3 \zeta_2^3 \right] + \mathbf{Te}^4 \left[-\frac{21}{40} \zeta_3 \zeta_2^2 - \frac{63}{64} \zeta_7 \right] \right. \\
 &\quad \left. + \mathbf{Te}^6 \left[\frac{3}{8} \zeta_3 \zeta_2 + \frac{1}{16} \zeta_5 \right] + \mathbf{Te}^8 \left[-\frac{1}{16} \zeta_3 \right] \right) \\
 \mathfrak{P}_{*14} &= g_{*2}^7 \left(\mathbf{Te}^3 \left[\frac{105}{16} \zeta_5^2 - \zeta_3^2 \zeta_2^2 - \frac{189}{32} \zeta_7 \zeta_3 \right] \right. \\
 &\quad \left. + \mathbf{Te}^5 \left[\frac{1}{2} \zeta_3^2 \zeta_2 - 2\zeta_5 \zeta_3 \right] + \mathbf{Te}^7 \left[\frac{1}{8} \zeta_3^2 \right] \right)
 \end{aligned}$$

Table 21: \mathfrak{p}_* up to weight 15 for $f = \log$ with $g(z) = z \left[1 + 3 g_{*3} z^{-3} \right]^{\frac{1}{3}}$.

$$\begin{aligned} \mathfrak{P}_{*3} &= g_{*3} \mathbf{Te} \\ \mathfrak{P}_{*6} &= g_{*3}^2 \left(\mathbf{Te}^2[-6\zeta_3] \right) \\ \mathfrak{P}_{*9} &= g_{*3}^3 \left(\mathbf{Te}^2 \left[36\zeta_3^2 - \frac{32}{5}\zeta_2^3 \right] + \mathbf{Te}^4 \left[-\frac{1}{5}\zeta_2^2 \right] + \mathbf{Te}^6 \left[-\frac{1}{3}\zeta_2 \right] \right) \\ \mathfrak{P}_{*12} &= g_{*3}^4 \left(\mathbf{Te}^2 \left[\frac{576}{5}\zeta_3\zeta_2^3 - 216\zeta_3^3 - 210\zeta_9 \right] \right. \\ &\quad \left. + \mathbf{Te}^4 \left[\frac{18}{5}\zeta_3\zeta_2^2 + 14\zeta_7 \right] + \mathbf{Te}^6 \left[6\zeta_3\zeta_2 - \frac{10}{3}\zeta_5 \right] \right) \\ \mathfrak{P}_{*15} &= g_{*3}^5 \left(\mathbf{Te}^2 \left[1296\zeta_3^4 + 3780\zeta_9\zeta_3 - 140\zeta_7\zeta_5 - \frac{23054144}{125125}\zeta_2^6 - \frac{6912}{5}\zeta_3^2\zeta_2^3 \right. \right. \\ &\quad \left. \left. - 420\zeta_{10,2}^{\text{ev}} \right] + \mathbf{Te}^4 \left[\frac{1332224}{28875}\zeta_2^5 - \frac{216}{5}\zeta_3^2\zeta_2^2 + 60\zeta_5^2 - 238\zeta_7\zeta_3 + 49\zeta_{8,2}^{\text{ev}} \right] \right. \\ &\quad \left. + \mathbf{Te}^6 \left[\frac{1007}{1575}\zeta_2^4 - 72\zeta_3^2\zeta_2 + \frac{190}{3}\zeta_5\zeta_3 - \frac{50}{3}\zeta_{6,2}^{\text{ev}} \right] + \mathbf{Te}^8 \left[\frac{193}{75}\zeta_2^3 \right] \right. \\ &\quad \left. + \mathbf{Te}^{10} \left[\frac{16}{15}\zeta_2^2 \right] + \mathbf{Te}^{12} \left[\frac{7}{45}\zeta_2 \right] \right) \end{aligned}$$

10 Synopsis

10.1 Diffeos, collectors, connectors, invariants

Given a general local identity-tangent mapping f of $\mathbb{C}_\infty \mapsto \mathbb{C}_\infty$, whether of tangency order 1 (*i.e.* $f(z) - z \sim Cst$) or of order $p > 1$ (*i.e.* $f(z) - z \sim Cst z^{1-p}$), what can be said of its **analytic invariants**? What are the most natural, complete systems $\{A_\omega, \omega \in \Omega\}$ of invariants? What methods are there for computing these A_ω , singly or collectively? How do these methods compare as to efficiency? Above all, on the more theoretical side: which are the most explicit and/or economical formulae for expanding the A_ω into convergent series of f -dependent inputs (such as the Taylor coefficients of f) and f -independent, universal constants?

Practically all natural, complete systems $\{A_\omega, \omega \in \Omega\}$ of invariants consist of the Fourier coefficients of the so-called **connectors** $\pi(z)$ – *i.e.* trigonometric Fourier series which *connect* the various sectorial normalisations of f with their immediate neighbours. Although these invariant *connectors* are totally independent and mutually unrelated, they all derive from a more basic object, the **collector** $\mathfrak{p}(z)$, which is unique and “of one piece”, but unfortunately not invariant. The *collector*, with its natural expansions into series of multitangents *or* monotangents, is a natural intermediary between f and the invariant-carrying *connectors*.

10.2 Affiliates, generators, mediators

The *analytic* invariants $A_\omega(f)$ are also *holomorphic* in f as long as f ranges through a fixed formal conjugacy class $\mathbb{G}^{(p,\rho)}$ of \mathbb{G} , where $p \in \mathbb{N}^*$ is the *tangency order* and $\rho \in \mathbb{C}$ the *iteration residue*. Thus, for elements of the prototypical class $\mathbb{G}^{(1,0)}$, which may be written as $f = l \circ g$ with $l(z) = z + 1$ and $g(z) = z + \mathcal{O}(z^{-2})$, the invariants $A_\omega(f)$ as well as the connector $\pi(z)$ and collector $\mathfrak{p}(z)$ that carry them, must be *entire functions* of g , hence of each of g 's coefficients g_n .

Now, given any analytic function $\gamma(t) := \sum_{0 \leq r} \gamma_r t^r$, we can associate with f, g, π, \mathfrak{p} the so-called *affiliates* $f_\diamond, g_\diamond, \pi_\diamond, \mathfrak{p}_\diamond$ defined via the corresponding substitution operators F, G, Π, \mathfrak{P} .⁹⁹

Three types of affiliates are of special relevance:

- (i) the *infinitesimal generators* $f_*, g_*, \pi_*, \mathfrak{p}_*$, with $\gamma(t) = \log(1 + t)$.
- (ii) the *first or main mediators* $f_\sharp, g_\sharp, \pi_\sharp, \mathfrak{p}_\sharp$, with $\gamma(t) = \frac{t}{1 + \frac{1}{2}t}$.
- (iii) the *second mediators* $f_{\sharp\sharp}, g_{\sharp\sharp}, \pi_{\sharp\sharp}, \mathfrak{p}_{\sharp\sharp}$, with $\gamma(t) = \frac{(1+t)^2 - 1}{(1+t)^2 + 1}$.

Each of the three series $f_*, f_\sharp, f_{\sharp\sharp}$ is resurgent and verifies resurgence equations ruled by (and yielding) the invariants $A_\omega(f)$. Here, f_* is by far the best choice.

The three series $g_*, g_\sharp, g_{\sharp\sharp}$ are resurgent, too, but with resurgence coefficients $A_\omega(g)$ totally unrelated to the $A_\omega(f)$. The usefulness of $g_*, g_\sharp, g_{\sharp\sharp}$, however, lies elsewhere – namely in their providing a bridge, first to the collectors $\mathfrak{p}_*, \mathfrak{p}_\sharp, \mathfrak{p}_{\sharp\sharp}$ and then to the connectors $\pi_*, \pi_\sharp, \pi_{\sharp\sharp}$. Here, the best choice is not g_* , but g_\sharp , with $g_{\sharp\sharp}$ the second best choice.

As for the three connectors $\pi_*, \pi_\sharp, \pi_{\sharp\sharp}$, each is as good as the other, since their Fourier coefficients stand in bi-polynomial correspondence with one another.

10.3 Main alien operators

To each type of *affiliate* f_\diamond there naturally corresponds a specific system of *alien operators* $\{\Delta_\omega^\diamond, \omega \in \mathbb{C}_\bullet\}$.

The alien counterpart of the infinitesimal *generators* f_* is the system $\{\Delta_\omega, \omega \in \mathbb{C}_\bullet\}$ of (standard) *alien derivations*.

The alien counterparts of the *mediators* f_\sharp and $f_{\sharp\sharp}$ are the systems of so-called *medial alien operators*¹⁰⁰ $\{\Delta_\omega^\sharp, \omega \in \mathbb{C}_\bullet\}$ and $\{\Delta_\omega^{\sharp\sharp}, \omega \in \mathbb{C}_\bullet\}$. Although these medial operators are not exact derivations (they possess

⁹⁹ Thus $f_\diamond(z) := F_\diamond \cdot z$ with $F_\diamond := \gamma(F - 1)$.

¹⁰⁰ These *medial operators* bear no relation to the so-called *median convolution average*.

more complex co-products), they are in a sense more basic than the alien derivations Δ_ω , and simpler too, at least in many respects, such as numerical computations. They occur naturally in several unrelated contexts and deserve to have their own niche within alien calculus.

10.4 Main moulds

To each type of *affiliate* f_\diamond there also correspond specific mouldian *symmetry types* which extend the familiar four-type landscape of *alternall/symmetral* and *alternell/symmetrel*. In the present instance, they also bring order and structure into the plethora of auxiliary moulds required for expanding the invariants $A_\omega(f)$. Here are the main moulds:¹⁰¹

- (i) The scalar multizetas $ze^\bullet, za^\bullet, zo^\bullet$. They are the mainstay of this investigation, being the transcendental ingredient of the $A_\omega(f)$.
- (ii) The multitangents $Tee^\bullet(z), Taa^\bullet(z), Too^\bullet(z)$. They are meromorphic, 1-periodic functions of z . It is through their Fourier coefficients that the multizetas smuggle their way into invariant analysis.
- (iii) The multizetaic resurgence monomials $\widetilde{Se}^\bullet(z), \widetilde{Sa}^\bullet(z), \widetilde{So}^\bullet(z)$, which are related – *in several ways* – to both the scalar multizetas and the multitangents.

These very basic moulds give rise to interesting combinatorial developments, such as the conversion formulae from Taa^\bullet and Too^\bullet to Tee^\bullet . We may note that, here again, the multitangents Too^\bullet , *i.e.* precisely the ones associated with an ‘exotic’ symmetry type, turn out to be the most useful.

10.5 Main results

Half the results presented in this paper deal with somewhat tangential issues – the mould machinery, the alien operators, the attendant combinatorics, etc. Regarding the core concern of the investigation – the expansion-description of the holomorphic invariants – we may point to the following:

We derive explicit and optimal¹⁰² expansions for the collectors and connectors of $f = l \circ g$ in their three main variants: first directly from g to π, \mathfrak{p} , next from g_* to π_*, \mathfrak{p}_* , lastly from g_\sharp to $\pi_\sharp, \mathfrak{p}_\sharp$. We even examine the general, affiliate-based scheme, from g_\diamond to $\pi_\diamond, \mathfrak{p}_\diamond$, the better to bring out the ‘specialness’ of the three main schemes.

¹⁰¹ The vowels ‘e’ and ‘a’ connote, as usual, alternality/symmetrelity or alternality/symmetry, whereas the vowel ‘o’ points to less common symmetry types, related to the mediators.

¹⁰² *Optimal* in the sense of *incapable of further simplification*.

We also detain ourselves over the ramified case ($p > 1$) and the far-going changes it brings: the *finite* reduction of multitanents to monotanents breaks down; the procedure for recovering the multitanents from their singular parts completely changes; the Fourier coefficients of the multitanents are no longer expressible as finite sums of multizetas, not even \mathbb{Q} -indexed ones.

We describe the growth properties of each invariant $A_\omega(f)$ as an entire function of exponential type in the Taylor coefficients of f .

We review various natural groups of formal germs, strictly larger than the group \mathbb{G}_0 of analytic germs, yet close enough to \mathbb{G}_0 to possess non-trivial analytic classes and holomorphic invariants $A_\omega(f)$. We characterize \mathbb{G}_{0++} , the largest of all such groups; and \mathbb{G}_{0+} , the largest of all *self-replicating groups*, whose elements produce connectors which, after rescaling, still belong to the group, and in turn produce their own connectors, *ad infinitum*. These developments may be taken as an introduction to the subject of *phantom holomorphic dynamics*.

We also stress the distinction between the *arithmetical* and *dynamical* monics. They are the same objects, but viewed differently:

- (i) the former as ingredients of the Stokes constants, in which capacity they are rigidly determined.
- (ii) the latter as ingredients of the holomorphic invariants, the sole demand on them being that of *making the invariants invariant*.

We show how the systems of (finite or infinite) relations that constrain the monics *change* depending on which perspective we adopt. Most noticeably, the finite, algebraic constraints on the *dynamical* monics turn out to be significantly weaker than those on their *arithmetical* counterpart.

References

- [1] O. BOUILLOT, *Invariants analytiques des difféomorphismes et multizêtas*, Orsay PhD, 19.10.2011, available as PDF on O. Bouillot's homepage.
- [2] X. BUFF, J. ECALLE, A. EPSTEIN, *Limits of degenerate parabolic quadratic rational maps*, *Geom. Funct. Anal.* **23** (2013), 42–95.
- [3] J. ECALLE, “Théorie des invariants holomorphes”, Thèse d’Etat, Orsay-Paris-Sud, 1974.
- [4] J. ECALLE, *Algèbres de fonctions résurgentes*. *Pub. Math. Orsay* (1981).
- [5] J. ECALLE, *Les fonctions résurgentes appliquées à l’itération*. *Pub. Math. Orsay* (1981).

- [6] J. ECALLE, *L'équation du pont et la classification analytique des objets locaux*. Pub. Math. Orsay (1985).
- [7] J. ECALLE, *Six lectures on transseries, analysable functions and the constructive proof of Dulac's conjecture*, In: "Bifurcation and Periodic Orbits of Vector Fields", D. Schlomiuk ed., Kluwer, 1993, 75–184.
- [8] J. ECALLE, *Cohesive functions and weak accelerations*, Journal d'Analyse Mathématique **60** (1993), 71–97.
- [9] J. ECALLE, *Twisted Resurgence Monomials and canonical synthesis of Local Objects*, Proc. of the June 2002 Edinburgh conference on Analysable Functions (ICMS workshop), World Scientific.
- [10] J. ECALLE, *The flexion structure and dimorphy: flexion units, singularators, generators, and the enumeration of multizeta irreducibles*, In: "Dynamics, Geometry and PDEs; Generalized Borel Summation", O. Costin, F. Fauvet, F. Menous, D. Sauzin (eds.).
- [11] P. FATOU, *Sur les solutions uniformes de certaines équations fonctionnelles*, C. R. Acad. Sci. Paris, **143** (1906), 546–548.
- [12] M. SHISHIKURA, *On the bifurcation of parabolic fixed points of rational maps*, Lecture Notes for the 19th Brazilian Mathematical Colloquium, 1993, IMPA.

The resurgent approach to topological string theory

Ricardo Couso-Santamaría

Abstract. In these notes I describe practical applications of resurgence to topological strings, a theory that enjoys connections with matrix models, enumerative and complex geometry, and strong/weak dualities in Physics. Starting from the asymptotic series representation of the free energy I outline recent results which are first steps for arriving at a transseries, which should in principle contain all the nonperturbative information of the theory.

1 Introduction

The goal of these notes is to present an overview of the work developed in [7,8] about the applications of resurgence to topological string theory. These references are not pieces of mathematics but physics work so they sit on a lower step in the staircase of rigor that has the work of Écalle at the top [12]. The objective then is to introduce the ideas and techniques that have been quite useful in understanding and uncovering nonperturbative effects in physical theories, and to put part of the focus on issues that could be taken as working problems for the resurgent mathematician. A nice companion to this article is [21], which assumes no familiarity with resurgence or topological strings.

The ultimate application of resurgence to Physics would be the use resurgent techniques to define and compute nonperturbative observables of a given physical theory. See [11] for an overview of the role of resurgence in Physics. By nonperturbative I mean valid for any value of the interaction couplings, small or large. (In Mathematics we denote this coupling by x^{-1} while in Physics we may call it g_s .) However, such an ambitious goal could not completely work in general for physical and technical reasons. Resurgence can capture nonperturbative information about a system and store it in the form of a *transseries*. This is a *formal*

object in a variable x built out of exponentials and powers,

$$\varphi = \sum_{n=0}^{\infty} \sigma^n e^{-nAx} \sum_{g=0}^{\infty} x^{-g} \varphi_g^{(n)}, \quad \sigma, A, \varphi_g^{(n)} \in \mathbb{C}. \quad (1.1)$$

The notation here is the following: A is called the instanton action in physical contexts and I will stick to that name; n labels instanton numbers, where $n = 0$ denotes the perturbative sector; σ is called the transseries parameter and is not constrained at the formal level. Transseries can be more general including many instanton actions, A_α , and associated sectors labeled by vectors \mathbf{n} with natural numbers as entries. They can also allow for other transseries monomials besides exponentials, such as logarithms, $\log x$. See for example [6, 13].

The computation of the transseries can be quite challenging in practice. Even if we have surpassed that obstacle we still have to perform the task of resumming the trans series into a function of x that would eventually define the physical observable φ_{phys} . The resummation handles each asymptotic series $\sum_{g=0}^{\infty} x^{-g} \varphi_g^{(n)}$ for every n to produce a finite number for a given x . However we still have to determine the value of the transseries parameter σ . For this we need some *physical input*, such as a boundary condition for φ_{phys} at infinity. This last step is important because resurgence alone cannot choose between all the possible nonperturbative completions. When we lack knowledge about the nonperturbative regime of a physical theory we may not have a way to determine the right completion.

In sight of such a disheartening picture we could just turn to other techniques sometimes available in Physics such as the strong/weak coupling duality or integrability, but we would be missing on the information revealable by resurgence and displayed in the transseries. To illustrate what I mean by the *resurgent approach* let us have a look at Figure 1.1 where I show a practical route from an asymptotic series of perturbative nature, $\varphi^{(0)}$, to a full nonperturbative physical quantity, φ . This approach will not always be successful but it is always worth trying.

The starting point in most physical problems is a finite sequence of perturbative coefficients, $\varphi_g^{(0)}$. How one arrives at these quantities and how many of them can be computed depends very much on the problem. The asymptotic nature of the resurgent approach focuses strongly on behaviors at large order g , so the more coefficients we have the more precise our numerical results will be. For generic quantum field theories computing $\varphi_g^{(0)}$ for even moderate g requires calculating a large amount of Feynman diagrams — roughly $g!$ of them. For theories like topological strings we rely on the recursive properties of the coefficients — like

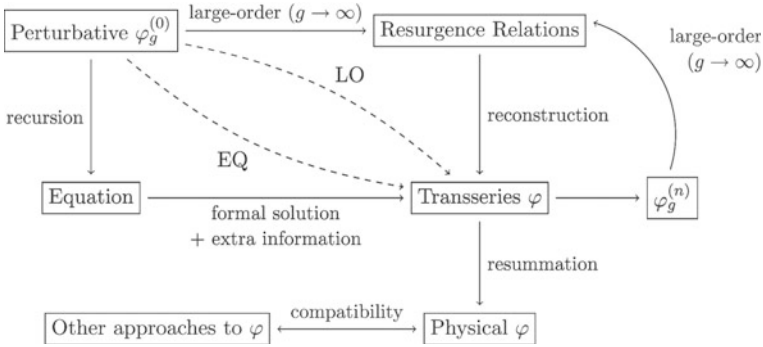


Figure 1.1. The resurgent diagram describes schematically the routes to the transseries starting from perturbation theory, namely EQ and LO, as well as the feedback triangle on the right-hand side and the resummation at the bottom.

the holomorphic anomaly equations, see later — to bypass Feynman diagrams altogether.

If our goal is to build a transseries by studying perturbative data alone we have two routes, which generically complement each other. They are labeled LO and EQ in Figure 1.1.

Route EQ, if available, is the fastest way to the transseries. We may take it if we can find an equation of some type that the perturbative asymptotic series, $\varphi^{(0)}(x)$, satisfies. The easiest way is to find a recursion relation between the coefficients $\varphi_g^{(0)}$ and build an equation from it. The next step is to promote this equation to be valid not only perturbatively but also for a transseries like (1.1). After this, computing coefficients $\varphi_g^{(n)}$ is basically a mechanical task.

To give a somewhat trivial example consider the list perturbative coefficients

$$0, 1, -1, 3, -11, 51, -283, \dots \tag{1.2}$$

that come from solving a Riccati equation in power series. Even if we did not know that such equation was behind these numbers it would not be too unlikely to find a (nonlinear) relation for them, namely

$$\varphi_0^{(0)} = 0, \quad \varphi_1^{(0)} = 1, \quad \varphi_g^{(0)} = -g\varphi_{g-1}^{(0)} + \sum_{h=0}^g \varphi_h^{(0)}\varphi_{g-1-h}^{(0)}, \tag{1.3}$$

and eventually arrive at the equation

$$\varphi^{(0)'}(x) = \varphi^{(0)}(x) - \varphi^{(0)}(x)^2/x - 1/x. \tag{1.4}$$

After this we can just drop the perturbative superscript and plug in a transseries ansatz. This would tell us that the *instanton action* in (1.1)

is $A = -1$ and that the following coefficients are

$$\text{one-instanton, } \varphi_g^{(1)}: \quad 1, 2, 1, \frac{4}{3}, \dots \quad (1.5)$$

$$\text{two-instanton, } \varphi_g^{(2)}: \quad -1, -5, -14, -\frac{122}{3}, \dots \quad (1.6)$$

and so on.

The route labeled LO (after large order) deals with the perturbative coefficients and nothing else. The goal is to determine, with as much detail as possible, how the coefficients $\varphi_g^{(0)}$ grow with g , because in those details are hidden the nonperturbative coefficients. This is what the theory of resurgence tells us that generically happens. So, following with the example, if we take the Riccati numbers (1.2) and pretend for a moment to forget their origin, we can analyze numerically their dependence in the index g . After some numerical computations we would find

$$\begin{aligned} \varphi_g^{(0)} &\sim \frac{\sinh(\pi)}{\pi} \left[\frac{g!}{(-1)^g} 1 + \frac{(g-1)!}{(-1)^{g-1}} 2 + \frac{(g-2)!}{(-1)^{g-2}} 1 + \frac{(g-3)!}{(-1)^{g-3}} \frac{4}{3} + \dots \right] \\ &+ \left(\frac{\sinh(\pi)}{\pi} \right)^2 \left[\frac{g!}{(2(-1))^g} (-1) + \frac{(g-1)!}{(2(-1))^{g-1}} (-5) \right. \\ &+ \left. \frac{(g-2)!}{(2(-1))^{g-2}} (-14) + \frac{(g-3)!}{(2(-1))^{g-3}} \left(-\frac{122}{3} \right) + \dots \right] + \dots \\ &= \sum_{n=1}^{\infty} \frac{S_1^n}{2\pi i} \sum_{h=0}^{\infty} \frac{(g-h)!}{(nA)^{g-h}} \varphi_h^{(n)} \quad \text{as } g \rightarrow \infty. \end{aligned} \quad (1.7)$$

Thus we find, in a very neat and organized fashion, all the nonperturbative information we were looking for. As an extra bit we obtain the Stokes constant S_1 , a quantity intrinsic to the problem that dictates how different resummations are related to each other. See [?] for a rigorous resurgent treatment of the Riccati equation. Let us stress now two important facts about the LO route.

The first is that the relation between $\varphi_g^{(0)}$ and $\varphi_h^{(n)}$ displayed in (1.7) for the Riccati example is generic. The presence of factorials of decreasing intensity and the instanton action in the denominator is a general consequence of resurgence and we expect to find relations similar to these for other problems. That a relation exists between perturbative and nonperturbative data is not that surprising given the existence of route EQ. What may be regarded as unexpected and useful is that the form of (1.7) is valid for a large class of problems.

The second point is that the route LO is essentially a numeric approach to the problem of finding the transseries, but one that is always available if

we can work with enough perturbative coefficients and precision. Practical concerns in this area include the use of convergence acceleration techniques like Richardson extrapolation, see [5].

The roads labeled LO and EQ describe the square in Figure 1.1. There is also a triangle between the transseries, the nonperturbative coefficients $\varphi_g^{(n)}$ (read out from the transseries), and new resurgence relations for $\varphi_g^{(n)}$ when g is large. The latter are quite similar in form to that in (1.7): the lhs is $\varphi_g^{(n)}$ and the rhs involves factorials, instanton actions, Stokes constants, and other coefficients $\varphi_h^{(m)}$. Since we have one such resurgence relation for each instanton number n the complete set of equations imposes quite a constraint on the coefficients of the transseries. This is a property of resurgence that we can take advantage of in problems where the roads LO and EQ do not yield as much information as we wanted (*e.g.*, due to numerical obstacles) or when that information is incomplete (*e.g.*, we cannot determine the coefficients completely). That will be the case in topological string theory.

The bottom part of the diagram deals with the resummation of the transseries, the determination of the transseries parameter σ , and the related issue of Stokes phenomena. I will not cover these topics here because for topological string theory the problem is still under investigation (see however the recent article [9]). I will just mention that to transform a formal transseries into an actual function we use Borel resummation on each of the asymptotic series $\varphi^{(n)}(x)$, see for example the second part of [20]. This resummation process can lead to an ambiguous answer at each instanton sector n . The cure to this problem comes from applying Borel resummation to the complete transseries, that is, Borel–Écalle resummation. It can be a nontrivial step to prove that the resummation is free of the ambiguities.

In the lucky cases in which we have access to alternative descriptions of our theories we can compare the resummed transseries with these other predictions. This can be a crucial step in determining the correct element in the family of transseries parametrized by σ .

2 Basics of topological strings

The first question that comes to mind is why apply the resurgent approach to topological string theory. The answer is twofold.

First of all, topological string theory is a subject of interest by theoretical physicists and mathematicians alike due to its central role in mirror symmetry, in understanding questions of the full string theory and M-theory and their dualities, as well as the connections with random matrix theory/matrix models. See [17] for details. Topological string theory is

defined from first principles as a perturbative expansion in a small parameter, g_s , called the string coupling constant. This series turns out to be asymptotic due to the factorial growth of the coefficients (Gevrey-1). Although the nonperturbative nature of the theory has been probed through several avenues, a general nonperturbative definition of topological strings is lacking. Nevertheless some proposals have appeared, at least for large classes of theories, that could fill this void, see for example [18] for a recent approach. This problem of finding a nonperturbative completion for a theory is one for which resurgence can provide valuable insight.

This leads us to the second part of our answer. The perturbative topological string coefficients can be computed very efficiently in some cases and that is the starting point we need for the resurgent approach along the LO route. Moreover I will show that the EQ road is also available. That is, there is an equation that generalizes the perturbative recursion — the *holomorphic anomaly equation* — and that computes many ingredients of the transseries.

Perturbative topological string theories are defined on top of topological field theories of maps from Riemann surfaces to Calabi–Yau manifolds (CY). They come in two kinds, A and B, defined on different CYs but related by mirror symmetry. This means that the two free energies, on the A and B side, will agree as formal asymptotic series once we have figured out the relation between the two geometries, also known as the mirror map,

$$F^{(0),A}(g_s, t) \xleftrightarrow[\text{map}]{\text{mirror}} F^{(0),B}(g_s, z), \quad t = t(z) \quad (2.1)$$

The dependence on the geometries appears through moduli, which are variables that capture the Kähler structure (parametrized by t) of the A-model CY, or the complex structure (parametrized by z) on the B-model CY. This means that these asymptotic series come in families labeled by t or z , and we have to regard the coefficients $F_g^{(0)}$ as functions, not just numbers. Moreover, the dependence on the moduli is not holomorphic, so \bar{t} and \bar{z} also appear. Taking $\bar{z} \rightarrow 0$ we obtain a holomorphic limit¹ of the free energies. For the A model this limit has the form

$$\mathcal{F}_g^{(0),A}(g_s, t) = \sum_{g=0}^{\infty} g_s^{2g-2} \sum_{d=1}^{\infty} N_{g,d} e^{-dt}, \quad (2.2)$$

¹ The holomorphic limit is not unique but attached to the notion of frame which will be ignored for the sake of clarity and brevity. We use curly \mathcal{F} to indicate holomorphic, while roman F to denote holomorphic and nonholomorphic dependence.

where $N_{g,d} \in \mathbb{Q}$ are the famous Gromov–Witten invariants. These count, in the appropriate sense, holomorphic maps from complex curves of genus g into the CY with fixed degree or homology class d .

The A-side of things is not kind towards the resurgent approach because the calculations there are hard. The B-model is far more welcoming thanks to the existence of the holomorphic anomaly equations that relate free energies of different orders, [3, 4]. They are roughly of the form

$$\partial_{\bar{z}} F_g^{(0)} \simeq \partial_z^2 F_{g-1}^{(0)} + \sum_{h=1}^{g-1} \partial_z F_h^{(0)} \partial_{\bar{z}} F_{g-h}^{(0)}, \quad (2.3)$$

and they can be solved recursively in g . The expressions for $F_g^{(0)}$ can be expressed quite compactly if we use an auxiliary (set of) variable(s), $S(z, \bar{z})$, rather than \bar{z} . In these variables the perturbative free energies have a dependence that is polynomial in S and rational in z with coefficients in \mathbb{Q} .

About solving the holomorphic anomaly equations I only want to mention that integration produces a constant, or rather a function of z but not of \bar{z} . This is called the *holomorphic ambiguity*. Finding what it is requires nontrivial knowledge about $\mathcal{F}_g^{(0)}$ at particular values of z called the large-radius point and the conifold point. For certain CY geometries, or toric type, this knowledge is believed to be enough to fix the ambiguity for all orders [1, 15]. A particularly simple geometry in this class is called local \mathbb{P}^2 (along with its mirror) for which over a hundred perturbative free energies were computed in [8] and were used for the resurgent analysis.

Recall that our goal is to exploit these perturbative coefficients to uncover the underlying transseries. That means finding instanton actions, A_α (one or several, and their modulus dependence) and higher instanton coefficients $F_g^{(n)}(z, S)$, for $n \neq 0$. Taking the LO route alone would be hopeless because it is mainly a numerical enterprise and we have to keep track of two variables, z and S . Fortunately the path along EQ will be opened once we extend the validity of the holomorphic anomaly equations past perturbation theory.

3 Resurgent approach to topological strings

At this point of the discussion we are sitting on the upper left corner of the diagram in figure 1.1. We need to make progress in making EQ available while already cranking the numerical machine of LO. We also have to start making predictions of what we should find. What particular functions of z and S should the instanton actions be? How many of them are there? What about higher instanton coefficients? The first two questions

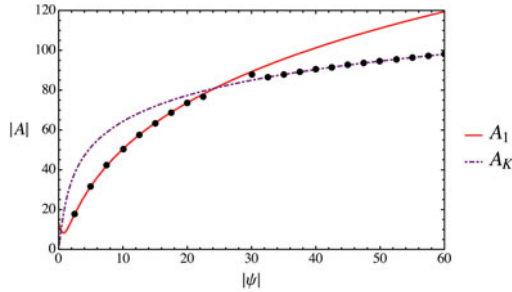


Figure 3.1. Dominant instanton actions obtained from large order growth of perturbative free energies for different values of the complex modulus $\psi = z^{-1/3}$. A_1 dominates for small ψ (around conifold point at $\psi = 1$), and A_K dominates for large ψ (around large-radius point at $\psi = \infty$). Since the actions are holomorphic these results can be obtained for any value of the propagator. In the transition region, around $|\psi| \simeq 25$, the two actions have similar weights in the large-order growth of $F_g^{(0)}$ and the numerics get worse.

can be guessed from previous experience in other theories, particularly from matrix models. There it was understood that instanton actions, A_α , are periods of the underlying geometry (the so called spectral curve), that is, integrals along cycles of the relevant differential form in the theory. Moreover, the periods are holomorphic and can be computed right after we know what CY we are working with [10]. We only need to find what particular linear combination of periods is realized as an instanton action, since only a small number of cycles are independent. The LO approach can tell us this numerically.

For local \mathbb{P}^2 there are three independent periods that are computed from the so-called Picard–Fuchs equations. A possible basis for the periods is

$$(t(z), t_c(z), 1) \quad (3.1)$$

where t is the Kähler modulus and t_c is the called the flat coordinate around the conifold point. They can be written in terms of hypergeometric functions with respect to z . From a LO analysis of the free energies we find two instanton actions as shown in Figure 3.1.

$$A_K = 4\pi^2 i t(z), \quad A_1 = \frac{2\pi i}{\sqrt{3}} t_c(z). \quad (3.2)$$

Due to their geometric origin as periods they are labeled Kähler and conifold. But we should not be too confident that our job finding actions is over because some, with a larger absolute value, could be lurking behind the dominant ones. To understand this remark notice that when we have several instanton actions and their corresponding sectors the large-order

growth of $F_g^{(0)}$ will include all of them. However, the order in which they appear will depend on the relative size of the actions because A_α enters the resurgence relation as A_α^{-g} , so the smallest it is in absolute value the more it contributes as $g \rightarrow \infty$. Some actions might always be larger than the dominant ones so they will only be seen as exponentially suppressed contributions in g .

Let us now deal with the one-instanton sectors associated to the actions we have found. Now we have no external insight as to what they should be so it is time to explore EQ. The logic to use here is the same as that in the Riccati example: take your perturbative recursion and make it into a single equation for $F^{(0)}(g_s, z, S^{zz})$; then drop the perturbative superscript, plug in your transseries ansatz and solve for the coefficients.

What worked like a charm for Riccati is going to fall short for topological strings and the holomorphic anomaly equations. First of all we are going to inherit the holomorphic ambiguity problem at every instanton level n and order g . For Riccati the only ambiguity lied in the first coefficient $\varphi_0^{(1)}$ but it was conventionally set to 1, transferring the ambiguity to the transseries parameter σ . The difference between both examples has to do with the nature of the equations. While Riccati is a differential equation in x , the resurgent variable, the extended holomorphic anomaly equations are only algebraic in g_s (and differential in z and S). This also means that the number of transseries parameters is not determined by the equations.

We find that the EQ route is not as powerful as we would have wanted and leaves several parts of the transseries undetermined:

- Number of transseries parameters: several transseries *ansätze* can solve the equations, with or without logarithmic transmonomials.
- Holomorphic ambiguities: recursive integration produces ambiguities that need to be fixed.
- Instanton actions: equations only impose that they are holomorphic, what at least is in agreement with their interpretation as periods.

To arrive at the box ‘Transseries F ’ in the resurgent diagram we need to complement EQ with the LO path and some amount of guess work on numerical results. Also, as we start making progress with this strategy we can activate the feedback triangle

$$F_g^{(n)} \longrightarrow \text{Resurgence Relations} \longrightarrow \text{Transseries } F \longrightarrow F_g^{(n)}. \quad (3.3)$$

This loop will act both as a source of information and as a consistency check because transseries coefficients appear multiple times in resurgence relations, as we mentioned in the introduction.

There is a big caveat here, though, one that we have not talked about yet. We do not know what the resurgence relations look like exactly for topological string theory. It is not an option here to derive a bridge equation that links alien and ordinary derivatives, as is done many examples such as Riccati, due to the nature of the holomorphic anomaly equations in relation to g_s . So we work on the assumption that the relations will be similar to those derived from a bridge equation because the bridge equation does appear in closely related theories like Painlevé equations and matrix models. See [19] for a review on the relation between topological strings and matrix models, and [2, 14] for a resurgent treatment of Painlevé I equation and the quartic matrix model.

3.1 Main results

Here are the main results we find for the CY geometry of local \mathbb{P}^2 . They start to paint the picture of what the transseries for the free energy looks like. Any attempt to obtain a nonperturbative value of the free energy from resurgence will have to use the results described below. In particular it will be crucial to know which actions and their corresponding transseries sector can contribute to a Borel-Écalle resummation of the transseries.

Holomorphic ambiguities. We can solve the extended holomorphic anomaly equations up to the holomorphic ambiguity and understand the dependence of the solutions on z and S , although the resulting expressions are not very illuminating.

To fix the ambiguities we look at what happens in the holomorphic limit near the large-radius and conifold points. More precisely we take the holomorphic limit of a resurgent relation linking perturbative and nonperturbative free energies.

$$\mathcal{F}_g^{(0)} \sim \frac{\Gamma(2g-1)}{A^{2g-1}} \frac{S_1}{2\pi i} \mathcal{F}_0^{(1)} \Rightarrow \frac{S_1}{2\pi i} \mathcal{F}_0^{(1)} = \lim_{g \rightarrow \infty} \frac{A^{2g-1}}{\Gamma(2g-1)} \mathcal{F}_g^{(0)}. \quad (3.4)$$

Since we know how holomorphic perturbative free energies behave at these special points we can extract results for the nonperturbative free energies using large-order limits. This can sometimes be done analytically and others numerically, but it is enough to fix ambiguities. We will comment on the fact that the Stokes constant cannot be disentangled from the ambiguity later.

Further instanton actions. We find two other instanton actions, A_2 and A_3 , besides A_K and A_1 . See Figure 3.2. They are also related to the

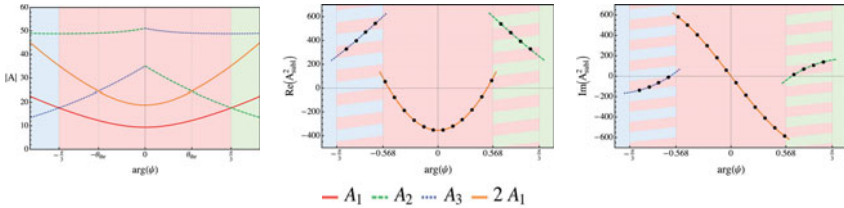


Figure 3.2. Instanton actions A_2 , A_3 , associated to conifold points, lie almost always behind A_1 and can only be seen as subleading contributions to $F_g^{(0)}$ when g is large. In these figures we fix $|\psi| = 2$ and vary $\arg(\psi)$. We also check that a 2-instanton sector contributes as well with action $2A_1$.

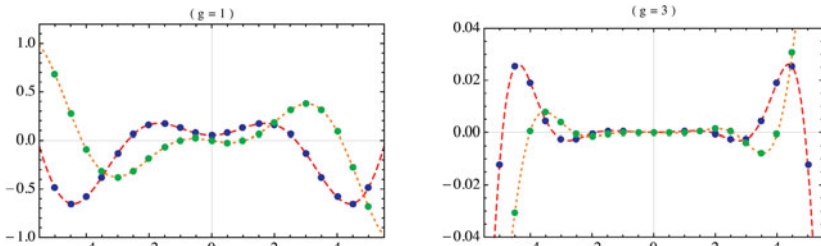


Figure 3.3. Representation of the real (red, dashed) and imaginary (orange, pointed) parts of $F_g^{(1)}(\psi, S^{zz})$ (wrt action A_1 and $g = 1, 3$) for $\psi = 2$ and free S . The blue and green plots show the numerical checks from large-order lying on top of the analytic expressions computed from the extended holomorphic anomaly equations. The dependence in the propagator is exponential (hence the oscillations) times polynomial (hence the changes in amplitude).

conifold point which, using the right coordinate $\psi = z^{-1/3}$, becomes three conifold points, one for each instanton action.

Since there can only be three independent cycles for this geometry there is a relation between all actions. It is $A_1 + A_2 + A_3 + A_K = 0$. This suggests that the transseries is resonant, provided that all actions here mentioned give rise to transseries sectors of their own.

Numerical checks. Inasmuch as we can carry out LO we find that all free energies $F_g^{(n)}$ we come across can be computed, up to ambiguity, from EQ. See an example of the numerical checks in Figure 3.3. This gives credit to the extended holomorphic anomaly equations we obtained out of the perturbative regime alone.

3.2 Open issues

Along the resurgent path we encountered several problems, some technical and some genuinely interesting from the resurgent viewpoint. I think they are both worth describing.

Numerical constraints. The numerical approach has an expiration date from the start. A finite amount of data can only give a finite number results of approximate precision. Taking large-order limits imposes a toll on precision that can only be kept at bay if we identify in closed form the numerical approximations we obtain for $A_\alpha, F_h^{(n)}, h = 0, 1, 2, \dots$

On the other hand we also want to compute nonperturbative energies from the extended holomorphic anomaly equations and analyze their own resurgent properties (c.f., triangle in the resurgent diagram), but this turns out to be computationally more demanding than perturbation theory was. Eventually one is forced to perform a numerical integration of the equations around particular values of z .

Unfamiliar resurgence relation. Let us think about Riccati again for a moment, and in particular about the asymptotics of the perturbative and one-instanton sectors. They have the form, suppressing Stokes constants,

$$\varphi_g^{(0)} \sim \sum_{h=0}^{\infty} \frac{\Gamma(g+1-h)}{A^{g+1-h}} \varphi_h^{(1)} + \sum_{h=0}^{\infty} \frac{\Gamma(g-h)}{(2A)^{g-h}} \varphi_h^{(2)} + \dots \quad (3.5)$$

$$\varphi_g^{(1)} \sim \sum_{h=0}^{\infty} \frac{\Gamma(g+1-h)}{A^{g+1-h}} \varphi_h^{(2)} + \dots \quad (3.6)$$

Note how $\varphi_0^{(2)}$ appears on both equations. This is a consequence of the bridge equation and quite a natural one because no other ingredients are available to play with. For topological strings and local \mathbb{P}^2 in particular, we find²

$$F_g^{(0)} \sim \sum_{h=0}^{\infty} \frac{\Gamma(2g-1-h)}{A_1^{2g-1-h}} F_h^{(1e_1)} + \sum_{h=0}^{\infty} \frac{\Gamma(2g-1-h)}{(2A_1)^{2g-1-h}} \tilde{F}_h^{(2e_1)} + \dots \quad (3.7)$$

$$F_g^{(1e_1)} \sim \sum_{h=0}^{\infty} \left\{ \frac{\Gamma(g+1-h)}{(A_1)^{g+1-h}} \widehat{F}_h^{(2e_1)} + \frac{\Gamma(g+1-h)}{(-A_1)^{g+1-h}} \widehat{F}_h^{(e_{1,1})} \right\} + \dots \quad (3.8)$$

The two 2-instanton coefficients in the analogous slots are in fact distinct. Their being different comes from the way their ambiguities are fixed, either imposing that the holomorphic limit is zero (for \tilde{F}) or that it is a particular and natural quantity that generalizes the 1-instanton case (for \widehat{F}). Both equations can be checked numerically. The question is

² Notation: $(1e_1) = (1, 0, 0, \dots)$, $(2e_1) = (2, 0, 0, \dots)$, $(e_{1,1}) = (1, 1, 0, \dots)$, where the first entry corresponds to A_1 and the second to $-A_1$.

then, why are there two types of 2-instanton free energy and how can we interpret them? Do both of them appear in the transseries?

With respect to this last question we can suspect that the bottom part of the resurgent diagram could be useful to provide some insight. If we manage to resum the transseries we may find that one or both of these sectors are needed to reproduce the full physical observable.

Disappearance of A_K in the Borel plane. Instanton actions depend on the complex structure z and so their strength (measured in absolute value) varies as we move in the z -plane (or the ψ -plane). This means that in one place A_K can be dominant over (less strong than) A_1 or the other way around. The dominant one controls the large-order growth of $F_g^{(0)}$ as $g \rightarrow \infty$. Since we have analytic expressions for the actions we can predict which one will be dominant in which areas. For small ψ or large z , it should be A_K the dominant action but we find numerically that $F_g^{(0)}$ is controlled by A_1 . How can this be? We look at the Borel plane of $F^{(0)}$, that is, we plot the singularities of the Borel transform of $F^{(0)}$ with respect to g_s (numerically using Padé approximants). Singularities are related to instanton actions. There we can see how, as we vary ψ , the singularities move. The closer to the origin the more dominant they are. We find that the singularity for A_K disappears when we dial ψ towards 0 even before it has the chance to become dominant. See Figure 3.4.³ That is why we do not find it in the numerical analysis. However, we do not yet understand the mechanism controlling the disappearance, though it may be related to higher order Stokes phenomenon [16].

Stokes constants. A natural problem in resurgence is the computation of Stokes constants. For the Riccati equation one can guess the value for S_1 from the numerics or formally prove what this value is. In the approach to topological strings we have to rely on numerics alone. However, we have already used the information contained in the large-order numerics to fix the holomorphic ambiguity and there is none left to find S_1 and other Stokes constants. Equivalently, we can only have expressions for the product of the ambiguity and the Stokes constants but not for the two separately. What we can show using LO and EQ is that S_1 does not carry dependence on z or S .

³ The perturbative free energy is an asymptotic series in g_s^2 , while higher instanton sectors depend on g_s . This implies that the instanton actions come in pairs of opposite signs.

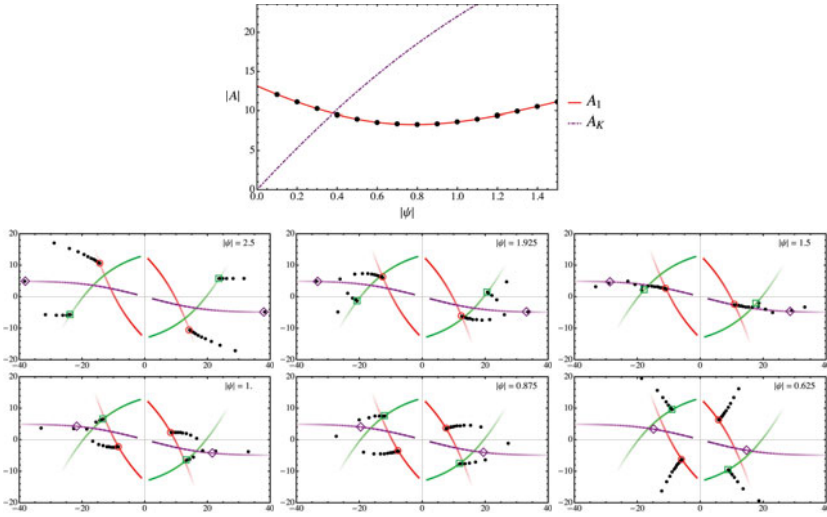


Figure 3.4. Above: the analytic expressions for A_1 and A_K , in absolute value, showing the would be transition in dominance if A_K did not disappear as a Borel singularity. Below: a sequence of frames showing the disappearance of the singularity as ψ decreases. We show A_K as a purple diamond, A_1 as a red circle, and A_3 as a green square, as well as their opposite values.

4 Conclusions

In the pages above I have described the basics of what resurgence can tell us about topological string theory in the nonperturbative regime. Many details have been simplified or skipped altogether. They can be found in [7,8]. The main goal has been to discuss the ideas summarized in the resurgent approach diagram in Figure 1.1, as they are applied to topological strings.

If we had to assign just one label for this work it would probably be ‘experimental mathematics’, because although our target theory is topological strings and the mathematical framework is resurgence, the techniques we use can be aimed at other targets and the results obtained are suggestive rather than rigorous. Formal theorems and proofs should follow to set on firm grounds the evidence here exposed and shed light on the issues yet to be understood. And while in other parts of Physics not everything can be made rigorous the case of topological strings is singular because it sits comfortably on the boundary of Physics and Mathematics.

In this way it should be shown if the free energy is resurgent and of which kind. The resurgent relations between different coefficients should be completely understood and the Stokes constants identified. We should also aspire to understand the physical interpretation or realization of the

nonperturbative data in the transseries. Avenues to explore, some of them under development, include the eventual resummation of the transseries, the relation with other nonperturbative approach to topological strings, and the possible consequences of resurgence in enumerative geometry.

The applications of resurgence in Physics have increased considerably in the past decade, but this trend will only finally take off when physicists see clear and accessible examples of the usefulness of resurgence. The exchange of ideas that took place at the conference ‘Resurgence, Physics and Numbers’ is a big step towards this goal.

References

- [1] M. ALIM, J. D. LANGE and P. MAYR, *Global properties of topological string amplitudes and orbifold invariants*, JHEP **1003** (2010), 113.
- [2] I. ANICETO, R. SCHIAPPA and M. VONK, *The resurgence of instantons in string theory*, Commun. Num. Theor. Phys. **6** (2012), 339–496.
- [3] M. BERSHADSKY, S. CECOTTI, H. OOGURI and C. VAFA, “Holomorphic anomalies in topological field theories,” Nucl.Phys. **B405** (1993), 279–304.
- [4] M. BERSHADSKY, S. CECOTTI, H. OOGURI and C. VAFA, *Kodaira –Spencer theory of gravity and exact results for quantum string amplitudes*, Commun. Math. Phys. **165** (1994), 311–428.
- [5] E. CALICETI, M. MEYER-HERMANN, P. RIBECA, A. SURZHYKOV and U. JENTSCHURA, *From useful algorithms for slowly convergent series to physical predictions based on divergent perturbative expansions*, Physics Reports **446** (2007), 1 – 96.
- [6] O. COSTIN, “Asymptotics and Borel Summability”, Monographs and Surveys in Pure and Applied Mathematics 141. CRC Press, 2012.
- [7] R. COUSO-SANTAMARÍA, J. D. EDELSTEIN, R. SCHIAPPA and M. VONK, *Resurgent transseries and the holomorphic anomaly*, Annales Henri Poincaré (2015), 1–69, in press. arXiv:1308.1695
- [8] R. COUSO-SANTAMARÍA, J. D. EDELSTEIN, R. SCHIAPPA and M. VONK, *Resurgent transseries and the holomorphic anomaly: nonperturbative closed strings in local $\mathbb{C}P^2$* , Commun. Math. Phys. **338** (2015), 285–346.
- [9] R. COUSO-SANTAMARÍA, M. MARIÑO and R. SCHIAPPA, *Resurgence matches quantization*, J. Physics A: Math. Theor. **50** (2017), 14, 145402.

- [10] N. DRUKKER, M. MARIÑO and P. PUTROV, *Nonperturbative aspects of ABJM theory*, JHEP **1111** (2011), 141.
- [11] G. V. DUNNE, “Resurgence and Non-Perturbative Physics.”. Lectures at CERN Winter School on Supergravity, Strings, and Gauge Theory, 2014.
- [12] J. ÉCALLE, *Les fonctions récurrentes*, Publ. Math. d’Orsay, **81-05** (1981), **81-06** (1981), **85-05** (1985).
- [13] G. A. EDGAR, *Transseries for beginners*, Real Anal. Exchange **35** (2009), 253–310.
- [14] S. GAROUFALIDIS, A. ITS, A. KAPAEV and M. MARIÑO, *Asymptotics of the instantons of Painlevé I*, Int. Math. Res. Not. **2012** (2012), 561–606.
- [15] B. HAGHIGHAT, A. KLEMM and M. RAUCH, *Integrability of the holomorphic anomaly equations*, JHEP **0810** (2008), 097.
- [16] C. J. HOWLS, P. J. LANGMAN and A. B. OLDE DAALHUIS, *On the higher-order Stokes phenomenon*, In: “Proceedings of the Royal Society of London A: Mathematical, Physical and Engineering Sciences”, The Royal Society, Vol. 460, 2004, 2285–2303.
- [17] K. HORI, S. KATZ, A. KLEMM, R. PANDHARIPANDE, R. THOMAS, C. VAFA, R. VAKIL and E. ZASLOW, “Mirror Symmetry” Clay Mathematics Monographs, Vol. 1, 2003.
- [18] M. MARIÑO, *Spectral theory and mirror symmetry*, arXiv:1506.07757v4.
- [19] M. MARINO, *Les Houches lectures on matrix models and topological strings*, arXiv:hep-th/0410165.
- [20] C. MITSCHI and D. SAUZIN, “Divergent series, summability and resurgence. I. Monodromy and resurgence”, with a foreword by Jean-Pierre Ramis and a preface by Éric Delabaere, Michèle Loday-Richaud, Claude Mitschi and David Sauzin, Lecture Notes in Mathematics, Vol. 2153, Springer, [Cham], 2016, xxi + 298 pp.
- [21] M. VONK, *Resurgence and topological strings*, In: “String Math.”, 2014 Edmonton, Alberta, Canada, June 9-13, 2014, 221.

WKB and resurgence in the Mathieu equation

Gerald V. Dunne and Mithat Ünsal

Abstract. In this paper, based on lectures by the authors at the May 2015 workshop *Resurgence, Physics and Numbers*, at the Centro di Ricerca Matematica Ennio De Giorgio of the Scuola Normale Superiore in Pisa, we explain the origin of resurgent trans-series in the Mathieu equation spectral problem, using uniform WKB and all-orders (exact) WKB. Exact quantization conditions naturally arise, and their expansion in the weak coupling regime produces resurgent trans-series expressions which exhibit precise relations between different instanton sectors. Indeed, the perturbative expansion encodes all orders of the multi-instanton expansion, an explicit realization of the general concept of “resurgence”. We also discuss the transition from weak to strong coupling, an explicit realization of “instanton condensation”.

1 Introduction

1.1 Some Motivation from Physics and Mathematics

Asymptotic analysis is a cornerstone of physics, providing accurate expansions when certain dimensionless combinations of physical parameters are large or small. Such expansions are often divergent, and these divergent expansions contain a wealth of information, in addition to giving numerically accurate estimates in the appropriate limiting regimes. The modern mathematical theory of resurgent asymptotics, based on Borel-Ecalle summation, is based on trans-series expansions, in which formal (divergent) series expansions in a small parameter are extended to trans-series expansions that also include summations over exponentially suppressed non-perturbative terms, as well as possible summations over powers of logarithms [1–5]. While this mathematical theory arose from quite abstract origins, it now appears that it is surprisingly well suited to many problems in physics. For example, in the language of quantum field theory, *multi-instanton calculus* is a trans-series expansion, involving a sum over an infinite set of non-perturbative multi-instanton sectors, each of which is multiplied by a fluctuation series, and some of which are multiplied by series of logarithms, due to quasi-zero modes. In another

context, it is well known in physics that summation of classes of Feynman diagrams often leads to series in powers of logarithms. From the physics perspective, the primary new idea from the formal theory of resurgence is the notion that there should generically be precise relationships between the fluctuations about different non-perturbative sectors, including the vacuum sector (“perturbation theory”). Viewed from the path integral, this is quite unexpected. In these lectures we explain in simple terms how this type of structure arises, using the classic example of instantons in the quantum spectral problem for the periodic cosine potential, known in mathematics as the Mathieu equation [6–11]. Using various forms of WKB, extended to all orders, we show how the trans-series structure arises. In the process, we find that not only is there a natural underlying trans-series, but there are concrete quantitative relations between different instanton sectors. Indeed, in an extreme manifestation of resurgence, we show that all orders of the trans-series are encoded in a subtle way in the divergent perturbative expansion itself. Here we explain what we mean by this somewhat dramatic claim. We use the language of the underlying differential equation, but these conclusions are even more interesting when translated into the path integral formalism. We propose that these ideas could in fact be used as a means to provide a sensible mathematical definition of the path integral, even in Minkowski space, and moreover a definition that provides also a means of making quantitative computations. One of the primary motivations is that in many physics applications it would be desirable to have better control over the analytic continuation of path integrals, for example for studying real-time processes, quantum transport, or finite density systems. One of the main mathematical advantages of a trans-series, compared to just an ordinary divergent series, is that the trans-series is designed to encode the proper analytic continuation properties of the function it is describing. This sounds appealing, but it is a notoriously difficult problem in path integrals, so we are motivated to understand as much of this trans-series structure as possible, in a well-defined concrete example. That is the purpose of these lectures.

The study of resurgent trans-series in quantum spectral problems began with the pioneering work of Bogomolny and Fateev, and Zinn-Justin, Brézin, Parisi, Voros et al [12–17] (for an excellent review see [18]), as well as in the mathematical literature from the work of Pham, Ramis, Dillinger, Delabaere, Berry, Howls, Aoki, Takei et al [19–24]. It also became clear from the work of Kruskal and Costin and co-workers, that resurgent asymptotic analysis is a powerful tool in studying the asymptotics of nonlinear differential equations [3, 24, 25]. More recently, in physics, Mariño, Schiappa and Weiss showed that the resurgent approach yields interesting new insights in the study of matrix models and string

theory [26,27]. Since then there has been a flourishing activity involving applications in matrix models, string theory, quantum gauge theory and sigma models, as well as new results in quantum mechanics [28–39]. In these lectures, our goal is quite modest: study a well-known and widely relevant system, the Mathieu equation, and understand it in great detail. Surprisingly, through the eyes of resurgence we are able to see new results in this very old problem.

Two further pieces of motivation are the following general questions:

- What can weak coupling analysis tell us about strong coupling ?
- Can weak coupling and strong coupling be related, even if the degrees of freedom re-organize themselves in a very non-trivial way, for example across a transition ?

We will be able to phrase these questions more precisely in the context of the Mathieu system, and see that resurgent asymptotic analysis provides precise answers.

1.2 Resurgent trans-series in quantum spectral problems

In this paper we concentrate on trans-series expressions for energy eigenvalues in certain quantum mechanical spectral problems, more specifically the Schrödinger equation for the periodic cosine (Mathieu) potential.

$$-\frac{\hbar^2}{2} \frac{d^2}{dx^2} \psi(x) + \cos(x) \psi(x) = u \psi(x). \quad (1.1)$$

This is an example of a more general class of quantum mechanical (QM) spectral problems with potentials having degenerate harmonic minima. In these cases it is known that standard Rayleigh-Schrödinger perturbation theory leads to a perturbative series that is not only divergent, but also Borel non-summable, in the sense that the expansion coefficients grow factorially fast in magnitude and do not alternate in sign [13, 14, 40–43]. Thus, naive Borel summation leads to a non-perturbative imaginary part for the energy, which moreover is ambiguous. This is doubly problematic: not only is it ambiguous, but these systems are stable, and therefore the energy should be real. (Contrast with the case of a cubic oscillator [44], or an inverted-double-well quartic oscillator [45], where the system is unstable and the imaginary part has a natural physical interpretation.) The resurgent trans-series expression for the energy resolves these apparent inconsistencies, because the perturbative series is only one part of the full trans-series, and the ambiguous imaginary non-perturbative term arising from Borel summation of perturbation theory is exactly cancelled by a corresponding term in a higher non-perturbative sector. Resurgence implies that these cancellations occur to all orders, leading to a full

trans-series that is not only real, but also unambiguous. This means that perturbation theory on its own is incomplete, while the full trans-series is complete. For a clear and exhaustive analysis of how these cancellations occur for general real trans-series we refer the reader to [46].

In the context of the Mathieu equation, consider performing perturbation theory within one of the potential wells, perturbing about the N^{th} energy level of the unperturbed harmonic well, leading to a perturbative expression of the form

$$u_{\text{pert}}(\hbar, N) = \sum_{n=0}^{\infty} \hbar^n u_n(N). \quad (1.2)$$

Notice that the system can be scaled in such a way that the sole parameter in the equation is \hbar , and the “semiclassical limit” of small \hbar refers to the situation where the potential wells are deep. (See Section 2.1 below.) The perturbative coefficients $u_n(N)$ are simple polynomials in the level number N , and can be computed by straightforward iterative procedures. For potentials with degenerate harmonic minima, the perturbative expansion (1.2) is not Borel summable, which means that on its own it is incomplete and indeed inconsistent. This is true not just for the ground state ($N = 0$), but also for higher states, so long as $N \ll 1/\hbar$, as discussed in more detail in Section 5 below. This situation can be remedied by recognizing that the full expansion of the energy at small coupling is in fact of the “trans-series” form:

$$u_{\text{trans}}(\hbar, N) = \sum_{k=0}^{\infty} \sum_{n=0}^{\infty} \sum_{l=1}^{k-1} c_{k,n,l}(N) \hbar^n \left(\frac{1}{\hbar^{N+1/2}} \exp \left[-\frac{S}{\hbar} \right] \right)^k \left(\ln \left[-\frac{1}{\hbar} \right] \right)^l. \quad (1.3)$$

Perturbation theory corresponds to the “zero-instanton sector”, $k = 0$, with coefficients $c_{0,n,0}(N) \equiv u_n(N)$. The higher ($k \geq 1$) instanton terms of the trans-series involve a sum over non-perturbative factors $\exp[-k S/\hbar]$, multiplied by prefactors that are themselves series in \hbar and in $\ln(1/\hbar)$. Note that the sum over logarithms in (1.3) begins in the $k = 2$ sector: physically, these logarithms arise from the interaction between instantons and anti-instantons, which requires $k \geq 2$.

The basic building blocks of the trans-series, \hbar , $\exp[-S/\hbar]$ and $\ln(1/\hbar)$, are called “trans-monomials”, and are familiar from physical examples. The parameter S in (1.3) is a numerical constant, the single-instanton action. With our choice of scaling of the Mathieu equation, $S = 8$ [see equation (2.7) below]. Remarkably, the expansion coefficients $c_{k,n,l}(N)$ of the trans-series are intertwined amongst themselves, in such a way that the ‘necessary’ cancellations occur in order to render the full

trans-series real and unambiguous. In practice, this works as follows: a Borel analysis of the perturbative series requires an analytic continuation in \hbar , producing non-perturbative imaginary parts, but these are precisely cancelled by the imaginary parts associated with the $\ln(-1/\hbar)$ factors in the non-perturbative portion of the trans-series. Similarly, the fluctuations about the single instanton sector, given by the coefficients $c_{1,n,0}$, are also divergent, and Borel summation of these fluctuations produces new imaginary parts, but these are cancelled by terms in the $k = 3$ sector. And so on. Ambiguities only arise if you look at just one isolated portion of the trans-series expansion, for example just the perturbative part, or just some particular multi-instanton sector. When viewed as a whole, the analytic continuation of the trans-series expression is real, unique and exact.

An important first step in our argument is a seemingly small and innocent shift of emphasis from much of the previous work studying the divergence of perturbation theory in quantum spectral problems, which has often concentrated on low-lying energy levels or bands, such as the ground state or lowest band. In order to see the full structure of the trans-series it proves useful to consider the spectral energy eigenvalue not just as a function of the small coupling (which we can take here as \hbar : see the scaling defined in Section 2.1 below), but also of the level or band number, N , an integer that labels the perturbative energy level or band. The fact that there exists such a label is physically clear for problems with degenerate harmonic minima, corresponding just to the unperturbed harmonic oscillator level number. Mathematically, it is clear from oscillation theorems for Sturm-Liouville type problems in one dimension. Thus we view the energy eigenvalue u in (1.1) as a function of two variables:

$$u = u(\hbar, N). \quad (1.4)$$

This immediately defines three interesting, and quite distinct, spectral regions:

1. $N\hbar \ll 1$: weak coupling, far below the barrier;
2. $N\hbar \sim O(1)$: intermediate coupling, near the barrier top;
3. $N\hbar \gg 1$: strong coupling, far above the barrier.

Note that even the physical language used to describe the different spectral regions is very different. In the weak coupling region the states are described as superpositions of localized atomic states in the so-called “tight-binding approximation”, while at strong-coupling the states are more naturally treated as using the “nearly-free electron” picture of weakly perturbed free states [47]. Near the barrier top, neither of these approximations is satisfactory, and there is a complicated re-arrangement

of degrees of freedom, a concrete realization of the phenomenon of “instanton condensation” [48–52]. Correspondingly, the expansions of the energy in these three regions are quite different, and yet they are all related. One of the main motivations of this work is to understand in more precise detail how this transition from weak- to strong-coupling occurs. In particular, we are motivated by the close analogy to so-called “large N ” techniques in quantum gauge theories and matrix models [53].

So far, the discussion sounds somewhat trivial. But the new result that we wish to describe is that by considering the dependence of $u(\hbar, N)$ on *both* \hbar and N we find that there is a direct quantitative relation between perturbation theory and the all-orders multi-instanton trans-series expression. For example, one explicit consequence of this relation is a dramatically improved description of the one-instanton sector.

New Result for Mathieu Spectrum [54, 55]: The leading exponential (“one-instanton”) splitting of the N^{th} band in the weak-coupling regime where $N\hbar \ll 1$ can be written, including the series of fluctuations,

$$u(\hbar, N) = u_{\text{pert}}(\hbar, N) \pm \frac{\hbar}{\sqrt{2\pi}} \frac{1}{N!} \left(\frac{32}{\hbar}\right)^{N+\frac{1}{2}} \exp\left[-\frac{S}{\hbar}\right] \mathcal{P}_{\text{inst}}(\hbar, N) + \dots \quad (1.5)$$

where the fluctuation factor $\mathcal{P}_{\text{inst}}(\hbar, N)$ is expressed entirely in terms of the perturbative expansion $u_{\text{pert}}(\hbar, N)$:

$$\begin{aligned} & \mathcal{P}_{\text{inst}}(\hbar, N) \\ &= \frac{\partial u_{\text{pert}}(\hbar, N)}{\partial N} \exp\left[S \int_0^{\hbar} \frac{d\hbar}{\hbar^3} \left(\frac{\partial u_{\text{pert}}(\hbar, N)}{\partial N} - \hbar + \frac{(N + \frac{1}{2}) \hbar^2}{S}\right)\right], \\ & S \equiv S_{\text{instanton}} = 8. \end{aligned} \quad (1.6)$$

This result (1.5, 1.6) agrees with the fluctuation series derived from the asymptotics of Mathieu functions [60], and also with a recent 3-loop computation for $N = 0$ [61], as discussed below in Section 4.3. The interesting new thing in (1.5, 1.6) is that the fluctuation series $\mathcal{P}_{\text{inst}}(\hbar, N)$ is expressed solely in terms of the perturbative fluctuation series $u_{\text{pert}}(\hbar, N)$. Thus, there is a direct relation between the fluctuations about the zero-instanton sector (*i.e.*, perturbation theory, $u_{\text{pert}}(\hbar, N)$), and the fluctuations about the one-instanton sector, $\mathcal{P}_{\text{inst}}(\hbar, N)$. This is an explicit example of resurgence, quite different from the early term/late term relations that have been studied previously. This ‘constructive’ form of resurgence appears to have first been noticed in formulas for the ionization rate for hydrogenic atoms [56], a result that motivated a systematic study by Álvarez and Casares in the context of one dimensional oscillators [57, 58], in which such explicit perturbative/non-perturbative relations were found in the cubic and quartic oscillator systems.

The first factor in (1.6), $\partial u_{\text{pert}}/\partial N$, is a density-of-states factor that is well known at leading order in \hbar [69, 70], but the remaining exponential factor in (1.6) is new [54, 55]. Similar relations can be derived expressing the fluctuations in any higher-instanton sector exactly in terms of the fluctuations about the zero-instanton sector (*i.e.*, perturbation theory). Furthermore, there are similar results for other potentials [40, 43, 45, 57, 58]. This is remarkable: it says that perturbation theory, $u(\hbar, N)$, encodes everything! One simply has to know how to decode this information.

In Section 2 we review basic known facts about the Mathieu spectrum. In Sections 3 - 5 we illustrate and derive the results (1.5, 1.6) in the context of the Schrödinger equation for these quantum mechanical systems, but the result is even more interesting when interpreted in the language of the path integral approach to the same spectral problem, as discussed in Section 6. This is in fact our main motivation, as we wish to develop a deeper insight into the general structure of semiclassical expansions, having in mind potential applications to quantum field theory.

2 Basic facts about the Mathieu spectrum

Here we summarize the basic classic results concerning the spectrum of the Mathieu equation (see, *e.g.* [6–11, 60]).

2.1 Notation and Scaling

The Mathieu equation describes the nonlinear oscillator problem, and has a wide array of applications [9, 11]. We write the Mathieu equation in the Schrödinger equation form (1.1), but by simple changes of variables, this becomes the standard textbook form of the Mathieu equation [11]:

$$\frac{d^2\psi}{dz^2} + (A - 2Q \cos(2z)) \psi = 0 \longleftrightarrow -\frac{\hbar^2}{2} \frac{d^2\psi}{dx^2} + \cos(x)\psi = u\psi. \quad (2.1)$$

(We use capital letters A and Q , rather than the conventional lower-case ones, to avoid confusion with symbols a and q , which have special meaning in the related gauge theory discussion.) So we can translate back and forth between notations with the identifications:

$$Q = \frac{4}{\hbar^2}, \quad A = \frac{8u}{\hbar^2}. \quad (2.2)$$

We also wish to compare with the important work of Zinn-Justin and Jentschura [42], who used yet another scaling:

$$\begin{aligned} & \left(-\frac{1}{2} \frac{d^2}{dx^2} + \frac{1}{8g} \sin^2(2\sqrt{g}x) \right) \psi = E_{ZJJ} \psi \\ & \longleftrightarrow \left(-\frac{(16g)^2}{2} \frac{d^2}{dx^2} + \cos(x) \right) \psi = (16gE_{ZJJ} - 1)\psi. \end{aligned} \quad (2.3)$$

Thus \hbar plays the role of a coupling constant g :

$$\hbar = 16g \quad , \quad u = -1 + 16g E_{ZJJ} = -1 + \hbar E_{ZJJ}. \quad (2.4)$$

The Mathieu system has a QM spectrum consisting of an infinite series of bands and gaps (also known as regions of stability and instability), as shown in Figure 2.1. Low in the spectrum the bands are very narrow, and high in the spectrum the gaps are very narrow. The transition between these two behaviors occurs near the top of the potential barrier, at $u = 1$, where the bands and gaps are of approximately equal width. These features are explained quantitatively below, in Section 5. We are particularly interested in the transition between the two extreme regions, which occurs near $u = 1$, the maximum of the potential $\cos x$.

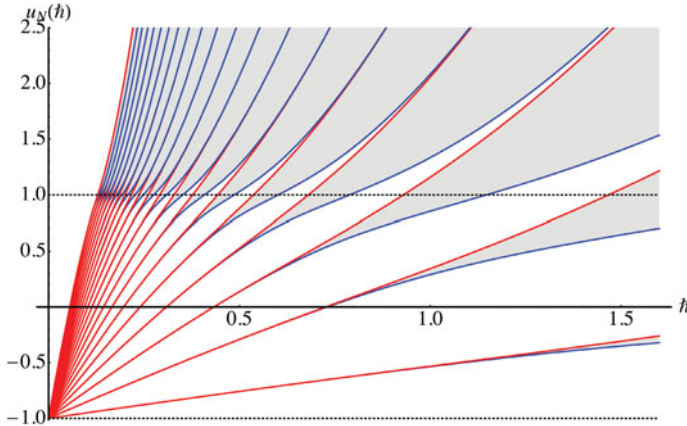


Figure 2.1. The energy spectrum of the Mathieu equation, as a function of the parameter \hbar . The *regions of stability* (the bands) are shaded, with lower edges shown as solid (blue) lines, and top edges shown as solid (red) lines. The bands are separated by *regions of instability* (gaps), which are unshaded. The first 20 bands are shown. At small \hbar , the bands are exponentially narrow, and the band *location* follows the linear behavior in (2.6). High in the spectrum, the gaps are exponentially narrow, and the gap *location* follows the quadratic behavior in (2.10). The maximum and minimum of the potential, at $u = \pm 1$, are shown as dotted lines. Note the smooth transition, near $u \sim 1$, between narrow bands at small \hbar , and narrow gaps at large \hbar . In this region, the bands and gaps are of equal width, and are not exponentially narrow, as discussed Section 5.3.

2.2 Weak coupling: $N\hbar \ll 1$

At small \hbar , with $N\hbar \ll 1$, we effectively have far-separated harmonic wells, with high barriers between them. Then perturbation theory in a given well, starting with the N^{th} harmonic oscillator level, leads to the

following perturbative expression [7–9, 11, 60]:

$$\begin{aligned}
 u_{\text{pert}}(\hbar, N) \sim & -1 + \hbar \left[N + \frac{1}{2} \right] - \frac{\hbar^2}{16} \left[\left(N + \frac{1}{2} \right)^2 + \frac{1}{4} \right] \\
 & - \frac{\hbar^3}{16^2} \left[\left(N + \frac{1}{2} \right)^3 + \frac{3}{4} \left(N + \frac{1}{2} \right) \right] \\
 & - \frac{\hbar^4}{16^3} \left[\frac{5}{2} \left(N + \frac{1}{2} \right)^4 + \frac{17}{4} \left(N + \frac{1}{2} \right)^2 + \frac{9}{32} \right] \\
 & - \frac{\hbar^5}{16^4} \left[\frac{33}{4} \left(N + \frac{1}{2} \right)^5 + \frac{205}{8} \left(N + \frac{1}{2} \right)^3 + \frac{405}{64} \left(N + \frac{1}{2} \right) \right] - \dots
 \end{aligned} \tag{2.5}$$

This expansion is indeed of the form of the perturbative expansion (1.2), where at n^{th} order of perturbation theory, the expansion coefficient $u_n(N)$ is a polynomial of degree n in the level number N . There is an implicit assumption here that $N\hbar \ll 1$.

For fixed N , the $u_n(N)$ are non-alternating in sign and diverge factorially fast [41, 54, 55, 60]:

$$u_n(N) \sim -\frac{2^{2N}}{\pi (N!)^2} \frac{\Gamma(n + 2N + 1)}{16^{n+2N+1}}, \quad n \rightarrow \infty. \tag{2.6}$$

This means that the perturbative expansion is Borel non-summable, and so the perturbative expression (2.6) must be extended to a trans-series. The rate of divergence (2.6) of perturbation theory has a characteristic form, with the factor 16 being equal to twice the instanton action, where the instanton action for the Mathieu potential is:

$$S \equiv S_{\text{instanton}} = \sqrt{2} \int_{-\pi}^{\pi} dx \sqrt{\cos(x) + 1} = 8. \tag{2.7}$$

In this spectral regime, well below the barrier top, the spectrum consists of narrow bands, whose central location is given by (2.6), and whose widths are given by the classic result [7, 9, 11, 60]

$$\begin{aligned}
 \Delta u_{\text{band}}(\hbar, N) \sim & \frac{2\hbar}{\sqrt{2\pi}} \frac{1}{N!} \left(\frac{32}{\hbar} \right)^{N+1/2} \exp \left[-\frac{8}{\hbar} \right] \left\{ 1 - \frac{\hbar}{32} \left[3 \left(N + \frac{1}{2} \right)^2 \right. \right. \\
 & \left. \left. + 4 \left(N + \frac{1}{2} \right) + \frac{3}{4} \right] + O(\hbar^2) \right\}. \tag{2.8}
 \end{aligned}$$

Physically, we interpret this as a non-perturbative single instanton term [62, 63], including the fluctuations about the single-instanton. This *single-instanton* effect is real and unambiguous. The factor 8 in the exponent is the instanton action for the Mathieu potential in (2.7).

2.3 Strong Coupling: $N\hbar \gg 1$

In the strong coupling regime, $N\hbar \gg 1$, far above the barrier top, the spectral behavior is completely different, as can be seen immediately from Figure 2.1. We can probe this region by taking \hbar large, keeping N small and fixed, in which case the gap edges are (see [11], converted to our notation):

$$\begin{aligned}
 u_0 &= \frac{\hbar^2}{8} \left(0 - \frac{1}{\hbar^2} + \frac{7}{4\hbar^6} - \frac{58}{9\hbar^{10}} + \frac{68687}{2304\hbar^{14}} + \dots \right) \\
 u_1^{(-)} &= \frac{\hbar^2}{8} \left(1 - \frac{4}{\hbar^2} - \frac{2}{\hbar^4} + \frac{1}{\hbar^6} - \frac{1}{6\hbar^8} - \frac{11}{36\hbar^{10}} + \frac{49}{144\hbar^{12}} \right. \\
 &\quad \left. - \frac{55}{576\hbar^{14}} - \frac{83}{540\hbar^{16}} + \dots \right) \\
 u_1^{(+)} &= \frac{\hbar^2}{8} \left(1 + \frac{4}{\hbar^2} - \frac{2}{\hbar^4} - \frac{1}{\hbar^6} - \frac{1}{6\hbar^8} + \frac{11}{36\hbar^{10}} + \frac{49}{144\hbar^{12}} \right. \\
 &\quad \left. + \frac{55}{576\hbar^{14}} - \frac{83}{540\hbar^{16}} + \dots \right) \\
 u_2^{(-)} &= \frac{\hbar^2}{8} \left(4 - \frac{4}{3\hbar^4} + \frac{5}{54\hbar^8} - \frac{289}{19440\hbar^{12}} + \frac{21391}{6998400\hbar^{16}} + \dots \right) \\
 u_2^{(+)} &= \frac{\hbar^2}{8} \left(4 + \frac{20}{3\hbar^4} - \frac{763}{54\hbar^8} + \frac{1002401}{19440\hbar^{12}} - \frac{1669068401}{6998400\hbar^{16}} + \dots \right) \\
 u_3^{(-)} &= \frac{\hbar^2}{8} \left(9 + \frac{1}{\hbar^4} - \frac{1}{\hbar^6} + \frac{13}{80\hbar^8} + \frac{5}{16\hbar^{10}} - \frac{1961}{5760\hbar^{12}} \right. \\
 &\quad \left. + \frac{609}{6400\hbar^{14}} + \dots \right) \\
 u_3^{(+)} &= \frac{\hbar^2}{8} \left(9 + \frac{1}{\hbar^4} + \frac{1}{\hbar^6} + \frac{13}{80\hbar^8} - \frac{5}{16\hbar^{10}} - \frac{1961}{5760\hbar^{12}} \right. \\
 &\quad \left. - \frac{609}{6400\hbar^{14}} + \dots \right) \\
 u_4^{(-)} &= \frac{\hbar^2}{8} \left(16 + \frac{8}{15\hbar^4} - \frac{317}{3375\hbar^8} + \frac{80392}{5315625\hbar^{12}} + \dots \right) \\
 u_4^{(+)} &= \frac{\hbar^2}{8} \left(16 + \frac{8}{15\hbar^4} + \frac{433}{3375\hbar^8} - \frac{45608}{5315625\hbar^{12}} + \dots \right). \quad (2.9)
 \end{aligned}$$

This is the regime where the kinetic energy dominates the potential energy, so the energy eigenvalues are obtained by perturbing around the (degenerate) free-particle-on-a-circle states, with the potential $\frac{2}{\hbar^2} \cos(x)$

treated as a perturbation. The expansions (2.9) are *convergent*, with a radius of convergence that increases quadratically with the level index N . They are conventionally expressed as continued-fraction representations of the eigenvalues, generated by a Fourier decomposition of the gap-edge eigenfunctions, and these continued-fraction expressions are themselves convergent [6, 8, 9, 11]. Nevertheless, despite these convergence properties, there are also non-perturbative effects, associated with the narrow splittings of the spectral gaps in this spectral region, as seen in Figure 2.1.

Rather than taking $\hbar \gg 1$ with N fixed, the high spectral region could also be probed by taking $\hbar \rightarrow 0$ and $N \rightarrow \infty$, but with $N\hbar \gg 1$ fixed. This is motivated by analogous “large- N ” expansions in quantum gauge theories and matrix models [53]. We will see that this is a surprisingly close analogy to the Mathieu spectrum. In this limit, for large level number $N \gg 1/\hbar$, the continued-fraction expressions for the energy eigenvalues give approximate expressions for the energy of the N^{th} gap as [11]:

$$u(\hbar, N) \sim \frac{\hbar^2}{8} \left(N^2 + \frac{1}{2(N^2-1)} \left(\frac{2}{\hbar} \right)^4 + \frac{5N^2+7}{32(N^2-1)^3(N^2-4)} \left(\frac{2}{\hbar} \right)^8 + \frac{9N^4+58N^2+29}{64(N^2-1)^5(N^2-4)(N^2-9)} \left(\frac{2}{\hbar} \right)^{12} + \dots \right). \quad (2.10)$$

This is an expansion in powers of $(2/\hbar)^4$. We observe that the n^{th} coefficient has poles at certain integer values of $N \leq n$, so the expression (2.10) should really be interpreted as an expansion about $N = \infty$. We discuss this further in Section 5.4. We also note that similar expansions, with coefficients with analogous poles, occur in gauge theory large- N expansions [64–66].

The strong-coupling expansion (2.10) does not fully describe the spectrum. It does not distinguish between the gap edges, $u_N^{(\pm)}$. Furthermore, the \hbar dependence of the expansion (2.10) is different from that in (2.9). For a given N , there is a non-perturbative splitting of the gap, occurring at order $1/\hbar^{2N}$. Thus, as the level index N increases, the gap splitting occurs at higher orders in perturbation theory, becoming exponentially small [11]:

$$\begin{aligned} \Delta u_{\text{gap}}(\hbar, N) &\sim \frac{\hbar^2}{4} \frac{1}{(2^{N-1}(N-1)!)^2} \left(\frac{2}{\hbar} \right)^{2N} \left[1 + \mathcal{O} \left(\left(\frac{2}{\hbar} \right)^4 \right) \right] \\ &\sim \frac{N\hbar^2}{2\pi} \left(\frac{e}{N\hbar} \right)^{2N}, \quad N \gg 1. \end{aligned} \quad (2.11)$$

Note that this has the same form as the non-perturbative effects in the large- N expansion of the Gross-Witten-Wadia unitary matrix model, in the strong coupling phase [48, 49, 65].

These strong-coupling results are very different from the weak-coupling expressions described in Section 2.2. The expansions are convergent rather than divergent, and the expansions do not appear to have a trans-series structure. Nevertheless, we show below in Section 5.4 that in fact a more natural way to interpret the expressions (2.9) is as trans-series [67].

2.4 Theorems Concerning Band and Gap Widths

Here we summarize the known rigorous estimates of the widths of bands and gaps (stability or instability regions) for the Mathieu problem. These generalize to the more general case of a periodic potential with a unique minimum in each period.

Band-Width Theorem [Harrell [77], Weinstein-Keller [69], Connor et al [70]]: For a periodic potential with a unique minimum in each period, the width of the N^{th} band has the leading behavior

$$\begin{aligned} \Delta u_{\text{band}} &\sim \frac{2}{\pi} \frac{\partial u}{\partial N} \exp \left[-\frac{1}{\hbar} S \right] (1 + O(\hbar)) \\ S &= \int_{\text{turning points}} \sqrt{V(x) - V_{\min}} dx \end{aligned} \quad (2.12)$$

where the exponent involves the action under the barrier. For the Mathieu equation, this produces the leading part of expression (2.8), as we discuss in Section 5. Our new result (1.5, 1.6) refines this estimate considerably, giving all the $O(\hbar)$ corrections, and moreover expresses these corrections entirely in terms of the perturbative series.

Gap-Width Theorem [Dykhne [68], Weinstein-Keller [69], Connor et al [70], Avron and Simon [78]]: For a periodic potential with a unique minimum in each period, the width of the N^{th} gap for $u \gg V_{\max}$ has the leading behavior:

$$\begin{aligned} \Delta u_{\text{gap}} &\sim \frac{2}{\pi} \frac{\partial u}{\partial N} \exp \left[-\frac{1}{\hbar} \text{Im} \tilde{S} \right] (1 + O(\hbar)) \\ \tilde{S} &= \int_{\text{complex turning points}} \sqrt{V(x) - V_{\min}} dx \end{aligned} \quad (2.13)$$

where the exponent now involves the action on a cycle connecting complex turning points. For the Mathieu equation, this produces the leading part of expression (2.11), as we discuss in Section 5.

Note the remarkable fact that these leading expressions (2.12, 2.13) for the band width and gap width have a common form, just with different turning points. This will be explained in Section 5. This gap-width result can also be extended, along the lines of (1.5, 1.6) for the bands [67].

3 Uniform WKB for the Mathieu equation

In this Section we outline our first approach to the spectrum, which demonstrates how a trans-series expression such as (1.3) arises for the energy levels, in the weak coupling regime where $\hbar N \ll 1$. Here we outline the overall strategy and summarize a few technical details. For further details, see [54, 55]. The resurgent structure of the Mathieu equation system has also been studied in [59].

3.1 Strategy of uniform WKB

Uniform WKB is a well-known approach [73–75], based on the simple idea of mapping the Schrödinger problem to a known “comparison problem”. Since the wells are harmonic, the relevant comparison problem is the harmonic oscillator system, whose eigenfunctions are parabolic cylinder functions. In the context of resurgence theory, the explicit use of uniform WKB was introduced by Álvarez et al in the study of quantum anharmonic oscillators [57, 58, 76]. The novelty of [40, 43, 57, 58, 76] is that the uniform WKB expansion is extended well beyond the leading terms studied in [73–75], which reveals a surprising new layer of rich mathematical structure.

The comparison mapping is achieved by making a parabolic uniform WKB ansatz for the wave-function:

$$\psi(x) = \frac{1}{\sqrt{\varphi'(x)}} D_\nu \left(\frac{1}{\sqrt{\hbar}} \varphi(x) \right). \quad (3.1)$$

Here D_ν is the parabolic cylinder function [6, 80], and ν is an ansatz parameter whose physical meaning will become clear below. It is closely related to the band label N . This uniform WKB ansatz converts the linear Schrödinger equation for $\psi(x)$ into a nonlinear equation for the argument function $\varphi(x)$, which can then be solved perturbatively. Straightforward local analysis near the (harmonic) potential minimum leads to a perturbative expansion of the energy:

$$u = u_{\text{pert}}(\hbar, \nu) = \sum_{n=0}^{\infty} \hbar^n u_n(\nu). \quad (3.2)$$

The coefficient $u_n(\nu)$ is a polynomial, of degree n , in the ansatz parameter ν . In the $\hbar \rightarrow 0$ limit, the ansatz parameter ν tends to an integer N , labelling the unperturbed harmonic oscillator energy level. In fact, when $\nu = N$, the expansion (3.2) coincides precisely with the result $u_{\text{pert}}(\hbar, N)$ of Rayleigh-Schrödinger perturbation theory in (1.2). As mentioned in the Introduction, this perturbative series expression is incomplete, and indeed ill-defined, because the series is not Borel summable. This is not particularly surprising because so far the analysis has been purely *local*, making no reference to the existence of neighboring degenerate minima of the potential. To determine the energy spectrum properly we must impose a *global* boundary condition that relates one minimum to another.

This global condition implies that ν is only *exponentially close* to the integer N , with a small correction that is a function of both N and \hbar [54,55]:

$$\nu_{\text{global}}(\hbar, N) = N + \delta\nu(\hbar, N) \quad (3.3)$$

The correction term $\delta\nu(\hbar, N)$ has a trans-series form:

$$\delta\nu(\hbar, N) = \sum_{k=1}^{\infty} \sum_{n=0}^{\infty} \sum_{l=1}^{k-1} d_{k,n,l}(N) \left(\frac{1}{\hbar^{N+1/2}} \exp\left[-\frac{S}{\hbar}\right] \right)^k \left(\ln\left[-\frac{1}{\hbar}\right] \right)^l \hbar^n. \quad (3.4)$$

As explained below, this trans-series structure follows directly from the properties of the parabolic cylinder functions, and it is therefore generic for potentials with degenerate harmonic minima.

The global boundary condition determines the ansatz parameter ν as a function of \hbar and N , as in (3.3, 3.4), and then the trans-series form of the energy eigenvalue follows immediately by inserting this into the formal perturbative series expansion:

$$u_{\text{trans}}(N, \hbar) = u_{\text{pert}}(\hbar, N + \delta\nu(N, \hbar)) = \sum_{n=0}^{\infty} \hbar^n u_n(N + \delta\nu(N, \hbar)). \quad (3.5)$$

Recall that the coefficients $u_n(\nu)$ are polynomials. We are using the fact that a formal expansion of a trans-series is itself a trans-series.

This uniform WKB approach explains in very elementary terms why the energy generically has a trans-series form for potentials with degenerate harmonic classical minima: all properties of the $\hbar \rightarrow 0$ limit are simply mapped to the resurgent asymptotic properties of the parabolic cylinder functions. All analytic continuations needed to analyze questions of resurgence and cancellation of ambiguities are ultimately expressed in terms of the well-known analytic continuation properties of the parabolic cylinder functions.

3.2 Perturbative expansion of the uniform WKB ansatz

The parabolic cylinder function $D_\nu(z)$ satisfies the differential equation

$$\frac{d^2}{dz^2} D_\nu(z) + \left(\nu + \frac{1}{2} - \frac{z^2}{4} \right) D_\nu(z) = 0. \quad (3.6)$$

Therefore the uniform WKB ansatz (3.1) converts the linear Schrödinger equation (1.1) to a non-linear equation for the argument function $\varphi(x)$:

$$V(x) - u - \frac{1}{8} \varphi^2 (\varphi')^2 + \frac{\hbar}{2} \left(\nu + \frac{1}{2} \right) (\varphi')^2 + \frac{\hbar^2}{4} \sqrt{\varphi'} \left(\frac{\varphi''}{(\varphi')^{3/2}} \right)' = 0. \quad (3.7)$$

Notice that the ansatz parameter ν appears in this nonlinear equation, whereas it does not appear in the original Schrödinger equation. This nonlinear equation can be solved using simultaneous perturbative expansions for $\varphi(x)$ and u :

$$u = u_0 + \hbar u_1 + \hbar^2 u_2 + \dots \quad (3.8)$$

$$\varphi(x) = \varphi_0(x) + \hbar \varphi_1(x) + \hbar^2 \varphi_2(x) + \dots \quad (3.9)$$

Note that the expansion coefficients u_n and $\varphi_n(x)$ also depend on the ansatz parameter ν , simply because they come from solving the equation (3.7), in which the parameter ν now appears.

3.2.1 Leading order of the perturbative expansion The leading order of (3.7) determines $\varphi_0(x)$ and u_0 :

$$\varphi_0^2 (\varphi_0')^2 = 8(V(x) - u_0). \quad (3.10)$$

It is notationally simpler in this case to shift the coordinate x by π so that the minimum of the potential is at $x = 0$. Thus we take $V(x) = -\cos x$. Clearly the spectrum is unchanged by this shift. Requiring regular behavior at $x = 0$ we determine

$$u_0 = -1 \quad (3.11)$$

$$\varphi_0(x) = 4\sqrt{2} \sin\left(\frac{x}{4}\right). \quad (3.12)$$

Physically, we understand $u_0 = -1$ simply as the reference energy of the bottom of the potential well.

3.2.2 First order of the perturbative expansion At $O(\hbar)$, again imposing regularity at $x = 0$, we find straightforwardly

$$u_1 = \nu + \frac{1}{2} \quad (3.13)$$

$$\varphi_1(x) = \frac{(\nu + \frac{1}{2}) \ln \cos \frac{x}{4}}{2\sqrt{2} \sin \frac{x}{4}}. \quad (3.14)$$

Once again, the result $u_1 = \nu + \frac{1}{2}$ is clear: it just gives the harmonic energies $\hbar(\nu + \frac{1}{2})$, above the reference energy at the bottom of the well: to this order $u(\nu, \hbar) = -1 + \hbar(\nu + \frac{1}{2}) + \dots$

3.2.3 Higher orders of the perturbative expansion This perturbative expansion can be extended to any desired order. One finds that the energy $u(\nu, \hbar)$ has an expansion of the form

$$u_{\text{pert}}(\hbar, \nu) = -1 + \hbar \left(\nu + \frac{1}{2} \right) - \sum_{n=2}^{\infty} \hbar^n P_n \left(\nu + \frac{1}{2} \right) \quad (3.15)$$

where P_n is a polynomial of degree n , with definite parity. Explicitly, the first few terms are:

$$\begin{aligned} u_{\text{pert}}(\hbar, \nu) \sim & -1 + \hbar \left[\nu + \frac{1}{2} \right] - \frac{\hbar^2}{16} \left[\left(\nu + \frac{1}{2} \right)^2 + \frac{1}{4} \right] \\ & - \frac{\hbar^3}{16^2} \left[\left(\nu + \frac{1}{2} \right)^3 + \frac{3}{4} \left(\nu + \frac{1}{2} \right) \right] \\ & - \frac{\hbar^4}{16^3} \left[\frac{5}{2} \left(\nu + \frac{1}{2} \right)^4 + \frac{17}{4} \left(\nu + \frac{1}{2} \right)^2 + \frac{9}{32} \right] \\ & - \frac{\hbar^5}{16^4} \left[\frac{33}{4} \left(\nu + \frac{1}{2} \right)^5 + \frac{205}{8} \left(\nu + \frac{1}{2} \right)^3 + \frac{405}{64} \left(\nu + \frac{1}{2} \right) \right] - \dots \quad (3.16) \end{aligned}$$

Replacing ν by an integer quantum number N , this expansion (3.16) agrees with the result (2.6) of Rayleigh-Schrödinger perturbation theory about the N^{th} harmonic oscillator level. But, as before, this is a formal, divergent asymptotic expansion, which moreover is not Borel summable, so this is not the whole story. We are missing the information about the fact that the spectrum consists of *bands*, not of discrete levels. This omission is because we have not yet applied the correct physical boundary conditions.

3.3 Global boundary condition: connecting different minima

To fully determine the spectrum, we need to extend the previous *local* analysis, in the neighborhood of a minimum of the potential, with *global* information about how neighboring minima are related.

It is well known (see Figure 2.1) that each perturbative level labeled by the integer index N splits into a continuous band of states (in classical language these are the “stability regions” of the Mathieu equation). In the QM Schrödinger context this phenomenon arises from the Bloch condition:

$$\psi(x + 2\pi) = e^{i\theta} \psi(x) \quad (3.17)$$

where θ is a real angular parameter that labels states within a given band of the spectrum. Conventional Floquet analysis [6, 9–11, 79] expresses this Bloch boundary condition in terms of the discriminant. Define two independent solutions $\psi_1(x)$ and $\psi_2(x)$, normalized as follows at some arbitrary chosen point (which we take here to be at $x = -\pi$, the center of a barrier between two potential minima: recall that here we are taking the potential $V(x) = -\cos x$):

$$\begin{pmatrix} \psi_1(-\pi) & \psi_1'(-\pi) \\ \psi_2(-\pi) & \psi_2'(-\pi) \end{pmatrix} = \begin{pmatrix} 1 & 0 \\ 0 & 1 \end{pmatrix}. \quad (3.18)$$

Then, using the symmetry of the Mathieu potential, we can re-write the Bloch condition in the compact form [11]:

$$\cos \theta = \psi_1(\pi). \quad (3.19)$$

This is the *exact quantization condition*, which determines the band spectrum. To make this exact quantization condition practically useful, we need a way to evaluate the right-hand-side of (3.19). This can be done numerically, or using asymptotics, as we do in this paper. The band-edge states correspond to $\theta = 0$ or $\theta = \pi$, and are periodic or anti-periodic functions, respectively. For other values of θ the wavefunctions are quasi-periodic (see (3.17)), corresponding to states within a given band. All this is very well known.

Now let us apply this global boundary condition (3.19) to the uniform WKB ansatz (3.1). First, define even and odd functions

$$f_{\pm}(x) = \frac{1}{\sqrt{\varphi'(x)}} \left(D_{\nu} \left(\frac{\varphi(x)}{\sqrt{\hbar}} \right) \pm D_{\nu} \left(-\frac{\varphi(x)}{\sqrt{\hbar}} \right) \right) \quad (3.20)$$

where we have used the fact that $\varphi(x)$ is odd, and $\varphi'(x)$ is even, on the interval $x \in [-\pi, \pi]$. Then the normalized basis functions in (3.18) are

$$\psi_1(x) = \frac{1}{\mathcal{W}} (f'_-(-\pi) f_+(x) - f'_+(-\pi) f_-(x)) \quad (3.21)$$

$$\psi_2(x) = \frac{1}{\mathcal{W}} (-f_-(-\pi) f_+(x) + f_+(-\pi) f_-(x)) \quad (3.22)$$

where \mathcal{W} is the (constant) Wronskian:

$$\mathcal{W} \equiv f_+(x) f'_-(x) - f'_+(x) f_-(x) = -\sqrt{\frac{8\pi}{\hbar}} \frac{1}{\Gamma(-\nu)}. \quad (3.23)$$

Then the exact (Bloch) quantization condition (3.19) can be written (in two equivalent forms):

$$\cos \theta = 1 + \frac{2}{\mathcal{W}} f'_+(\pi) f_-(\pi) \quad (3.24)$$

$$= -1 + \frac{2}{\mathcal{W}} f'_-(\pi) f_+(\pi). \quad (3.25)$$

Thus, the global boundary condition is imposed at the midpoint between two neighboring perturbative vacua: $x_{\text{midpoint}} = \pi$. Moreover, the global condition is expressed in terms of parabolic cylinder functions evaluated at x_{midpoint} . This Bloch condition results in the perturbative energy level splitting into a continuous band, with states within the band labeled by the angular parameter θ . The bottom of the lowest band has $\theta = 0$ and its wave function is an even function, while the top of the lowest band has $\theta = \pi$ and its wave function is an odd function. For such band-edge states the Bloch conditions (3.24, 3.25) take a simpler form:

$$(\text{even state}) : f_-(\pi) = 0 \quad (3.26)$$

$$(\text{odd state}) : f_+(\pi) = 0. \quad (3.27)$$

Using the uniform WKB ansatz (3.20) we find that these band edges are determined by the exact condition:

$$D_\nu \left(\frac{\varphi(\pi)}{\sqrt{\hbar}} \right) = \pm D_\nu \left(-\frac{\varphi(\pi)}{\sqrt{\hbar}} \right). \quad (3.28)$$

Now we come to the main point. The argument $\varphi(\pi)$, just like the perturbative expansion of the energy in (3.16), is a Borel non-summable series in \hbar , with leading term being non-zero: $\varphi_0(\pi) = 4$. Thus, as $\hbar \rightarrow 0$ we are interested in the asymptotics of the parabolic cylinder functions

at large magnitude of their argument. But in order to make sense of the Borel non-summable series we must analytically continue in \hbar off the Stokes line, the positive real axis, $\hbar > 0$. Then the argument of the parabolic cylinder functions in (3.28) becomes complex, and we need to use the asymptotics of these functions off the real axis [6, 11]:

$$D_\nu(z) \sim z^\nu e^{-z^2/4} (1 + \dots) + e^{\pm i\pi\nu} \frac{\sqrt{2\pi}}{\Gamma(-\nu)} z^{-1-\nu} e^{z^2/4} (1 + \dots),$$

$$\frac{\pi}{2} < \pm \arg(z) < \pi. \quad (3.29)$$

The sign here depends on which way we continue off the real axis. The ellipsis denote known fluctuation terms [6, 11, 54]. Thus, we see that the exact quantization condition for the band edges (3.28) requires a balance between the two exponential terms in (3.29). Had we been on the real axis, we would eliminate the growing exponential in (3.29) by setting ν equal to a non-negative integer, but this is just perturbation theory. Balancing the two exponentials expresses the exact quantization condition in the following form:

$$\frac{(e^{\pm i\pi} \hbar)^\nu}{\Gamma(-\nu)} = \pm (\varphi(\pi))^{2\nu+1} \frac{e^{-\frac{1}{2} \frac{\varphi^2(\pi)}{\hbar}}}{\sqrt{2\pi \hbar}} (1 + \dots). \quad (3.30)$$

Expanding about an integer, writing $\nu = N + \delta\nu$, and the fact that $\frac{\varphi^2(\pi)}{2\hbar} = \frac{8}{\hbar} - (\nu + \frac{1}{2}) \ln 2 + \dots$, we find the exponentially small shift in (3.3). The higher order terms generate powers of $\ln \hbar$ (for further details, see [54]). Thus we see immediately how the trans-series structure arises: inserting $\nu = N + \delta\nu(\hbar, N)$ into the formal expansion (3.2, 3.16), we generate a trans-series expression for u , of the form (1.3). By construction, all analytic continuations are self-consistent, because we have simply used the analytic continuation properties of the parabolic cylinder functions. All higher fluctuation terms can be deduced straightforwardly from the fluctuations of the parabolic cylinder functions.

This *resurgence* procedure works because the global boundary condition is expressed in terms of parabolic cylinder functions of $1/\hbar$, and for these functions the analytic continuation properties are rigorously known. Thus, trans-series expressions of the form (1.3) also arise for other potentials with harmonic minima. Ambiguities only arise if you first expand the global boundary condition and look at just one isolated portion of the resulting trans-series expansion, for example just the perturbative part, or

just some particular multi-instanton sector. When viewed as a whole, the analytic continuation of the trans-series expression is unique and exact, and leads to real and unambiguous energy eigenvalues.

4 Relating perturbative and non-perturbative sectors

4.1 Results of Zinn-Justin and Jentschura

We now compare with the beautiful results of Zinn-Justin and Jentschura (ZJJ) [42]. (Recall Equations (2.3, 2.4), which translate between their notation for the Mathieu equation and ours.) ZJJ conjectured an exact quantization condition of the form:

$$\left(\frac{32}{\hbar}\right)^{-B_{\text{ZJJ}}} \frac{e^{\frac{1}{2}A_{\text{ZJJ}}}}{\Gamma(\frac{1}{2}-B_{\text{ZJJ}})} + \left(-\frac{32}{\hbar}\right)^{-B_{\text{ZJJ}}} \frac{e^{-\frac{1}{2}A_{\text{ZJJ}}}}{\Gamma(\frac{1}{2}+B_{\text{ZJJ}})} = \frac{2\cos\theta}{\sqrt{2\pi}} \quad (4.1)$$

where θ is the Bloch angle, and $A_{\text{ZJJ}}(\hbar, E)$ and $B_{\text{ZJJ}}(\hbar, E)$ are functions of energy that need to be computed. ZJJ derived the following expansions (we rewrite the following expressions in terms of $\hbar \equiv 16g$ instead of g):

$$\begin{aligned} B_{\text{ZJJ}}(\hbar, E) &= E + \frac{\hbar}{16} \left(\frac{1}{4} + E^2\right) + \left(\frac{\hbar}{16}\right)^2 \left(\frac{5E}{4} + 3E^3\right) \\ &\quad + \left(\frac{\hbar}{16}\right)^3 \left(\frac{17}{32} + \frac{35E^2}{4} + \frac{25E^4}{2}\right) \\ &\quad + \left(\frac{\hbar}{16}\right)^4 \left(\frac{721E}{64} + \frac{525E^3}{8} + \frac{245E^5}{4}\right) + \dots \quad (4.2) \end{aligned}$$

$$\begin{aligned} A_{\text{ZJJ}}(\hbar, E) &= \frac{16}{\hbar} + \frac{\hbar}{16} \left(\frac{3}{4} + 3E^2\right) + \left(\frac{\hbar}{16}\right)^2 \left(\frac{23E}{4} + 11E^3\right) \\ &\quad + \left(\frac{\hbar}{16}\right)^3 \left(\frac{215}{64} + \frac{341E^2}{8} + \frac{199E^4}{4}\right) \\ &\quad + \left(\frac{\hbar}{16}\right)^4 \left(\frac{4487E}{64} + 326E^3 + \frac{1021E^5}{4}\right) + \dots \quad (4.3) \end{aligned}$$

ZJJ showed that expanding the transcendental quantization condition (4.1) leads to a trans-series expression for the energy eigenvalue, and made extensive numerical checks of the associated resurgent cancellations. We also note that the computation of $B_{\text{ZJJ}}(\hbar, E)$ is straightforward, while $A_{\text{ZJJ}}(\hbar, E)$ is considerably more involved [42].

4.2 Inversion and a surprise

Consider inverting the expression for $B_{ZJJ}(E, \hbar)$, to express it as $E_{ZJJ}(\hbar, B)$ [54,55]:

$$\begin{aligned} E_{ZJJ}(\hbar, B) = & B - \frac{\hbar}{16} \left(B^2 + \frac{1}{4} \right) - \left(\frac{\hbar}{16} \right)^2 \left(B^3 + \frac{3B}{4} \right) \\ & - \left(\frac{\hbar}{16} \right)^3 \left(\frac{5B^4}{2} + \frac{17B^2}{4} + \frac{9}{32} \right) \\ & - \left(\frac{\hbar}{16} \right)^4 \left(\frac{33B^5}{4} + \frac{205B^3}{8} + \frac{405B}{64} \right) - \dots \quad (4.4) \end{aligned}$$

We see that this agrees with the perturbative weak coupling expansion (2.6), with the definitions (2.4) and the identification of B with the band label number N :

$$B = N + \frac{1}{2}. \quad (4.5)$$

Thus, computing the function $B_{ZJJ}(\hbar, E)$ is equivalent to computing Rayleigh-Schrödinger perturbation theory. These are the fluctuations about the perturbative vacuum.

Using (4.4), the non-perturbative function $A_{ZJJ}(\hbar, E)$ in (4.3) can be re-expressed as a function of B :

$$\begin{aligned} A_{ZJJ}(\hbar, B) = & \frac{16}{\hbar} + \frac{\hbar}{16} \left(3B^2 + \frac{3}{4} \right) + \left(\frac{\hbar}{16} \right)^2 \left(5B^3 + \frac{17B}{4} \right) \\ & + \left(\frac{\hbar}{16} \right)^3 \left(\frac{55B^4}{4} + \frac{205B^2}{8} + \frac{135}{64} \right) \\ & + \left(\frac{\hbar}{16} \right)^4 \frac{9}{64} (336B^5 + 1120B^3 + 327B) + \dots \quad (4.6) \end{aligned}$$

Notice the striking similarities between terms in the expansions of $A_{ZJJ}(\hbar, B)$ and $E_{ZJJ}(\hbar, B)$. To see this explicitly, we compute:

$$\begin{aligned} \frac{\partial E_{ZJJ}(\hbar, B)}{\partial B} = & 1 - \frac{\hbar}{8} B - \left(\frac{\hbar}{16} \right)^2 \left(3B^2 + \frac{3}{4} \right) \\ & - \left(\frac{\hbar}{16} \right)^3 \left(10B^3 + \frac{17B}{2} \right) \\ & - \left(\frac{\hbar}{16} \right)^4 \left(\frac{165B^4}{4} + \frac{615B^2}{8} + \frac{405}{64} \right) - \dots \quad (4.7) \end{aligned}$$

and compare this with

$$\begin{aligned}
 -\frac{\hbar^2}{16} \frac{\partial A_{ZJJ}(\hbar, B)}{\partial \hbar} &= 1 - \left(\frac{\hbar}{16}\right)^2 \left(3B^2 + \frac{3}{4}\right) \\
 &\quad - \left(\frac{\hbar}{16}\right)^3 \left(10B^3 + \frac{17B}{2}\right) \\
 &\quad - \left(\frac{\hbar}{16}\right)^4 \left(\frac{165B^4}{4} + \frac{615B^2}{8} + \frac{405}{64}\right) - \dots \quad (4.8)
 \end{aligned}$$

We deduce the remarkably simple relation:

$$\frac{\partial E_{ZJJ}}{\partial B} = -\frac{\hbar}{16} \left(2B + \hbar \frac{\partial A_{ZJJ}}{\partial \hbar}\right). \quad (4.9)$$

It is straightforward to check this to higher orders in \hbar .

In other words, the non-perturbative function $A_{ZJJ}(\hbar, B)$, and therefore also $A_{ZJJ}(\hbar, E)$, can be deduced immediately from knowledge of the perturbative energy $E_{ZJJ}(\hbar, B)$. Thus, only one of the two functions $B_{ZJJ}(\hbar, E)$ and $A_{ZJJ}(\hbar, E)$ is actually needed to generate the entire trans-series. Note that this fact is not at all obvious when these functions are written in terms of E as $B_{ZJJ}(\hbar, E)$ and $A_{ZJJ}(\hbar, E)$, as in (4.2, 4.3), but become clear when everything is expressed in terms of B , as in (4.4, 4.6). We will understand the reason for this in Section 5. The implication of this fact is that the exact quantization condition (4.1) involves only one function. See for example Eq. (68) in [54].

4.3 Implications and two independent confirmations

This relation between the A_{ZJJ} and B_{ZJJ} functions has some remarkable implications. Recall that the function $E_{ZJJ}(\hbar, B)$ describes the fluctuations about the perturbative vacuum, while $A_{ZJJ}(\hbar, B)$ describes the fluctuations about the single-instanton [42, 55]. For example, the single-instanton fluctuation factor comes from

$$\begin{aligned}
 \frac{\partial E_{ZJJ}}{\partial B} e^{-\frac{1}{2}A_{ZJJ}} &\sim e^{-8/\hbar} \left(1 - \frac{\hbar}{8}B - \dots\right) \left(1 - \frac{\hbar}{32} \left(3B^2 + \frac{3}{4}\right) - \dots\right) \\
 &= e^{-8/\hbar} \left(1 - \frac{\hbar}{32} \left(3B^2 + 4B + \frac{3}{4}\right) - \dots\right) \quad (4.10)
 \end{aligned}$$

in agreement with the fluctuation factor in (2.8). At first sight, it looks from (4.10) as though one needs *both* $E_{ZJJ}(\hbar, B)$ and $A_{ZJJ}(\hbar, B)$ in order to compute the fluctuations about the single-instanton sector. But because of the simple relation (4.9) between $E_{ZJJ}(\hbar, B)$ and $A_{ZJJ}(\hbar, B)$, it is

enough to know just $E_{ZJJ}(\hbar, B)$, which means just knowing perturbation theory.

Combining these facts, and re-writing in terms of the energy eigenvalue u , we arrive at the result written in the compact form (1.5, 1.6). For example, going to the next higher order in \hbar we find:

$$\begin{aligned} \Delta u_{\text{band}}(\hbar, N) \sim & \frac{2\hbar}{\sqrt{2\pi}} \frac{1}{N!} \left(\frac{32}{\hbar}\right)^{N+1/2} \exp\left[-\frac{8}{\hbar}\right] \\ & \times \left\{ 1 - \frac{\hbar}{32} \left[3\left(N + \frac{1}{2}\right)^2 + 4\left(N + \frac{1}{2}\right) + \frac{3}{4} \right] \right. \\ & + \frac{\hbar^2}{32768} \left(144\left(N + \frac{1}{2}\right)^4 + 64\left(N + \frac{1}{2}\right)^3 \right. \\ & \left. \left. - 312\left(N + \frac{1}{2}\right)^2 - 176\left(N + \frac{1}{2}\right) - 87 \right) + O(\hbar^3) \right\}. \end{aligned} \quad (4.11)$$

We stress that this is a completely constructive relationship. Given some number of orders of the perturbative expansion $u_{\text{pert}}(\hbar, N)$ about the perturbative vacuum, from (1.5, 1.6) we can immediately write down the same number of orders of the fluctuations about the single-instanton sector. In (4.11) we have shown the first few orders of this fluctuation.

Moreover, this relation between perturbative and non-perturbative effects extends throughout the entire trans-series, to all higher multi-instanton sectors [55]. They are all encoded in the perturbative series $u_{\text{pert}}(\hbar, N)$. Therefore, the fluctuations about the single-instanton saddle, and all other non-perturbative saddles, are precisely encoded in the fluctuations about the perturbative vacuum. This surprising result is in fact consistent with the ambitious goal of resurgence, which claims that the expansion about one saddle contains, in principle, information about the expansions around other saddles, provided one knows how different saddles are connected. This connection is provided by the exact quantization condition (3.19), which is itself a statement of the Bloch boundary condition [55].

At the one-instanton level, we have two independent confirmations of this result. Long ago, in a truly remarkable paper, Dingle and Müller computed many orders of the series corrections to the exponential band splitting, directly from the asymptotics of the Mathieu differential equation [60]. We can compare (4.11) with equation (72) of [60], and after adjusting notation (their $q_0 \equiv (2N + 1)$, and their $h \equiv 2/\hbar$) we see complete agreement. This comparison can easily be carried out to higher orders.

From the physics perspective, an even more interesting comparison is to a recent direct brute-force Feynman diagram computation of the fluctuations about the single-instanton sector, to three loop order [61] (the corresponding result has also been confirmed for the double-well system [61]). Specifically, for the single-instanton expansion of the lowest ($N = 0$) band, the diagrammatic computation found the fluctuation factor (translated to our normalizations: their $g \equiv \hbar/8$):

$$\exp\left[-\frac{8}{\hbar}\right]\left[1-\frac{7}{8}\left(\frac{\hbar}{8}\right)-0.460937498\left(\frac{\hbar}{8}\right)^2-\dots\right]. \quad (4.12)$$

This diagrammatic computation involved more than 20 three-loop Feynman diagrams, each involving propagators in the presence of an instanton, and only some of these diagrams could be evaluated exactly. Hence the third coefficient is only known numerically. This field-theoretic result should be compared with the fluctuation factor in (4.11) with $N = 0$:

$$\exp\left[-\frac{8}{\hbar}\right]\left[1-\frac{7}{8}\left(\frac{\hbar}{8}\right)-\frac{59}{128}\left(\frac{\hbar}{8}\right)^2-\dots\right]. \quad (4.13)$$

We see agreement up to 7 decimal places. Considering the complexity of the Feynman diagrammatic approach [61], compared with the simplicity of the result (1.6), we see that resurgence is telling us something quite novel and non-trivial about perturbation theory. Furthermore, we note that in the diagrammatic computation, certain diagrams evaluated to numbers involving zeta values, but these all presumably cancel in the end because the final coefficient is rational. This is surprisingly reminiscent of such cancellations found in QFT at higher loops, a fact that has fascinating number theoretic and combinatorial implications [81].

It is also interesting to compare the result (1.5, 1.6) with the theorems of Harrell, Weinstein-Keller and Connor et al [69,70,77] listed in Section 2.4. These results give one part of the prefactor to leading order, namely the density of states factor $\partial u/\partial N$, but do not say anything about higher orders in \hbar . Presumably there is a strong theorem here awaiting a more rigorous proof.

5 All-orders WKB analysis of the Mathieu equation: actions and dual actions

There is another, complementary, WKB approach to this problem, often called “exact WKB”, or “all-orders WKB” [24]. While the uniform WKB approach has the advantage that it explains straightforwardly where the

trans-series structure comes from in the weak-coupling spectral region, the all-orders WKB has an advantage that it can easily describe both high and low energy, and even energies near the top of the barrier. There is also an interesting connection to low energy behavior of certain supersymmetric quantum field theories [38,83–89].

We begin with Dunham’s all-orders WKB action [80,90]:

$$a(\hbar, u) = \frac{\sqrt{2}}{2\pi} \left(\oint_C \sqrt{u - V} dx - \frac{\hbar^2}{2^6} \oint_C \frac{(V')^2}{(u - V)^{5/2}} dx - \frac{\hbar^4}{2^{13}} \oint_C \left(\frac{49(V')^4}{(u - V)^{11/2}} - \frac{16V'V'''}{(u - V)^{7/2}} \right) dx - \dots \right) \quad (5.1)$$

where the contour integral encircles the turning points. The leading term is just the familiar WKB action. We write this expansion as a formal series in powers of \hbar^2 , with coefficients that are functions of the energy u :

$$a(\hbar, u) = \sum_{n=0}^{\infty} \hbar^{2n} a_n(u). \quad (5.2)$$

Remarkably, the higher-order WKB actions can be obtained by acting on these leading WKB actions with differential operators with respect to the energy u [38,84,85]. This follows from the fact that for $V = \cos(x)$, the numerators in (5.1), which are given by the derivatives of V , can be re-expressed as polynomials of V . Therefore by differentiating $\sqrt{u - V}$ with respect to u , and taking appropriate combinations, one can generate the integrands in (5.1) up to total derivatives which vanish after integrating around the turning points. For example, at the next two orders:

$$a_1(u) = \frac{1}{48} \left(2u \frac{d^2}{du^2} + \frac{d}{du} \right) a_0(u) \quad (5.3)$$

$$a_2(u) = \frac{1}{2^9 45} \left(28u^2 \frac{d^4}{du^4} + 120u \frac{d^3}{du^3} + 75 \frac{d^2}{du^2} \right) a_0(u). \quad (5.4)$$

In fact, $a_0(u)$ satisfies a 2nd-order Picard-Fuchs equation (5.11), so these can be further simplified, but we do not need this fact here.

The all-orders WKB expression for the *location* of a narrow band or gap can be expressed as [80,90]:

$$a(\hbar, u) = \begin{cases} N \hbar & \text{(gap)} \\ (N + \frac{1}{2}) \hbar & \text{(band)}. \end{cases} \quad (5.5)$$

This “all-orders Bohr-Sommerfeld” formula relates a complicated expression in the energy, u , and coupling, \hbar , to an integer that labels the

band or gap. This can be inverted to express the energy as a function of N and \hbar . For example, when $u \approx -1$, we can expand and invert, which leads to the perturbative expansion (2.6), as we illustrate in the next sub-section. Alternatively, we can expand at $u \gg 1$ and then invert, which leads to the strong-coupling expansion (2.10), as we illustrate in the following sub-section. Expanding near the barrier top, $u \approx 1$, yields information about the spectrum in this regime.

All this is perturbative information, obtained from the formal all-orders WKB expansion (5.1) in powers of \hbar . But, as is clear from the Mathieu spectrum shown in Figure 1, we are also interested in non-perturbative information related to the width of the bands and gaps, whose central locations are given by (5.5). This non-perturbative information can be extracted from the same all-orders expansion (5.1), but with different contours, now encircling the other turning points; for example, for the energy range below the barrier top, the new turning points are those associated with tunneling through the barrier between two adjacent wells. For energies above the barrier top, these turning points merge and go into the complex plane, and this expression continues smoothly. Thus, we write this “dual” action as

$$a^D(\hbar, u) = \frac{\sqrt{2}}{2\pi} \left(\oint_{C_D} \sqrt{u - V} dx - \frac{\hbar^2}{2^6} \oint_{C_D} \frac{(V')^2}{(u - V)^{5/2}} dx - \frac{\hbar^4}{2^{13}} \oint_{C_D} \left(\frac{49(V')^4}{(u - V)^{11/2}} - \frac{16V'V'''}{(u - V)^{7/2}} \right) dx - \dots \right) \quad (5.6)$$

integrated over the dual integration cycle C_D , which encircles these dual turning points. For the Mathieu problem there are just two independent cycles, C and C_D , and they correspond to the generators of the two cycles of the underlying torus. Note that the higher-order WKB dual actions can also be obtained from the leading one by acting with certain differential operators: in fact, since the only difference is the different cycles, the relations have exactly the same form as in (5.4), with a_n replaced with a_n^D . With proper analytic continuation, this quantization condition permits smooth transitions and dualities between the various spectral regions, connecting weak and strong coupling, and also the bottom and top of the wells. The distinction between the various regions is encoded in the location of the turning points in the complex plane, and the associated Stokes lines. For energies inside the wells there are real turning points. As the energy approaches the barrier top, the turning points come together and coalesce, and move apart again along the imaginary axis for energy above the barrier top.

Given this dual action, there is an elegant compact formula (2.12) for the leading width of a *band*, for energies well below the potential barrier (*i.e.* here $-1 \leq u \ll 1$). In terms of the action and dual action, this leading order result reads:

$$\Delta u_{\text{band}} \sim \frac{2}{\pi} \frac{\partial u}{\partial N} e^{-\frac{2\pi}{\hbar} \text{Im} a_0^D} \sim \frac{\hbar}{\pi} \frac{\partial u}{\partial a_0} e^{-\frac{2\pi}{\hbar} \text{Im} a_0^D}. \quad (5.7)$$

There is also an elegant compact formula (2.13) for the leading width of a *gap*, for energies well above the potential barrier (*i.e.* here $u \gg 1$). In terms of the action and dual action, this leading order result reads:

$$\Delta u_{\text{gap}} \sim \frac{2}{\pi} \frac{\partial u}{\partial N} e^{-\frac{2\pi}{\hbar} \text{Im} a_0^D} \sim \frac{\hbar}{\pi} \frac{\partial u}{\partial a_0} e^{-\frac{2\pi}{\hbar} \text{Im} a_0^D}. \quad (5.8)$$

Notice that these formula are the same! Furthermore, notice that the prefactor can be interpreted as a frequency, and the exponential factor as a probability of tunneling through the barrier: for band widths, the tunneling is between real turning points, but for gap widths it is tunneling between complex turning points. The energy dependence of a_0 and a_0^D is very different in the different spectral regions, and this explains the difference between the final expressions (2.8, 2.11) for the Mathieu band and gap widths, even though they come from expressions with a common form.

5.1 Weak coupling

The leading order terms of the actions are expressed in terms of elliptic integrals

$$a_0(u) = \frac{\sqrt{2}}{\pi} \int_{-1}^u dy \sqrt{\frac{y-u}{y^2-1}} = \frac{4}{\pi} \left(\mathbb{E} \left(\frac{1+u}{2} \right) - \frac{1}{2}(1-u) \mathbb{K} \left(\frac{1+u}{2} \right) \right) \quad (5.9)$$

$$a_0^D(u) = -\frac{\sqrt{2}}{\pi} \int_u^1 dy \sqrt{\frac{y-u}{y^2-1}} = -\frac{4i}{\pi} \left(\mathbb{E} \left(\frac{1-u}{2} \right) - \frac{1}{2}(1+u) \mathbb{K} \left(\frac{1-u}{2} \right) \right). \quad (5.10)$$

These actions are two independent solutions of the second-order Picard-Fuchs equation:

$$\frac{d^2 a_0}{du^2} = \frac{1}{4(1-u^2)} a_0(u) \quad (5.11)$$

and consequently they satisfy the Wronskian relation

$$a_0(u) \frac{da_0^D(u)}{du} - a_0^D(u) \frac{da_0(u)}{du} = \frac{2i}{\pi} \quad (5.12)$$

which simply expresses the Legendre relation [here \mathbb{K}' denotes $\mathbb{K}(1-k^2)$, using the conventions of [11]]:

$$\mathbb{E}\mathbb{K}' + \mathbb{E}'\mathbb{K} - \mathbb{K}\mathbb{K}' = \frac{\pi}{2}. \quad (5.13)$$

The higher-order WKB actions can be obtained by the action of certain differential operators on $a_0(u)$ or $a_0^D(u)$, as noted above in (5.4). For example, the first two next-to-leading order actions calculated from (5.4) are

$$a_1(u) = \frac{1}{48\pi(1-u^2)} \left((1-u)\mathbb{K}\left(\frac{1+u}{2}\right) + 2u\mathbb{E}\left(\frac{1+u}{2}\right) \right) \quad (5.14)$$

$$a_2(u) = -\frac{1}{46080\pi(1-u^2)^3} \left[(1-u)(4u^3 + 93u^2 - 60u + 75)\mathbb{K}\left(\frac{1+u}{2}\right) + 2(4u^4 - 153u^2 - 75)\mathbb{E}\left(\frac{1+u}{2}\right) \right] \quad (5.15)$$

and similarly for $a_1^D(u)$ and $a_2^D(u)$.

5.1.1 Band center location from Bohr-Sommerfeld at weak coupling The all-orders Bohr-Sommerfeld expression (5.5) that identifies u with the center of the band is:

$$\frac{\hbar}{2} \left(N + \frac{1}{2} \right) = a(u, \hbar) \equiv \sum_{n=0}^{\infty} \hbar^{2n} a_n(u). \quad (5.16)$$

The WKB actions $a_n(u)$ can be expanded near the bottom of the wells, $u \sim -1$:

$$a_0(u) \sim \frac{u+1}{2} + \frac{(u+1)^2}{32} + \frac{3(u+1)^3}{512} + \frac{25(u+1)^4}{16384} + \frac{245(u+1)^5}{524288} + \dots \quad (5.17)$$

$$a_1(u) \sim \frac{1}{128} + \frac{5(u+1)}{2048} + \frac{35(u+1)^2}{32768} + \frac{525(u+1)^3}{1048576} + \frac{8085(u+1)^4}{33554432} + \dots \quad (5.18)$$

$$a_2(u) \sim \frac{17}{262144} + \frac{721(u+1)}{8388608} + \frac{10941(u+1)^2}{134217728} + \frac{141757(u+1)^3}{2147483648} + \frac{3342339(u+1)^4}{68719476736} + \dots \quad (5.19)$$

Inserting these expansions into the all-orders Bohr-Sommerfeld expression (5.16) we obtain:

$$\begin{aligned}
 N + \frac{1}{2} &= \frac{2}{\hbar} (a_0(u) + \hbar^2 a_1(u) + \hbar^4 a_2(u) + \dots) \\
 &\sim \frac{1}{\hbar} \left((u+1) + \frac{(u+1)^2}{16} + \frac{3(u+1)^3}{256} + \frac{25(u+1)^4}{8192} \right. \\
 &\quad \left. + \frac{245(u+1)^5}{262144} + \dots \right) \\
 &\quad + 2\hbar \left(\frac{1}{128} + \frac{5(u+1)}{2048} + \frac{35(u+1)^2}{32768} + \frac{525(u+1)^3}{1048576} \right. \\
 &\quad \left. + \frac{8085(u+1)^4}{33554432} + \dots \right) \\
 &\quad + 2\hbar^3 \left(\frac{17}{262144} + \frac{721(u+1)}{8388608} + \frac{10941(u+1)^2}{134217728} \right. \\
 &\quad \left. + \frac{141757(u+1)^3}{2147483648} + \frac{3342339(u+1)^4}{68719476736} + \dots \right) \\
 &\quad + \dots \tag{5.20}
 \end{aligned}$$

This expresses the band label N as a formal series in \hbar , with coefficients that are functions of the energy u . To compare with perturbation theory, we invert to write the energy u as a formal series in \hbar , with coefficients that are functions of the band label N . Doing so, we obtain precisely the perturbative expansion (2.6). Notice, that in this latter formal series, the coefficients of the formal series in \hbar are simple polynomials in $(N + \frac{1}{2})$. Also recall that this perturbative expansion (2.6) is non-Borel-summable in this regime where $N\hbar \ll 1$.

5.1.2 Band width at weak coupling The exponentially narrow band widths can be evaluated using the dual actions. In the weak-coupling region,

$$u \sim -1 + 2a_0(u) + \dots = -1 + \hbar \left(N + \frac{1}{2} \right) + \dots \tag{5.21}$$

$$\pi \operatorname{Im}[a_0^D] \sim 4 + \frac{1+u}{2} \left(\ln \left(\frac{1+u}{32} \right) - 1 \right) + \dots \tag{5.22}$$

Therefore, from (5.7) we obtain the band width estimate (using Stirling's formula in the last step):

$$\begin{aligned}\Delta u_{\text{band}} &\sim \frac{2\hbar}{\pi} \left(\frac{\hbar(N + \frac{1}{2})}{32e} \right)^{-(N + \frac{1}{2})} e^{-8/\hbar} \\ &\sim \sqrt{\frac{2}{\pi}} \frac{2^{4(N+1)}}{N!} \left(\frac{2}{\hbar} \right)^{N - \frac{1}{2}} e^{-8/\hbar}\end{aligned}\quad (5.23)$$

in agreement with (2.8).

5.2 Strong coupling

5.2.1 Gap center location from Bohr-Sommerfeld at strong coupling In the strong coupling region (*i.e.* $u \gg 1$, or $N\hbar \gg 1$) the all-orders Bohr-Sommerfeld condition (5.5) that identifies u with the center of the gap reads

$$\frac{\hbar}{2}N = a(u, \hbar) \equiv \sum_{n=0}^{\infty} \hbar^{2n} a_n(u) \quad (5.24)$$

The WKB actions $a_n(u)$ can be expanded for $u \gg 1$ as:

$$a_0(u) \sim \sqrt{2u} \left(1 - \frac{1}{16u^2} - \frac{15}{1024u^4} - \frac{105}{16384u^6} - \dots \right) \quad (5.25)$$

$$a_1(u) \sim -\frac{1}{16(2u)^{5/2}} \left(1 + \frac{35}{32u^2} + \frac{1155}{1024u^4} + \frac{75075}{65536u^6} + \dots \right) \quad (5.26)$$

$$a_2(u) \sim -\frac{1}{64(2u)^{7/2}} \left(1 + \frac{273}{64u^2} + \frac{5005}{512u^4} + \frac{2297295}{131072u^6} + \dots \right). \quad (5.27)$$

Combining these expansions we find

$$\begin{aligned}N &= \frac{2}{\hbar} (a_0(u) + \hbar^2 a_1(u) + \hbar^4 a_2(u) + \dots) \\ &\sim \frac{2\sqrt{2u}}{\hbar} \left[1 - \frac{1}{16u^2} - \frac{15}{1024u^4} - \frac{105}{16384u^6} - \frac{15015}{4194304u^8} - \dots \right] \\ &\quad - \frac{\hbar}{8(2u)^{5/2}} \left[1 + \frac{35}{32u^2} + \frac{1155}{1024u^4} + \frac{75075}{65536u^6} + \frac{4849845}{4194304u^8} + \dots \right] \\ &\quad - \frac{\hbar^3}{32(2u)^{7/2}} \left[1 + \frac{273}{64u^2} + \frac{5005}{512u^4} + \frac{2297295}{131072u^6} + \frac{115426311}{4194304u^8} + \dots \right] \\ &\quad - \dots\end{aligned}\quad (5.28)$$

This expresses the band label N as a formal series in \hbar , with coefficients that are functions of the energy u . To compare with the strong-coupling expansion, we invert to write the energy u as a formal series in \hbar , with coefficients that are functions of the band label N . This leads to (here we have defined the “action” $a \equiv \frac{N\hbar}{2}$):

$$u \sim \left[\frac{a^2}{2} + \frac{1}{4a^2} + \frac{5}{64} \frac{1}{a^6} + \frac{9}{128} \frac{1}{a^{10}} + \dots \right] + \hbar^2 \left[\frac{1}{16a^4} + \frac{21}{128} \frac{1}{a^8} + \frac{55}{128} \frac{1}{a^{12}} + \dots \right] + \dots \quad (5.29)$$

$$\begin{aligned} &\sim \frac{1}{2} \left(\frac{N\hbar}{2} \right)^2 + \frac{1}{4} \left(\frac{2}{N\hbar} \right)^2 \frac{1}{\left(1 - \frac{\hbar^2}{(N\hbar)^2} \right)} \\ &+ \frac{5}{64} \left(\frac{2}{N\hbar} \right)^6 \frac{\left(1 + \frac{7\hbar^2}{5(N\hbar)^2} \right)}{\left(1 - \frac{\hbar^2}{(N\hbar)^2} \right)^3 \left(1 - \frac{4\hbar^2}{(N\hbar)^2} \right)} + \dots \quad (5.30) \end{aligned}$$

We recognize precisely the strong-coupling expansion (2.10). Thus, the all-orders-WKB action $a(u, \hbar)$ determines the (convergent) expansion of the location of the gap high up in the spectrum.

5.2.2 Gap width at strong coupling Despite these expressions (for the center of the N^{th} gap) being convergent, there are still non-perturbatively small corrections associated with the narrow gaps high in the spectrum (see Figure 2.1). Expanding the leading actions in this spectral region we find

$$u \sim \frac{1}{2} a_0^2 + \dots = \frac{\hbar^2}{8} N^2 + \dots \quad (5.31)$$

$$\pi \mathcal{I}m[a_0^D] \sim \sqrt{2u} (\ln(8u) - 2) + \dots \quad (5.32)$$

Therefore, from (5.8) we obtain the gap width estimate:

$$\Delta u_{\text{gap}} \sim \frac{\hbar^2 N}{2\pi} \left(\frac{e}{\hbar N} \right)^{2N} \quad (5.33)$$

in agreement with (2.11). Thus, the formulas (5.7, 5.8) have the correct form in both extreme limits, in one case referring to the width of a band, and in the other to the width of a gap.

5.3 Intermediate coupling: instanton condensation near the barrier top

Near the barrier top, where $u \sim 1$, there is a transition from the divergent perturbative behavior characteristic of the weak coupling region, to the convergent perturbative expansions characteristic of the strong-coupling region. As is clear from the plots in Figures 2.1 and 5.1, the transition is smooth, but connecting the regions requires careful interpretation of the various expansions. Of particular interest are the different mechanisms by which non-perturbative terms arise in the different physical regions. For example, the general expressions for the exponentially narrow width of a band (5.7) deep in the weak coupling region, and of a gap (5.8) high in the strong coupling region, are not valid in the region in the vicinity of the barrier top, because the single-instanton factor $\exp\left[-\frac{2\pi}{\hbar} \text{Im } a_0^D\right]$ is no longer exponentially small. Thus, the explicit expressions (2.8) and (2.11) are not accurate in this region of the spectrum. Physically, this is a region of “instanton condensation”. This is of particular interest as it is a direct analogue of an instanton condensation phenomenon observed in matrix models and 2d gauge theories [48–52].

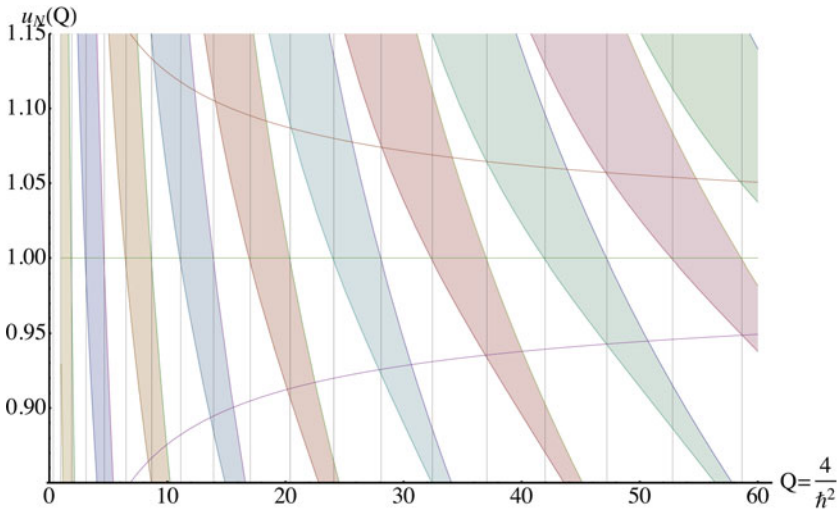


Figure 5.1. The bands (shaded) and gaps, as a function of the parameter $Q \equiv \frac{4}{\hbar^2}$, near the barrier top $u = 1$. The vertical lines denote the values $Q = \frac{\pi^2}{16} \left(N \pm \frac{1}{4}\right)^2$, where N is the band label, and which agree accurately with the points at which the band/gap edges intersect the line $u = 1$. The curved solid lines show the expressions in (5.41), which gives the gap splitting at the top of a band, centered at $u = 1$. This leading expression fits the exact curves quite well.

In the spectral region near $u \sim 1$:

$$a_0 \sim \frac{4}{\pi} + \frac{u-1}{2\pi} \left[\ln \left(\frac{32}{u-1} \right) + 1 \right] + \dots \quad (5.34)$$

$$-ia_0^D \sim \frac{1}{2}(u-1) + \dots \quad (5.35)$$

The fact that a_0^D vanishes at $u = 1$ implies that the single-instanton approximations (2.8, 2.11) are no longer good, as the exponentially small instanton factor $\exp \left[-\frac{2\pi}{\hbar} \text{Im} a_0^D \right]$ is now of order 1. The fact that $a_0(u)$ tends to a non-zero constant implies the leading scaling between N and \hbar in this region:

$$N + \frac{1}{2} \sim \frac{8}{\pi \hbar} \quad (\text{band center at } u = 1) \quad (5.36)$$

$$N \sim \frac{8}{\pi \hbar} \quad (\text{gap center at } u = 1). \quad (5.37)$$

We had already expected that the barrier top would be in the vicinity of $N \sim 1/\hbar$, but the behavior $a_0(u) \sim 4/\pi$ fixes the non-trivial coefficient to be $8/\pi$. We can now use these estimates (5.36, 5.37) in either the weak-coupling expansion (2.6) or the strong coupling expansion (2.10) to obtain two very different looking expressions for the energy at the top of the barrier:

$$\begin{aligned} u_{\text{weak}} &\sim -1 + \frac{8}{\pi} \left[1 - \frac{1}{16} \frac{8}{\pi} - \frac{1}{2^8} \left(\frac{8}{\pi} \right)^2 - \frac{5}{2^{14}} \left(\frac{8}{\pi} \right)^3 \right. \\ &\quad \left. - \frac{33}{2^{18}} \left(\frac{8}{\pi} \right)^4 - \dots \right] + \mathcal{O}(\hbar) \\ &= 1 + \mathcal{O}(\hbar) \end{aligned} \quad (5.38)$$

$$\begin{aligned} u_{\text{strong}} &\sim \frac{1}{2} \left[\left(\frac{4}{\pi} \right)^2 + \frac{1}{2} \left(\frac{\pi}{4} \right)^2 + \frac{5}{32} \left(\frac{\pi}{4} \right)^6 + \frac{9}{64} \left(\frac{\pi}{4} \right)^{10} + \dots \right] + \mathcal{O}(\hbar) \\ &= 1 + \mathcal{O}(\hbar). \end{aligned} \quad (5.39)$$

It is interesting that these two different expansions agree at $u \sim 1$, but there are corrections $\sim \mathcal{O}(\hbar)$, corresponding to the band and gap widths in the vicinity of the barrier top.

The estimates in (5.36, 5.37) can be refined further: the *edges* of the bands/gaps when $u = 1$ are given by (see also [69]):

$$N \pm \frac{1}{4} \sim \frac{8}{\pi \hbar} \quad (\text{band/gap edge at } u = 1) \quad (5.40)$$

as shown in Figure 5.1. In this figure, showing the bands (shaded) and gaps (unshaded), plotted as a function of the parameter $Q = \frac{4}{\hbar^2}$ that appears in the Mathieu equation (2.1, 2.2), we see clearly that at one of these edges, the band and the gap immediately above and below have equal width. Physically, this is directly related to the fact that the discriminant can be expressed in terms of the reflection and transmission amplitudes [71], and the fact that at the top of an inverted harmonic barrier the reflection and transmission probabilities are equal, both being $1/2$ [72]. Relatively little is known rigorously about the corrections to this behavior of the band/gap widths in this region, even though in some sense it is the most interesting region physically [38, 69, 70]. The results of Weinstein and Keller imply that the small \hbar behavior for the upper band edges has leading behavior

$$u \sim 1 \pm \frac{\pi \hbar}{16} + \dots \quad (5.41)$$

These lines are shown in Figure 5.1, and we see that they do indeed intersect the upper band edges quite accurately. It would be interesting to investigate more precisely the band and gap widths in this region.

5.4 Summary of different behaviors of Mathieu spectrum in different regions

It is worth comparing the form of the expressions for the energy in the three different spectral regions.

- **Weak coupling:** $N\hbar \ll 1$, deep inside the wells, far below the barrier top. Here the band edge energy eigenvalues $u^{(\pm)}(\hbar, N)$ are expressed as a resurgent trans-series:

$$u^{(\pm)}(\hbar, N) \sim \sum_{n=0}^{\infty} u_n(N) \hbar^n \pm \frac{32}{\sqrt{\pi} N!} \left(\frac{32}{\hbar} \right)^{N-1/2} \exp \left[-\frac{8}{\hbar} \right] \sum_{n=0}^{\infty} d_n(N) \hbar^n + \dots \quad (5.42)$$

The first term is the formal perturbative series, $u_{\text{pert}}(\hbar, N)$, which is divergent and Borel non-summable. The leading Borel poles occur at the two-instanton location. The first, one-instanton, exponential correction in (5.42) gives the leading band width. Furthermore, the expansion coefficients $u_n(N)$ and $d_n(N)$ are explicitly related: the $d_n(N)$ are fully determined by the $u_n(N)$, as in (1.5, 1.6).

- **Strong coupling:** $N\hbar \gg 1$, far above the barrier top. Here the gap edges are conventionally written as the convergent expansions (2.9).

This raises an obvious question: how can such convergent expansions smoothly connect to the trans-series expansion (5.42) below the barrier top? In fact [38], one can re-write the expansions (2.9) in the following suggestive form:

$$u^{(\pm)}(\hbar, N) = \frac{\hbar^2 N^2}{8} \sum_{n=0}^{N-1} \frac{\alpha_n(N)}{\hbar^{4n}} \pm \frac{\hbar^2}{8} \frac{\left(\frac{2}{\hbar}\right)^{2N}}{(2^{N-1}(N-1)!)^2} \sum_{n=0}^{N-1} \frac{\beta_n(N)}{\hbar^{4n}} + \dots \quad (5.43)$$

where the coefficient functions $\alpha_n(N)$ and $\beta_n(N)$ are rational functions of the gap label N , but have poles at the two-instanton location. Thus the expansions truncate at $n = N$. Note that this has a similar form to the trans-series in (5.42). As $N \rightarrow \infty$, the polynomial expansions in $\frac{1}{\hbar^4}$ extend to infinite series. Remarkably, with this re-arrangement we find once again that the expansion coefficients $\alpha_n(N)$ and $\beta_n(N)$ are explicitly related: the $\beta_n(N)$ are fully determined by the $\alpha_n(N)$. Thus, the strong-coupling expansions can also be written in a form that matches the trans-series structure of the weak-coupling region [67].

• **Transition region: intermediate coupling:** $N\hbar \sim \frac{8}{\pi}$, near the barrier top. This is the instanton condensation region, where the single-instanton exponential factor becomes of order 1, so that all instanton orders need to be taken into account. Here, relatively little is known precisely. One concrete statement is that the bands and gaps in this region have equal width at leading order, and this width is $O(\hbar)$, for example as in (5.41).

6 Path integral interpretation: steepest descents and Lefschetz thimbles

We have used WKB techniques in the framework of differential equations to derive the new result (1.5, 1.6), which relates higher orders of the non-perturbative trans-series expansion to the perturbative series. But the result is even more interesting when viewed from the equivalent path integral language. Here, different instanton sectors correspond to different saddle points of the path integral, and so we learn that there is a saddle point expansion of the path integral representation of the quantum resolvent, in which the fluctuations about different saddle points are directly related to one another. In practice, this has been confirmed by the work of [61] because their diagrammatic computation of the fluctuations about the one-instanton sector is based on a perturbative expansion of the path integral about the one-instanton sector. But the fact that this computation is so technically difficult means that there should be a simpler way to understand the final result. We propose that this is an example where

a saddle point expansion in terms of Lefschetz thimbles can be implemented explicitly.

To illustrate the basic idea, we turn back to a zero-dimensional example, and recall the results of Berry and Howls [19] concerning an all-orders steepest descents expansion of an ordinary contour integral. They considered a contour integral of the form

$$I^{(n)}(\hbar) = \int_{C_n} dz e^{-\frac{1}{\hbar} f(z)} = \frac{1}{\sqrt{1/\hbar}} \exp\left[-\frac{1}{\hbar} f_n\right] T^{(n)}(\hbar) \quad (6.1)$$

where the contour C_n follows the steepest descent path through the saddle point z_n of the function $f(z)$. The first two factors on the RHS are the dominant exponential term and the Gaussian fluctuation prefactor. The remaining factor, $T^{(n)}(\hbar)$, is a formal series in \hbar , and represents all orders of the perturbative fluctuations about this saddle point. Physicists typically just keep the exponential and the Gaussian prefactor. Berry and Howls [19] point out that there is a great deal of interesting information encoded in the further fluctuations $T^{(n)}(\hbar)$. For example, under relatively mild assumptions about the function $f(z)$, one can show by straightforward contour deformation that the fluctuations about different saddle points are directly related. This is a manifestation of Darboux's theorem: the fluctuations about a given point are governed by the nearest singularity, which here is the nearest (connected) saddle point [19]. This fact can be expressed as the following integral transform:

$$T^{(n)}(\hbar) = \frac{1}{2\pi i} \sum_m (-1)^{\gamma_{nm}} \int_0^\infty \frac{dv}{v} \frac{e^{-v}}{1 - \hbar v/(F_{nm})} T^{(m)}\left(\frac{F_{nm}}{v}\right) \quad (6.2)$$

where the sum is over all other saddles topologically connected to the n^{th} saddle, and the γ_{nm} determine the orientations of the deformed steepest descent contours. Here $F_{nm} \equiv f_m - f_n$ is the difference of the exponents at the saddle points z_m and z_n . An immediate consequence of this result is that if we write the fluctuation about the n^{th} saddle as

$$T^{(n)}(\hbar) \sim \sum_{r=0}^{\infty} T_r^{(n)} \hbar^r \quad (6.3)$$

then expanding both sides of (6.2) we find a relation between the fluctuation coefficients around saddle points z_n and z_m :

$$T_r^{(n)} \sim \frac{(r-1)!}{2\pi i} \sum_m \frac{(-1)^{\gamma_{nm}}}{(F_{nm})^r} \left[T_0^{(m)} + \frac{F_{nm}}{(r-1)} T_1^{(m)} + \frac{(F_{nm})^2}{(r-1)(r-2)} T_2^{(m)} + \dots \right], \quad r \rightarrow \infty. \quad (6.4)$$

Notice the universal large-order factorial divergence of fluctuations, and more importantly notice that this says that fluctuations about *neighboring* saddles are explicitly related.

For full details see [19], but here it is more appropriate to illustrate how this works with some examples. Consider the zero-dimensional “partition function” for the Mathieu system, writing the periodic potential as $V(z) = \sin^2(z)$:

$$Z(\hbar) = \int_{-\pi/2}^{\pi/2} dz e^{-\frac{1}{\hbar} \sin^2(z)}. \quad (6.5)$$

There are two saddle points: $z_0 = 0$ and $z_1 = \frac{\pi}{2}$. It is straightforward to generate the “perturbative expansion” about the “vacuum” saddle point at $z_0 = 0$. The expansion coefficients in (6.3) for $n = 0$ are:

$$\begin{aligned} T_r^{(0)} &= \frac{\Gamma(r + \frac{1}{2})^2}{\sqrt{\pi} \Gamma(r+1)} \\ &\sim \frac{(r-1)!}{\sqrt{\pi}} \left(1 - \frac{\frac{1}{4}}{(r-1)} + \frac{\frac{9}{32}}{(r-1)(r-2)} - \frac{\frac{75}{128}}{(r-1)(r-2)(r-3)} + \dots \right). \end{aligned} \quad (6.6)$$

$r \rightarrow \infty$

It is also straightforward to generate the fluctuation expansion about the “non-perturbative saddle” at $z_1 = \frac{\pi}{2}$:

$$T^{(1)}(\hbar) \sim i \sqrt{\pi} \left(1 - \frac{1}{4} g^2 + \frac{9}{32} g^4 - \frac{75}{128} g^6 + \dots \right). \quad (6.7)$$

Comparing coefficients, we see that the low-order coefficients of the fluctuations about the non-perturbative saddle z_1 govern the large-order behavior of the fluctuations about the vacuum saddle z_0 . Below we consider a more interesting example where there are three saddles.

This is a general feature of a wide class of ordinary exponential integrals: fluctuations around different saddles are quantitatively related. In studying path integrals, and especially semiclassical multi-instanton expansions of path integrals, we often motivate our formal manipulations by analogy with steepest descents asymptotic analysis of ordinary integrals. Thus, it is a reasonable question to ask whether or not something like this could possibly occur for (infinite dimensional!) path integrals. This leads to the theory of infinite dimensional Morse Theory and Lefschetz thimbles. Even the generalization from a one-dimensional integral to a multi-dimensional integral introduces interesting and highly non-trivial

effects [91–94]. There are many more subtleties in going from finite to infinite dimensions [95–97].

Instead of delving into this unresolved issue, let us illustrate what happens when you ask this question about the Mathieu system. Here we have done the calculation without using the path integral, but we can re-interpret the results in path integral terms. Specifically, consider the Schrödinger problem with periodic potential $V(x) = \sin^2(x)$. The large order growth of the perturbative expansion coefficients for the ground state energy is [41]

$$c_n \sim n! \left(1 - \frac{5}{2} \cdot \frac{1}{n} - \frac{13}{8} \cdot \frac{1}{n(n-1)} - \dots \right). \quad (6.8)$$

This is the large-order growth of the fluctuation about the vacuum saddle point, for the ground state energy. Next, we can inspect the multi-instanton trans-series expansion for the same physical quantity, the ground state energy, and look for the fluctuations about the ‘nearest’ saddle point with the same quantum numbers as the perturbative vacuum. This is the instanton/anti-instanton saddle point, and we find [55]

$$\text{Im } E_0 \sim \pi e^{-2\frac{1}{2\hbar}} \left(1 - \frac{5}{2} \cdot \hbar - \frac{13}{8} \cdot \hbar^2 - \dots \right). \quad (6.9)$$

Notice the correspondence of the factors appearing in these different expansions, about different saddles. This is very surprising. It means that to some degree the basic resurgent relation between large-order behavior of fluctuations about one saddle and low-orders of fluctuations about a neighboring saddle is indeed inherited by the path integral. (This is not just a feature of the Mathieu system: a similar relation holds also for the double-well potential).

To emphasize that this structure could be quite general we consider a further example that has the interesting feature of having more saddle points. Let us generalize the zero-dimensional example above, by replacing the periodic Mathieu potential $V(x) = \sin^2(x)$ by the doubly-periodic elliptic potential of Lamé type [98]:

$$V(x) = \text{sd}^2(x|m) \quad , \quad 0 \leq m \leq 1 \quad (6.10)$$

where $0 \leq m \leq 1$ is the elliptic parameter. Note that this potential interpolates smoothly between the periodic Mathieu case, $V(x) = \sin^2(x)$, when $m = 0$ and the “Sinh-Gordon” potential, $V(x) = \sinh^2(x)$, when $m = 1$. We write the zero dimensional partition function as the trace over the period:

$$Z(\hbar|m) = \frac{1}{\sqrt{\hbar\pi}} \int_{-\mathbb{K}}^{\mathbb{K}} dz e^{-\frac{1}{\hbar} \text{sd}^2(z|m)}. \quad (6.11)$$

This has the following “perturbative expansion” about the “vacuum saddle” at $z = 0$.

$$Z_{\text{pert}}(\hbar|m) = \sum_{n=0}^{\infty} a_n^{(0)}(m) \hbar^n. \quad (6.12)$$

For example, at some chosen values of m we have:

$$\begin{aligned} Z_{\text{pert}}(\hbar|0) &= 1 + \frac{1}{4}\hbar + \frac{9}{32}\hbar^2 + \frac{75}{128}\hbar^3 + \frac{3675}{2048}\hbar^4 + \frac{59535}{8192}\hbar^5 + \dots \\ Z_{\text{pert}}(\hbar|1) &= 1 - \frac{1}{4}\hbar + \frac{9}{32}\hbar^2 - \frac{75}{128}\hbar^3 + \frac{3675}{2048}\hbar^4 - \frac{59535}{8192}\hbar^5 + \dots \\ Z_{\text{pert}}\left(\hbar\left|\frac{1}{4}\right.\right) &= 1 + \frac{1}{8}\hbar + \frac{9}{64}\hbar^2 + \frac{105}{512}\hbar^3 + \frac{1995}{4096}\hbar^4 + \frac{48195}{32768}\hbar^5 + \dots \\ Z_{\text{pert}}\left(\hbar\left|\frac{3}{4}\right.\right) &= 1 - \frac{1}{8}\hbar + \frac{9}{64}\hbar^2 - \frac{105}{512}\hbar^3 + \frac{1995}{4096}\hbar^4 - \frac{48195}{32768}\hbar^5 + \dots \\ Z_{\text{pert}}\left(\hbar\left|\frac{1}{2}\right.\right) &= 1 + 0\hbar + \frac{3}{32}\hbar^2 + 0\hbar^3 + \frac{315}{2048}\hbar^4 + 0\hbar^5 + \dots \end{aligned} \quad (6.13)$$

These perturbative expansions are divergent for all m , but are non-alternating for $m < 1/2$, and alternating for $m > 1/2$. This latter fact reflects the duality relation: $Z(\hbar|m) = Z(-\hbar|1 - m)$, which follows from a property of the Jacobi elliptic function sd .

The “action” function $V(z)$ has two different types of non-trivial saddles, one set along the real axis and another on the imaginary axis. Their relative distance from the vacuum saddle at $z = 0$ is governed by the value of the elliptic parameter m . At the real saddle point $z_1 = \mathbb{K}(m)$, we have the action $S_1 = \frac{1}{1-m}$, while at the imaginary saddle at $z_2 = i\mathbb{K}(1 - m)$ we have $S_2 = -\frac{1}{m}$. These two different saddles can be seen in the large-order behavior of the perturbative fluctuation coefficients. Numerically, by studying the large-order behavior of the expansion coefficients about $z_0 = 0$, one finds [98]

$$a_n^{(0)}(m) \sim \frac{(n-1)!}{\pi} \left(S_1^{n+1/2}(m) + (-1)^n |S_2|^{n+1/2}(m) \right) \quad (6.14)$$

For $m < \frac{1}{2}$, S_1 dominates and the $a_n^{(0)}(m)$ are non-alternating in sign. For $m > \frac{1}{2}$, S_2 dominates and the $a_n^{(0)}(m)$ alternate in sign. For $m = \frac{1}{2}$, S_1 and S_2 are equal in magnitude, and the odd terms vanish due to interference cancellations. Thus both the real and complex saddles influence the large-order growth of the fluctuations about the trivial vacuum saddle at $z_0 = 0$. This is an explicit example of the sum of neighboring saddles in (6.4).

Actually, this relation can be made even more precise [98], noting that the fluctuations about the saddles $z_1 = \mathbb{K}(m)$ and $z_2 = i\mathbb{K}(1 - m)$ can be written as

$$Z^{(1)}(\hbar|m) = i e^{-S_1/\hbar} \sum_{n=0}^{\infty} a_n^{(1)}(m) \hbar^n \tag{6.15}$$

$$Z^{(2)}(\hbar|m) = i e^{-S_2/\hbar} \sum_{n=0}^{\infty} a_n^{(2)}(m) \hbar^n \tag{6.16}$$

and one finds an exact resurgence relation:

$$Z^{(0)}(\hbar|m) = \frac{2}{2\pi i} \sum_{k \in \{1,2\}} \int_0^{\infty} \frac{dv}{v} \frac{1}{1 - \hbar v} Z^{(k)}(v|m) \tag{6.17}$$

and an exact relation between the expansion coefficients $a_n^{(k)}$:

$$a_n^{(0)}(m) = \sum_{j=0}^{n-1} \frac{(n - j - 1)!}{\pi} \left(\frac{a_j^{(1)}(m)}{S_1^{n-j}} + \frac{a_j^{(2)}(m)}{S_2^{n-j}} \right). \tag{6.18}$$

Now we can ask again how much of this resurgent structure is inherited by the *path integral* version of this problem. The partition function is now an *infinite dimensional functional integral*:

$$Z(\hbar|m) = \int \mathcal{D}x e^{-S[x]} = \int \mathcal{D}x e^{-\int d\tau \left(\frac{1}{4} \dot{x}^2 + \frac{1}{\hbar} \text{sd}^2(\sqrt{\hbar}x|m) \right)}. \tag{6.19}$$

As before for the Mathieu case, we illustrate our point using the simplest observable, the perturbative ground state energy, for which we find perturbative expansions as functions of m . For several selected values of m the first few terms are:

$$\begin{aligned} E^{(0)}(\hbar|0) &= 1 - \frac{1}{4}\hbar - \frac{1}{16}\hbar^2 - \frac{3}{64}\hbar^3 - \frac{53}{1024}\hbar^4 - \frac{297}{4096}\hbar^5 - \dots \\ E^{(0)}(\hbar|1) &= 1 + \frac{1}{4}\hbar - \frac{1}{16}\hbar^2 + \frac{3}{64}\hbar^3 - \frac{53}{1024}\hbar^4 + \frac{297}{4096}\hbar^5 - \dots \\ E^{(0)}\left(\hbar \left| \frac{1}{4} \right. \right) &= 1 - \frac{1}{8}\hbar - \frac{11}{128}\hbar^2 - \frac{3}{128}\hbar^3 - \frac{889}{32768}\hbar^4 - \frac{225}{8192}\hbar^5 - \dots \\ E^{(0)}\left(\hbar \left| \frac{3}{4} \right. \right) &= 1 + \frac{1}{8}\hbar - \frac{11}{128}\hbar^2 + \frac{3}{128}\hbar^3 - \frac{889}{32768}\hbar^4 + \frac{225}{8192}\hbar^5 - \dots \\ E^{(0)}\left(\hbar \left| \frac{1}{2} \right. \right) &= 1 + 0\hbar - \frac{3}{32}\hbar^2 + 0\hbar^3 - \frac{39}{2048}\hbar^4 + 0\hbar^5 - \dots \end{aligned} \tag{6.20}$$

These expansions are remarkably similar to the zero dimensional expansions of the zero dimensional partition function in (6.13). For example, we again observe the duality relation: $E^{(0)}(\hbar|m) = E^{(0)}(-\hbar|1-m)$, and the perturbative expansions are non-alternating for $m < \frac{1}{2}$, but alternating for $m > \frac{1}{2}$.

The Lamé potential is doubly periodic, in the complex plane. This means that there are two types of instantons: real instantons and complex “ghost” instantons. The real instantons tunnel between minima of the potential along the real axis, while the complex instantons tunnel between saddles along the imaginary axis. The associated classical actions are:

$$S_{\mathcal{I}}(m) = \frac{2 \arcsin(\sqrt{m})}{\sqrt{m(1-m)}} \quad (6.21)$$

$$S_{\mathcal{G}}(m) = \frac{-2 \arcsin(\sqrt{1-m})}{\sqrt{m(1-m)}}. \quad (6.22)$$

Then one can study the large order growth of the perturbative expansion coefficients for the ground state energy and one finds that both the real and complex instantons contribute to this large-order behavior [98]:

$$a_n(m) \sim -\frac{16}{\pi} n! \left(\frac{1}{(S_{\mathcal{I}\bar{\mathcal{I}}}(m))^{n+1}} - \frac{(-1)^{n+1}}{|S_{\mathcal{G}\bar{\mathcal{G}}}(m)|^{n+1}} \right). \quad (6.23)$$

This is remarkable. It means that the complex instantons directly affect perturbation theory, even though they are not in the original path integral measure, which is a sum over all real paths. The close resemblance to the resurgent structure of the zero-dimensional analogue system [see Eq. (6.14)] strongly suggests once more that analytic continuation of path integrals may inherit resurgent structure.

Thus we would be tempted to define a path integral by its resurgent thimble expansion:

$$\int \mathcal{D}A e^{-\frac{1}{\hbar}S[A]} = \sum_{\text{thimbles } k} \mathcal{N}_k e^{-\frac{i}{\hbar}S_{\text{imag}}[A_k]} \int_{\Gamma_k} \mathcal{D}A e^{-\frac{1}{\hbar}S_{\text{real}}[A]} \quad (6.24)$$

where the sum over Lefschetz thimbles is the analogue of the sum over steepest descent contours, but now is a sum over functional steepest descents contours, or thimbles. This type of expansion is purely formal, but the previous two examples illustrate that there is some truth to it. We take this as motivation to formalize such expansions more rigorously.

7 Conclusion

In these lectures we have reviewed a number of different approaches to the general question of resurgent asymptotic expansions for spectral problems, using the Mathieu equation as a concrete example. We have found several interesting new facts, which we believe motivate a more rigorous mathematical analysis of these problems. We hope we have convinced the reader, both physicist and mathematician alike, that there are some interesting new features still lurking in this very old problem, waiting to be made more precise. One of the main conclusions is that there is more structure when one considers the eigenvalue u as a function of two variables, both the level/band/gap label N as well as the coupling \hbar . This has surprisingly close analogies with “large- N ” methods in physics [53]. This also motivates the problem of understanding better the mathematical properties of trans-series of more than one variable. The path integral interpretation of these results, and the close relation to multi-instanton calculus for quantum field theories (both supersymmetric and non-supersymmetric), encourages us to reconsider more seriously the question of defining an all-orders steepest descents expansion of path integrals. Some initial work along these lines has appeared recently [99].

ACKNOWLEDGEMENTS. We thank the organizers, in particular Frédéric Fauvet and David Sauzin, for organizing such an interesting workshop in such an inspiring location. We acknowledge support from the US DOE grants DE-SC0010339 (GD) and DE-SC0013036 (MÜ). M.Ü.’s work was partially supported by the Center for Mathematical Sciences and Applications at Harvard University.

References

- [1] J. ÉCALLE, “Les Fonctions Resurgentes”, Vols. I - III, Publ. Math. Orsay, 1981.
- [2] D. SAUZIN, “Resurgent Functions and Splitting Problems”, RIMS Kokyuroku 1493 (2005), 0706.0137.
- [3] O. COSTIN, “Asymptotics and Borel Summability”, Chapman & Hall/CRC, 2009.
- [4] E. DELABAERE, *Introduction to the Ecalle theory*, In: “Computer Algebra and Differential Equations”, **193**, London Math. Soc., Lecture Note Series, Cambridge University Press, 1994, 59.
- [5] B. Y. STERNIN and V. E. SHATALOV, “Borel-Laplace Transform and Asymptotic Theory: Introduction to Resurgent Analysis”, CRC, 1996.

- [6] E. T. WHITTAKER and G. N. WATSON, “A Course of Modern Analysis”, Cambridge Univ. Press, 1902.
- [7] S. GOLDSTEIN, *Mathieu functions*, Trans. Camb. Philos. Soc. **23** (1927), 303–336.
- [8] N. W. MCLACHLAN, “Theory and Application of Mathieu Functions”, Clarendon Press, Oxford, 1947.
- [9] J. MEIXNER and F. W. SCHÄPFKE, “Mathieusche Funktionen und Sphäroidfunktionen”, Springer-Verlag, Berlin, 1954.
- [10] W. MAGNUS and S. WINKLER, “Hill’s Equation”, John Wiley & Sons, New York, 1966.
- [11] G. WOLF, “Mathieu Functions and Hill’s Equation”, Chapter 28 of NIST Digital Library of Mathematical Functions, <http://dlmf.nist.gov/28>.
- [12] R. BALIAN, G. PARISI and A. VOROS, *Discrepancies from asymptotic series and their relation to complex classical trajectories*, Phys. Rev. Lett. **41** (1978), 1141; “Quartic Oscillator,” in Marseille 1978, Proceedings, *Feynman Path Integrals*.
- [13] E. B. BOGOMOLNY, *Calculation of instanton - anti-instanton contributions in quantum mechanics*, Phys. Lett. **B91** (1980), 431.
- [14] J. ZINN-JUSTIN, *Multi-instanton contributions in quantum mechanics*, Nucl. Phys. B **192** (1981), 125.
- [15] A. VOROS, *The return of the quartic oscillator. The complex WKB method*, Ann. de l’I. H. Poincaré, A **39** (1983), 211.
- [16] I. I. BALITSKY and A. V. YUNG, *Instanton molecular vacuum in $N=1$ supersymmetric quantum mechanics*, Nucl. Phys. B **274** (1986), 475.
- [17] J. ZINN-JUSTIN, “Quantum Field Theory and Critical Phenomena”, Oxford, 2002.
- [18] J. C. LE GUILLOU and J. ZINN-JUSTIN, “Large Order behavior of Perturbation Theory”, North-Holland, Amsterdam, 1990.
- [19] M. V. BERRY and C. J. HOWLS, “Hyperasymptotics”, Proc. R. Soc. A **430**, 653 (1990); “Hyperasymptotics for integrals with saddles”, Proc. R. Soc. A **434**, 657 (1991); M. V. BERRY, *Asymptotics, superasymptotics, hyperasymptotics ...*, In: *Asymptotics Beyond All Orders*, H. Segur *et al.* (eds.), Plenum Press, New York, 1991.
- [20] J-P. RAMIS, *Séries divergentes et théories asymptotiques*, In: “Séries divergentes et procédés de resommation”, Journées X UPS, July 1991.
- [21] E. DELABAERE, *Spectre de l’opérateur de Schrödinger stationnaire unidimensionnel à potentiel polynôme trigonométrique*, C. R. Acad. Sci. Paris **314** (1992), 807.

- [22] E. DELABAERE, H. DILLINGER and F. PHAM, *Exact semiclassical expansions for one-dimensional quantum oscillators*, J. Math. Phys. **38** (1997), 6126; E. DELABAERE and F. PHAM, *Resurgent methods in semi-classical asymptotics*, Ann. de l'I. H. Poincaré, A **71** (1999), 1.
- [23] T. AOKI, T. KAWAI and Y. TAKEI, *Algebraic analysis of singular perturbations: On exact WKB analysis*, RIMS-947; T. KAWAI and Y. TAKEI, *Secular equations through the exact WKB analysis*, RIMS, Kyoto University, 1991.
- [24] C. J. HOWLS, T. KAWAI and Y. TAKEI (eds.), "Towards the Exact WKB Analysis of Differential Equations, Linear or Non-Linear", Kyoto University Press, 1999.
- [25] O. COSTIN, *Exponential asymptotics, transseries, and generalized Borel summation for analytic rank one systems of ODE's*, IMRN **8**, (1995); O. COSTIN and M. D. KRUSKAL, *Optimal uniform estimates and rigorous asymptotics beyond all orders for a class of ODE's*, Proc. Roy. Soc. Lond. **452** (1996); O. COSTIN and M. D. KRUSKAL, *On optimal truncation of divergent series solutions of nonlinear differential systems; Berry smoothing*, Proc. R. Soc. Lond. A **455** (1999), 1931-1956.
- [26] M. MARINO, R. SCHIAPPA and M. WEISS, *Nonperturbative effects and the large-order behavior of matrix models and topological strings*, Commun. Num. Theor. Phys. **2** (2008), 349–419,
- [27] M. MARINO, R. SCHIAPPA and M. WEISS, *Multi-instantons and multi-cuts*, J. Math. Phys. **50** (2009), 052301.
- [28] S. PASQUETTI and R. SCHIAPPA, *Borel and Stokes nonperturbative phenomena in topological string theory and $c=1$ matrix models*, Annales Henri Poincaré **11** (2010), 351.
- [29] I. ANICETO, R. SCHIAPPA and M. VONK, *The resurgence of instantons in string theory*, Commun. Num. Theor. Phys. **6** (2012), 339–496.
- [30] M. MARIÑO, *Lectures on non-perturbative effects in large N gauge theories, matrix models and strings*, Fortsch. Phys. **62** (2014), 455–540.
- [31] P. C. ARGYRES and M. ÜNSAL, *The semi-classical expansion and resurgence in gauge theories: new perturbative, instanton, bion, and renormalon effects*, JHEP **1208** (2012), 063, [1206.1890]; P. ARGYRES and M. ÜNSAL, *A semiclassical realization of infrared renormalons*, Phys.Rev.Lett. **109** (2012), 121601, [arXiv:1204.1661].
- [32] G. V. DUNNE and M. ÜNSAL, *Continuity and Resurgence: towards a continuum definition of the $CP(N-1)$ model*, Phys.Rev.

- D87** (2013), 025015, [1210.3646 [hep-th]]; G. V. DUNNE and M. ÜNSAL, *Resurgence and trans-series in quantum field theory: the CP(N-1) model*, JHEP **1211** (2012), 170, [1210.2423 [hep-th]].
- [33] A. CHERMAN, D. DORIGONI, G. V. DUNNE and M. ÜNSAL, *Resurgence in quantum field theory: nonperturbative effects in the principal Chiral model*, Phys. Rev. Lett. **112** (2014), 021601, [1308.0127]; A. CHERMAN, D. DORIGONI and M. ÜNSAL, *Decoding perturbation theory using resurgence: Stokes phenomena, new saddle points and Lefschetz thimbles*, JHEP **1510** (2015), 056, [1403.1277 [hep-th]].
- [34] T. MISUMI, M. NITTA and N. SAKAI, *Neutral bions in the $\mathbb{C}P^{N-1}$ model*, JHEP **1406** (2014), 164, [1404.7225]; T. MISUMI, M. NITTA and N. SAKAI, *Classifying bions in Grassmann sigma models and non-Abelian gauge theories by D-branes*, PTEP **2015** (2015), 033B02, [1409.3444]; M. NITTA, *Fractional instantons and bions in the O(N) model with twisted boundary conditions*, JHEP **03** (2015), 108, [1412.7681].
- [35] I. ANICETO, J. G. RUSSO and R. SCHIAPPA, *Resurgent analysis of localizable observables in supersymmetric gauge theories*, JHEP **1503** (2015), 172, [1410.5834 [hep-th]].
- [36] R. COUSO-SANTAMARÍA, J. D. EDELSTEIN, R. SCHIAPPA and M. VONK, *Resurgent transseries and the holomorphic anomaly: nonperturbative closed strings in local $\mathbb{C}P^2$* , Commun. Math. Phys. **338** (2015), 285, [1407.4821 [hep-th]].
- [37] R. COUSO-SANTAMARÍA, R. SCHIAPPA and R. VAZ, *Finite N from resurgent large N*, Annals Phys. **356** (2015), 1, [1501.01007 [hep-th]].
- [38] G. BAŞAR and G. V. DUNNE, *Resurgence and the Nekrasov-Shatashvili limit: connecting weak and strong coupling in the Mathieu and Lamé systems*, JHEP **1502** (2015), 160, [1501.05671 [hep-th]].
- [39] G. V. DUNNE and M. ÜNSAL, *Resurgence and dynamics of O(N) and Grassmannian sigma models*, JHEP **1509** (2015), 199, [1505.07803 [hep-th]].
- [40] E. BREZIN, G. PARISI and J. ZINN-JUSTIN, *Perturbation theory at large orders for potential with degenerate minima*, Phys. Rev. D **16** (1977), 408.
- [41] M. STONE and J. REEVE, *Late terms in the asymptotic expansion for the energy levels of a periodic potential*, Phys. Rev. D **18** (1978), 4746.
- [42] J. ZINN-JUSTIN and U. D. JENTSCHURA, *Multi-instantons and exact results I: conjectures, WKB expansions, and instanton in-*

- teractions, *Annals Phys.* **313** (2004), 197, [quant-ph/0501136]; *Multi-instantons and exact results II: Specific cases, higher-order effects, and numerical calculations*, *Annals Phys.* **313** (2004), 269, [quant-ph/0501137].
- [43] M. UNSAL, *Theta dependence, sign problems and topological interference*, *Phys. Rev. D* **86** (2012), 105012, [1201.6426 [hep-th]].
- [44] A. I. VAINSHTEIN, *Decaying systems and divergence of perturbation theory*, Novosibirsk Report, December 1964, reprinted in Russian, with an English translation by M. Shifman, In: “Proceedings of QCD2002/ArkadyFest”, K. A. Olive *et al.* (eds.), World Scientific, Singapore, 2002.
- [45] C. M. BENDER and T. T. WU, *An harmonic oscillator*, *Phys. Rev.* **184** (1969), 1231; *Anharmonic oscillator 2: a study of perturbation theory in large order*, *Phys. Rev. D* **7** (1973), 1620.
- [46] I. ANICETO and R. SCHIAPPA, *Nonperturbative ambiguities and the reality of resurgent transseries*, *Commun. Math. Phys.* **335** (2015), 183, [1308.1115 [hep-th]].
- [47] C. KITTEL, “Introduction to Solid State Physics, Wiley, New York.
- [48] D. J. GROSS and E. WITTEN, *Possible third order phase transition in the large N lattice gauge theory*, *Phys. Rev. D* **21** (1980), 446.
- [49] S. R. WADIA, *A study of $U(N)$ lattice gauge theory in 2-dimensions*, 1212.2906 [hep-th], an edited version of unpublished 1979 preprint, EFI-79/44-CHICAGO; S. R. WADIA, *$N = \infty$ phase transition in a class of exactly soluble model lattice gauge theories*, *Phys. Lett. B* **93** (1980), 403.
- [50] H. NEUBERGER, *Nonperturbative contributions in models with a nonanalytic behavior at infinite N* , *Nucl. Phys. B* **179** (1981), 253.
- [51] D. J. GROSS and A. MATYTSIN, *Instanton induced large N phase transitions in two-dimensional and four-dimensional QCD*, *Nucl. Phys. B* **429** (1994), 50, [hep-th/9404004]; *Some properties of large N two-dimensional Yang-Mills theory*, *Nucl. Phys. B* **437** (1995), 541, [hep-th/9410054].
- [52] E. WITTEN, *On quantum gauge theories in two-dimensions*, *Commun. Math. Phys.* **141** (1991), 153.
- [53] M. MARIÑO, “Instantons and Large N : An Introduction to Non-Perturbative Methods in Quantum Field Theory”, Cambridge University Press, 2015.
- [54] G. V. DUNNE and M. ÜNSAL, *Uniform WKB, multi-instantons, and resurgent trans-series*, *Phys. Rev. D* **89** (2014), no. 10, 105009, [1401.5202 [hep-th]].

- [55] G. V. DUNNE and M. ÜNSAL, *Generating nonperturbative physics from perturbation theory*, Phys. Rev. D **89** (2014), no. 4, 041701, [1306.4405 [hep-th]].
- [56] N. HOE, B. D'ETAT, J. GRUMBERG, M. CABY, E. LÉBOUCHER and G. COULAUD, *Stark effect of hydrogenic ions*, Phys. Rev. A **25** (1982), 891.
- [57] G. ALVAREZ and C. CASARES, *Exponentially small corrections in the asymptotic expansion of the eigenvalues of the cubic anharmonic oscillator*, J. Phys. A: Math. Gen. **33** (2000), 5171; *Uniform asymptotic and JWKB expansions for anharmonic oscillators*, J. Phys. A: Math. Gen. **33** (2000), 2499.
- [58] G. ALVAREZ, C. J. HOWLS and H. J. SILVERSTONE, *Anharmonic oscillator discontinuity formulae up to second exponentially small order*, J. Phys. A: Math. Gen. **35** (2002), 4003.
- [59] T. MISUMI, M. NITTA and N. SAKAI, *Resurgence in sine-Gordon quantum mechanics: Exact agreement between multi-instantons and uniform WKB*, JHEP **1509** (2015), 157, [1507.00408 [hep-th]].
- [60] R. B. DINGLE and H. J. W. MÜLLER, *Asymptotic expansions of Mathieu functions and their characteristic numbers*, J. reine angew. Math. **211** (1962), 11.
- [61] M. A. ESCOBAR-RUIZ, E. SHURYAK and A. V. TURBINER, *Three-loop correction to the instanton density. II. The sine-Gordon potential*, Phys. Rev. D **92** (2015), no. 2, 025047, [1505.05115 [hep-th]]; *Three-loop correction to the instanton density. I. The quartic double well potential*, Phys. Rev. D **92** (2015), no. 2, 025046 [1501.03993 [hep-th]].
- [62] S. COLEMAN, "Aspects of Symmetry: Selected Erice Lectures", Cambridge University Press, 1988.
- [63] H. NEUBERGER, *Semiclassical calculation of the energy dispersion relation in the valence band of the quantum pendulum*, Phys. Rev. D **17** (1978), 498.
- [64] B. DE WIT and G. 'T HOOFT, *Nonconvergence of the $1/N$ expansion for $SU(N)$ gauge fields on a lattice*, Phys. Lett. B **69** (1977), 61.
- [65] YA. GOLDSCHMIDT, *$1/N$ expansion in two-dimensional lattice gauge theory*, J. Math. Phys. **21** (1980), 1842.
- [66] S. SAMUEL, *$u(n)$ integrals, $1/n$, and the Dewit-'t Hooft anomalies*, J. Math. Phys. **21** (1980), 2695.
- [67] G. BAŞAR, G. V. DUNNE and M. ÜNSAL, to appear.

- [68] A. M. DYKHNE, *Quasiclassical particles in a one-dimensional periodic potential*, Sov. Phys. JETP **13** (1961), 999 [J. Exptl. Theoret. Phys. **40**, 1423 (1961)].
- [69] M. I. WEINSTEIN and J. B. KELLER, *Hill's equation with a large potential*, SIAM J. Appl. Math. **45** (1985), 200; *Asymptotic behavior of stability regions for Hill's equation*, SIAM J. Appl. Math. **47** (1987), 941.
- [70] J. N. L. CONNOR, T. UZER, R. A. MARCUS and A. D. SMITH, *Eigenvalues of the Schrödinger equation for a periodic potential with nonperiodic boundary conditions: A uniform semiclassical analysis*, J. Chem. Phys. **80** (1984), 5095.
- [71] J. B. KELLER, *Discriminant, transmission coefficient, and stability bands of Hill's equation*, J. Math. Phys. **25** (1984), 2903.
- [72] K. W. FORD, D. L. HILL, M. WAKANO and J. A. WHEELER, *Quantum effects near a barrier maximum*, Ann. Phys. **7** (1959), 239.
- [73] R. E. LANGER, *The asymptotic solutions of certain linear ordinary differential equations of the second order*, Trans. Am. Math. Soc. **36** (1934), 90.
- [74] T. M. CHERRY, *Expansions in terms of parabolic cylinder functions*, Proc. Edinburgh Math. Soc. **8** (1948), 50.
- [75] S. C. MILLER and R. H. GOOD, *A WKB-type approximation to the Schrödinger equation*, Phys. Rev. **91** (1953), 174.
- [76] G. ÁLVAREZ, *Langer-Cherry derivation of the multi-instanton expansion for the symmetric double well*, J. Math. Phys. **45** (2004), 3095.
- [77] E. M. HARRELL, *The band-structure of a one-dimensional, periodic system in a scaling limit*, Ann. Phys. **119** (1979), 351.
- [78] J. AVRON and B. SIMON, *The asymptotics of the gap in the Mathieu equation*, Ann. Phys. **134** (1981), 76.
- [79] K. KONISHI and G. PAFFUTI, "Quantum Mechanics: A New Introduction", Oxford University Press, 2009.
- [80] C. M. BENDER and S. ORZSAG, "Advanced Mathematical Methods for Scientists and Engineers", Wiley, New York, 1999.
- [81] D. J. BROADHURST, R. DELBOURGO and D. KREIMER, *Unknotting the polarized vacuum of quenched QED*, Phys. Lett. B **366** (1996), 421, [hep-ph/9509296]; D. J. BROADHURST and D. KREIMER, *Association of multiple zeta values with positive knots via Feynman diagrams up to 9 loops*, Phys. Lett. B **393** (1997), 403, [hep-th/9609128].
- [82] R. B. DINGLE, "Asymptotic Expansions: their Derivation and Interpretation", Academic Press, 1973.

- [83] N. A. NEKRASOV and S. L. SHATASHVILI, *Quantization of integrable systems and four dimensional gauge theories*, In: “Proceedings of 16th International Congress on Mathematical Physics”, P. Exner (ed.), World Scientific, 2010, 0908.4052 [hep-th].
- [84] A. MIRONOV and A. MOROZOV, *Nekrasov functions and exact Bohr-Zommerfeld integrals*, JHEP **1004** (2010), 040, 0910.5670 [hep-th].
- [85] W. HE and Y. G. MIAO, *Magnetic expansion of Nekrasov theory: the $SU(2)$ pure gauge theory*, Phys. Rev. D **82** (2010), 025020, 1006.1214 [hep-th].
- [86] M. X. HUANG, A. K. KASHANI-POOR and A. KLEMM, *The Ω deformed B-model for rigid $\mathcal{N} = 2$ theories*, Annales Henri Poincaré **14** (2013), 425, 1109.5728 [hep-th]; M. X. HUANG, *On Gauge Theory and Topological String in Nekrasov-Shatashvili Limit*, JHEP **1206** (2012), 152, 1205.3652 [hep-th].
- [87] A. K. KASHANI-POOR and J. TROOST, *The toroidal block and the genus expansion*, JHEP **1303** (2013), 133, 1212.0722 [hep-th]; *Pure $\mathcal{N} = 2$ super Yang-Mills and exact WKB*, JHEP **1508** (2015), 160, 1504.08324 [hep-th].
- [88] D. KREFL, *Non-perturbative quantum geometry*, JHEP **1402** (2014), 084, 1311.0584 [hep-th]; *Non-perturbative quantum geometry II*, JHEP **1412** (2014), 118, 1410.7116 [hep-th].
- [89] A. GORSKY and A. MILEKHIN, *RG-Whitham dynamics and complex Hamiltonian systems*, Nucl. Phys. B **895** (2015), 33, 1408.0425 [hep-th].
- [90] J. L. DUNHAM, *The Wentzel-Brillouin-Kramers method of solving the wave equation*, Phys. Rev. **41** (1932), 713.
- [91] M. V. FEDORYUK, *The saddle-point method*, Izdat. “Nauka,” Moscow, MR 58:22580 (1977).
- [92] V. L. ARNOLD, A. N. VARCHENKO and S. M. GUSEIN-ZADE, “Singularities of Differentiable Maps. Volume 2, Monodromy and Asymptotics of Integrals”, “Nauka”, Moscow, 1984 (Russian), English transl., Birkhäuser, Basel, 1988.
- [93] F. PHAM, *Vanishing homologies and the n variable saddlepoint method*, Proc. Symp. Pure Math. **2** (1983), no. 40, 319–333.
- [94] E. DELABAERE and C. J. HOWLS, *Global asymptotics for multiple integrals with boundaries*, Duke Math. J. **112** (2002), 199–264.
- [95] E. WITTEN, *A new look at the path integral of quantum mechanics*, <http://arxiv.org/abs/1009.6032> arXiv:1009.6032.
E. WITTEN, *Analytic continuation of Chern-Simons theory*, AMS/

- IP Stud. Adv. Math. **50** (2011), 347–446,
[<http://arxiv.org/abs/1001.2933>arXiv:1001.2933].
- [96] G. GURALNIK and Z. GURALNIK, *Complexified path integrals and the phases of quantum field theory*, Annals Phys. **325** (2010), 2486–2498, [0710.1256]
- [97] M. KONTSEVICH, “Resurgence from the Path Integral Perspective”, Talk at Perimeter Institute, 2012; “Exponential Integrals”, Talks at Simons Center and at IHES, 2014, 2015; “On Non-perturbative Quantization, Fukaya Categories and Resurgence”, Talk at Simons Center, 2015.
- [98] G. BAŞAR, G. V. DUNNE and M. ÜNSAL, *Resurgence theory, ghost-instantons, and analytic continuation of path integrals*, JHEP **1310** (2013), 041, [1308.1108 [hep-th]].
- [99] A. BEHTASH, G. V. DUNNE, T. SCHAEFER, T. SULEJMANPASIC and M. ÜNSAL, *Complexified path integrals, exact saddles and supersymmetry*, Phys. Rev. Lett. **116** (2016), 011601 [1510.00978 [hep-th]]; *Toward Picard-Lefschetz theory of path integrals, complex saddles and resurgence*, Annals of Mathematical Sciences and Applications **2** (2017), 95–212. 1510.03435 [hep-th].

Renormalised conical zeta values

Li Guo, Sylvie Paycha and Bin Zhang

Abstract. Conical zeta values associated with rational convex polyhedral cones generalise multiple zeta values. We renormalise conical zeta values at poles by means of a generalisation of Connes and Kreimer's Algebraic Birkhoff Factorisation. This paper serves as a motivation for and an application of this generalised renormalisation scheme. The latter also yields an Euler-Maclaurin formula on rational convex polyhedral lattice cones which relates exponential sums to exponential integrals. When restricted to Chen cones, it reduces to Connes and Kreimer's Algebraic Birkhoff Factorisation for maps with values in the algebra of ordinary meromorphic functions in one variable.

1 Introduction

Multiple zeta values (MZVs) are special values of the multiple zeta function at integral arguments. Their study which has been very active for over two decades arose interest from both mathematics and physics. At arguments where the multiple zeta functions are divergent, renormalisation methods borrowed from quantum field theory have been adapted to extract information from the divergence, including the stuffle and/or shuffle relations known to be satisfied by convergent MZVs. See for example [4,10,14,16]. MZVs were generalised by Terasoma [15] to conical zeta values (CZVs) which were studied in [6,12,15,17,18] in the contexts of cyclotomic multiple zeta values and Witten multiple zeta values.

To a rational convex polyhedral cone $C \subset \mathbb{R}^k$ and the interior C° of C , one assigns the conical zeta value (CZV)¹

$$\zeta(C; \vec{s}) := \zeta^\circ(C; \vec{s}) := \sum_{(n_1, \dots, n_k) \in C^\circ \cap \mathbb{Z}^k} n_1^{-s_1} \cdots n_k^{-s_k}$$

¹ This definition differs from Terasoma's in [15] by the fact that we do not take linear combinations amongst the n_j 's, however it can easily be shown that the two definitions generate the same sets of CZVs.

at $\vec{s} = (s_1, \dots, s_k) \in \mathbb{Z}^k$ if the series is convergent. Here the stuffle and shuffle relations of MZVs are replaced by the open and closed subdivision properties discussed in [6]. We investigate divergent CZVs along the lines of the renormalisation methods implemented in previous works to study divergent MZVs.

More precisely, the purpose of this paper is threefold, we

- (a) regularise the corresponding divergent expressions at $s_i \leq 0$ by means of a Laplace-type regularisation:

$$(\varepsilon_1, \dots, \varepsilon_k) \mapsto \sum_{(n_1, \dots, n_k) \in C^\circ \cap \mathbb{Z}^k} \frac{e^{\varepsilon_1 n_1 + \dots + \varepsilon_k n_k}}{n_1^{s_1} \dots n_k^{s_k}};$$

- (b) justify the need for a multivariate regularisation, the usual single variable regularisation ($\varepsilon_i = \lambda_i \varepsilon$) being too restrictive to be implemented on all cones;
- (c) compare the multivariate and univariate approach for Chen cones, where the CZVs amount to MZVs.

A natural idea is to apply Connes and Kreimer's Algebraic Birkhoff Factorisation [2], see also [13]. One of the main ingredients needed for such a factorisation is a coalgebra structure on the source space - here the space of lattice cones - of the maps to be renormalised. In [8] we showed that the space of lattice cones carries a cograded, coaugmented, connected coalgebra structure; in the present paper, we show that this coalgebra can be enlarged to a differential coalgebra structure (Theorem 3.5).

Due to the geometric nature of convex cones, which is reflected in the specific coproduct built on the corresponding space of lattice cones, one cannot implement a univariate regularisation, namely one depending on a single parameter ε , as Connes and Kreimer did in their Algebraic Birkhoff Factorisation on Feynman graphs. The coproduct we use involves transverse cones built by means of an orthogonal projection, so we need a regularisation procedure which can be implemented for all cones under consideration, as well as their faces, together with the transverse cones to their faces. For a small enough family of lattice cones, such as the family of lattice Chen cones (see Equation 3.3), their faces and the transverse lattice cones to their faces, one can use a univariate regularisation, in which case the regularised maps take values in Laurent series. Connes and Kreimer's Algebraic Birkhoff Factorisation can then be applied to the coalgebra of lattice cones modulo a minor adjustment due to the absence of a product on the space of such cones. However, to deal with general convex cones and the transverse cones to their faces, we need (Remark 4.1) a multivariate regularisation (Equation (5.1)) which

involves a vector parameter $\vec{\varepsilon} = (\varepsilon_1, \dots, \varepsilon_k) \in \mathbb{C}^k$. The regularised maps we build this way take values in the space of multivariate meromorphic germs at zero with linear poles (Proposition-Definition 5.4), which we investigated in [7].

Specifically, to renormalise divergent CZVs associated to lattice cones (C, Λ) , we implement a generalisation (Theorem 2.5) of Connes and Kreimer's Algebraic Birkhoff Factorisation device [2] to the map on the coalgebra of lattice cones defined by an exponential sum $S(C, \Lambda)$ on the lattice cones (C, Λ) . The generalised Algebraic Birkhoff Factorisation carried out in [8] applies to maps with a

- source space that is not any longer a Hopf algebra needed to handle exponential sums acting on the colagebra of lattice cones, which is only equipped with a partial product,
- target space that is not any longer a Rota-Baxter algebra required to handle exponential sums with values in the algebra of multivariate meromorphic functions.

In the present paper, we further generalise the coalgebra of cones on which we implement the Algebraic Birkhoff Factorisation equipping it with an additional differential structures. Indeed, in view of renormalising CZVs, not only do we need to renormalise the exponential sums but also their derivatives with respect to the regularisation parameter. Hence the need for an additional differential structure which comes with a decoration \vec{s} leading to decorated (open) lattice cones $((C, \Lambda); \vec{s})$ (compare with Definition 2.8 in [6]).

This renormalisation procedure (Theorem 5.7) implemented on the exponential sums $S((C, \Lambda); \vec{s})$ associated with decorated lattice cones $((C, \Lambda); \vec{s})$ implies an Euler-Maclaurin formula (Equation 6.1) on lattice cones [8] which relates exponential sums to the corresponding exponential integrals. The renormalised CZV $\zeta^{\text{ren}}((C, \Lambda), \vec{s})$ associated with a decorated lattice cone $((C, \Lambda); \vec{s})$ are derived (Equation (4.2)) from the factors entering the factorisation formula of the associated exponential sum $S((C, \Lambda); \vec{s})$.

On the smaller coalgebra of lattice Chen cones, the multivariate regularisation procedure implemented on the algebra of all convex lattice cones, can be reduced to a univariate regularisation procedure by specifying one direction of regularisation $\vec{\varepsilon} := \vec{a} \varepsilon$ for some fixed vector \vec{a} . Then (Proposition 6.2) our renormalisation procedure amounts to the usual Algebraic Birkhoff Factorisation on the maps given by the exponential sums on the lattice cones, with values in Laurent series, thus independent of the choice of the direction \vec{a} . As a by-product, our geometric renormalisation procedure therefore yields renormalised MZVs at negative integers

as the special case of renormalised CZVs associated with lattice Chen cones. However, these renormalised MZVs do not satisfy the stuffle relations [9] due to the use of the coproduct on Chen cones which involves an orthogonal complement map. Thus, the renormalised MZVs we obtain here by a geometric approach as particular instances of CZVs differ from the ones derived in [14] and [10] by an alternative algebro-combinatorial approach. As observed in [8], the renormalised CZVs derived here by means of a multivariate Algebraic Birkhoff Factorisation, can alternatively be derived directly from the derivatives of the exponential sums on cones by means of the projection onto the holomorphic part of the meromorphic germs they give rise to. In this respect, the multivariate parametrisation approach – imposed here by the geometric nature of the cones – bares over the univariate one, the advantage that renormalisation then amounts to a projection on the target space of multivariate meromorphic germs without the need for an Algebraic Birkhoff Factorisation. So, not only is the multivariate approach necessary when dealing with the space of all cones, but it is also very useful in so far as it suggests a possible way to circumvent the use of an Algebraic Birkhoff Factorisation.

2 Generalised Algebraic Birkhoff Factorisation

Let us first recall the Algebraic Birkhoff Factorisation of Connes and Kreimer’s renormalisation scheme [2], which we shall then generalise in order to later renormalise divergent CZVs.

Theorem 2.1. *Let H be a commutative connected graded Hopf algebra and (R, P) be a Rota-Baxter algebra of weight -1 , $\varphi : H \rightarrow R$ be an algebra homomorphism.*

- (a) *There are algebra homomorphisms $\varphi_- : H \rightarrow \mathbf{k} + P(R)$ and $\varphi_+ : H \rightarrow \mathbf{k} + (\text{id} - P)(R)$ such that*

$$\varphi = \varphi_-^{*(-1)} * \varphi_+. \quad (2.1)$$

Here $\varphi_-^{(-1)}$ is the inverse of φ_- with respect to the convolution product.*

- (b) *If P is idempotent: $P^2 = P$, then the decomposition in (a) is unique.*

It is easy to see that P is a Rota-Baxter operator of weight -1 if and only if $\text{id} - P$ is and P is idempotent if and only if $\text{id} - P$ is. Thus by exchanging P and $\text{id} - P$, we obtain a variation of the Algebraic Birkhoff Factorisation in Theorem 2.1 [3]:

$$\varphi = \tilde{\varphi}_+^{*(-1)} * \tilde{\varphi}_-, \quad (2.2)$$

where $\tilde{\varphi}_+ : H \rightarrow \mathbf{k} + (\text{id} - P)(R)$ and $\tilde{\varphi}_- : H \rightarrow \mathbf{k} + P(R)$.

On the one hand, in [8], we generalised the Algebraic Birkhoff Factorisation of Connes-Kreimer’s renormalisation scheme for connected coalgebras without the need for either a Hopf algebra in the source or a Rota-Baxter algebra in the target. On the other hand, we provided the following differential variant in [11].

Theorem 2.2. *If (H, d) is in addition a differential Hopf algebra (R, P, ∂) is a commutative differential Rota-Baxter algebra, and φ is a differential algebra homomorphism, then φ_- and φ_+ are also differential algebra homomorphisms.*

In order to explore the structure of renormalised CZVs, we combine these two generalisations.

Definition 2.3. A **differential cograded, coaugmented, connected coalgebra** is a cograded, coaugmented, connected coalgebra $(\mathbf{C} = \bigoplus_{n \geq 0} \mathbf{C}^{(n)}, \Delta, \varepsilon, u)$ with linear maps $\delta_\sigma : \mathbf{C} \rightarrow \mathbf{C}$ for σ in an index set Σ such that

$$\begin{aligned} \Delta \delta_\sigma &= (\text{id} \otimes \delta_\sigma + \delta_\sigma \otimes \text{id}) \Delta, \\ \delta_\sigma(\mathbf{C}^{(n)}) &\subseteq \mathbf{C}^{(n+1)}, \\ \delta_\sigma \delta_\tau &= \delta_\tau \delta_\sigma, \\ \sigma, \tau &\in \Sigma. \end{aligned} \tag{2.3}$$

The linear maps $\delta_\sigma, \sigma \in \Sigma$, are called **coderivations** on \mathbf{C} .

It follows from the definition that δ_σ stabilises $\ker \varepsilon$. Recall the counit property of ε for Δ :

$$\beta_\ell = (\varepsilon \otimes \text{id})\Delta, \quad \beta_r = (\text{id} \otimes \varepsilon)\Delta, \tag{2.4}$$

where

$$\beta_\ell : \mathbf{C} \rightarrow \mathbf{k} \otimes \mathbf{C}, x \mapsto 1 \otimes x, \quad \beta_r : \mathbf{C} \rightarrow \mathbf{C} \otimes \mathbf{k}, x \mapsto x \otimes 1,$$

with

$$\beta_\ell^{-1} : \mathbf{k} \otimes \mathbf{C} \rightarrow \mathbf{C}, a \otimes x \mapsto ax, \quad \beta_r^{-1} : \mathbf{C} \otimes \mathbf{k} \rightarrow \mathbf{C}, x \otimes a \mapsto ax.$$

Lemma 2.4. *For a differential cograded, coaugmented, connected coalgebra $(\mathbf{C}, \Delta, \varepsilon, u)$ with coderivations $\delta_\sigma, \sigma \in \Sigma$, we have $\varepsilon \delta_\sigma = 0$.*

Proof. Apply $\varepsilon \otimes \varepsilon$ to the two sides of the identity $\Delta \delta_\sigma = (\text{id} \otimes \delta_\sigma + \delta_\sigma \otimes \text{id})\Delta$. By the counit property in Equation (2.4), on the left hand side we have

$$(\varepsilon \otimes \varepsilon)\Delta \delta_\sigma = (\varepsilon \otimes \text{id})(\text{id} \otimes \varepsilon)\Delta \delta_\sigma = (\varepsilon \otimes \text{id})\beta_r \delta_\sigma = (\varepsilon \delta_\sigma \otimes \text{id})\beta_r.$$

Similarly on the right hand side we have

$$\begin{aligned} (\varepsilon \otimes \varepsilon)(\text{id} \otimes \delta_\sigma + \delta_\sigma \otimes \text{id})\Delta &= (\varepsilon \otimes \varepsilon \delta_\sigma)\Delta + (\varepsilon \delta_\sigma \otimes \varepsilon)\Delta \\ &= (1 \otimes \varepsilon \delta_\sigma)\beta_\ell + (\varepsilon \delta_\sigma \otimes 1)\beta_r. \end{aligned}$$

Thus we obtain $(1 \otimes \varepsilon \delta_\sigma)\beta_\ell = 0$. Hence $\varepsilon \delta_\sigma = 0$. \square

As we shall argue later on, the renormalisation of CZVs requires the following generalised version of the Algebraic Birkhoff Factorisation and its differential variant to connected coalgebras in the source space, which are not necessarily Hopf algebras, and algebras in the target space which are not necessarily Rota-Baxter algebras. Further, we will generalise the the variation of Algebraic Birkhoff Factorisation in Equation (2.2) in order to derive the Euler-Maclaurin formula in Section 5.2.

Theorem 2.5. *Let $\mathbf{C} = \bigoplus_{n \geq 0} \mathbf{C}^{(n)}$ be a differential cograded, coaugmented, connected coalgebra with coderivations $\delta_\sigma, \sigma \in \Sigma$. Let A be a unitary differential algebra with derivations $\partial_\sigma, \sigma \in \Sigma$. Let $A = A_1 \oplus A_2$ be a linear decomposition such that $1_A \in A_1$ and*

$$\partial_\sigma(A_i) \subseteq A_i, \quad i = 1, 2, \quad \sigma \in \Sigma.$$

Let P be the projection of A to A_1 along A_2 and the set $\mathcal{G}(\mathbf{C}, A)$ of linear maps $\varphi : \mathbf{C} \rightarrow A$ such that $\varphi(\mathbf{I}) = 1_A$ where $\mathbf{I} = u(1)$. Given $\varphi \in \mathcal{G}(\mathbf{C}, A)$ such that $\partial_\sigma \varphi = \varphi \delta_\sigma, \sigma \in \Sigma$, define maps $\varphi_i \in \mathcal{G}(\mathbf{C}, A), i = 1, 2$, by the following recursive formulae on $\ker \varepsilon$:

$$\varphi_1(x) = -P\left(\varphi(x) + \sum_{(x)} \varphi_1(x')\varphi(x'')\right), \quad (2.5)$$

$$\varphi_2(x) = (\text{id}_A - P)\left(\varphi(x) + \sum_{(x)} \varphi_1(x')\varphi(x'')\right). \quad (2.6)$$

Here $\sum_{(x)} x' \otimes x'' := \Delta(x) - | \otimes x - x \otimes |$ is the reduced coproduct.

- (a) We have $\varphi_i(\ker \varepsilon) \subseteq A_i$ (hence $\varphi_i : \mathbf{C} \rightarrow \mathbf{k}1_A + A_i$ with $\varphi_i(\mathbf{I}) = 1_A$) and $\delta_\sigma \varphi_i = \varphi_i \delta_\sigma, i = 1, 2, \sigma \in \Sigma$. Moreover,

$$\varphi = \varphi_1^{*(-1)} * \varphi_2 \quad (2.7)$$

- (b) φ_1 and φ_2 are the unique maps in $\mathcal{G}(\mathbf{C}, A)$ such that $\varphi_i(\ker \varepsilon) \subseteq A_i$ for $i = 1, 2$, and Equation (2.7) holds.
(c) If moreover A_1 is a subalgebra of A then $\varphi_1^{*(-1)}$ lies in $\mathcal{G}(\mathbf{C}, A_1)$.

Remark 2.6.

- With the notations of Theorem 2.1, we observe that Equation (2.7) with $\varphi_1 = \varphi_-$ yields Equation (2.1) usually seen in the literature whereas setting $\varphi_1 = \varphi_+$ amounts to Equation (2.2), which we will apply in Section 5.2.
- When the coderivations δ_σ and derivations ∂_σ , $\sigma \in \Sigma$, are taken to be the zero maps, we obtain the generalisation [8, Theorem 4.4] of the Algebraic Birkhoff Factorisation of Connes and Kreimer [2] which does not involve the differential structure, for maps from a connected coalgebra (which is not necessarily equipped with a product) to a decomposable unitary algebra (which does not necessarily decompose into a sum of two subalgebras). This also generalises the differential Algebraic Birkhoff Factorisation in [11].

Proof. The proof follows the same argument as the one for [8, Theorem 4.4] and will be omitted. \square

3 A differential coalgebraic structure on lattice cones

We now apply the general setup in the last section to lattice cones.

3.1 Lattice cones

We begin with recalling the notion and basic properties of lattice cones. See [8] for details. In a finite dimensional real vector space, a **lattice** is a finitely generated subgroup which spans the whole space over \mathbb{R} . Such a pair, namely a real vector space equipped with a lattice is called a **lattice vector space**. Let $V_1 \subset V_2 \subset \dots$ be a family of finite dimensional real vector spaces, and let Λ_k be a lattice in V_k such that $\Lambda_k = \Lambda_{k+1} \cap V_k$. The vector space $V := \bigcup_{k=1}^{\infty} V_k$ and the corresponding lattice $\Lambda := \bigcup_{k=1}^{\infty} \Lambda_k$ are equipped with their natural filtration. Such a pair (V, Λ) is called a **filtered lattice space**. Usually we work in $(\mathbb{R}^\infty, \mathbb{Z}^\infty)$ with $V_k = \mathbb{R}^k$, Λ_k the standard lattice \mathbb{Z}^k , and $\{e_1, e_2, \dots\}$ the standard basis.

For a filtered lattice space (V, Λ) , a point/vector in Λ is called a **lattice point/vector**, a rational multiple of an integer point/vector is called a **rational lattice point/vector**.

For a subset S of V , let $\text{lin}(S)$ denote its \mathbb{R} -linear span. In this paper, we only consider subspaces of V spanned by rational lattice vectors.

Let $V := \bigcup_{k \geq 1} V_k$ with $\Lambda = \bigcup_{k \geq 1} \Lambda_k$ be a filtered lattice space. An **inner product** $Q(\cdot, \cdot) = (\cdot, \cdot)$ on V is a sequence of inner products

$$Q_k(\cdot, \cdot) = (\cdot, \cdot)_k : V_k \otimes V_k \rightarrow \mathbb{R}, \quad k \geq 1,$$

that is compatible with the inclusion $j_k : V_k \hookrightarrow V_{k+1}$ and whose restriction to $\Lambda \otimes \mathbb{Q}$ and hence Λ takes values in \mathbb{Q} . A filtered lattice space together with an inner product is called a **filtered lattice Euclidean space**.

Let L be a subspace of V_k . Set

$$L^{\perp_k^Q} := \{v \in V_k \mid Q_k(v, u) = 0 \text{ for all } u \in L\}.$$

The inner product Q_k gives the direct sum decomposition $V_k = L \oplus L^{\perp_k^Q}$ and hence the orthogonal projection

$$\pi_{k, L^\perp}^Q : V_k \rightarrow L^{\perp_k^Q} \tag{3.1}$$

along L as well as an isomorphism

$$\iota_{k, L}^Q : V_k/L \rightarrow L^{\perp_k^Q}.$$

Also, the induced isomorphism $Q_k^* : V_k \rightarrow V_k^*$ yields an embedding $V_k^* \hookrightarrow V_{k+1}^*$. We refer to the direct limit $V^{\otimes} := \bigcup_{k=1}^\infty V_k^* = \varinjlim V_k^*$ as the **filtered dual space** of V . We henceforth take $V_k = \mathbb{R}^k$ and fix an inner product $Q(\cdot, \cdot) = (\cdot, \cdot)$ on V^{\otimes} dropping the superscript Q to simplify notations.

We collect basic definitions and facts on lattice cones that will be used in this paper, see [6] for a detailed discussion.

- (a) By a **cone** in V_k we mean a **closed convex (polyhedral) cone** in V_k , namely the convex set

$$\langle v_1, \dots, v_n \rangle := \mathbb{R}\{v_1, \dots, v_n\} = \mathbb{R}_{\geq 0}v_1 + \dots + \mathbb{R}_{\geq 0}v_n, \tag{3.2}$$

where $v_i \in V_k, i = 1, \dots, n$.

- (b) A cone is called **rational** if the v_i 's in Equation (3.2) are in Λ_k . This is equivalent to requiring that the vectors are in $\Lambda_k \otimes \mathbb{Q}$.
- (c) A **subdivision** of a cone C is a set $\underline{C} = \{C_1, \dots, C_r\}$ of cones such that
 - (i) $C = \bigcup_{i=1}^r C_i$,
 - (ii) C_1, \dots, C_r have the same dimension as C , and
 - (iii) C_1, \dots, C_r intersect along their faces, *i.e.*, $C_i \cap C_j$ is a face of both C_i and C_j .

We will use $\mathcal{F}^o(\underline{C})$ denote the set of faces of C_1, \dots, C_r that are not contained in any proper face of C .

- (d) A **lattice cone** in V_k is a pair (C, Λ_C) with C a cone in V_k and Λ_C a lattice in $\text{lin}(C)$ generated by rational vectors.

- (e) A **face** of a lattice cone (C, Λ_C) is the lattice cone (F, Λ_F) where F is a face of C and $\Lambda_F := \Lambda_C \cap \text{lin}(F)$.
- (f) A **primary generating set** of a lattice cone (C, Λ_C) is a generating set $\{v_1, \dots, v_n\}$ of C such that
- (i) $v_i \in \Lambda_C, i = 1, \dots, n$,
 - (ii) there is no real number $r_i \in (0, 1)$ such that $r_i v_i$ lies in Λ_C , and
 - (iii) none of the generating vectors v_i is a positive linear combination of the others.
- (g) A lattice cone (C, Λ_C) is called **strongly convex** (resp. **simplicial**) if C is. A lattice cone (C, Λ_C) is called **smooth** if the additive monoid $\Lambda_C \cap C$ has a monoid basis. In other words, there are linearly independent rational lattice vectors v_1, \dots, v_ℓ such that $\Lambda_C \cap C = \mathbb{Z}_{\geq 0}\{v_1, \dots, v_\ell\}$.
- (h) A Chen cone is a smooth cone in \mathbb{R}^∞ of the form

$$C_k^{\text{Chen}} := \langle e_1, e_1 + e_2, \dots, e_1 + \dots + e_k \rangle. \quad (3.3)$$

Note that the faces of a Chen cone $\langle e_1, e_1 + e_2, \dots, e_1 + \dots + e_k \rangle$ are of the form $\langle e_1 + \dots + e_{i_1}, e_1 + \dots + e_{i_2}, \dots, e_1 + \dots + e_{i_l} \rangle$ for some indices $1 \leq i_1 < \dots < i_l \leq k$, so they are not Chen cones in general.

- (i) A **subdivision** of a lattice cone (C, Λ_C) is a set of lattice cones $\{(C_i, \Lambda_{C_i}) \mid 1 \leq i \leq r\}$ such that $\{C_i \mid 1 \leq i \leq r\}$ is a subdivision of C and $\Lambda_{C_i} = \Lambda_C$ for all $1 \leq i \leq r$.
- (j) Let F be a face of a cone $C \subseteq V_k$. The **transverse cone** $t(C, F)$ to F is the projection $\pi_{k, F^\perp}(C)$ of C in $\text{lin}(F)^\perp \subseteq V_k$, where $\pi_{k, F^\perp} = \pi_{k, \text{lin}(F)^\perp}$.
- (k) Let (F, Λ_F) be a face of the lattice cone (C, Λ_C) . The **transverse lattice cone** $(t(C, F), \Lambda_{t(C, F)})$ along the face (F, Λ_F) is the projection of (C, Λ_C) on $\text{lin}(F)^\perp \subseteq V_k$. More precisely,

$$(t(C, F), \Lambda_{t(C, F)}) := (\pi_{k, F^\perp}(C), \pi_{k, F^\perp}(\Lambda_C)). \quad (3.4)$$

We also use the notation $t((C, \Lambda_C), (F, \Lambda_F))$ to denote the transverse lattice cone.

As in the case of ordinary cones, we have the following property which will later be used to extend by linearity the exponential sum from smooth lattice cones to any lattice cone, it generalises known results for ordinary cones, see, e.g. [5, Example 2, page 48].

Proposition 3.1. *Any lattice cone can be subdivided into smooth lattice cones.*

Proposition 3.2. [8] *Transverse cones enjoy the following properties. Let F be a face of a cone C .*

- (a) **(Transitivity)** $t(C, F) = t(t(C, F'), t(F, F'))$ if F' is a face of F .
- (b) **(Compatibility with the partial order)** We have $\{H \preceq t(C, F)\} = \{t(G, F) \mid F \leq G \leq C\}$.
- (c) **(Compatibility with the dimension filtration)** $\dim(C) = \dim(F) + \dim(t(C, F))$ for any face F of C .

To the first two properties, there are corresponding properties for lattice cones:

- (d) **(Transitivity)** $t((C, \Lambda_C), (F, \Lambda_F)) = t(t((C, \Lambda_C), (F', \Lambda_{F'})), t((F, \Lambda_F), (F', \Lambda_{F'})))$ if $(F', \Lambda_{F'})$ is a face of (F, Λ_F) .
- (e) **(Compatibility with the partial order)** We have

$$\begin{aligned} & \{(H, \Lambda_H) \preceq t((C, \Lambda_C), (F, \Lambda_F))\} \\ & = \{t((G, \Lambda_G), (F, \Lambda_F)) \mid (F, \Lambda_F) \preceq (G, \Lambda_G) \preceq (C, \Lambda_C)\}. \end{aligned}$$

3.2 The coalgebra of lattice cones

Let \mathfrak{C}_k denote the set of lattice cones in V_k , $k \geq 1$. The natural inclusions $\mathfrak{C}_k \rightarrow \mathfrak{C}_{k+1}$ induced by the natural inclusions $V_k \rightarrow V_{k+1}$, $\Lambda_k \rightarrow \Lambda_{k+1}$, $k \geq 1$, give rise to the direct limit $\mathfrak{C} = \varinjlim \mathfrak{C}_k = \cup_{k \geq 1} \mathfrak{C}_k$.

We equip the \mathbb{Q} -linear space $\mathbb{Q}\mathfrak{C}$ generated by \mathfrak{C} with a coproduct by means of transverse lattice cones [8]. The maps

$$\begin{aligned} \Delta : \mathbb{Q}\mathfrak{C} &\longrightarrow \mathbb{Q}\mathfrak{C} \otimes \mathbb{Q}\mathfrak{C}, \\ (C, \Lambda_C) &\mapsto \sum_{F \leq C} (t(C, F), \Lambda_{t(C, F)}) \otimes (F, \Lambda_C \cap \text{lin}(F)), \end{aligned} \tag{3.5}$$

$$\varepsilon : \mathbb{Q}\mathfrak{C} \longrightarrow \mathbb{Q}, \quad (C, \Lambda_C) \longmapsto \begin{cases} 1, & C = \{0\}, \\ 0, & C \neq \{0\}, \end{cases} \tag{3.6}$$

and

$$u : \mathbb{Q} \rightarrow \mathbb{Q}\mathfrak{C}, \quad 1 \mapsto (\{0\}, \{0\}) \tag{3.7}$$

define a cograded, coaugmented, connected coalgebra with the grading

$$\mathbb{Q}\mathfrak{C} = \bigoplus_{n \geq 0} \mathbb{Q}\mathfrak{C}^{(n)}, \tag{3.8}$$

where

$$\mathfrak{C}^{(n)} := \{(C, \Lambda_C) \in \mathfrak{C} \mid \dim C = n\}, \quad n \geq 0.$$

Corollary 3.3. *For a given lattice cone (C, Λ_C) , the subspace*

$$\bigoplus_{F \preceq C} \mathbb{Q}(F, \Lambda_C \cap \text{lin}(F)) \oplus \bigoplus_{F' \preceq F \preceq C} \mathbb{Q}(t(F, F'), \Lambda_{t(F, F')})$$

of $\mathbb{Q}\mathcal{C}$ is a subcoalgebra of $\mathbb{Q}\mathcal{C}$.

Now we work in the filtered lattice Euclidean space $(\mathbb{R}^\infty, \mathbb{Z}^\infty)$ with $V_k = \mathbb{R}^k$, Λ_k the standard lattice \mathbb{Z}^k , and $\{e_1, e_2, \dots\}$ the standard basis. Let $\mathbb{Z}_{\leq 0}^\infty := \varinjlim \mathbb{Z}_{\leq 0}^k$. For any element $\vec{s} = (s_i) \in \mathbb{Z}_{\leq 0}^\infty$, we set $|\vec{s}| := \sum |s_i|$.

On the space $\mathbb{Q}\mathcal{D}\mathcal{C}$ freely generated by the set

$$\mathcal{D}\mathcal{C} := \mathcal{C} \times \mathbb{Z}_{\leq 0}^\infty$$

of **decorated (open) lattice cones**, there is a family of linear operators

$$\delta_i : \mathbb{Q}\mathcal{D}\mathcal{C} \rightarrow \mathbb{Q}\mathcal{D}\mathcal{C}, \quad ((C, \Lambda_C); \vec{s}) \mapsto ((C, \Lambda_C); \vec{s} - e_i). \quad (3.9)$$

By an inductive argument on $|\vec{s}|$, we obtain

Lemma 3.4. *For $(C, \Lambda_C) \in \mathcal{C}$, $k \geq 1$ and $\vec{s} \in \mathbb{Z}_{\leq 0}^k$, we have*

$$((C, \Lambda_C); \vec{s}) = \delta_1^{-s_1} \dots \delta_k^{-s_k} ((C, \Lambda_C); \vec{0}).$$

We next extend the coproduct Δ on $\mathbb{Q}\mathcal{C}$ to a coproduct on $\mathbb{Q}\mathcal{D}\mathcal{C}$, still denoted by Δ . We proceed by induction on $n := |\vec{s}|$. For $n = 0$, we have $\vec{s} = \vec{0}$ and define

$$\Delta \left((C, \Lambda_C); \vec{0} \right) = \sum \left((C_{(1)}, \Lambda_{C_{(1)}}); \vec{0} \right) \otimes \left((C_{(2)}, \Lambda_{C_{(2)}}); \vec{0} \right),$$

using the coproduct $\Delta(C, \Lambda_C) = \sum (C_{(1)}, \Lambda_{C_{(1)}}) \otimes (C_{(2)}, \Lambda_{C_{(2)}})$ on $\mathbb{Q}\mathcal{C}$ define in Equation (3.5).

Assume that the coproduct Δ has been defined for $((C, \Lambda_C); \vec{s})$ with $|\vec{s}| = \ell$ for $\ell \geq 0$. Consider $((C, \Lambda_C); \vec{s}) \in \mathcal{D}\mathcal{C}$ with $\vec{s} \in \mathbb{Z}_{\leq 0}^k$, $|\vec{s}| = \ell + 1$. Then there is some i such that $s_i \leq -1$ and we define

$$\begin{aligned} \Delta((C, \Lambda_C); \vec{s}) &= (\Delta \delta_i)((C, \Lambda_C); \vec{s} + e_i) \\ &:= (D_i \Delta)((C, \Lambda_C); \vec{s} + e_i), \end{aligned} \quad (3.10)$$

where $D_i = \delta_i \otimes 1 + 1 \otimes \delta_i$. Explicitly, we have

$$\Delta((C, \Lambda_C); \vec{s}) = D_1^{-s_1} \dots D_k^{-s_k} \Delta((C, \Lambda_C); \vec{0}). \quad (3.11)$$

The counit ε in Equation (2.4) is trivially extended to a map on $\mathbb{Q}\mathfrak{D}\mathfrak{C}$ for which we use the same notation

$$\begin{aligned} \varepsilon : \mathbb{Q}\mathfrak{D}\mathfrak{C} &\rightarrow \mathbb{Q}, \\ \varepsilon((C, \Lambda_C); \vec{s}) &= \begin{cases} 1, & ((C, \Lambda_C); \vec{s}) = ((\{0\}, \{0\}); \vec{0}), \\ 0, & \text{otherwise.} \end{cases} \end{aligned} \quad (3.12)$$

In particular, ε vanishes on cones of positive dimension. In view of the canonical embedding $\mathfrak{C} \rightarrow \mathfrak{D}\mathfrak{C}$, the unit u defined in Equation (2.4) can be seen as the map

$$u : \mathbb{Q} \rightarrow \mathbb{Q}\mathfrak{D}\mathfrak{C}, \quad 1 \mapsto ((\{0\}, \{0\}); 0). \quad (3.13)$$

Denote

$$\mathfrak{D}\mathfrak{C}^{(n)} := \{((C, \Lambda_C); \vec{s}) \mid \dim C + |\vec{s}| = n\}, \quad n \geq 0. \quad (3.14)$$

Then by definition, we have $\mathfrak{D}\mathfrak{C}^{(0)} = \{((\{0\}, \{0\}); 0)\}$ and $\delta_i(\mathfrak{D}\mathfrak{C}^{(n)}) \subseteq \mathfrak{D}\mathfrak{C}^{(n+1)}$, $n \geq 0$.

Theorem 3.5. *Let Δ, ε, u be as defined in Equations (3.11), (3.12) and (3.13). Equipped with the grading as in Equation (3.14) and the derivations in Equation (3.9), the quadruple $(\mathbb{Q}\mathfrak{D}\mathfrak{C}, \Delta, \varepsilon, u)$ becomes a differential cograded, coaugmented, connected coalgebra.*

Proof. The first equation in Equation (2.3) is just Equation (3.10). The other equations follow from the definitions.

We prove the coassociativity by induction on $|\vec{s}|$ with the initial case $|\vec{s}| = 0$ given by the coassociativity of Δ on $\mathbb{Q}\mathfrak{C}$, where a lattice cone $(C, \Lambda_C) \in \mathfrak{C}$ is identified with $((C, \Lambda_C); \vec{0})$.

Suppose the coassociativity has been proved for vectors $\vec{s} \in \mathbb{Z}_{\leq 0}^k$ with $|\vec{s}| = n \geq 0$ and let $\vec{s} \in \mathbb{Z}_{\leq 0}^k$ with $|\vec{s}| = n + 1$. Then there is some index i with $s_i \leq -1$. By the induction hypothesis, we have $(\Delta \otimes \text{id})\Delta((C, \Lambda_C); \vec{s} + \vec{e}_i) = (\text{id} \otimes \Delta)\Delta((C, \Lambda_C); \vec{s} + \vec{e}_i)$. It follows that

$$\begin{aligned} &(\Delta \otimes \text{id})\Delta((C, \Lambda_C); \vec{s}) \\ &= (\Delta \otimes \text{id})D_i\Delta((C, \Lambda_C); \vec{s} + \vec{e}_i) \\ &= (\delta_i \otimes \text{id} \otimes \text{id} + \text{id} \otimes \delta_i \otimes \text{id} + \text{id} \otimes \text{id} \otimes \delta_i)(\Delta \otimes \text{id})\Delta((C, \Lambda_C); \vec{s} + \vec{e}_i) \\ &= (\delta_i \otimes \text{id} \otimes \text{id} + \text{id} \otimes \delta_i \otimes \text{id} + \text{id} \otimes \text{id} \otimes \delta_i)(\text{id} \otimes \Delta)\Delta((C, \Lambda_C); \vec{s} + \vec{e}_i) \\ &= (\text{id} \otimes \Delta)D_i\Delta((C, \Lambda_C); \vec{s} + \vec{e}_i) \\ &= (\text{id} \otimes \Delta)\Delta((C, \Lambda_C); \vec{s}). \end{aligned}$$

This proves the coassociativity.

We also prove the counit property $(\varepsilon \otimes \text{id}) \Delta = \beta_\ell$ by induction on $|\vec{s}|$ with the initial case $|\vec{s}| = 0$ given by the counit property on $\mathbb{Q}\mathcal{C}$. Suppose that the property is proved for lattice cones with $|\vec{s}| = \ell \geq 0$. Then for $((C, \Lambda_C); \vec{s}) \in \mathcal{D}\mathcal{C}$ with $|\vec{s}| = \ell + 1$, there is some $1 \leq i \leq k$ such that $s_i \leq -1$. Then

$$\begin{aligned} (\varepsilon \otimes \text{id})\Delta((C, \Lambda_C); \vec{s}) &= (\varepsilon \otimes \text{id})(\delta_i \otimes \text{id} + \text{id} \otimes \delta_i)\Delta((C, \Lambda_C); \vec{s} + e_i) \\ &= (\varepsilon \delta_i \otimes \text{id} + \varepsilon \otimes \delta_i)\Delta((C, \Lambda_C); \vec{s} + e_i) \\ &= (\varepsilon \otimes \delta_i)\Delta((C, \Lambda_C); \vec{s} + e_i) \\ &= (\text{id} \otimes \delta_i)(\varepsilon \otimes \text{id})\Delta((C, \Lambda_C); \vec{s} + e_i) \\ &= (\text{id} \otimes \delta_i)\beta_\ell((C, \Lambda_C); \vec{s} + e_i) \\ &= \beta_\ell \delta_i((C, \Lambda_C); \vec{s} + e_i) \\ &= \beta_\ell((C, \Lambda_C); \vec{s}). \end{aligned}$$

This completes the induction. The proof of $(\text{id} \otimes \varepsilon) \Delta = \beta_r$ is similar.

From the fact that $\mathbb{Q}\mathcal{D}\mathcal{C}$ is cograded with the grading in Equation (3.14), we have

$$\mathbb{Q}\mathcal{D}\mathcal{C} = \mathbb{Q}u(1) \oplus \ker \varepsilon$$

and $\mathbb{Q}\mathcal{D}\mathcal{C}^{(0)} = \{((\{0\}, \{0\}); (0))\}$. Hence $\mathbb{Q}\mathcal{D}\mathcal{C}$ is connected. \square

Corollary 3.6. *Let $\mathcal{C}\mathfrak{h}$ be the set of lattice Chen cones, their faces and their transverse lattice cones in $(\mathbb{R}^\infty, \mathbb{Z}^\infty)$ and $\mathcal{D}\mathcal{C}\mathfrak{h} = \mathcal{C}\mathfrak{h} \times \mathbb{Z}_{\leq 0}^\infty$, then $\mathbb{Q}\mathcal{C}\mathfrak{h}$ and $\mathbb{Q}\mathcal{D}\mathcal{C}\mathfrak{h}$ are sub-coalgebras of $\mathbb{Q}\mathcal{D}\mathcal{C}$.*

4 Renormalisation on Chen cones

We want to renormalise MZVs, so we consider the space $\mathbb{Q}\mathcal{D}\mathcal{C}\mathfrak{h}$. For a lattice cone (C, Λ_C) with interior (C°, Λ_C) , one way to regularise the sum

$$\sum_{\vec{n} \in C^\circ \cap \Lambda_C} 1$$

is to introduce a linear form α on V_k and a parameter ε , and then define

$$\phi(C, \Lambda_C) := \sum_{\vec{n} \in C^\circ \cap \Lambda_C} e^{\alpha(\vec{n})\varepsilon}.$$

Usually, we assume that α is rational, that is $\alpha(\vec{n}) \in \mathbb{Q}$ for all $\vec{n} \in \Lambda_k$.

A problem arises with this regularisation: a necessary condition for $S(C, \Lambda_C)(\varepsilon)$ to be a Laurent series in ε is $\ker(\alpha) \cap C^\circ \cap \Lambda_C = \{0\}$, for otherwise there are infinite many 1's in the summation.

Remark 4.1.

- (a) For a single lattice cone, it is easy to find such a linear function α , but problems can arise to find a linear function well suited for a family of lattice cones. For the family \mathfrak{C} , it is impossible to find a universal α ; take any $v \in \ker(\alpha)$, then α vanishes on $\langle v \rangle$.
- (b) For the family of cones in the first orthant, it is also impossible to find a universal α . This can be reduced to the two dimensional case. Any rational vector v in the open upper half plane defines a cone $\langle v \rangle$ in the first quadrant or a transverse cone $\langle v \rangle = t(C, f)$ of a face f of a two dimensional cone C in the first quadrant. Choosing v in $\ker(\alpha)$ implies that α vanishes on $\langle v \rangle$. This extends to the closed upper half-plane since $\langle e_1 \rangle$ is a cone in the first quadrant.

However, it is possible to find such an α for a small enough family, for example the family \mathfrak{Ch} .

Proposition 4.2. *A linear form $\alpha = \sum a_i e_i^*$ is negative on all cones in \mathfrak{Ch} if and only if $a_i < a_{i+1} < 0$ for $i \in \mathbb{N}$.*

Proof. In order to give the proof, we first determine the form of the transverse cones to faces of a Chen cone $C := \langle v_1, \dots, v_k \rangle$, where we have set $v_i := e_1 + \dots + e_i$ for $i \geq 1$. For positive integers $p < q$, denote $[p, q] := [p, p+1, \dots, q]$, and $v_{[p,q]} = v_p, v_{p+1}, \dots, v_q$. Then a face of C is of the form

$$F = \langle v_{[j_0, i_1]}, v_{[j_1, i_2]}, \dots, v_{[j_n, i_{n+1}]} \rangle,$$

$$0 =: i_0 \leq j_0 \leq i_1 \leq j_1 \leq i_2 \leq j_2 \leq \dots \leq i_{n-1} \leq j_{n-1} \leq i_n \leq j_n \leq i_{n+1} \leq j_{n+1} := k+1.$$

Here $p \leq q$ means $p+2 \leq q$. Then the transverse cone is generated by $\pi_{F^\perp}(v_m)$ with $i_\ell < m < j_\ell$, for $0 \leq \ell \leq n+1$ with $i_\ell \leq j_\ell$.

First let us compute $\pi_{F^\perp}(e_m)$ for $i_\ell < m < j_\ell$, for $0 \leq \ell \leq n+1$ with $i_\ell \leq j_\ell$. We know that

(a1) if $\ell = 0, i_0 \leq j_0$, then

$$e_m = \frac{j_0 - i_0 - 1}{j_0 - i_0} (e_m - e_{j_0}) - \frac{1}{j_0 - i_0} \sum_{i_0 < t < j_0, t \neq m} (e_t - e_{j_0}) + \frac{1}{j_0 - i_0} (v_{j_0});$$

(a2) if $0 < \ell < n+1, i_\ell \leq j_\ell$, then

$$e_m = \frac{j_\ell - i_\ell - 1}{j_\ell - i_\ell} (e_m - e_{j_\ell}) - \frac{1}{j_\ell - i_\ell} \sum_{i_\ell < t < j_\ell, t \neq m} (e_t - e_{j_\ell})$$

$$+ \frac{1}{j_\ell - i_\ell} (v_{j_\ell}) - \frac{1}{j_\ell - i_\ell} (v_{i_\ell});$$

(b) if $\ell = n + 1, i_{n+1} \leq j_{n+1}$, then

$$e_m = e_m.$$

For $0 \leq \ell < n + 1$ and $i_\ell < t < j_\ell$, there is $(e_t - e_{j_\ell}) \perp \text{lin}(F)$. For $\ell = n + 1$ and $i_{n+1} < t < j_{n+1}$, there is $e_t \perp \text{lin}(F)$. Thus for the projection of e_m we have

(a) if $0 \leq \ell < n + 1, i_\ell \leq j_\ell, i_\ell < m < j_\ell$, then

$$\pi_{F^\perp}(e_m) = \frac{j_\ell - i_\ell - 1}{j_\ell - i_\ell} (e_m - e_{j_\ell}) - \frac{1}{j_\ell - i_\ell} \sum_{i_\ell < t < j_\ell, t \neq m} (e_t - e_{j_\ell});$$

(b) if $\ell = n + 1, i_{n+1} \leq j_{n+1}, i_{n+1} < m < j_{n+1}$, then

$$\pi_{F^\perp}(e_m) = e_m.$$

Therefore,

(a) if $0 \leq \ell < n + 1, i_\ell \leq j_\ell, i_\ell < m < j_\ell$, then

$$\begin{aligned} \pi_{F^\perp}(v_m) &= \frac{j_\ell - m}{j_\ell - i_\ell} \sum_{i_\ell < t \leq m} (e_t - e_{j_\ell}) - \frac{m - i_\ell}{j_\ell - i_\ell} \sum_{m < t < j_\ell} (e_t - e_{j_\ell}) \\ &= \frac{j_\ell - m}{j_\ell - i_\ell} \sum_{i_\ell < t \leq m} e_t - \frac{m - i_\ell}{j_\ell - i_\ell} \sum_{m < t \leq j_\ell} e_t; \end{aligned}$$

(b) if $\ell = n + 1, i_{n+1} \leq j_{n+1}, i_{n+1} < m < j_{n+1}$, then $\pi_{F^\perp}(v_m) = e_{i_{n+1}+1} + \dots + e_m$.

We are now ready to prove the proposition, noting that α is negative on a transverse cone if and only if it is so on its generators $\pi_{F^\perp}(v_m), i_\ell < m < j_\ell, 0 \leq \ell \leq n + 1$.

Let α be negative on all transverse cones to faces of the cone $C = \langle v_1, \dots, v_k \rangle, k \geq 1$. Then the transverse cone for the face $\langle v_1, \dots, \hat{v}_i, \dots, v_k \rangle$ (the cone spanned by v_1, \dots, v_k except $v_i, i = 1, \dots, k - 1$, is spanned by $\frac{1}{2}(e_i - e_{i+1})$, by the above Case (a). Then applying α to this transverse cone, we have $a_i < a_{i+1}$. Now for the cone $\langle v_1, \dots, v_{k-1} \rangle$, by Case (b), the transverse cone is generated by e_k , applying α yields $a_k < 0$. This is what we need.

Conversely, suppose that $\alpha = \sum a_i e_i^*$ satisfies $a_i < a_{i+1} < 0$. Clearly, α is negative on C and its faces. It is also negative on $\pi_{F^\perp}(v_m)$ in Case (b). For $\pi_{F^\perp}(v_m)$ in Case (a), using the fact

$$\frac{j_\ell - m}{j_\ell - i_\ell} \sum_{i_\ell < t \leq m} 1 = \frac{m - i_\ell}{j_\ell - i_\ell} \sum_{m < t \leq j_\ell} 1,$$

we find $\alpha(\pi_{F^\perp}(v_m)) < 0$. Therefore α is negative on all transverse cones. \square

We now fix a linear function $\alpha = \sum a_i e_i^*$ with $a_i < a_{i+1} < 0$, and for $((C, \Lambda_C), \vec{s}) \in \mathfrak{DC}\mathfrak{h}$, we set

$$\phi((C, \Lambda_C), \vec{s}) = \sum_{\vec{n} \in \Lambda_C \cap C^o} \frac{e^{\alpha(\vec{n})\varepsilon}}{\vec{n}^{\vec{s}}}, \quad (4.1)$$

where we have set $\vec{n}^{\vec{s}} = n_1^{s_1} \cdots n_k^{s_k}$ with $\vec{n} := (n_1, \dots, n_k) \in \Lambda_C$ and $\vec{s} = (s_1, \dots, s_k) \in \mathbb{Z}_{\leq 0}^k$.

Applying the same proof as for Lemma 4.4 in [8], we have

Lemma 4.3. *The image $\phi((C, \Lambda_C), \vec{s})$ is a meromorphic function in ε for any decorated lattice cone $((C, \Lambda_C), \vec{s})$ in $\mathfrak{DC}\mathfrak{h}$.*

This gives rise to a linear map:

$$\phi : \mathbb{Q}\mathfrak{DC}\mathfrak{h} \rightarrow \mathbb{C}[\varepsilon^{-1}, \varepsilon]$$

to which we can then apply Connes-Kreimer's renormalisation scheme on the coalgebra of Chen cones as in Theorem 2.5, without bothering about the product structure. So, applying the induction formula with $(R, P) = (\mathbb{C}[\varepsilon^{-1}, \varepsilon], -\pi_+)$, where π_+ is the projection to the holomorphic part, we have

$$\phi = \phi_-^{*(-1)} * \phi_+,$$

where $\phi_-^{*(-1)}$ is the holomorphic part and ϕ_+ is the polar part. Here ϕ_- takes values in $\mathbb{C}[[\varepsilon]]$ and ϕ_+ takes values in $\mathbb{C}[\varepsilon^{-1}]$.

Let us define renormalised MZVs as

$$\zeta^{\text{ren}}((C, \Lambda_C), \vec{s}) := \phi_-^{*(-1)}((C, \Lambda_C), \vec{s})(0). \quad (4.2)$$

We will see that the renormalised MZVs do not depend on the parameters a_i , a fact which might seem surprising at first glance and that will be proved in the sequel. An important consequence is that the parameters can be seen as formal parameters, thus allowing for a regularisation in a more general situation than the one of Chen cones considered here.

5 Renormalised CZVs

As we previously discussed, it is impossible to find a universal linear function α which would regularise all lattice cones simultaneously, but it is possible to find one for the family of Chen cones; in the Chen cone case, we renormalise along a direction $\vec{a} := (a_1, a_2, \dots)\varepsilon$. Since the parameter ε can be viewed as a re-scaling of variables, this suggests to replace the parameters $\vec{a} := (a_1, a_2, \dots, a_k)$ by the variables

$\vec{\varepsilon} = \sum \varepsilon_i e_i^* \in V^*$, where $\varepsilon_1 := a_1 \varepsilon, \varepsilon_2 := a_2 \varepsilon, \dots, \varepsilon_k := a_k \varepsilon$, and to define

$$S_k^o((C, \Lambda_C); \vec{s})(\vec{\varepsilon}) := \sum_{\vec{n} \in \Lambda_C \cap C^o} \frac{e^{\langle \vec{n}, \vec{\varepsilon} \rangle}}{\vec{n}^{\vec{s}}} = \sum_{(n_1, \dots, n_k) \in C^o \cap \Lambda_C} \frac{e^{n_1 \varepsilon_1 \dots n_k \varepsilon_k}}{n_1^{s_1} \dots n_k^{s_k}} \quad (5.1)$$

for a strongly convex lattice cone (for example, a simplicial cone) $(C, \Lambda_C) \in \mathfrak{C}$ with $C \subset \mathbb{R}^k$ and where we have set $\vec{n}^{\vec{s}} = n_1^{s_1} \dots n_k^{s_k}$ with $\vec{n} := (n_1, \dots, n_k) \in \Lambda_C$ and $\vec{s} = (s_1, \dots, s_k) \in \mathbb{Z}_{\leq 0}^k$.

The sum (5.1) is absolutely convergent on

$$\check{C}^- := \left\{ \vec{\varepsilon} := \sum_{i=1}^k \varepsilon_i e_i^* \mid \langle \vec{x}, \vec{\varepsilon} \rangle < 0 \text{ for all } \vec{x} \in C \right\},$$

which has dimension k .

Remark 5.1. With our convention that $0^s = 1$ for s with $\text{Re}(s) \leq 0$, the function $S_k^o((C, \Lambda_C); \vec{s})(\vec{\varepsilon})$ in the variables $\vec{\varepsilon} = \sum \varepsilon_i e_i^*$ does not depend on the choice of $k \geq 1$ such that $C \subseteq V_k$ and $\vec{s} \in \mathbb{Z}_{\leq 0}^k$. Thus we will suppress the subscript k in the sum.

Choosing the above multivariate regularisation implies that – in contrast to Connes and Kreimer’s renormalisation scheme – the range space is no longer the space of Laurent series. The new target space is a space of multivariate meromorphic germs discussed in [7] which is not a Rota-Baxter algebra, thus requiring² the generalised version of Connes and Kreimer’s renormalisation scheme corresponding to Theorem 2.5.

5.1 Regularisations

The function $S^o((C, \Lambda_C), \vec{s})$ is a very specific type of meromorphic function, for it has linear poles. We briefly review the relevant definitions, and refer the reader to [7] for a more detailed discussion.

Definition 5.2. Let k be a positive integer.

- (a) A **germ of meromorphic functions at 0** on \mathbb{C}^k is the quotient of two holomorphic functions in a neighborhood of 0 inside \mathbb{C}^k .

² As observed in [8], the renormalised CZVs we derive here by means of a multivariate Algebraic Birkhoff Factorisation, can alternatively be derived directly from the derivatives of the exponential sums on cones by means of the projection onto the holomorphic part of the meromorphic germs they give rise to, an alternative renormalisation method which gives rise to the same CZVs.

- (b) A germ of meromorphic functions $f(\vec{\varepsilon})$ on \mathbb{C}^k is said to have **linear poles at zero with rational coefficients** if there exist vectors $L_1, \dots, L_n \in \Lambda_k \otimes \mathbb{Q}$ (possibly with repetitions) such that $f \prod_{i=1}^n L_i$ is a holomorphic germ at zero whose Taylor expansion under a basis of Λ_k has rational coefficients.
- (c) We will denote by $\mathcal{M}_{\mathbb{Q}}(\mathbb{C}^k)$ the set of germs of meromorphic functions on \mathbb{C}^k with linear poles at zero with rational coefficients. It is a linear subspace over \mathbb{Q} .

Composing with the projection $\mathbb{C}^{k+1} \rightarrow \mathbb{C}^k$ dual to the inclusion $j_k : \mathbb{C}^k \rightarrow \mathbb{C}^{k+1}$ then yields the embedding

$$\mathcal{M}_{\mathbb{Q}}(\mathbb{C}^k) \hookrightarrow \mathcal{M}_{\mathbb{Q}}(\mathbb{C}^{k+1}),$$

thus giving rise to the direct limit

$$\mathcal{M}_{\mathbb{Q}}(\mathbb{C}^{\infty}) := \varinjlim \mathcal{M}_{\mathbb{Q}}(\mathbb{C}^k) = \bigcup_{k=1}^{\infty} \mathcal{M}_{\mathbb{Q}}(\mathbb{C}^k).$$

Fix an inner product $Q(\cdot, \cdot)$ in $(\mathbb{R}^{\infty}, \mathbb{Z}^{\infty})$, a polar germ is a meromorphic germ at zero of the form

$$\frac{h(\ell_1, \dots, \ell_m)}{L_1^{s_1} \cdots L_n^{s_n}},$$

where

- (a) h lies in $\mathcal{M}_{\mathbb{Q},+}(\mathbb{C}^m)$,
- (b) $\ell_1, \dots, \ell_m, L_1, \dots, L_n$ lie in $\Lambda_k \otimes \mathbb{Q}$, with L_1, \dots, L_n linearly independent, such that

$$Q(\ell_i, L_j) = 0 \quad \text{for all } (i, j) \in [m] \times [n];$$

- (c) s_1, \dots, s_n are positive integers.

The subspace of $\mathcal{M}_{\mathbb{Q}}(\mathbb{C}^{\infty})$ generated by all polar germs is denoted by $\mathcal{M}_{\mathbb{Q},-}(\mathbb{C}^{\infty})$. Let $\mathcal{M}_{\mathbb{Q},+}(\mathbb{C}^{\infty})$ be the algebra of holomorphic germs.

Proposition 5.3 ([7]). *For any given inner product $Q(\cdot, \cdot)$ on \mathbb{R}^{∞} , there is a direct sum decomposition*

$$\mathcal{M}_{\mathbb{Q}}(\mathbb{C}^{\infty}) = \mathcal{M}_{\mathbb{Q},-}(\mathbb{C}^{\infty}) \oplus \mathcal{M}_{\mathbb{Q},+}(\mathbb{C}^{\infty}).$$

Thus we have the projection map

$$\pi_+ : \mathcal{M}_{\mathbb{Q}}(\mathbb{C}^{\infty}) \rightarrow \mathcal{M}_{\mathbb{Q},+}(\mathbb{C}^{\infty}). \quad (5.2)$$

One advantage to work with this multivariate regularisation is that the target space is stable under partial derivatives, and we thus have a linear map compatible with coderivatives. The partial derivation

$$\partial_i = \frac{\partial}{\partial \varepsilon_i},$$

combined with the usual subdivision techniques implemented to define exponential sums and integrals on cones (see e.g. [1])

Proposition 5.4. *For any smooth lattice cone (C, Λ_C) , the image $S^o((C, \Lambda_C); \vec{s})(\vec{\varepsilon})$ defines an element in $\mathcal{M}_{\mathbb{Q}}(\mathbb{C}^\infty)$. For a general lattice cone (C, Λ_C) , the germ of functions*

$$\sum_{F \in \mathcal{F}^o(C)} S^o((F, \Lambda_F); \vec{s})$$

does not depend on the choice of the subdivision $\underline{C} = \{(C_i, \Lambda_{C_i})\}$ of (C, Λ_C) into smooth lattice cones in Proposition 3.1.

Thanks to Proposition 5.4, we extend (5.1) to any lattice cone setting

$$S^o((C, \Lambda_C); \vec{s}) := \sum_{F \in \mathcal{F}^o(C)} S^o((F, \Lambda_F); \vec{s}),$$

for any subdivision $\underline{C} = \{(C_i, \Lambda_{C_i})\}$ of (C, Λ_C) into smooth lattice cones.

Proof. We first prove this for a smooth lattice cone (C, Λ_C) with $|\vec{s}| = 0$. Let $C = \langle v_1, \dots, v_m \rangle$ with $\{v_1, \dots, v_m\}$ being a basis of Λ_C . Since an element \vec{x} in $C \cap \Lambda_C$ can be written in a unique way as $\sum_{j=1}^m n_j v_j$ where $n_j \in \mathbb{Z}_{\geq 0}$, we have for $\vec{\varepsilon} = \sum_{j=1}^m \varepsilon_j e_j^* \in \check{C}^-$,

$$\begin{aligned} S^o(C, \Lambda_C)(\vec{\varepsilon}) &:= \prod_{j=1}^m \sum_{n_j \in \mathbb{Z}_{\geq 1}} e^{n_j \langle v_j, \vec{\varepsilon} \rangle} \\ &= \prod_{j=1}^m \frac{e^{\langle v_j, \vec{\varepsilon} \rangle}}{1 - e^{\langle v_j, \vec{\varepsilon} \rangle}} = \prod_{j=1}^m \frac{e^{L_j(\vec{\varepsilon})}}{1 - e^{L_j(\vec{\varepsilon})}}, \end{aligned} \tag{5.3}$$

where $L_j(\vec{\varepsilon}) = \langle v_j, \vec{\varepsilon} \rangle$. They are holomorphic on \check{C}^- and extend to germs of meromorphic functions on \mathbb{C}^k with simple linear poles at $L_1(\vec{\varepsilon}) = 0, \dots, L_n(\vec{\varepsilon}) = 0$.

Indeed, from the generating power series $\frac{x}{e^x - 1} = \sum_{n=0}^\infty B_n \frac{x^n}{n!}$ of Bernoulli numbers, we have that $\frac{1}{1 - e^x} = -\frac{1}{x} \frac{x}{e^x - 1}$ is in $\mathcal{M}_{\mathbb{Q}}(\mathbb{C})$. Then the same

holds for $\frac{e^x}{1-e^x} = \frac{1}{1-e^x} - 1$. Thus for each linear form L on \mathbb{C}^k with rational coefficients, both $\frac{L}{1-e^L}$ and $\frac{e^L}{1-e^L}$ are in $\mathcal{M}_{\mathbb{Q}}(\mathbb{C}^k)$.

For a smooth lattice cone, the conclusion that $S^o(C, \Lambda_C)(\vec{\varepsilon})$ lies in $\mathcal{M}_{\mathbb{Q}}(\mathbb{C}^k)$ follows from Equation (5.3) since $\mathcal{M}_{\mathbb{Q}}(\mathbb{C}^k)$ is closed under multiplication.

Next for a smooth lattice cone (C, Λ_C) and $\vec{s} \in \mathbb{Z}_{\leq 0}^k$. Notice that by definition, $S^o(C, \Lambda_C)(\vec{\varepsilon})$ is absolutely convergent on \check{C}^- . The same holds for

$$\sum_{\vec{n} \in C^o \cap \Lambda_C} \partial_{\vec{\varepsilon}}^{-\vec{s}} e^{\langle \vec{n}, \vec{\varepsilon} \rangle} = \sum_{\vec{n} \in C^o \cap \Lambda_C} \vec{n}^{-\vec{s}} e^{\langle \vec{n}, \vec{\varepsilon} \rangle},$$

so that on \check{C}^- , we have

$$\partial_{\vec{\varepsilon}}^{-\vec{s}} S^o(C, \Lambda_C)(\vec{\varepsilon}) = \sum_{\vec{n} \in C^o \cap \Lambda_C} \vec{n}^{-\vec{s}} e^{\langle \vec{n}, \vec{\varepsilon} \rangle} = S^o((C, \Lambda_C); \vec{s})(\vec{\varepsilon}).$$

This shows that $S^o((C, \Lambda_C); \vec{s})(\vec{\varepsilon})$ and $S^c((C, \Lambda_C); \vec{s})(\vec{\varepsilon})$ lie in $\mathcal{M}_{\mathbb{Q}}(\mathbb{C}^k)$.

Now for a general lattice cone (C, Λ_C) , suppose $\underline{C}' = \{C'_1, \dots, C'_r\}$ is another subdivision of C into smooth lattice cones. Let $\underline{C}'' = \{C''_1, \dots, C''_{r''}\}$ be a common refinement of the two subdivisions into smooth lattice cones, which exists by Lemma 2.3 in [6]. Then for any element $F \in \mathcal{F}^o(\underline{C})$, the subdivision $\underline{C}'' = \{C''_1, \dots, C''_{r''}\}$ induces a subdivision $\underline{D}^F = \{D^F_1, \dots, D^F_{r''}\}$ of F^o by some elements of $\mathcal{F}^o(\underline{C}'')$. Then we have

$$C^o = \bigcup_{F \in \mathcal{F}^o(\underline{C})} F^o = \bigcup_{F \in \mathcal{F}^o(\underline{C})} \bigcup_{G \in \mathcal{F}^o(\underline{D}^F)} G^o = \bigcup_{G \in \mathcal{F}^o(\underline{C}'')} G^o.$$

Therefore on \check{C}^- , we have

$$\sum_{F \in \mathcal{F}^o(\underline{C})} S^o((F, \Lambda_C \cap \text{lin}(F)); \vec{s}) = \sum_{G \in \mathcal{F}^o(\underline{C}'')} S^o((G, \Lambda_C \cap \text{lin}(G)); \vec{s}).$$

By the same argument, the above equation holds when \underline{C}'' is replaced by \underline{C}' . This gives what we need.

Noting that faces of a smooth lattice cone are smooth, we know for any lattice cone (C, Λ_C) , $S^o((C, \Lambda_C); \vec{s})(\vec{\varepsilon}) \in \mathcal{M}_{\mathbb{Q}}(\mathbb{C}^\infty)$. □

Consequently, we have a linear map

$$S^o : \mathbb{Q}\mathcal{DC} \rightarrow \mathcal{M}_{\mathbb{Q}}(\mathbb{C}^\infty), \quad ((C, \Lambda_C); \vec{s}) \mapsto S^o((C, \Lambda_C); \vec{s}).$$

By definition, the following conclusion holds.

Corollary 5.5. *Let (C, Λ_C) be a lattice cone and let $\underline{C} = \{(C_1, \Lambda_{C_1}), \dots, (C_r, \Lambda_{C_r})\}$ be a subdivision of C . Then for $\vec{s} \in \mathbb{Z}_{\leq 0}^k$ we have*

$$S^o((C, \Lambda_C); \vec{s}) = \sum_{F \in \mathcal{F}^o(\underline{C})} S^o((F, \Lambda_C \cap \text{lin}(F)); \vec{s})$$

in $\mathcal{M}_{\mathbb{Q}}(\mathbb{C}^\infty)$.

By an analytic continuation argument, we have the following relations among regularised CZVs.

Proposition 5.6. *For the linear map*

$$S^o : \mathbb{Q}\mathcal{DC} \rightarrow \mathcal{M}_{\mathbb{Q}}(\mathbb{C}^\infty)$$

and any $i \in \mathbb{Z}_{>0}$,

$$S^o \delta_i = \partial_i S^o.$$

That means that for any $((C, \Lambda_C), \vec{s})$ in \mathcal{DC} , we have

$$S^o((C, \Lambda_C); \vec{s})(\vec{\varepsilon}) = \partial^{-\vec{s}} S^o(C, \Lambda_C)(\vec{\varepsilon}),$$

where $\partial^{-\vec{s}} = \partial_1^{-s_1} \dots \partial_k^{-s_k}$.

Proof. For a given $\vec{s} \in \mathbb{Z}_{\leq 0}^k$ and a simplicial lattice cone $(C, \Lambda_C) \in \mathcal{C}$ with $C \subset \mathbb{R}^k$, by absolute convergence we have

$$\partial_i S^o((C, \Lambda_C); \vec{s})(\vec{\varepsilon}) = S^o((C, \Lambda_C); \vec{s} - e_i)(\vec{\varepsilon}) = S^o(\delta_i((C, \Lambda_C); \vec{s}))(\vec{\varepsilon})$$

for $\vec{\varepsilon} \in \check{C}^-$. Therefore by analytic continuation, in $\mathcal{M}_{\mathbb{Q}}(\mathbb{C}^\infty)$, we have

$$\partial_i S^o((C, \Lambda_C); \vec{s})(\vec{\varepsilon}) = S^o(\delta_i((C, \Lambda_C); \vec{s}))(\vec{\varepsilon}),$$

that is,

$$S^o \delta_i = \partial_i S^o$$

for any simplicial lattice cone. Then by definition of S^o , $S^o \delta_i = \partial_i S^o$ holds in general. □

5.2 Renormalisation

When V is equipped with two inner products (which might be taken to be the same), we can use one to construct the coalgebra $\mathbb{Q}\mathcal{DC}$ from transverse lattice cones introduced in Section 2 and use the other one to construct the decomposition

$$\mathcal{M}_{\mathbb{Q}}(\mathbb{C}^\infty) = \mathcal{M}_{\mathbb{Q},+}(\mathbb{C}^\infty) \oplus \mathcal{M}_{\mathbb{Q},-}(\mathbb{C}^\infty)$$

in Proposition 5.3. Since $\mathcal{M}_{\mathbb{Q},+}(\mathbb{C}^\infty)$ is a unitary subalgebra, the Algebraic Birkhoff Factorisation in Theorem 2.5 applies, with $\mathbf{C} = \mathbb{Q}\mathcal{D}\mathcal{C}$ and

$$\begin{aligned} A &= \mathcal{M}_{\mathbb{Q}}(\mathbb{C}^\infty), \\ A_1 &= \mathcal{M}_{\mathbb{Q},+}(\mathbb{C}^\infty), \\ A_2 &= \mathcal{M}_{\mathbb{Q},-}(\mathbb{C}^\infty), \\ P &= \pi_+ : \mathcal{M}_{\mathbb{Q}}(\mathbb{C}^\infty) \rightarrow \mathcal{M}_{\mathbb{Q},+}(\mathbb{C}^\infty). \end{aligned}$$

We have chosen A_1 to be the holomorphic part since it contains the unit. See the remark after Theorem 2.5 for this nonorthodox choice of A_1 . We consequently obtain the following theorem.

Theorem 5.7 (Algebraic Birkhoff Factorisation for CZVs). *For the linear map*

$$S^o : \mathbb{Q}\mathcal{D}\mathcal{C} \rightarrow \mathcal{M}_{\mathbb{Q}}(\mathbb{C}^\infty),$$

there exist unique linear maps $S_1^o : \mathbb{Q}\mathcal{D}\mathcal{C} \rightarrow \mathcal{M}_{\mathbb{Q},+}(\mathbb{C}^\infty)$ and $S_2^o : \mathbb{Q}\mathcal{D}\mathcal{C} \rightarrow \mathbb{Q} + \mathcal{M}_{\mathbb{Q},-}(\mathbb{C}^\infty)$, with $S_1^o(\{0\}, \{0\}) = 1$, $S_2^o(\{0\}, \{0\}) = 1$, such that

$$S^o = (S_1^o)^{*(-1)} * S_2^o. \quad (5.4)$$

The same theorem applies to the sub-coalgebra $\mathbb{Q}\mathcal{C}$, which yields a factorisation of $S^o : \mathbb{Q}\mathcal{C} \rightarrow \mathcal{M}_{\mathbb{Q}}(\mathbb{C}^\infty)$, giving rise to two linear maps $S_1^o : \mathbb{Q}\mathcal{C} \rightarrow \mathcal{M}_{\mathbb{Q},+}(\mathbb{C}^\infty)$ and $S_2^o : \mathbb{Q}\mathcal{C} \rightarrow \mathbb{Q} + \mathcal{M}_{\mathbb{Q},-}(\mathbb{C}^\infty)$. We can legitimately use the same notation as in Theorem 5.7 since they correspond to the restriction of the linear maps in Theorem 5.7 as a result of the uniqueness of the factorisation.

In [8], we identify S_2^o with the exponential integral and give a formula for

$$\mu^o(C, \Lambda_C) := (S_1^o)^{*(-1)}(C, \Lambda_C)$$

as follows.

Proposition 5.8. *As a linear map on $\mathbb{Q}\mathcal{C}$, we have*

$$\begin{aligned} S_2^o &= I, \\ \mu^o &= \pi_+ S^o. \end{aligned}$$

Here I is the exponential integral on lattice cones [8] defined as follows on simplicial cones and then extended to any cone by the subdivision

property. If $v_1, \dots, v_k \in \Lambda_C$ is a set of primary generators of a simplicial cone C , and u_1, \dots, u_k a basis of Λ_C , for $1 \leq i \leq k$, let $v_i = \sum_{j=1}^k a_{ji} u_j$, $a_{ji} \in \mathbb{Z}$. Define linear functions $L_i := L_{v_i} := \sum_{j=1}^k a_{ji} \langle u_j, \vec{\varepsilon} \rangle$ and let $w(C, \Lambda_C)$ denote the absolute value of the determinant of the matrix $[a_{ij}]$, then

$$I(C, \Lambda_C)(\vec{\varepsilon}) := (-1)^k \frac{w(C, \Lambda_C)}{L_1 \cdots L_k}. \tag{5.5}$$

Proposition 5.8 can be generalised to $\mathbb{Q}\mathfrak{DC}$ as follows.

Proposition 5.9. *For $((C, \Lambda_C); \vec{s}) \in \mathbb{Q}\mathfrak{DC}$, we have*

$$\begin{aligned} S_1^o((C, \Lambda_C); \vec{s}) &= \partial^{-\vec{s}} S_1^o(C, \Lambda_C), \\ S_2^o((C, \Lambda_C); \vec{s}) &= \partial^{-\vec{s}} S_2^o(C, \Lambda_C) \end{aligned} \tag{5.6}$$

and

$$\mu^o = \pi_+ S^o. \tag{5.7}$$

Proof. By Proposition 5.6, S^o are compatible with the coderivations on $\mathbb{Q}\mathfrak{DC}$ and derivations on $\mathcal{M}_{\mathbb{Q}}(\mathbb{C}^\infty)$. The conclusion then follows from Theorem 2.5. \square

For $((C, \Lambda_C); \vec{s}) \in \mathfrak{DC}$ the expressions $\mu^o((C, \Lambda_C); \vec{s}) = (S_1^o)^{*(-1)}((C, \Lambda_C); \vec{s})$ in the Algebraic Birkhoff Factorisation of S^o is a germ of holomorphic functions which we can therefore evaluate at 0.

Definition 5.10. The value

$$\zeta^o((C, \Lambda_C); \vec{s}) := (S_1^o)^{*(-1)}((C, \Lambda_C); \vec{s})(0)$$

is called the **renormalised open CZV** of (C, Λ_C) at \vec{s} .

In particular, this definition applies to cones in \mathfrak{Ch} and $\mathfrak{DC}\mathfrak{h}$.

Corollary 5.11. *The germs of functions $(S_1^o)^{*(-1)}(C, \Lambda_C)$ are generating functions of renormalised open CZVs at nonpositive integers. More precisely, for a lattice cone $(C, \Lambda_C) \in \mathfrak{C}$, we have*

$$(S_1^o)^{*(-1)}(C, \Lambda_C)(\vec{\varepsilon}) = \sum_{\vec{r} \in \mathbb{Z}_{\geq 0}^k} \zeta^o((C, \Lambda_C); -\vec{r}) \frac{\vec{\varepsilon}^{\vec{r}}}{\vec{r}!}. \tag{5.8}$$

Proof. By Equation (5.6), we have

$$\partial_{\vec{\varepsilon}}^{\vec{r}} (S_1^o)^{*(-1)}(C, \Lambda_C)(0) = (S_1^o)^{*(-1)}((C, \Lambda_C); -\vec{r})(0) = \zeta^o((C, \Lambda_C); -\vec{r}),$$

as needed. \square

6 Comparison of the two renormalisation schemes

So far, we have two approaches to renormalise sums on Chen cones, which can be related by means of a restriction $\vec{\varepsilon} = \vec{a} \varepsilon$ along a direction \vec{a} : the first one by which the Algebraic Birkhoff Factorisation procedure is implemented after restricting, the second one by which the Algebraic Birkhoff Factorisation procedure is implemented before restricting.

Under the restriction along a direction \vec{a} , the splittings of the target space in the two approaches differ as it can be seen in the following counterexample which shows that evaluation $\mathcal{E}_{\vec{a}}$ along a given direction $\vec{a} \varepsilon$ does not commute with the projection π_+ :

$$\pi_+ \circ \mathcal{E}_{\vec{a}} \neq \mathcal{E}_{\vec{a}} \circ \pi_+,$$

where the projection π_+ on the left hand side is the one on $\mathcal{M}_{\mathbb{Q}}(\mathbb{C}^\infty)$ and the one on the right hand side is on $\mathcal{M}_{\mathbb{Q}}(\mathbb{C})$.

Counterexample 6.1. Let $f(\varepsilon_1, \varepsilon_2) := \frac{\varepsilon_1}{\varepsilon_2}$, then

$$\pi_+ \circ \mathcal{E}_{\vec{a}}(f) = \frac{a_1}{a_2} \neq 0 = \mathcal{E}_{\vec{a}} \circ \pi_+(f).$$

But surprisingly, these two renormalisation procedures give the same renormalised values for Chen cones.

Proposition 6.2. *For Chen cones, the factorisations obtained by*

- *first implementing the Algebraic Birkhoff Factorisation on the exponential sum S^o and then restricting along a direction $\vec{a}\varepsilon$, and*
- *first restricting the exponential sum S^o along a direction $\vec{a}\varepsilon$ and then implementing the Algebraic Birkhoff Factorisation*

coincide.

Proof. We first investigate the first renormalisation procedure. Since the Algebraic Birkhoff Factorisation applied to the exponential sum S^o on cones boils down to the Euler-Maclaurin formula on cones [8], we have that on \mathbb{QC}

$$S^o = \mu^o * I, \tag{6.1}$$

where $*$ is the convolution associated with the coproduct on lattice cones. For any lattice cone (C, Λ_C) , $\mu^o(C, \Lambda_C)$ is holomorphic and $I(C, \Lambda_C)$ is a \mathbb{Q} -linear combination of expressions of the form $\frac{1}{L_1 \cdots L_m}$ where L_1, \dots, L_m are m linearly independent linear forms on some V_k . By Proposition 5.9, differentiating yields for any lattice cone (C, Λ_C) and any \vec{s} , a holomorphic function $\mu^o((C, \Lambda_C); \vec{s})$ and a sum $I((C, \Lambda_C); \vec{s})$

of expressions of the form $\frac{c}{L_1^{s_1} \dots L_m^{s_m}}$ where L_1, \dots, L_m are m linearly independent linear forms on some V_k and s_1, \dots, s_m non-negative integers. Now, restricting along the direction $\vec{\varepsilon} = \vec{a} \varepsilon$ yields for any lattice cone (C, Λ_C) and \vec{s} , a map $\mu^0((C, \Lambda_C); \vec{s})|_{\vec{\varepsilon}=\vec{a}\varepsilon}$ in $\mathbb{Q}[[\varepsilon]]$. Furthermore, the restriction $I((C, \Lambda_C); \vec{s})|_{\vec{\varepsilon}=\vec{a}\varepsilon}$ lies in $\mathbb{Q}[\varepsilon^{-1}]\varepsilon^{-1}$ if $((C, \Lambda_C); \vec{s}) \neq ((\{0\}, \{0\}), \vec{0})$ as a sum of restricted fractions. So if we let

$$\tilde{\mu}((C, \Lambda_C); \vec{s})(\varepsilon) = \mu^0((C, \Lambda_C); \vec{s})(\vec{\varepsilon})|_{\vec{\varepsilon}=\vec{a}\varepsilon},$$

and

$$\tilde{I}((C, \Lambda_C); \vec{s})(\varepsilon) = I((C, \Lambda_C); \vec{s})(\vec{\varepsilon})|_{\vec{\varepsilon}=\vec{a}\varepsilon},$$

with $\phi((C, \Lambda_C); \vec{s})(\varepsilon) = S^o((C, \Lambda_C); \vec{s})(\vec{\varepsilon})|_{\vec{\varepsilon}=\vec{a}\varepsilon}$ as in (4.1), we have

$$\phi = \tilde{\mu} * \tilde{I},$$

where $\tilde{\mu}((C, \Lambda_C); \vec{s}) \in \mathbb{Q}[[\varepsilon]]$ and $\tilde{I}((C, \Lambda_C); \vec{s}) \in \mathbb{Q} + \mathbb{Q}[\varepsilon^{-1}]\varepsilon^{-1}$.

The alternative renormalisation procedure is to implement Algebraic Birkhoff Factorisation on the restricted map ϕ , which yields a factorisation

$$\phi = \phi_-^{*(-1)} * \phi_+,$$

with $\phi_-^{*(-1)}((C, \Lambda_C); \vec{s}) \in \mathbb{C}[[\varepsilon]]$, and $\phi_+((C, \Lambda_C); \vec{s}) \in \mathbb{C}[\varepsilon^{-1}]$.

Thus both factorisations are for linear maps between the same spaces. Now the standard argument of the uniqueness of the Algebraic Birkhoff Factorisation then shows that the two factorisations coincide. \square

Corollary 6.3. *The renormalised MZVs do not depend on the parameters a_1, a_2, \dots .*

Let us illustrate the two approaches on a simple example. To simplify notations, for k linear forms L_1, \dots, L_k , we set

$$[L_1, \dots, L_k] := \frac{e^{L_1}}{1 - e^{L_1}} \frac{e^{L_1+L_2}}{1 - e^{L_1+L_2}} \dots \frac{e^{L_1+L_2+\dots+L_k}}{1 - e^{L_1+L_2+\dots+L_k}}. \tag{6.2}$$

and

$$\frac{e^\varepsilon}{1 - e^\varepsilon} = -\frac{1}{\varepsilon} + h(\varepsilon). \tag{6.3}$$

Example 6.4. For $k = 2$ and the Chen cone $\langle e_1, e_1 + e_2 \rangle$, we have

$$S^o(\langle e_1, e_1 + e_2 \rangle, \Lambda_2) = [\varepsilon_1, \varepsilon_2],$$

$$\begin{aligned} \pi_+([\varepsilon_1, \varepsilon_2]) &= \pi_+ \left(\left(-\frac{1}{\varepsilon_1} + h(\varepsilon_1) \right) \left(-\frac{1}{\varepsilon_1 + \varepsilon_2} + h(\varepsilon_1 + \varepsilon_2) \right) \right) \\ &= \pi_+ \left(-\frac{h(\varepsilon_1 + \varepsilon_2)}{\varepsilon_1} - \frac{h(\varepsilon_1)}{\varepsilon_1 + \varepsilon_2} + h(\varepsilon_1)h(\varepsilon_1 + \varepsilon_2) \right) \\ &= -\frac{h(\varepsilon_1 + \varepsilon_2) - h(\varepsilon_2)}{\varepsilon_1} - \frac{h(\varepsilon_1) - h\left(\frac{\varepsilon_1 - \varepsilon_2}{2}\right)}{\varepsilon_1 + \varepsilon_2} + h(\varepsilon_1)h(\varepsilon_1 + \varepsilon_2). \end{aligned}$$

So

$$\begin{aligned} \pi_+([\varepsilon_1, \varepsilon_2])|_{(a_1\varepsilon, a_2\varepsilon)} &= -\frac{h((a_1 + a_2)\varepsilon) - h(a_2\varepsilon)}{a_1\varepsilon} \\ &\quad - \frac{h(a_1\varepsilon) - h\left(\frac{(a_1 - a_2)\varepsilon}{2}\right)}{(a_1 + a_2)\varepsilon} \\ &\quad + h(a_1\varepsilon)h((a_1 + a_2)\varepsilon). \end{aligned}$$

Evaluating at $\varepsilon = 0$ yields

$$\begin{aligned} \zeta(0, 0) &= -\frac{(a_1 + a_2) - a_2}{a_1} h'(0) - \frac{\frac{a_1 + a_2}{2}}{a_1 + a_2} h'(0) + h(0)^2 \\ &= -\frac{3}{2} h'(0) + h(0)^2 = \frac{3}{8}. \end{aligned}$$

On the other hand, to use formula (4.2) to find $\phi_-^{*(-1)}$ needs more involved computations. We easily get

$$\phi_-^{*(-1)}(\langle e_1 \rangle, \mathbb{Z}e_1) = h(a_1\varepsilon),$$

and

$$\phi_-^{*(-1)}(\langle e_1 + e_2 \rangle, \mathbb{Z}(e_1 + e_2)) = h((a_1 + a_2)\varepsilon).$$

The reduced coproduct applied to the two dimensional Chen cone reads

$$\begin{aligned} \Delta'(\langle e_1, e_1 + e_2 \rangle, \Lambda_2) &= (\langle e_2 \rangle, \mathbb{Z}e_2) \otimes (\langle e_1 \rangle, \mathbb{Z}e_1) \\ &\quad + \left(\langle e_1 - e_2 \rangle, \mathbb{Z}\frac{e_1 - e_2}{2} \right) \otimes (\langle e_1 + e_2 \rangle, \mathbb{Z}(e_1 + e_2)). \end{aligned}$$

Thus

$$\begin{aligned}
 & \phi_{-}(\langle e_1, e_1 + e_2 \rangle, \Lambda_2) \\
 = & -P \left(\left(-\frac{1}{a_1 \varepsilon} + h(a_1 \varepsilon) \right) \left(-\frac{1}{(a_1 + a_2) \varepsilon} + h((a_1 + a_2) \varepsilon) \right) \right. \\
 & \left. + \left(-h(a_2 \varepsilon) \right) \left(-\frac{1}{a_1 \varepsilon} + h(a_1 \varepsilon) \right) \right. \\
 & \left. + \left(-h((a_1 - a_2) \varepsilon / 2) \right) \left(-\frac{1}{(a_1 + a_2) \varepsilon} + h((a_1 + a_2) \varepsilon) \right) \right) \\
 = & \frac{h((a_1 + a_2) \varepsilon) - h(a_2 \varepsilon)}{a_1 \varepsilon} + \frac{h(a_1 \varepsilon) - h((a_1 - a_2) \varepsilon / 2)}{(a_1 + a_2) \varepsilon} \\
 & - h(a_1 \varepsilon) h((a_1 + a_2) \varepsilon) \\
 & + h(a_2 \varepsilon) h(a_1 \varepsilon) + h((a_1 - a_2) \varepsilon / 2) h((a_1 + a_2) \varepsilon).
 \end{aligned}$$

Now by the equation

$$\begin{aligned}
 & \phi_{-}(\langle e_1, e_1 + e_2 \rangle, \Lambda_2) + \phi_{-}^{*(-1)}(\langle e_1, e_1 + e_2 \rangle, \Lambda_2) \\
 & + \phi_{-}(\langle e_2 \rangle, \mathbb{Z} e_2) \phi_{-}^{*(-1)}(\langle e_1 \rangle, \mathbb{Z} e_1) \\
 & + \phi_{-} \left(\langle e_1 - e_2 \rangle, \mathbb{Z} \frac{e_1 - e_2}{2} \right) \phi_{-}^{*(-1)}(\langle e_1 + e_2 \rangle, \mathbb{Z}(e_1 + e_2)) \\
 = & 0,
 \end{aligned}$$

we have

$$\begin{aligned}
 \phi_{-}^{*(-1)}(\langle e_1, e_1 + e_2 \rangle, \Lambda_2) = & -\frac{h((a_1 + a_2) \varepsilon) - h(a_2 \varepsilon)}{a_1 \varepsilon} \\
 & - \frac{h(a_1 \varepsilon) - h\left(\frac{(a_1 - a_2) \varepsilon}{2}\right)}{(a_1 + a_2) \varepsilon} \\
 & + h(a_1 \varepsilon) h((a_1 + a_2) \varepsilon).
 \end{aligned}$$

This agrees with $\pi_{+}([\varepsilon_1, \varepsilon_2])|_{(a_1 \varepsilon, a_2 \varepsilon)}$.

ACKNOWLEDGEMENTS. The authors thank Kavli Institute for Theoretical Physics China (KITPC) and Morningside Center of Mathematics (MCM) in Beijing where part of the work was carried out. The second author thanks Sichuan University, Lanzhou University and Capital Normal University for their kind hospitality. The authors thank the referee for helpful suggestions.

References

- [1] A. BARVINOK, “Integer Points in Polyhedra”, Zurich Lectures in Advanced Mathematics, European Mathematical Society, 2008.
- [2] A. CONNES and D. KREIMER, *Hopf algebras, renormalisation and noncommutative neometry*, Comm. Math. Phys. **199** (1988), 203–242.
- [3] K. EBRAHIMI-FARD, L. GUO and D. KREIMER, *Spitzer’s identity and the algebraic Birkhoff decomposition in p QFT*, J. Phys. A: Math. Gen. **37** (2004), 11037–11052.
- [4] K. EBRAHIMI-FARD, D. MANCHON, J. SINGER and J. ZHAO, *Transfer group for renormalized multiple zeta values*, arXiv:1510.09159 [math.NT].
- [5] W. FULTON, “Introduction to Toric Varieties”, Princeton University Press, 1993.
- [6] L. GUO, S. PAYCHA and B. ZHANG, *Conical zeta values and their double subdivision relations*, Adv. Math. **252** (2014), 343–381.
- [7] L. GUO, S. PAYCHA and B. ZHANG, *A conical approach to Laurent expansions for multivariate meromorphic germs with linear poles*, arXiv:1501.00426 v2.
- [8] L. GUO, S. PAYCHA and B. ZHANG, *Algebraic Birkhoff factorisation and the Euler-Maclaurin formula on cones*, Duke Math J. **166** (2017), 537–571.
- [9] L. GUO, S. PAYCHA and B. ZHANG, *Counting an infinite number of points: a testing ground for renormalisation methods*, arXiv:1501.00429.
- [10] L. GUO and B. ZHANG, *Renormalisation of multiple zeta values*, J. Algebra **319** (2008), 3770–3809.
- [11] L. GUO and B. ZHANG, *Differential Birkhoff decomposition and renormalisation of multiple zeta values*, J. Number Theory **128** (2008), 2318–2339.
- [12] Y. KOMORI, K. MATSUMOTO and H. TSUMURA, *On Witten multiple zeta-functions associated with semisimple Lie algebras V* , Glasgow Mathematical Journal **57** (2015), 107–130.
- [13] D. MANCHON, *Hopf algebras, from basics to applications to renormalisation*, Comptes-rendus des Rencontres mathématiques de Glanon 2001 (2003); “Hopf Algebras in Renormalisation”, Handbook of algebra, Vol. 5, M. Hazewinkel (ed.), 2008.
- [14] D. MANCHON and S. PAYCHA, *Nested sums of symbols and renormalised multiple zeta values*, Int. Math. Res. Papers **24** (2010), 4628–4697.

- [15] T. TERASOMA, *Rational convex cones and cyclotomic multiple zeta values*, arXiv:math/0410306.
- [16] J. ZHAO, *Renormalization of multiple q -zeta values*, *Acta Mathematica Sinica* **24** (2008), 1593–1616.
- [17] J. ZHAO, *Alternating Euler sums and special values of Witten multiple zeta function attached to $\mathfrak{so}(5)$* , *J. Aust. Math. Soc.* **89** (2010), 419–430.
- [18] J. ZHAO and X. ZHOU, *Witten multiple zeta values attached to $\mathfrak{sl}(4)$* , *Tokyo J. of Math.* **34** (2011), 135–152.

Combinatorics of Poincaré s and Schröder s equations

Frédéric Menous, Jean-Christophe Novelli and Jean-Yves Thibon

Abstract. We investigate the combinatorial properties of the functional equation $\phi[h(z)] = h(qz)$ for the conjugation of a formal diffeomorphism ϕ of \mathbb{C} to its linear part $z \mapsto qz$. This is done by interpreting the functional equation in terms of symmetric functions, and then lifting it to noncommutative symmetric functions. We describe explicitly the expansion of the solution in terms of plane trees and prove that its expression on the ribbon basis has coefficients in $\mathbb{N}[q]$ after clearing the denominators $(q)_n$. We show that the conjugacy equation can be lifted to a quadratic fixed point equation in the free triduplicial algebra on one generator. This can be regarded as a q -deformation of the duplicial interpretation of the noncommutative Lagrange inversion formula. Finally, these calculations are interpreted in terms of the group of the operad of Stasheff polytopes, and are related to Ecalle's arborified expansion by means of morphisms between various Hopf algebras of trees.

1 Introduction

Algebraic identities between generic formal power series can often be interpreted as identities between symmetric functions. This is the case, for example, with the Lagrange inversion formula (see, *e.g.*, [34, Example 24, page 35, Example 25, page 132], [30, Section 2.4], and [31]). The problem can be stated as follows. Given

$$\varphi(z) = \sum_{n \geq 0} \varphi_n z^n \quad (\varphi_0 \neq 0) \tag{1.1}$$

find the coefficients g_n of the unique power series

$$g(z) = \sum_{n \geq 0} g_n z^{n+1} \quad \text{satisfying} \quad z = \frac{g(z)}{\varphi(g(z))}. \tag{1.2}$$

We can assume that $\varphi_0 = 1$ and that

$$\varphi(g) = \sum_{n \geq 0} h_n(X) g^n = \prod_{n \geq 1} (1 - g x_n)^{-1} =: \sigma_g(X) \quad (1.3)$$

is the generating series of the homogeneous symmetric functions of an infinite set of variables X . In λ -ring notation, the solution reads

$$g_n = \frac{1}{n+1} h_n((n+1)X) \quad (1.4)$$

(recall that $\sigma_t(nX) = \sigma_t(X)^n$, see, e.g., [34, page 25]). On this expression, it is clear that g_n is Schur positive, in fact, it is the Frobenius characteristic of the permutation representation of \mathfrak{S}_n on the set PF_n of parking functions of length n . These calculations can be lifted to the algebra of noncommutative symmetric functions, and the result is then interpreted in terms of representations of 0-Hecke algebras. This in turn leads to various combinatorial interpretations, to q -analogues, and to a new interpretation of the antipode of the Hopf algebra of noncommutative formal diffeomorphisms [39].

There is another functional equation which can be investigated in this setting. Given a formal diffeomorphism

$$\phi(z) = \sum_{n \geq 0} \phi_n z^{n+1} \quad \text{with } \phi_0 = q \neq 0, \quad (1.5)$$

one may look for a formal diffeomorphism tangent to identity

$$h(z) = \sum_{n \geq 0} g_n z^{n+1} = z g(z) \quad (g_0 = 1), \quad (1.6)$$

conjugating ϕ to its linear part

$$h^{-1} \circ \phi \circ h(z) = qz \text{ or equivalently } \phi[h(z)] = h(qz) = qz g(qz). \quad (1.7)$$

In terms of symmetric functions, we can assume that

$$\phi(z) = qz \sigma_z(X) \quad (1.8)$$

so that the conjugacy equation reads

$$\phi[h(z)] = qh(z) \sigma_{h(z)}(X) = qz \sum_{n \geq 0} g_n (qz)^n, \quad (1.9)$$

and interpreting g_n as symmetric functions $g_n(X)$, we can get rid of z by homogeneity (since $g_n(zX) = z^n g_n(X)$). Our functional equation reads now

$$g(X) \sigma_{g(X)} = g(qX). \quad (1.10)$$

We can lift this to noncommutative symmetric functions, for example as

$$g(qA) = \sum_{n \geq 0} S_n(A)g(A)^{n+1}. \quad (1.11)$$

For $q = 0$, this reduces to the functional equation for the antipode of the noncommutative Faà di Bruno Hopf algebra [2,39], so that this problem can indeed be regarded as a generalisation of the noncommutative Lagrange inversion.

The conjugacy equation for h is often called Poincaré's equation, and the equivalent one for h^{-1} , Schröder's equation. Indeed, it has been first discussed by Schröder [43], who discovered a few explicit solutions, which are still essentially the only known ones. It is easy to show the existence and unicity of a formal solution when q is not a root of unity. The analyticity of the solution for $|q| \neq 1$ has been established by Koenigs [28]. It is interesting that this result can be easily proved by means of inequalities involving the Schröder numbers [33], defined by the same Schröder in a totally different context [42]. Much more difficult is Siegel's proof of convergence in the case $q = e^{2\pi i\theta}$ with θ satisfying a diophantine condition [44] (see also [16] for a modern proof under Bruno's condition). Again in this case, the Schröder numbers play a crucial role in the majorations.

We shall see that analyzing the conjugacy equation at the level of the noncommutative Faà di Bruno algebra provides a simple explanation of this fact, by letting Schröder trees appear naturally in the iterative solution of a q -difference equation. The resulting expressions turn out to be identical to those produced by Ecalle's arborification method [14–16]. This coincidence will be explained in Section 11, where it will be proved that both methods can be interpreted in terms of calculations in the group of an operad and in related Hopf algebras.

Identifying the noncommutative Faà di Bruno algebra with noncommutative symmetric functions as in [39], we have several bases at our disposal. The solution g of the noncommutative Poincaré equation is naturally expressed in the complete basis S^I . After clearing out the denominators $(q; q)_n$, it turns out that its homogeneous components g_n are positive on the ribbon basis. This unexpected fact suggests that these should be the graded characteristics of some projective modules over 0-Hecke algebra, a conjecture that we expect to investigate in another paper. This positivity property will be proved in two different ways. We shall first recast the conjugacy equation as a quadratic fixed point problem, by means of the triduplicial operations introduced in [40]. On the ribbon basis, the quadratic map is manifestly positive. Next, comparing the binary tree expansion with the previous one based on reduced

plane trees, we obtain a natural bijection between these trees and hypoplactic classes of parking functions (*aka* parking quasi-ribbons or segmented nondecreasing parking functions). This solves a problem which was left open in [38], and provides a bijection similar to the duplicial bijection of [40] between nondecreasing parking functions and binary trees.

In Section 6, we describe the expansion of g_n on the ribbon basis. The numerator of each coefficient is a q -analogue of $n!$, recording a statistic on permutations which is explicitly described.

In Section 7, we discuss Schröder's equation at the level of noncommutative symmetric functions. It leads to a different combinatorics. There is no natural expansion on trees, but instead, there is a rather explicit algebraic formula for the coefficients, which amounts to applying a simple linear transformation to a famous sequence of noncommutative symmetric functions, the q -Klyachko elements $K_n(q)$ [19, 29], which occur as well as Lie idempotents in descent algebras or as noncommutative Hall-Littlewood functions [24]. It is then shown in Section 8 that the same coefficients arise when the problem is considered from the point of view of mould calculus and differential operators. Thus, at least for this problem, the mould calculus approach can be seen to be dual to that relying on the noncommutative Faà di Bruno algebra.

The rest of the paper is devoted to the explanation of the coincidence between the coefficients of our first plane tree expansion, and Ecalle's arborified coefficients. The short story is that on the one hand, the paper [15] provides an interpretation of the arborification method as a lift of the original problem to an equation in the group of characters of a Connes-Kreimer algebra. On the other hand, our version with plane trees of the functional equation can be naturally interpreted in the group of a free operad. This group turns out to be isomorphic to the group of characters of a Hopf algebra of reduced plane forests, which admits a surjective morphism to the previous Connes-Kreimer algebra.

Section 9 provides some background on the operad of reduced plane trees. It is a free operad with one generator in each degree $n \geq 2$, also known as the operad of Stasheff polytopes, or as a free S -magmatic operad [26, 32]. We describe the associated group, and prove that it is isomorphic to the group of characters of the Hopf algebra of reduced plane trees of [12].

In Section 10, we explain the encoding of the previous group by means of Polish codes of trees, and illustrate the method on the cases of Lagrange inversion and of the Poincaré equation.

In Section 11, we recall the Hopf algebraic interpretation of the arborification method [15, 16], and prove that the skeleton map already in-

troduced in [39] induces a morphism of Hopf algebras between reduced plane forests and the \mathbb{N}^* -decorated Connes-Kreimer algebra.

In Section 12, we review briefly the interpretation of Lagrange inversion and of Cayley's formula for the solution of a generic differential equation in terms of an operad on (non-reduced) plane trees.

Finally, it is generally interesting to look at the images of formal series in combinatorial Hopf algebras under various characters. In the Appendix (Section 13), we review a few examples of explicit solutions of the conjugacy equation. Apart from the trivial case of linear fractional transformations $\phi(z) = qz/(1-z)$ (corresponding to the alphabet $A = \{1\}$), there is the already nontrivial case of the logistic map $\phi(z) = qz(1-z)$, corresponding to $A = \{-1\}$, for which explicit solutions (already given by Schröder) are known for $q = -2, 2, 4$. The case $A = \mathbb{E}$, corresponding to $\phi(z) = qze^z$ is not explicitly solved, but it leads to interesting statistics on pairs of permutations. These examples are investigated numerically in [7–10].

2 Notations

This paper is a continuation of [39, 40]. Our notations for ordinary symmetric functions are as in [34], and for noncommutative symmetric functions as in [19, 29].

The classical algebra of symmetric functions, denoted by Sym or $Sym(X)$, is a free associative and commutative graded algebra with one generator in each degree:

$$Sym = \mathbb{C}[h_1, h_2, \dots] = \mathbb{C}[e_1, e_2, \dots] = \mathbb{C}[p_1, p_2, \dots] \quad (2.1)$$

where the h_n are the complete homogeneous symmetric functions, the e_n the elementary symmetric functions, and the p_n the power sums.

Its usual bialgebra structure is defined by the coproduct

$$\Delta_0 h_n = \sum_{i=0}^n h_i \otimes h_{n-i} \quad (h_0 = 1) \quad (2.2)$$

which allows to interpret it as the algebra of polynomial functions on the multiplicative group

$$G_0 = \{a(z) = \sum_{n \geq 0} a_n z^n \mid a_0 = 1\} \quad (2.3)$$

of formal power series with constant term 1: h_n is the coordinate function

$$h_n : a(z) \longmapsto a_n. \quad (2.4)$$

Indeed, $h_n(a(z)b(z)) = (\Delta_0 h_n)(a(z) \otimes b(z))$.

But h_n can also be interpreted as a coordinate on the group

$$G_1 = \{A(z) = \sum_{n \geq 0} a_n z^{n+1} \ (a_0 = 1)\} \tag{2.5}$$

of formal diffeomorphisms tangent to identity, under functional composition. Again with $h_n(A(z)) = a_n$ and $h_n(A(z)B(z)) = \Delta_1(A(z) \otimes B(z))$, the coproduct is now

$$\Delta_1 h_n = \sum_{i=0}^n h_i \otimes h_{n-i}((i + 1)X) \ (h_0 = 1) \tag{2.6}$$

where $h_n(mX)$ is defined as the coefficient of t^n in $(\sum h_k t^k)^m$. The resulting bialgebra is known as the Faà di Bruno algebra [27].

These constructions can be repeated word for word with the algebra Sym of noncommutative symmetric functions. It is a free associative (and noncommutative) graded algebra with one generator S_n in each degree, which can be interpreted as above if the coefficients a_n belong to a noncommutative algebra. In this case, G_0 is still a group, but G_1 is not, as its composition is not anymore associative. However, the coproduct Δ_1

$$\Delta_1 S_n = \sum_{i=0}^n S_i \otimes S_{n-i}((i + 1)A) \ (S_0 = 1) \tag{2.7}$$

remains coassociative, and Sym endowed with this coproduct is a Hopf algebra, known as Noncommutative Formal Diffeomorphisms [2, 39], or as the noncommutative Faà di Bruno algebra [13].

The classical trick of regarding a generic series as a series of symmetric functions amounts to working in one of these Hopf algebras. The occurrence of trees in the solutions of certain problems can be traced back to the existence of Hopf algebras morphisms between these algebras and various Hopf algebras of trees.

Recall that bases of Sym_n are labelled by compositions I of n . The noncommutative complete and elementary functions are denoted by S_n and Λ_n , and the notation S^I means $S_{i_1} \cdots S_{i_r}$. The ribbon basis is denoted by R_I . The notation $I \vDash n$ means that I is a composition of n . The conjugate composition is denoted by I^\sim . The product formula for ribbons is

$$R_I R_J = R_{IJ} + R_{I \triangleright J} \tag{2.8}$$

where for $I = (i_1, \dots, i_r)$ and $J = (j_1, \dots, j_s)$,

$$IJ = (i_1, \dots, i_r, j_1, \dots, j_s) \text{ and } I \triangleright J = (i_1, \dots, i_r + j_1, \dots, j_s). \tag{2.9}$$

The graded dual of Sym is $Q\text{Sym}$ (quasi-symmetric functions). The dual basis of (S^I) is (M_I) (monomial), and that of (R_I) is (F_I) .

The *evaluation* $\text{Ev}(w)$ of a word w over a totally ordered alphabet A is the sequence $(|w|_a)_{a \in A}$ where $|w|_a$ is the number of occurrences of a in w . The *packed evaluation* $I = \text{pEv}(w)$ is the composition obtained by removing the zeros in $\text{Ev}(w)$.

Two permutations $\sigma, \tau \in \mathfrak{S}_n$ are said to be *sylvester-equivalent* if the decreasing binary trees¹ of σ^{-1} and τ^{-1} have the same shape. The generating function of the number of inversions on a sylvester class is given by the q -hook-length formula [1, 25].

3 Recursive solution of Poincaré's equation

Equation (1.11) can be written as a q -difference equation

$$g(qA) - g(A) = \sum_{n \geq 1} S_n(A)g(A)^{n+1}. \quad (3.1)$$

Introducing a homogeneity parameter t , we have

$$g(qtA) - g(tA) = \sum_{n \geq 1} t^n S_n(A)g(tA)^{n+1}. \quad (3.2)$$

Let g_n be the term of degree n in g , so that

$$g(tA) = \sum_{n \geq 1} t^n g_n(A). \quad (3.3)$$

Comparing the homogeneous components in both sides of (3.2), one gets a triangular system allowing to compute the g_n recursively. For $n \leq 3$:

$$\begin{aligned} g_0 &= 1, \\ (q-1)g_1 &= S_1, \\ (q^2-1)g_2 &= 2S_1g_1 + S_2, \\ (q^3-1)g_3 &= 2S_1g_2 + S_1g_1^2 + 3S_2g_1 + S_3. \end{aligned} \quad (3.4)$$

Define

$$q_n = q^n - 1, \quad (q)_n = q_n q_{n-1} \cdots q_1 \quad \text{and} \quad \tilde{g}_n = (q)_n g_n \quad (3.5)$$

¹ The decreasing tree $T(w)$ of a word without repeated letters $w = unv$ and maximal letter n is the binary tree with root n and left and right subtrees $T(u)$ and $T(v)$.

The first \tilde{g}_n are then

$$\begin{aligned} \tilde{g}_1 &= S_1, \\ \tilde{g}_2 &= (q - 1)S_2 + 2S^{11}, \\ \tilde{g}_3 &= (q)_2S_3 + 3(q^2 - 1)S^{21} + 2(q - 1)S^{12} + (5 + q)S^{111}. \end{aligned} \tag{3.6}$$

On the ribbon basis of **Sym**, the expression is quite remarkable:

$$\begin{aligned} \tilde{g}_1 &= S_1, \\ \tilde{g}_2 &= (q + 1)R_2 + 2R_{11}, \\ \tilde{g}_3 &= (1 + q)(1 + q + q^2)R_3 + (2 + q + 3q^2)R_{21} \\ &\quad + 3(1 + q)R_{12} + (5 + q)R_{111}. \end{aligned} \tag{3.7}$$

Indeed, \tilde{g}_n is a linear combination of ribbons with positive coefficients which are all q -analogues of $n!$. Note that it is immediate, by induction on n , that $\tilde{g}_n|_{q=1} = n!S_1^n$, but it is not clear that the coefficients are in $\mathbb{N}[q]$. A combinatorial interpretation of these coefficients will be given below (Theorem 6.4).

4 A tree-expanded solution

In order to solve (3.2), define a q -integral by²

$$\int_a^b t^{n-1} d_q t = \left[\frac{t^n}{q^n - 1} \right]_a^b \tag{4.1}$$

and a q -difference operator

$$\Delta_q f(t) = \frac{f(qt) - f(t)}{t}. \tag{4.2}$$

Then,

$$\Delta_q \int_0^t f(s) d_q s = f(t) \tag{4.3}$$

so that g is the unique solution of the fixed point equation

$$g(tA) = g_0 + \sum_{n \geq 1} S_n(A) \int_0^t s^{n-1} g(sA)^{n+1} d_q s. \tag{4.4}$$

² This is just the ordinary q -integral up to conjugation by the transformation $t \mapsto (q - 1)t$.

This equation is of the form

$$g = g_0 + \sum_{n \geq 2} F_n(g, \dots, g) \tag{4.5}$$

where

$$F_n(x_1, \dots, x_n) = S_{n-1} \int_0^1 s^{n-2} x_1(s) \cdots x_n(s) d_q s \tag{4.6}$$

is an n -linear operator. The solution can therefore be expanded as a sum over reduced plane trees (plane trees in which all internal vertices have at least two descendants), which will be called *Schröder trees* in the sequel.

Proceeding as in [39], we introduce another indeterminate S_0 (non-commuting with the other S_n) and set $g_0 = S_0$. The solution is then a linear combinations of monomials S^I where I is a vector of nonnegative integers, with $i_1 > 0$.

The first \tilde{g}_n are then

$$\begin{aligned} \tilde{g}_1 &= S^{100} \\ \tilde{g}_2 &= (q-1)S^{2000} + S^{11000} + S^{10100} \\ \tilde{g}_3 &= (q)_2 S^{30000} + (q^2-1)(S^{210000} + S^{201000} + S^{200100}) \\ &\quad + (q-1)(S^{120000} + S^{102000}) \\ &\quad + S^{1110000} + S^{1101000} + S^{1011000} + S^{1010100} + (q+1)S^{1100100}. \end{aligned} \tag{4.7}$$

We can interpret each S_i as the symbol of an $(i + 1)$ -ary operation in Polish notation. Then, \tilde{g}_n is a sum over Polish codes of Schröder trees as in [39, Figure 4]:

$$\tilde{g}_2 = (q-1) \begin{array}{c} 2 \\ / \quad | \quad \backslash \\ 0 \quad 0 \quad 0 \end{array} + \begin{array}{c} 1 \\ / \quad \backslash \\ 0 \quad 0 \end{array} + \begin{array}{c} 1 \\ / \quad \backslash \\ 0 \quad 1 \\ / \quad \backslash \\ 0 \quad 0 \end{array} \tag{4.8}$$

$$= (q-1)S^{2000} + S^{11000} + S^{10100}. \tag{4.9}$$

The exponent vectors I encoding Schröder trees as above will be referred to as *Schröder pseudocompositions*.

From (4.6), we have:

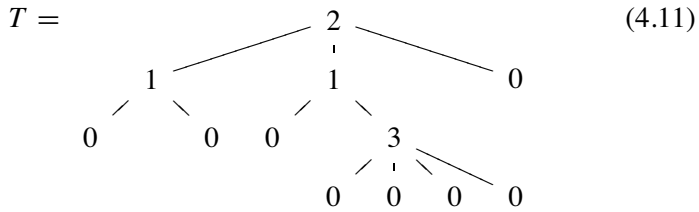
Theorem 4.1. *Let I be a Schröder pseudocomposition, and $T(I)$ be the tree encoded by I . The coefficient of S^I in g is*

$$m_I(q) = \prod_{v \in T(I)} \frac{1}{q^{\phi(v)-1}} \tag{4.10}$$

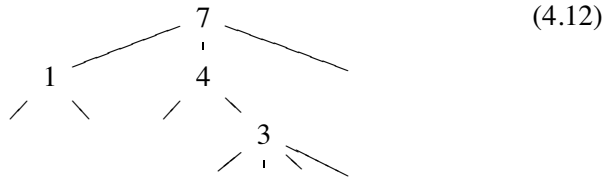
where v runs over the internal vertices of $T(I)$ and $\phi(v)$ is the number of leaves of the subtree of v .

Note 4.2. These coefficients are precisely those obtained by Ecalle’s arborification method [14–16]. This coincidence will be explained in Section 11.

Example 4.3. For



decorating each internal vertex v with the number $\phi(v) - 1$, we obtain



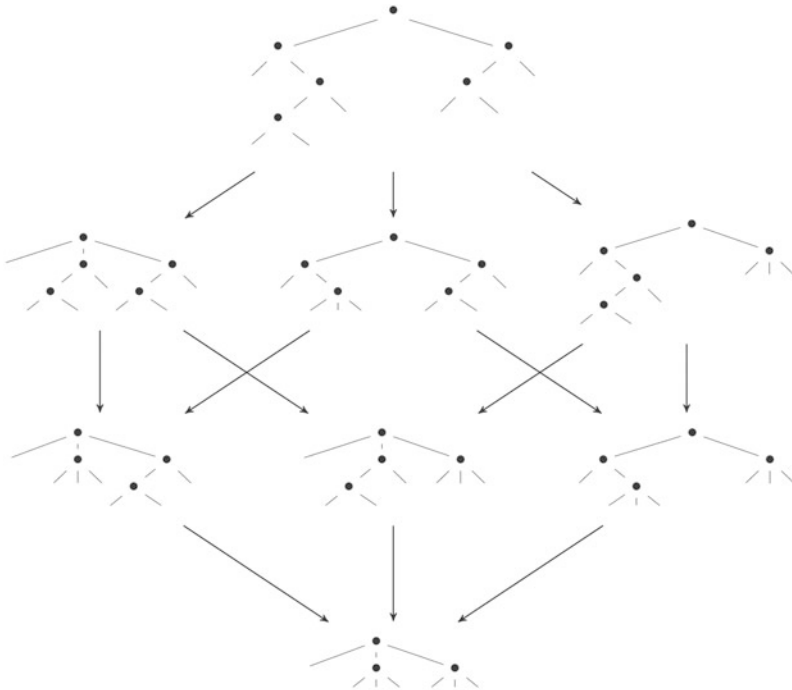
so that

$$m_{210010300000} = \frac{1}{q_7 q_4 q_3 q_1}. \tag{4.13}$$

Note 4.4. The I whose nonzero entries are all equal to 1 correspond to binary trees. The anti-refinements $J \preceq I$ of such an I , obtained by summing consecutive nonzero entries in all possible ways, correspond to the trees $T(J)$ obtained by contracting (internal) left edges in all possible ways in $T(I)$. This procedure provides a way to group Schröder trees

into classes labelled by binary trees. An algebraic interpretation of these groups will be provided below.

Example 4.5. The contractions of the binary tree $T(1101100011000)$ are



which are respectively, reading the diagram by rows,
 $T(201100011000)$, $T(110200011000)$, $T(110110002000)$,
 $T(20200011000)$, $T(20110002000)$, $T(11020002000)$,
 and $T(2020002000)$.

5 A binary tree expansion

5.1 A bilinear map on Sym

The preceding remark (Note 4.4) suggests that, as in the case of Lagrange inversion, the conjugacy equation can be cast as a quadratic fixed point problem. This is easily done at the level of noncommutative symmetric functions.

Let Ω be the linear operator on Sym introduced in [38,39], and defined by

$$\Omega S^{(i_1, \dots, i_r)} = S^{(i_1+1, i_2, \dots, i_r)}. \quad (5.1)$$

Writing

$$g(qtA) - g(tA) = \sum_{n \geq 1} t^n S_n(A) g(tA)^{n+1} \tag{5.2}$$

$$= \left(\sum_{n \geq 1} t^n S_n(A) g(tA)^n \right) g(tA) \tag{5.3}$$

$$= t S_1(A) g(tA)^2 + t \left(\sum_{n \geq 2} t^{n-1} S_n(A) g(tA)^n \right) g(tA) \tag{5.4}$$

$$= t S_1(A) g(tA)^2 + t \Omega \left[\sum_{n \geq 1} t^n S_n(A) g(tA)^{n+1} \right] g(tA) \tag{5.5}$$

$$= t S_1(A) g(tA)^2 + t \Omega [g(qtA) - g(tA)] g(tA) \tag{5.6}$$

we see that g is the unique solution of the quadratic functional equation

$$g(tA) = 1 + \int_0^t (S_1(A)g(sA) + t\Omega\Delta_q g(sA)) g(sA) d_qs \tag{5.7}$$

of the form

$$g = 1 + \mathbf{B}_q(g, g). \tag{5.8}$$

The bilinear map \mathbf{B}_q has a simple expression in the complete basis. For two compositions $I \models i$ and $J \models j$,

$$\mathbf{B}_q(S^I, S^J) = \int_0^1 (S_1 S^I S^J s^{i+j} + \Omega S^I (q^i - 1) s^i S^J s^j) d_qs \tag{5.9}$$

$$= \frac{S^{1IJ} + q_i \Omega S^{IJ}}{q_{i+j+1}}. \tag{5.10}$$

It follows that in the ribbon basis

$$\mathbf{B}_q(R_I, R_J) = \frac{(R_{1I} + q^i R_{1 \triangleright I}) R_J}{q_{i+j+1}}. \tag{5.11}$$

As a consequence, the coefficients of \tilde{g}_n on the ribbon basis are in $\mathbb{N}[q]$. A combinatorial interpretation will be provided below.

For example, with $g_0 = 1$, we have,

$$\begin{aligned} g_1 &= \mathbf{B}_q(g_0, g_0) \\ g_2 &= \mathbf{B}_q(g_0, g_1) + \mathbf{B}_q(g_1, g_0) \\ g_3 &= \mathbf{B}_q(g_0, g_2) + \mathbf{B}_q(g_1, g_1) + \mathbf{B}_q(g_2, g_0) \end{aligned} \tag{5.12}$$

so that one gets

$$\begin{aligned}
 \tilde{g}_1 &= q_1 \mathbf{B}_q(\tilde{g}_0, \tilde{g}_0) \\
 \tilde{g}_2 &= q_2(\mathbf{B}_q(\tilde{g}_0, \tilde{g}_1) + \mathbf{B}_q(\tilde{g}_1, \tilde{g}_0)) \\
 \tilde{g}_3 &= q_3(\mathbf{B}_q(\tilde{g}_0, \tilde{g}_2) + \frac{q_2}{q_1} \mathbf{B}_q(\tilde{g}_1, \tilde{g}_1) + \mathbf{B}_q(\tilde{g}_2, \tilde{g}_0))
 \end{aligned} \tag{5.13}$$

and

$$\begin{aligned}
 \tilde{g}_1 &= S_1 \\
 \tilde{g}_2 &= (S^{11}) + (S^{11} + q_1 S_2) \\
 \tilde{g}_3 &= (2S^{111} + q_1 S^{12}) + \frac{q_2}{q_1} (S^{111} + q_1 S^{21}) \\
 &\quad + (2S^{111} + q_1 S^{12} + 2q_2 S^{21} + q_1 q_2 S_3) \\
 &= q_1 q_2 S_3 + 3q_2 S^{21} + 2q_1 S^{12} + \left(\frac{q_2}{q_1} + 4 \right) S^{111},
 \end{aligned} \tag{5.14}$$

which coincides with (3.6).

5.2 Triduplicial expansion

These equations can be lifted to Schröder trees, by setting as above $g_0 = S_0$ and using (5.9) without modification. We recover then the same expressions for g_n as in the previous section.

Indeed, start again with (5.13) and $\tilde{g}_0 = g_0 = S_0$. We then have

$$\begin{aligned}
 \tilde{g}_1 &= S^{100}, \\
 \tilde{g}_2 &= (S^{10100}) + (S^{11000} + q_1 S^{2000}), \\
 \tilde{g}_3 &= (S^{1010100} + S^{1011000} + q_1 S^{102000}) + \frac{q_2}{q_1} (S^{1100100} + q_1 S^{200100}) \\
 &\quad + \left(S^{1101000} + S^{1110000} + q_1 S^{120000} \right. \\
 &\quad \left. + q_2 S^{201000} + q_2 S^{210000} + q_1 q_2 S^{30000} \right),
 \end{aligned} \tag{5.15}$$

which again gives back (4.7).

Now, (5.11) can be lifted in another way. Indeed, in the same way as Lagrange inversion is directly related to Catalan numbers (in the guise of nondecreasing parking functions) and to the free duplicial algebra on one generator **CQSym** [40], we find here the little Schröder numbers which are related to the free triduplicial algebra on one generator (defined in [40]), into which **CQSym** is naturally embedded.

More precisely, the co-hypoplactic subalgebra of **QSym**, denoted by **SQSym** in [38], spanned by hypoplactic classes of parking functions (parking quasi-ribbons), has been identified in [40] as the free triduplicial algebra on one generator. Its graded dimension is given by the number of Schröder trees, but no natural bijection between these trees and parking quasi-ribbons had been known up to now. However, this algebra has a basis \mathbf{P}_α which is mapped to the ribbon basis R_I by a Hopf algebra morphism χ . This suggests that the operations on ribbons involved in (5.11) might be the image under χ of triduplicial operations on parking quasi-ribbons and that an analogue of the S -basis should exist in **SQSym**. We shall see that this is indeed the case, by means of bijections between three families of Schröder objects: parking quasi-ribbons, Schröder trees, and Schröder pseudo-compositions. These bijections will allow to transport the triduplicial structure on the latter objects.

Recall from [38] that hypoplactic classes of parking functions are represented as parking quasi-ribbons, or segmented nondecreasing parking functions, *i.e.*, nondecreasing parking functions with bars allowed between different values, for example

$$\{1\}, \quad \{11, 12, 1|2\}, \quad (5.16)$$

$$\{111, 112, 11|2, 113, 11|3, 122, 1|22, 123, 1|23, 12|3, 1|2|3\}. \quad (5.17)$$

With a parking quasi-ribbon α , we associate the elements

$$\mathbf{P}_\alpha := \sum_{\bar{\mathbf{a}}=\alpha} \mathbf{F}_{\mathbf{a}}, \quad (5.18)$$

where $\bar{\mathbf{a}}$ denotes the hypoplactic class of \mathbf{a} . For example,

$$\mathbf{P}_{11|3} = \mathbf{F}_{131} + \mathbf{F}_{311}, \quad \mathbf{P}_{113} = \mathbf{F}_{113}. \quad (5.19)$$

The product formula in this basis is

$$\mathbf{P}_\alpha \mathbf{P}_\beta = \mathbf{P}_{\alpha|\beta'} + \mathbf{P}_{\alpha \cdot \beta'} \quad (5.20)$$

where $\beta' = \beta[|\alpha|]$ (*i.e.*, the word formed by the entries of β shifted by the length of α), and the dot denotes concatenation. The triduplicial operations on parking quasi-ribbons are defined by [40]

$$\alpha < \beta = \alpha \cdot \beta[\max(\alpha) - 1], \quad (5.21)$$

$$\alpha \circ \beta = \alpha | \beta[|\alpha|], \quad (5.22)$$

$$\alpha > \beta = \alpha \cdot \beta[|\alpha|]. \quad (5.23)$$

One easily checks that they satisfy the seven triduplicial relations

$$\begin{aligned}
 (x \prec y) \prec z &= x \prec (y \prec z) \\
 (x \circ y) \circ z &= x \circ (y \circ z) \\
 (x \succ y) \succ z &= x \succ (y \succ z) \\
 (x \succ y) \prec z &= x \succ (y \prec z) \\
 (x \circ y) \prec z &= x \circ (y \prec z) \\
 (x \succ y) \circ z &= x \succ (y \circ z) \\
 (x \circ y) \succ z &= x \circ (y \succ z).
 \end{aligned} \tag{5.24}$$

In order to define the triduplicial operations on Schröder pseudocompositions, we first need a bijection, which will be described below.

5.3 A bijection between parking quasiribbons and Schröder trees

The bijection between Schröder pseudocompositions and Schröder trees is trivial, as it is essentially the Polish notation for the tree. The difficult point is the correspondence between trees and parking quasi-ribbons.

Among all Schröder trees, we have binary trees, and among parking quasi-ribbons, we have parking quasi-ribbons without bars, that are non-decreasing parking functions. Both are counted by Catalan numbers.

We shall first describe the bijection from binary trees to parking quasi-ribbons without bars. Its extension to all Schröder trees will then be straightforward. Let ϕ be this bijection. It is recursively defined as follows. Set $\phi(\emptyset) = \emptyset$ and $\phi(\bullet) = 1$.

Given a tree T with left and right subtrees respectively T_1 and T_2 , we have

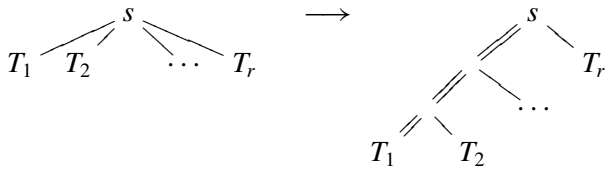
$$\phi(T) = \phi(T_2) \cdot (\phi(T_1)[\max(\phi(T_2)) - 1]) \cdot (|T_1| + \max(\phi(T_2))), \tag{5.25}$$

with the convention that, if T_2 is empty, $\max(\phi(T_2)) = 1$, and the dot denotes concatenation. This operation can also be described as collecting the vertices of T recursively by visiting first its right subtree, then its left subtree and finally its root, with the rules that a leaf takes the value of the last visited vertex (1 if there were none) and an internal vertex gets as value the size of its left subtree added to the value of its right son (added to 1 if there is no right son).

Example 5.1. We have

$$\begin{array}{c}
 & & 8 & & \\
 & \swarrow & & \searrow & \\
 6 & & & & 5 \\
 \swarrow \searrow & & & & \swarrow \searrow \\
 6 & & 4 & & 4 \\
 \swarrow & & & & \swarrow \searrow \\
 5 & & & & 2 \\
 & & & & \swarrow \searrow \\
 & & & & 1 & & 1
 \end{array}
 \longrightarrow 1124455668. \quad (5.26)$$

Let us now extend ϕ to all Schröder trees. First, Schröder trees are in bijection with binary trees with two-colored left edges: if an internal node s has more than two children with corresponding subtrees T_1, T_2, \dots, T_r , draw $r - 1$ left edges (of the second color) from s and attach to the new r nodes the r subtrees in order, as in a binary tree:



This amounts to reverting the contraction process described in Note 4.4.

Having computed this tree, send it with the previous bijection to a non-decreasing parking function, and insert a bar between two letters if they are separated by a left branch of the second color.

Example 5.2. The continuation of (5.26) is

$$\begin{array}{c}
 & & 8 & & \\
 & \swarrow & & \searrow & \\
 6 & & & & 5 \\
 \swarrow \searrow & & & & \swarrow \searrow \\
 6 & & 4 & & 4 \\
 \swarrow & & & & \swarrow \searrow \\
 5 & & & & 2 \\
 & & & & \swarrow \searrow \\
 & & & & 1 & & 1
 \end{array}
 \longrightarrow
 \begin{array}{c}
 & & 8 & & \\
 & \swarrow & & \searrow & \\
 6 & & & & 5 \\
 \swarrow \searrow & & & & \swarrow \searrow \\
 6 & & 4 & & 4 \\
 \swarrow & & & & \swarrow \searrow \\
 5 & & & & 2 \\
 & & & & \swarrow \searrow \\
 & & & & 1 & & 1
 \end{array}
 \longrightarrow 11|244|5566|8. \quad (5.27)$$

Theorem 5.3. *The previous algorithm provides a bijection between Schröder trees and parking quasi-ribbons.*

Before proving the theorem, let us describe the inverse bijection $\psi = \phi^{-1}$ from nondecreasing parking functions to binary trees. Set $\psi(1) = \emptyset$. Let $p = a_1 \dots a_r$ be a nondecreasing parking function. Let $w =$

$w_1 \dots w_{r-1}$ be the word such that $w_k = a_k + r - 1 - k$. Let ℓ be greatest index of w such that $a_\ell = a_{\ell+1}$ and $w_\ell = a_r$ (as $a_0 = 1$, if ℓ does not exist, set $\ell = 0$). Then compute recursively the images of $a_1 \dots a_\ell$ as the right subtree of the root, and of $(a_{\ell+1} \dots a_{r-1})[a_\ell - 1]$ as the left subtree of the root.

Example 5.4. Consider all nondecreasing parking functions $112445566X$, where X is bound by the constraint of being a nondecreasing parking function, so that $X \in \{6, 7, 8, 9, 10\}$. The word w is the same for all those parking functions, namely **988988776**, where we write in boldface the w_k such that $a_k = a_{k+1}$. Note that the 6 can be bold or not depending on the value of X : if X is 6, it is indeed in bold. Now, the index ℓ is well-defined in all the examples, so that we can separate the word and apply it recursively:

$$\begin{aligned} 1124455666 &\longrightarrow_{\ell=9} (\emptyset, 112445566) \\ 1124455667 &\longrightarrow_{\ell=8} (1, 11244556) \\ 1124455668 &\longrightarrow_{\ell=6} (122, 112445) & (5.28) \\ 1124455669 &\longrightarrow_{\ell=4} (12233, 1124) \\ 11244556610 &\longrightarrow_{\ell=0} (112445566, \emptyset) \end{aligned}$$

Proof. Let us now prove that ϕ is indeed a bijection and that its inverse is ψ as claimed.

First, the values of ϕ are clearly nondecreasing parking functions.

For ψ , the crucial point is to prove that it is well-defined (see (5.28) for an illustration).

Given a nondecreasing parking function $p = a_1 \dots a_r$, the allowed values for a_r are in the interval $[a_{r-1}, r]$. And this interval corresponds precisely to the values taken by the subword of w obtained by selecting the indices i such that $a_i = a_{i+1}$. Indeed, any of these values belong to this interval, since all values of w do. Conversely, a direct induction on the length of p implies the result, since the only question concerns the index $r - 1$ which is considered in the subword of w iff $a_{r-1} = a_r$. Finally, if one splits p after the rightmost occurrence w_ℓ of such a value, both the prefix of p and its suffix $a_{\ell+1} \dots a_{r-1}$ are parking functions: it is obvious for the prefix and is easy for the suffix, since we considered the *rightmost occurrence*. This occurrence has only strictly smaller values to its left ($w_i - w_{i+1}$ can be at most 1), so that the shifted suffix is a parking function. Now, by definition, the values of ψ are binary trees, so that at this point, we have maps going from each set to the other. Let us now see why they are inverses of each other.

Both maps are recursive, so we just need to prove that they are inverse of each other on the first step. Let $p = a_1 \dots a_r$ be a nondecreasing

parking function which is the image under ϕ of a binary tree T having T_1 and T_2 as left and right subtrees. Since a_r is the sum of the size of T_1 and of the maximal value of $\phi(T_2)$, a_r corresponds to the value w_ℓ in the word w where ℓ is the size of T_2 and $r - \ell - 1$ is the size of T_1 . Now, this value ℓ necessarily satisfies $a_\ell = a_{\ell+1}$, since a_ℓ is the maximal value M of T_2 and $a_{\ell+1} = 1 + M - 1$. Finally, among all indices k satisfying $a_k = a_{k+1}$ and $w_k = w_\ell$, ℓ is the only one such that the suffix $a_{\ell+1} \dots a_{r-1}$ is a parking function, since any other occurrence in w has one equal value to its right, which contradicts the fact of being a nondecreasing parking function.

Since ϕ and ψ both have the right image sets and $\psi \circ \phi$ is the identity map on binary trees, they both are bijections, inverses of each other.

Finally, let us see why the extension of ϕ to Schröder trees is a bijection. First, all left branches relate numbers that cannot be equal, so that separations on nondecreasing parking functions are made between non equal letters, which is the required condition about parking quasi-ribbons. The converse is also true: the number of left branches in a binary tree T is equal to the number of different letters plus one in $\phi(T)$. So the map from binary trees with two-colored left branches to parking quasi-ribbons is a bijection and the composition of both bijections through the middle object of binary trees with two-colored left branches is still a bijection. □

5.4 Triduplicial operations on Schröder pseudocompositions

Now that we have a bijection between parking quasiribbons and Schröder pseudocompositions, we can translate the triduplicial operations initially defined on parking quasiribbons to Schröder pseudocompositions.

Definition 5.5. Let I and J be two Schröder pseudocompositions. Define J' such that $J = J'0^m$ and J' does not end by a 0.

Then

$$I \prec J = J \triangleright I = J'0^{m-1}.I \tag{5.29}$$

$$I \circ J = J' \triangleright I \cdot 0^{m-1} \tag{5.30}$$

$$I \succ J = J' \cdot I \cdot 0^{m-1}. \tag{5.31}$$

Example 5.6. Denoting by a the parking quasi-ribbon 1 and by x the pseudocomposition 100,

$$a \prec a = 11 \quad x \prec x = 10100 \tag{5.32}$$

$$a \circ a = 1|2 \quad x \circ x = 2000 \tag{5.33}$$

$$a \succ a = 12 \quad x \succ x = 11000, \tag{5.34}$$

which coincide with the bijection described in the previous section.

Theorem 5.7. *The operations above endow the set of Schröder pseudocompositions with the structure of a triduplicial algebra, freely generated by $x = 100$.*

Proof. This is a direct consequence of the translation of the triduplicial operations on Schröder pseudocompositions.

We shall prove it for each rule. Operation \prec on parking quasi-ribbons is defined by $\alpha \prec \beta = \alpha \cdot \beta[\max(\alpha) - 1]$ and via the bijection ψ extended to parking quasi-ribbons, it corresponds to glueing the image of α to the rightmost leaf of β so that, on Schröder pseudocompositions, one obtains $J'.0^{m-1}.I$.

Operations \circ and \succ on parking quasi-ribbons are defined by $\alpha \circ \beta = \alpha | \beta[|\alpha|]$ and $\alpha \succ \beta = \alpha \cdot \beta[|\alpha|]$ and via the bijection ψ extended to parking quasi-ribbons, it corresponds to putting the image of α as the left child of the rightmost internal node labelled 1 of the image of β (which is also the last visited internal node of the tree in Polish notation) with an edge of the natural color (for \succ) or of the second color (for \circ). The translation on Schröder pseudocompositions is straightforward. \square

Define now an order \leq on parking quasiribbons by the cover relation

$$\beta \succ \alpha \quad \text{if } \alpha = uv, \beta = u|v' \tag{5.35}$$

with $v' = v$ if the last letter of u is smaller than the first letter of v , and $v' = v[1]$ otherwise.

For example, the predecessors of $11|23$ are $11|2|3$ and $1|2|34$.

With this order, we can define a basis \mathbf{S}^α by

$$\mathbf{S}^\alpha = \sum_{\alpha \leq \beta} \mathbf{P}_\beta. \tag{5.36}$$

For example,

$$\mathbf{S}^1 = \mathbf{P}_1, \mathbf{S}^{11} = \mathbf{P}_{11} + \mathbf{P}_{1|2}, \mathbf{S}^{12} = \mathbf{P}_{12} + \mathbf{P}_{1|2}, \mathbf{S}^{1|2} = \mathbf{P}_{1|2} \tag{5.37}$$

and

$$\mathbf{S}^{11|23} = \mathbf{P}_{11|23} + \mathbf{P}_{1|2|34} + \mathbf{P}_{11|2|3} + \mathbf{P}_{1|2|3|4}. \tag{5.38}$$

The Hopf epimorphism $\chi : \mathbf{SQSym} \rightarrow \mathbf{Sym}$ is defined by

$$\chi(\mathbf{P}_\alpha) = R_{I\sim} \tag{5.39}$$

where I is the bar composition of α whose parts are the lengths of the factors between the bars, e.g., for $\alpha = 111|24|5$, $I = 321$.

It is then clear that

$$\chi(\mathbf{S}^\alpha) = S^{I^\sim}. \tag{5.40}$$

For $U_m \in \mathbf{SQSym}_m$ and $V_n \in \mathbf{SQSym}_n$, define

$$B_q(U_m, V_n) = q_{m+n+1} \mathbf{B}_q(U_m, V_n), \tag{5.41}$$

where \mathbf{B}_q is defined after Eq. (5.8). Then, in the bases \mathbf{P} and \mathbf{S} with both indexations:

$$B_q(\mathbf{S}^\alpha, \mathbf{S}^\beta) = q_{|\alpha|} \mathbf{S}^{\beta < (\alpha \circ 1)} + \mathbf{S}^{\beta < (\alpha > 1)} \tag{5.42}$$

$$B_q(\mathbf{S}^I, \mathbf{S}^J) = q_{|I|} \Omega \mathbf{S}^{IJ} + \mathbf{S}^{IJ} \tag{5.43}$$

$$B_q(\mathbf{P}_\alpha, \mathbf{P}_\beta) = q^{|\alpha|} \mathbf{P}_{\beta < (\alpha \circ 1)} + \mathbf{P}_{\beta < (\alpha > 1)} + q^{|\alpha|} \mathbf{P}_{\beta \circ \alpha \circ 1} + \mathbf{P}_{\beta \circ \alpha > 1} \tag{5.44}$$

$$B_q(\mathbf{P}_I, \mathbf{P}_J) = q^{|I|} \mathbf{P}_{\Omega I J} + \mathbf{P}_{1 I J} + q^{|I|} P_{1 \triangleright J' \triangleright I 0^m} + \mathbf{P}_{1 J' \triangleright I 0^m} \tag{5.45}$$

where, as above, $J = J'0^m$ and J' does not end by a 0.

For example, one can recover the computation of \tilde{g}_3 in (5.15): start from the expression of \tilde{g}_1 and \tilde{g}_2 in this same equation and then compute \tilde{g}_3 according to Eq. (5.13):

The first term is $B_q(\tilde{g}_0, \tilde{g}_2)$:

$$\begin{aligned} B_q(S_0, S^{10100}) &= q_0 S^{110100} + S^{1010100} = S^{1010100}, \\ B_q(S_0, S^{11000}) &= q_0 S^{111000} + S^{1011000} = S^{1011000}, \\ B_q(S_0, S^{2000}) &= q_0 S^{12000} + S^{102000} = S^{102000}. \end{aligned} \tag{5.46}$$

Note that some S^I here are not indexed by Schröder pseudocompositions, but these terms eventually disappear as their coefficient is $q_0 = q^0 - 1 = 0$. The second term is $B_q(\tilde{g}_1, \tilde{g}_1)$:

$$B_q(S^{100}, S^{100}) = q_1 S^{200100} + S^{1100100}. \tag{5.47}$$

The third term is $\mathbf{B}_q(\tilde{g}_2, \tilde{g}_0)$:

$$\begin{aligned} B_q(S^{10100}, S_0) &= q_2 S^{201000} + S^{1101000}, \\ B_q(S^{11000}, S_0) &= q_2 S^{210000} + S^{1110000}, \\ B_q(S^{2000}, S_0) &= q_2 S^{30000} + S^{120000}, \end{aligned} \tag{5.48}$$

so that we recover (5.15).

6 Expansion on the ribbon basis

The expression of g in Sym is recovered by setting $S_0 = 1$. As in the case of the Lagrange series, it is interesting to expand g on the ribbon basis. As we have already seen before, the first terms are

$$\tilde{g}_1 = R_1, \tag{6.1}$$

$$\tilde{g}_2 = (1 + q)R_2 + 2R_{11}, \tag{6.2}$$

$$\begin{aligned} \tilde{g}_3 = & (1 + q)(1 + q + q^2)R_3 + (2 + q + 3q^2)R_{21} \\ & + 3(1 + q)R_{12} + (5 + q)R_{111}. \end{aligned} \tag{6.3}$$

We can observe that each coefficient is a q -analogue of $n!$. We shall now prove this fact, and describe the relevant statistics on permutations.

For a pseudo-composition I , let \hat{I} be the ordinary composition obtained by removing the zero entries.

For a binary tree $t = T(I)$, set

$$P_t = \sum_{J \leq I} m_J(q) S^J \tag{6.4}$$

For a pseudo-composition J encoding a tree $T(J)$, let

$$d_J = \sum_{v \in T(J)} (\phi(v) - 1) \tag{6.5}$$

Then, the coefficient of R_K in $(q)_n P_t$ is equal to

$$(q)_n m_I(q) q^{d_I - d_J} \tag{6.6}$$

where J is the coarsest anti-refinement of I such that $K \leq \hat{J}$. Indeed, R_K will then occur in all the refinements of J , and if I' is such a refinement, then,

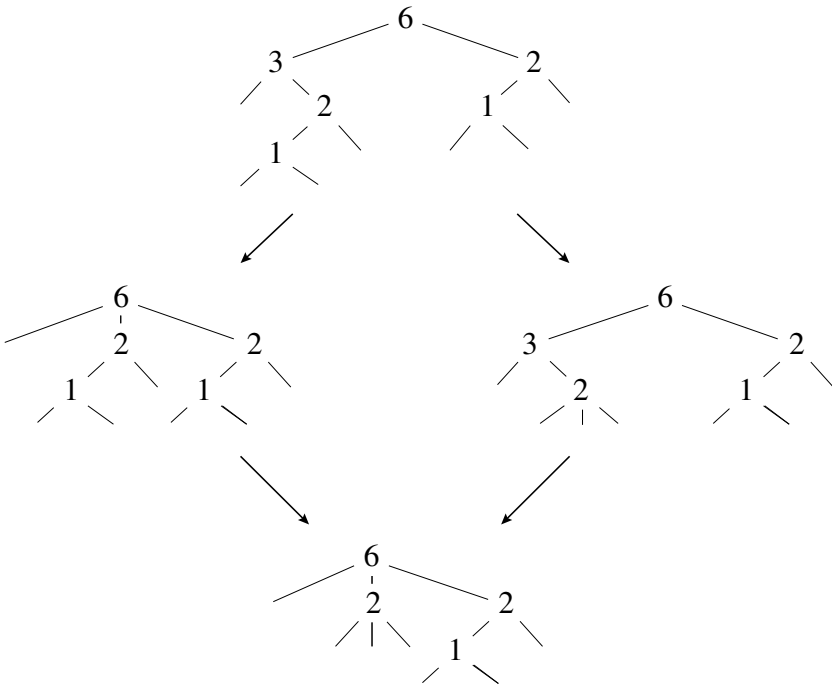
$$m_{I'}(q) = m_I(q) \prod_{v \in C(I, I')} q_{\phi(v)-1} \tag{6.7}$$

where $C(I, I')$ is the set of vertices of $T(I)$ which have been contracted in $T(I')$. Thus, factoring the coefficient $m_I(q)$, we see that R_K picks up a factor

$$\prod_i (q_i + 1)^{n_i} = q^{d_I - d_J} \quad \text{if} \quad \frac{m_J(q)}{m_I(q)} = \prod_i q_i^{n_i} \tag{6.8}$$

when summing over the Boolean lattice of refinements of J .

Example 6.1. For $I = (1101100011000)$ and $K = (51)$, we have $J = (20200011000)$, and on the picture (extracted from 4.5)



we can read that the coefficient of R_{51} in the projection of $(q)_6 P_T(1101100011000)$ on Sym is

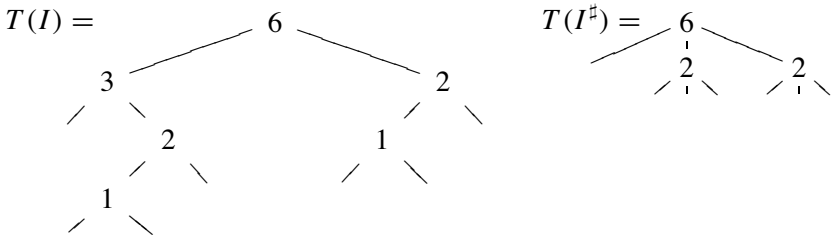
$$\frac{(q)_6}{q_6 q_3 q_2^2 q_1^2} q^4 = \frac{q_5 q_4}{q_2 q_1} q^4 = q^{10} + 2q^8 + q^9 + 2q^7 + 2q^6 + q^5 + q^4. \quad (6.9)$$

For a pseudo-composition I , let I^\sharp be its coarsest anti-refinement. The polynomial

$$(q)_n m_I(q) q^{d_I - d_{I^\sharp}} \quad (6.10)$$

is, up to left-right symmetry, the q -hook-length formula for the binary tree $T(I)$ [1, 25] (with its leaves removed). Indeed, for a vertex v of a binary tree $t = T(I)$, $d_I - d_{I^\sharp}$ coincides with the number of internal nodes of its left subtree.

Example 6.2. Continuing with $I = (110110011000)$, $I^\sharp = (2020002000)$,

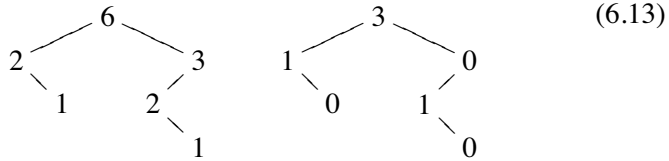


(6.11)

and (6.10) yields

$$\frac{(q)_6}{q_6 q_3 q_2^2 q_1^2} q^{6+3+2+1+2+1-(6+2+2)} = \frac{q_5 q_4}{q_2 q_1} q^{3+1+1} = \frac{q_5 q_4}{q_2 q_1} q^5 \quad (6.12)$$

which is the q -hook-length formula for the left-right flip



of the skeleton of $T(I)$. Indeed, the power of q is $3 + 1 + 1 = 5$ (given by the sum of the sizes of the right subtrees), and the denominator is $q_6 q_2 q_1 q_3 q_2 q_1$ (recording the sizes of all the subtrees).

Thus, up to a fixed power of q , this expression enumerates by number of non-inversions the permutations in the sylvester class labelled by the binary tree $T(I)$.

Summing over all binary trees, we see that each coefficient $c_K(q)$ of R_K in \tilde{g}_n is indeed a q -analogue of $n!$.

Translating these results at the level of permutations yields the following description of the expansion of \tilde{g}_n on the ribbon basis of **Sym**:

Definition 6.3. Let σ be a permutation and let α be the top of its sylvester class, that is, the permutation with the smallest number of inversions in its sylvester class. Let $I = (i_1, \dots, i_r)$ be a composition and let D be the descent set of the conjugate \bar{I} . Define $C_I(\sigma)$ as

$$q^{\text{inv}(\sigma) - \text{inv}(\alpha)} q^{\text{inv}(\alpha, D)}, \quad (6.14)$$

where $\text{inv}(\alpha, D)$ is the number of pairs $(i < j)$ such that $\alpha_i > \alpha_j$ and $j \in D$.

Theorem 6.4. The coefficient of R_I in the expansion of \tilde{g}_n is equal to

$$\sum_{\sigma \in \mathfrak{S}_n} C_I(\sigma). \quad (6.15)$$

For example, here are the tables for $n = 3$ and $n = 4$ of all coefficients C_I , where permutations are grouped by sylvester classes.

σ/I	3	21	12	111
123	1	1	1	1
132	q	q	1	1
312	q^2	q^2	q	q
213	q	1	q	1
231	q^2	q^2	1	1
321	q^3	q^2	q	1

(6.16)

σ/I	4	31	22	211	13	121	112	1111
1234	1	1	1	1	1	1	1	1
1243	q	q	q	q	1	1	1	1
1423	q^2	q^2	q^2	q^2	q	q	q	q
4123	q^3	q^3	q^3	q^3	q^2	q^2	q^2	q^2
1324	q	q	1	1	q	q	1	1
3124	q^2	q^2	q	q	q^2	q^2	q	q
1342	q^2	q^2	q^2	q^2	1	1	1	1
3142	q^3	q^3	q^3	q^3	q	q	q	q
3412	q^4	q^4	q^4	q^4	q^2	q^2	q^2	q^2
1432	q^3	q^3	q^2	q^2	q	q	1	1
4132	q^4	q^4	q^3	q^3	q^2	q^2	q	q
4312	q^5	q^5	q^4	q^4	q^3	q^3	q^2	q^2
2134	q	1	q	1	q	1	q	1
2143	q^2	q	q^2	q	q	1	q	1
2413	q^3	q^2	q^3	q^2	q^2	q	q^2	q
4213	q^4	q^3	q^4	q^3	q^3	q^2	q^3	q^2
2314	q^2	q^2	1	1	q^2	q^2	1	1
2341	q^3	q^3	q^3	q^3	1	1	1	1
2431	q^4	q^4	q^3	q^3	q	q	1	1
4231	q^5	q^5	q^4	q^4	q^2	q^2	q	q
3214	q^3	q^2	q	1	q^3	q^2	q	1
3241	q^4	q^3	q^4	q^3	q	1	q	1
3421	q^5	q^5	q^3	q^3	q^2	q^2	1	1
4321	q^6	q^5	q^4	q^3	q^3	q^2	q	1

(6.17)

7 Schröder's equation for the inverse of h

Let now $f = h^{-1}$ where $h^{-1} \circ \phi \circ h(z) = qz$ or equivalently

$$f \circ \phi(w) = qf(w) \quad (w = h(z)). \quad (7.1)$$

This is Schröder's equation. In the noncommutative setting, with again $\phi(z) = qz\sigma_z(A)$, it becomes

$$\sum_{k \geq 0} f_k q^{k+1} w^{k+1} \sigma_w((k+1)A) = q \sum_{n \geq 0} f_n w^{n+1} \quad (7.2)$$

which translates into the recurrence relation

$$f_n = \sum_{k+l=n} q^k f_k S_l((k+1)A). \quad (7.3)$$

Theorem 7.1. *Let L be the linear endomorphism of Sym defined by*

$$\begin{aligned} L(S^I) &= S_{i_1}(A) S_{i_2}((i_1+1)A) S_{i_3}((i_1+i_2+1)A) \\ &\quad \cdots S_{i_r}((i_1+\cdots+i_{r-1}+1)A). \end{aligned} \quad (7.4)$$

Then,

$$\begin{aligned} f_n &= L\left(S_n\left(\frac{A}{1-q}\right)\right) \\ &= \sum_{I \models n} \frac{q^{\text{maj}(I)}}{(1-q^{i_1})(1-q^{i_1+i_2})\cdots(1-q^{i_1+\cdots+i_r})} L(S^I), \end{aligned} \quad (7.5)$$

where $A/(1-q)$ and maj is defined as in [29, 6.1]³.

For example,

$$f_1 = \frac{1}{1-q} S_1(A) \quad (7.6)$$

$$f_2 = \frac{1}{1-q^2} S^2(A) + \frac{q}{(1-q)(1-q^2)} S_1(A) S_1(2A) \quad (7.7)$$

$$\begin{aligned} f_3 &= \frac{1}{1-q^3} S_3(A) + \frac{q^2}{(1-q^2)(1-q^3)} S_2(A) S_1(3A) \\ &\quad + \frac{q}{(1-q)(1-q^3)} S_1(A) S_2(2A) \\ &\quad + \frac{q^3}{(1-q)(1-q^2)(1-q^3)} S_1(A) S_1(2A) S_1(3A) \end{aligned} \quad (7.8)$$

³ $\text{maj}(I)$ is the sum of the descents of I , i.e., $\text{maj}(I) = (r-1)i_1 + (r-2)i_2 + \cdots + i_{r-1}$ if $I = (i_1, \dots, i_r)$.

Proof. Replacing $S_l((k + 1)A)$ by $S_l(A)$ in (7.3), we obtain a recurrence relation satisfied by the expansion on the basis S^I of the $S_n(A/(1 - q))$. To recover f_n from this expression, we just have to replace each factor S_{i_k} of S^I by $S_{i_k}((i_1 + \dots + i_{k-1} + 1)A)$. \square

Note 7.2. The noncommutative symmetric function

$$K_n(q) = (q)_n S_n \left(\frac{A}{1 - q} \right) = \sum_{I \models n} q^{\text{maj}(I)} R_I \tag{7.9}$$

is the q -Klyachko function. For q a primitive n th root of 1, it is mapped to Klyachko’s Lie idempotent in the descent algebra of the symmetric group [19, 29]. It is also a noncommutative analogue of the Hall-Littlewood function Q'_{1^n} [24].

Naturally, we may also choose to define f by

$$f_n = \sum_{k+l=n} q^k S_l((k + 1)A) f_k. \tag{7.10}$$

With this choice

$$f = \left(L \left(\overline{\sigma_1 \left(\frac{A}{1 - q} \right)} \right) \right) \tag{7.11}$$

and it is what we obtain by mould calculus in the next section (the bar involution is defined by $\overline{S^I} = S^{\bar{I}}$, where \bar{I} is the mirror composition).

8 A noncommutative mould expansion

Ecalte’s approach to the linearization equation (1.7) is to find a closed expression of the substitution automorphism

$$H : \psi \longmapsto \psi \circ h \tag{8.1}$$

as a differential operator. The idea is to look for an expansion of the form

$$H = \sum_I \mathcal{M}_I U^I \tag{8.2}$$

where $I = (i_1, \dots, i_r)$ runs over all compositions, $U^I = U_{i_1} \dots U_{i_r}$ as usual, and the U_n are the homogeneous component of the differential operator

$$U : \psi \longmapsto \psi \circ u, \quad \text{where } \phi(z) = qu(z), \tag{8.3}$$

given by the Taylor expansion at z of $\psi(z + (u(z) - z))$,

$$U_n = \sum_{I \models n} \frac{u^I}{\ell(I)} z^{n+\ell(I)} \partial_z^{\ell(I)}. \tag{8.4}$$

In this setting, the functional equation (1.7) reads

$$HUM_q = M_qH, \quad \text{where } (M_q\psi)(z) = \psi(qz). \quad (8.5)$$

We have already identified our generic power series $\phi(z)$ with $qz\sigma_z(X)$, so that $u_n = h_n(X)$. A natural noncommutative analogue is to set $u_n = S_n(A)$. There is another way to introduce noncommutative symmetric functions in this problem. The substitution maps U and H , being automorphisms, are grouplike elements in the Hopf algebra of differential operators. So, it is natural to introduce a second alphabet B (commuting with A) and to identify U_n with $S_n(B)$. The problem amounts to looking for H as an element of (the completion of) $\text{Sym}(A) \otimes \text{Sym}(B)$. Let us write it as $H(B)$, regarded as a symmetric function of B with coefficients in $\text{Sym}(A)$. Then (8.5) reads now

$$H(B)\sigma_1(B) = H(qB). \quad (8.6)$$

This is solved by

$$H(B) = \prod_{i \geq 0}^{\leftarrow} \lambda_{-q^i}(B) = \cdots \lambda_{-q^2}(B)\lambda_{-q}(B)\lambda_{-1}(B) \quad (8.7)$$

which may be denoted by

$$H(B) = \sigma_1\left(\frac{B}{q-1}\right) \quad (8.8)$$

Setting $F = H^{-1}$, we have that

$$F(B) = \sigma_1(B)\sigma_q(B)\sigma_{q^2}(B)\cdots \quad (8.9)$$

is the image of $\sigma_1(A/(1-q))$ (in the sense of [29]) by the bar involution $S^I \mapsto \overline{S^I}$, so that

$$F_n = \sum_{I \models n} \frac{q^{\text{maj}(I)}}{(1-q^{i_1})(1-q^{i_1+i_2})\cdots(1-q^n)} S^{\overline{I}}, \quad (8.10)$$

The function $f(z)$ is obtained by acting on the identity: $f(z) = Fz$. This is obtained from

$$U^I z = \overline{L(S^{\overline{I}}(A))} z^{|I|+1}. \quad (8.11)$$

Indeed,

$$\begin{aligned} U_n z^m &= \sum_{I \models n} \frac{S^I}{\ell(I)!} \frac{m!}{(m-\ell(I))!} z^{m+n} \\ &= \sum_{I \models n} M_I(m) S^I z^{m+n} = S_n(mA) z^{m+n}. \end{aligned} \quad (8.12)$$

9 The operad of reduced plane trees

9.1 A free operad

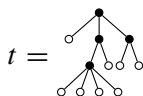
We shall now investigate the relation between our Schröder tree expansion (Section 4) and Ecalle’s arborification. So far, the S^I with I a Schröder pseudocomposition have been interpreted as elements of the free triduplial algebra **SQSym**. They can also be interpreted as elements of a free operad (see [3, 5]). We shall see that this operad, which is based on reduced plane trees, is also related to the noncommutative version of the Hopf algebra of formal diffeomorphisms tangent to identity [2].

The set of reduced plane trees with n leaves will be denoted denoted by PT_n , and PT denotes the union $\bigcup_{n \geq 1} \text{PT}_n$.

The number of leaves of a tree t will be called its degree $d(t)$, and we define the grading $\text{gr}(t)$ of a tree as its degree minus 1. In low degrees we have

$$\text{PT}_1 = \{\circ\}, \text{PT}_2 = \left\{ \begin{array}{c} \bullet \\ \diagup \quad \diagdown \\ \circ \quad \circ \end{array} \right\}, \text{PT}_3 = \left\{ \begin{array}{c} \bullet \\ \diagup \quad \diagdown \\ \bullet \quad \circ \\ \diagup \quad \diagdown \\ \circ \quad \circ \end{array}, \begin{array}{c} \bullet \\ \diagup \quad \diagdown \\ \circ \quad \bullet \\ \diagup \quad \diagdown \\ \circ \quad \circ \end{array}, \begin{array}{c} \bullet \\ \diagup \quad \diagdown \\ \circ \quad \circ \\ \diagup \quad \diagdown \\ \bullet \quad \bullet \end{array} \right\}, \dots \quad (9.1)$$

The leaves (in white in the pictures) are also called external vertices whilst the other vertices (in black) are said to be internal (note that \circ has no internal vertex). For instance, the tree



has degree $d(t) = 8$, grading $\text{gr}(t) = 7$ and $i(t) = 4$ internal vertices.

Definition 9.1. The free non- Σ operad \mathcal{S} in the category of vector spaces is the vector space

$$\mathcal{S} = \bigoplus_{n \geq 1} \mathcal{S}_n \text{ where } \mathcal{S}_n = \text{CPT}_n. \quad (9.2)$$

The composition operations

$$\mathcal{S}_n \otimes \mathcal{S}_{k_1} \otimes \dots \otimes \mathcal{S}_{k_n} \longrightarrow \mathcal{S}_{k_1 + \dots + k_n} \quad (n \geq 1, k_i \geq 1) \quad (9.3)$$

map the tensor product of trees $t_0 \otimes t_1 \otimes \dots \otimes t_n$ to the tree $t_0 \circ (t_1, \dots, t_n)$ obtained by replacing the leaves of t_0 , from left to right, by the trees t_1, \dots, t_n .

For instance,

$$\circ \circ (\circ, \circ) = \circ \circ \circ \circ \circ \quad (9.4)$$

The tree \circ of PT_1 is the unit of this composition. A proof of its associativity can be found in [3] or [5], where this operad is called a free \mathcal{S} -magmatic operad. Note that \mathcal{S} is also called the operad of Stasheff polytopes (see [26,32]) so that the letter \mathcal{S} can stand for Stasheff or Schröder as well.

9.2 The group of the operad

Let $\hat{\mathcal{S}}$ be the completion of the vector space \mathcal{S} with respect to the grading $gr(t) = d(t) - 1$. The group of the operad \mathcal{S} is defined as:

Definition 9.2. Let

$$G_{\text{ncdiff}} = \left\{ \circ + \sum_{n \geq 2} p(n), \quad p(n) \in \mathcal{S}_n \right\} \subset \hat{\mathcal{S}} \quad (9.5)$$

endowed with the composition product

$$p \circ q = q + \sum_{n \geq 2} p(n) \circ \underbrace{(q, \dots, q)}_n \in G_{\text{ncdiff}} \quad (9.6)$$

for $p = \circ + \sum_{n \geq 2} p(n)$ and $q \in G_{\text{ncdiff}}$.

This is indeed a group (see e.g., [5]). Elements of G_{ncdiff} can be described by their coordinates

$$p = \sum_{t \in PT} p_t t \quad \text{and} \quad q = \sum_{t \in PT} q_t t. \quad (9.7)$$

(with $q_\circ = p_\circ = 1$) so that the coordinates of $r = p \circ q$ are given by

$$r_t = \sum_{t = t_0 \circ (t_1, \dots, t_n)} p_{t_0} q_{t_1} \dots q_{t_n} \quad (9.8)$$

This expression involves the so-called admissible cuts defining the coproduct in Hopf algebras of the Connes-Kreimer family. It suggests that the elements of G_{ncdiff} can be interpreted as characters of the bialgebra defined as follows.

Let

$$\overline{T}(\mathcal{S}) = \bigoplus_{p \geq 1} \mathcal{S}^{\otimes p} \tag{9.9}$$

be the reduced tensor algebra over \mathcal{S} (whose basis is given by plane forests $f = t_1 \cdot \dots \cdot t_k$) equipped with the coalgebra structure defined on trees by

$$\tilde{\Delta}(t) = \sum_{t=t_0 \circ (t_1, \dots, t_n)} t_0 \otimes (t_1 \cdot \dots \cdot t_n) \tag{9.10}$$

where \cdot means concatenation, and then extended as an algebra morphism on $\overline{T}(\mathcal{S})$. For example,

$$\tilde{\Delta} \left(\begin{array}{c} \circ \\ / \quad \backslash \\ \circ \quad \circ \end{array} \right) = \circ \otimes \begin{array}{c} \circ \\ / \quad \backslash \\ \circ \quad \circ \end{array} + \begin{array}{c} \circ \\ / \quad \backslash \\ \circ \quad \circ \end{array} \otimes \begin{array}{c} \circ \\ / \quad \backslash \\ \circ \quad \circ \end{array} \cdot \circ + \begin{array}{c} \circ \\ / \quad \backslash \\ \circ \quad \circ \end{array} \otimes \circ \cdot \circ \cdot \circ \cdot \circ \tag{9.11}$$

It is then clear that any $p \in G_{\text{ncdiff}}$ can be identified as the algebra morphism φ_p defined by

$$\varphi_p(t) = p_t \tag{9.12}$$

so that, if $r = p \circ q$, then

$$\varphi_{p \circ q} = \varphi_r = \varphi_p * \varphi_q = \mu \circ (\varphi_p \otimes \varphi_q) \circ \tilde{\Delta} \tag{9.13}$$

where $*$ is the usual convolution product for a bialgebra, and μ is the multiplication of \mathbb{C} . Note that if $\bigwedge(t_1 \cdot t_2 \cdot \dots \cdot t_n)$ (with $n \geq 2$) is the tree obtained by grafting the trees t_1, \dots, t_n to a common root (in other words, $\bigwedge(t_1 \cdot t_2 \cdot \dots \cdot t_n) = c_n \circ (t_1, \dots, t_n)$, where c_n is the corolla with n leaves) the map $\tilde{\Delta}$ is the unique algebra map such that

$$\tilde{\Delta}(\circ) = \circ \otimes \circ, \tag{9.14}$$

$$\begin{aligned} \tilde{\Delta} \left(\bigwedge(t_1, \dots, t_n) \right) &= \circ \otimes \bigwedge(t_1, \dots, t_n) \\ &+ \left(\bigwedge \otimes \text{Id} \right) \circ \tilde{\Delta}(t_1 \cdot t_2 \cdot \dots \cdot t_n) \end{aligned} \tag{9.15}$$

9.3 The Hopf algebra of reduced plane trees and its characters

The quotient of the bialgebra $\overline{T}(\mathcal{S})$ by the relations $t \cdot \circ = \circ \cdot t = t$ is a graded unital algebra \mathcal{H}_{PT} , spanned by \circ and the forests $t_1 \cdot t_2 \cdot \dots \cdot t_n$ with $t_i \in \cup_{n \geq 2} \text{PT}_n$, with \circ as unit.

It is a Hopf algebra for the coproduct defined on trees by

$$\Delta(t) = (p \otimes p) \circ \tilde{\Delta}(t) \tag{9.16}$$

where p is the projection from $\overline{T}(\mathcal{S})$ to \mathcal{H}_{PT} .

In the former example:

$$\Delta \left(\begin{array}{c} \circ \\ \diagup \quad \diagdown \\ \circ \quad \circ \\ \diagup \quad \diagdown \\ \circ \quad \circ \end{array} \right) = \circ \otimes \begin{array}{c} \circ \\ \diagup \quad \diagdown \\ \circ \quad \circ \end{array} + \begin{array}{c} \circ \\ \diagup \quad \diagdown \\ \circ \quad \circ \end{array} \otimes \begin{array}{c} \circ \\ \diagup \quad \diagdown \\ \circ \quad \circ \end{array} + \begin{array}{c} \circ \\ \diagup \quad \diagdown \\ \circ \quad \circ \end{array} \otimes \circ. \tag{9.17}$$

It is now clear that the group G_{ncdiff} is precisely the group of characters of this Hopf algebra (for $p \in G_{\text{ncdiff}}, \varphi_p(\circ) = 1$).

This Hopf algebra was first considered in [12] (with the opposite coproduct $P \circ \Delta$, where $P(u \otimes v = v \otimes u)$), where it is called the Hopf algebra of reduced plane trees $\mathcal{H}_{\text{pl}}^{\text{red}}$. The coproduct can be described in terms of admissible cuts of a tree $t \in \text{PT}$, *i.e.*, (possibly empty) subsets c of edges *not connected to a leaf* with the rule that along any path from the root of t to any of its leaves, there is at most one edge in c . The edges in c are naturally ordered from left to right. To any admissible cut c corresponds a unique subforest $P^c(t)$, the *pruning*, concatenation of the subtrees obtained by cutting the edges in c , in the order defined above. The coproduct can then be defined by:

$$\Delta(t) = \sum_{c \in \text{Adm } t} R^c(t) \otimes P^c(t), \tag{9.18}$$

where $R^c(t)$ is the trunk, obtained by replacing each subtree of $P^c(t)$ with a single leaf.

So far, we have defined the group of the operad of Stasheff polytopes (or Schröder trees), and shown that it coincides with the group of characters of the Hopf algebra of reduced plane trees. We shall see that it is also a group of *formal noncommutative diffeomorphisms* related to the noncommutative Lagrange inversion (see [39]) and to the noncommutative version of Poincaré's equation.

10 Noncommutative formal diffeomorphisms

10.1 A group of noncommutative diffeomorphisms

As pointed out in [2], it is possible to consider formal diffeomorphisms in one variable with coefficients in an associative algebra, but if this algebra is not commutative, the set of such diffeomorphisms is not anymore a group because associativity is broken. Nevertheless, there is still a noncommutative version of the Faà di Bruno Hopf algebra.

We can recover a group by regarding the coefficients as well as the variable as formal noncommutative variables. Heuristically, let us start with a fixed diffeomorphism u of

$$G_{\text{diff}} = \{u(z) = z + \sum_{n \geq 1} u_n z^{n+1} \in \mathbb{C}[[z]]\} \tag{10.1}$$

in the variable z with coefficients u_n . Consider now that z is replaced by S_0 and that each u_n is replaced by a variable S_n . We get a series

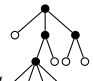
$$g_c = S_0 + \sum_{n \geq 1} S_n S_0^{n+1} \tag{10.2}$$

in an infinity of noncommuting variables. Nothing prevents us from “iterating” g_c as we would do with an ordinary power series

$$\begin{aligned} g_c \circ g_c &= g_c + \sum_{n \geq 1} S_n g_c^{n+1} \\ &= S_0 + S_1 S_0^2 + S_2 S_0^3 + S_1(S_1 S_0^2) S_0 + S_1 S_0(S_1 S_0^2) + \dots \end{aligned} \tag{10.3}$$

Further iterations lead to words in the variables S_0, S_1, \dots indexed by Schröder pseudocompositions, which will eventually represent all reduced plane trees.

Let $S^\circ = S_0$ and, if $t = \wedge(t_1, \dots, t_n)$, $S^t = S_{n-1} S^{t_1} \dots S^{t_n}$. We recover the correspondence with Polish codes. For example,



$$= S_2 S_0 S_1 S_3 S_0 S_0 S_0 S_0 S_0 S_1 S_0 S_0 = S^{201300000100} \tag{10.4}$$

Identifying trees with their Polish codes, the group G_{ncdiff} can be described as

$$G_{\text{ncdiff}} = \left\{ g = \sum_{t \in \text{PT}} g_t S^t, g_t \in \mathbb{C}, g_\circ = 1 \right\} \subset \mathbb{C}\langle\langle S_0, S_1, \dots \rangle\rangle \tag{10.5}$$

where $\mathbb{C}\langle\langle S_0, S_1, \dots \rangle\rangle$ is the completion of the algebra of polynomials, with respect to the degree in S_0 .

If we set $g = g(S_0, S_1, \dots) = g(S_0; \mathbf{S})$ ($\mathbf{S} = S_1, \dots$), then,

Theorem 10.1. *The composition $f \circ g = h$ in G_{ncdiff} is given by*

$$h(S_0; \mathbf{S}) = f(g; \mathbf{S}). \tag{10.6}$$

In other words we substitute g to the variable S_0 in f . Graphically we substitute trees to leaves. It is easy to check that this group coincides with the previous one. If

$$g = \sum_{t \in \text{PT}} g_t S^t, f = \sum_{t \in \text{PT}} f_t S^t, h = f \circ g = \sum_{t \in \text{PT}} h_t S^t \in G_{\text{ncdiff}}, \tag{10.7}$$

then h_t is a sum of contributions from f and g . The contributions to h_t can be

- $f_t S^t$ if we substitute the S_0 part of g to any S_0 (a leaf) of the term $f_t S^t$ of f .
- $g_t S^t$ if we substitute the term $g_t S^t$ of g to the S_0 part of f
- $f_{t_0} g_{t_1} \dots g_{t_n} S^t$ if when substituting (from left to right) the terms $g_{t_1} S^{t_1}, \dots, g_{t_n} S^{t_n}$ to n S_0 variables (leaves) in $f_{t_0} S^{t_0}$, we get the monomial S^t .

This means that

$$h_t = \sum_{(t_0; t_1 \dots t_n) = (R^c(t); P^c(t))} f_{t_0} g_{t_1} \dots g_{t_n} \quad (10.8)$$

which is precisely the convolution of characters in \mathcal{H}_{PT} .

In the sequel, we shall denote by the same letter (for instance g) an element of G_{ncdiff} regarded as a series of trees

$$g = \sum_t g_t t, \quad (10.9)$$

as a series of noncommutative monomials

$$g = \sum_t g_t S^t, \quad (10.10)$$

or as the character g sending t on g_t .

10.2 Inversion in G_{ncdiff} and Lagrange inversion

One can compute the compositional inverse of f_c (defined by $f_t = 1$ if t is a corolla and 0 otherwise). This yields a signed series involving all trees.

Consider the series

$$f_c = S^\circ + \sum_{n \geq 1} S^{\wedge(\circ^{n+1})}. \quad (10.11)$$

We shall work here in $\overline{T}(\mathcal{S})$ (where \circ is not the unit). Let $i(t)$ be the number of internal vertices of a tree t . The inverse of f_c is then given by

$$g_c = \sum_{t \in PT} (-1)^{i(t)} S^t \quad (10.12)$$

since

$$g_c = S_0 + \sum_{n \geq 1} \sum_{\substack{t = \wedge(t_1 \dots t_{n+1}) \\ t_i \in \text{PT}}} (-1)^{i(t)} S^{\wedge(t_1 \dots t_{n+1})} \tag{10.13}$$

$$= S_0 + \sum_{n \geq 1} \sum_{\substack{t = \wedge(t_1 \dots t_{n+1}) \\ t_i \in \text{PT}}} (-1)^{1+i(t_1)+\dots+i(t_{n+1})} S_n S^{t_1} \dots S^{t_{n+1}} \tag{10.14}$$

$$= S_0 - \sum_{n \geq 1} S_n g_c^{n+1} \tag{10.15}$$

so that $S_0 = g_c + \sum_{n \geq 1} S_n g_c^{n+1} = f_c \circ g_c$.

In order to establish a link with the noncommutative analogue of Lagrange inversion (see [39]), we can look for the compositional inverse of

$$f_L = \left(1 + \sum_{n \geq 1} S_n S_0^n \right)^{-1} \cdot S_0 \in G_{\text{ncdiff}}, \tag{10.16}$$

where the exponent -1 means here the multiplicative inverse as a formal power series. Working with trees, consider the series of trees L such that

$$L = \circ + \sum_{k \geq 1} \bigwedge (L^{\cdot k} \cdot \circ) \tag{10.17}$$

then $L = \sum L^t t$ with $L^t = 1$ or 0 .

The inverse g_L of f_L is $\sum L^t S^t$. Indeed,

$$g_L = S^\circ + \sum_{k \geq 1} S^{\wedge(L^{\cdot k} \cdot \circ)} \tag{10.18}$$

$$= S_0 + \sum_{k \geq 1} S_k g_L^k S_0 \tag{10.19}$$

$$= \left(1 + \sum_{n \geq 1} S_n g_L^n \right) S_0 \tag{10.20}$$

and obviously $f_L \circ g_L = S_0$.

Apart from \circ , all the trees of PT occurring in g_L are such that the rightmost subtree of each internal vertex is a leaf (S_0). Let PT_L be the set of such trees, and let α be the map sending \circ to itself and $t \in \text{PT}_L$ to the tree (with possible unary internal vertices) obtained by removing all the rightmost leaves of its internal vertices. We obtain in this way the tree expansion of Section 5.3 in [39].

One can also define S^t for such trees. Now

$$\alpha(L) = \circ + \sum_{n \geq 1} \bigwedge (\alpha(L)^{\cdot n}) \tag{10.21}$$

and if we replace trees by their Polish codes, the resulting series g satisfies

$$g = S_0 + \sum_{n \geq 1} S_n g^n, \tag{10.22}$$

the functional equation considered in [39]. This correspondence will be explained in details in Section 12, using a group morphism from G_{ncdiff} to the group G_C of the Catalan operad.

10.3 The conjugacy equation

Let Y be the grading operator on trees ($Y(t) = (d(t) - 1)t$), and let $q^Y(t) = q^{d(t)-1}t$. The noncommutative analogue of the conjugacy equation can be written as

$$g(qS_0; \mathbf{S}) = qg_c(g; \mathbf{S}) \tag{10.23}$$

where the initial diffeomorphism is the corolla series. This equation also reads

$$q^{-1}g(qS_0; \mathbf{S}) = q^Y g = g_c \circ g. \tag{10.24}$$

It is not difficult to compute the coefficients of the solution $g = \sum_t c_t(q)t$, noticing that $c_\circ(q) = 1$ and, if $t = \wedge(t_1, \dots, t_n)$ then,

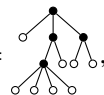
$$q^{d(t)-1}c_t(q) = c_t(q) + c_{t_1}(q) \dots c_{t_n}(q). \tag{10.25}$$

As we have already seen, the coefficients have the closed form

$$c_t(q) = \prod_{v \in t} \frac{1}{q^{\phi(v)-1} - 1} \tag{10.26}$$

where v runs over the internal vertices of t and $\phi(v)$ is the number of leaves of the subtree of v .

For example, for

$t =$


$c_t(q) = \frac{1}{(q^7 - 1)(q - 1)(q^4 - 1)(q^3 - 1)}. \tag{10.27}$

Surprisingly, the same coefficients appear in the commutative case, in Ecalle's arborified solution of the conjugacy equation, which has been interpreted in [15] in terms of characters on the Connes-Kreimer Hopf algebra \mathcal{H}_{CK} of (non plane) rooted trees decorated by positive integers. We shall see that there is indeed a kind of noncommutative arborification, which will be eventually explained by a morphism of Hopf algebras.

11 Commutative versus noncommutative

11.1 Commutative diffeomorphisms and the Connes-Kreimer algebra

In this section we recall briefly how certain (commutative) formal diffeomorphisms can be obtained as characters of a Hopf algebra (see [15] and [16]), in particular the solution of the conjugacy equation

$$qu(h(z)) = h(qz) \tag{11.1}$$

where u and h are formal diffeomorphisms of G_{diff} (tangent to the identity). The use of trees to encode diffeomorphisms appears in [14] and is related to differential operators indexed by trees, an idea originally due to Cayley.

We shall rely upon the references [6], [17] and [18], except that we use the opposite coproduct, in order to avoid antimorphisms.

A rooted tree⁴ T is a connected and simply connected set of oriented edges and vertices such that there is precisely one distinguished vertex (the root) with no incoming edge. A forest F is a (commutative) monomial in rooted trees.

Let $l(F)$ be the number of vertices in F . One can decorate a forest by \mathbb{N}^* , that is, with each vertex v of F , we associate an element n_v of \mathbb{N}^* . We denote by $\mathcal{T}_{\mathbb{N}}$ (resp. $\mathcal{F}_{\mathbb{N}}$) the set of decorated trees (resp. forests). It includes the empty tree, denoted by \emptyset . As for sequences, if a forest F is decorated by n_1, \dots, n_s ($l(F) = s$), we write

$$|F| = n_1 + \dots + n_s. \tag{11.2}$$

For n in \mathbb{N}^* , the operator B_n^+ associates with a forest of decorated trees the tree with root decorated by n connected to the roots of the forest : $B_n^+(\emptyset)$ is the tree with one vertex decorated by n . For example,

$$B_n^+ \left(\begin{array}{cc} \begin{array}{c} n_4 \\ \bullet \\ | \\ n_5 \end{array} & \begin{array}{c} n_1 \\ \bullet \\ \diagup \quad \diagdown \\ n_3 \quad n_2 \end{array} \end{array} \right) = \begin{array}{c} n \\ \bullet \\ \diagup \quad \diagdown \\ n_4 \quad n_1 \\ \bullet \quad \bullet \\ | \quad | \\ n_5 \quad n_3 \end{array} \tag{11.3}$$

The linear span \mathcal{H}_{CK} of $\mathcal{F}_{\mathbb{N}}$ is the graded Connes-Kreimer Hopf algebra of trees decorated by \mathbb{N}^* for the product

$$\pi(F_1 \otimes F_2) = F_1 F_2 \tag{11.4}$$

and the unit \emptyset .

⁴ Not to be confused with rooted plane trees, of which Schröder trees are a special case.

The coproduct Δ can be defined by induction

$$\Delta(\emptyset) = \emptyset \otimes \emptyset, \tag{11.5}$$

$$\Delta(T_1 \dots T_k) = \Delta(T_1) \dots \Delta(T_k), \tag{11.6}$$

$$\Delta(B_n^+(F)) = \emptyset \otimes B_n^+(F) + (B_n^+ \otimes \text{Id}) \circ \Delta(F). \tag{11.7}$$

There exists a combinatorial description of this coproduct (see [17]). For a given tree $T \in \mathcal{T}_{\mathbb{N}}$, an admissible cut c is a subset of its vertices such that, on the path from the root to an element of c , no other vertex of c is encountered. For such an admissible cut, $P^c(T)$ is the product of the subtrees of T whose roots are in c and $R^c(T)$ is the remaining tree, once these subtrees have been removed. With these definitions, for any tree T , we have

$$\Delta(T) = \sum_{c \text{ adm.}} R^c(T) \otimes P^c(T). \tag{11.8}$$

For example,

$$\begin{aligned} \Delta \left(\begin{array}{c} n_1 \\ \swarrow \quad \searrow \\ n_3 \quad n_2 \end{array} \right) &= \begin{array}{c} n_1 \\ \swarrow \quad \searrow \\ n_3 \quad n_2 \end{array} \otimes \emptyset + \begin{array}{c} n_1 \\ | \\ n_3 \end{array} \otimes \bullet_{n_2} + \begin{array}{c} n_1 \\ | \\ n_2 \end{array} \otimes \bullet_{n_3} \\ &+ \bullet_{n_1} \otimes \bullet_{n_2} \bullet_{n_3} + \emptyset \otimes \begin{array}{c} n_1 \\ \swarrow \quad \searrow \\ n_3 \quad n_2 \end{array} \end{aligned}$$

Definition 11.1. Given a formal diffeomorphism

$$u(z) = z + \sum_{n \geq 1} u_n z^{n+1}, \tag{11.9}$$

we associate with any tree T (see [15, 16, 36, 37]) a monomial $A_T(z)$ recursively defined as follows:

- For the empty tree $A_{\emptyset}(z) = z$,
- If $T = B_+^n(\emptyset)$ then $A_T(z) = u_n z^{n+1}$,
- If $T = B_+^n(F)$ where $F = T_1^{a_1} \dots T_k^{a_k}$ is a non empty product of k distinct decorated trees, with multiplicities a_1, \dots, a_k ($a_1 + \dots + a_k = s$), then

$$A_T(z) = \frac{1}{a_1! \dots a_k!} A_{T_1}^{a_1}(z) \dots A_{T_k}^{a_k}(z) (\partial_z^{a_1 + \dots + a_k} u_n z^{n+1}) \tag{11.10}$$

The main result is then:

Theorem 11.2. *The map ρ_u sending a character φ of \mathcal{H}_{CK} to the formal diffeomorphism of G_{diff}*

$$\rho_u(\varphi)(z) = \sum_{T \in \mathcal{T}_{\mathbb{N}}} \varphi(T) A_T(z) \tag{11.11}$$

is a group homomorphism from the group of characters G_{CK} of \mathcal{H}_{CK} to G_{diff} .

See [15, 16, 36, 37] for proofs.

Going back to the equation $u(h(z)) = q^{-1}h(qz)$, one can observe that

- $u = \rho_u(\varphi_0)$, where φ_0 is the character given by $\varphi_0(T) = 1$ (resp. 0) if $T = \emptyset$ or $T = B_+^n(\emptyset)$ (resp. otherwise).
- If the conjugating h is given by a character θ ($h = \rho_u(\theta)$) then $q^{-1}h(qz)$ is given by the character $\theta \circ q^Y$ where $q^Y(F) = q^{|F|}F$.

Therefore, the conjugacy equation can be lifted to the character equation

$$\varphi_0 * \theta = \theta \circ q^Y. \tag{11.12}$$

This equation is easily solved. For a tree $T = B_+^n(T_1 \dots T_s)$, we get

$$(q^{|T|} - 1)\theta(T) = \theta(T_1) \dots \theta(T_s) \tag{11.13}$$

so that

$$\theta(T) = \prod_{v \in T} \frac{1}{q^{|T_v|} - 1} \tag{11.14}$$

where T_v is the subtree of T whose root is the vertex v .

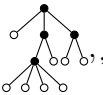
A more explicit expression can be found in [16]. Such “arborified” expressions are useful for analysis since they allow to prove the analyticity of the conjugating map under some diophantine conditions on q (ensuring a geometric growth of the numbers $\theta(T)$, see e.g., [16]).

11.2 Relating \mathcal{H}_{CK} and \mathcal{H}_{PT}

The similarity of the coefficients $c_r(q)$ and $\theta(T)$ suggests a link between both versions of the conjugacy equation, which turns out to be understandable at the level of Hopf algebras.

Theorem 11.3. *Let sk (for “skeleton”) be the map defined from PT to $\mathcal{T}_{\mathbb{N}}$ by $\text{sk}(\circ) = \emptyset$ and, if $t = \bigwedge(t_1, \dots, t_n)$ ($n \geq 2$), then $\text{sk}(t) = B_+^{n-1}(\text{sk}(t_1) \dots \text{sk}(t_n))$.*

This map extends naturally to an algebra morphism from \mathcal{H}_{PT} to \mathcal{H}_{CK} which is actually a Hopf algebra morphism.

For example if $t =$ ,

$$T = \text{sk}(t) = \begin{array}{c} & 2 & \\ & \bullet & \\ & / \quad \backslash & \\ 1 & & 1 \\ | & & \\ \bullet & & \\ | & & \\ 3 & & \end{array} \quad (11.15)$$

The proof follows immediately by comparing the recursive (or combinatorial) definition of the coproducts.

This Hopf morphism induces a group morphism sk^* sending a character $\varphi \in G_{CK}$ to the character $\text{sk}^*(\varphi) = \varphi \circ \text{sk}$. It sends the character θ to the character defined by

$$g = \sum_t c_t(q)t. \quad (11.16)$$

In other words, for any reduced plane tree t , $c_t(q) = \theta(\text{sk}(t))$.

11.3 The final diagram

Let us summarize the situation:

- We have a noncommutative analogue of the conjugacy equation whose solution is a character on \mathcal{H}_{PT} defined by the coefficients $c_t(q)$,
- In the commutative case, the solution can be computed as a character on \mathcal{H}_{CK} ,
- Both characters are related by the group morphism sk^* .

There is also a morphism from G_{ncdiff} to G_{diff} , so that we also get the solution in the commutative case. For $u \in G_{\text{diff}}$, the algebra map α_u sending S_0 to z and S_n to u_n defines a group morphism and, if we denote by $g_c \in G_{\text{ncdiff}}$ the sum of all corollas, then $\alpha_u(g_c) = u$. This morphism also sends the solution of the noncommutative conjugacy equation to the solution of the commutative one.

The final picture is then:

Theorem 11.4. *The diagram*

$$\begin{array}{ccc} G_{CK} & \xrightarrow{\text{sk}^*} & G_{\text{ncdiff}} \\ & \searrow \rho_u & \downarrow \alpha_u \\ & & G_{\text{diff}} \end{array} \quad (11.17)$$

is commutative.

Proof. Consider a character $\varphi \in G_{CK}$. Then, on the one hand

$$\rho_u(\varphi) = \sum_T \varphi(T) A_T(z) \tag{11.18}$$

and, on the other hand, as $\phi = \text{sk}^*(\varphi)$ ($\phi(t) = \varphi(\text{sk}(t))$),

$$\alpha_u(\phi) = \alpha_u \left(\sum_t \phi(t) S^t \right) = \sum_T \varphi(T) \alpha_u \left(\sum_{\text{sk}(t)=T} S^t \right). \tag{11.19}$$

The above diagram commutes if, for any tree T ,

$$A_T(z) = \alpha_u \left(\sum_{\text{sk}(t)=T} S^t \right). \tag{11.20}$$

The result is obvious for $T = \emptyset$, and for any tree $C_n = B_n^+(\emptyset)$, since $A_{C_n}(z) = u_n z^{n+1}$ and the only reduced tree with such a skeleton is the corolla c_{n+1} :

$$\alpha_u(S^{c_{n+1}}) = \alpha_u(S_n S_0^{n+1}) = u_n z^{n+1} = A_{C_n}(z). \tag{11.21}$$

Now, from Definition 11.1, if $T = B_n^+(T_1^{a_1} \dots T_k^{a_k})$ where T_1, \dots, T_k are distinct rooted trees, then

$$A_T(z) = \binom{n+1}{a_1, a_2, \dots, a_k} A_{T_1}^{a_1}(z) \dots A_{T_k}^{a_k}(z) u_n z^{n+1-a_1-\dots-a_k}. \tag{11.22}$$

Let

$$X_0 = S_0 \text{ and } X_i = \sum_{\text{sk}(t)=T_i} S^t. \tag{11.23}$$

If $W(a_0, a_1, \dots, a_k)$ is the set of all possible words obtained by concatenating a_i copies of X_i , then

$$\sum_{\text{sk}(t)=T} S^t = \sum_{w \in W(n+1-a_1-\dots-a_k, a_1, \dots, a_k)} S_n w \tag{11.24}$$

since a tree has skeleton T if and only if it can be written $c_n \circ (t_1, \dots, t_n)$ for the operadic composition, where the n -tuple (t_1, \dots, t_n) contains exactly a_i trees with skeleton T_i and $n + 1 - a_1 - \dots - a_k$ trees \circ . There are

exactly $\binom{n+1}{a_1, a_2, \dots, a_k}$ such n -tuples, and, by induction,

$$\begin{aligned} & \alpha_u \left(\sum_{\text{sk}(t)=T} S^t \right) \\ &= A_{T_1}^{a_1}(z) \dots A_{T_k}^{a_k}(z) u_n z^{n+1-a_1-\dots-a_k} \left(\sum_{w \in W(n+1-a_1-\dots-a_k, a_1, \dots, a_k)} 1 \right) \\ &= A_T(z) \end{aligned} \tag{11.25}$$

□

12 The Catalan operad

The preceding considerations can be repeated almost word for word for the free operad on one generator in each degree

$$\mathcal{C} = \bigoplus_{n \geq 1} \mathbb{C} \mathcal{T}_n \tag{12.1}$$

where \mathcal{T}_n denotes the set of all plane trees on n vertices:

$$\mathcal{T}_1 = \{\bullet\}, \mathcal{T}_2 = \left\{ \begin{array}{c} \bullet \\ \vdots \\ \bullet \end{array} \right\}, \mathcal{T}_3 = \left\{ \begin{array}{c} \bullet \\ \swarrow \quad \downarrow \\ \bullet \quad \bullet \end{array} \right\}, \mathcal{T}_4 = \left\{ \begin{array}{c} \bullet \\ \swarrow \quad \downarrow \quad \searrow \\ \bullet \quad \bullet \quad \bullet \end{array} \right\}, \dots \tag{12.2}$$

endowed with the same composition as in \mathcal{S} . We shall call it the *Catalan operad*, although it probably has other names [5, 26].

General plane trees can be represented by their Polish codes, as monomials S^I , where S_n is now the symbol of an n -ary operation, that is $S^\bullet = S_0$ and $S^{B_+(t_1, \dots, t_k)} = S_k S^{t_1} \dots S^{t_k}$. For instance,

$$S \begin{array}{c} \bullet \\ \swarrow \quad \downarrow \\ \bullet \quad \bullet \end{array} = S^{3100200}. \tag{12.3}$$

As observed in [39], these I are also the evaluation vectors on nondecreasing parking functions.

The discussion of Lagrange inversion and related problems given in [39] can be interpreted as calculations in the group $G_{\mathcal{C}}$ of this operad. The functional equation

$$g = \sum_{n \geq 0} S_n g^n \tag{12.4}$$

can be rewritten as

$$(S_0 - S^{10} - S^{200} - \dots) \circ g = S_0 \tag{12.5}$$

so that it amounts to inverting the series

$$f = S_0 - \sum_{n \geq 1} S^{n0^n} \tag{12.6}$$

in the group $G_{\mathcal{C}}$. The relation with the computations in Section 10.2 can be elucidated with the help of a surjective group morphism from G_{ncdiff} to $G_{\mathcal{C}}$. Recall that PT_L is the set of Schröder trees such that the rightmost

subtree of each internal vertex is a leaf. Let α be the map which sends \circ to \bullet and any other tree t of PT :

- to the the plane tree obtained by removing all the rightmost leaves of its internal vertices if t is in PT_L ,
- to 0 otherwise.

This map is surjective on plane trees and induces a linear map on monomials in S_0, S_1, \dots which happens to be a group morphism from G_{ncdiff} to G_C . If we still denote by α this morphism, then, since

$$\alpha(g_c) = \alpha \left(S^\circ + \sum_{n \geq 1} S^{\wedge(\circ^{n+1})} \right) = S_0 + \sum_{n \geq 1} S^{n0^n} \in G_C, \quad (12.7)$$

$$\alpha(g_L) = \alpha \left(\left(1 + \sum_{n \geq 1} S_n S_0^n \right)^{-1} S_0 \right) = S_0 - \sum_{n \geq 1} S^{n0^n} \in G_C. \quad (12.8)$$

we can obtain the composition inverse of these series of G_C as $\alpha(f_c)$ and $\alpha(f_L)$, which gives back the formulas of [39].

The functional equation for g can also be written

$$g = S_0 + \Omega g \cdot g =: S_0 + B(g, g) \quad (12.9)$$

Each plane tree in the solution of (12.4) corresponds to a unique binary tree $B_T(S_0)$ in the solution of (12.9). This induces a bijection between plane trees and binary trees: writing (see (5.1))

$$B(S^I, S^J) = \Omega S^I S^J, \quad (12.10)$$

there is a unique way to decompose a plane tree S^I on n vertices as

$$S^I = B(S^{I_1}, S^{I_2}) \quad (12.11)$$

so that recursively

$$S^I = B_T(S_0, \dots, S_0) \quad (12.12)$$

for a unique binary tree T with $n - 1$ internal vertices. For example,

$$S^{\bullet} = S^{10} = B(S_0, S_0), \quad (12.13)$$

$$S^{\bullet} \begin{array}{l} \diagup \\ \bullet \\ \diagdown \end{array} = S^{200} = B(S^{10}, S_0) = B(B(S_0, S_0), S_0), \quad (12.14)$$

$$S^{\bullet} \begin{array}{l} \bullet \\ \bullet \\ \bullet \end{array} = S^{110} = B(S_0, S^{10}) = B(S_0, B(S_0, S_0)) \quad (12.15)$$

We recover in this way the classical rotation correspondence.

In fact, if, in the one to one correspondence with plane tree, $S^{t_1} = S^{t_1}$ and $S^{t_2} = S^{t_2}$, the tree corresponding to $S^t = B(S^{t_1}, S^{t_2}) = \Omega S^t S^J$ is $t = B_+(B_-(t_1), t_2)$. Using this trick we get for instance

$$S^{3100200} = S^{\bullet} \begin{array}{c} \diagup \quad \diagdown \\ \bullet \quad \bullet \end{array} \begin{array}{c} \diagup \quad \diagdown \\ \bullet \quad \bullet \end{array} = B(S^{\bullet} \begin{array}{c} \diagup \quad \diagdown \\ \bullet \quad \bullet \end{array}, S^{\bullet} \begin{array}{c} \diagup \quad \diagdown \\ \bullet \quad \bullet \end{array}) = B(B(S^{\bullet} \begin{array}{c} \diagup \quad \diagdown \\ \bullet \quad \bullet \end{array}, S^{\bullet}), B(S^{\bullet} \begin{array}{c} \diagup \quad \diagdown \\ \bullet \quad \bullet \end{array}, S^{\bullet})) \quad (12.16)$$

that corresponds finally to the binary tree $B(B(B(S_0, B(S_0, S_0)), S_0), B(B(S_0, S_0), S_0))$:



Another question which can be investigated in this context is the formal solution of the generic differential equation

$$\frac{dx}{ds} = f(x(s)), \quad x(0) = x_0. \quad (12.18)$$

Rather than stating Cayley's formula for $x^{(k)}$ in terms of rooted trees and derivatives, we shall write down a noncommutative version involving plane trees and the coefficients of the generic power series f . Assuming without loss of generality that $x_0 = 0$, we can look for a series $X(s) \in G_C$ satisfying

$$\frac{dX}{ds} = \sum_{n \geq 0} S_n X(s)^n. \quad (12.19)$$

Thus,

$$X(s) = S_0 s + \sum_{n \geq 1} S_n \int_0^s X(u)^n du =: \sum_{n \geq 1} X_n \frac{s^n}{n!} \quad (12.20)$$

and solving iteratively as usual, we get successively

$$X_1 = S_0, \quad (12.21)$$

$$X_2 = S^{10}, \quad (12.22)$$

$$X_3 = 2S^{200} + S^{110}, \quad (12.23)$$

$$X_4 = 6S^{3000} + 3S^{2100} + 3S^{2010} + 2S^{1200} + S^{1110}. \quad (12.24)$$

Identifying as before trees and their Polish codes,

$$X_n = \sum_{t \in \mathcal{T}_n} c_t S^t \quad (12.25)$$

and setting

$$F_n(Y_1, \dots, Y_n) = S_n \int_0^s Y_1(u) \cdots Y_n(u) du \tag{12.26}$$

we have

$$X_{n+1} = \sum_{k=1}^n \sum_{i_1+\dots+i_k=n} F_k \left(X_{i_1} \frac{s^{i_1}}{i_1!}, \dots, X_{i_k} \frac{s^{i_k}}{i_k!} \right), \tag{12.27}$$

which gives for the coefficient c_t of $t = B_+(t_1, \dots, t_k) \in \mathcal{T}_{n+1}$

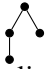
$$c_t \frac{s^{n+1}}{(n+1)!} = \int_0^s c_{t_1} \cdots c_{t_k} \frac{u^{|t_1|+\dots+|t_k|}}{|t_1|! \cdots |t_k|!} du \tag{12.28}$$

so that

$$c_t = \binom{n}{|t_1|, \dots, |t_k|} c_{t_1} \cdots c_{t_k} \tag{12.29}$$

which is clearly the recursion for the number of decreasing (or increasing) labellings of t , also given by the hook-length formula

$$c_t = (n+1)! \prod_{v \in t} \frac{1}{h_v} \tag{12.30}$$

where h_v is the number of nodes of the subtree with root v . For instance, for the tree  that corresponds to the monomial S^{2100} , there are 3 decreasing labellings:

$$\begin{array}{c} 4 \\ / \quad \backslash \\ 2 \quad 3 \\ | \\ 1 \end{array} , \quad \begin{array}{c} 4 \\ / \quad \backslash \\ 3 \quad 2 \\ | \\ 1 \end{array} , \quad \begin{array}{c} 4 \\ / \quad \backslash \\ 3 \quad 1 \\ | \\ 2 \end{array} . \tag{12.31}$$

Replacing each S_k by $\frac{f^{(k)}}{k!}$, we recover Cayley's formula for $x^{(n)}$,

$$\frac{d^n x}{ds^n} = \sum_{|t|=n} a(t) \delta_t, \tag{12.32}$$

where

$$a(t) = \frac{|t|!}{t! |S_t|}, \tag{12.33}$$

S_t being the symmetry group of t ,

$$B_+(t_1, \dots, t_n)! = |B_+(t_1, \dots, t_n)| \cdot t_1! \cdots t_n!, \quad \bullet! = 1. \tag{12.34}$$

and the elementary differentials are defined by [4]

$$\delta_{\bullet}^i = f^i, \quad \delta_{B_+(t_1, \dots, t_n)}^i = \sum_{j_1, \dots, j_n=1}^N (\delta_{t_1}^{j_1} \cdots \delta_{t_n}^{j_n}) \partial_{j_1} \cdots \partial_{j_n} f^i \quad (12.35)$$

In particular, the solution is given by

$$x(s) = x_0 + \sum_t \frac{s^{|t|}}{|t|!} a(t) \delta_t(0) \quad (12.36)$$

For example,

$$\begin{aligned} x^{(4)} &= f'''(f, f, f) + 3f''(f, f'(f)) \\ &\quad + f'(f''(f, f)) + f'(f'(f'(f))). \end{aligned} \quad (12.37)$$

Note that with the interpretation of S_n as an n -linear operation, our formal calculations are valid for $x \in \mathbb{R}^N$: we can write the Taylor expansion of f as

$$f(x) = F_0 + F_1(x) + F_2(x, x) + F_3(x, x, x) + \cdots \quad (12.38)$$

without expliciting the expression of F_n in terms of partial derivatives.

Once again, the functional equation (12.19) can be recast as a quadratic fixed point problem:

$$\begin{aligned} \frac{dX}{ds} &= S_0 + (S_1 + S_2X(s) + S_3X^2(s) + \cdots)X(s) \\ &= S_0 + (\Omega X'(s))X(s) \end{aligned} \quad (12.39)$$

so that

$$X(s) = S_0s + \int_0^s \Omega X'(u) \cdot X(u) du = S_0s + \mathbf{B}(X(s), X(s)) \quad (12.40)$$

The bilinear map \mathbf{B} acts on trees by

$$\mathbf{B}\left(S^i \frac{s^i}{i!}, S^j \frac{s^j}{j!}\right) = \binom{i+j}{i, j} \Omega S^{i+j} \frac{s^{i+j+1}}{(i+j+1)!} \quad (12.41)$$

13 Appendix: numerical examples

In the case of Lagrange inversion, comparison between the formal non-commutative solution and numerical examples (specializations of the alphabet, or characters) leads to interesting insights. We shall give here a (short) list of known workable examples.

13.1 Warmup: $A = 1$

The alphabet $A = 1$ is defined by $S_n(1) = 1$ for all n . In this case,

$$\phi(z) = \frac{qz}{1-z} = qz\sigma_z(1) \quad (13.1)$$

is a Möbius transformation, and it is trivial to conjugate it to its linear part when $q \neq 1$. However, it is a good exercise to work out the series solution. We have

$$S_n(m) = \binom{n+m-1}{n} \text{ so that } L(S^I)(1) = \frac{n!}{i_1! \cdots i_r!} = n!S^I(\mathbb{E}) \quad (13.2)$$

where \mathbb{E} is defined by $S_n(\mathbb{E}) = 1/n!$. Hence,

$$f(z) = \int_0^\infty e^{-t} L\left(z\sigma_{zt}\left(\frac{\mathbb{E}}{1-q}\right)\right) dt = \frac{z}{1-\frac{z}{1-q}}. \quad (13.3)$$

13.2 The logistic map: $A = -1$

The logistic map is defined by

$$\phi(z) = qz(1-z) = qz\sigma_z(-1). \quad (13.4)$$

Indeed, by definition, $\sigma_z(-1)$ is the inverse of $\sigma_z(1)$, so that $S_1(-1) = -1$ and $S_n(-1) = 0$ for $n > 1$.

The recurrence for $g_n(-1)$ is here

$$(1-q^n)g_n = \sum_{k=0}^{n-1} g_k g_{n-1-k} \quad (13.5)$$

yielding

$$\begin{aligned} g_1 &= \frac{1}{1-q}, \\ g_2 &= \frac{2}{(1-q)(1-q^2)}, \\ g_3 &= \frac{5+q}{(1-q)(1-q^2)(1-q^3)}, \dots \end{aligned} \quad (13.6)$$

the numerator being a q -analogue of $n!$.

For $q = -2, 2, 4$, these series have explicit forms in terms of elementary functions:

$$\begin{aligned} q = -2: f(z) &= \frac{\sqrt{3}}{6} \left(2\pi - 3 \arccos \left(z - \frac{1}{2} \right) \right), h(z) = \frac{1}{2} - \cos \left(\frac{2z}{\sqrt{3}} + \frac{\pi}{3} \right), \\ q = 2: f(z) &= -\frac{1}{2} \ln(1-2z), h(z) = \frac{1}{2} (1 - e^{-2z}), \\ q = 4: f(z) &= (\arcsin \sqrt{z})^2, h(z) = (\sin \sqrt{z})^2. \end{aligned} \quad (13.7)$$

Numerical investigations, including a conjecture for the radius of convergence in the general case, can be found in [7, 8].

13.3 The Ricker map: $A = \mathbb{E}$

This case corresponds to

$$\phi(z) = qze^z. \quad (13.8)$$

No closed expression is known for f or g , but a numerical study can be found in [7].

We have

$$\begin{aligned} S_n(m\mathbb{E}) &= \frac{m^n}{n!}, \text{ so that } L(S^l) \\ &= \frac{1^{i_1}(i_1+1)^{i_2}(i_1+i_2+1)^{i_3} \cdots (i_1+\cdots+i_{r-1}+1)^{i_r}}{i_1!i_2! \cdots i_r!} \end{aligned} \quad (13.9)$$

and we can compute

$$\begin{aligned} f_1 &= \frac{1}{1-q}, \\ f_2 &= \frac{3q+1}{2!(1-q)(1-q^2)}, \\ f_3 &= \frac{16q^3+11q^2+8q+1}{3!(1-q)(1-q^2)(1-q^3)}, \cdots \end{aligned} \quad (13.10)$$

The numerators are q -analogues of $(n!)^2$, whose combinatorial interpretation requires further investigations.

References

- [1] A. BJÖRNER and M. WACHS, *q*-Hook length formulas for forests, J. Combin. Theory Ser. A **52** (1989), 165–187.

- [2] C. BROUDER, A. FRABETTI and C. KRATTENTHALER, *Noncommutative Hopf algebra of formal diffeomorphisms*, QA/0406117, 2004 - arxiv.org
- [3] E. BURGUNDER and R. HOLTkamp, *Partial magmatic bialgebras*, Homology, Homotopy Appl. **10** (2008), no. 2, 59–81.
- [4] J. C. BUTCHER, “Numerical Methods for Ordinary Differential Equations”, (2nd ed.), John Wiley & Sons Ltd. (2008), ISBN 978-0-470-72335-7.
- [5] F. CHAPOTON, *Operads and algebraic combinatorics of trees*, Sém. Lothar. Combin. **58** (2007/08).
- [6] A. CONNES and D. KREIMER, *Hopf algebras, renormalization and noncommutative geometry*, In: “Quantum Field Theory: Perspective and Prospective” (Les Houches, 1998), Vol. 530 of *NATO Sci. Ser. C Math. Phys. Sci.*, Kluwer Acad. Publ., Dordrecht, 1999, 59–108.
- [7] T. L. CURTRIGHT and C. K. ZACHOS, *Evolution profiles and functional equations*, J. Phys. A **42** (2009), 485208.
- [8] T. L. CURTRIGHT and C. K. ZACHOS, *Chaotic maps, Hamiltonian flows, and holographic methods*, J. Phys A **43** (2010), 445101, 15pp.
- [9] T. L. CURTRIGHT, X. JIN and C. K. ZACHOS, *Approximate solutions of functional equations*, preprint (2011), arXiv:1105.3664.
- [10] T. L. CURTRIGHT and A. VEITIA, *Logistic map potentials*, preprint (2010), arXiv:1005.5030.
- [11] G. DUCHAMP, F. HIVERT and J.-Y. THIBON, *Noncommutative symmetric functions VI: free quasi-symmetric functions and related algebras*, Internat. J. Alg. Comput. **12** (2002), 671–717.
- [12] K. EBRAHIMI-FARD and D. MANCHON, *On an extension of Knuth’s rotation correspondence to reduced planar trees*, J. Noncommut. Geom. **8** (2014), 303–320.
- [13] K. EBRAHIMI-FARD, A. LUNDERVOLD and D. MANCHON, *Noncommutative Bell polynomials, quasideterminants and incidence Hopf algebras*, arXiv:1402.4761.
- [14] J. ÉCALLE, *Singularités non abordables par la géométrie*, Ann. Inst. Fourier (Grenoble) **42** (1992), 73–164.
- [15] F. FAUVET and F. MENOUS, *Ecalle’s arborification-coarborification transforms and Connes-Kreimer Hopf algebra*, Ann. Sci. Ecole Normale Sup. **50** (2017), 35–83.
- [16] F. FAUVET, F. MENOUS and D. SAUZIN, *Explicit linearization of one-dimensional germs through tree-expansions*, Bull. of the Soc. Math. de France, to appear.
- [17] L. FOISSY *Les algèbres de Hopf des arbres enracinés décorés. I*, Bull. Sci. Math., **126** (2002), 193–239.

- [18] L. FOISSY, *Les algèbres de Hopf des arbres enracinés décorés. II*, Bull. Sci. Math., **126** (2002), 249–288.
- [19] I.M. GELFAND, D. KROB, A. LASCOUX, B. LECLERC, V. S. RETAKH, and J.-Y. THIBON, *Noncommutative symmetric functions*, Adv. in Math. **112** (1995), 218–348.
- [20] I. GESSEL, *Noncommutative Generalization and q -analog of the Lagrange Inversion Formula*, Trans. Amer. Math. Soc. **257** (1980), no. 2, 455–482.
- [21] R. GROSSMAN and R. G. LARSON, *Hopf-algebraic structure of families of trees*, J. Algebra **126** (1989), 184–210.
- [22] R. GROSSMAN and R. G. LARSON, *Hopf-algebraic structure of combinatorial objects and differential operators*, Israel J. Math. **72** (1990), 109–117.
- [23] M. HAIMAN, *Conjectures on the quotient ring by diagonal invariants*, J. Algebraic Combin. **3** (1994), 17–36.
- [24] F. HIVERT, *Hecke algebras, difference operators, and quasi-symmetric functions*, Adv. Math. **155** (2000), 181–238.
- [25] F. HIVERT, J.-C. NOVELLI and J.-Y. THIBON, *Trees, functional equations and combinatorial Hopf algebras*, Europ. J. Combin. **29** (2008), 1682–1695.
- [26] R. HOLTkamp, *On Hopf algebra structures over free operads*, Adv. Math. **207** (2006), 544–565.
- [27] S. A. JONI and G.-C. ROTA, *Coalgebras and bialgebras in combinatorics*, Contemp. Math. **6** (1982), 1–47.
- [28] G. KOENIGS, *Recherches sur les intégrales de certaines équations fonctionnelles*, Ann. Sci. Ecole Norm. Sup. **1** (1884) supplém., 1–14.
- [29] D. KROB, B. LECLERC and J.-Y. THIBON, *Noncommutative symmetric functions II: Transformations of alphabets*, Intern. J. Alg. Comput. **7** (1997), 181–264.
- [30] A. LASCOUX, “Symmetric Functions and Combinatorial Operators on Polynomials”, CBMS Regional Conference Series in Mathematics, Vol. 99, American Math. Soc., Providence, RI, 2003.
- [31] C. LENART, *Lagrange inversion and Schur functions*, J. Algebraic Combin. **11** (2000), 69–78.
- [32] J.-L. LODAY, *The diagonal of the Stasheff polytope*, In: “Higher Structures in Geometry and Physics”, Vol. 287 of Progr. Math., Birkhäuser/Springer, New York, 2011, 269–292.
- [33] S. MARMI, *An Introduction To Small Divisors*, arXiv:math/0009232.
- [34] I.G. MACDONALD, “Symmetric Functions and Hall Polynomials”, 2nd ed., Oxford University Press, 1995.

- [35] F. MENOUS, *Formulas for the Connes-Moscovici Hopf algebra*, In: *Combinatorics and Physics*, Vol. 539 of *Contemp. Math.*, Amer. Math. Soc., Providence, RI, 2011, 269–285.
- [36] F. MENOUS, *An example of local analytic q -difference equation: analytic classification*, *Ann. Fac. Sci. Toulouse Math.* (6) **15** (2006), 773–814.
- [37] F. MENOUS, *On the stability of some groups of formal diffeomorphisms by the Birkhoff decomposition*. *Adv. Math.* **216** (2007), 1–28.
- [38] J.-C NOVELLI and J.-Y. THIBON, “A Hopf Algebra of Parking Functions”, *Proc. FPSAC/SFCA 2004*, Vancouver (electronic).
- [39] J.-C NOVELLI and J.-Y. THIBON, *Noncommutative symmetric functions and Lagrange inversion*, *Adv. Appl. Math.* **40** (2008), 8–35.
- [40] J.-C NOVELLI and J.-Y. THIBON, *Duplicial algebras and Lagrange inversion*, arXiv:1209.5959.
- [41] F. PANAITÉ, *Relating the Connes-Kreimer and Grossman-Larson Hopf algebras built on rooted trees*, *Lett. Math. Phys.* **51** (2000), 211–219.
- [42] E. SCHRÖDER, *Vier combinatorische Probleme*, *Zeitschrift für Angewandte Mathematik und Physik* **15** (1870), 361–376.
- [43] E. SCHRÖDER, *Über iterierte Funktionen*, *Math. Ann.* **3** (1871), 296–322.
- [44] C. L. SIEGEL, *Iteration of analytic functions*, *Ann. of Math. Second Series* **43** (1942), 607–612.
- [45] N. J. A. SLOANE, *The On-Line Encyclopedia of Integer Sequences*, <http://oeis.org+>.

CRM Series

Publications by the Ennio De Giorgi Mathematical Research Center Pisa

The Ennio De Giorgi Mathematical Research Center in Pisa, Italy, was established in 2001 and organizes research periods focusing on specific fields of current interest, including pure mathematics as well as applications in the natural and social sciences like physics, biology, finance and economics. The CRM series publishes volumes originating from these research periods, thus advancing particular areas of mathematics and their application to problems in the industrial and technological arena.

Published volumes

1. *Matematica, cultura e società 2004* (2005). ISBN 88-7642-158-0
2. *Matematica, cultura e società 2005* (2006). ISBN 88-7642-188-2
3. M. GIAQUINTA, D. MUCCI, *Maps into Manifolds and Currents: Area and $W^{1,2}$ -, $W^{1/2}$ -, BV-Energies*, 2006. ISBN 88-7642-200-5
4. U. ZANNIER (editor), *Diophantine Geometry*. Proceedings, 2005 (2007). ISBN 978-88-7642-206-5
5. G. MÉTIVIER, *Para-Differential Calculus and Applications to the Cauchy Problem for Nonlinear Systems*, 2008. ISBN 978-88-7642-329-1
6. F. GUERRA, N. ROBOTTI, *Ettore Majorana. Aspects of his Scientific and Academic Activity*, 2008. ISBN 978-88-7642-331-4
7. Y. CENSOR, M. JIANG, A.K. LOUIS (editors), *Mathematical Methods in Biomedical Imaging and Intensity-Modulated Radiation Therapy (IMRT)*, 2008. ISBN 978-88-7642-314-7
8. M. ERICSSON, S. MONTANGERO (editors), *Quantum Information and Many Body Quantum systems*. Proceedings, 2007 (2008). ISBN 978-88-7642-307-9
9. M. NOVAGA, G. ORLANDI (editors), *Singularities in Nonlinear Evolution Phenomena and Applications*. Proceedings, 2008 (2009). ISBN 978-88-7642-343-7
– *Matematica, cultura e società 2006* (2009). ISBN 88-7642-315-4
10. H. HOSNI, F. MONTAGNA (editors), *Probability, Uncertainty and Rationality*, 2010. ISBN 978-88-7642-347-5

11. L. AMBROSIO (editor), *Optimal Transportation, Geometry and Functional Inequalities*, 2010. ISBN 978-88-7642-373-4
- 12*. O. COSTIN, F. FAUVET, F. MENOUS, D. SAUZIN (editors), *Asymptotics in Dynamics, Geometry and PDEs; Generalized Borel Summation*, vol. I, 2011. ISBN 978-88-7642-374-1, e-ISBN 978-88-7642-379-6
- 12**. O. COSTIN, F. FAUVET, F. MENOUS, D. SAUZIN (editors), *Asymptotics in Dynamics, Geometry and PDEs; Generalized Borel Summation*, vol. II, 2011. ISBN 978-88-7642-376-5, e-ISBN 978-88-7642-377-2
13. G. MINGIONE (editor), *Topics in Modern Regularity Theory*, 2011. ISBN 978-88-7642-426-7, e-ISBN 978-88-7642-427-4
– *Matematica, cultura e società 2007-2008* (2012). ISBN 978-88-7642-382-6
14. A. BJORNER, F. COHEN, C. DE CONCINI, C. PROCESI, M. SALVETTI (editors), *Configuration Spaces*, Geometry, Combinatorics and Topology, 2012. ISBN 978-88-7642-430-4, e-ISBN 978-88-7642-431-1
15. A. CHAMBOLLE, M. NOVAGA E. VALDINOCI (editors), *Geometric Partial Differential Equations*, 2013. ISBN 978-88-7642-343-7, e-ISBN 978-88-7642-473-1
16. J. NEŠETŘIL, M. PELLEGRINI (editors), *The Seventh European Conference on Combinatorics, Graph Theory and Applications*, EuroComb 2013. ISBN 978-88-7642-524-0, e-ISBN 978-88-7642-525-7
17. L. AMBROSIO (editor), *Geometric Measure Theory and Real Analysis*, 2014. ISBN 978-88-7642-522-6, e-ISBN 978-88-7642-523-3
18. J. MATOUŠEK, J. NEŠETŘIL, M. PELLEGRINI (editors), *Geometry, Structure and Randomness in Combinatorics*, 2015. ISBN 978-88-7642-524-0, e-ISBN 978-88-7642-525-7
19. N. FUSCO, A. PRATELLI (editors), *Free Discontinuity Problems*, 2016. ISBN 978-88-7642-592-9, e-ISBN 978-88-7642-593-6
20. F. FAUVET, D. MANCHON, S. MARMI, D. SAUZIN (editors), *Resurgence, Physics and Numbers*, 2017. ISBN 978-88-7642-612-4, e-ISBN 978-88-7642-613-1

Volumes published earlier

Dynamical Systems. Proceedings, 2002 (2003)

Part I: *Hamiltonian Systems and Celestial Mechanics*.

ISBN 978-88-7642-259-1

Part II: *Topological, Geometrical and Ergodic Properties of Dynamics*.

ISBN 978-88-7642-260-1

Matematica, cultura e società 2003 (2004). ISBN 88-7642-129-7

Ricordando Franco Conti, 2004. ISBN 88-7642-137-8

N.V. KRYLOV, *Probabilistic Methods of Investigating Interior Smoothness of Harmonic Functions Associated with Degenerate Elliptic Operators*, 2004. ISBN 978-88-7642-261-1

Phase Space Analysis of Partial Differential Equations. Proceedings, vol. I, 2004 (2005). ISBN 978-88-7642-263-1

Phase Space Analysis of Partial Differential Equations. Proceedings, vol. II, 2004 (2005). ISBN 978-88-7642-263-1